Santanu Saha Ray

Nonlinear Differential Equations in Physics

Novel Methods for Finding Solutions

Springer

Nonlinear Differential Equations in Physics

Santanu Saha Ray

Nonlinear Differential Equations in Physics

Novel Methods for Finding Solutions

Springer

Santanu Saha Ray
Department of Mathematics
National Institute of Technology Rourkela
Odisha, India

ISBN 978-981-15-1655-9 ISBN 978-981-15-1656-6 (eBook)
https://doi.org/10.1007/978-981-15-1656-6

This Springer imprint is published by the registered company Springer Nature Singapore Pte Ltd.
The registered company address is: 152 Beach Road, #21-01/04 Gateway East, Singapore 189721, Singapore

Preface

This book provides brief introduction to the fractional derivatives and preliminaries of local fractional calculus and presents an overview of wavelets in mathematical preliminaries. The need of the present work for the scientific and engineering community also has been discussed succinctly in the book.

In Chap. 1, various analytical and numerical methods for solving partial and fractional differential equations have been discussed along with some numerical methods for solving stochastic point kinetics equations. In Chap. 2, the utilization of new approaches of decomposition method in getting solutions for partial and fractional differential equations has been discussed. In this regard, a modified decomposition method has been newly applied for solving coupled Klein–Gordon–Schrödinger equations. In Chap. 3, the generalized order operational matrix of Haar wavelet has been used for finding the numerical solution of Bagley–Torvik equation. Next, the solutions of the Haar wavelet method are compared with OHAM as well as with the exact solutions for the fractional Fisher-type equation. The generalized order operational matrix of the Haar wavelet has been proposed for first time by the author for finding the numerical solution of Bagley–Torvik equation. In Chap. 4, an investigation into solutions of Riesz space fractional differential equations by using various numerical methods has been presented. In application, the solution of inhomogeneous fractional diffusion equation with Riesz space fractional derivative has been presented by utilizing an explicit finite difference scheme with shifted Grünwald approximation technique.

In Chap. 5, the exact solutions of fractional differential equations have been reported. Methods like first integral method, classical Kudryashov method, modified Kudryashov method, and mixed dn-sn method have been utilized here for getting new exact solutions of fractional differential equations. Also, the fractional complex transform with the local fractional derivatives has been used here for the reduction of fractional differential equations to integer-order ordinary differential equations. In Chap. 6, the generalized Jacobi elliptic function expansion method has been used for getting new exact solutions of the coupled Schrödinger–Boussinesq equations (CSBEs). Moreover, by numerical results, it has been shown that the nature of the solutions is doubly periodic. For justifying the nature of the solutions

as doubly periodic, the numerical results have also been presented in this work. In Chap. 7, new techniques, viz. modified fractional reduced differential transform method (MFRDTM) and coupled fractional reduced differential transform method (CFRDTM), are proposed for the first time for solving fractional differential equations. In view of that, the fractional KdV equation has been solved by using the modified fractional reduced differential transform method (MFRDTM). Furthermore, convergence analysis and error estimate for MFRDTM and CFRDTM have been presented in this chapter. The main advantages of the methods emphasize the fact that they provide explicit analytical approximate solutions and also numerical solutions elegantly.

In Chap. 8, Riesz fractional coupled Schrödinger–KdV equations have been solved by implementing a new approach, viz. time-splitting spectral method. In order to verify the results, it has been also solved by an implicit finite difference method by using fractional centered difference approximation for Riesz fractional derivative. The obtained results manifest that the proposed time-splitting spectral method is very effective and simple for obtaining approximate solutions of Riesz fractional coupled Schrödinger–KdV equations. In the last chapter, the stochastic point kinetics equations in nuclear reactor dynamics have been solved by using Euler–Maruyama and strong order 1.5 Taylor numerical methods. From the obtained results, it has been concluded that Euler–Maruyama and strong order 1.5 Taylor numerical methods perform an effective calculation in comparison with stochastic piecewise constant approximations method. So the proposed method is efficient and a powerful tool for solving the stochastic point kinetics equations. This work has been universally recognized as a benchmark work of the author in this field.

Rourkela, India Santanu Saha Ray

Acknowledgements

I take this opportunity to express my sincere gratitude to Dr. R. K. Bera, former Professor and Head, Department of Science, National Institute of Technical Teacher's Training and Research, Kolkata, and Dr. K. S. Chaudhuri, Professor, Department of Mathematics, Jadavpur University, Kolkata, for their encouragement in the preparation of this book. I also express my sincere gratitude to Director of National Institute of Technology Rourkela, Odisha, for his kind cooperation in this regard. I received considerable assistance from my colleagues in the Department of Mathematics, National Institute of Technology Rourkela, Odisha.

I wish to express my sincere thanks to several people involved in the preparation of this book. Moreover, I am especially grateful to Springer for their cooperation in all aspects of the production of this book. Last but not least, special mention should be made of my parents and my beloved wife, Lopamudra, for their patience, unequivocal support, and encouragement throughout the period of my work. I also acknowledge the allowance of my son, Sayantan, for not sparing my juxtaposition in his childhood playtime and valuable educational activities. I look forward to receiving comments and suggestions on the work from the readers.

Rourkela, India Santanu Saha Ray

Contents

About the Author

Santanu Saha Ray is Professor and Head of the Department of Mathematics, National Institute of Technology Rourkela, Odisha, India. An elected Fellow of the Institute of Mathematics and its Applications, UK, since 2018, Prof. Saha Ray is also a member of the Society for Industrial and Applied Mathematics (SIAM), American Mathematical Society (AMS) and the International Association of Engineers (IAENG). With over 18 years of experience in teaching undergraduate and graduate students and 17 years of research in mathematics, his focus areas are fractional calculus, differential equations, wavelet transforms, stochastic differential equations, integral equations, nuclear reactor kinetics with simulation, numerical analysis, operations research, mathematical modeling, mathematical physics, and computer applications.

The editor-in-chief of the *International Journal of Applied and Computational Mathematics* and associate editor of *Mathematical Sciences* (both published by Springer), Prof. Saha Ray has published research papers in various international journals of repute. In addition, he has authored six books: one with Springer and five with other publishers—*Graph Theory with Algorithms and Its Applications: In Applied Science and Technology* (Springer); *Fractional Calculus with Applications for Nuclear Reactor Dynamics*; *Numerical Analysis with Algorithms and Programming*; *Wavelet Methods for Solving Partial Differential Equations and Fractional Differential Equations*; *Generalized Fractional Order Differential Equations Arising in Physical Models*; and *Novel Methods for Solving Linear and Nonlinear Integral Equations* (with other publishers). He has served as principal investigator for various sponsored research projects funded by government agencies. He received an IOP Publishing Top Cited Author Award in 2018, which recognizes outstanding authors using citations recorded in Web of Science.

List of Figures

List of Tables

Chapter 1
Mathematical Preliminaries

1.1 Overview

The main objective is to propose novel analytical and numerical techniques to find the solutions of partial, stochastic, and fractional-order differential equations arising in physical problems. Most of the physical phenomena that arise in mathematical physics and engineering fields can be best described by the nonlinear partial differential equations. The problems arise in different areas of applied mathematics, physics, and engineering, including fluid dynamics, nonlinear optics, solid mechanics, plasma physics, quantum field theory, and condensed-matter physics, can be modeled by partial differential equations [1–3]. Many problems of physical interest are described by partial differential equations. The usual procedures necessarily change the actual problems in essential ways in order to make it mathematically tractable by the conventional methods. Unfortunately, these changes necessarily deviate the actual solutions; therefore, they can differ, sometimes seriously, from the actual physical behavior. Physically accurate and correct solutions can be obtained by avoiding these limitations, which would add an important advancement to our insights into the natural behavior of physical systems. Consequently, it would potentially enhance the scientific and technological breakthroughs for solving nonlinear physical problems.

Nowadays, the subject of fractional calculus and its applications has gained considerable popularity and importance during the past three decades or so, mainly due to its demonstrated applications in various seemingly diverse and widespread fields of science and engineering [4–12]. It deals with derivatives and integrals of arbitrary orders. In many cases, the real physical processes could be modeled in a reliable manner using fractional-order differential equations rather than integer-order equations [4–6].

In this context, the local fractional calculus theory is very important for modeling problems for fractal mathematics and engineering on Cantorian space in fractal media [13–15]. Most nonlinear physical phenomena that appear in many

S. Saha Ray, *Nonlinear Differential Equations in Physics*,
https://doi.org/10.1007/978-981-15-1656-6_1

areas of scientific fields, in particular in modeling anomalous dynamics of complex systems, neutron diffusion and transport, control theory, viscoelasticity, rheology, signal processing, biomechanics, plasma physics, solid state physics, fluid dynamics, optical fibers, mathematical biology, and chemical kinetics, can be best modeled by nonlinear fractional partial differential equations.

Various important phenomena in electromagnetics, viscoelasticity, fluid mechanics, electrochemistry, advection-diffusion models, biological population models, optics and signals processing are well described by fractional differential equations [4–6, 9–12]. But it is quite difficult to get the exact solutions of nonlinear fractional differential equations. For that reason, we need a reliable and efficient technique for the solution of fractional differential equations.

Stochastic differential equations (SDEs) [16–20] occur where a system described by differential equations is influenced by random noise. Typically, SDEs contain a variable which represents random white noise calculated as the derivative of Brownian motion or the Wiener process. However, other types of random behavior are possible. Stochastic differential equation (SDE) models play a prominent role in a range of application areas, including biology, chemistry, epidemiology, mechanics, microelectronics, economics, and finance.

The aim of this book is to develop and improve significantly analytical and numerical techniques in order to have advanced approaches to reinforce and complement classical methods. The improved and developed techniques have been examined to be reliable, accurate, effective, and efficient in both the analytic and numerical purposes.

The present research work focuses on new development of valuable analytical and numerical techniques that have been examined for effectiveness and reliability over other existing methods.

1.2 Introduction to Fractional Calculus

Fractional differential operators have a long history, having been mentioned by Leibniz in a letter to L'Hospital in 1695. Referring to the question of fractional-order differentiation, Leibniz wrote, "It will lead to a paradox, from which one-day useful consequences will be drawn." Early mathematicians who contributed to the study of fractional differential operators include Liouville, Riemann, and Holmgrem (See [8] for a history of the development of fractional differential operators). A number of definitions for the fractional derivative have been emerged over the years: Grünwald–Letnikov fractional derivative, Riemann–Liouville fractional derivative, and the Caputo fractional derivative [4–6, 8].

The fractional differential equations appear more and more frequently in different research areas and engineering applications. An effective and easy-to-use method for solving such equations is needed. It should be mentioned that from the viewpoint of fractional calculus applications in physics, chemistry, and engineering, it was undoubtedly the book written by Oldham and Spanier [6] which played an

outstanding role in the development of this subject. Moreover, it was the first book that was entirely devoted to a systematic presentation of the ideas, methods, and applications of the fractional calculus.

Later, there appeared several fundamental works on various aspects of the fractional calculus including an extensive survey on fractional differential equations by Podlubny [4], Miller and Ross [5], and others. Furthermore, several references to the books by Oldham and Spanier [6], Podlubny [4], and Miller and Ross [5] show that applied scientists need first of all an easy introduction to the theory of fractional derivatives and fractional differential equations, which could help them in their initial steps to adopting the fractional calculus as a method of research.

1.2.1 Fractional Derivative and Integration

Fractional calculus has been used to model physical and engineering processes which are found to be best described by fractional differential equations. For that reason, we need a reliable and efficient technique for the solution of fractional differential equations. The fractional calculus has gained considerable importance during the past decades mainly due to its applications in diverse fields of science and engineering.

Definition 1 A real function $f(t)$, $t > 0$ is said to be in the space C_γ, $\gamma \in \mathsf{R}$ if there exists a real number $p(> \gamma)$, such that $f(t) = t^p f_1(t)$, where $f_1(t) \in C[0, \infty]$ and it is said to be in the space C_γ^m iff $f^{(m)} \in C_m$, $m \in \mathrm{N}$.

Riemann–Liouville Integral and Derivative Operator

The most frequently encountered definition of an integral of fractional order is the Riemann–Liouville integral [4].

The fractional-order Riemann–Liouville integral of order $\alpha(>0)$, of a function $f \in C_\gamma$, $\gamma \geq -1$ is defined as

$$J^\alpha f(t) = \frac{1}{\Gamma(\alpha)} \int_0^t (t-\tau)^{\alpha-1} f(\tau)\, \mathrm{d}\tau, \quad t > 0, \quad \alpha \in R^+. \tag{1.1}$$

where R^+ is the set of positive real numbers.

Remark 1 For $f \in C_\gamma$, $\gamma \geq -1$, we have the following property

$$J^\alpha t^\beta = \frac{\Gamma(\beta+1)\, t^{\beta+\alpha}}{\Gamma(\beta+\alpha+1)}, \ \beta > -1, \ \alpha > -1-\beta.$$

Definition 2 The left-hand side and right-hand side Riemann–Liouville fractional integral of a function $f \in C_\gamma$, $(\gamma \geq -1)$ are defined as

$$ {}_{-\infty}J_t^\alpha f(t) = \frac{1}{\Gamma(m-\alpha)} \int_{-\infty}^{t} (t-\tau)^{m-\alpha-1} f(\tau)\, \mathrm{d}\tau,\ m-1<\alpha<m,\ m \in N, \quad (1.2) $$

and

$$ {}_tJ_\infty^\alpha f(t) = \frac{(-1)^m}{\Gamma(m-\alpha)} \int_{t}^{\infty} (\tau-t)^{m-\alpha-1} f(\tau)\, \mathrm{d}\tau, \quad \text{for} \quad m-1<\alpha<m,\ m \in N \quad (1.3) $$

respectively.

Definition 3 Riemann–Liouville fractional derivative of order α ($\alpha > 0$ and $\alpha \in \boldsymbol{R}^+$) is defined as

$$ \begin{aligned} D^\alpha f(t) &= D^m J^{m-\alpha} f(t) \\ &= \begin{cases} \frac{1}{\Gamma(m-\alpha)} \frac{\mathrm{d}^m}{\mathrm{d}t^m} \int_0^t (t-\tau)^{(m-\alpha-1)} f(\tau)\mathrm{d}\tau, & \text{if } m-1<\alpha<m, m \in \boldsymbol{N} \\ \frac{\mathrm{d}^m f(t)}{dt^m}, & \text{if } \alpha = m,\ m \in \boldsymbol{N} \end{cases} \end{aligned} \quad (1.4) $$

Definition 4 The left Riemann–Liouville fractional derivative of order $\alpha(m-1<\alpha<m,\ m \in N)$ can be defined as

$$ {}_{-\infty}D_t^\alpha f(t) = \frac{1}{\Gamma(m-\alpha)} \frac{\mathrm{d}^m}{\mathrm{d}t^m} \int_{-\infty}^{t} (t-\tau)^{m-\alpha-1} f(\tau)\mathrm{d}\tau,\ m-1<\alpha<m,\ m \in N \quad (1.5) $$

Definition 5 The right Riemann–Liouville fractional derivative of order $\alpha(m-1<\alpha<m,\ m \in N)$ can be defined as

$$ {}_tD_\infty^\alpha f(t) = \frac{(-1)^m}{\Gamma(m-\alpha)} \frac{\mathrm{d}^m}{\mathrm{d}t^m} \int_{t}^{\infty} (\tau-t)^{m-\alpha-1} f(\tau)\mathrm{d}\tau,\ m-1<\alpha<m,\ m \in N. \quad (1.6) $$

Remark 2 One of the interesting properties of the Riemann–Liouville fractional derivative is the derivative of a constant which is not zero. So mathematically, it can be written as

$$ D_t^\alpha C = \frac{Ct^{-\alpha}}{\Gamma(1-\alpha)}, \quad (1.7) $$

where C is a constant.

The Semi-group Property of the Fractional Integral Operator

If $\mathrm{Re}(\alpha) > 0$ and $\mathrm{Re}(\beta) > 0$ then the equation $J^{\alpha}J^{\beta}g(t) = J^{\beta}J^{\alpha}g(t) = J^{\alpha+\beta}g(t)$ is satisfied at almost every point $t \in [a,\ b]$ for $f(t) \in L_p[a,b](1 \le p \le \alpha)$. If $\alpha + \beta > 1$, then $J^{\alpha}J^{\beta}g(t) = J^{\beta}J^{\alpha}g(t) = J^{\alpha+\beta}g(t)$ held at any point of $[a,b]$.

Caputo Fractional Derivative

The fractional derivative, introduced by Caputo [4] in the late sixties, is called Caputo fractional derivative. The fractional derivative of $f(t)$ in the Caputo sense is defined by

$$\begin{aligned} D_t^{\alpha} f(t) &= J^{m-\alpha} D^m f(t) \\ &= \begin{cases} \frac{1}{\Gamma(m-\alpha)} \int_0^t (t-\tau)^{(m-\alpha-1)} \frac{\mathrm{d}^m f(\tau)}{\mathrm{d}\tau^m} \mathrm{d}\tau, & \text{if } m-1 < \alpha < m,\ m \in \boldsymbol{N}, \\ \frac{\mathrm{d}^m f(t)}{\mathrm{d}t^m}, & \text{if } \alpha = m,\ m \in \boldsymbol{N}, \end{cases} \end{aligned} \tag{1.8}$$

where the parameter α is the order of the derivative and is allowed to be real or even complex. In this paper, only real and positive α will be considered.

For the Caputo's derivative, we have

$$D^{\alpha} C = 0, \quad (C \text{ is a constant}) \tag{1.9}$$

$$D^{\alpha} t^{\beta} = \begin{cases} 0, & \beta \le \alpha - 1, \\ \frac{\Gamma(\beta+1)t^{\beta-\alpha}}{\Gamma(\beta-\alpha+1)}, & \beta > \alpha - 1. \end{cases} \tag{1.10}$$

Similar to integer-order differentiation, Caputo's derivative is linear.

$$D^{\alpha}(\gamma f(t) + \delta g(t)) = \gamma D^{\alpha} f(t) + \delta D^{\alpha} g(t), \tag{1.11}$$

where γ and δ are constants, and satisfies so-called Leibnitz's rule.

$$D^{\alpha}(g(t)f(t)) = \sum_{k=0}^{\infty} \binom{\alpha}{k} g^{(k)}(t) D^{\alpha-k} f(t), \tag{1.12}$$

if $f(\tau)$ is continuous in [0,t] and $g(\tau)$ has continuous derivatives sufficient number of times in $[0,\ t]$.

Lemma 1: Let $\mathrm{Re}(\alpha) > 0$ and let $n = [\mathrm{Re}(\alpha)] + 1$ for $\alpha \notin \boldsymbol{N}_0 = \{0, 1, 2, \ldots\}$; $n = \alpha$ for $\alpha \in \boldsymbol{N}_0$. If $f(t) \in AC^n[a,\ b]$(the space of functions $f(t)$ which are absolutely continuous and possess continuous derivatives up to order $n-1$ on $[a,b]$) or $f(t) \in C^n[a,\ b]$ (the space of functions $f(t)$ which are n times continuously differentiable on $[a,b]$), then

$$ {}^{C}D_t^{\alpha} J^{\alpha} f(t) = f(t), \tag{1.13} $$

$$ J^{\alpha} {}^{C}D_t^{\alpha} f(t) = f(t) - \sum_{k=0}^{n-1} \frac{t^k}{k!} f^{(k)}(0+), \; t > 0. \tag{1.14} $$

Proof Let $\alpha \notin \boldsymbol{N}_0$. Since $f(t) \in AC^n[a, b]$, the Caputo derivative ${}^{C}D_t^{\alpha} f(t)$ is continuous on $[a, b]$, i.e., ${}^{C}D_t^{\alpha} f(t) \in C[a, b]$.

Now, according to the definition of Caputo derivative Eq. (1.8),

$$ \begin{aligned} {}^{C}D_t^{\alpha} J^{\alpha} f(t) &= J^{n-\alpha} D^n J^{\alpha} f(t) \\ &= J^{n-\alpha} J^{\alpha-n} f(t), \text{ by the property } J^{\alpha-n} f(t) = D^n J^{\alpha} f(t) \\ &= f(t). \end{aligned} $$

Thus, Eq. (1.13) has been derived.

Again, according to the definition of Caputo derivative Eq. (1.8),

$$ \begin{aligned} J^{\alpha} {}^{C}D_t^{\alpha} f(t) &= J^{\alpha} J^{n-\alpha} D^{(n)} f(t) \\ &= J^n D^{(n)} f(t), \quad \text{using the semi-group property in (1.1)} \\ J^{\alpha} J^{n-\alpha} &= J^n \\ &= f(t) - \sum_{k=0}^{n-1} \frac{t^k f^{(k)}(0+)}{\Gamma(k+1)}. \end{aligned} $$

Hence, Eq. (1.14) has been obtained. ■

Theorem 1.1 (*Generalized Taylor's formula* [21])
Suppose that $D_a^{k\alpha} f(t) \in C(a, b]$ *for* $k = 0, 1, \ldots, n+1$, *where* $0 < \alpha \leq 1$, *we have*

$$ f(t) = \sum_{i=0}^{n} \frac{(t-a)^{i\alpha}}{\Gamma(i\alpha+1)} \left[D_a^{i\alpha} f(t) \right]_{t=a} + \Re_n^{\alpha}(t; a), \tag{1.15} $$

with $\Re_n^{\alpha}(t; a) = \frac{(t-a)^{(n+1)\alpha}}{\Gamma((n+1)\alpha+1)} \left[D_a^{(n+1)\alpha} f(t) \right]_{t=\xi}, \quad a \leq \xi \leq t, \forall t \in (a, b],$

where $D_a^{k\alpha} = D_a^{\alpha}.D_a^{\alpha}.D_a^{\alpha}...D_a^{\alpha}$ (k times).

Proof The proof of the Theorem 1.1 can be found from Theorem 3 in Ref. [21]. ■

Grünwald–Letnikov Fractional Derivative

The Grünwald–Letnikov fractional derivative was first introduced by Anton Karl Grünwald (1838–1920) from Prague, in 1867 and by Aleksey Vasilyevich Letnikov

(1837–1888) from Moscow in 1868. The Grünwald–Letnikov fractional derivative is based on finite differences, which is equivalent to the Riemann–Liouville definition.

The Grünwald–Letnikov fractional derivative of an order $\alpha(>0)$ [4, 8, 22] is defined as

$$ {}_aD_t^{\alpha} f(t) = \lim_{\substack{h \to 0 \\ mh = t-a}} h^{-q} \sum_{r=0}^{m} \omega_r^q f(t - rh), \tag{1.16} $$

where $\omega_r^q = (-1)^r \binom{q}{r}$.

$$ \omega_0^q = 1 \text{ and } \omega_r^q = \left(1 - \frac{q+1}{r}\right) \omega_{r-1}^q,\ r = 1, 2, \ldots \tag{1.17} $$

Riesz Fractional Integral and Derivative

In this section, some significant definitions, viz. the right Riemann–Liouville derivative, left Riemann–Liouville derivative, Riesz fractional derivative, and Riesz fractional integral which are to be used subsequently in consequent chapters, have been presented.

Definition 6 Riesz fractional integral [4, 8, 23, 24] of the order α, $n-1 \le \alpha < n$ of a function $f \in C_\gamma$, $(\gamma \ge -1)$ is defined as

$$ \begin{aligned} {}_0^R J_x^{\alpha} f(x) &= c_\alpha \left({}_{-\infty}J_x^{\alpha} + {}_xJ_{\infty}^{\alpha} \right) f(x) \\ &= \frac{c_\alpha}{\Gamma(\alpha)} \int_{-\infty}^{+\infty} |x - \zeta|^{\alpha - 1} f(\zeta)\, \mathrm{d}\zeta, \end{aligned} $$

where $c_\alpha = \frac{1}{2\cos\left(\frac{\pi\alpha}{2}\right)}$, $\alpha \neq 1$.

Here, ${}_{-\infty}J_t^{\alpha}$, ${}_tJ_{\infty}^{\alpha}$ are the left-hand and right-hand side Riemann–Liouville fractional integral operators defined in definition 2.

Definition 7 The Riesz fractional derivative of order α $(n-1 < \alpha \le n, n \in \mathbb{N})$ on the infinite domain $-\infty < t < \infty$ of a function $f \in C_\gamma$, $(\gamma \ge -1)$ is defined as [4, 8, 23–25]

$$ \frac{\mathrm{d}^{\alpha} f(x)}{\mathrm{d}|x|^{\alpha}} = -c_\alpha \left({}_{-\infty}D_x^{\alpha} f(x) + {}_xD_{\infty}^{\alpha} f(x) \right), \tag{1.18} $$

where $c_\alpha = \frac{1}{2\cos\left(\frac{\pi\alpha}{2}\right)}$, $\alpha \neq 1$.

Here, ${}_{-\infty}D_t^\alpha$ and ${}_tD_\infty^\alpha$ are the left-hand and right-hand side Riemann–Liouville fractional differential operators defined in definitions 4 and 5, respectively.

In case of $a \leq t \leq b$ (i.e., t defined in a finite interval), the Riesz fractional derivative of order α $(n-1 < \alpha \leq n, n \in \mathsf{N})$ can be written as

$$\frac{\mathrm{d}^\alpha f(t)}{\mathrm{d}|x|^\alpha} = -\frac{1}{2\cos\left(\frac{\alpha\pi}{2}\right)}\left({}_aD_x^\alpha f(x) + {}_xD_b^\alpha f(x)\right),$$

where

$${}_aD_x^\alpha f(x) = \frac{1}{\Gamma(n-\alpha)}\frac{\mathrm{d}^n}{\mathrm{d}x^n}\int_a^x \frac{f(\zeta)\mathrm{d}\zeta}{(x-\zeta)^{1-n+\alpha}},$$

$${}_xD_b^\alpha f(x) = \frac{(-1)^n}{\Gamma(n-\alpha)}\frac{\mathrm{d}^n}{\mathrm{d}x^n}\int_x^b \frac{f(\zeta)\mathrm{d}\zeta}{(\zeta-x)^{1-n+\alpha}}.$$

Lemma 2 *For a function $\phi(t)$ defined on the infinite domain $(-\infty < x < \infty)$, the following equality holds*:

$$-(-\Delta)^{\frac{\alpha}{2}}\phi(x) = -c_\alpha({}_{-\infty}D_x^\alpha + {}_xD_\infty^\alpha)\phi(x) = \frac{\mathrm{d}^\alpha}{\mathrm{d}|x|^\alpha}\phi(x), \text{for } n-1 < \alpha \leq n,\ n \in \mathsf{N}. \tag{1.19}$$

Proof According to Samko et al. [8], a fractional power of the Laplace operator is defined as follows:

$$-(-\Delta)^{\frac{\alpha}{2}}\phi(x) = -F^{-1}|\xi|^\alpha \mathbf{F}(\phi(x)), \tag{1.20}$$

where F and F^{-1} denote the Fourier transform and inverse Fourier transform of $f(x)$, respectively. Hence, we have

$$-(-\Delta)^{\frac{\alpha}{2}}\phi(x) = -\frac{1}{2\pi}\int_{-\infty}^{\infty} \mathrm{e}^{-it\xi}|\xi|^\alpha \int_{-\infty}^{\infty} \mathrm{e}^{i\xi\eta}\phi(\eta)\mathrm{d}\eta\mathrm{d}\xi.$$

Supposing that $\phi(x)$ vanishes at $x = \pm\infty$, the integration by parts yields

$$\int_{-\infty}^{\infty} \mathrm{e}^{i\xi\eta}\phi(\eta)\mathrm{d}\eta = -\frac{1}{i\xi}\int_{-\infty}^{\infty} \mathrm{e}^{i\xi\eta}\phi'(\eta)\mathrm{d}\eta.$$

Thus, we obtain

$$-(-\Delta)^{\frac{\alpha}{2}}\phi(x) = -\frac{1}{2\pi}\int_{-\infty}^{\infty}\phi'(\eta)\left[i\int_{-\infty}^{\infty}e^{i\xi(\eta-t)}\frac{|\xi|^{\alpha}}{\xi}\mathrm{d}\xi\right]\mathrm{d}\eta.$$

Let $I = i\int_{-\infty}^{\infty}\mathrm{e}^{i\xi(\eta-x)}\frac{|\xi|^{\alpha}}{\xi}\mathrm{d}\xi$, then

$$I = i\left[-\int_{0}^{\infty}\mathrm{e}^{i\xi(x-\eta)}\xi^{\alpha-1}\mathrm{e}\xi + \int_{0}^{\infty}\mathrm{e}^{i\xi(\eta-x)}\xi^{\alpha-1}\mathrm{d}\xi\right],$$

for $0<\alpha<1$, we have

$$I = i\left[\frac{-\Gamma(\alpha)}{[i(\eta-x)]^{\alpha}} + \frac{\Gamma(\alpha)}{[i(x-\eta)]^{\alpha}}\right] = \frac{\mathrm{sign}(x-\eta)\Gamma(\alpha)\Gamma(1-\alpha)}{|x-\eta|^{\alpha}\Gamma(1-\alpha)}\left[i^{1-\alpha}+(-i)^{1-\alpha}\right].$$

Using $\Gamma(\alpha)\Gamma(1-\alpha) = \frac{\pi}{\sin(\pi\alpha)}$ and $i^{1-\alpha}+(-i)^{1-\alpha} = 2\sin\left(\frac{\alpha\pi}{2}\right)$, we obtain

$$I = \frac{\mathrm{sign}(x-\eta)\pi}{\cos\left(\frac{\alpha\pi}{2}\right)|x-\eta|^{\alpha}\Gamma(1-\alpha)}.$$

Hence, for $0<\alpha<1$

$$\begin{aligned}-(-\Delta)^{\frac{\alpha}{2}}\phi(x) &= -\frac{1}{2\pi}\int_{-\infty}^{\infty}\phi'(\eta)\frac{\mathrm{sign}(x-\eta)\pi}{\cos\left(\frac{\alpha\pi}{2}\right)|x-\eta|^{\alpha}\Gamma(1-\alpha)}\mathrm{d}\eta\\ &= -\frac{1}{2\cos\left(\frac{\alpha\pi}{2}\right)}\left[\frac{1}{\Gamma(1-\alpha)}\int_{-\infty}^{x}\frac{\phi'(\eta)}{(x-\eta)^{\alpha}}\mathrm{d}\eta - \frac{1}{\Gamma(1-\alpha)}\int_{x}^{\infty}\frac{\phi'(\eta)}{(\eta-x)^{\alpha}}\mathrm{d}\eta\right].\end{aligned}$$

Following [1, 3], for $0<\alpha<1$, the Grünwald–Letnikov fractional derivative in $[a,x]$ is given by

$${}_aD_x^{\alpha}\phi(x) = \frac{\phi(a)(x-a)^{-\alpha}}{\Gamma(1-\alpha)} + \frac{1}{\Gamma(1-\alpha)}\int_{a}^{x}\frac{\phi'(\eta)}{(t-\eta)^{\alpha}}\mathrm{d}\eta.$$

Therefore, if $\phi(x)$ tends to zero for $a\to-\infty$, then we have

$${}_{-\infty}D_x^{\alpha}\phi(x) = \frac{1}{\Gamma(1-\alpha)}\int_{-\infty}^{x}\frac{\phi'(\eta)}{(x-\eta)^{\alpha}}\mathrm{d}\eta.$$

Similarly, if $\phi(x)$ tends to zero for $b \to +\infty$, then we have

$$ {}_{x}D_{\infty}^{\alpha}\phi(x) = \frac{-1}{\Gamma(1-\alpha)} \int_{x}^{\infty} \frac{\phi'(\eta)}{(\eta - x)^{\alpha}} \mathrm{d}\eta. $$

Hence, if $\phi(x)$ is continuous and $\phi(x)$ is integrable for $x \geq a$, then for every $\alpha (0 < \alpha < 1)$, the Riemann–Liouville derivative exists and coincides with the Grünwald–Letnikov derivative. Finally, for $0 < \alpha < 1$, we have

$$ -(-\Delta)^{\frac{\alpha}{2}}\phi(x) = -\frac{1}{2\cos\left(\frac{\alpha\pi}{2}\right)} \left[{}_{-\infty}D_{x}^{\alpha}\phi(x) + {}_{x}D_{\infty}^{\alpha}\phi(x) \right] = \frac{\mathrm{d}^{\alpha}}{\mathrm{d}|x|^{\alpha}}\phi(x), $$

where ${}_{-\infty}D_{x}^{\alpha}\phi(x) = \frac{1}{\Gamma(1-\alpha)} \frac{\mathrm{d}}{\mathrm{d}x} \int_{-\infty}^{x} \frac{\phi(\eta)\mathrm{d}\eta}{(x-\eta)^{\alpha}}$ and ${}_{x}D_{\infty}^{\alpha}\phi(x) = \frac{-1}{\Gamma(1-\alpha)} \frac{\mathrm{d}}{\mathrm{d}x} \int_{x}^{\infty} \frac{\phi(\eta)\mathrm{d}\eta}{(\eta-x)^{\alpha}}$.

Following a similar argument, for $1 < \alpha < 2$, we can obtain

$$ -(-\Delta)^{\frac{\alpha}{2}}\phi(x) = -\frac{1}{2\cos\left(\frac{\alpha\pi}{2}\right)} \left[{}_{-\infty}D_{x}^{\alpha}\phi(x) + {}_{x}D_{\infty}^{\alpha}\phi(x) \right] = \frac{\mathrm{d}^{\alpha}}{\mathrm{d}|x|^{\alpha}}\phi(x), $$

where ${}_{-\infty}D_{x}^{\alpha}\phi(x) = \frac{1}{\Gamma(2-\alpha)} \frac{\mathrm{d}^2}{\mathrm{d}x^2} \int_{-\infty}^{x} \frac{\phi(\eta)\mathrm{d}\eta}{(x-\eta)^{\alpha-1}}$ and ${}_{x}D_{\infty}^{\alpha}\phi(x) = \frac{1}{\Gamma(2-\alpha)} \frac{\mathrm{d}^2}{\mathrm{d}x^2} \int_{t}^{\infty} \frac{\phi(\eta)\mathrm{d}\eta}{(\eta-x)^{\alpha-1}}$.

Finally, for $n-1 < \alpha < n$, we have

$$ -(-\Delta)^{\frac{\alpha}{2}}\phi(x) = -\frac{1}{2\cos\left(\frac{\alpha\pi}{2}\right)} \left[{}_{-\infty}D_{x}^{\alpha}\phi(x) + {}_{x}D_{\infty}^{\alpha}\phi(t) \right] = \frac{\mathrm{d}^{\alpha}}{\mathrm{d}|x|^{\alpha}}\phi(x), $$

where ${}_{-\infty}D_{x}^{\alpha}\phi(x) = \frac{1}{\Gamma(n-\alpha)} \frac{\mathrm{d}^n}{\mathrm{d}x^n} \int_{-\infty}^{x} \frac{\phi(\zeta)\mathrm{d}\zeta}{(x-\zeta)^{\alpha+1-n}}$ and ${}_{x}D_{\infty}^{\alpha}\phi(x) = \frac{(-1)^n}{\Gamma(n-\alpha)} \frac{\mathrm{d}^n}{\mathrm{d}x^n} \int_{t}^{\infty} \frac{\phi(\zeta)\mathrm{d}\zeta}{(\zeta-x)^{\alpha+1-n}}$.

Remark 3 For a function $f(t)$ defined on the finite interval $[0, L]$, the result in Eq. (1.19) holds by setting

$$ \phi^{*}(t) = \begin{cases} \phi(t) & t \in (0, L), \\ 0 & t \notin (0, L). \end{cases} $$

That is $\phi^{*}(t) = 0$ on the boundary points and beyond the boundary points.

Definition 8 Riesz–Feller fractional derivative proposed by Feller [24] is a generalization of the Riesz fractional derivative. For $0 < \alpha \leq 2$, $\alpha \neq 1$ and free parameter θ, $|\theta| \leq \min\{\alpha, 2-\alpha\}$, the Riesz–Feller fractional derivative is defined as [26]

$$ {}^{F}D_{\theta}^{\alpha}\psi(x) = (C_{+}(\alpha,\theta)D_{+}^{\alpha} + C_{-}(\alpha,\theta)D_{-}^{\alpha})\psi(x), \tag{1.21} $$

where the coefficients $C_{\pm}(\alpha,\theta)$ are given by

$$C_{+}(\alpha,\theta)=\frac{\sin\left((\alpha-\theta)\frac{\pi}{2}\right)}{\sin(\alpha\pi)},\ C_{-}(\alpha,\theta)=\frac{\sin\left((\alpha+\theta)\frac{\pi}{2}\right)}{\sin(\alpha\pi)},$$

and D_{+}^{α} and D_{-}^{α} are the left- and right-sided Weyl fractional derivatives of order α, defined for $x\in\mathsf{R}$ and $\alpha>0$, $n-1<\alpha\leq n$, $n\in N$ as

$$(D_{+}^{\alpha})\psi(x):=\left(\frac{\mathrm{d}}{\mathrm{d}x}\right)^{n}\left(I_{+}^{n-\alpha}\psi\right)(x), \tag{1.22}$$

$$(D_{-}^{\alpha})\psi(x):=\left(\frac{\mathrm{d}}{\mathrm{d}x}\right)^{n}\left(I_{-}^{n-\alpha}\psi\right)(x). \tag{1.23}$$

In the above formulae, $I_{\pm}^{n-\alpha}$ are the left- and right-sided Weyl fractional integrals given by

$$I_{+}^{\alpha}\psi(x)=\frac{1}{\Gamma(\alpha)}\int_{-\infty}^{x}(x-\zeta)^{\alpha-1}\psi(\zeta)\mathrm{d}\zeta, \tag{1.24}$$

and

$$I_{-}^{\alpha}\psi(x)=\frac{1}{\Gamma(\alpha)}\int_{x}^{\infty}(\zeta-x)^{\alpha-1}\psi(\zeta)\mathrm{d}\zeta. \tag{1.25}$$

1.2.2 Preliminaries of Local Fractional Calculus

In this section, the basic definitions and some elementary properties of local fractional derivative have been briefly discussed.

Local Fractional Continuity of a Function

Definition 9 Suppose that $f(x)$ is defined throughout some interval containing x_0 and all points near x_0, then $f(x)$ is said to be local fractional continuous at $x=x_0$, denoted by $\lim_{x\to x_0}f(x)=f(x_0)$, if to each positive ε and some positive constant k corresponds some positive δ such that [27–29]

$$|f(x)-f(x_0)|<k\varepsilon^{\alpha},\quad 0<\alpha\leq 1, \tag{1.26}$$

whenever $|x-x_0|<\delta,\ \varepsilon,\ \delta>0$ and $\varepsilon,\ \delta\in\mathsf{R}$. Consequently, the function $f(x)$ is called local fractional continuous on the interval (a,b), denoted by

$$f(x)\in C_\alpha(a,b), \tag{1.27}$$

where α is fractal dimension with $0<\alpha\leq 1$.

Definition 10 A function $f(x):\mathsf{R}\to\mathsf{R},\ X\mapsto f(X)$ is called a nondifferentiable function of exponent α, $0<\alpha\leq 1$, which satisfies Hölder function of exponent α, then for $x,y\in X$, we have [27–29]

$$|f(x)-f(y)|\leq C|x-y|^\alpha. \tag{1.28}$$

Definition 11 A function $f(x):\mathsf{R}\to\mathsf{R}\ X\mapsto f(X)$ is called to be local fractional continuous of order α, $0<\alpha\leq 1$, or shortly α-local fractional continuous, when we have [27–29]

$$f(x)-f(x_0)=O((x-x_0)^\alpha). \tag{1.29}$$

Remark 4 A function $f(x)$ is said to be in the space $C_\alpha[a,b]$ if and only if it can be written as [27–29]

$$f(x)-f(x_0)=O((x-x_0)^\alpha),$$

with any $x_0\in[a,b]$ and $0<\alpha\leq 1$.

Theorem 1.2 (*Generalized Hadamard's Theorem*) [30]

Any function $f(x)\in C^\alpha(I)$ in a neighborhood of a point x_0 can be decomposed in the form

$$f(x)=f(x_0)+\frac{(x-x_0)^\alpha}{\Gamma(1+\alpha)}g(x),$$

where $g(x)\in C^{m\alpha}(I)$ (the space of functions which are m times α th differentiable on $I\subset\mathsf{R}$).

Local Fractional Derivative

If a function is not differentiable at $x=x_0$, but has a fractional derivative of order α at this point, then it is locally equivalent to the function

$$f(x)=f(x_0)+\frac{(x-x_0)^\alpha}{\Gamma(\alpha+1)}f^{(\alpha)}(x_0)+O\Big((x-x_0)^{2\alpha}\Big), \tag{1.30}$$

Definition 12 Following to Eq. (1.30), the local fractional derivative of $f(x) \in C_\alpha(a,b)$ of order α at $x = x_0$ is defined as [27–29]

$$f^{(\alpha)}(x_0) = \left.\frac{\mathrm{d}^\alpha f(x)}{\mathrm{d}x^\alpha}\right|_{x=x_0} = \lim_{x\to x_0} \frac{\Delta^\alpha(f(x) - f(x_0))}{(x-x_0)^\alpha}, \tag{1.31}$$

where $\Delta^\alpha(f(x) - f(x_0)) \cong \Gamma(1+\alpha)(f(x) - f(x_0))$ and $0 < \alpha \leq 1$.

Another definition of local fractional derivative has been proposed by Kolwankar and Gangal [31] by means of theory on the Cantor space, which is given as follows.

Definition 13 Local fractional derivative of order $\alpha(0 < \alpha < 1))$ of a function $f \in C^0 : \mathsf{R} \to \mathsf{R}$ is defined as

$$D^\alpha f(x) = \lim_{\zeta \to x} D_x^\alpha (f(\zeta) - f(x)), \tag{1.32}$$

if the limit exist in $\mathsf{R} \cup \infty$.

If $f(x)$ is differentiable at the point other than $x = x_0$, with nonzero value of the derivative, then it can be approximated locally as

$$f(x) = f(x_0) + f'(x_0)(x - x_0) + o(x - x_0). \tag{1.33}$$

So the local fractional derivative of $f(x)$ at $x = x_0$ becomes

$$\begin{aligned} D^\alpha f(x_0) &= \lim_{x\to x_0} \frac{d^\alpha (f(x) - f(x_0))}{d(x-x_0)^a} \\ &= f'(x_0) \lim_{x\to x_0} \frac{d^\alpha (x - x_0)}{d(x-x_0)^a} \end{aligned} \tag{1.34}$$

Remark 5 The following rules are hold [13]

(1) $\frac{\mathrm{d}^\alpha x^{k\alpha}}{dx^\alpha} = \frac{\Gamma(1+k\alpha)}{\Gamma(1+(k-1)\alpha)} x^{(k-1)\alpha}$;

(2) $\frac{\mathrm{d}^\alpha E_\alpha(kx^\alpha)}{\mathrm{d}x^\alpha} = kE_\alpha(kx^\alpha)$, k is a constant.

Remark 6 [13, 27–29]

(I) If $y(x) = (f \circ u)(x)$ where $u(x) = g(x)$, then we have

$$\frac{\mathrm{d}^\alpha y(x)}{\mathrm{d}x^\alpha} = f^{(\alpha)}(g(x)) \left(g^{(1)}(x)\right)^\alpha, \tag{1.35}$$

when $f^{(\alpha)}(g(x))$ and $g^{(1)}(x)$ exist.

(II) If $y(x) = (f \circ u)(x)$ where $u(x) = g(x)$, then we have

$$\frac{\mathrm{d}^{\alpha} y(x)}{\mathrm{d}x^{\alpha}} = f^{(1)}(g(x))g^{(\alpha)}(x), \tag{1.36}$$

when $f^{(1)}(g(x))$ and $g^{(\alpha)}(x)$ exist.

1.3 Wavelets

Nowadays, wavelets [32] have found their place in many applications for a wide range of engineering disciplines. Wavelets are very effectively used in signal analysis for waveform demonstration and segmentations (separation or partition), time-frequency analysis, and fast algorithms for easy execution. Wavelets allow accurate depiction of a variety of functions and operators. With the widespread applications of wavelet methods for solving difficult problems in diverse fields of science and engineering such as wave propagation, data compression, image processing, pattern recognition, computer graphics and in medical technology, these methods have been implemented to develop accurate and fast algorithms for solving integral, differential, and integro-differential equations, especially those whose solutions are highly localized in position and scale [32, 33]. Using the powerful multiresolution analysis, one can represent a function by a finite sum of components at different resolutions so that each component can be adaptively processed based on the objectives of the application. This capability of representing functions compactly and in several levels of resolutions is the major strength of the wavelet analysis.

The word "*wavelet*" has been derived from the French word "*ondelette,*" which means "small wave." An oscillatory function $\psi(x) \in L^2(\mathsf{R})$ with zero mean and compact support is a wavelet if it has the following desirable characteristics:

(i) Smoothness: $\psi(x)$ is n times differentiable, and their derivatives are continuous.

(ii) Localization: $\psi(x)$ is well localized in both time and frequency domains, i.e., $\psi(x)$ and its derivatives must decay rapidly. For frequency localization, $\widehat{\Psi}(\omega)$ must decay sufficiently fast as $\omega \to \infty$ and that $\widehat{\Psi}(\omega)$ becomes flat in the neighborhood of $\omega = 0$. The flatness is associated with the number of vanishing moments of $\psi(x)$, i.e.,

$$\int_{-\infty}^{\infty} x^k \psi(x)\mathrm{d}x = 0 \quad \text{or equivalently } \frac{\mathrm{d}^k}{\mathrm{d}\omega^k}\widehat{\Psi}(\omega) = 0 \text{ for } k = 0, 1, \ldots, n$$

in the sense that larger the number of vanishing moments, more is the flatness when ω is small.

(iii) The admissibility condition

$$\int_{-\infty}^{\infty} \frac{\left|\hat{\Psi}(\omega)\right|}{|\omega|} \mathrm{d}\omega < \infty$$

suggests that $\left|\widehat{\Psi}(\omega)\right|$ decay at least as $|\omega|^{-1}$ or $|x|^{\varepsilon-1}$ for $\varepsilon > 0$.

Although most of the numerical methods have been successfully applied for many linear and nonlinear differential equations, they have also some drawbacks in regions where singularities or sharp transitions occur. In those cases, the solutions may be oscillating and for an accurate representation of the results, adaptive numerical schemes must be used which complicates the solution. To overcome the above difficulty, wavelet transform [32, 34] methods are quite useful.

1.3.1 Wavelet Transform

Morlet and Grossmann [35, 36] first introduced the concept of wavelets in the early 1980s. Since then, a lot of researchers were involved in the development of wavelets. Some notable contributors include Morlet and Grossmann [36] for formulation of continuous wavelet transform (CWT), Stromberg [37] for early works on discrete wavelet transform (DWT), Meyer [38] and Mallat [39] for multiresolution analysis using wavelet transform, and Daubechies [40] for proposal of orthogonal compactly supported wavelets. Thereafter, a lot of work has been done both on development and application of wavelet analysis on a wide variety of problems like signal and image processing, data condensation, and solution of differential equations.

In 1982, Jean Morlet, a French geophysical engineer, first introduced the concept of wavelets as a family of functions constructed from dilation and translation of a single function known as the "mother wavelet" $\psi(t)$. They are defined by

$$\psi_{a,b}(t) = \frac{1}{\sqrt{|a|}} \psi\left(\frac{t-b}{a}\right), \quad a, b \in \mathsf{R},\ a \neq 0 \tag{1.37}$$

where a is called a scaling parameter which measures the degree of compression or scale, and b is a translation or shifting parameter that determines the location of the wavelet. If $|a| < 1$, the wavelet (1.37) is the compressed version of the mother

wavelet and corresponds mainly to higher frequencies. On the other hand, when $|a| > 1$, $\psi_{a,b}(t)$ has a larger time width than $\psi(t)$ and corresponds to lower frequencies. Thus, wavelets have time widths adapted to their frequencies, which is the main reason for the success of the Morlet wavelets in signal processing and time-frequency signal analysis. It can be noted that the resolution of wavelets at different scales varies in the time and frequency domains as governed by the Heisenberg uncertainty principle. At large scale, the solution is coarse in the time domain and fine in the frequency domain. As the scale decreases, the resolution in the time domain becomes finer while that in the frequency domain becomes coarser.

The success of Morlet's numerical algorithms encouraged Grossmann, a French theoretical physicist, to make an extensive study of the Morlet wavelet transform which led to the recognition that wavelets $\psi_{a,b}(t)$ correspond to a square integrable representation of the affine group. Grossmann was concerned with the wavelet transform of $f \in L^2(\mathsf{R})$ defined by

$$\mathscr{W}_{\psi}[f](a,b) = \left(f, \psi_{a,b}\right) = \frac{1}{\sqrt{|a|}} \int_{-\infty}^{\infty} f(t)\overline{\psi\left(\frac{t-b}{a}\right)}\,\mathrm{d}t, \tag{1.38}$$

where $\psi_{a,b}(t)$ plays the same role as the kernel $\mathrm{e}^{i\omega t}$ in the Fourier transform. The continuous wavelet transform $\mathscr{W}_{\psi}$ is linear. The inverse wavelet transform can be defined so that f can be reconstructed by means of the formula

$$f(t) = C_{\psi}^{-1} \int_{-\infty}^{\infty} \int_{-\infty}^{\infty} \mathscr{W}_{\psi}[f](a,b)\psi_{a,b}(t)(a^{-2}\mathrm{d}a)\mathrm{d}b \tag{1.39}$$

provided C_{ψ} satisfies the so-called admissibility condition, that is,

$$C_{\psi} = 2\pi \int_{-\infty}^{\infty} \frac{\left|\widehat{\Psi}(\omega)\right|^2}{|\omega|}\mathrm{d}\omega < \infty, \tag{1.40}$$

where $\widehat{\Psi}(\omega)$ is the Fourier transform of the mother wavelet $\psi(t)$.

Grossmann's ingenious work revealed that certain algorithms that decompose a signal on the whole family of scales can be utilized as an efficient tool for multiscale analysis. In practical applications, the continuous wavelet can be computed at discrete grid points. For this, a general wavelet ψ can be defined by replacing a with $a_0^m (a_0 \neq 0, 1)$, b with $nb_0a_0^m (b_0 \neq 0)$, where m and n are integers and making

$$\psi_{m,n}(t) = a_0^{-m/2}\psi(a_0^{-m}t - nb_0). \tag{1.41}$$

The discrete wavelet transform of f is defined as

$$\bar{f}(m,n) = \mathcal{W}[f](m,n) = (f, \psi_{m,n}) = \int_{-\infty}^{\infty} f(t)\bar{\psi}_{m,n}(t)\mathrm{d}t \tag{1.42}$$

where $\psi_{m,n}(t)$ is given in Eq. (1.41).

The series

$$\sum_{m,n=-\infty}^{\infty} \bar{f}(m,n)\psi_{m,n}(t) \tag{1.43}$$

is called the wavelet series of f, and the functions $\{\psi_{m,n}(t)\}$ are called the discrete wavelets or simply wavelets. To compute the wavelet transform of a function at some point in the time-scale plane, we do not need to know the function values for the entire time axis. All we need is the function at those values of time at which the wavelet is nonzero. Consequently, the evaluation of the wavelet transform can be done almost in real time.

It is known that the continuous wavelet transform is a two-parameter representation of a function. In many practical applications particularly in signal processing, data are represented by a finite number of values, so it is essential and often expedient to consider the discrete version of the continuous wavelet transform. From a mathematical perspective, continuous representation of a function of two continuous parameters a, b in Eq. (1.38) can be converted into a discrete one by assuming that a and b take only integral values as given in Eq. (1.41). In general, the function f belonging to the Hilbert space, $L^2(\mathsf{R})$ can be completely determined by its discrete wavelet transform if the wavelets form a complete system in $L^2(\mathsf{R})$. In other words, if the wavelets form an orthonormal basis of $L^2(\mathsf{R})$, then they are complete and f can be reconstructed from its discrete wavelet transform $\{\bar{f}(m,n) = (f, \psi_{m,n})\}$ by means of the formula

$$f(t) = \sum_{m,n=-\infty}^{\infty} (f, \psi_{m,n})\psi_{m,n}(t), \tag{1.44}$$

provided the wavelets form an orthonormal basis.

Alternatively, the function f can be determined by the formula

$$f(t) = \sum_{m,n=-\infty}^{\infty} (f, \psi_{m,n})\bar{\psi}_{m,n}(t), \tag{1.45}$$

provided the wavelets form a basis and $\{\bar{\psi}_{m,n}(t)\}$ is the dual basis.

For some particular choice of ψ and a_0, b_0, the $\psi_{m,n}$ constitute an orthonormal basis for $L^2(\mathsf{R})$. If $a_0 = 2$ and $b_0 = 1$, then there exists a function ψ with good time-frequency localization properties such that

$$\psi_{m,n}(t) = 2^{-m/2}\psi(2^{-m}t - n) \tag{1.46}$$

form an orthonormal basis for $L^2(\mathsf{R})$. These $\{\psi_{m,n}(t)\}$ are known as the Littlewood–Paley wavelets. It has good space-frequency localization, given in the following representation of f as

$$f(t) = \sum_{m,n} \big(f, \psi_{m,n}\big)\psi_{m,n}(t). \tag{1.47}$$

An orthodox example of a wavelet ψ for which $\psi_{m,n}$ constitute an orthonormal basis of $L^2(\mathsf{R})$ is the Haar wavelet

$$\psi(t) = \begin{cases} 1, & 0 \le t < \frac{1}{2} \\ -1, & \frac{1}{2} \le t < 1 \\ 0, & \text{otherwise} \end{cases}. \tag{1.48}$$

Historically, the Haar basis is the first orthonormal wavelet basis that was invented long before the concept of wavelet was introduced. The joint venture of Morlet and Grossmann led to a detailed mathematical study of the wavelet transforms and applications.

Wavelet techniques enable us to divide a complicated function into several simpler ones and study them separately. This property, along with a fast wavelet algorithm, makes these techniques very attractive for analysis and synthesis. Unlike Fourier-based analyses that use global (nonlocal) sine and cosine functions as bases, wavelet analysis uses bases that are localized in time and frequency to more effectively represent nonstationary signals. As a result, a wavelet representation is much more compact and easier for implementation. Using the powerful multiresolution analysis, one can represent a function by a finite sum of components at different resolutions so that each component can be adaptively processed based on the objectives of the application. This capability of representing functions compactly and in several levels of resolutions is the major strength of the wavelet analysis.

1.3.2 Orthonormal Wavelets

The orthonormal wavelets with good time-frequency localization are found to play a significant role in wavelet theory and have a great variety of applications. In general, the theory of wavelets instigates with a single function $\psi \in L^2(\Re)$, and a

family of functions $\psi_{m,n}$ is constructed from this single function ψ by the operation of binary dilation (i.e., dilation by 2^m) and dyadic translation of $n2^{-m}$ so that

$$\begin{aligned}\psi_{m,n}(t) &= 2^{\frac{m}{2}}\psi\left(2^m\left(t-\frac{n}{2^m}\right)\right), \quad m,n \in \mathrm{Z} \\ &= 2^{\frac{m}{2}}\psi(2^m t - n),\end{aligned} \tag{1.49}$$

where the factor $2^{\frac{m}{2}}$ is introduced to ensure orthonormality.

Definition 14 Orthonormal Wavelet A wavelet $\psi \in L^2(\mathsf{R})$ is called an orthonormal, if the family of functions $\psi_{m,n}$, generated from ψ, is an orthonormal basis of $L^2(\mathsf{R})$; that is,

$$\langle \psi_{i,j}, \psi_{m,n} \rangle = \delta_{i,m}\delta_{j,n}, \quad i,j,m,n \in \mathbf{Z}.$$

Definition 15 Semi-orthogonal Wavelet A wavelet $\psi \in L^2(\mathsf{R})$ is called an semi-orthogonal wavelet [33], if the family $\{\psi_{m,n}\}$ satisfies the following condition,

$$\langle \psi_{i,j}, \psi_{m,n} \rangle = 0,\ i \neq m,\ i,j,m,n \in \mathbf{Z}.$$

Obviously, every semi-orthogonal wavelets generate an orthogonal decomposition of $L^2(\mathsf{R})$, and every orthonormal wavelet is also a semi-orthogonal wavelet.

Construction of Orthonormal Wavelets

The construction of an orthonormal wavelet, viz. the Haar wavelet, is discussed by using the properties of scaling functions and filters. The scaling function ϕ satisfies the dilation equation as

$$\phi(t) = \sqrt{2}\sum_{n=-\infty}^{\infty} c_n \phi(2t-n), \tag{1.50}$$

where the coefficients c_n are given by

$$c_n = \sqrt{2}\int_{-\infty}^{\infty} \phi(t)\phi(2t-n)\mathrm{d}t. \tag{1.51}$$

Evaluating the above integral given in Eq. (1.51), with $\phi = \chi_{[0,1)}$, gives c_n as follows:

$$c_0 = c_1 = \frac{1}{\sqrt{2}} \quad \text{and} \quad c_n = 0 \quad \text{for} \quad n \neq 0, 1.$$

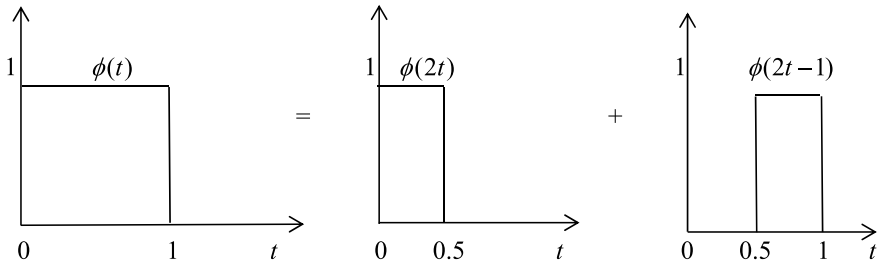

Fig. 1.1 Two-scale relation of $\phi(t) = \phi(2t) + \phi(2t-1)$

Here $\chi_{[0,1)}$ denotes the characteristic function given by

$$\chi_{[0,1)}(t) = \begin{cases} 1, & 0 \le t < 1 \\ 0, & \text{otherwise} \end{cases}.$$

Hence, the dilation equation becomes

$$\phi(t) = \phi(2t) + \phi(2t-1). \tag{1.52}$$

This means that $\phi(t)$ is a linear combination of the even and odd translates of $\phi(2t)$ and satisfies a very simple two-scale relation (1.52), which is shown in Fig. 1.1.

Thus, the Haar mother wavelet is obtained as a simple two-scale relation

$$\begin{aligned} \psi(t) &= \phi(2t) - \phi(2t-1) \\ &= \chi_{[0,0.5)} - \chi_{[0.5,1)} \end{aligned} \tag{1.53}$$

$$= \begin{cases} 1, & 0 \le t < \frac{1}{2} \\ -1, & \frac{1}{2} \le t < 1 \\ 0, & \text{otherwise} \end{cases} \tag{1.54}$$

This two-scale relation (1.53) of ψ is represented in Fig. 1.2.

1.3.3 Multiresolution Analysis

In 1989, Stephane Mallat and Yves Meyer introduced the idea of multiresolution analysis (MRA) [33, 34]. The fundamental idea of MRA is to represent a function as a limit of successive approximations, each of which is a "smoother" version of the original function. The successive approximations correspond to different resolutions, which lead to the name multiresolution analysis as a formal approach to construct orthogonal wavelet bases utilizing a definite set of rules. It also provides

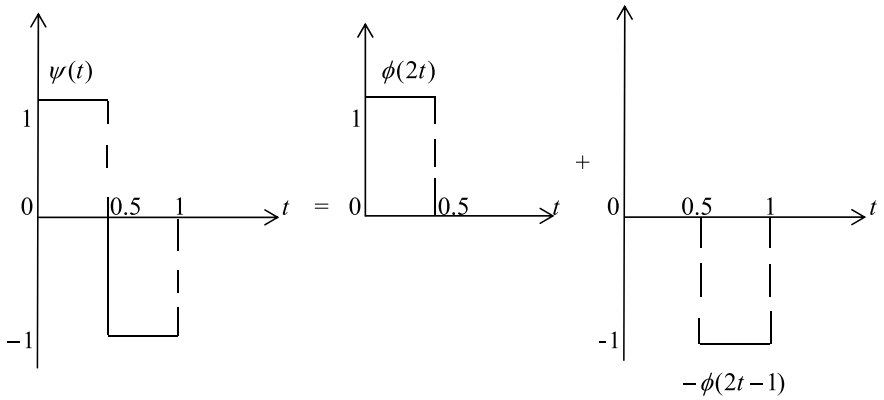

Fig. 1.2 Two-scale relation of $\psi(t) = \phi(2t) - \phi(2t-1)$

the existence of so-called scaling functions and scaling filters which are then used for the construction of wavelets and fast numerical algorithms. In applications, it is an effective mathematical framework for the hierarchical decomposition of a signal or an image into components of different scales represented by a sequence of function spaces on R.

Any wavelet, orthogonal or semi-orthogonal, generates a direct sum decomposition of $L^2(\mathsf{R})$. For each $j \in \mathrm{Z}$,, let us consider the closed subspaces

$$V_j = \ldots \oplus W_{j-2} \oplus W_{j-1}, \quad j \in \mathsf{Z},$$

of $L^2(\mathsf{R})$. A set of subspaces $\{V_j\}_{j\in\mathbf{Z}}$ is said to be MRA of $L^2(\mathsf{R})$ if it possesses the following properties:

(i) $V_j \subset V_{j+1}, \quad \forall j \in \mathsf{Z}$,
(ii) $\bigcup_{j\in\mathrm{Z}} V_j$ is dense in $L^2(\mathsf{R})$,
(iii) $\bigcap_{j\in\mathrm{Z}} V_j = \{0\}$,
(iv) $V_{j+1} = V_j \oplus W_j$,
(v) $f(t) \in V_j \Leftrightarrow f(2t) \in V_{j+1}, \quad \forall j \in \mathsf{Z}$.

Properties (ii)–(v) state that $\{V_j\}_{j\in\mathrm{Z}}$ is a nested sequence of subspaces that effectively covers $L^2(\mathsf{R})$ That is, every square integrable function can be approximated as closely as desired by a function that belongs to at least one of the subspaces V_j. A function $\varphi \in L^2(\mathsf{R})$ is called a scaling function if it generates the nested sequence of subspaces V_j and satisfies the dilation equation, namely

$$\varphi(t) = \sum_k p_k \varphi(at - k), \tag{1.55}$$

with $p_k \in l^2$ and a being any rational number.

For each scale j, since $V_j \subset V_{j+1}$, there exists a unique orthogonal complementary subspace W_j of V_j in V_{j+1}. This subspace W_j is called wavelet subspace and is generated by $\psi_{j,k} = \psi(2^j t - k)$, where $\psi \in L^2$ is called the wavelet. From the above discussion, these results follow easily

- $V_{j_1} \cap V_{j_2} = V_{j_2}$, $j_1 > j_2$,
- $W_{j_1} \cap W_{j_2} = 0$, $j_1 \neq j_2$,
- $V_{j_1} \cap W_{j_2} = 0$, $j_1 \leq j_2$.

Mathematically, the fundamental idea of multiresolution analysis is to represent a function or signal as a limit of successive approximations, each of which is a finer version of the function. These successive approximations correspond to different levels of resolutions. Thus, multiresolution analysis is a formal approach to constructing orthonormal wavelet bases using a definite set of rules and procedures. The key feature of this analysis is to describe mathematically the process of studying signals or images at different time scales. From the point of view of practical applications, MRA is a really effective mathematical framework for the hierarchical decomposition of an image or signal into components of different scales or frequencies.

In recent years, there have been many developments and new applications of wavelet analysis for describing complex algebraic functions and analyzing empirical continuous data obtained from many kinds of signals at different scales of resolutions. The wavelet-based approximations of ordinary and partial differential equations have been attracting the attention, since the contribution of orthonormal bases of compactly supported wavelet by Daubechies and multiresolution analysis-based fast wavelet transform algorithm by Beylkin et al. [41] gained momentum to make wavelet approximations attractive.

In order to solve partial differential equations by numerical methods, the unknown solution can be represented by wavelets of different resolutions, resulting in a multigrid representation. The dense matrix resulting from an integral operator can be sparsified using wavelet-based thresholding techniques to attain an arbitrary degree of solution accuracy. The main feature of wavelets is its ability to convert the given differential and integral equations to a system of linear or nonlinear algebraic equations that can be solved by numerical methods.

1.4 New Analytical and Numerical Techniques for Partial and Fractional Differential Equations

1.4.1 Introduction

The purpose of this section is to deliver a brief description of various analytical and numerical methods for solving partial and fractional differential equations. The present research work focuses on new development of valuable analytical and numerical techniques that have been examined for effectiveness and reliability over other existing methods. Also, various analytical methods such as first integral method (FIM) [42–46], optimal homotopy asymptotic method (OHAM) [47, 48], homotopy analysis method (HAM) [49], variational iteration method (VIM) [50, 51], and homotopy perturbation method (HPM) [52, 53] are used to compare the accuracy of solutions for numerous partial as well as fractional differential equations with the results obtained by the proposed techniques. The applicability of these proposed methods has been examined for solving nonlinear partial differential equations (PDEs) and fractional partial differential equations (FPDEs). The main aim is to develop and improve significantly analytical and numerical techniques in order to have advanced approaches to reinforce and complement classical methods. The improved and developed techniques have been examined to be reliable, accurate, effective, and efficient in both the analytic and numerical purposes. Thus, the goal of this work is to encourage the researcher to get familiar with the beauty as well as the effectiveness of these analytical and numerical techniques in the study of nonlinear physical phenomena.

1.4.2 Modified Decomposition Method

Let us consider the following system of coupled partial differential equations

$$\begin{aligned} L_{tt}u &= L_{xx}u - u + N(u,v), \\ L_t v &= iL_{xx}v + iM(u,v), \end{aligned} \tag{1.56}$$

where $L_t \equiv \frac{\partial}{\partial t}$, $L_{tt} \equiv \frac{\partial^2}{\partial t^2}$, and $L_{xx} \equiv \frac{\partial^2}{\partial x^2}$ symbolize the linear differential operators, and the notations $N(u,v) = |v|^2$ and $M(u,v) = uv$ symbolize the nonlinear operators.

Applying the twofold integration inverse operator $L_{tt}^{-1} \equiv \int_0^t \int_0^t (\bullet) \mathrm{d}t\mathrm{d}t$ to the system (1.56) and using the specified initial conditions yields

$$\begin{aligned} u(x,t) &= u(x,0) + tu_t(x,0) + L_{tt}^{-1}L_{xx}u - L_{tt}^{-1}u + L_{tt}^{-1}N(u,v), \\ v(x,t) &= v(x,0) + iL_t^{-1}L_{xx}v + iL_t^{-1}M(u,v). \end{aligned} \tag{1.57}$$

The Adomian decomposition method [54, 55] assumes an infinite series of solutions for unknown function $u(x,t)$ and $v(x,t)$ given by

$$\begin{aligned} u(x,t) &= \sum_{n=0}^{\infty} u_n(x,t), \\ v(x,t) &= \sum_{n=0}^{\infty} v_n(x,t). \end{aligned} \tag{1.58}$$

and nonlinear operators $N(u,v) = |v|^2$ and $M(u,v) = uv$ by the infinite series of Adomian's polynomials given by

$$N(u,v) = \sum_{n=0}^{\infty} A_n(u_0,u_1,\ldots,u_n,v_0,v_1,\ldots,v_n),\ M(u,v) = \sum_{n=0}^{\infty} B_n(u_0,u_1,\ldots,u_n,v_0,v_1,\ldots,v_n),$$

where A_n and B_n are the appropriate Adomian polynomial which is generated according to algorithm determined in [54, 55]. For the nonlinear operator $N(u,v)$, these polynomials can be defined as

$$A_n(u_0,u_1,\ldots,u_n,v_0,v_1,\ldots,v_n) = \frac{1}{n!}\frac{\mathrm{d}^n}{\mathrm{d}\lambda^n}\left[N\left(\sum_{k=0}^{\infty}\lambda^k u_k, \sum_{k=0}^{\infty}\lambda^k v_k\right)\right]_{\lambda=0},\ n \geq 0 \tag{1.59}$$

Similarly for the nonlinear operator $M(u,v)$,

$$B_n(u_0,u_1,\ldots,u_n,v_0,v_1,\ldots,v_n) = \frac{1}{n!}\frac{\mathrm{d}^n}{\mathrm{d}\lambda^n}\left[M\left(\sum_{k=0}^{\infty}\lambda^k u_k, \sum_{k=0}^{\infty}\lambda^k v_k\right)\right]_{\lambda=0},\ n \geq 0 \tag{1.60}$$

These formulae are easy to set computer code to get as many polynomials as we need in the calculation of the numerical as well as explicit solutions. For the sake of convenience of the readers, we can give the first few Adomian polynomials for $N(u,v) = |v|^2$, $M(u,v) = uv$ of the nonlinearity as

$$\begin{aligned} A_0 &= v_0\overline{v}_0, \\ A_1 &= v_1\overline{v}_0 + v_0\overline{v}_1, \\ A_2 &= v_2\overline{v}_0 + v_0\overline{v}_2 + v_1\overline{v}_1, \\ &\cdots \end{aligned}$$

and

$$\begin{aligned} B_0 &= u_0v_0, \\ B_1 &= u_1v_0 + u_0v_1, \\ B_2 &= u_2v_0 + u_0v_2 + u_1v_1, \\ &\cdots \end{aligned}$$

and so on, and the rest of the polynomials can be constructed in a similar manner.

Substituting the initial conditions into Eq. (1.57) and consequently identifying the zeroth components u_0 and v_0, then we obtain the subsequent components by the following recursive equations by using the standard ADM

$$\begin{aligned} u_{n+1} &= L_{tt}^{-1}L_{xx}u_n - L_{tt}^{-1}u_n + L_{tt}^{-1}A_n\ ,\ n \geq 0, \\ v_{n+1} &= iL_t^{-1}L_{xx}v_n + iL_t^{-1}B_n\ ,\ n \geq 0. \end{aligned} \tag{1.61}$$

Recently, Wazwaz [56] proposed that the construction of the zeroth component of the decomposition series can be defined in a slightly different way. In [56], he assumed that if the zeroth component $u_0 = g$ and the function g are possible to divide into two parts such as g_1 and g_2, the one can formulate the recursive algorithm for u_0 and general term u_{n+1} in a form of the modified recursive scheme as follows:

$$\begin{aligned} u_0 &= g_1 \\ u_1 &= g_2 + L_{tt}^{-1}L_{xx}u_0 - L_{tt}^{-1}u_0 + L_{tt}^{-1}A_0 \\ u_{n+1} &= L_{tt}^{-1}L_{xx}u_n - L_{tt}^{-1}u_n + L_{tt}^{-1}A_n\ ,\ n \geq 1 \end{aligned} \tag{1.62}$$

Similarly, if the zeroth component $v_0 = g'$ and the function g' are possible to divide into two parts such as g_1' and g_2', the one can formulate the recursive algorithm for v_0 and general term v_{n+1} in a form of the modified recursive scheme as follows:

$$\begin{aligned} v_0 &= g_1', \\ v_1 &= g_2' + iL_t^{-1}L_{xx}v_0 + iL_t^{-1}B_0, \\ v_{n+1} &= iL_t^{-1}L_{xx}v_n + iL_t^{-1}B_n\ ,\quad n \geq 1. \end{aligned} \tag{1.63}$$

This type of modification is giving more flexibility to the ADM in order to solve complicate nonlinear differential equations. In many cases, the modified decomposition scheme avoids unnecessary computation especially in the calculation of the

Adomian polynomials. The computation of these polynomials will be reduced very considerably by using the MDM.

It is worth noting that the zeroth components u_0 and v_0 are defined; then, the remaining components u_n and v_n, $n \geq 1$ can be completely determined. As a result, the components $u_0, u_1, \ldots,$ and $v_0, v_1, \ldots,$ are identified, and the series solutions thus entirely determined. However, in many cases, the exact solution in a closed form may be obtained.

The decomposition series (1.58) solutions generally converge very rapidly in real physical problems [55]. The rapidity of this convergence means that few terms are required. The convergence of this method has been rigorously established by Cherruault [57], Abbaoui and Cherruault [58, 59], and Himoun et al. [60]. The practical solutions will be the n-term approximations φ_n and ψ_n

$$\begin{aligned} \phi_n &= \sum_{i=0}^{n-1} u_i(x,t), \ n \geq 1, \\ \psi_n &= \sum_{i=0}^{n-1} v_i(x,t), \ n \geq 1, \end{aligned} \tag{1.64}$$

with

$$\begin{aligned} \lim_{n\to\infty} \phi_n &= u(x,t), \\ \lim_{n\to\infty} \psi_n &= v(x,t). \end{aligned}$$

1.4.3 New Two-Step Adomian's Decomposition Method

First, consider a one-dimensional fractional diffusion equation considered in [61]

$$\frac{\partial u(x,t)}{\partial t} = \mathrm{d}(x) \frac{\partial^{\alpha} u(x,t)}{\partial x^{\alpha}} + q(x,t) \tag{1.65}$$

on a finite domain $x_L < x < x_R$ with $1 < \alpha \leq 2$. Here, $\mathrm{d}(x) > 0$ is the diffusion coefficient (or diffusivity), and α denotes the order of Riemann fractional derivative.

In this case, for solving Eq. (1.65), Adomian's decomposition method has been adopted. In light of this method, we assume that

$$u = \sum_{n=0}^{\infty} u_n \tag{1.66}$$

to be the solution of Eq. (1.65).

Now, Eq. (1.65) can be rewritten as

$$L_t u(x,t) = \mathrm{d}(x) D_x^{\alpha} u(x,t) + q(x,t), \tag{1.67}$$

where $L_t \equiv \frac{\partial}{\partial t}$ which is an easily invertible linear operator, and $D_x^{\alpha}(\bullet)$ is the Riemann–Liouville derivative of order α.

Therefore, by Adomian's decomposition method, we can write

$$u(x,t) = u(x,0) + L_t^{-1}\left(\mathrm{d}(x) D_x^{\alpha}\left(\sum_{n=0}^{\infty} u_n\right)\right) + L_t^{-1}(q(x,t)). \tag{1.68}$$

Each term of series (1.66) is given by the standard Adomian decomposition method recurrence relation

$$\begin{aligned} u_0 &= f, \\ u_{n+1} &= L_t^{-1}\left(\mathrm{d}(x) D_x^{\alpha} u_n\right), \quad n \geq 0, \end{aligned} \tag{1.69}$$

where $f = u(x,0) + L_t^{-1}(q(x,t))$.

It is worth noting that once the zeroth component u_0 is defined, then the remaining components u_n, $n \geq 1$ can be completely determined; each term is computed by using the previous term. As a result, the components $u_0, u_1, \ldots$ are identified, and the series solutions thus entirely determined. However, in many cases, the exact solution in a closed form may be obtained.

Recently, Wazwaz [56] proposed that the construction of the zeroth component u_0 of the decomposition series can be defined in a slightly different way. In [56], he assumed that if the zeroth component $u_0 = f$ and the function f is possible to divide into two parts such as f_1 and f_2, then one can formulate the recursive algorithm for u_0 and general term u_{n+1} in a form of the modified decomposition method (MDM) recursive scheme as follows:

$$\begin{aligned} u_0 &= f_1, \\ u_1 &= f_2 + L_t^{-1}\left(\mathrm{d}(x) D_x^{\alpha} u_n\right), \\ u_{n+1} &= L_t^{-1}\left(\mathrm{d}(x) D_x^{\alpha} u_n\right) \quad n \geq 1. \end{aligned} \tag{1.70}$$

Comparing the recursive scheme (1.69) of the standard Adomain method with the recursive scheme (1.70) of the modified technique leads to the conclusion that in Eq. (1.69), the zeroth component was defined by the function f, whereas in Eq. (1.70), the zeroth component u_0 is defined only by a part f_1 of f. The remaining part f_2 of f is added to the definition of the component u_1 in Eq. (1.70). Although the modified technique needs only a slight variation from the standard Adomian decomposition method, the results are promising in that it minimizes the size of calculations needed and will accelerate the convergence. The modification could lead to a promising approach for many applications in applied science.

The decomposition series solution (1.66) generally converges very rapidly in real physical problems [54, 55]. The rapidity of this convergence means that few

terms are required. The convergence of this method has been rigorously established by Cherruault [57], Abbaoui and Cherruault [58, 59], and Himoun et al. [60]. The practical solution will be the n-term approximation ϕ_n

$$\phi_n = \sum_{i=0}^{n-1} u_i(x,t), \quad n \geq 1, \tag{1.71}$$

with

$$\lim_{n\to\infty} \phi_n = u(x,t).$$

Luo [46] presented the theoretical support of how the exact solution can be achieved by using only two iterations in the modified decomposition method. In detail, it is possible because all other components vanish, if the zeroth component is equal to the exact solution.

Although the modified decomposition method may provide the exact solution by using two iterations only, the criterion of dividing the function f into two practical parts, and the case where f consists only of one term remains unsolved so far. The two-step Adomian decomposition method (TSADM) overcomes the difficulties arising in the modified decomposition method.

In the following, Luo [62] presents the two-step Adomian decomposition method. For the convenience of the reader, we consider the differential equation

$$Lu + Ru + Nu = g, \tag{1.72}$$

where L is the highest order derivative which is assumed to be easily invertible, R is a linear differential operator of order less than L, Nu represents the nonlinear terms, and g is the source term.

The main ideas of the two-step Adomian decomposition method are as follows:

(I) Applying the inverse operator L^{-1} to g, and using the given conditions, we obtain $\varphi = \phi + L^{-1}g$, where the function ϕ represents the term arising from using the given conditions, all are assumed to be prescribed.
Let

$$\varphi = \sum_{i=0}^{m} \varphi_i, \tag{1.73}$$

where $\phi_0, \phi_1, \ldots, \phi_m$ are the terms arising from integrating the source term g and from using the given conditions. Based on this, we define $u_0 = \varphi_k + \cdots + \varphi_{k+s}$, where $k = 0, 1, \ldots, m$, $s = 0, 1, \ldots, m-k$. Then, we verify that u_0 satisfies the original equation Eq. (1.72) and the given conditions by substitution, once the exact solution is obtained, we stop. Otherwise, we go to the following step two.

(II) We set $u_0 = \varphi$ and continue with the standard Adomian recursive relation $u_{k+1} = -L^{-1}(Ru_k) - L^{-1}(A_k)$, $k \geq 0$.

Next, consider a two-dimensional fractional diffusion equation considered in [63]

$$\frac{\partial u(x,y,t)}{\partial t} = \mathrm{d}(x,y)\frac{\partial^{\alpha} u(x,y,t)}{\partial x^{\alpha}} + \mathrm{e}(x,y)\frac{\partial^{\beta} u(x,y,t)}{\partial y^{\beta}} + q(x,y,t), \tag{1.74}$$

on a finite rectangular domain $x_L < x < x_H$ and $y_L < y < y_H$, with fractional orders $1 < \alpha \leq 2$ and $1 < \beta \leq 2$, where the diffusion coefficients $d(x, y) > 0$ and $e(x, y) > 0$. The "forcing" function $q(x, y, t)$ is used to represent sources and sinks.

Now, following the similar argument for one-dimensional fractional diffusion equation, for Eq. (1.74) using Adomian's decomposition method, we can obtain

$$\begin{aligned} u(x,y,t) = u(x,y,0) &+ L_t^{-1}\left(\mathrm{d}(x,y)D_x^{\alpha}\left(\sum_{n=0}^{\infty} u_n\right)\right) + L_t^{-1}\left(\mathrm{e}(x,y)D_y^{\beta}\left(\sum_{n=0}^{\infty} u_n\right)\right) \\ &+ L_t^{-1}(q(x,y,t)). \end{aligned} \tag{1.75}$$

The standard Adomian decomposition method recurrence scheme is

$$\begin{aligned} u_0 &= f, \\ u_{n+1} &= L_t^{-1}\left(\mathrm{d}(x,y)D_x^{\alpha}u_n\right) + L_t^{-1}\left(\mathrm{e}(x,y)D_y^{\beta}u_n\right), \quad n \geq 0, \end{aligned} \tag{1.76}$$

where $f = u(x,y,0) + L_t^{-1}(q(x,y,t))$.

The modified decomposition method (MDM) recursive scheme is as follows

$$\begin{aligned} u_0 &= f_1, \\ u_1 &= f_2 + L_t^{-1}\left(\mathrm{d}(x,y)D_x^{\alpha}u_0\right) + L_t^{-1}\left(\mathrm{e}(x,y)D_y^{\beta}u_0\right), \\ u_{n+1} &= L_t^{-1}\left(\mathrm{d}(x,y)D_x^{\alpha}u_n\right) + L_t^{-1}\left(\mathrm{e}(x,y)D_y^{\beta}u_n\right), \ n \geq 1. \end{aligned} \tag{1.77}$$

Compared to the standard Adomian method and the modified method, we can see that the two-step Adomian method may provide the solution by using two iterations only.

1.4.4 New Approach for Adomian's Decomposition Method

Let us consider the following space fractional diffusion equation

$$\frac{\partial u(x,t)}{\partial t} = \kappa D_x^{\alpha} u(x,t), \quad 0 < x < L, \quad t \geq 0, \quad 1 < \alpha \leq 2, \tag{1.78}$$

with the following boundary conditions

$$\frac{\partial u(0,t)}{\partial x} = \frac{\partial u(L,t)}{\partial x} = 0, \quad t \geq 0, \tag{1.79}$$

and initial condition

$$u(x,0) = f(x), \quad 0 \leq x \leq L, \tag{1.80}$$

where κ is the diffusion coefficient and D_x^{α} is Caputo fractional derivative of order α.

Therefore, after considering the initial condition $u(x,0) = f(x)$ as Fourier cosine series, we can take

$$u(x,0) = \frac{\pi^2}{3} + \sum_{n=1}^{\infty} \frac{2}{L} \int_0^L f(\xi) \cos\left(\frac{n\pi\xi}{L}\right) \mathrm{d}\xi \cos_{\gamma}\left(\frac{n\pi x}{L}\right), \tag{1.81}$$

where $\cos_{\gamma}\left(\frac{n\pi x}{L}\right)$ is the generalized cosine function defined in [8] and $\gamma = \alpha/2$, $\gamma \in \left(\frac{1}{2}, 1\right]$.

It is known that $D_x^{\gamma} \sin_{\gamma} x = \cos_{\gamma} x$, $\lim_{\gamma \to 1} \sin_{\gamma} x = \sin x$, and $D_x^{\gamma} \sin_{\gamma} x = \cos_{\gamma} x$, where $\cos_{\gamma} x = \sum_{n=0}^{\infty} \frac{(-1)^n x^{2n\gamma}}{\Gamma(2n\gamma + 1)}$.

According to the Adomian decomposition method, we can write

$$u(x,t) = u(x,0) + L_t^{-1}(\mathrm{d} D_x^{\alpha} u(x,t)), \tag{1.82}$$

where

$$\begin{aligned}
u_0 &= u(x,0) = \frac{\pi^2}{3} + \sum_{n=1}^{\infty} \frac{2}{L} \int_0^L f(\xi) \cos\left(\frac{n\pi\xi}{L}\right) \mathrm{d}\xi \cos_{\gamma}\left(\frac{n\pi x}{L}\right), \\
u_1 &= L_t^{-1}(\mathrm{d} D_x^{\alpha} u_0), \\
u_2 &= L_t^{-1}(\mathrm{d} D_x^{\alpha} u_1), \\
u_3 &= L_t^{-1}(\mathrm{d} D_x^{\alpha} u_2),
\end{aligned}$$

and so on.

The practical solution will be the n-term approximation ϕ_n

$$\phi_n = \sum_{i=0}^{n-1} u_i(x,t), \quad n \geq 1 \tag{1.83}$$

with

$$\lim_{n\to\infty} \phi_n = u(x,t).$$

1.4.5 Modified Homotopy Analysis Method with Fourier Transform

To describe the basic idea, let us consider the following fractional differential equation

$$N[u(x,t)] = 0, \tag{1.84}$$

where N is a nonlinear differential operator containing Riesz fractional derivative defined in Eq. (1.18), x and t denote independent variables and $u(x,t)$ is an unknown function. For simplicity, we ignore all boundary or initial conditions, which can be treated in a similar way.

Then, applying Fourier transform and using Eq. (1.20), we can reduce fractional differential Eq. (1.84) to the following Fourier transformed the differential equation

$$N[\hat{u}(k,t)] = 0, \tag{1.85}$$

where $\hat{u}(k,t)$ is the Fourier transform of $u(x,t)$.

By means of the HAM [64, 65], one first constructs the zeroth-order deformation equation of Eq. (1.85) as

$$(1-p)L[\phi(k,t;p) - \hat{u}_0(k,t)] = p\hbar N[\phi(k,t;p)], \tag{1.86}$$

where L is an auxiliary linear operator, $\phi(k,t;p)$ is an unknown function, $\hat{u}_0(k,t)$ is an initial guess of $\hat{u}(k,t)$, $\hbar \neq 0$ is an auxiliary parameter, and $p \in [0,1]$ is the embedding parameter. For the sake of convenience, the expression in nonlinear operator form has been modified in HAM. In this modified homotopy analysis method, the nonlinear term appeared in expression for nonlinear operator form has been expanded using Adomian's type of polynomials as $\sum_{n=0}^{\infty} A_n p^n$ [55].

Obviously, when $p = 0$ and $p = 1$, we have

$$\phi(k,t;0) = \hat{u}_0(k,t), \ \phi(k,t;1) = \hat{u}(k,t), \tag{1.87}$$

respectively. Thus, as p increases from 0 to 1, the solution $\phi(k,t;p)$ varies from the initial guess $\hat{u}_0(k,t)$ to the solution $\hat{u}(k,t)$. Expanding $\phi(x,t;p)$ in Taylor series with respect to the embedding parameter p, we have

$$\phi(k,t;p) = \hat{u}_0(k,t) + \sum_{m=1}^{+\infty} p^m \hat{u}_m(k,t), \tag{1.88}$$

where $\hat{u}_m(k,t) = \frac{1}{m!}\frac{\partial^m}{\partial p^m}\phi(k,t;p)\Big|_{p=0}$.

The convergence of the series (1.88) depends upon the auxiliary parameter $\hbar$. If it is convergent at $p = 1$, we have

$$\hat{u}(k,t) = \hat{u}_0(k,t) + \sum_{m=1}^{+\infty} \hat{u}_m(k,t),$$

which must be one of the solutions of the original nonlinear equation.

Differentiating the zeroth-order deformation Eq. (1.86) m times with respect to p and then setting $p = 0$ and finally dividing them by $m!$, we obtain the following mth-order deformation equation

$$L[\hat{u}_m(k,t) - \chi_m \hat{u}_{m-1}(k,t)] = \hbar \Re_m(\hat{u}_0, \hat{u}_1, \ldots, \hat{u}_{m-1}), \tag{1.89}$$

where

$$\Re_m(\hat{u}_0, \hat{u}_1, \ldots, \hat{u}_{m-1}) = \frac{1}{(m-1)!}\frac{\partial^{m-1} N[\phi(k,t;p)]}{\partial p^{m-1}}\Big|_{p=0}$$

and

$$\chi_m = \begin{cases} 1, & m > 1 \\ 0, & m \le 1 \end{cases}. \tag{1.90}$$

It should be noted that $\hat{u}_m(k,t)$ for $m \ge 1$ is governed by the linear Eq. (1.89) which can be solved by symbolic computational software. Then, by applying inverse Fourier transformation, we can get $u_m(x,t)$.

1.4.6 *Modified Fractional Reduced Differential Transform Method*

Consider the following general nonlinear partial differential equation:

$$Lu(x,t) + Ru(x,t) + Nu(x,t) = g(x,t), \tag{1.91}$$

with initial condition

$$u(x,0) = f(x),$$

where $L \equiv D_t^{\alpha}$ is an easily invertible linear operator, R is the remaining part of the linear operator, $Nu(x,t)$ is a nonlinear term, and $g(x,t)$ is an inhomogeneous term.

We can look for the solution $u(x,t)$ of the Eq. (1.91) in the form of the fractional power series:

$$u(x,t) = \sum_{k=0}^{\infty} U_k(x) t^{\alpha k}, \tag{1.92}$$

where t-dimensional spectrum function $U_k(x)$ is the transformed function of $u(x,t)$.

Now, let us write the nonlinear term

$$N(u,t) = \sum_{n=0}^{\infty} A_n(U_0(x), U_1(x), \cdots, U_n(x))\, t^{n\alpha}, \tag{1.93}$$

where A_n is the appropriate Adomian's polynomials [55]. In this specific nonlinearity, we use the general form of the formula for A_n Adomian's polynomials as

$$A_n(U_0(x), U_1(x), \cdots, U_n(x)) = \frac{1}{n!}\frac{\mathrm{d}^n}{\mathrm{d}\lambda^n}\left[N\left(\sum_{i=0}^{\infty} \lambda^i U_i(x)\right)\right]_{\lambda=0}. \tag{1.94}$$

Now, applying Riemann–Liouville integral J^{α} both sides of Eq. (1.91), we have

$$u(x,t) = \Phi + J^{\alpha} g(x,t) - J^{\alpha} Ru(x,t) - J^{\alpha} Nu(x,t), \tag{1.95}$$

where from the initial condition $\Phi = u(x,0) = f(x)$.

Substituting Eqs. (1.92) and (1.93), for $u(x,t)$ and $N(u,t)$, respectively, in Eq. (1.95) yields

$$\sum_{k=0}^{\infty} U_k(x) t^{\alpha k} = f(x) + J^{\alpha}\left(\sum_{k=0}^{\infty} G_k(x) t^{\alpha k}\right) - J^{\alpha}\left(R\left(\sum_{k=0}^{\infty} U_k(x) t^{\alpha k}\right)\right) - J^{\alpha}\left(\sum_{k=0}^{\infty} A_k(x) t^{\alpha k}\right),$$

where $g(x,t) = \left(\sum_{k=0}^{\infty} G_k(x) t^{\alpha k}\right)$, and $G_k(x)$ is the transformed function of $g(x,t)$.

After carry out Riemann–Liouville integral J^{α}, we obtain

$$\sum_{k=0}^{\infty} U_k(x)\, t^{\alpha k} = f(x) + \left(\sum_{k=0}^{\infty} G_k(x) \frac{t^{\alpha(k+1)}\Gamma(\alpha k+1)}{\Gamma(\alpha(k+1)+1)}\right) - \left(R\left(\sum_{k=0}^{\infty} U_k(x) \frac{t^{\alpha(k+1)}\Gamma(\alpha k+1)}{\Gamma(\alpha(k+1)+1)}\right)\right) - \left(\sum_{k=0}^{\infty} A_k(x) \frac{t^{\alpha(k+1)}\Gamma(\alpha k+1)}{\Gamma(\alpha(k+1)+1)}\right).$$

Finally, equating coefficients of like powers of t, we derive the following recursive formula

$$U_0(x) = f(x),$$

and

$$\begin{aligned} U_{k+1}(x) =& G_k(x) \frac{\Gamma(\alpha k+1)}{\Gamma(\alpha(k+1)+1)} - R\left(U_k(x) \frac{\Gamma(\alpha k+1)}{\Gamma(\alpha(k+1)+1)}\right) \\ & - A_k(x) \frac{\Gamma(\alpha k+1)}{\Gamma(\alpha(k+1)+1)}, \quad k \geq 0. \end{aligned} \tag{1.96}$$

Using the known $U_0(x)$, all components $U_1(x), U_2(x), \cdots, U_n(x), \cdots,$, etc., are determinable by using Eq. (1.96).

Substituting these $U_0(x), U_1(x), U_2(x), \cdots, U_n(x), \cdots,$, etc., in Eq. (1.92), the approximate solution can be obtained as

$$\tilde{u}_p(x,t) = \sum_{m=0}^{p} U_m(x)\, t^{m\alpha}, \tag{1.97}$$

where p is the order of approximate solution.

Therefore, the corresponding exact solution is given by

$$u(x,t) = \lim_{p\to\infty} \tilde{u}_p(x,t). \tag{1.98}$$

1.4.7 Coupled Fractional Reduced Differential Transform Method

In order to introduce coupled fractional reduced differential transform, two cases are considered.

For Functions with Two Independent Variables

In this case, $U(h, k-h)$ is considered as the coupled fractional reduced differential transform of $u(x,t)$. If the function $u(x,t)$ is analytic and differentiated continuously

with respect to time t, then we define the fractional coupled reduced differential transform of $u(x,t)$ as

$$U(h,k-h)=\frac{1}{\Gamma(h\alpha+(k-h)\beta+1)}\left[D_t^{(h\alpha+(k-h)\beta)}u(x,t)\right]_{t=0}, \tag{1.99}$$

whereas the inverse transform of $U(h,k-h)$ is

$$u(x,t)=\sum_{k=0}^{\infty}\sum_{h=0}^{k}U(h,k-h)t^{h\alpha+(k-h)\beta}, \tag{1.100}$$

which is one of the solutions of coupled fractional differential equations.

Theorem 1.3 *Suppose that $U(h,k-h)$ and $V(h,k-h)$ are coupled fractional reduced differential transform of functions $u(x,t)$ and $v(x,t)$, respectively.*

(i) *If $u(x,t)=f(x,t)\pm g(x,t)$,* then $U(h,k-h)=F(h,k-h)\pm G(h,k-h)$.

(ii) *If $u(x,t)=af(x,t)$, where $a\in\mathsf{R}$, then $U(h,k-h)=aF(h,k-h)$.*

(iii) If $f(x,t)=u(x,t)v(x,t)$, *then* $F(h,k-h)=\sum_{l=0}^{h}\sum_{s=0}^{k-h}U(h-l,s)V(l,k-h-s)$.

(iv) *If $f(x,t)=D_t^{\alpha}u(x,t)$, then*

$$F(h,k-h)=\frac{\Gamma((h+1)\alpha+(k-h)\beta+1)}{\Gamma(h\alpha+(k-h)\beta+1)}U(h+1,k-h).$$

(v) If $f(x,t)=D_t^{\beta}v(x,t)$, then

$$F(h,k-h)=\frac{\Gamma(h\alpha+(k-h+1)\beta+1)}{\Gamma(h\alpha+(k-h)\beta+1)}V(h,k-h+1).$$

Proof of Theorem 1.3 (i)

If $u(x,t)=f(x,t)\pm g(x,t)$, then according to Eq. (1.99)

$$\begin{aligned} U(h,k-h) &= \frac{1}{\Gamma(h\alpha+(k-h)\beta+1)}\left[D_t^{(h\alpha+(k-h)\beta)}(f(x,t)\pm g(x,t))\right]_{t=0} \\ &= \frac{1}{\Gamma(h\alpha+(k-h)\beta+1)}\left[D^{(h\alpha+(k-h)\beta)}f(x,t)\right]_{t=0} \\ &\pm \frac{1}{\Gamma(h\alpha+(k-h)\beta+1)}\left[D^{(h\alpha+(k-h)\beta)}g(x,t)\right]_{t=0} \end{aligned}$$

Therefore, in view of Eq. (1.99),

$$U(h,k-h) = F(h,k-h) \pm G(h,k-h)$$

where $F(h,k-h) = \frac{1}{\Gamma(h\alpha+(k-h)\beta+1)}\left[D^{(h\alpha+(k-h)\beta)}f(x,t)\right]_{t=0}$
and $G(h,k-h) = \frac{1}{\Gamma(h\alpha+(k-h)\beta+1)}\left[D^{(h\alpha+(k-h)\beta)}g(x,t)\right]_{t=0}$

Proof of Theorem 1.3 (ii)

If $u(x,t) = af(x,t)$ where $a \in \mathsf{R}$, then according to Eq. (1.99)

$$\begin{aligned} U(h,k-h) &= \frac{1}{\Gamma(h\alpha+(k-h)\beta+1)}\left[D^{(h\alpha+(k-h)\beta)}af(x,t)\right]_{t=0} \\ &= a\left(\frac{1}{\Gamma(h\alpha+(k-h)\beta+1)}\left[D^{(h\alpha+(k-h)\beta)}f(x,t)\right]_{t=0}\right) \\ &= aF(h,k-h) \end{aligned}$$

Proof of Theorem 1.3 (iii)

According to Eq. (1.100)

$$\begin{aligned} f(x,t) &= U(0,0)V(0,0) + (U(1,0)V(0,0) + U(0,0)V(1,0))t^{\alpha} \\ &\quad + \{U(0,1)V(0,0) + U(0,0)V(0,1)\}t^{\beta} \\ &\quad + (U(1,0)V(0,1) + U(0,1)V(1,0) + U(1,1)V(0,0) + U(0,0)V(1,1))t^{\alpha+\beta} + \cdots \\ &= \sum_{k=0}^{\infty}\sum_{h=0}^{k}\left(\sum_{l=0}^{h}\sum_{s=0}^{k-h}U(h-l,s)V(l,k-h-s)\right)t^{h\alpha+(k-h)\beta} \end{aligned}$$

Hence, $F(h,k-h) = \sum_{l=0}^{h}\sum_{s=0}^{k-h}U(h-l,s)V(l,k-h-s)$, identified in view of Eq. (1.100).

Proof of Theorem 1.3 (iv)

If $f(x,t) = D_t^{\alpha} u(x,t)$, then according to Eq. (1.99)

$$\begin{aligned} F(h,k-h) &= \frac{1}{\Gamma(h\alpha+(k-h)\beta+1)}\left[D_t^{(h+1)\alpha+(k-h)\beta}u(x,t)\right]_{t=0} \\ &= \frac{\Gamma((h+1)\alpha+(k-h)\beta+1)}{\Gamma(h\alpha+(k-h)\beta+1)}\left[\frac{1}{\Gamma((h+1)\alpha+(k-h)\beta+1)}D_t^{(h+1)\alpha+(k-h)\beta}u(x,t)\right]_{t=0} \\ &= \frac{\Gamma((h+1)\alpha+(k-h)\beta+1)}{\Gamma(h\alpha+(k-h)\beta+1)}U(h+1,k-h) \end{aligned}$$

where $U(h+1,k-h) = \left[\frac{1}{\Gamma((h+1)\alpha+(k-h)\beta+1)}D_t^{(h+1)\alpha+(k-h)\beta}u(x,t)\right]_{t=0}$

Proof of Theorem 1.3 (v)

If $f(x,t) = D_t^{\beta} v(x,t)$, then according to Eq. (1.99)

$$\begin{aligned} F(h,k-h) &= \frac{1}{\Gamma(h\alpha+(k-h)\beta+1)}\left[D_t^{(h\alpha+(k-h+1)\beta)}v(x,t)\right]_{t=0} \\ &= \frac{\Gamma(h\alpha+(k-h+1)\beta+1)}{\Gamma(h\alpha+(k-h)\beta+1)}\left[\frac{1}{\Gamma(h\alpha+(k-h+1)\beta+1)}D_t^{(h\alpha+(k-h+1)\beta)}v(x,t)\right]_{t=0} \\ &= \frac{\Gamma(h\alpha+(k-h+1)\beta+1)}{\Gamma(h\alpha+(k-h)\beta+1)}V(h,k-h+1) \end{aligned}$$

where $V(h,k-h+1) = \left[\frac{1}{\Gamma(h\alpha+(k-h+1)\beta+1)}D_t^{(h\alpha+(k-h+1)\beta)}v(x,t)\right]_{t=0}$

For Functions with Three Independent Variables

In this case, $U(h,k-h)$ is considered as the coupled fractional reduced differential transform of $u(x,y,t)$. If the function $u(x,y,t)$ is analytic and differentiated continuously with respect to time t, then we define the fractional coupled reduced differential transform of $u(x,y,t)$ as

$$U(h,k-h) = \frac{1}{\Gamma(h\alpha+(k-h)\beta+1)}\left[D_t^{(h\alpha+(k-h)\beta)}u(x,y,t)\right]_{t=0}, \tag{1.101}$$

whereas the inverse transform of $U(h,k-h)$ is

$$u(x,y,t) = \sum_{k=0}^{\infty}\sum_{h=0}^{k} U(h,k-h)t^{h\alpha+(k-h)\beta}, \tag{1.102}$$

which is one of the solutions of coupled fractional differential equations.

Theorem 1.4. *Suppose that $U(h,k-h)$ and $V(h,k-h)$ are coupled fractional reduced differential transform of functions $u(x,y,t)$ and $v(x,y,t)$, respectively.*

(i) *If* $u(x,y,t) = f(x,y,t) \pm g(x,y,t)$, *then* $U(h,k-h) = F(h,k-h) \pm G(h,k-h)$.

(ii) If $u(x,y,t) = af(x,y,t)$, *where* $a \in \mathsf{R}$, *then* $U(h,k-h) = aF(h,k-h)$.

(iii) *If* $f(x,y,t) = u(x,y,t)v(x,y,t)$, then $F(h,k-h) = \sum_{l=0}^{h}\sum_{s=0}^{k-h} U(h-l,s)V(l,k-h-s)$.

(iv) If $f(x,y,t) = D_t^{\alpha}u(x,y,t)$, *then*

$$F(h,k-h) = \frac{\Gamma((h+1)\alpha + (k-h)\beta + 1)}{\Gamma(h\alpha + (k-h)\beta + 1)} U(h+1,k-h).$$

(v) If $f(x,y,t) = D_t^{\beta}v(x,y,t)$, then

$$F(h,k-h) = \frac{\Gamma(h\alpha + (k-h+1)\beta + 1)}{\Gamma(h\alpha + (k-h)\beta + 1)} V(h,k-h+1).$$

The proofs of Theorem 1.4 (i), (ii) and (iv), (v) can be obtained in a similar manner as done for the functions with two independent variables.

Proof of Theorem 1.4 (iii)

$$\begin{aligned}
f(x,y,t) &= u(x,y,t)v(x,y,t) \\
&= \left(\sum_{k=0}^{\infty}\sum_{h=0}^{k} U(h,k-h)t^{h\alpha+(k-h)\beta}\right)\left(\sum_{k=0}^{\infty}\sum_{h=0}^{k} V(h,k-h)t^{h\alpha+(k-h)\beta}\right) \\
&= U(0,0)V(0,0) + (U(1,0)V(0,0) + U(0,0)V(1,0))t^{\alpha} + (U(0,1)V(0,0) + U(0,0)V(0,1))t^{\beta} \\
&\quad + (U(1,0)V(0,1) + U(0,1)V(1,0) + U(1,1)V(0,0) + U(0,0)V(1,1))t^{\alpha+\beta} + \ldots \\
&= \sum_{k=0}^{\infty}\sum_{h=0}^{k}\left(\sum_{l=0}^{h}\sum_{s=0}^{k-h} U(h-l,s)V(l,k-h-s)\right)t^{h\alpha+(k-h)\beta}.
\end{aligned}$$

Hence,

$$F(h,k-h) = \sum_{l=0}^{h}\sum_{s=0}^{k-h} U(h-l,s)V(l,k-h-s).$$

1.4.8 Optimal Homotopy Asymptotic Method

The OHAM was introduced and developed by Merinca et al. [66]. In OHAM, the control and adjustment of the convergence region are provided in a convenient way.

To illustrate the basic ideas of optimal homotopy asymptotic method [67, 68], we consider the following nonlinear differential equation

$$A(u(x,t)) + g(x,t) = 0,\ x \in \Omega \tag{1.103}$$

with the boundary conditions

$$B\left(u, \frac{\partial u}{\partial t}\right) = 0, \quad x \in \Gamma \tag{1.104}$$

where A is a differential operator, B is a boundary operator, $u(x,t)$ is an unknown function, Γ is the boundary of the domain Ω, and $g(x,t)$ is a known analytic function.

The operator A can be decomposed as

$$A = L + N, \tag{1.105}$$

where L is a linear operator and N is a nonlinear operator.

We construct a homotopy $\varphi(x,\, t\,;\, p) : \Omega \times [0,1] \to \Re$ which satisfies

$$\begin{aligned} H(\varphi(x,\, t\,;\, p), p) &= (1-p)[L(\varphi(x,\, t\,;\, p)) + g(x,t)] \\ &\quad - H(p)[A(\varphi(x,\, t\,;\, p)) + g(x,t)] = 0, \end{aligned} \tag{1.106}$$

where $p \in [0,\, 1]$ is an embedding parameter, $H(p)$ is a nonzero auxiliary function for $p \neq 0$ and $H(0) = 0$. When $p = 0$ and $p = 1$,, we have $\varphi(x,\, t\,;\, 0) = u_0(x,t)$ and $\varphi(x,\, t\,;\, 1) = u(x,t)$, respectively.

Thus, as p varies from 0 to 1, the solution $\varphi(x,\, t\,;\, p)$ approaches from $u_0(x,t)$ to $u(x,t)$.

Here $u_0(x,t)$ is obtained from Eqs. (1.106) and (1.104) with $p = 0$ yields

$$L(\varphi(x,\, t\,;\, 0)) + g(x,t) = 0, \qquad B\left(u_0, \frac{\partial u_0}{\partial t}\right) = 0. \tag{1.107}$$

The auxiliary function $H(p)$ is chosen in the form

$$H(p) = pC_1 + p^2C_2 + p^3C_3 + \ldots \tag{1.108}$$

where $C_1,\, C_2, C_3,\, \ldots$ are constants to be determined. To get an approximate solution, $\tilde{\varphi}(x,\, t\,;\, p, C_1, C_2, C_3, \ldots)$ is expanded in a series about p as

$$\tilde{\varphi}(x,\, t\,;\, p, C_1, C_2, C_3, \ldots) = u_0(x,t) + \sum_{i=1}^{\infty} u_i(x,t,C_1,C_2,C_3,\ldots)p^i. \tag{1.109}$$

Substituting Eq. (1.109) in Eq. (1.106) and equating the coefficients of like powers of p, we will have the following equations

$$L(u_1(x,\,t)+g(x,t))=C_1N_0(u_0(x,\,t)),\qquad B\left(u_1,\frac{\partial u_1}{\partial t}\right)=0. \tag{1.110}$$

$$\begin{aligned}&L(u_2(x,\,t))-L(u_1(x,\,t))=C_2N_0(u_0(x,\,t))+C_1(L(u_1(x,\,t))+N_1(u_0(x,\,t),u_1(x,\,t))),\\&B\left(u_2,\frac{\partial u_2}{\partial t}\right)=0.\end{aligned} \tag{1.111}$$

and hence, the general governing equations for $u_j(x,t)$ are given by

$$\begin{aligned}L\big(u_j(x,\,t)\big)=&L\big(u_{j-1}(x,\,t)\big)+C_jN_0(u_0(x,\,t))\\&+\sum_{i=1}^{j-1}C_i\big[L\big(u_{j-1}(x,\,t)\big)+N_{j-1}\big(u_0(x,\,t),\,\ldots,u_{j-1}(x,\,t)\big)\big]\,;\end{aligned} \tag{1.112}$$

$j=2,3,\ldots$

where $N_j\big(u_0(x,\,t),\,\ldots,u_j(x,\,t)\big)$ is the coefficient of p^j in the expansion of $N(\varphi(x,\,t\,;\,p))$ about the embedding parameter p and

$$N(\varphi(x,\,t\,;\,p,C_1,C_2,C_3,\ldots))=N_0(u_0(x,\,t))+\sum_{j=1}^{\infty}N_j\big(u_0,u_1,\,\ldots,\,u_j\big)p^j. \tag{1.113}$$

It is observed that the convergence of the series (1.109) depends upon the auxiliary constants $C_1,C_2,C_3,\ldots$.

The approximate solution of Eq. (1.103) can be written in the following form

$$\tilde{u}(x,\,t\,;\,C_1,C_2,C_3,\ldots)=u_0(x,t)+\sum_{j=1}^{n-1}u_j(x,t,C_1,C_2,C_3,\ldots). \tag{1.114}$$

Substituting Eq. (1.114) in Eq. (1.103), we get the following expression for the residual

$$R_n(x,\,t\,;C_1,C_2,C_3,\ldots)=L(\tilde{u}(x,\,t\,;C_1,C_2,C_3,\ldots))+N(\tilde{u}(x,\,t\,;C_1,C_2,C_3,\ldots))+g(x,t). \tag{1.115}$$

If $R_n(x,\,t\,;C_1,C_2,C_3,\ldots)=0$,, then $\tilde{u}(x,\,t\,;C_1,C_2,C_3,\ldots)$ is the exact solution. Generally, such case does not arise for nonlinear problems. The nth-order approximate solution given by Eq. (1.114) depends on the auxiliary constants $C_1,C_2,C_3,\ldots$, and these constants can be optimally determined by various methods such as weighted residual least square method, Galerkin's method, and collocation method.

The convergence of the nth approximate solution depends upon the optimal values of the unknown constants $C_1, C_2, C_3, \ldots$. When the convergence control constants $C_1, C_2, C_3, \ldots$ are known by the above-mentioned methods, then the approximate solution of Eq. (1.103) is well determined.

1.4.9 First Integral Method

Let us consider the time fractional differential equation with independent variables $x = (x_1, x_2, \ldots, x_m, t)$ and a dependent variable u.

$$P(u, D_t^{\alpha}u, u_{x_1}, u_{x_2}, u_{x_3}, D_t^{2\alpha}u, u_{x_1x_1}, u_{x_1x_2}, u_{x_2x_2}, u_{x_3x_3}, \ldots) = 0, \quad 0 < \alpha \leq 1 \tag{1.116}$$

where $D_t^{\alpha}u$ is the fractional modified Riemann–Liouville derivatives of u.

Using the variable transformation

$$u(x_1, x_2, \ldots, x_m, t) = U(\xi), \quad \xi = x_1 + l_1x_2 + \ldots + l_{m-1}x_m + \frac{\lambda t^{\alpha}}{\Gamma(1+\alpha)}, \tag{1.117}$$

where k, l_i, and λ are constants to be determined later; the fractional differential Eq. (1.117) is reduced to a nonlinear ordinary differential equation

$$H = (U(\xi), U'(\xi), U''(\xi), \ldots). \tag{1.118}$$

We assume that Eq. (1.117) has a solution in the form

$$U(\xi) = X(\xi), \tag{1.119}$$

and introduce a new independent variable $Y(\xi) = U_{\xi}(\xi)$, which leads to a new system of ODEs of the form

$$\begin{aligned} \frac{\mathrm{d}X(\xi)}{\mathrm{d}\xi} &= Y(\xi), \\ \frac{\mathrm{d}Y(\xi)}{\mathrm{d}\xi} &= G(X(\xi), Y(\xi)). \end{aligned} \tag{1.120}$$

Now, let us recall the first integral method [69]. By using the division theorem for two variables in the complex domain $\mathbb{C}$ which is based on the Hilbert's Nullstellensatz Theorem [70], we can obtain one first integral to Eq. (1.120) which can reduce Eq. (1.118) to a first-order integrable ordinary differential equation. An exact solution to Eq. (1.116) is then obtained by solving this equation directly.

Theorem 1.5 (*Division theorem) Suppose that* $Q(x, y)$ *and* $R(x, y)$ *are polynomials in* $\mathbb{C}[[x, y]]$, and $Q(x, y)$ is *irreducible in* $\mathbb{C}[[x, y]]$. *If* $R(x, y)$ *vanishes at all zero points of* $Q(x, y)$, *then there exists a polynomial* $H(x, y)$ *in* $\mathbb{C}[[x, y]]$ *such that*

$$R(x,y) = Q(x,y)H(x,y). \tag{1.121}$$

The division theorem follows immediately from the Hilbert's Nullstellensatz theorem from the ring theory of commutative algebra [70–72].

Theorem 1.6 *(Hilbert's Nullstellensatz theorem, see* [70]**)** *Let K be a field and L be an algebraic closure of K. Then*

(i) *Every ideal* γ *of* $K[X_1, X_2, \ldots, X_n]$ *not containing* 1 *admits at least one zero in* L^n.
(ii) *Let* $x = (x_1, x_2, \ldots, x_n)$ *and* $y = (y_1, y_2, \ldots, y_n)$ *be two elements of* L^n*; for the set of polynomials of* $K[X_1, X_2, \ldots, X_n]$ *zero at x to be identical with the set of polynomials of* $K[X_1, X_2, \ldots, X_n]$ *zero at y, it is necessary and sufficient that there exists an K-automorphism S of L such that* $y_i = S(x_i)$ for $1 \le i \le n$.
(iii) *For an ideal* α *of* $K[X_1, X_2, \ldots, X_n]$ *to be maximal, it is necessary and sufficient that there exists an x in* L^n *such that* α *is the set of polynomials of* $K[X_1, X_2, \ldots, X_n]$ *zero at x.*
(iv) *For a polynomial Q of* $K[X_1, X_2, \ldots, X_n]$ *to be zero on the set of zeros in* L^n *of an ideal* γ *of* $K[X_1, X_2, \ldots, X_n]$*, it is necessary and sufficient that there exists an integer* $m > 0$ *such that* $Q^m \in \gamma$."

Using the ring conception of commutative algebra, Feng [69] *first proposed the first integral method in solving Burgers–KdV equation. The basic idea of this method is to construct the first integral with polynomial coefficients of an explicit form to an equivalent autonomous planar system by using the division theorem.*

1.4.10 Haar Wavelets and the Operational Matrices

Morlet (1982) [33] first introduced the idea of wavelets as a family of functions constructed from dilation and translation of a single function called the "mother wavelet." Haar wavelet functions have been used from 1910 and were introduced by the Hungarian mathematician Alfred Haar [73]. Haar wavelets (which are Daubechies wavelets of order 1) consist of piecewise constant functions on the real line that can take only three values, i.e., 0, 1, and −1 and are therefore the simplest orthonormal wavelets with a compact support. Haar wavelet method to be used due to the following features: simpler and fast, flexible, convenient, small computational costs, and computationally attractive. The Haar functions are a family of switched rectangular waveforms where amplitudes can differ from one function to another.

The Haar wavelet family for $x \in [0, 1)$ is defined as follows [74]

$$h_i(x) = \begin{cases} 1 & x \in [\xi_1, \xi_2) \\ -1 & x \in [\xi_2, \xi_3) \\ 0 & \text{else where} \end{cases} \tag{1.122}$$

where

$$\xi_1 = \frac{k}{m},\ \xi_2 = \frac{k+0.5}{m},\ \xi_3 = \frac{k+1}{m}.$$

In these formulae integer $m = 2^j,\ j = 0, 1, 2, \ldots, J$ indicates the level of the wavelet; $k = 0, 1, 2, \ldots, m-1$ is the translation parameter. The maximum level of resolution is J. The index i is calculated from the formula $i = m + k + 1$; in the case of minimal values $m = 1,\ k = 0$, we have $i = 2$. The maximal value of $i = 2M = 2^{J+1}$. It is assumed that the value $i = 1$ corresponds to the scaling function for which

$$h_i(x) = \begin{cases} 1 & \text{for } x \in [0, 1) \\ 0 & \text{elsewhere.} \end{cases} \tag{1.123}$$

In the following analysis, integrals of the wavelets are defined as

$$p_i(x) = \int_0^x h_i(x)\mathrm{d}x, \quad q_i(x) = \int_0^x p_i(x)\mathrm{d}x,\ r_i(x) = \int_0^x q_i(x)\mathrm{d}x.$$

This can be done with the aid of (1.122)

$$p_i(x) = \begin{cases} x - \xi_1 & \text{for } x \in [\xi_1, \xi_2) \\ \xi_3 - x & \text{for } x \in [\xi_2, \xi_3) \\ 0 & \text{elsewhere} \end{cases}. \tag{1.124}$$

$$q_i(x) = \begin{cases} 0 & \text{for } x \in [0, \xi_1) \\ \frac{1}{2}(x - \xi_1)^2 & \text{for } x \in [\xi_1, \xi_2) \\ \frac{1}{4m^2} - \frac{1}{2}(\xi_3 - x)^2 & \text{for } x \in [\xi_2, \xi_3) \\ \frac{1}{4m^2} & \text{for } x \in [\xi_3, 1] \end{cases}. \tag{1.125}$$

$$r_i(x) = \begin{cases} \frac{1}{6}(x - \xi_1)^3 & \text{for } x \in [\xi_1, \xi_2) \\ \frac{1}{4m^2}(x - \xi_2) + \frac{1}{6}(\xi_3 - x)^3 & \text{for } x \in [\xi_2, \xi_3) \\ \frac{1}{4m^2}(x - \xi_2) & \text{for } x \in [\xi_3, 1) \\ 0 & \text{elsewhere} \end{cases}. \tag{1.126}$$

The collocation points are defined as

$$x_l = \frac{l - 0.5}{2M}, \qquad l = 1,\ 2,\ \ldots,\ 2M.$$

It is expedient to introduce the $2M \times 2M$ matrices **H**, **P**, **Q,** and **R** with the elements $H(i,l) = h_i(x_l),\ P(i,l) = p_i(x_l),\ Q(i,l) = q_i(x_l)$, and $R(i,l) = r_i(x_l)$, respectively.

In 2012, the generalized Haar wavelet operational matrix of integration has been derived by the learned researcher Saha Ray [75]. Usually, the Haar wavelets are defined for the interval $t \in [0,\ 1)$, but in general case $t \in [A,\ B]$, we divide the interval $[A,\ B]$ into m equal subintervals; each of width $\Delta t = (B - A)/m$. In this case, the orthogonal set of Haar functions is defined in the interval $[A,\ B]$ by [75]

$$h_0(t) = \begin{cases} 1 & t \in [A, B], \\ 0 & \text{elsewhere} \end{cases}. \tag{1.127}$$

and

$$h_i(t) = \begin{cases} 1, & \zeta_1(i) \le t < \zeta_2(i) \\ -1, & \zeta_2(i) \le t < \zeta_3(i) \\ 0, & \text{otherwise} \end{cases}. \tag{1.128}$$

where

$$\begin{aligned} \zeta_1(i) &= A + \left(\frac{k-1}{2^j}\right)(B - A) = A + \left(\frac{k-1}{2^j}\right) m\Delta t, \\ \zeta_2(i) &= A + \left(\frac{k-(1/2)}{2^j}\right)(B - A) = A + \left(\frac{k-(1/2)}{2^j}\right) m\Delta t, \\ \zeta_3(i) &= A + \left(\frac{k}{2^j}\right)(B - A) = A + \left(\frac{k}{2^j}\right) m\Delta t, \end{aligned}$$

for $i = 1, 2, \cdots, m$, $m = 2^J$ and J is a positive integer which is called the maximum level of resolution. Here j and k represent the integer decomposition of the index i, i.e., $i = k + 2^j - 1$, $0 \le j < i$, and $1 \le k < 2^j + 1$.

The mutual orthogonalities of all Haar wavelets can be expressed as

$$\int_a^b h_m(t) h_n(t) \mathrm{d}t = (b - a) 2^{-j} \delta_{mn} = \begin{cases} (b-a)2^{-j}, & m = n = 2^j + k \\ 0, & m \ne n \end{cases}.$$

Function Approximation

Any function $y(t) \in L^2([0,\ 1))$ can be expanded into Haar wavelets by [76]

$$y(t) = c_0 h_0(t) + c_1 h_1(t) + c_2 h_2(t) + \cdots, \quad \text{where } c_j = \int_0^1 y(t) h_j(t) \mathrm{d}t. \tag{1.129}$$

If $y(t)$ is approximated as piecewise constant in each subinterval, the sum in Eq. (1.129) may be terminated after m terms, and consequently, we can write discrete version in the matrix form as

$$\mathbf{Y} \approx \left(\sum_{i=0}^{m-1} c_i h_i(t_l) \right)_{1\times m} = \mathbf{C}_m^T \mathbf{H}_m, \tag{1.130}$$

where $\mathbf{Y}$ and $\mathbf{C}_m^T$ are the m-dimensional row vectors.

Here $\mathbf{H}_m$ is the Haar wavelet matrix of order m defined by $\mathbf{H}_m = [\boldsymbol{h}_0, \boldsymbol{h}_1, \cdots, \boldsymbol{h}_{m-1}]^T$, i.e.

$$\mathrm{H}_m = \begin{bmatrix} \boldsymbol{h}_0 \\ \boldsymbol{h}_1 \\ \cdots \\ \boldsymbol{h}_{m-1} \end{bmatrix} = \begin{bmatrix} h_{0,0} & h_{0,1} & \cdots & h_{0,m-1} \\ h_{1,0} & h_{1,1} & \cdots & h_{1,m-1} \\ \vdots & \vdots & & \vdots \\ h_{m-1,0} & h_{m-1,1} & \cdots & h_{m-1,m-1} \end{bmatrix}. \tag{1.131}$$

where $\boldsymbol{h}_0, \boldsymbol{h}_1, \cdots, \boldsymbol{h}_{m-1}$ are the discrete form of the Haar wavelet bases.

The collocation points are given by

$$t_l = A + (l - 0.5)\Delta t,\ l = 1, 2,\ \cdots, m. \tag{1.132}$$

Operational Matrix of the General-Order Integration

The integration of the $\mathbf{H}_m(t) = [h_0(t),\ h_1(t), \ldots, h_{m-1}(t)]^T$ can be approximated by [77]

$$\int_0^t \mathbf{H}_m(\tau)\mathrm{d}\tau \cong \mathbf{Q}\mathbf{H}_m(t), \tag{1.133}$$

where $\mathbf{Q}$ is called the Haar wavelet operational matrix of integration which is a square matrix of m-dimension. To derive the Haar wavelet operational matrix of the general order of integration, we recall the fractional integral of order $\alpha(>0)$ which is defined by Podlubny [4]

$$J^{\alpha} f(t) = \frac{1}{\Gamma(\alpha)} \int_0^t (t-\tau)^{\alpha-1} f(\tau)\mathrm{d}\tau,\ \alpha > 0,\ \alpha \in \mathsf{R}^+ \tag{1.134}$$

where R^+ is the set of positive real numbers.

The operational matrix for a general order was first time derived by learned researcher Saha Ray [75]. The Haar wavelet operational matrix $\mathbf{Q}^{\alpha}$ for integration of the general order α is given by [75]

$$\mathbf{Q}^{\alpha}\mathbf{H}_m(t) = J^{\alpha}\mathbf{H}_m(t) = [J^{\alpha}h_0(t), J^{\alpha}h_1(t), \ldots, J^{\alpha}h_{m-1}(t)]^T.$$

Thus,

$$\mathbf{Q}^{\alpha}\mathbf{H}_m(t) = [Qh_0(t), Qh_1(t), \cdots, Qh_{m-1}(t)]^T. \tag{1.135}$$

where

$$Qh_0(t) = \begin{cases} \frac{t^{\alpha}}{\Gamma(1+\alpha)}, & t \in [A,\ B], \\ 0, & \text{elsewhere} \end{cases}. \tag{1.136}$$

and

$$Qh_i(t) = \begin{cases} 0, & A \le t < \zeta_1(i), \\ \phi_1, & \zeta_1(i) \le t < \zeta_2(i), \\ \phi_2, & \zeta_2(i) \le t < \zeta_3(i), \\ \phi_3, & \zeta_3(i) \le t < B, \end{cases}. \tag{1.137}$$

where

$$\phi_1 = \frac{(t-\zeta_1(i))^{\alpha}}{\Gamma(\alpha+1)},$$
$$\phi_2 = \frac{(t-\zeta_1(i))^{\alpha}}{\Gamma(\alpha+1)} - 2\frac{(t-\zeta_2(i))^{\alpha}}{\Gamma(\alpha+1)},$$
$$\phi_3 = \frac{(t-\zeta_1(i))^{\alpha}}{\Gamma(\alpha+1)} - 2\frac{(t-\zeta_2(i))^{\alpha}}{\Gamma(\alpha+1)} + \frac{(t-\zeta_3(i))^{\alpha}}{\Gamma(\alpha+1)}.$$

for $i = 1, 2, \cdots, m$, $m = 2^J$ and J is a positive integer, called the maximum level of resolution. Here j and k represent the integer decomposition of the index i, i.e.$i = k + 2^j - 1$, $0 \le j < i$ and $1 \le k < 2^j + 1$.

1.5 Numerical Methods for Solving Stochastic Point Kinetics Equation

The point kinetics equations are the most essential model in the field of nuclear science and engineering. The modeling of these equations intimates the time-dependent behavior of a nuclear reactor [78–81]. Noise in reactors can be described by conventional point reactor kinetic equations (PRKE) with fluctuation

introduced in some of the parameters. Such equations may be referred to as stochastic point reactor kinetic equations. Power reactor noise analysis may be viewed as study of a reactor's response to a stochastic reactivity or source input. The difficulty of solving stochastic point reactor kinetic equations arises from the fact that they are nonlinear. The stochastic behavior of a point reactor is modeled with a system of Itô stochastic differential equations.

The point kinetics equations model a system of interacting populations, specifically the populations of neutrons and delayed neutron precursors. The dynamical process explained by the point kinetics equations is stochastic in nature. The neutron density and delayed neutron precursor concentrations differ randomly with respect to time. At the levels of high power, random behavior is imperceptible. But at low-power levels, such as at the beginning, random fluctuation in the neutron density and neutron precursor concentrations can be crucial.

The numerical solutions for neutron population density and sum of precursors concentration population density have been solved with stochastic piecewise constant approximation (PCA) method and Monte Carlo computations by using different step reactivity functions [81]. The derivation and the solution for stochastic neutron point kinetics equation have elaborately described in the work of [82] by considering the same parameters and different step reactivity with Euler–Maruyama method and strong order 1.5 Taylor method. It can be observed that the numerical methods like Euler–Maruyama method and strong order 1.5 Taylor method are likely reliable with stochastic PCA method and Monte Carlo computations. Here, Euler–Maruyama method and Taylor 1.5 strong order approximations method have been applied efficiently and conveniently for the solution of the stochastic point kinetics equation.

In the present investigation, the main attractive advantage, of these computational numerical methods, is their elegant applicability for solving stochastic point kinetics equations in a simple and efficient way.

1.5.1 Wiener Process

A standard Wiener process (often called Brownian motion) on the interval $[0, T]$ is a continuous time stochastic process $W(t)$ that depends continuously on $t \in [0, T]$ and satisfies the following properties [82–85]

(i) $W(0) = 0$ (with probability 1).

(ii) For $0 \leq s \leq t \leq T$, the increment $W(t) - W(s)$ is normally distributed with mean $E(W(t)) = 0$, variance $E(W(t) - W(s))^2 = |t - s|$, and covariance $E(W(t)W(s)) = \min(t, s)$; equivalently $W(t) - W(s) \sim \sqrt{t - s}N(0, 1)$ where $N(0, 1)$ denotes a normal distribution with zero mean and unit variance.

(iii) For $0 \leq s < t < u < v \leq T$, the increments $W(t) - W(s)$ and $W(v) - W(u)$ are independent. For the computational purpose, it is useful to consider

discredited Brownian motion, where $W(t)$ is specified at discrete t values. We thus set $\Delta t = T/N$ for some positive integer N and let $W_i = W(t_i)$ with $t_i = i\Delta t$. We discretize the Wiener process with time step Δt as $W_i = W_{i-1} + dW_i i = 1, 2, \ldots, N$, where each $dW_i \sim \sqrt{\Delta t} N(0, 1)$.

Stochastic differential equation (SDE) models play a prominent role in a range of application areas, including biology, chemistry, epidemiology, mechanics, microelectronics, economics, and finance.

An Itô process (or stochastic integral) $X = \{X_t, t \geq 0\}$ has the form [82–85]

$$X_t = X_0 + \int_0^t a(X_s)\mathrm{d}s + \int_0^t b(X_s)\mathrm{d}W_s, \quad \text{for } t \geq 0. \tag{1.138}$$

It consists of an initial value $X_0 = x_0$, which may be random, a slowly varying continuous component called the drift and rapid varying continuous random component called the diffusion. The second integral in Eq. (1.138) is an Itô stochastic integral with respect to the Wiener process $W = \{W_t, t \geq 0\}$. The integral equation in Eq. (1.138) is often written in the differential form

$$\mathrm{d}X_t = a(X_t)\mathrm{d}t + b(X_t)\mathrm{d}W_t, \tag{1.139}$$

Then Eq. (1.139) is called stochastic differential equation (or Itô stochastic differential equation). Here Euler–Maruyama Method and the order 1.5 Strong Taylor methods have been described which are used later for solving a stochastic point kinetics equation.

1.5.2 Euler–Maruyama Method

The Euler–Maruyama approximation is the simplest time-discrete approximations of an Itô process. Let $\{Y_\tau\}$ be an Itô process on $\tau \in [t_0, T]$ satisfying the stochastic differential equation (SDE)

$$\begin{cases} \mathrm{d}Y_\tau = a(\tau, Y_\tau)\mathrm{d}\tau + b(\tau, Y_\tau)\mathrm{d}W_\tau \\ Y_{t_0} = Y_0 \end{cases}. \tag{1.140}$$

For a given time discretization

$$t_0 = \tau_0 < \tau_1 < \cdots < \tau_n = T, \tag{1.141}$$

an Euler approximation is a continuous time stochastic process $\{X(\tau), t_0 \leq \tau \leq T\}$ satisfying the iterative scheme [84, 85]

$$X_{n+1} = X_n + a(\tau_n, X_n)\Delta\tau_{n+1} + b(\tau_n, X_n)\Delta W_{n+1}, \tag{1.142}$$

for $n = 0, 1, 2, \ldots, N-1$, with initial value

$$X_0 = X(\tau_0),$$

where $X_n = X(\tau_n)$, $\Delta\tau_{n+1} = \tau_{n+1} - \tau_n$, and $\Delta W_{n+1} = W(\tau_{n+1}) - W(\tau_n)$. Here, each random number ΔW_n is computed as $\Delta W_n = \eta_n\sqrt{\Delta\tau_n}$, where η_n is chosen from the standard normal distribution $N(0, 1)$.

We have considered the equidistant discretized times

$\tau_n = \tau_0 + n\Delta$ with $\Delta = \Delta_n = \frac{(T-\tau_0)}{N}$ for some integer N large enough so that $\Delta \in (0, 1)$.

1.5.3 Order 1.5 Strong Taylor Method

Here we consider Taylor approximation having strong order $\alpha = 1.5$. The order 1.5 strong Taylor scheme can be obtained by adding more terms from Itô–Taylor expansion to the Milstein scheme [84, 85]. The order 1.5 strong Itô–Taylor scheme is

$$\begin{aligned} Y_{n+1} = Y_n + a\Delta_n + b\Delta W_n + \frac{1}{2}bb_x(\Delta W_n^2 - \Delta_n) + a_x b\Delta Z_n + \frac{1}{2}(aa_x + \frac{1}{2}b^2 a_{xx})\Delta_n^2 \\ + (ab_x + \frac{1}{2}b^2 b_{xx})(\Delta W_n\Delta_n - \Delta Z_n) + \frac{1}{2}b(bb_{xx} + b_x^2)(\frac{1}{3}\Delta W_n^2 - \Delta_n)\Delta W_n \end{aligned} \tag{1.143}$$

for $n = 0, 1, 2, \ldots, N-1$, with initial value

$$Y_0 = Y(\tau_0) \text{ and } \Delta_n = \Delta\tau_n.$$

Here, partial derivatives are denoted by subscripts, and the random variable ΔZ_n is normally distributed with mean $E(\Delta Z_n) = 0$ and variance $E(\Delta Z_n^2) = \frac{1}{3}\Delta\tau_n^3$ and correlated with ΔW_n by covariance

$$E(\Delta Z_n \Delta W_n) = \frac{1}{2}\Delta\tau_n^2.$$

We can generate ΔZ_n as

$$\Delta Z_n = \frac{1}{2}\Delta\tau_n(\Delta W_n + \Delta V_n/\sqrt{3}), \tag{1.144}$$

where ΔV_n is chosen independently from $\sqrt{\Delta\tau_n}\, N(0,1)$. Here the approximation $Y_n = Y(\tau_n)$ is the continuous time stochastic process $\{Y(\tau),\ t_0 \le \tau \le T\}$, the time-step size $\Delta\tau_n = \tau_n - \tau_{n-1}$, and $\Delta W_n = W(\tau_n) - W(\tau_{n-1})$.

References

1. Wazwaz, A.M.: Partial Differential Equations: methods and Applications. Balkema, Lisse (2002)
2. Debnath, L.: Nonlinear Partial Differential Equations for Scientists and Engineers. Birkhäuser, Boston (2005)
3. Wazwaz, A.M.: Partial Differential Equations and Solitary Waves Theory. Springer, Berlin Heidelberg (2009)
4. Podlubny, I.: Fractional Differential Equations. Academic Press, New York (1999)
5. Miller, K.S., Ross, B.: An Introduction to the Fractional Calculus and Fractional Differential Equations. Wiley, New York (1993)
6. Oldham, K.B., Spainer, J.: The Fractional Calculus. Academic Press, New York (1974)
7. Debnath, L.: Integral Transforms and Their Applications. CRC Press, Boca Raton (1995)
8. Samko, S.G., Kilbas, A.A., Marichev, O.I.: Fractional Integrals and derivatives: Theory and Applications. Taylor and Francis, London (1993)
9. Saha Ray, S.: Fractional Calculus with applications for Nuclear Reactor Dynamics. CRC Press, Taylor and Francis Group, Boca Raton (2015)
10. Kilbas, A.A., Srivastava, H.M., Trujillo, J.J.: Theory and Applications of Fractional Differential Equations. Elsevier Science and Tech, Amsterdam (2006)
11. Gorenflo, R., Mainardi, F.: Fractional calculus: integral and differential equations of fractional order. In: Carpinteri, A., Mainardi, F. (eds.) Fractals and Fractional Calculus in Continuum Mechanics, pp. 223–276. Springer, Vienna (1997)
12. Mainardi, F.: Fractional calculus: some basic problems in continuum and statistical mechanics. In: Carpinteri, A., Mainardi, F. (eds.) Fractals and Fractional Calculus in Continuum Mechanics, pp. 291–348. Springer, Vienna (1997)
13. Hu, M.S., Baleanu, D., Yang, X.J.: One-phase problems for discontinuous heat transfer in fractal media. Math. Probl. Eng. **2013**, 1–3 (2013). (358473)
14. Su, W.H., Yang, X.J., Jafari, H., Baleanu, D.: Fractional complex transform method for wave equations on Cantor sets within local fractional differential operator. Adv. Differ. Equ. **97**, 1–8 (2013)
15. Yang, X.J., Baleanu, D., Srivastava, H.M.: Local Fractional Integral Transforms and Their Applications. Academic Press, Elsevier (2015)
16. Øksendal, B.: Stochastic Differential Equations: An Introduction with Applications. Springer, Berlin, Heidelberg, NewYork (1998)
17. Platen, E.: An introduction to numerical methods for stochastic differential equations. Acta Numer. **8**, 197–246 (1999)
18. Holden, H., Øksendal, B., Ubøe, J., Zhang, T.: Stochastic Partial Differential Equations: A Modeling, White Noise Functional Approach. Springer, New York (2010)
19. Lord, G.J., Powell, C.E., Shardlow, T.: An Introduction to Computational Stochastic PDEs. Cambridge University Press, New York, USA (2014)
20. Kloeden, P.E., Pearson, R.A.: The numerical solution of stochastic differential equations. ANZIAM J. **20**(1), 8–12 (1977)
21. Odibat, Z.M., Shawagfeh, N.T.: Generalized Taylor's formula. Appl. Math. Comput. **186**(1), 286–293 (2007)
22. Ray, S.S., Sahoo, S.: Generalized Fractional Order Differential Equations Arising in Physical Models. CRC Press, Boca Raton (2018)

23. Shen, S., Liu, F., Anh, V.: Fundamental solution and discrete random walk model for a time-space fractional diffusion equation of distributed order. J. Appl. Math. Comput. **28**(1–2), 147–164 (2008)
24. Herrmann, R.: Fractional Calculus: An Introduction for Physicists. World Scientific, Singapore (2011)
25. Yang, Q.: Novel Analytical and Numerical Methods for Solving Fractional Dynamical System. Queensland University of Technology (2010)
26. Al-Saqabi, B., Boyadjiev, L., Luchko, Y.: Comments on employing the Riesz-Feller derivative in the Schrödinger equation. Eur. Phys. J. Spec. Top. **222**(8), 1779–1794 (2013)
27. Yang, X.J.: Advanced Local Fractional Calculus and Its Applications. World Science Publisher, New York (2012)
28. Yang, X.J.: A short note on local fractional calculus of function of one variable. J. Appl. Libr. Inf. Sci. **1**(1), 1–13 (2012)
29. Yang, X.J.: The zero-mass renormalization group differential equations and limit cycles in non-smooth initial value problems. Prespacetime J. **3**(9), 913–923 (2012)
30. Jumarie, G.: Table of some basic fractional calculus formulae derived from a modified Riemann-Liouville derivative for non-differentiable functions. Appl. Math. Lett. **22**(3), 378–385 (2009)
31. Kolwankar, K.M., Gangal, A. D.: Fractional differentiability of nowhere differentiable functions and dimensions. Chaos Interdisc. J. Nonlinear Sci. **6**(4), 505–513 (1996)
32. Debnath, L.: Wavelet Transforms and Their Applications. Birkhäuser, Boston (2002)
33. Chui, C.K.: An Introduction to Wavelets. Academic Press, London (1992)
34. Saha, R.S., Gupta, A.K.: Wavelet Methods for Solving Partial Differential Equations and Fractional Differential Equations. Chapman and Hall/CRC, New York (2018)
35. Morlet, J., Arens, G., Fourgeau, I., Giard, D.: Wave propagation and sampling theory. Geophysics **47**, 203–236 (1982)
36. Grossmann, A., Morlet, J.: Decomposition of Hardy functions into square integrable wavelets of constant shape. SIAM J. Math. Anal. **15**, 723–736 (1984)
37. Stromberg, J.: A modified Franklin system and higher order systems of *Rn* as unconditional bases for Hardy spaces. In: Beckner, W., et al. (eds.) Conference in Harmonic Analysis in Honor of A. Zygmund, vol. 2, pp. 475-493. Wadsworth Mathematics Series (1982)
38. Meyer, Y: Principe d'incertitude, bases hilbertiennes et alg´ebres d'operateurs. Seminaire Bourbaki **28**, 209–223 (1986)
39. Mallat, S.G.: Multiresolution approximations and wavelet orthonormal bases of $L^2(\Re)$. Trans. Am. Math. Soc. **315**(1), 69–87 (1989)
40. Daubechies, I.: Ten Lectures on Wavelets. Society for Industrial and Applied Mathematics, Philadelphia (1992)
41. Beylkin, G., Coifman, R., Rokhlin, V.: Fast wavelet transforms and numerical algorithms. Commun. Pure Appl. Math. **44**(2), 141–183 (1991)
42. Raslan, K.R.: The first integral method for solving some important nonlinear partial differential equations. Nonlinear Dynam. **53**, 281–286 (2008)
43. Abbasbandy, S., Shirzadi, A.: The first integral method for modified Benjamin–Bona–Mahony equation. Commun. Nonlinear Sci. Numer. Simul. **15**, 1759–1764 (2010)
44. Lu, B.: The first integral method for some time fractional differential equations. J. Math. Anal. Appl. **395**, 684–693 (2012)
45. Jafari, H., Soltani, R., Khalique, C.M., Baleanu, D.: Exact solutions of two nonlinear partial differential equations by using the first integral method. Bound. Value Prob. **2013**, 117 (2013)
46. Bekir, A., Güner, Ö., Ünsal, Ö.: The first integral method for exact solutions of nonlinear fractional differential equations. J. Comput. Nonlinear Dyn. **10**(021020), 1–5 (2015)
47. Marinca, V., Herisanu, N.: An optimal homotopy asymptotic method for solving nonlinear equations arising in heat transfer. Int. Commun. Heat Mass Transfer **35**, 710–715 (2008)
48. Marinca, V., Herisanu, N.: Nonlinear Dynamical Systems in Engineering. Springer, Berlin (2011)

49. Liao, S.: On the homotopy analysis method for nonlinear problems. Appl. Math. Comput. **147**, 499–513 (2004)
50. He, J.H.: A new approach to nonlinear partial differential equations. Commun. Nonlinear Sci. Numer. Simul. **2**(4), 230–235 (1997)
51. Tatari, M., Dehghan, M.: On the convergence of He's variational iteration method. J. Comput. Appl. Math. **207**, 121–128 (2007)
52. He, J.H.: Homotopy perturbation technique. Comput. Methods Appl. Mech. Eng. **178**, 257–262 (1999)
53. Ghorbani, A.: Beyond Adomian polynomials: He polynomials. Chaos Solitons Fractals **39**, 1486–1492 (2009)
54. Adomian, G.: Nonlinear Stochastic Systems Theory and Applications to Physics. Kluwer Academic Publishers, The Netherlands (1989)
55. Adomian, G.: Solving Frontier Problems of Physics: The Decomposition Method. Kluwer Academic Publishers, Boston (1994)
56. Wazwaz, A.M.: A Reliable Modification of Adomian Decomposition Method. Appl. Math. Comp. **102**(1), 77–86 (1999)
57. Cherruault, Y.: Convergence of Adomian's method. Kybernetes **18**, 31–38 (1989)
58. Abbaoui, K., Cherruault, Y.: Convergence of Adomian's Method Applied to Differential Equations. Comput. Math. Appl. **28**(5), 103–109 (1994)
59. Abbaoui, K., Cherruault, Y.: New ideas for proving convergence of decomposition methods. Comput. Math. Appl. **29**, 103–108 (1995)
60. Himoun, N., Abbaoui, K., Cherruault, Y.: New results of convergence of adomian's method. Kybernetes **28**(4–5), 423–429 (1999)
61. Meerschaert, M.M., Scheffler, H., Tadjeran, C.: Finite difference methods for two-dimensional fractional dispersion equation. J. Comput. Phys. **211**, 249–261 (2006)
62. Luo, X.-G.: A two-step Adomian decomposition method. Appl. Math. Comput. **170**(1), 570–583 (2005)
63. Tadjeran, C., Meerschaert, M.M., Scheffler, H.: A second-order accurate numerical approximation for the fractional diffusion equation. J. Comput. Phys. **213**, 205–213 (2006)
64. Liao, S.: Beyond Perturbation: Introduction to the Modified Homotopy Analysis Method. Chapman and Hall/CRC Press, Boca Raton (2003)
65. Liao, S.: The Proposed Homotopy Analysis Techniques for the Solution of Nonlinear Problems, Ph.D. Thesis, Shanghai Jiao Tong University, Shanghai (1992) (in English)
66. Marinca, V., Herisanu, N., Bota, C., Marinca, B.: An optimal homotopy asymptotic method applied to the steady flow of fourth-grade fluid past a porous plate. Appl. Math. Lett. **22**(2), 245–251 (2009)
67. Shah, R.A., Islam, S., Siddiqui, A.M., Haroon, A.: Optimal homotopy asymptotic method solution of unsteady second grade fluid in wire coating analysis. J. KSIAM **15**(3), 201–222 (2011)
68. Ghoreishi, M., Ismail, AIBMd, Alomari, A.K., Bataineh, A.S.: The comparison between homotopy analysis method and optimal homotopy asymptotic method for nonlinear age-structured population models. Commun. Nonlinear Sci. Numer. Simul. **17**, 1163–1177 (2012)
69. Feng, Z.S.: The first integral method to study the Burgers-KdV equation. J. Phys. A: Math. Gen. **35**, 343–349 (2002)
70. Bourbaki, N.: Commutative algebra. Addison-Wesley, Paris (1972)
71. Feng, Z., Wang, X.: Explicit exact solitary wave solutions for the Kundu equation and the derivative Schrödinger equation. Phys. Scr. **64**(1), 7–14 (2001)
72. Feng, Z., Roger, K.: Traveling waves to a Burgers–Korteweg–de Vries-type equation with higher-order nonlinearities. J. Math. Anal. Appl. **328**(2), 1435–1450 (2007)
73. Haar, A.: Zur theorie der orthogonalen Funktionsysteme. Math. Anal. **69**, 331–371 (1910)
74. Lepik, Ü.: Numerical solution of evolution equations by the Haar Wavelet method. Appl. Math. Comput. **185**, 695–704 (2007)

75. Saha Ray, S.: On Haar wavelet operational matrix of general order and its application for the numerical solution of fractional Bagley Torvik equation. Appl. Math. Comput. **218**, 5239–5248 (2012)
76. Chen, C.F., Hsiao, C.H.: Haar wavelet method for solving lumped and distributed parameter-systems. IEE Proc.-Control Theory Appl. **144**(1), 87–94 (1997)
77. Saha Ray, S., Patra, A.: Haar wavelet operational methods for the numerical solutions of Fractional order nonlinear oscillatory Van der Pol system. Appl. Math. Comput. **220**, 659–667 (2013)
78. Hetrick, D.L.: Dynamics of Nuclear Reactors. American Nuclear Society, Chicago, London (1993)
79. Duderstadt, J.J., Hamilton, L.J.: Nuclear Reactor Analysis. Wiley, Michigan (1976)
80. Kinard, M., Allen, K.E.J.: Efficient numerical solution of the point kinetics equations in nuclear reactor dynamics. Ann. Nucl. Energy **31**, 1039–1051 (2004)
81. Hayes, J.G., Allen, E.J.: Stochastic point-kinetics equations in nuclear reactor dynamics. Ann. Nucl. Energy **32**, 572–587 (2005)
82. Saha Ray, S.: Numerical Simulation of Stochastic point kinetic equation in the dynamical system of nuclear reactor. Ann. Nucl. Energy **49**, 154–159 (2012)
83. Higham, D.J.: An algorithmic introduction to numerical simulation of stochastic differential equations. SIAM Rev. **43**, 525–546 (2001)
84. Sauer, T.: Numerical solution of stochastic differential equation in finance. Handb. Comput. Finance **64**, 529–550 (2012)
85. Kloeden, P.E., Platen, E.: Numerical Solution of Stochastic Differential Equations. Springer, New York (1992)

Chapter 2
New Approaches for Decomposition Method for the Solution of Differential Equations

2.1 Introduction

In many practical applications regarding the field of science and engineering, the physical systems are modeled by nonlinear partial differential equations (NLPDEs). These equations play a significant role in modeling problems in science and engineering. Many physical phenomena of the physical problems arising in various fields of science and engineering can be elegantly investigated by the NPDEs. Furthermore, NPDEs are widely used to describe complex phenomena in various fields of sciences, such as physics, biology, and chemistry and engineering. Because, in many of the cases exact solutions are very difficult or even impossible to obtain for NPDEs, the approximate analytical solutions are particularly important for the study of dynamic systems for analyzing their physical nature. In the case of approximate analytical solutions, the success of a certain approximation method depends on the nonlinearities that occur in the studied problem, and thus a general algorithm for the construction of such approximate solutions do not exist in the general cases. Various methods have been devised to find the exact and approximate solutions of nonlinear partial differential equations in order to impart a great deal of information for understanding physical phenomena arising in numerous scientific and engineering fields. The investigation of the analytical solutions of NPDEs plays a prominent role in the study of nonlinear physical phenomena.

In this chapter, the modified decomposition method has been implemented for solving a coupled Klein-Gordon Schrödinger equation. In this purpose, a system of coupled Klein-Gordon Schrödinger equation with appropriate initial values has been solved by using the modified decomposition method. The proposed method does not need linearization, weak nonlinearity assumptions or perturbation theory.

Spatially fractional order diffusion equations are generalizations of classical diffusion equations which are increasingly used in modeling practical superdiffusive problems in fluid flow, finance and other areas of application. This chapter presents the analytical solutions of space fractional diffusion equations by two-step Adomian

S. Saha Ray, *Nonlinear Differential Equations in Physics*,
https://doi.org/10.1007/978-981-15-1656-6_2

decomposition method (TSADM). By using initial conditions, the explicit solutions of the equations have been presented in the closed form and then their solutions have been represented graphically. The solution procedures of a one-dimensional and a two-dimensional fractional diffusion equation are presented to show the application of the present technique. The solutions obtained by the standard decomposition method have been numerically evaluated and presented in the form of tables and then compared with those obtained by TSADM. After examining the results, it manifests that the present TSADM performs extremely well in terms of efficiency and simplicity.

This chapter also presents the new approach of the Adomian decomposition method (ADM) for the solution of space fractional diffusion equation with insulated ends. A typical example of special interest with fractional space derivative of order α, $1 < \alpha \leq 2$ is considered in the present analysis and solved by ADM after expressing the initial condition as Fourier series. The explicit solution of space fractional diffusion equation has been presented in the closed form and then the numerical solution has been represented graphically. The behaviour of Adomian solutions and the effects of different values of α are shown graphically.

2.2 Outline of the Present Study

The aim of the present chapter is to focus on the study of nonlinear partial differential equations (NLPDEs) that have particular applications appearing in engineering and applied sciences. The analytical approximate methods have been used for solving some specific nonlinear partial differential equations like coupled nonlinear Klein-Gordon-Schrödinger equations, space fractional diffusion equations on finite domain, space fractional diffusion equation with insulated ends, which have a wide variety of applications in physical models.

2.2.1 Coupled Nonlinear Klein–Gordon–Schrödinger Equations

The coupled nonlinear Klein–Gordon–Schrödinger (K-G-S) equations are considered in the following form:

$$\begin{aligned} &u_{tt} - u_{xx} + u - |v|^2 = 0 \\ &iv_t + v_{xx} + uv = 0. \end{aligned} \tag{2.1}$$

The modified decomposition method has been applied for solving coupled Klein-Gordon-Schrödinger equations which play an important role in modern physics.

Darwish and Fan [1] have been proposed an algebraic method to obtain the explicit exact solutions for coupled Klein-Gordon-Schrödinger (K-G-S) equations. Recently, the Jacobi elliptic function expansion method has been applied to obtain the solitary wave solutions for coupled K-G-S equations [2]. Hioe [3] has obtained periodic solitary waves for two coupled nonlinear Klein–Gordon and Schrödinger equations. Bao and Yang [4] have presented efficient, unconditionally stable and accurate numerical methods for approximations of the Klein-Gordon-Schrödinger equations. In order to determine the explicit series solutions of the coupled K-G-S equations, the notion of Adomian's decomposition method (in short ADM) [5, 6] has been used. Without the use of any linearization or transformation method, the ADM accurately computes the series solution. The ADM method which is of great interest to applied sciences [5–7], provides the solution in a rapidly convergent series with components that can be elegantly computed. The nonlinear equations are solved easily and elegantly without linearizing the problem by using the ADM [5, 6]. Large classes of linear and nonlinear differential equations, both ordinary as well as partial, can be solved by the Adomian decomposition method [5–41]. A reliable modification of Adomian decomposition method has been done by Wazwaz [42]. The decomposition method provides an effective procedure for analytical solution of a wide and general class of dynamical systems representing real physical problems [5–10, 12, 14–20, 23–25, 28–38, 40, 41]. This method efficiently works for initial-value or boundary-value problems and for linear or nonlinear, ordinary or partial differential equations and even for stochastic systems. Moreover, we have the advantage of a single global method for solving ordinary or partial differential equations as well as many types of other equations. Recently, the solution of the fractional differential equation has been obtained through the Adomian decomposition method by the researchers [38–40]. The method has features in common with many other methods, but it is distinctly different on close examinations, and one should not be misled by apparent simplicity into superficial conclusions [5, 6].

In the present chapter, the modified decomposition method (in short MDM) has been used to obtain the analytical approximate solutions of the coupled sine-Gordon equations (2.1).

2.2.2 *Space Fractional Diffusion Equations on Finite Domain*

Fractional diffusion equations are used to model problems in physics [43–45], finance [46–49], and hydrology [50–54]. Fractional space derivatives may be used to formulate anomalous dispersion models, where a particle plume spreads at a rate that is different than the classical Brownian motion model. When a fractional derivative of order $1 < \alpha < 2$ replaces the second derivative in a diffusion or dispersion model, it leads to a superdiffusive flow model. Nowadays, fractional

diffusion equation plays important roles in modeling anomalous diffusion and subdiffusion systems, description of fractional random walk, the unification of diffusion and wave propagation phenomenon, see, e.g., the reviews in [43–58], and references therein.

A one-dimensional fractional diffusion equation has been considered as in [59]

$$\frac{\partial u(x,t)}{\partial t} = d(x)\frac{\partial^{\alpha} u(x,t)}{\partial x^{\alpha}} + q(x,t), \tag{2.2}$$

on a finite domain $x_L < x < x_R$ with $1 < \alpha \leq 2$. It is to be assumed that the diffusion coefficient (or diffusivity) $d(x) > 0$. We also assume an initial condition $u(x, t = 0) = s(x)$ for $x_L < x < x_R$ and Dirichlet boundary conditions of the form $u(x_L, t) = 0$ and $u(x_R, t) = b_R(t)$. Equation (2.2) uses a Riemann fractional derivative of order α.

Also, a two-dimensional fractional diffusion equation has been considered as in [60]

$$\frac{\partial u(x,y,t)}{\partial t} = d(x,y)\frac{\partial^{\alpha} u(x,y,t)}{\partial x^{\alpha}} + e(x,y)\frac{\partial^{\beta} u(x,y,t)}{\partial y^{\beta}} + q(x,y,t), \tag{2.3}$$

on a finite rectangular domain $x_L < x < x_H$ and $y_L < y < y_H$, with fractional orders $1 < \alpha \leq 2$ and $1 < \beta \leq 2$, where the diffusion coefficients $d(x, y) > 0$ and $e(x, y) > 0$. The 'forcing' function $q(x, y, t)$ can be used to represent sources and sinks. We will assume that this fractional diffusion equation has a unique and sufficiently smooth solution under the following initial and boundary conditions. Assume the initial condition $u(x, y, t = 0) = f(x, y)$ for $x_L < x < x_H$, $y_L < y < y_H$, and Dirichlet boundary condition $u(x, y, t) = B(x, y, t)$ on the boundary (perimeter) of the rectangular region $x_L < x < x_H$, $y_L < y < y_H$, with the additional restriction that $B(x_L, y, t) = B(x, y_L, t) = 0$. In physical applications, this means that the left/lower boundary is set far away enough from an evolving plume that no significant concentrations reach that boundary. The classical dispersion equation in two dimensions is given by $\alpha = \beta = 2$. The values of $1 < \alpha < 2$, or $1 < \beta < 2$ model a super-diffusive process in that coordinate. Equation (2.3) also uses Riemann fractional derivatives of order α and β.

In this chapter, the new two-step Adomian Decomposition Method (ADM) [6] has been used to obtain the solutions of the fractional diffusion equations (2.2) and (2.3).

2.2.3 *Space Fractional Diffusion Equation with Insulated Ends*

The fractional differential equations appear more and more frequently in different research areas and engineering applications. Nowadays, fractional diffusion equation plays important roles in modeling anomalous diffusion and subdiffusion

systems, description of fractional random walk, the unification of diffusion and wave propagation phenomenon, see, e.g. the reviews in [43, 44, 55–58, 61], and references therein.

In this chapter, the following space fractional diffusion equation with insulated ends has been considered [62]

$$\frac{\partial u(x,t)}{\partial t} = dD_x^{\alpha} u(x,t), \quad 0 < x < L, \quad t \geq 0, \quad 1 < \alpha \leq 2, \tag{2.4}$$

where d is the diffusion coefficient and D_x^{α} is Caputo fractional derivative of order α, which is defined as [63]

$$D_x^{\alpha} f(x) = \begin{cases} \frac{\mathrm{d}^m f(x)}{\mathrm{d}x^m}, & \alpha = m \in N \\ \frac{1}{\Gamma(m-\alpha)} \int_0^x (x-\xi)^{m-\alpha-1} \frac{\mathrm{d}^m f(\xi)}{\mathrm{d}\xi^m} \mathrm{d}\xi, & m-1 < \alpha < m, \ m \in N. \end{cases} \tag{2.5}$$

We further consider the following Dirichlet's boundary conditions

$$\frac{\partial u(0,t)}{\partial x} = \frac{\partial u(L,t)}{\partial x} = 0, \quad t \geq 0, \tag{2.6}$$

and initial condition

$$u(x,0) = f(x), \quad 0 \leq x \leq L \tag{2.7}$$

In the present chapter, the Adomian decomposition method (ADM) [5, 6] with a simple variation has been used to obtain the analytical approximate solution of space fractional diffusion equation (2.4) with insulated ends.

2.3 Analysis of Proposed Methods

In this section, the analysis of modified decomposition method (MDM), the new two-step Adomian Decomposition Method, and Adomian decomposition method with a simple variation have been presented for solving the above physical problems.

2.3.1 A Modified Decomposition Method for Coupled K-G-S Equations

The coupled K-G-S equations (2.1) can be written in the following operator form

$$\begin{aligned} L_{tt}u &= L_{xx}u - u + N(u,v) \\ L_t v &= iL_{xx}v + iM(u,v) \end{aligned} \tag{2.8}$$

where $L_t \equiv \frac{\partial}{\partial t}$, $L_{tt} \equiv \frac{\partial^2}{\partial t^2}$ and $L_{xx} \equiv \frac{\partial^2}{\partial x^2}$ symbolize the linear differential operators and the notations $N(u,v) = |v|^2$ and $M(u,v) = uv$ symbolize the nonlinear operators.

Applying the two-fold integration inverse operator $L_{tt}^{-1} \equiv \int_0^t \int_0^t (.)\mathrm{d}t\mathrm{d}t$ to the system (2.8) and using the specified initial conditions yields

$$\begin{aligned} u(x,t) &= u(x,0) + tu_t(x,0) + L_{tt}^{-1}L_{xx}u - L_{tt}^{-1}u + L_{tt}^{-1}N(u,v) \\ v(x,t) &= v(x,0) + iL_t^{-1}L_{xx}v + iL_t^{-1}M(u,v). \end{aligned} \tag{2.9}$$

The Adomian decomposition method [5, 6] assumes an infinite series of solutions for unknown function $u(x,t)$ and $v(x,t)$ given by

$$\begin{aligned} u(x,t) &= \sum_{n=0}^{\infty} u_n(x,t), \\ v(x,t) &= \sum_{n=0}^{\infty} v_n(x,t), \end{aligned} \tag{2.10}$$

and nonlinear operators $N(u,v) = |v|^2$ and $M(u,v) = uv$ by the infinite series of Adomain polynomials given by

$$\begin{aligned} N(u,v) &= \sum_{n=0}^{\infty} A_n(u_0, u_1, \ldots, u_n, v_0, v_1, \ldots, v_n); \\ M(u,v) &= \sum_{n=0}^{\infty} B_n(u_0, u_1, \ldots, u_n, v_0, v_1, \ldots, v_n), \end{aligned}$$

where A_n and B_n are the appropriate Adomian's polynomial which are generated according to algorithm determined in [5, 6]. For the nonlinear operator $N(u,v)$, these polynomials can be defined as

$$A_n(u_0, u_1, \ldots, u_n, v_0, v_1, \ldots, v_n) = \frac{1}{n!}\frac{d^n}{d\lambda^n}\left[N\left(\sum_{k=0}^{\infty}\lambda^k u_k, \sum_{k=0}^{\infty}\lambda^k v_k\right)\right]_{\lambda=0}, \quad n \geq 0. \tag{2.11}$$

Similarly for the nonlinear operator $M(u,v)$,

$$B_n(u_0, u_1, \ldots, u_n, v_0, v_1, \ldots, v_n) = \frac{1}{n!}\frac{d^n}{d\lambda^n}\left[M\left(\sum_{k=0}^{\infty}\lambda^k u_k, \sum_{k=0}^{\infty}\lambda^k v_k\right)\right]_{\lambda=0}, \quad n \geq 0. \tag{2.12}$$

These formulae are easy to set computer code to get as many polynomials as we need in the calculation of the numerical as well as explicit solutions. For the sake of convenience of the readers, we can give the first few Adomian polynomials for $N(u,v) = |v|^2$, $M(u,v) = uv$ of the nonlinearity as

$$\begin{aligned}
&A_0 = v_0\overline{v}_0,\\
&A_1 = v_1\overline{v}_0 + v_0\overline{v}_1,\\
&A_2 = v_2\overline{v}_0 + v_0\overline{v}_2 + v_1\overline{v}_1,\\
&\ldots\\
&\text{and}\\
&B_0 = u_0v_0,\\
&B_1 = u_1v_0 + u_0v_1,\\
&B_2 = u_2v_0 + u_0v_2 + u_1v_1,\\
&\ldots
\end{aligned}$$

and so on, the rest of the polynomials can be constructed in a similar manner.

Substituting the initial conditions into Eq. (2.9) and identifying the zeroth components u_0 and v_0, we then obtain the subsequent components by using the following recursive equations according to the standard ADM

$$\begin{aligned}
u_{n+1} &= L_{tt}^{-1}L_{xx}u_n - L_{tt}^{-1}u_n + L_{tt}^{-1}A_n, \quad n \geq 0,\\
v_{n+1} &= iL_t^{-1}L_{xx}v_n + iL_t^{-1}B_n, \quad n \geq 0.
\end{aligned} \tag{2.13}$$

Recently, Wazwaz [42] proposed that the construction of the zeroth component of the decomposition series can be defined in a slightly different way. In [42], he assumed that if the zeroth component $u_0 = g$ and the function g is possible to divide into two parts such as g_1 and g_2, the one can formulate the recursive algorithm for u_0 and general term u_{n+1} in a form of the modified recursive scheme as follows:

$$\begin{aligned}
u_0 &= g_1,\\
u_1 &= g_2 + L_{tt}^{-1}L_{xx}u_0 - L_{tt}^{-1}u_0 + L_{tt}^{-1}A_0,\\
u_{n+1} &= L_{tt}^{-1}L_{xx}u_n - L_{tt}^{-1}u_n + L_{tt}^{-1}A_n, \quad n \geq 1.
\end{aligned} \tag{2.14}$$

Similarly, if the zeroth component $v_0 = g'$ and the function g' is possible to divide into two parts such as g_1' and g_2', the one can formulate the recursive algorithm for v_0 and general term v_{n+1} in a form of the modified recursive scheme as follows:

$$\begin{aligned} v_0 &= g_1', \\ v_1 &= g_2' + iL_t^{-1}L_{xx}v_0 + iL_t^{-1}B_0, \\ v_{n+1} &= iL_t^{-1}L_{xx}v_n + iL_t^{-1}B_n, \quad n \geq 1. \end{aligned} \tag{2.15}$$

This type of modification is giving more flexibility to the ADM in order to solve complicate nonlinear differential equations. In many cases, the modified decomposition scheme avoids unnecessary computation especially in the calculation of the Adomian polynomials. The computation of these polynomials will be reduced very considerably by using the MDM.

It is worth noting that the zeroth components u_0 and v_0 are defined then the remaining components u_n and v_n, $n \geq 1$ can be completely determined. As a result, the components $u_0, u_1, \ldots,$ and $v_0, v_1, \ldots,$ are identified and the series solutions thus entirely determined. However, in many cases, the exact solution in a closed form may be obtained.

The decomposition series solutions (2.10) generally converge very rapidly in real physical problems [6]. The rapidity of this convergence means that few terms are required. The convergence of this method has been rigorously established by Cherruault [64], Abbaoui and Cherruault [65, 66] and Himoun et al. [67]. The practical solutions will be the n-term approximations ϕ_n and ψ_n

$$\begin{aligned} \phi_n &= \sum_{i=0}^{n-1} u_i(x,t), \quad n \geq 1, \\ \psi_n &= \sum_{i=0}^{n-1} v_i(x,t), \quad n \geq 1. \end{aligned} \tag{2.16}$$

with

$$\begin{aligned} \lim_{n\to\infty} \phi_n &= u(x,t), \\ \lim_{n\to\infty} \psi_n &= v(x,t). \end{aligned} \tag{2.17}$$

2.3.2 The Two-Step Adomian Decomposition Method

Equation (2.2) can be rewritten as

$$L_t u(x,t) = d(x) D_x^{\alpha} u(x,t) + q(x,t) \tag{2.18}$$

where $L_t \equiv \frac{\partial}{\partial t}$ which is an easily invertible linear operator, $D_x^{\alpha}(.)$ is the Riemann-Liouville derivative of order α.

The solution $u(x,t)$ of Eq. (2.18) is represented by the decomposition series

$$u = \sum_{n=0}^{\infty} u_n. \tag{2.19}$$

Now, operating L_t^{-1} both sides of Eq. (2.18) and then substituting Eq. (2.19) yields

$$u(x,t) = u(x,0) + L_t^{-1}\left(d(x)D_x^{\alpha}\left(\sum_{n=0}^{\infty} u_n\right)\right) + L_t^{-1}(q(x,t)) \tag{2.20}$$

Each term of series (2.19) is given by the standard ADM recurrence relation

$$\begin{aligned} u_0 &= f, \\ u_{n+1} &= L_t^{-1}\left(d(x)D_x^{\alpha}u_n\right), \quad n \geq 0 \end{aligned} \tag{2.21}$$

where $f = u(x,0) + L_t^{-1}(q(x,t))$.

It is worth noting that once the zeroth component u_0 is defined, then the remaining components u_n, $n \geq 1$ can be completely determined; each term is computed by using the previous term. As a result, the components $u_0, u_1, \ldots$ are identified and the series solutions thus entirely determined. However, in many cases, the exact solution in a closed form may be obtained.

Without loss of generality let us assume that the zeroth component $u_0 = f$ and the function f is possible to divide into two parts such as f_1 and f_2, then one can formulate the recursive algorithm for u_0 and general term u_{n+1} in a form of the modified decomposition method (MDM) recursive scheme as follows:

$$\begin{aligned} u_0 &= f_1 \\ u_1 &= f_2 + L_t^{-1}\left(d(x)D_x^{\alpha}u_n\right) \\ u_{n+1} &= L_t^{-1}\left(d(x)D_x^{\alpha}u_n\right), \quad n \geq 1. \end{aligned} \tag{2.22}$$

Comparing the recursive scheme (2.21) of the standard Adomain method with the recursive scheme (2.22) of the modified technique leads to the conclusion that in Eq. (2.21) the zeroth component was defined by the function f, whereas in Eq. (2.22), the zeroth component u_0 is defined only by a part f_1 of f. The remaining part f_2 of f is added to the definition of the component u_1 in Eq. (2.22). Although the modified technique needs only a slight variation from the standard Adomian decomposition method, the results are promising in that it minimizes the size of calculations needed and will accelerate the convergence. The modification could lead to a promising approach for many applications in applied science.

The decomposition series solution (2.19) generally converges very rapidly in real physical problems [5, 6]. Here also, the practical solution will be the n-term approximation ϕ_n

$$\phi_n = \sum_{i=0}^{n-1} u_i(x,t), \quad n \geq 1 \tag{2.23}$$

with

$$\lim_{n\to\infty} \phi_n = u(x,t). \tag{2.24}$$

Luo [68] presented the theoretical support of how the exact solution can be achieved by using only two iterations in the modified decomposition method. In detail, it is possible because all other components vanish if the zeroth component is equal to the exact solution.

Although the modified decomposition method may provide the exact solution by using two iterations only, the criterion of dividing the function f into two practical parts, and the case where f consists only of one term remains unsolved so far. The two-step Adomian decomposition method (TSADM) overcomes the difficulties arising in the modified decomposition method.

In the following, Luo [68] presents the two-step Adomian decomposition method. For the convenience of the reader, we consider the differential equation

$$Lu + Ru + Nu = g, \tag{2.25}$$

where L is the highest order derivative which is assumed to be easily invertible, R is a linear differential operator of order less than L, Nu represents the nonlinear terms, and g is the source term.

The main ideas of the two-step Adomian decomposition method are:

1. Applying the inverse operator L^{-1} to g, and using the given conditions we obtain

$$\varphi = \phi + L^{-1}g,$$

where the function ϕ represents the term arising from using the given conditions, all are assumed to be prescribed.
Let

$$\varphi = \sum_{i=0}^{m} \varphi_i, \tag{2.26}$$

where $\phi_0, \phi_1, \ldots, \phi_m$ are the terms arising from integrating the source term g and from using the given conditions. Based on this, we define $u_0 = \varphi_k + \ldots + \varphi_{k+s}$ where $k = 0, 1, \ldots, m$, $s = 0, 1, \ldots, m-k$. Then we verify that u_0 satisfies the original equation Eq. (2.25) and the given conditions by substitution, once the exact solution is obtained, we stop. Otherwise, we go to the following step two.

2. We set $u_0 = \varphi$ and continue with the standard Adomian recursive relation

$$u_{k+1} = -L^{-1}(Ru_k) - L^{-1}(A_k), \quad k \geq 0.$$

Similarly, for Eq. (2.3), we can obtain

$$\begin{aligned} u(x,y,t) = u(x,y,0) + L_t^{-1}\left(d(x,y)D_x^{\alpha}\left(\sum_{n=0}^{\infty} u_n\right)\right) \\ + L_t^{-1}\left(e(x,y)D_y^{\beta}\left(\sum_{n=0}^{\infty} u_n\right)\right) + L_t^{-1}(q(x,y,t)). \end{aligned} \tag{2.27}$$

Now, the standard Adomian decomposition method recurrence scheme is

$$\begin{aligned} u_0 &= f, \\ u_{n+1} &= L_t^{-1}\left(d(x,y)D_x^{\alpha}u_n\right) + L_t^{-1}\left(e(x,y)D_y^{\beta}u_n\right), \quad n \geq 0, \end{aligned} \tag{2.28}$$

where $f = u(x,y,0) + L_t^{-1}(q(x,y,t))$.

In the other hand, the modified decomposition method recursive scheme is as follows

$$\begin{aligned} u_0 &= f_1 \\ u_1 &= f_2 + L_t^{-1}\left(d(x,y)D_x^{\alpha}u_0\right) + L_t^{-1}\left(e(x,y)D_y^{\beta}u_0\right) \\ u_{n+1} &= L_t^{-1}\left(d(x,y)D_x^{\alpha}u_n\right) + L_t^{-1}\left(e(x,y)D_y^{\beta}u_n\right), \quad n \geq 1. \end{aligned} \tag{2.29}$$

Compared to the standard Adomian method and the modified method, we can see that the two-step Adomian method may provide the solution by using two iterations only.

2.3.3 *ADM with a Simple Variation for Space Fractional Diffusion Model*

Equation (2.4) can be written as

$$L_t u(x,t) = dD_x^{\alpha}u(x,t), \tag{2.30}$$

where $L_t \equiv \frac{\partial}{\partial t}$ which is an easily invertible linear operator, $D_x^{\alpha}(\cdot)$ is the Caputo fractional derivative of order α.

If $f(x)$ is a periodic function with period L, then the Fourier Cosine series of $f(x)$ in $[0, L]$ can be obtained as

$$f(x) = \frac{\pi^2}{3} + \sum_{n=1}^{\infty} \frac{2}{L} \int_0^L f(\xi) \cos\left(\frac{n\pi\xi}{L}\right) \mathrm{d}\xi \cos\left(\frac{n\pi x}{L}\right). \tag{2.31}$$

The Fourier Cosine series is well adapted to functions whose first order derivatives are zero at the endpoints $x = 0$ and $x = L$ of the interval $[0, L]$, since all the basis functions $\cos\left(\frac{n\pi x}{L}\right)$ have this property.

Therefore, after considering the initial condition $u(x, 0) = f(x)$ as Fourier Cosine series, we can take

$$u(x, 0) = \frac{\pi^2}{3} + \sum_{n=1}^{\infty} \frac{2}{L} \int_0^L f(\xi) \cos\left(\frac{n\pi\xi}{L}\right) \mathrm{d}\xi \cos_\gamma\left(\frac{n\pi x}{L}\right), \tag{2.32}$$

where $\cos_\gamma\left(\frac{n\pi x}{L}\right)$ is the Generalized Cosine function defined in [69] and $\gamma = \alpha/2$, $\gamma \in (\frac{1}{2}, 1]$.

It is known that

$$D_x^\gamma \sin_\gamma x = \cos_\gamma x, \lim_{\gamma \to 1} \sin_\gamma x = \sin x$$

and

$$D_x^\gamma \sin_\gamma x = \cos_\gamma x,$$

where $\cos_\gamma x = \sum_{n=0}^{\infty} \frac{(-1)^n x^{2n\gamma}}{\Gamma(2n\gamma + 1)}$.

According to the Adomian decomposition method, we can write,

$$u(x, t) = u(x, 0) + L_t^{-1}(\mathrm{d} D_x^\alpha u(x, t)), \tag{2.33}$$

where

$$\begin{aligned}
u_0 &= u(x, 0) \\
&= \frac{\pi^2}{3} + \sum_{n=1}^{\infty} \frac{2}{L} \int_0^L f(\xi) \cos\left(\frac{n\pi\xi}{L}\right) \mathrm{d}\xi \cos_\gamma\left(\frac{n\pi x}{L}\right), \\
u_1 &= L_t^{-1}(\mathrm{d} D_x^\alpha u_0), \\
u_2 &= L_t^{-1}(\mathrm{d} D_x^\alpha u_1), \\
u_3 &= L_t^{-1}(\mathrm{d} D_x^\alpha u_2),
\end{aligned}$$

and so on.

The decomposition series solution

$$u = \sum_{n=0}^{\infty} u_n,$$

generally converges very rapidly in real physical problems [6]. The practical solution will be the n-term approximation ϕ_n

$$\phi_n = \sum_{i=0}^{n-1} u_i(x,t), \quad n \geq 1 \tag{2.34}$$

with

$$\lim_{n\to\infty} \phi_n = u(x,t). \tag{2.35}$$

2.4 Solutions of Coupled Klein–Gordon–Schrödinger Equations

In this section, the modified decomposition method has been used for getting the analytical approximate solutions for the coupled K-G-S equations (2.1).

2.4.1 Implementation of MDM for Analytical Approximate Solutions of Coupled K-G-S Equations

We first consider the coupled K-G-S equations (2.1) with the initial conditions

$$\begin{aligned} &u(x,0) = 6B^2 \sec h^2(Bx), \quad u_t(x,0) = -12B^2 c \sec h^2(Bx)\tanh(Bx), \\ &v(x,0) = 3B \sec h^2(Bx)\mathrm{e}^{idx}, \end{aligned} \tag{2.36}$$

where $B(\geq 1/2)$, c and d are arbitrary constants.

Using (2.14) and (2.15) with (2.11) and (2.12) respectively and considering $c = \frac{\sqrt{4B^2-1}}{2}$, $d = -\frac{c}{2B}$ for the coupled K-G-S equations (2.1) and initial conditions (2.36) gives

$$
\begin{aligned}
u_0 &= 0,\\
u_1 &= u(x,0) + tu_t(x,0) + L_{tt}^{-1}L_{xx}u_0 - L_{tt}^{-1}u_0 + L_{tt}^{-1}A_0\\
&= 6B^2\sec h^2(Bx) - 12B^2ct\sec h^2(Bx)\tanh(Bx),\\
u_2 &= L_{tt}^{-1}L_{xx}u_1 - L_{tt}^{-1}u_1 + L_{tt}^{-1}A_1\\
&= t^2(-3B^2\sec h^2(Bx) - 9B^4\sec h^4(Bx) + 3B^4\cosh(3Bx)\sec h^5(Bx))\\
&\quad + t^3(-2B^4c\sec h^5(Bx)(-11\sinh(Bx) + \sinh(3Bx))\\
&\quad + 2B^2c\sec h^2(Bx)\tanh(Bx)),
\end{aligned}
$$

and

$$
\begin{aligned}
v_0 &= 0,\\
v_1 &= v(x,0) + iL_t^{-1}L_{xx}v_0 + iL_t^{-1}B_0\\
&= 3B\sec h^2(Bx)\mathrm{e}^{idx},\\
v_2 &= iL_t^{-1}L_{xx}v_1 + iL_t^{-1}B_1\\
&= -3iB\mathrm{e}^{idx}t\sec h^2(Bx)(2B^2\sec h^2(Bx) + (d + 2iB\tanh^2(Bx))^2)
\end{aligned}
$$

and so on, in this manner, the other components of the decomposition series can be easily obtained of which $u(x,t)$ and $v(x,t)$ were evaluated in the following series form

$$
\begin{aligned}
u(x,t) &= 6B^2\sec h^2(Bx) - 12B^2ct\sec h^2(Bx)\tanh(Bx)\\
&\quad + t^2(-3B^2\sec h^2(Bx) - 9B^4\sec h^4(Bx) + 3B^4\cosh(3Bx)\sec h^5(Bx))\\
&\quad + t^3(-2B^4c\sec h^5(Bx)(-11\sinh(Bx) + \sinh(3Bx)) + 2B^2c\sec h^2(Bx)\tanh(Bx)) + \cdots,\\
v(x,t) &= 3B\sec h^2(Bx)\mathrm{e}^{idx}
\end{aligned}
\tag{2.37}
$$

$$
-3iB\mathrm{e}^{idx}t\sec h^2(Bx)(2B^2\sec h^2(Bx) + (d + 2iB\tanh^2(Bx))^2) + \cdots. \tag{2.38}
$$

follow immediately with the aid of *Mathematica* [70].

2.4.2 Numerical Results and Discussion for Coupled K-G-S Equations

In this section, we analyze the numerical solutions for coupled K-G-S equations obtained by the modified decomposition method.

The numerical simulations using MDM

In the present numerical experiment, Eqs. (2.37) and (2.38) have been used to draw the graphs as shown in Figs. 2.1, 2.2, 2.3 and 2.4 respectively.

The numerical solutions of the coupled K-G-S equations (2.1) have been shown in Figs. 2.1, 2.2, 2.3 and 2.4 with the help of five-term and four-term approximations ϕ_5 and ψ_4 for the decomposition series solutions of $u(x,t)$ and $v(x,t)$ respectively. In the present numerical computation, we have assumed $B = 0.575$.

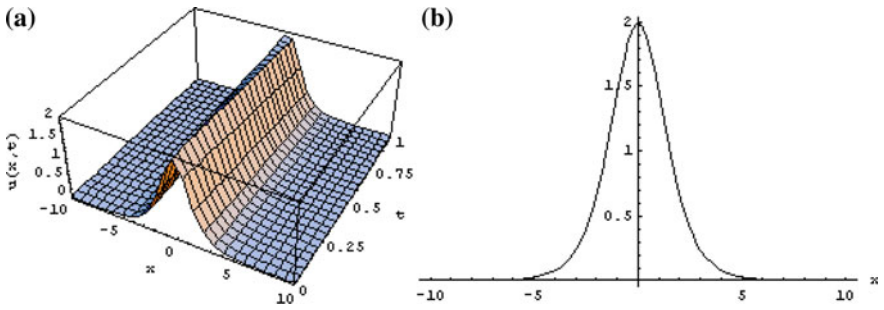

Fig. 2.1 **a** The decomposition method solution for $u(x,t)$, **b** Corresponding 2D solution for $u(x,t)$ when $t = 0$

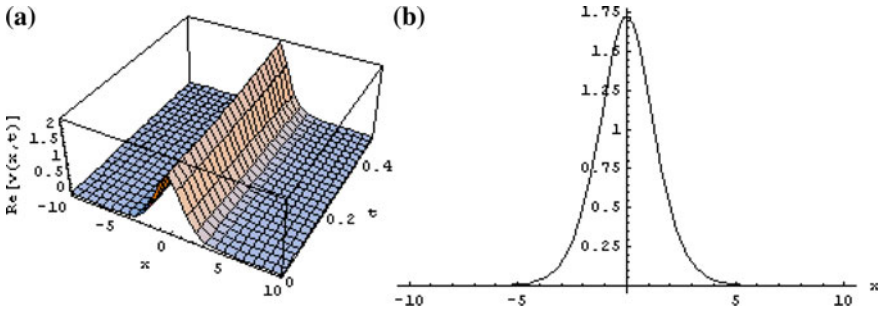

Fig. 2.2 **a** The decomposition method solution for $\mathrm{Re}(v(x,t))$, **b** Corresponding 2D solution for $\mathrm{Re}(v(x,t))$ when $t = 0$

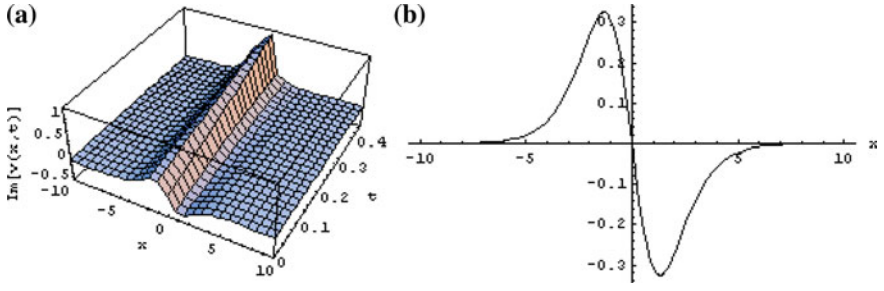

Fig. 2.3 **a** The decomposition method solution for $\mathrm{Im}(v(x,t))$, **b** Corresponding 2D solution for $\mathrm{Im}(v(x,t))$ when $t = 0$

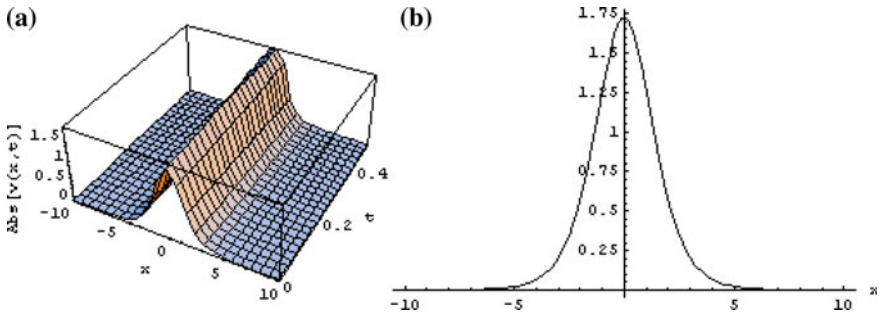

Fig. 2.4 **a** The decomposition method solution for $\mathrm{Abs}(v(x,t))$, **b** Corresponding 2D solution for $\mathrm{Abs}(v(x,t))$ when $t = 0$

2.5 Implementation of Two-Step Adomian Decomposition Method for Space Fractional Diffusion Equations on a Finite Domain

In this section, the new two-step Adomian decomposition method has been implemented for the solutions of one-dimensional and two-dimensional space fractional diffusion equations with finite domain respectively.

2.5.1 Solution of One-Dimensional Space Fractional Diffusion Equation

Let us consider the one-dimensional fractional diffusion equation (2.2), as taken in [59]

$$\frac{\partial u(x,t)}{\partial t} = d(x)\frac{\partial^{1.8} u(x,t)}{\partial x^{1.8}} + q(x,t), \tag{2.39}$$

on a finite domain $0 < x < 1$, with the diffusion coefficient

$$d(x) = \Gamma(2.2)x^{2.8}/6 = 0.183634x^{2.8},$$

the source/sink function

$$q(x,t) = -(1+x)\mathrm{e}^{-t}x^3,$$

the initial condition

$$u(x,0) = x^3, \quad \text{for } 0 < x < 1$$

and the boundary conditions

$$u(0,t) = 0, u(1,t) = \mathrm{e}^{-t}, \quad \text{for } t > 0.$$

Now, Eq. (2.39) can be rewritten in operator form as

$$L_t u(x,t) = d(x) D_x^{1.8} u(x,t) + q(x,t), \tag{2.40}$$

where $L_t \equiv \frac{\partial}{\partial t}$ symbolizes the easily invertible linear differential operator, $D_x^{1.8}(.)$ is the Riemann–Liouville derivative of order 1.8.

Applying the one-fold integration inverse operator $L_t^{-1} \equiv \int_0^t (.)\mathrm{d}t$ to Eq. (2.40) and using the specified initial condition yields

$$\begin{aligned} u(x,t) &= u(x,0) + L_t^{-1}\left(d(x) D_x^{1.8}\left(\sum_{n=0}^{\infty} u_n\right)\right) + L_t^{-1}(q(x,t)) \\ &= \mathrm{e}^{-t}x^3 + \mathrm{e}^{-t}x^4 - x^4 + L_t^{-1}\left(d(x) D_x^{1.8}\left(\sum_{n=0}^{\infty} u_n\right)\right). \end{aligned} \tag{2.41}$$

The standard Adomian decomposition method:

$$\begin{aligned} u_0 &= \mathrm{e}^{-t}x^3 + \mathrm{e}^{-t}x^4 - x^4, \\ u_1 &= L_t^{-1}\left(\frac{\Gamma(2.2)x^{2.8}}{6}\frac{\partial^{1.8}u_0}{\partial x^{1.8}}\right) \\ &= (-\mathrm{e}^{-t}+1)x^4 + \frac{4(-\mathrm{e}^{-t}+1-t)x^5}{2.2}, \\ u_2 &= L_t^{-1}\left(\frac{\Gamma(2.2)x^{2.8}}{6}\frac{\partial^{1.8}u_1}{\partial x^{1.8}}\right) \\ &= \frac{4(\mathrm{e}^{-t}+t-1)x^5}{2.2} + \frac{80\left(\mathrm{e}^{-t} - \frac{t^2}{2!} + t - 1\right)x^6}{3.2 \times 2.2^2}, \\ u_3 &= L_t^{-1}\left(\frac{\Gamma(2.2)x^{2.8}}{6}\frac{\partial^{1.8}u_2}{\partial x^{1.8}}\right) \\ &= \frac{80\left(-\mathrm{e}^{-t} + \frac{t^2}{2!} - t + 1\right)x^6}{3.2 \times 2.2^2} + \frac{80\Gamma(6)\left(-\mathrm{e}^{-t} - \frac{t^3}{3!} + \frac{t^2}{2!} - t + 1\right)x^7}{4.2 \times 3.2^2 \times 2.2^3}, \end{aligned}$$

and so on.

Therefore, according to the decomposition method, the two-term approximation ϕ_2 is

$$\begin{aligned}\phi_2 &= u_0 + u_1 \\ &= \mathrm{e}^{-t}x^3 + \frac{4(-\mathrm{e}^{-t}+1-t)x^5}{2.2}.\end{aligned} \tag{2.42}$$

Therefore, the three-term approximation ϕ_3 is

$$\begin{aligned}\phi_3 &= u_0 + u_1 + u_2 \\ &= \mathrm{e}^{-t}x^3 + \frac{80\left(\mathrm{e}^{-t} - \frac{t^2}{2!} + t - 1\right)x^6}{3.2 \times 2.2^2}.\end{aligned} \tag{2.43}$$

Therefore, according to the decomposition method, the four-term approximation ϕ_4 is

$$\begin{aligned}\phi_4 &= u_0 + u_1 + u_2 + u_3 \\ &= \mathrm{e}^{-t}x^3 + \frac{80\Gamma(6)\left(-\mathrm{e}^{-t} - \frac{t^3}{3!} + \frac{t^2}{2!} - t + 1\right)x^7}{4.2 \times 3.2^2 \times 2.2^3}\end{aligned} \tag{2.44}$$

The TSADM:

Using the scheme (2.26) of TSADM, we have

$$\varphi = \varphi_0 + \varphi_1 + \varphi_2,$$

where $\varphi_0 = \mathrm{e}^{-t}x^3$, $\varphi_1 = \mathrm{e}^{-t}x^4$, $\varphi_2 = -x^4$.

Clearly, φ_1 and φ_2 do not satisfy the initial condition $u(x,0) = x^3$. By selecting $u_0 = \varphi_0$ and verifying that u_0 justifies Eq. (2.39) and satisfies the initial as well as boundary conditions, we obtain the following terms from the recursive scheme of MDM

$$\begin{aligned}u_0 &= \mathrm{e}^{-t}x^3, \\ u_1 &= \mathrm{e}^{-t}x^4 - x^4 + L_t^{-1}\left(\frac{\Gamma(2.2)x^{2.8}}{6}\frac{\partial^{1.8}u_0}{\partial x^{1.8}}\right) \\ &= \mathrm{e}^{-t}x^4 - x^4 - (\mathrm{e}^{-t}-1)x^4 \\ &= 0 \\ u_2 &= L_t^{-1}\left(\frac{\Gamma(2.2)x^{2.8}}{6}\frac{\partial^{1.8}u_1}{\partial x^{1.8}}\right) \\ &= 0\end{aligned}$$

and so on.

Therefore, the solution is

$$u(x,t) = \mathrm{e}^{-t}x^3 \tag{2.45}$$

The solution (2.45) can be verified through substitution in Eq. (2.39).

2.5.2 Solution of Two-Dimensional Space Fractional Diffusion Equation

Let us consider the two-dimensional fractional diffusion equation Eq. (1.2), as in [60]

$$\frac{\partial u(x,y,t)}{\partial t} = d(x,y)\frac{\partial^{1.8}u(x,y,t)}{\partial x^{1.8}} + e(x,y)\frac{\partial^{1.6}u(x,y,t)}{\partial y^{1.6}} + q(x,y,t), \tag{2.46}$$

on a finite rectangular domain $0<x<1$, $0<y<1$, for $0 \le t \le T_{\text{end}}$ with the diffusion coefficients

$$d(x,y) = \Gamma(2.2)x^{2.8}y/6,$$

and

$$e(x,y) = 2xy^{2.6}/\Gamma(4.6),$$

and the forcing function

$$q(x,y,t) = -(1+2xy)\mathrm{e}^{-t}x^3y^{3.6},$$

with the initial condition

$$u(x,y,0) = x^3y^{3.6},$$

and Dirichlet boundary conditions on the rectangle in the form $u(x,0,t) = u(0,y,t) = 0$, $u(x,1,t) = \mathrm{e}^{-t}x^3$, and $u(1,y,t) = \mathrm{e}^{-t}y^{3.6}$, for all $t \ge 0$.

Now, Eq. (2.46) can be rewritten in operator form as

$$L_t u(x,y,t) = d(x,y)D_x^{1.8}u(x,y,t) + e(x,y)D_y^{1.6}u(x,y,t) + q(x,y,t), \tag{2.47}$$

where $L_t \equiv \frac{\partial}{\partial t}$ symbolizes the easily invertible linear differential operator, $D_x^{1.8}(.)$ and $D_y^{1.6}(.)$ are the Riemann–Liouville derivatives of order 1.8 and 1.6 respectively.

Applying the one-fold integration inverse operator $L_t^{-1} \equiv \int_0^t (.)\mathrm{d}t$ to the Eq. (2.47) and using the specified initial condition yields

$$\begin{aligned}u(x,y,t) &= u(x,y,0) + L_t^{-1}\left(d(x,y)D_x^{1.8}\left(\sum_{n=0}^{\infty}u_n\right)\right)\\ &\quad + L_t^{-1}\left(e(x,y)D_y^{1.6}\left(\sum_{n=0}^{\infty}u_n\right)\right) + L_t^{-1}(q(x,y,t))\\ &= x^3y^{3.6}\mathrm{e}^{-t} + 2x^4y^{4.6}\mathrm{e}^{-t} - 2x^4y^{4.6} + L_t^{-1}\left(d(x,y)D_x^{1.8}\left(\sum_{n=0}^{\infty}u_n\right)\right)\\ &\quad + L_t^{-1}\left(e(x,y)D_y^{1.6}\left(\sum_{n=0}^{\infty}u_n\right)\right)\end{aligned} \tag{2.48}$$

The standard Adomian decomposition method:

$$\begin{aligned}u_0 &= x^3y^{3.6}\mathrm{e}^{-t} + 2x^4y^{4.6}\mathrm{e}^{-t} - 2x^4y^{4.6},\\ u_1 &= L_t^{-1}\left(\frac{\Gamma(2.2)x^{2.8}y}{6}\frac{\partial^{1.8}u_0}{\partial x^{1.8}}\right) + L_t^{-1}\left(\frac{2xy^{2.6}}{\Gamma(4.6)}\frac{\partial^{1.6}u_0}{\partial y^{1.6}}\right)\\ &= 2x^4y^{4.6}(-\mathrm{e}^{-t}+1) + \left(\frac{8}{2.2} + \frac{2\times 4.6}{3}\right)x^5y^{5.6}(-\mathrm{e}^{-t}+1-t)\\ &= 2x^4y^{4.6}(-\mathrm{e}^{-t}+1) + \frac{1106}{165}x^5y^{5.6}(-\mathrm{e}^{-t}+1-t),\\ u_2 &= L_t^{-1}\left(\frac{\Gamma(2.2)x^{2.8}y}{6}\frac{\partial^{1.8}u_1}{\partial x^{1.8}}\right) + L_t^{-1}\left(\frac{2xy^{2.6}}{\Gamma(4.6)}\frac{\partial^{1.6}u_1}{\partial y^{1.6}}\right)\\ &= \frac{1106}{165}x^5y^{5.6}(\mathrm{e}^{-t}-1+t) + \frac{9101827}{272250}x^6y^{6.6}\left(\mathrm{e}^{-t}-1+t-\frac{t^2}{2}\right)\end{aligned}$$

and so on.

Therefore, according to the decomposition method, the three-term approximation ϕ_3 is

$$\begin{aligned}\phi_3 &= u_0 + u_1 + u_2\\ &= x^3y^{3.6}\mathrm{e}^{-t} + \frac{9101827}{272250}x^6y^{6.6}\left(\mathrm{e}^{-t}-1+t-\frac{t^2}{2}\right)\end{aligned} \tag{2.49}$$

The TSADM:

Using the scheme (2.26) of TSADM, we have

$$\varphi = \varphi_0 + \varphi_1 + \varphi_2,$$

where $\varphi_0 = x^3y^{3.6}\mathrm{e}^{-t}$, $\varphi_1 = 2x^4y^{4.6}\mathrm{e}^{-t}$, $\varphi_2 = -2x^4y^{4.6}$.

Clearly, φ_1 and φ_2 do not satisfy the initial condition $u(x,y,0) = x^3y^{3.6}$. By selecting $u_0 = \varphi_0$ and verifying that u_0 justifies Eq. (2.46) and satisfies the initial as

well as boundary conditions, we obtain the following terms from the recursive scheme of MDM

$$\begin{aligned}
u_0 &= x^3 y^{3.6} \mathrm{e}^{-t}, \\
u_1 &= 2x^4 y^{4.6} \mathrm{e}^{-t} - 2x^4 y^{4.6} + L_t^{-1}\left(\frac{\Gamma(2.2)x^{2.8}y}{6}\frac{\partial^{1.8}u_0}{\partial x^{1.8}}\right) + L_t^{-1}\left(\frac{2xy^{2.6}}{\Gamma(4.6)}\frac{\partial^{1.6}u_0}{\partial y^{1.6}}\right) \\
&= 2x^4 y^{4.6} \mathrm{e}^{-t} - 2x^4 y^{4.6} - 2(\mathrm{e}^{-t} - 1)x^4 y^{4.6} \\
&= 0, \\
u_2 &= L_t^{-1}\left(\frac{\Gamma(2.2)x^{2.8}y}{6}\frac{\partial^{1.8}u_1}{\partial x^{1.8}}\right) + L_t^{-1}\left(\frac{2xy^{2.6}}{\Gamma(4.6)}\frac{\partial^{1.6}u_1}{\partial y^{1.6}}\right) \\
&= 0
\end{aligned}$$

and so on.

Therefore, the solution is

$$u(x, y, t) = x^3 y^{3.6} \mathrm{e}^{-t}. \tag{2.50}$$

The solution (2.50) can be verified through substitution in Eq. (2.46).

2.5.3 *Numerical Results and Discussion for Space Fractional Diffusion Equations*

In this section, the numerical solutions for space fractional diffusion equations obtained by proposed new two-step Adomian decomposition method have been analyzed. Also, an analysis for the comparison of errors between TSADM solution and standard Adomian decomposition method solution has been presented here.

The numerical simulations using TSADM

In this present numerical experiment, Eqs. (2.45) and (2.50) have been used to draw the graphs as shown in Figs. 2.5 and 2.6 respectively. Figure 2.5 shows the 3D surface solution $u(x, t)$ for one-dimensional fractional diffusion equation. On the other hand, Fig. 2.6 shows the 3D surface solution $u(x, y, t)$ for two-dimensional fractional diffusion equation.

Comparison of errors between TSADM solution and standard Adomian decomposition method solution

In this present analysis, the solutions of the two-step Adomian decomposition method have been compared with that obtained by standard Adomian decomposition method. Here we demonstrate the absolute errors by taking different values of x and t. Comparison results in Tables 2.1, 2.2, 2.3 and 2.4 exhibit that there is a good agreement between TSADM and standard Adomian decomposition method solutions.

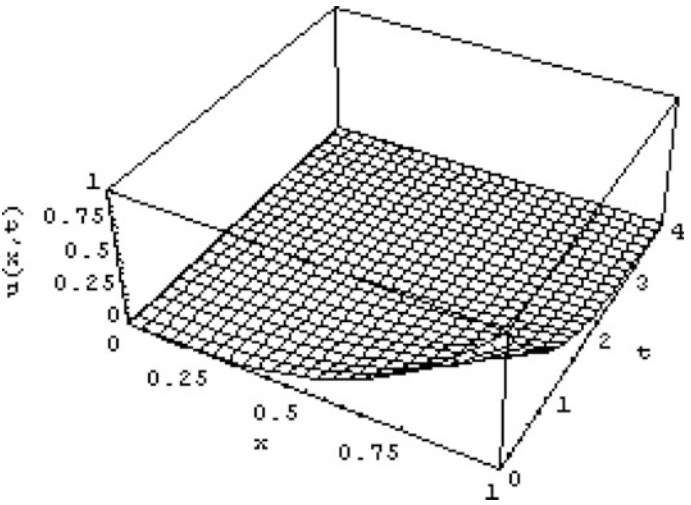

Fig. 2.5 Three dimensional surface solution $u(x,t)$ of one-dimensional fractional diffusion Eq. (2.39)

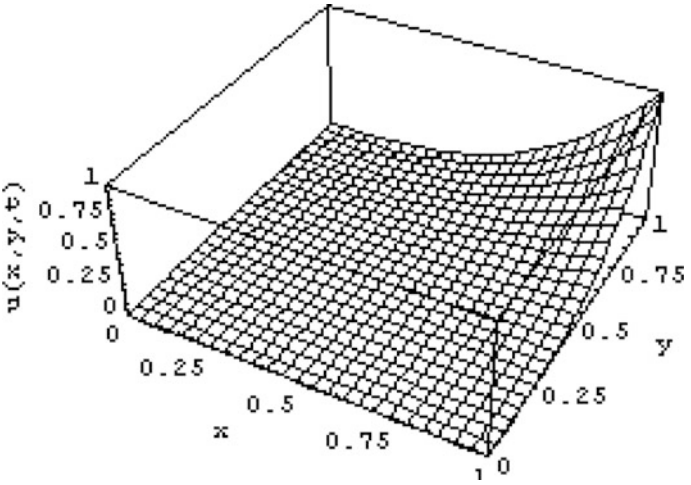

Fig. 2.6 Three dimensional surface solution $u(x,y,t)$ of two-dimensional fractional diffusion Eq. (2.46) at time $t = 1$

From Tables 2.1, 2.2 and 2.3, it can be observed that the standard Adomian decomposition method solution converges very slowly to the exact solution. On the other hand, TSADM requires only two iterations to achieve the exact solution. Therefore, TSADM is more effective and promising compared to standard Adomian decomposition method.

Table 2.1 Comparison between TSADM solution and standard Adomian decomposition method solution ϕ_2

(x, t)	Two-step Adomain decomposition method solution (exact solution $u(x,t) = e^{-t}x^3$)	Standard Adomian decomposition method two term solution ϕ_2	Absolute error $\lvert u - \phi_2 \rvert$
(0, 0)	0	0	0
(0.25, 0)	0.015625	0.015625	0
(0.5, 0)	0.125	0.125	0
(0.75, 0)	0.421875	0.421875	0
(1, 0)	1	1	0
(0, 1)	0	0	0
(0.25, 1)	0.00574812	0.00509492	0.000653195
(0.5, 1)	0.0459849	0.0250827	0.0209022
(0.75, 1)	0.155199	−0.00352725	0.158726
(0, 2)	0	0	0
(0.25, 2)	0.00211461	0.0000987486	0.00201587
(0.5, 2)	0.0169169	−0.0475908	0.0645077
(0.75, 2)	0.0570946	−0.432761	0.489855
(0, 3)	0	0	0
(0.25, 3)	0.000777923	−0.00286161	0.00363954
(0.5, 3)	0.00622338	−0.110242	0.116465

Table 2.2 Comparison between TSADM solution and standard Adomian decomposition method solution ϕ_3

(x, t)	Two-step Adomain decomposition method solution (exact solution $u(x,t) = e^{-t}x^3$)	Standard Adomian decomposition method three term solution ϕ_3	Absolute error $\lvert u - \phi_3 \rvert$
(0, 0)	0	0	0
(0.25, 0)	0.015625	0.015625	0
(0.5, 0)	0.125	0.125	0
(0.75, 0)	0.421875	0.421875	0
(1, 0)	1	1	0
(0, 1)	0	0	0
(0.25, 1)	0.00574812	0.0055815	0.000166612
(0.5, 1)	0.0459849	0.0353218	0.0106631
(0.75, 1)	0.155199	0.0337393	0.12146
(0, 2)	0	0	0
(0.25, 2)	0.00211461	0.00102422	0.00109039
(0.5, 2)	0.0169169	−0.0528681	0.0697851
(0, 3)	0	0	0
(0.25, 3)	0.000777923	−0.00231194	0.00308986
(0.5, 3)	0.00622338	−0.191528	0.197751

Table 2.3 Comparison between TSADM solution and standard Adomian decomposition method solution ϕ_4

(x, t)	Two-step Adomain decomposition method solution (exact solution $u(x,t) = e^{-t}x^3$)	Standard Adomian decomposition method four term solution ϕ_4	Absolute error $\lvert u - \phi_4 \rvert$
(0, 0)	0	0	0
(0.25, 0)	0.015625	0.015625	0
(0.5, 0)	0.125	0.125	0
(0.75, 0)	0.421875	0.421875	0
(1, 0)	1	1	0
(0, 1)	0	0	0
(0.25, 1)	0.00574812	0.00570392	0.0000442011
(0.5, 1)	0.0459849	0.0403272	0.00565774
(0.75, 1)	0.155199	0.0585313	0.0966678
(0, 2)	0	0	0
(0.25, 2)	0.00211461	0.00151496	0.000599653
(0.5, 2)	0.0169169	−0.0598386	0.0767556
(0, 3)	0	0	0
(0.25, 3)	0.000777923	−0.00184474	0.00262266
(0.5, 3)	0.00622338	−0.329478	0.335701

Table 2.4 Comparison between TSADM solution and standard Adomian decomposition method solution ϕ_3

$(x, y, t = 1)$	Two-step Adomain decomposition method solution (exact solution $u(x,y,t=1) = x^3y^3$)	Standard Adomian decomposition method three term solution ϕ_3	Absolute error $\lvert u - \phi_3 \rvert$
(0, 0.25, 1)	0	0	0
(0.25, 0.25, 1)	0.000039094	0.0000389794	0.0000001146
(0.5, 0.25, 1)	0.000312752	0.000305417	0.000007335
(0.75, 0.25, 1)	0.00105554	0.000971995	0.0000835416
(1, 0.25, 1)	0.00250201	0.00203262	0.000469391
(0, 0.5, 1)	0	0	0
(0.25, 0.5, 1)	0.000474043	0.000462926	0.0000111166
(0.5, 0.5, 1)	0.00379234	0.00308088	0.000711464
(0.75, 0.5, 1)	0.0127992	0.00469513	0.00810402
(1, 0.5, 1)	0.0303387	−0.015195	0.0455337
(0, 0.75, 1)	0	0	0
(0.25, 0.75, 1)	0.00204054	0.00187904	0.000161501
(0.5, 0.75, 1)	0.0163244	0.00598829	0.0103361
(0.75, 0.75, 1)	0.0550947	−0.0626396	0.117734
(0, 1, 1)	0	0	0
(0.25, 1, 1)	0.00574812	0.00466974	0.00107838
(0.5, 1, 1)	0.0459849	−0.0230313	0.0690162

From Table 2.4, it can be observed that the absolute errors for TSADM solution and standard Adomian decomposition method solution ϕ_3 are very small for small values of x and y. But as the values of x and y increase the absolute errors also increase.

2.6 Solution of Space Fractional Diffusion Equation with Insulated Ends

In this section, a variation of Adomian decomposition method has been proposed for getting analytical approximate solution of space fractional diffusion equation with insulated ends.

2.6.1 Implementation of the Present Method

Let us consider initial conditions

$$u(x,0) = x^2, \quad 0 \le x \le \pi \tag{2.51}$$

and boundary conditions

$$\frac{\partial u(0,t)}{\partial x} = \frac{\partial u(\pi,t)}{\partial x} = 0, \quad t \ge 0 \tag{2.52}$$

for Eq. (2.4), as taken in [62].

We see that $f(x) = x^2$ is a periodic function with period π. The Fourier sine series of $f(x)$ in [0, π] can be obtained as

$$f(x) = \frac{\pi^2}{3} + \sum_{n=1}^{\infty} \frac{4}{n^2}(-1)^n \cos nx. \tag{2.53}$$

Therefore, after considering $f(x)$ as Fourier Cosine series, we can take

$$u(x,0) = \frac{\pi^2}{3} + \sum_{n=1}^{\infty} \frac{4}{n^2}(-1)^n \cos_\gamma nx, \tag{2.54}$$

where $\cos_\gamma nx$ is the Generalized Cosine function and $\gamma = \alpha/2$, $\gamma \in (\frac{1}{2}, 1]$.

From Eq. (2.33), the following terms can be obtained

$$u_0 = u(x,0) = \frac{\pi^2}{3} + \sum_{n=1}^{\infty} \frac{4}{n^2}(-1)^n \cos_\gamma nx,$$

$$u_1 = L_t^{-1}(dD_x^\alpha u_0) = \frac{-td}{1!} \sum_{n=1}^{\infty} \frac{4}{n^2}(-1)^n n^{2\gamma} \cos_\gamma nx,$$

$$u_2 = L_t^{-1}(dD_x^\alpha u_1) = \frac{t^2 d^2}{2!} \sum_{n=1}^{\infty} \frac{4}{n^2}(-1)^n n^{4\gamma} \cos_\gamma nx,$$

$$u_3 = L_t^{-1}(dD_x^\alpha u_2) = -\frac{t^3 d^3}{3!} \sum_{n=1}^{\infty} \frac{4}{n^2}(-1)^n n^{6\gamma} \cos_\gamma nx$$

and so on.

Therefore, the solution is

$$\begin{aligned} u(x,t) &= \frac{\pi^2}{3} + \sum_{n=1}^{\infty} \frac{4}{n^2}(-1)^n \cos_\gamma nx \left(1 - \frac{tdn^{2\gamma}}{1!} + \frac{t^2 d^2 n^{4\gamma}}{2!} - \frac{t^3 d^3 n^{6\gamma}}{3!} + \cdots\right) \\ &= \frac{\pi^2}{3} + \sum_{n=1}^{\infty} \frac{4}{n^2}(-1)^n \cos_\gamma nx\, E_1(-tdn^{2\gamma}), \end{aligned}$$

where $E_\lambda(z)$ is the Mittag-Leffler function in one parameter.

$$\begin{aligned} &= \frac{\pi^2}{3} + \sum_{n=1}^{\infty} \frac{4}{n^2}(-1)^n \cos_\gamma nx\, \mathrm{e}^{-tdn^{2\gamma}} \\ &= \frac{\pi^2}{3} + \sum_{n=1}^{\infty} \frac{4}{n^2}(-1)^n \cos_{\alpha/2} nx\, \mathrm{e}^{-tdn^{\alpha}} \end{aligned} \tag{2.55}$$

The solution (2.55) can be verified through substitution in Eq. (2.4).

2.6.2 Numerical Results and Discussion

In this section, the numerical solutions of the space fractional diffusion equation with insulated ends obtained by the proposed method have been analyzed.

The numerical simulations for the proposed method

In this present numerical experiment, Eq. (2.55) has been used to draw the graphs as shown in Figs. 2.7, 2.8 and 2.9 for different fractional order values of α respectively. In this numerical analysis, we assume $d = 0.4$ for Eq. (2.4).

Figures 2.7, 2.8 and 2.9 show anomalous diffusion behaviour. These figures exhibit slow diffusion at the beginning and fast diffusion later. From these figures, it is also observed that diffusion behaviour increases as α increases.

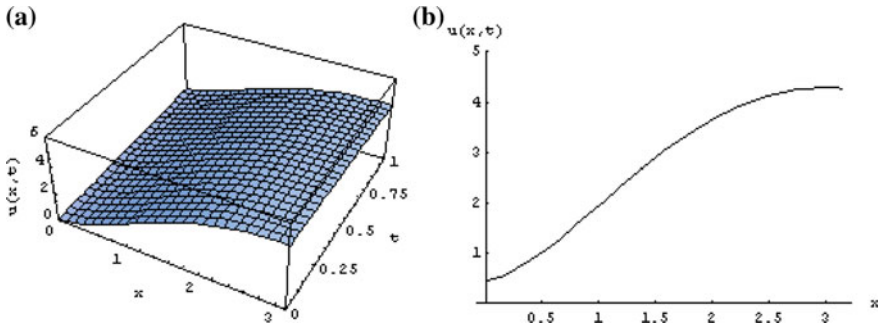

Fig. 2.7 **a** The 3D surface solution, **b** The corresponding 2D solution at $t = 0.5$, $d = 0.4$ and $\alpha = 1.5$

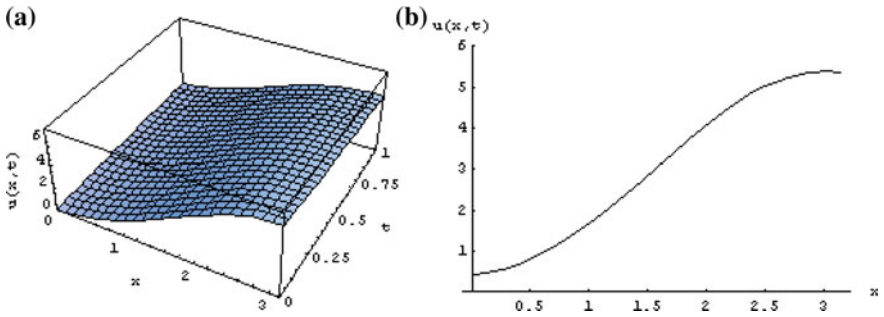

Fig. 2.8 **a** The 3D surface solution, **b** The corresponding 2D solution at $t = 0.5$, $d = 0.4$ and $\alpha = 1.75$

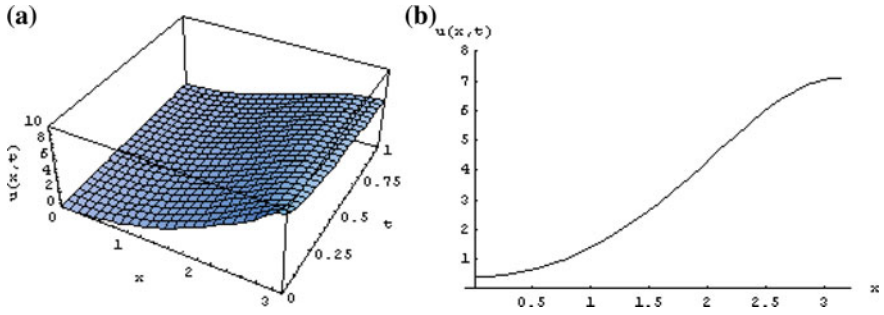

Fig. 2.9 **a** The 3D surface solution, **b** The corresponding 2D solution at $t = 0.5$, $d = 0.4$ and $\alpha = 2$

2.7 Conclusion

In the present chapter, the modified decomposition method has been used for finding the solutions for the coupled K-G-S equations with initial conditions. The approximate solutions to the coupled K-G-S equations have been calculated by using the MDM without any need of transformation techniques and linearization of the equations. Additionally, it does not need any discretization method to get numerical solutions. This proposed method thus eliminates the difficulties of massive computational work.

This chapter includes an analytical scheme to obtain the solutions of the one dimensional and two-dimensional fractional diffusion equations. Two typical examples have been discussed as illustrations. In this work, it has been established that TSADM is well suited to solve the fractional diffusion equation. TSADM proceeds in two steps. The first step consists of verifying that the zeroth component of the series solution includes the exact solution. Once the exact solution is obtained, we stop. Otherwise, we continue with the standard Adomian recursion relation in the second step.

In this chapter, TSADM has been applied for the solutions of space fractional diffusion equations. The TSADM may provide the solution by using two iterations only if compared with the standard Adomian method and the modified decomposition method. Moreover, the TSADM overcomes the difficulties arising in the modified decomposition method as discussed earlier. A comparison study between the TSADM and the standard decomposition method is conducted to illustrate the efficiency of the TSADM and the results obtained indicate that the TSADM is more feasible and effective.

This chapter also presents an analytical scheme to obtain the solution of space fractional diffusion equation with insulated ends by ADM with a simple variation. In the present analysis, a new approach of Adomian decomposition method has been successfully applied after expressing the initial condition as a Fourier series. The physical significance of the solution has been also presented graphically. The present work demonstrates that this proposed technique is well suited to solve the space fractional diffusion equation with insulated ends.

The proposed methods are straightforward, without restrictive assumptions and the components of the series solution can be easily computed using any mathematical symbolic package. Moreover, these methods do not change the problem into a convenient one for the use of linear theory. Therefore, they provide more realistic series solutions that generally converge very rapidly in real physical problems. When solutions are computed numerically, the rapid convergence is obvious. Moreover, no linearization or perturbation is required. It can avoid the difficulty of finding the inverse of the Laplace Transform and can reduce the labour of perturbation method. It is quite obvious to see that these methods are quite accurate, easy and efficient technique for solving fractional partial differential equations arising in physical problems.

As mentioned, the proposed methods avoid linearization and physically unrealistic assumptions. Furthermore, as the present methods do not require discretization of the variables, i.e., time and space, it is not affected by computational round off errors and one is not faced with the necessity of large computer memory and time. Consequently, the computational size will be reduced.

References

1. Darwish, A., Fan, E.G.: A series of new explicit exact solutions for the coupled Klein-Gordon-Schrödinger equations. Chaos. Soliton. Fractals. **20**, 609–617 (2004)
2. Liu, S., Fu, Z., Liu, S., Wang, Z.: The periodic solutions for a class of coupled nonlinear Klein-Gordon equations. Phys. Lett. A **323**, 415–420 (2004)
3. Hioe, F.T.: Periodic solitary waves for two coupled nonlinear Klein-Gordon and Schrödinger equations. J. Phys. A: Math. Gen. **36**, 7307–7330 (2003)
4. Bao, W., Yang, L.: Efficient and accurate numerical methods for the Klein-Gordon-Schrödinger equations. http://web.cz3.nus.edu.sg/∼bao/PS/KGS.pdf
5. Adomian, G.: Nonlinear stochastic systems theory and applications to physics. Kluwer Academic publishers, Netherlands (1989)
6. Adomian, G.: Solving frontier problems of physics: the decomposition method. Kluwer Academic Publishers, Boston (1994)
7. Wazwaz, A.M.: Partial differential equations: methods and applications. Balkema, Lisse, The Netherlands (2002)
8. Adomian, G.: An analytical solution of the stochastic Navier-Stokes system. Found. Phys. **21** (7), 831–843 (1991)
9. Adomian, G., Rach, R.: Linear and nonlinear Schrödinger equations. Found. Phys. **21**, 983–991 (1991)
10. Adomian, G.: Solution of physical problems by decomposition. Comput. Math. Appl. **27**(9–10), 145–154 (1994)
11. Adomian, G.: Solutions of nonlinear P.D.E. Appl. Math. Lett. **11**(3), 121–123 (1998)
12. Wazwaz, A.M.: The decomposition method applied to systems of partial differential equations and to the reaction—diffusion Brusselator model. Appl. Math. Comput. **110**(2–3), 251–264 (2000)
13. Wazwaz, A.M.: Approximate solutions to boundary value problems of higher order by the modified decomposition method. Comput. Math Appl. **40**(6–7), 679–691 (2000)
14. Wazwaz, A.M.: The modified decomposition method applied to unsteady flow of gas through a porous medium. Appl. Math. Comput. **118**(2–3), 123–132 (2001)
15. Wazwaz, A.M.: Construction of soliton solutions and periodic solutions of the Boussinesq equation by the modified decomposition method. Chaos. Solitons. Fractals. **12**(8), 1549–1556 (2001)
16. Wazwaz, A.M.: Construction of solitary wave solutions and rational solutions for the KdV equation by Adomian decomposition method. Chaos. Solitons. Fractals. **12**(12), 2283–2293 (2001)
17. Wazwaz, A.M.: A computational approach to soliton solutions of the Kadomtsev-Petviashvili equation. Appl. Math. Comput. **123**(2), 205–217 (2001)
18. Wazwaz, A.M., Gorguis, A.: An analytic study of fisher's equation by using Adomian decomposition method. Appl. Math. Comput. **154**(3), 609–620 (2004)
19. Wazwaz, A.M.: Analytical solution for the time-dependent Emden-Fowler type of equations by Adomian decomposition method. Appl. Math. Comput. **166**(3), 638–651 (2005)
20. Mavoungou, T., Cherruault, Y.: Solving frontier problems of physics by decomposition method: a new approach. Kybernetes **27**(9), 1053–1061 (1998)

21. Abbaoui, K., Cherruault, Y.: The decomposition method applied to the Cauchy problem. Kybernetes **28**, 103–108 (1999)
22. Khelifa, S., Cherruault, Y.: Approximation of the solution for a class of first order p.d.e. by Adomian method. Kybernetes **31**(3/4), 577–595 (2002)
23. Inc, M., Cherruault, Y.: A new approach to travelling wave solution of a fourth-order semilinear diffusion equation. Kybernetes **32**(9–10), 1492–1503 (2003)
24. Inc, M., Cherruault, Y., Abbaoui, K.: A computational approach to the wave equations: an application of the decomposition method. Kybernetes **33**(1), 80–97 (2004)
25. Inc, M., Cherruault, Y.: A reliable approach to the Korteweg-de Vries equation: an application of the decomposition method. Kybernetes **34**(7–8), 951–959 (2005)
26. Inc, M., Cherruault, Y.: A reliable method for obtaining approximate solutions of linear and nonlinear Volterra-Fredholm integro-differential equations. Kybernetes **34**(7–8), 1034–1048 (2005)
27. Kaya, D., Yokus, A.: A numerical comparison of partial solutions in the decomposition method for linear and nonlinear partial differential equations. Math. Comp. Simul. **60**(6), 507–512 (2002)
28. Kaya, D.: A numerical solution of the Sine-Gordon equation using the modified decomposition method. Appl. Math. Comp. **143**, 309–317 (2003)
29. Kaya, D., El-Sayed, S.M.: On a generalized fifth order KdV equations. Phys. Lett. A **310**(1), 44–51 (2003)
30. Kaya, D., El-Sayed, S.M.: An application of the decomposition method for the generalized KdV and RLW equations. Chaos. Solitons. Fractals. **17**(5), 869–877 (2003)
31. Kaya, D.: An explicit and numerical solutions of some fifth-order KdV equation by decomposition method. Appl. Math. Comp. **144**(2–3), 353–363 (2003)
32. Kaya, D.: Solitary wave solutions for a generalized Hirota-Satsuma coupled KdV equation. Appl. Math. Comp. **147**, 69–78 (2004)
33. Kaya, D.: A numerical simulation of solitary-wave solutions of the generalized regularized long-wave equation. Appl. Math. Comp. **149**(3), 833–841 (2004)
34. Kaya, D., Inan, I.E.: A numerical application of the decomposition method for the combined KdV–MKdV equation. Appl. Math. Comput. **168**(2), 915–926 (2005)
35. Geyikli, T., Kaya, D.: An application for a modified KdV equation by the decomposition method and finite element method. Appl. Math. Comput. **169**(2), 971–981 (2005)
36. El-Sayed, S.M., Kaya, D.: A numerical solution and an exact explicit solution of the NLS equation. Appl. Math. Comput. **172**(2), 1315–1322 (2006)
37. Kaya, D.: The exact and numerical solitary-wave solutions for generalized modified Boussinesq equation. Phys. Lett. A **348**(3–6), 244–250 (2006)
38. Ray, S.S., Bera, R.K.: Analytical solution of a dynamic system containing fractional derivative of order one-half by Adomian decomposition method. Trans. ASME J. Appl. Mech. **72**(2), 290–295 (2005)
39. Ray, S.S., Bera, R.K.: An approximate solution of a nonlinear fractional differential equation by Adomian decomposition method. Appl. Math. Comput. **167**(1), 561–571 (2005)
40. Ray, S.S., Bera, R.K.: Analytical solution of the Bagley Torvik equation by Adomian decomposition method. Appl. Math. Comput. **168**(1), 398–410 (2005)
41. Ray, S.S.: A numerical solution of the coupled Sine-Gordon equation using the modified decomposition method. Appl. Math. Comput. **175**(2), 1046–1054 (2006)
42. Wazwaz, A.M.: A Reliable Modification of Adomian decomposition method. Appl. Math. Comp. **102**(1), 77–86 (1999)
43. Metzler, R., Barkai, E., Klafter, J.: Anomalous diffusion and relaxation close to thermal equilibrium: a fractional Fokker-Planck equation approach. Phys. Rev. Lett. **82**(18), 3563–3567 (1999)
44. Metzler, R., Klafter, J.: The random walk's guide to Anomalous diffusion: a fractional dynamics approach. **339**(1), 1–77 (2000)

45. Metzler, R., Klafter, J.: The restaurant at the end of the random walk: recent developments in the description of anomalous transport by fractional dynamics. J. Phys. A **37**, R161–R208 (2004)
46. Gorenflo, R., Mainardi, F., Scalas, E., Raberto, M.: Fractional calculus and continuous time finance. III. The diffusion limit. Mathematical finance (Konstanz, 2000), Trends Math., Birkhuser, Basel. 171–180 (2001)
47. Mainardi, F., Raberto, M., Gorenflo, R., Scalas, E.: Fractional calculus and continuous-time finance II: the waiting-time distribution. Phys. A **287**, 468–481 (2000)
48. Scalas, E., Gorenflo, R., Mainardi, F.: Fractional calculus and continuous-time finance. Phys. A **284**, 376–384 (2000)
49. Raberto, M., Scalas, E., Mainardi, F.: Waiting-times and returns in high-frequency financial data: an empirical study. Phys. A **314**, 749–755 (2002)
50. Benson, D.A., Wheatcraft, S., Meerschaert, M.M.: Application of a fractional advection–dispersion equation. Water Resour. Res **36**, 1403–1412 (2000)
51. Baeumer, B., Meerschaert, M.M., Benson, D.A., Wheatcraft, S.W.: Subordinated advection—dispersion equation for contaminant transport. Water Resour. Res. **37**, 1543–1550 (2001)
52. Benson, D.A., Schumer, R., Meerschaert, M.M., Wheatcraft, S.W.: Fractional dispersion, Lévy motions, and the MADE tracer tests. Transp. Porous Media **42**, 211–240 (2001)
53. Schumer, R., Benson, D.A., Meerschaert, M.M., Wheatcraft, S.W.: Eulerian derivation of the fractional advection-dispersion equation. J. Contam. Hydrol. **48**, 9–88 (2001)
54. Schumer, R., Benson, D.A., Meerschaert, M.M., Baeumer, B.: Multiscaling fractional advection-dispersion equations and their solutions. Water Resour. Res. **39**, 1022–1032 (2003)
55. Mainardi, F.: Fractional calculus: some basic problems in continuum and statistical mechanics. In: Carpinteri, A., Mainardi, F. (eds.) Fractals and fractional calculus in continuum mechanics, pp. 291–348. Springer, Vienna (1997)
56. Mainardi, F., Pagnini, G.: The weight functions as solutions of the time-fractional diffusion equation. Appl. Math. Comput. **141**, 51–62 (2003)
57. Agrawal, O.P.: Solution for a fractional diffusion-wave equation defined in a bounded domain. Nonlinear Dyn. **29**, 145–155 (2002)
58. Schneider, W.R., Wyss, W.: Fractional diffusion and wave equations. J. Math. Phys. **30**, 134–144 (1989)
59. Meerschaert, M.M., Scheffler, H., Tadjeran, C.: Finite difference methods for two-dimensional fractional dispersion equation. J. Comput. Phys. **211**, 249–261 (2006)
60. Tadjeran, C., Meerschaert, M.M., Scheffler, H.: A second-order accurate numerical approximation for the fractional diffusion equation. J. Comput. Phys. **213**, 205–213 (2006)
61. Mainardi, F., Luchko, Y., Pagnini, G.: The fundamental solution of the space-time fractional diffusion equation. Fractional Calc. Appl Anal. **4**(2), 153–192 (2001)
62. Shen, S., Liu, F.: Error Analysis of an explicit finite difference approximation for the space fractional diffusion equation with insulated ends. ANZIAM J., **46**(E), C871-C887 (2005)
63. Podlubny, I.: Fractional differential equations. Academic Press, New York (1999)
64. Cherruault, Y.: Convergence of Adomian's method. Kybernetes **18**, 31–38 (1989)
65. Abbaoui, K., Cherruault, Y.: Convergence of Adomian's method applied to differential equations. Comput. Math. Applic. **28**(5), 103–109 (1994)
66. Abbaoui, K., Cherruault, Y.: New Ideas for proving convergence of decomposition methods. Comput. Math. Applic. **29**, 103–108 (1995)
67. Himoun, N., Abbaoui, K., Cherruault, Y.: New Results of Convergence of Adomian's Method. Kybernetes **28**(4–5), 423–429 (1999)
68. Luo, X.G.: A two-step Adomian decomposition method. Appl. Math. Comput. **170**(1), 570–583 (2005)
69. Samko, S.G., Kilbas, A.A., Marichev, O.I.: Fractional integrals and derivatives: theory and applications. Taylor and Francis, London (1993)
70. Wolfram, S.: Mathematica for Windows, Version 5.0, Wolfram Research, (2003)

Chapter 3
Numerical Solution of Fractional Differential Equations by Using New Wavelet Operational Matrix of General Order

3.1 Introduction

Fractional calculus is a field of applied mathematics that deals with derivatives and integrals of arbitrary orders (including complex orders). It is also known as generalized integral and differential calculus of arbitrary order [1, 2]. In the last few decades, fractional calculus has been extensively investigated due to their broad applications in mathematics, physics, and engineering such as viscoelasticity, diffusion of a biological population, signal processing, electromagnetism, fluid mechanics, electrochemistry, and so on. Fractional differential equations are extensively used in modeling of physical phenomena in various fields of science and engineering. Fractional calculus was described by Gorenflo and Mainardi [3] as the field of mathematical analysis which deals with investigation and applications of integrals and derivatives of arbitrary order.

Fractional calculus is in use for the past 300 years ago. And many great mathematicians [2] (pure and applied) such as N. H. Abel, M. Caputo, L. Euler, J. Fourier, A. K. Grünwald, J. Hadamard, G. H. Hardy, O. Heaviside, H. J. Holmgren, P. S. Laplace, G. W. Leibniz, A. V. Letnikov, J. Liouville, B. Riemann, M. Riesz, and H. Weyl made major contributions to the theory of fractional calculus.

The history of fractional calculus was started at the end of the seventeenth century, and the birth of fractional calculus was due to a letter exchange. At that time, scientific journals did not exist and scientists exchanged their information through letters. The first conference on fractional calculus and its applications was organized in June 1974 by B. Ross and held at the University of New Haven.

In recent years, fractional calculus has become the focus of interest for many researchers in different disciplines of applied science and engineering because of the fact that realistic modeling of a physical phenomenon can be successfully achieved by using fractional calculus.

S. Saha Ray, *Nonlinear Differential Equations in Physics*,
https://doi.org/10.1007/978-981-15-1656-6_3

The fractional derivative has been occurring in many physical problems such as frequency-dependent damping behavior of materials, motion of a large thin plate in a Newtonian fluid, creep and relaxation functions for viscoelastic materials, the $PI^{\lambda}D^{\mu}$ controller for the control of dynamical systems, etc. Phenomena in electromagnetics, acoustics, viscoelasticity, and electrochemistry and material science are also described by differential equations of fractional order. The solution of the differential equation containing fractional derivative is much involved.

Fractional calculus has been used to model physical and engineering processes that are found to be best described by fractional differential equations. For that reason, we need a reliable and efficient technique for the solution of fractional differential equations.

Recently, orthogonal wavelet bases are becoming more popular for numerical solutions of partial differential equations due to their excellent properties such as the ability to detect singularities, orthogonality, flexibility to represent a function at a different level of resolution and compact support. In recent years, there has been a growing interest in developing wavelet-based numerical algorithms for the solution of fractional-order partial differential equations. Among them, the Haar wavelet method is the simplest and is easy to use. Haar wavelets have been successfully applied for the solutions of ordinary and partial differential equations, integral equations, and integro-differential equations.

3.2 Outline of the Present Study

In this chapter, a numerical method based on the Haar wavelet operational method is applied to solve the Bagley–Torvik equation. In the present analysis, a new numerical technique based on Haar wavelet operational matrices of the general order of integration has been employed for the solution of fractional-order Bagley–Torvik equation. In this regard, a general procedure of obtaining this Haar wavelet operational matrix of integration Q^{α} of the general order α is derived. To the best information of the author, such correct general order operational matrix is not reported earlier in the open literature. In the present chapter, the Haar wavelet operational method has been applied for the numerical solution of the Bagley–Torvik equation and then compared with the analytical solution obtained by Podlubny [4].

Also, in this chapter, the fractional Fisher-type equation has been solved by using two reliable techniques, viz. Haar wavelet method and optimal homotopy asymptotic method (OHAM). Haar wavelet method is an efficient numerical method for the solution of fractional-order partial differential equation like Fisher type. The obtained results of the fractional Fisher-type equation are then compared with the optimal homotopy asymptotic method as well as with the exact solutions.

3.2.1 Fractional Dynamic Model of Bagley–Torvik Equation

Torvik and Bagley [5] derived a fractional differential equation of degree $\alpha = \frac{3}{2}$ for the description of the motion of an immersed plate in a Newtonian fluid [6]. The motion of a rigid plate of mass m and area A connected by a massless spring of stiffness k, immersed in a Newtonian fluid, was originally proposed by Bagley and Torvik.

A rigid plate of mass m immersed into an infinite Newtonian fluid as shown in Fig. 3.1. The plate is held at a fixed point by means of a spring of stiffness k. It is assumed that the motions of spring do not influence the motion of the fluid and that the area A of the plate is very large, such that the stress–velocity relationship is valid on both sides of the plate.

Let μ be the viscosity and ρ be the fluid density. The displacement of the plate y is described by

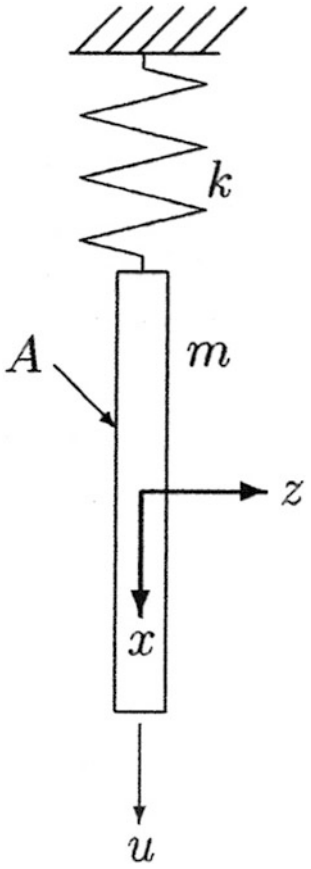

Fig. 3.1 Rigid plate of mass m immersed into a Newtonian fluid [6]

$$Ay''(t) + BD^{3/2}y(t) + Cy(t) = g(t), \quad y(0) = y'(0) = 0 \tag{3.1}$$

where $A = m, B = 2A\sqrt{\mu\rho}$, and $C = k$.

In the present analysis, the Haar wavelet method has been applied for the numerical solution of the Bagley–Torvik equation of fractional order. Then, the obtained numerical results have been also compared with the exact solutions.

3.2.2 Generalized Time Fractional Fisher-Type Equation

The generalized time fractional Fisher's biological population diffusion equation is given by

$$\frac{\partial^\alpha u}{\partial t^\alpha} = \frac{\partial^2 u}{\partial x^2} + F(u), \quad u(x,0) = \varphi(x) \tag{3.2}$$

where $u(x,t)$ denotes the population density and $t > 0, x \in \Re, F(u)$ is a continuous nonlinear function satisfying the following conditions $F(0) = F(1) = 0$, $F'(0) > 0 > F'(1)$. The derivative in Eq. (3.2) is the Caputo derivative of order α.

The aim of the present work is to implement Haar wavelet method and optimal homotopy asymptotic method (OHAM) in order to demonstrate the capability of these methods in handling nonlinear equations of arbitrary order so that one can apply it to various types of nonlinearity.

3.3 Haar Wavelets and the Operational Matrices

In this section, a brief survey is introduced for the Haar wavelet operational matrix method which is used to solve the fractional-order Bagley–Torvik equation and fractional Fisher-type equation. In this context, a short review of Haar wavelets and operational matrices has been discussed here.

3.3.1 Haar Wavelets

Haar functions have been used from 1910 when they were introduced by the Hungarian mathematician Alfred Haar. Haar wavelets are the simplest wavelets among various types of wavelets. They are step functions (piecewise constant

functions) on the real line that can take only three values, i.e., 0, 1, and −1. We use the Haar wavelet method due to the following features, simpler and fast, flexible, convenient, small computational costs, and computationally attractive.

The Haar functions are a family of switched rectangular waveforms where amplitudes can differ from one function to another. The orthogonal set of Haar functions are defined in the interval $[0, 1)$ by

$$h_0(t) = 1$$
$$h_i(t) = \begin{cases} 1, & \frac{k-1}{2^j} \le t < \frac{k-\frac{1}{2}}{2^j} \\ -1, & \frac{k-\frac{1}{2}}{2^j} \le t < \frac{k}{2^j} \\ 0, & \text{otherwise} \end{cases} \tag{3.3}$$

where $i = 1, 2, \ldots, m-1$, $m = 2^J$, and J is a positive integer. j and k represent the integer decomposition of the index i, i.e., $i = k + 2^j - 1$, $0 \le j < i$, and $1 \le k < 2^j + 1$.

Theoretically, this set of functions is complete. The first curve of Fig. 3.2 is that $h_0(t) = 1$ during the whole interval $[0, 1)$. It is called the scaling function. The second curve $h_1(t)$ is the fundamental square wave or the mother wavelet which also spans the whole interval $[0, 1)$. All the other subsequent curves are generated from $h_1(t)$ with two operations: translation and dilation. $h_2(t)$ is obtained from $h_1(t)$ with dilation, i.e., $h_1(t)$ is compressed from the whole interval $[0, 1)$ to the half interval $[0, 1/2]$ to generate $h_2(t)$ is the same as $h_2(t)$ but shifted(translated) to the right by 1/2. Similarly, $h_2(t)$ is compressed form a half interval to a quarter interval to generate $h_4(t)$. The function $h_4(t)$ s translated to the right by $1/4, 2/4, 3/4$ to generate $h_5(t)$, $h_6(t)$, $h_7(t)$, respectively.

In the construction, $h_0(t)$ is called the scaling function and $h_1(t)$ is the mother wavelet.

Usually, the Haar wavelets are defined for the interval $t \in [0, 1]$. In general case $t \in [A, B]$, we divide the interval $[A, B]$ into m equal subintervals; each of width $\Delta t = (B - A)/m$. In this case, the orthogonal set of Haar functions are defined in the interval $[A,\ B]$ by Saha Ray [7]

$$h_0(t) = \begin{cases} 1, & t \in [A, B] \\ 0, & \text{elsewhere} \end{cases},$$
$$h_i(t) = \begin{cases} 1, & \xi_1(i) \le t < \xi_2(i) \\ -1, & \xi_2(i) \le t < \xi_3(i) \\ 0, & \text{otherwise} \end{cases} \tag{3.4}$$

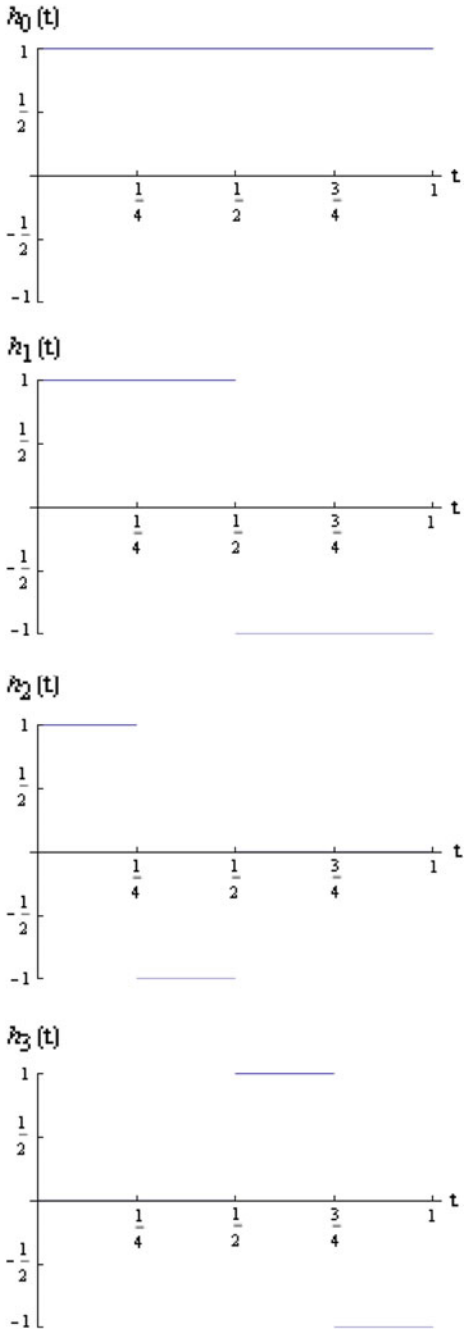

Fig. 3.2 Haar wavelet functions with $m = 8$

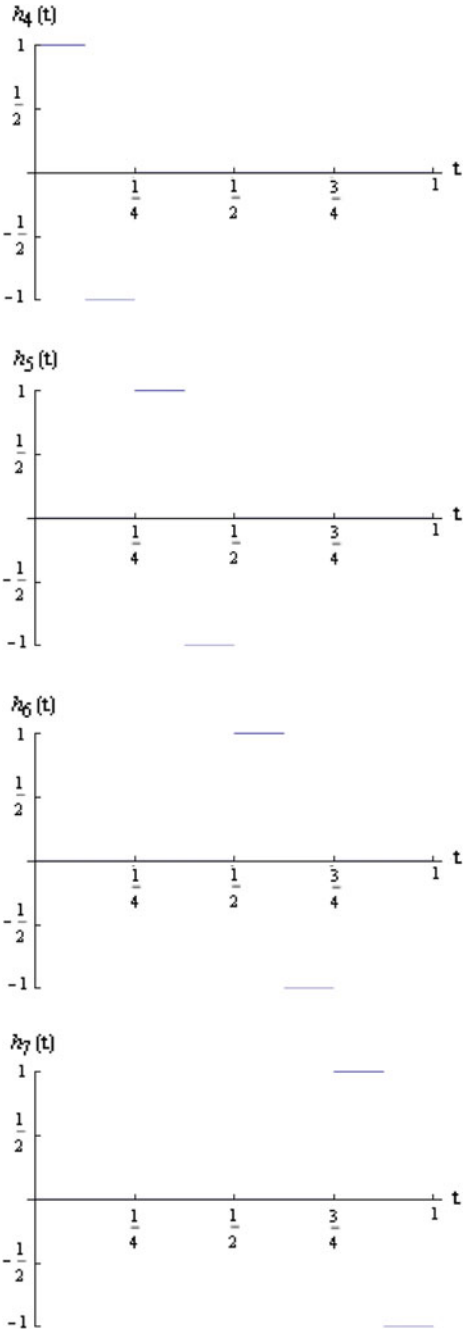

Fig. 3.2 (continued)

where

$$\xi_1(i) = A + \left(\frac{k-1}{2^j}\right)(B-A) = A + \left(\frac{k-1}{2^j}\right)m\Delta t,$$
$$\xi_2(i) = A + \left(\frac{k-\frac{1}{2}}{2^j}\right)(B-A) = A + \left(\frac{k-\frac{1}{2}}{2^j}\right)m\Delta t,$$
$$\xi_3(i) = A + \left(\frac{k}{2^j}\right)(B-A) = A + \left(\frac{k}{2^j}\right)m\Delta t,$$

for $i = 1, 2, \ldots, m$, $m = 2^J$, and J is a positive integer which is called the maximum level of resolution. Here, j and k represent the integer decomposition of the index i, i.e., $i = k + 2^j - 1$, $0 \le j < i$, and $1 \le k < 2^j + 1$.

In the following analysis, integrals of the wavelets are defined as

$$p_i(x) = \int_0^x h_i(x)\mathrm{d}x, \quad q_i(x) = \int_0^x p_i(x)\mathrm{d}x, \quad r_i(x) = \int_0^x q_i(x)\mathrm{d}x.$$

This can be done with the aid of (3.4)

$$p_i(x) = \begin{cases} x - \xi_1 & \text{for } x \in [\xi_1, \xi_2) \\ \xi_3 - x & \text{for } x \in [\xi_2, \xi_3) \\ 0 & \text{elsewhere} \end{cases} \tag{3.5}$$

$$q_i(x) = \begin{cases} 0 & \text{for } x \in [0, \xi_1) \\ \frac{1}{2}(x-\xi_1)^2 & \text{for } x \in [\xi_1, \xi_2) \\ \frac{1}{4m^2} - \frac{1}{2}(\xi_3 - x)^2 & \text{for } x \in [\xi_2, \xi_3) \\ \frac{1}{4m^2} & \text{for } x \in [\xi_3, 1] \end{cases} \tag{3.6}$$

$$r_i(x) = \begin{cases} \frac{1}{6}(x-\xi_1)^3 & \text{for } x \in [\xi_1,\ \xi_2) \\ \frac{1}{4m^2}(x-\xi_2) + \frac{1}{6}(\xi_3 - x)^3 & \text{for } x \in [\xi_2, \xi_3) \\ \frac{1}{4m^2}(x-\xi_2) & \text{for } x \in [\xi_3, 1) \\ 0 & \text{elsewhere} \end{cases} \tag{3.7}$$

The collocation points are defined as

$$x_l = \frac{l - 0.5}{2M}, \quad l = 1, 2, \ldots, 2M. \tag{3.8}$$

It is expedient to introduce the $2M \times 2M$ matrices **H**, **P**, **Q,** and ***R*** with the elements $H(i,l) = h_i(x_l)$, $P(i,l) = p_i(x_l)$, $Q(i,l) = q_i(x_l)$ and $R(i,l) = r_i(x_l)$, respectively.

3.3.2 Operational Matrix of the General Order Integration

In 2012, the generalized Haar wavelet operational matrix of integration has been devised first time ever by Saha Ray [7].

The integration of the $\mathbf{H}_m(t) = [h_0(t), h_1(t), \ldots, h_{m-1}(t)]^{\mathrm{T}}$ can be approximated by Chen and Hsiao [8]

$$\int_0^t \mathbf{H}_m(\tau)\mathrm{d}\tau \cong \mathbf{Q}\mathbf{H}_m(t), \tag{3.9}$$

where $\mathbf{Q}$ is called the Haar wavelet operational matrix of integration which is a square matrix of dimension $m \times m$.

Now, we shall derive the Haar wavelet operational matrix of the general order of integration. In this purpose, we first introduce the fractional integral of order α (>0) which is defined as Podlubny [4]

$$J^{\alpha}f(t) = \frac{1}{\Gamma(\alpha)}\int_0^t (t-\tau)^{\alpha-1}f(\tau)\mathrm{d}\tau, \quad t > 0, \quad \alpha \in \mathsf{R}^{+} \tag{3.10}$$

where R^{+} is the set of positive real numbers.

The Haar wavelet operational matrix Q^{α} of integration of the general order α is given by

$$\begin{aligned}\mathbf{Q}^{\alpha}\mathbf{H}_m(t) &= J^{\alpha}\mathbf{H}_m(t)\\ &= [J^{\alpha}h_0(t), J^{\alpha}h_1(t), \ldots, J^{\alpha}h_{m-1}(t)]^{\mathrm{T}}\\ &= [Qh_0(t), Qh_1(t), \ldots, Qh_{m-1}(t)]^{\mathrm{T}},\end{aligned}$$

where

$$\begin{aligned}Qh_0(t) &= \begin{cases}\frac{t^{\alpha}}{\Gamma(\alpha+1)}, & t \in [A, B]\\ 0, & \text{elsewhere}\end{cases},\\ Qh_i(t) &= \begin{cases}0, & A \le t < \xi_1(i)\\ f_1, & \xi_1(i) \le t < \xi_2(i)\\ f_2, & \xi_2(i) \le t < \xi_3(i)\\ f_3, & \xi_3(i) \le t < B\end{cases}\end{aligned} \tag{3.11}$$

where

$$f_1 = \frac{(t-\xi_1(i))^{\alpha}}{\Gamma(\alpha+1)},$$
$$f_2 = \frac{(t-\xi_1(i))^{\alpha}}{\Gamma(\alpha+1)} - 2\frac{(t-\xi_2(i))^{\alpha}}{\Gamma(\alpha+1)},$$
$$f_3 = \frac{(t-\xi_1(i))^{\alpha}}{\Gamma(\alpha+1)} - 2\frac{(t-\xi_2(i))^{\alpha}}{\Gamma(\alpha+1)} + \frac{(t-\xi_3(i))^{\alpha}}{\Gamma(\alpha+1)},$$

for $i = 1, 2, \ldots, m$, $m = 2^J$, and J is a positive integer. Here, j and k represent the integer decomposition of the index i, i.e., $i = k + 2^j - 1$, $0 \le j < i$, and $1 \le k < 2^j + 1$.

For instance, if $m = 4$, we have

$$\mathbf{Q}^{1/2}\mathbf{H}_4 = \begin{pmatrix} 0.398942 & 0.690988 & 0.892062 & 1.0555 \\ 0.398942 & 0.690988 & 0.0941775 & -0.326475 \\ 0.398942 & -0.106896 & -0.0909723 & -0.0376338 \\ 0 & 0 & 0.398942 & -0.106896 \end{pmatrix}$$

$$\mathbf{QH_4} = \begin{pmatrix} \frac{1}{8} & \frac{3}{8} & \frac{5}{8} & \frac{7}{8} \\ \frac{1}{8} & \frac{3}{8} & \frac{3}{8} & \frac{1}{8} \\ \frac{1}{8} & \frac{1}{8} & 0 & 0 \\ 0 & 0 & \frac{1}{8} & \frac{1}{8} \end{pmatrix}$$

$$\mathbf{Q}^2\mathbf{H}_4 = \begin{pmatrix} \frac{1}{128} & \frac{9}{128} & \frac{25}{128} & \frac{49}{128} \\ \frac{1}{128} & \frac{9}{128} & \frac{23}{128} & \frac{31}{128} \\ \frac{1}{128} & \frac{7}{128} & \frac{1}{16} & \frac{1}{16} \\ 0 & 0 & \frac{1}{128} & \frac{7}{128} \end{pmatrix}$$

Although, the learned researchers Chen and Hsiao [8], Kilicman and Zhour [9], Li and Zhao [10] and Bouafoura and Braiek [11] proposed the generalized operational matrix of integration which is an approximate matrix in nature. It is not the exact generalized operational matrix. Moreover, it has a drawback for obtaining the correct integer-order operational matrices from the generalized operational matrix.

In the present analysis, the derived Haar wavelet operational matrix of integration $\mathbf{Q}^{\alpha} = (\mathbf{Q}^{\alpha}\mathbf{H})H^{-1}$ of the general order α is the correct operational matrix. The above examples justify its correctness.

3.3.3 Function Approximation by Haar Wavelets

Any function $f(t) \in L^2([0,1))$ can be expanded into Haar wavelets by

$$y(t) = c_0 h_0(t) + c_1 h_1(t) + c_2 h_2(t) + \cdots \tag{3.12}$$

where $c_j = \int_0^1 y(t) h_j(t) \mathrm{d}t$.

If $y(t)$ is approximated as a piecewise constant in each subinterval, the sum in Eq. (3.12) may be terminated after m terms and consequently, we can write a discrete version in the matrix form as

$$\mathbf{Y} \approx \left(\sum_{i=0}^{m-1} c_i h_i(t_l) \right)_{1\times m} = \mathbf{C}^{\mathbf{T}} \mathbf{H}_m, \tag{3.13}$$

where $\mathbf{Y}$ is the discrete form of the continuous function $y(t)$, and $\mathbf{C}^{\mathbf{T}} = [c_0, c_1, \ldots, c_{m-1}]$ is called the coefficient vector of $\mathbf{Y}$ which can be calculated from $\mathbf{C}^{\mathbf{T}} = \mathbf{Y}.\mathbf{H}_m^{-1}$. $\mathbf{Y}$ and $\mathbf{C}^{\mathbf{T}}$ are both row vectors, and $\mathbf{H}_m$ is the Haar wavelet matrix of order $m = 2^J$, J is a positive integer and is defined by $\mathbf{H}_m = [\boldsymbol{h}_0, \boldsymbol{h}_1, \ldots, \boldsymbol{h}_{m-1}]^{\mathrm{T}}$

i.e.,

$$H_m = \begin{bmatrix} \boldsymbol{h}_0 \\ \boldsymbol{h}_1 \\ \cdots \\ \boldsymbol{h}_{m-1} \end{bmatrix} = \begin{bmatrix} h_{0,0} & h_{0,1} & \ldots & h_{0,m-1} \\ h_{1,0} & h_{1,1} & \ldots & h_{1,m-1} \\ \ldots. & & & \\ h_{m-1,0} & h_{m-1,1} & \ldots & h_{m-1,m-1} \end{bmatrix} \tag{3.14}$$

where $\boldsymbol{h}_0, \boldsymbol{h}_1, \ldots, \boldsymbol{h}_{m-1}$ are the discrete form of the Haar wavelet bases; the discrete values are taken from the continuous curves $h_0(t), h_1(t), \ldots, h_{m-1}(t)$, respectively.

The expansion of a given function $f(t)$ into the Haar wavelet series is

$$f(t) = \sum_{i=0}^{m-1} c_i h_i(t), \quad t \in [A, B] \tag{3.15}$$

where c_i are the wavelet coefficients.

In the present paper, we apply wavelet collocation method to determine the coefficients c_i. These collocation points are given by

$$t_l = A + (l - 0.5)\Delta t, \quad l = 1, 2, \ldots, m. \tag{3.16}$$

The discrete version of (3.15) is

$$f(t_l) = \sum_{i=0}^{m-1} c_i h_i(t_l). \tag{3.17}$$

Equation (3.17) can be written in the matrix form as

$$\hat{f} = \mathbf{C}^T \mathbf{H}_m. \tag{3.18}$$

where $\hat{f}$ and C^T are m-dimensional row vectors, and $\mathbf{H}_m$ is the Haar wavelet matrix of order m.

3.3.4 Convergence of Haar Wavelet Approximation

In this subsection, the convergence analysis for the Haar wavelet method has been employed.

Theorem 3.1 *Let, $f(x) \in L^2(R)$ be a continuous function defined in [0, 1). Then, the error at Jth level may be defined as*

$$E_J(x) = |f(x) - f_J(x)| = \left| f(x) - \sum_{i=1}^{2M} a_i h_i(x) \right| = \left| \sum_{i=2M}^{\infty} a_i h_i(x) \right|. \tag{3.19}$$

Then, the error norm at Jth level satisfies the following inequalities

$$\|E_J\| \leq \frac{K^2}{12} 2^{-2J}, \tag{3.20}$$

where $|f'(x)| \leq K$, for all $x \in (0,\ 1)$ and $K > 0$ and M is a positive number related to the Jth level resolution of the wavelet given by $M = 2^J$.

Proof The error at the Jth level of resolution is defined as

$$\begin{aligned} |E_J| &= |f(x) - f_J(x)| \\ &= \left| \sum_{i=2M}^{\infty} a_i h_i(x) \right|, \end{aligned}$$

where

$$f_J(x) = \sum_{i=0}^{2M-1} a_i h_i(x), \quad M = 2^J.$$

$$\begin{aligned}\|E_J\|^2 &= \int_{-\infty}^{\infty} \left(\sum_{i=2M}^{\infty} a_i h_i(x), \sum_{l=2M}^{\infty} a_l h_l(x) \right) \mathrm{d}x \\ &= \sum_{i=2M}^{\infty} \sum_{l=2M}^{\infty} a_i a_l \int_{-\infty}^{\infty} h_i(x) h_l(x) \mathrm{d}x \\ &\leq \sum_{i=2M}^{\infty} |a_i|^2.\end{aligned}$$

Now, $a_i = \int_0^1 2^{j/2} f(x) h(2^j x - k) \mathrm{d}x$,
where $h_i(x) = 2^{j/2} h(2^j x - k)$, $k = 0, 1, 2, \ldots, 2^j - 1$, $j = 0, 1, \ldots, J$ and

$$h\left(2^j x - k\right) = \begin{cases} 1, & k2^{-j} \leq x < \left(k + \frac{1}{2}\right)2^{-j} \\ -1, & \left(k + \frac{1}{2}\right)2^{-j} \leq x < (k+1)2^{-j} \\ 0, & \text{elsewhere} \end{cases}.$$

Therefore, applying integral mean value theorem, we obtain

$$\begin{aligned} a_i &= 2^{j/2} \left[\int_{k2^{-j}}^{(k+\frac{1}{2})2^{-j}} f(x)\mathrm{d}x - \int_{(k+\frac{1}{2})2^{-j}}^{(k+1)2^{-j}} f(x)\mathrm{d}x \right] \\ &= 2^{j/2} \left[\left(\left(k + \frac{1}{2}\right)2^{-j} - k2^{-j} \right) f(\xi_1) \right. \\ &\quad \left. - \left((k+1)2^{-j} - \left(k + \frac{1}{2}\right)2^{-j} \right) f(\xi_2) \right], \\ &\qquad \text{where} \quad \xi_1 \in \left(k2^{-j}, \left(k + \frac{1}{2}\right)2^{-j} \right) \text{ and} \\ &\qquad\quad \xi_2 \in \left(\left(k + \frac{1}{2}\right)2^{-j}, (k+1)2^{-j} \right) \end{aligned}$$

Consequently, applying Lagrange's mean value theorem, we have

$$a_i = 2^{-\frac{j}{2}-1} (\xi_1 - \xi_2)(f'(\xi)), \quad \text{where } \xi \in (\xi_1, \xi_2).$$

This implies that

$$\begin{aligned} a_i^2 &= 2^{-j-2} (\xi_2 - \xi_1)^2 f'(\xi)^2 \\ &\leq 2^{-j-2} 2^{-2j} K^2, \quad \text{since } |f'(x)| \leq K \\ &= 2^{-3j-2} K^2. \end{aligned}$$

Therefore,

$$\begin{aligned}
\|E_J\|^2 &\le \sum_{i=2M}^{\infty} a_i^2 \le \sum_{i=2M}^{\infty} 2^{-3j-2}K^2 \\
&= K^2 \sum_{j=J+1}^{\infty} \sum_{i=2^j}^{2^{j+1}-1} 2^{-3j-2} \\
&= K^2 \sum_{j=J+1}^{\infty} 2^{-3j-2}\left(2^{j+1} - 1 - 2^j + 1\right) \\
&= K^2 \sum_{j=J+1}^{\infty} (2^{-2j-1} - 2^{-2j-2}) \\
&= K^2 \sum_{j=J+1}^{\infty} 2^{-2j}(2^{-1} - 2^{-2}) \\
&= \frac{K^2}{4} \sum_{j=J+1}^{\infty} 2^{-2j} \\
&= \frac{K^2}{4} \frac{2^{-2(J+1)}}{\left(1 - \frac{1}{4}\right)} \\
&= \frac{K^2}{12} 2^{-2J}.
\end{aligned} \tag{3.21}$$

From the above Eq. (3.21), it is obvious that the error bound is inversely proportional to the level of resolution J of Haar wavelet. Hence, the accuracy in the wavelet method improves as we increase the level of resolution J.

3.4 Basic Idea of Optimal Homotopy Asymptotic Method

To illustrate the basic ideas of optimal homotopy asymptotic method, we consider the following nonlinear differential equation

$$A(u(x,t)) + g(x,t) = 0, x \in \Omega \tag{3.22}$$

with the boundary conditions

$$B\left(u, \frac{\partial u}{\partial t}\right) = 0, x \in \Gamma \tag{3.23}$$

where A is a differential operator, B is a boundary operator, $u(x,t)$ is an unknown function, Γ is the boundary of the domain Ω, and $g(x,t)$ is a known analytic function.

The operator A can be decomposed as

$$A = L + N, \tag{3.24}$$

where L is a linear operator, and N is a nonlinear operator.

We construct a homotopy $\varphi(x,t;p) : \Omega \times [0,1] \to \Re$ which satisfies

$$\begin{aligned} H(\varphi(x,t;p),p) &= (1-p)[L(\varphi(x,t;p)) + g(x,t)] \\ &\quad - H(p)[A(\varphi(x,t;p)) + g(x,t)] = 0, \end{aligned} \tag{3.25}$$

where $p \in [0,1]$ is an embedding parameter, and $H(p)$ is a nonzero auxiliary function for $p \neq 0$ and $H(0) = 0$. When $p = 0$ and $p = 1$, we have $\varphi(x,t;0) = u_0(x,t)$ and $\varphi(x,t;1) = u(x,t)$, respectively.

Thus as p varies from 0 to 1, the solution $\varphi(x,t;p)$ approaches from $u_0(x,t)$ to $u(x,t)$.

Here $u_0(x,t)$ is obtained from Eqs. (3.25) and (3.23) with $p = 0$ yields

$$L(\varphi(x,t;0)) + g(x,t) = 0, \quad B\left(u_0, \frac{\partial u_0}{\partial t}\right) = 0. \tag{3.26}$$

The auxiliary function $H(p)$ is chosen in the form

$$H(p) = pC_1 + p^2C_2 + p^3C_3 + \cdots, \tag{3.27}$$

where $C_1, C_2, C_3, \ldots$ are constants to be determined. To get an approximate solution, $\tilde{\varphi}(x,t;p,C_1,C_2,C_3,\ldots)$ is expanded in a series about p as

$$\tilde{\varphi}(x,t;p,C_1,C_2,C_3,\ldots) = u_0(x,t) + \sum_{i=1}^{\infty} u_i(x,t,C_1,C_2,C_3,\ldots)p^i. \tag{3.28}$$

Substituting Eq. (3.28) in Eq. (3.25) and equating the coefficients of like powers of p, we will have the following equations

$$L(u_1(x,t) + g(x,t)) = C_1N_0(u_0(x,t)), \quad B\left(u_1, \frac{\partial u_1}{\partial t}\right) = 0. \tag{3.29}$$

$$\begin{aligned} L(u_2(x,t)) - L(u_1(x,t)) &= C_2N_0(u_0(x,t)) \\ &\quad + C_1(L(u_1(x,t)) + N_1(u_0(x,t),u_1(x,t))), B\left(u_2, \frac{\partial u_2}{\partial t}\right) = 0. \end{aligned} \tag{3.30}$$

and hence, the general governing equations for $u_j(x,t)$ is given by

$$L\big(u_j(x,t)\big) = L\big(u_{j-1}(x,t)\big) + C_j N_0(u_0(x,t)) + \sum_{i=1}^{j-1} C_i\big[L\big(u_{j-1}(x,t)\big) + N_{j-1}\big(u_0(x,t),\ldots,u_{j-1}(x,t)\big)\big]; \quad j = 2,3,\ldots \tag{3.31}$$

where $N_j\big(u_0(x,t),\ldots,u_j(x,t)\big)$ is the coefficient of p^j in the expansion of $N(\varphi(x,t;p))$ about the embedding parameter p and

$$N(\varphi(x,t;p,C_1,C_2,C_3,\ldots)) = N_0(u_0(x,t)) + \sum_{j=1}^{\infty} N_j\big(u_0,u_1,\ldots,u_j\big)p^j. \tag{3.32}$$

It is observed that the convergence of the series (3.28) depends upon the auxiliary constants $C_1, C_2, C_3, \ldots$.

The approximate solution of Eq. (3.22) can be written in the following form

$$\tilde{u}(x,t;C_1,C_2,C_3,\ldots) = u_0(x,t) + \sum_{j=1}^{n-1} u_j(x,t,C_1,C_2,C_3,\ldots). \tag{3.33}$$

Substituting Eq. (3.33) in Eq. (3.22), we get the following expression for the residual

$$R_n(x,t;C_1,C_2,C_3,\ldots) = L(\tilde{u}(x,t;C_1,C_2,C_3,\ldots)) + N(\tilde{u}(x,t;C_1,C_2,C_3,\ldots)) + g(x,t). \tag{3.34}$$

If $R_n(x,t;C_1,C_2,C_3,\ldots) = 0$, then $\tilde{u}(x,t;C_1,C_2,C_3,\ldots)$ is the exact solution. Generally, such case does not arise for nonlinear problems. The nth-order approximate solution given by Eq. (3.33) depends on the auxiliary constants $C_1, C_2, C_3, \ldots$, and these constants can be optimally determined by various methods. Here, we apply the collocation method.

According to the collocation method, the optimal values of the constants $C_1, C_2, C_3, \ldots$ can be obtained by solving the following system of equations:

$$R_n\big(x_i,t_j;C_1,C_2,C_3,\ldots,C_{k^2}\big) = 0, \quad \text{for } i = 1,2,\ldots,k \text{ and } j = 1,2,\ldots,k \tag{3.35}$$

After obtaining the optimal values of the convergence control constants $C_1, C_2, C_3, \ldots$ by the above-mentioned method, the approximate solution of Eq. (3.22) is well determined.

3.5 Application of Haar Wavelet Method for the Numerical Solution of Bagley–Torvik Equation

In the present analysis, we are using the operational matrix of Haar wavelet for finding the numerical solution of Bagley–Torvik Equation, which arises, for instance, in modeling the motion of a rigid plate immersed in a Newtonian fluid.

Let us consider the Bagley–Torvik equation [4]

$$Ay''(t) + BD^{3/2}y(t) + Cy(t) = f(t), t > 0 \tag{3.36}$$

where

$$f(t) = \begin{cases} 8, & 0 \le t \le 1 \\ 0, & t > 1 \end{cases}$$

subject to initial conditions

$$y(0) = y'(0) = 0.$$

The Haar wavelet solution is sought in the form

$$y(t) = \sum_{i=0}^{m-1} c_i h_i(t), \tag{3.37}$$

which can be written in the matrix form as

$$y(t_l) = C^T H_m(t_l), \tag{3.38}$$

where t_l is the collocation points in Eq. (2.7), C^T is the m-dimensional row vector, and $H_m(t_l)$ is the Haar wavelet square matrix of order m.

Integrating Eq. (3.36), we get

$$A\int_0^t\int_0^t D^2y(t)\mathrm{d}t\,\mathrm{d}t + B\int_0^t\int_0^t D^{3/2}y(t)\mathrm{d}t\,\mathrm{d}t + C\int_0^t\int_0^t y(t)\mathrm{d}t\,\mathrm{d}t = \int_0^t\int_0^t f(t)\mathrm{d}t\,\mathrm{d}t.$$

This implies

$$A[y(t) - y(0) - t\,y'(0)] + BJ^{1/2}y(t) + C\int_0^t\int_0^t y(t)\mathrm{d}t\,\mathrm{d}t = \int_0^t\int_0^t f(t)\mathrm{d}t\,\mathrm{d}t.$$

Substituting the initial conditions, we obtain

$$Ay(t) + BJ^{1/2}y(t) + C\int_0^t \int_0^t y(t)\mathrm{d}t\,\mathrm{d}t = \int_0^t \int_0^t f(t)\mathrm{d}t\,\mathrm{d}t. \tag{3.39}$$

Now, expressing Eq. (3.38) into the discrete matrix form, we obtain

$$AC^T H_m(t_l) + BC^T Q^{1/2} H_m(t_l) + CC^T Q^2 H_m(t_l) = EH_m^{-1}(t_l) Q^2 H_m(t_l). \tag{3.40}$$

Since, $\int_0^t \int_0^t f(\mathrm{t})\mathrm{d}t\,\mathrm{d}t \cong c^T Q^2 H_m(t)$, where $c^T = EH_m^{-1}(t)$ and E is the discrete form of the function $f(t_l) = 8(u(t_l) - u(t_l - 1))$, where $u(t)$ is the Heaviside step function, for Eq. (3.36).

From Eq. (3.40), we have

$$C^T\left(AH_m(t_l) + BQ^{1/2}H_m(t_l) + CQ^2 H_m(t_l)\right) = EH_m^{-1}(t_l)Q^2 H_m(t_l). \tag{3.41}$$

Solving Eq. (3.41) for the coefficient row vector C^T, we get

$$C^T = EH_m^{-1}(t_l)Q^2 H_m(t_l)\left(AH_m(t_l) + BQ^{1/2}H_m(t_l) + CQ^2 H_m(t_l)\right)^{-1}. \tag{3.42}$$

Using Eq. (3.38), the Haar wavelet numerical solution is obtained as

$$y(t_l) = EH_m^{-1}(t_l)Q^2 H_m(t_l)\left(AH_m(t_l) + BQ^{1/2}H_m(t_l) + CQ^2 H_m(t_l)\right)^{-1} H_m(t_l). \tag{3.43}$$

Now, the analytical solution of Eq. (3.36) is [4]

$$y(t) = \int_0^t G_3(t-\tau) f(\tau)\mathrm{d}\tau, \tag{3.44}$$

where $G_3(t) = \frac{1}{A}\sum_{r=0}^{\infty} \frac{(-1)^r}{r!}\left(\frac{C}{A}\right)^r t^{2r+1} E^{(r)}_{\frac{1}{2},\frac{3}{2}r+2}\left(\frac{-B}{A}t^{1/2}\right)$, $E_{\lambda,\mu}(z)$ is called the Mittag–Leffler function in two parameters λ, μ (>0) [4] and

$$E^{(r)}_{\lambda,\mu}(y) \equiv \frac{\mathrm{d}^r}{\mathrm{d}y^r} E_{\lambda,\mu}(y) = \sum_{j=0}^{\infty} \frac{(j+r)!y^j}{j!\Gamma(\lambda j + \lambda r + \mu)}, \quad (r = 0, 1, 2, \ldots)$$

Then, Eq. (3.44) is reduced to

$$y(t) = 8[y_U(t) - y_U(t-1)], \quad \text{if } f(t) = 8(u(t) - u(t-1)) \tag{3.45}$$

where

$$y_U(t) = u(t)\left[\frac{1}{A}\sum_{r=0}^{\infty}\frac{(-1)^r}{r!}\left(\frac{C}{A}\right)^r t^{2(r+1)} E^{(r)}_{\frac{1}{2},\frac{3}{2}r+3}\left(\frac{-B}{A}t^{1/2}\right)\right].$$

The solution (3.45) is the analytical solution of Eq. (3.36).

3.5.1 Numerical Results and Discussions

In the present numerical computation, we have assumed $A = 1$, $B = 0.5$, and $C = 0.5$, as is taken in [4]. It is interesting to note that the graph obtained by Haar wavelet operation method almost coincides with that of [4] cited in Fig. 3.3.

Equations (3.43) and (3.45) have been used to draw the graphs as shown in Fig. 3.3. In Fig. 3.3, *y*app(t) and *y*ext(t) specify Haar wavelet numerical solution and analytical exact solution of Bagley–Torvik equation, respectively.

To have a comparison of the present analysis through Haar wavelet operational method with that of another available method [4], Table 3.1 creates to cite the absolute errors at the collocation points given by Eq. (3.16).

The R.M.S. error between the numerical solution and the exact solution is 0.204029. The above numerical experiments presented in this section were computed using Mathematica 7 [12].

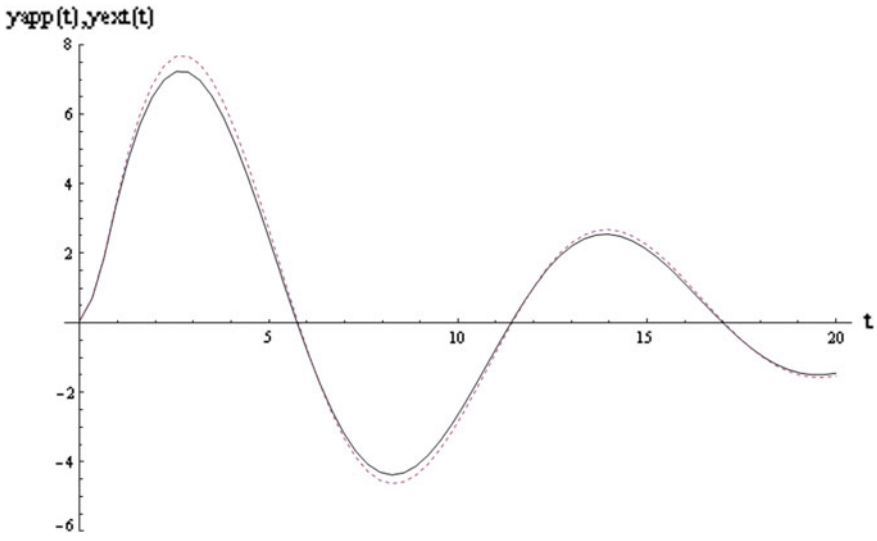

Fig. 3.3 Numerical solution *y*app(t) and analytical exact solution *y*ext(t) of Bagley–Torvik equation (black line for *y*app(t) and dash line for *y*ext(t))

Table 3.1 Absolute error between numerical solution and analytical exact solution

Sl. No.	Time (t)	Analytical exact solution	Numerical solution	Absolute error
1	0.15625	0.0871108	0.0794522	0.00765854
2	0.46875	0.721004	0.70136	0.0196437
3	0.78125	1.87889	1.85171	0.0271845
4	1.09375	3.43807	3.35895	0.0791208
5	1.40625	4.85696	4.67105	0.185911
6	1.71875	5.98737	5.71216	0.27521
7	2.03125	6.83165	6.48436	0.347298
8	2.34375	7.39045	6.98837	0.402077
9	2.65625	7.66909	7.22953	0.439556
10	2.96875	7.67925	7.21918	0.460064
11	3.28125	7.43909	6.97477	0.464314
12	3.59375	6.97278	6.51938	0.453404
13	3.90625	6.30966	5.88088	0.428782
14	4.21875	5.48313	5.09093	0.392194
15	4.53125	4.52949	4.18387	0.345618
16	4.84375	3.48673	3.19553	0.291196
17	5.15625	2.39322	2.16206	0.231159
18	5.46875	1.28657	1.11881	0.167756
19	5.78125	0.202504	0.0993191	0.103185
20	6.09375	−0.826127	−0.865657	0.03953
21	6.40625	−1.77019	−1.7489	0.0212933
22	6.71875	−2.60496	−2.52737	0.0775864
23	7.03125	−3.3106	−3.1827	0.127905
24	7.34375	−3.87253	−3.70144	0.171084
25	7.65625	−4.28152	−4.07526	0.206259
26	7.96875	−4.53369	−4.30082	0.232869
27	8.28125	−4.63032	−4.37967	0.250654
28	8.59375	−4.57747	−4.31783	0.259644
29	8.90625	−4.38554	−4.1254	0.260137
30	9.21875	−4.06866	−3.81598	0.252674
31	9.53125	−3.64404	−3.40603	0.238006
32	9.84375	−3.13126	−2.9142	0.217055
33	10.1563	−2.55149	−2.36062	0.190874
34	10.4688	−1.92678	−1.76617	0.160611
35	10.7813	−1.27925	−1.15179	0.12746
36	11.0938	−0.630455	−0.537829	0.0926261
37	11.4063	−0.00071872	0.056568	0.0572867
38	11.7188	0.591432	0.613989	0.0225565
39	12.0313	1.12973	1.11919	0.0105422
40	12.3438	1.60056	1.55946	0.0411051

(continued)

Table 3.1 (continued)

Sl. No.	Time (t)	Analytical exact solution	Numerical solution	Absolute error
41	12.6563	1.99321	1.92484	0.0683651
42	12.9688	2.30003	2.20832	0.0917076
43	13.2813	2.51652	2.40585	0.110679
44	13.5938	2.64127	2.51628	0.124988
45	13.9063	2.6758	2.54129	0.134509
46	14.2188	2.62437	2.4851	0.139268
47	14.5313	2.49368	2.35425	0.139437
48	14.8438	2.29251	2.15719	0.135316
49	15.1563	2.03131	1.90399	0.127317
50	15.4688	1.7218	1.60585	0.115943
51	15.7813	1.37652	1.27475	0.101767
52	16.0938	1.00838	0.922968	0.0854092
53	16.4063	0.630246	0.56273	0.0675157
54	16.7188	0.254542	0.205806	0.0487359
55	17.0313	−0.107127	−0.13683	0.0297033
56	17.3438	−0.444276	−0.455293	0.0110165
57	17.6563	−0.747806	−0.74103	0.00677619
58	17.9688	−1.01021	−0.987015	0.0231906
59	18.2813	−1.22569	−1.18788	0.0378169
60	18.5938	−1.3903	−1.33997	0.0503275
61	18.9063	−1.50186	−1.44138	0.0604813
62	19.2188	−1.56003	−1.49191	0.0681253
63	19.5313	−1.56614	−1.49294	0.0731934
64	19.8438	−1.52304	−1.44734	0.0757026

3.5.2 Error Estimate

The following table demonstrates the comparison between the numerical solution obtained by Haar wavelet and the analytical solution. The corresponding absolute errors are presented in Table 3.2.

Table 3.2 Comparison of error between the numerical solution and analytical exact solution for $t = 0, 1, 2, \ldots, 10$

Time t	Approximate solution of $y(t)$	Analytical solution of $y(t)$	Absolute error
0	8.88178×10^{-16}	0	8.88178×10^{-16}
1	3.53856	2.95258	0.585974
2	7.53718	6.76011	0.77707
3	8.2854	7.66614	0.61926
4	6.26126	6.07725	0.184014
5	2.53055	2.94394	0.41339
6	−1.49195	−0.525171	0.966783
7	−4.50898	−3.2463	1.26268
8	−5.72074	−4.55029	1.17045
9	−5.00085	−4.30286	0.697989
10	−2.84029	−2.84838	0.0080944

3.6 Solution of Fractional Fisher-Type Equation

In this section, the time fractional Fisher-type equation has been solved by reliable methods, namely the Haar wavelet method and OHAM, respectively.

3.6.1 Application of Haar Wavelet to Fractional Fisher-Type Equation

Consider the nonlinear diffusion equation of the Fisher type [13, 14]

$$\frac{\partial^{\alpha} u}{\partial t^{\alpha}} = \frac{\partial^2 u}{\partial x^2} + u(1-u)(u-a), \tag{3.46}$$

where $0 < \alpha \leq 1$, $0 \leq x \leq 1$, and $0 < a < 1$

with the initial condition

$$u(x,0) = \frac{1}{1 + \mathrm{Exp}\left[-\left(\frac{1}{\sqrt{2}}\right)x\right]}. \tag{3.47}$$

When $\alpha = 1$, the exact solution of Eq. (3.46) is given by Wazwaz and Gorguis [15], Liu [16]

$$u(x,t) = \frac{1}{1 + \mathrm{Exp}\left[-\left(\frac{x+ct}{\sqrt{2}}\right)\right]}, \tag{3.48}$$

where $c = \sqrt{2}\left(\frac{1}{2} - a\right)$.

Let us divide both space and time interval [0, 1] into m equal subintervals; each of width $\Delta = \frac{1}{m}$.

Haar wavelet solution of $u(x,t)$ is sought by assuming that $\frac{\partial^2 u(x,t)}{\partial x^2}$ can be expanded in terms of Haar wavelets as

$$\frac{\partial^2 u(x,t)}{\partial x^2} = \sum_{i=1}^{m}\sum_{j=1}^{m} c_{ij} h_i(x) h_j(t). \tag{3.49}$$

Integrating Eq. (3.49) twice w.r.t. x from 0 to x, we get

$$u(x,t) = \sum_{i=1}^{m}\sum_{j=1}^{m} c_{ij} Q^2 h_i(x) h_j(t) + q(t) + xp(t). \tag{3.50}$$

Putting $x = 0$, in Eq. (3.50), we get

$$q(t) = u(0,t). \tag{3.51}$$

Putting $x = 1$, in Eq. (3.50) we get

$$p(t) = u(1,t) - u(0,t) - \sum_{i=1}^{m}\sum_{j=1}^{m} c_{ij}\left[Q^2 h_i(x)\right]_{x=1} h_j(t). \tag{3.52}$$

Again $q(t) + xp(t)$ can be approximated using Haar wavelet function as

$$q(t) + xp(t) = \sum_{i=1}^{m}\sum_{j=1}^{m} r_{ij} h_i(x) h_j(t). \tag{3.53}$$

This implies

$$\begin{aligned} u(0,t) + x\left[u(1,t) - u(0,t) - \sum_{i=1}^{m}\sum_{j=1}^{m} c_{ij}\left[Q^2 h_i(x)\right]_{x=1} h_j(t)\right] \\ = \sum_{i=1}^{m}\sum_{j=1}^{m} r_{ij} h_i(x) h_j(t). \end{aligned} \tag{3.54}$$

Substituting Eq. (3.53) in Eq. (3.50), we get

$$u(x,t) = \sum_{i=1}^{m}\sum_{j=1}^{m} c_{ij} Q^2 h_i(x) h_j(t) + \sum_{i=1}^{m}\sum_{j=1}^{m} r_{ij} h_i(x) h_j(t). \tag{3.55}$$

The nonlinear term presented in Eq. (3.46) can be approximated using Haar wavelet function as

$$u(1-u)(u-a) = \sum_{i=1}^{m}\sum_{j=1}^{m} d_{ij}h_i(x)h_j(t). \tag{3.56}$$

Therefore,

$$\begin{aligned}
&\left(\sum_{i=1}^{m}\sum_{j=1}^{m} c_{ij}Q^2h_i(x)h_j(t) + \sum_{i=1}^{m}\sum_{j=1}^{m} r_{ij}h_i(x)h_j(t)\right)\\
&\left(1 - \sum_{i=1}^{m}\sum_{j=1}^{m} c_{ij}Q^2h_i(x)h_j(t) + \sum_{i=1}^{m}\sum_{j=1}^{m} r_{ij}h_i(x)h_j(t)\right)\\
&\left(\sum_{i=1}^{m}\sum_{j=1}^{m} c_{ij}Q^2h_i(x)h_j(t) + \sum_{i=1}^{m}\sum_{j=1}^{m} r_{ij}h_i(x)h_j(t) - a\right) = \sum_{i=1}^{m}\sum_{j=1}^{m} d_{ij}h_i(x)h_j(t)
\end{aligned} \tag{3.57}$$

Substituting Eqs. (3.49) and (3.56) in Eq. (3.46), we will have

$$\frac{\partial^\alpha u}{\partial t^\alpha} = \sum_{i=1}^{m}\sum_{j=1}^{m} c_{ij}h_i(x)h_j(t) + \sum_{i=1}^{m}\sum_{j=1}^{m} d_{ij}h_i(x)h_j(t)\,. \tag{3.58}$$

Now applying J^α to both sides of Eq. (3.58) yields

$$u(x,t) - u(x,0) = J_t^\alpha\left(\sum_{i=1}^{m}\sum_{j=1}^{m} c_{ij}h_i(x)h_j(t)\right) + J_t^\alpha\left(\sum_{i=1}^{m}\sum_{j=1}^{m} d_{ij}h_i(x)h_j(t)\right). \tag{3.59}$$

Substituting Eq. (8.44) and Eq. (3.55) in Eq. (3.59), we get

$$\begin{aligned}
\sum_{i=1}^{m}\sum_{j=1}^{m} c_{ij}Q^2h_i(x)h_j(t) + \sum_{i=1}^{m}\sum_{j=1}^{m} r_{ij}h_i(x)h_j(t)\\
- \frac{1}{1+\mathrm{e}^{-\left(\frac{1}{\sqrt{2}}\right)x}} = \sum_{i=1}^{m}\sum_{j=1}^{m} c_{ij}h_i(x)Q_t^\alpha h_j(t)\\
+ \sum_{i=1}^{m}\sum_{j=1}^{m} d_{ij}h_i(x)Q_t^\alpha h_j(t).
\end{aligned} \tag{3.60}$$

Now substituting the collocation points $x_l = \frac{l-0.5}{m}$ and $t_k = \frac{k-0.5}{m}$ for $l,k = 1,2,\ldots,m$ in Eqs. (3.54), (3.57), and (3.60), we have $3m^2$ equations in $3m^2$

unknowns in c_{ij}, r_{ij}, and d_{ij}. By solving this system of equations using mathematical software, the Haar wavelet coefficients c_{ij}, r_{ij}, and d_{ij} can be obtained.

3.6.2 Application of OHAM to Fractional Fisher-Type Equation

Using the optimal homotopy asymptotic method, the homotopy for Eq. (3.46) can be written as

$$(1-p)\frac{\partial^{\alpha}\varphi(x,t;p)}{\partial t^{\alpha}} = H(p)\left[\frac{\partial^{\alpha}\varphi(x,t;p)}{\partial t^{\alpha}} - \frac{\partial^{2}\varphi(x,t;p)}{\partial x^{2}} - \varphi(x,t;p)[1-\varphi(x,t;p)][\varphi(x,t;p)-a]\right] \tag{3.61}$$

Here,

$$\varphi(x,t;p) = u_0(x,t) + \sum_{i=1}^{\infty} u_i(x,t)p^i, \tag{3.62}$$

$$H(p) = pC_1 + p^2C_2 + p^3C_3 + \cdots, \tag{3.63}$$

$$N(\varphi(x,t;p)) = N_0(u_0(x,t)) + \sum_{k=1}^{\infty} N_k(u_0,u_1,\ldots,u_k)p^k. \tag{3.64}$$

Substituting Eqs. (3.62)–(3.64) in Eq. (3.61) and equating the coefficients of like powers of p, we have the following system of partial differential equations.

Coefficients of p^0:

$$\frac{\partial^{\alpha}u_0(x,t)}{\partial t^{\alpha}} = 0. \tag{3.65}$$

Coefficients of p^1:

$$\frac{\partial^{\alpha}u_1(x,t)}{\partial t^{\alpha}} - \frac{\partial^{\alpha}u_0(x,t)}{\partial t^{\alpha}} = C_1\left[\frac{\partial^{\alpha}u_0(x,t)}{\partial t^{\alpha}} - \frac{\partial^{2}u_0(x,t)}{\partial x^{2}} + au_0(x,t) - (u_0(x,t))^2(1+a) + (u_0(x,t))^3\right] \tag{3.66}$$

Coefficients of p^2:

$$\begin{aligned}\frac{\partial^\alpha u_2(x,t)}{\partial t^\alpha}-\frac{\partial^\alpha u_1(x,t)}{\partial t^\alpha}&=C_1\left[\frac{\partial^\alpha u_1(x,t)}{\partial t^\alpha}-\frac{\partial^2 u_1(x,t)}{\partial x^2}+au_1(x,t)\right.\\&\quad\left.-2u_0(x,t)u_1(x,t)(1+a)+3(u_0(x,t))^2u_1(x,t)\right]\\&\quad+C_2\left[\frac{\partial^\alpha u_0(x,t)}{\partial t^\alpha}-\frac{\partial^2 u_0(x,t)}{\partial x^2}\right.\\&\quad\left.+au_0(x,t)-(u_0(x,t))^2(1+a)+(u_0(x,t))^3\right]\end{aligned}\tag{3.67}$$

and so on.

For solving fractional Fisher-type equation using OHAM, we consider the initial condition Eq. (3.47) and solving Eqs. (3.65)–(3.67), we obtain

$$u_0(x,t)=\frac{1}{1+\mathrm{Exp}\left[-\left(\frac{1}{\sqrt{2}}\right)x\right]},\tag{3.68}$$

$$u_1(x,t)=\frac{C_1(2a-1)\mathrm{Exp}\left[\frac{x}{\sqrt{2}}\right]t^\alpha}{2\left(1+\mathrm{Exp}\left[\frac{x}{\sqrt{2}}\right]\right)^2\Gamma(1+\alpha)},\tag{3.69}$$

$$\begin{aligned}u_2(x,t)=u_1(x,t)+C_1&\left[u_1(x,t)-\frac{C_1(2a-1)\mathrm{Exp}\left[\frac{x}{\sqrt{2}}\right]\left(1-4\mathrm{Exp}\left[\frac{x}{\sqrt{2}}\right]+\mathrm{Exp}\left[\sqrt{2}x\right]\right)t^{2\alpha}}{4\left(1+\mathrm{Exp}\left[\frac{x}{\sqrt{2}}\right]\right)^4\Gamma(1+2\alpha)}\right.\\&+\frac{aC_1(2a-1)\mathrm{Exp}\left[\frac{x}{\sqrt{2}}\right]t^{2\alpha}}{2\left(1+\mathrm{Exp}\left[\frac{x}{\sqrt{2}}\right]\right)^2\Gamma(1+2\alpha)}-\frac{(1+a)C_1(2a-1)\mathrm{Exp}\left[\sqrt{2}x\right]t^{2\alpha}}{\left(1+\mathrm{Exp}\left[\frac{x}{\sqrt{2}}\right]\right)^3\Gamma(1+2\alpha)}\\&\left.+\frac{3C_1(2a-1)\mathrm{Exp}\left[\frac{3x}{\sqrt{2}}\right]t^{2\alpha}}{2\left(1+\mathrm{Exp}\left[\frac{x}{\sqrt{2}}\right]\right)^4\Gamma(1+2\alpha)}\right]\\&+C_2\left[-\frac{\partial^2 u_0(x,t)}{\partial x^2}+au_0(x,t)-(u_0(x,t))^2(1+a)+(u_0(x,t))^3\right]\frac{t^\alpha}{\Gamma(1+\alpha)}\end{aligned}\tag{3.70}$$

Using Eqs. (3.68)–(3.70) and consequently substituting in Eq. (3.33), the second-order approximate solution is obtained as follows

$$
\begin{aligned}
u(x,t) = {} & \frac{1}{1+\mathrm{Exp}\left[-\left(\frac{1}{\sqrt{2}}\right)x\right]} + \frac{C_1(2a-1)\mathrm{Exp}\left[\frac{x}{\sqrt{2}}\right]t^{\alpha}}{2\left(1+\mathrm{Exp}\left[\frac{x}{\sqrt{2}}\right]\right)^2\Gamma(1+\alpha)} + u_1(x,t) \\
& + C_1\left[u_1(x,t) - \frac{C_1(2a-1)\mathrm{Exp}\left[\frac{x}{\sqrt{2}}\right]\left(1-4\mathrm{Exp}\left[\frac{x}{\sqrt{2}}\right]+\mathrm{Exp}\left[\sqrt{2}x\right]\right)t^{2\alpha}}{4\left(1+\mathrm{Exp}\left[\frac{x}{\sqrt{2}}\right]\right)^4\Gamma(1+2\alpha)}\right. \\
& + \frac{aC_1(2a-1)\mathrm{Exp}\left[\frac{x}{\sqrt{2}}\right]t^{2\alpha}}{2\left(1+\mathrm{Exp}\left[\frac{x}{\sqrt{2}}\right]\right)^2\Gamma(1+2\alpha)} \\
& \left. - \frac{(1+a)C_1(2a-1)\mathrm{Exp}\left[\sqrt{2}x\right]t^{2\alpha}}{\left(1+\mathrm{Exp}\left[\frac{x}{\sqrt{2}}\right]\right)^3\Gamma(1+2\alpha)} + \frac{3C_1(2a-1)\mathrm{Exp}\left[\frac{3x}{\sqrt{2}}\right]t^{2\alpha}}{2\left(1+\mathrm{Exp}\left[\frac{x}{\sqrt{2}}\right]\right)^4\Gamma(1+2\alpha)}\right] + C_2\frac{t^{\alpha}}{\Gamma(1+\alpha)} \\
& \left[-\frac{\partial^2 u_0(x,t)}{\partial x^2} + au_0(x,t) - (u_0(x,t))^2(1+a) + (u_0(x,t))^3\right]
\end{aligned}
\tag{3.71}
$$

The optimal values of the convergence control constants C_1 and C_2 can be obtained using the collocation method from Eq. (3.35).

3.6.3 Numerical Results and Discussion

Table 3.3 shows the comparison of the approximate solutions of fractional Fisher-type Eq. (3.46) obtained by using the Haar wavelet method and OHAM at different values of x and t. Tables 3.4, 3.5, and 3.6 exhibit the comparison of approximate solutions obtained by Haar wavelet method and OHAM for fractional Fisher-type Eq. (3.46). The obtained results in Tables 3.3, 3.4, 3.5, and 3.6 demonstrate that these methods are well suited for solving fractional Fisher-type equation. Table 3.7 exhibits the L_2 and L_∞ error norm for fractional Fisher-type equation at different values of t and $\alpha = 1$. It can be easily observed from Table 3.7 that the solutions obtained by OHAM are more accurate than that of the Haar wavelet method.

In the case of fractional Fisher-type Eq. (3.46), Figs. 3.4, 3.5, 3.6, and 3.7 show the graphical comparison between the numerical solutions obtained by Haar wavelet method and exact solutions for different values of x and t for $\alpha = 1$.

Table 3.3 Absolute errors in the solution of fractional Fisher-type Eq. (3.46) using the Haar wavelet method and second-order OHAM at various points of x and t for $\alpha = 1$

x	$\lvert u_{\text{Exact}} - u_{\text{Haar}}\rvert$				$\lvert u_{\text{Exact}} - u_{\text{OHAM}}\rvert$			
	$t = 0.2$	$t = 0.4$	$t = 0.6$	$t = 0.8$	$t = 0.2$	$t = 0.4$	$t = 0.6$	$t = 0.8$
0.1	6.3532E−3	2.37818E−3	1.10276E−2	0.01313	1.15082E−6	2.2604E−5	9.065E−5	2.3096E−4
0.2	0.0157158	1.13279E−3	0.0156863	0.0202773	2.08404E−6	9.2861E−6	5.967E−5	1.7382E−4
0.3	0.0254058	8.69964E−4	0.0188795	0.0256173	5.29828E−6	4.1167E−6	2.814E−5	1.151E−4
0.4	0.0346376	3.18353E−3	0.0206902	0.0290465	8.45965E−6	1.7464E−5	3.605E−6	5.5364E−5
0.5	0.0392372	6.88463E−4	0.0293499	0.0394803	1.1537E−5	3.0617E−5	3.521E−5	4.6066E−6
0.6	0.0452261	1.29706E−3	0.0284296	0.0387295	1.45011E−5	4.3441E−5	6.635E−5	6.4167E−5
0.7	0.0486123	0.00292683	0.0260098	0.0356642	1.73248E−5	5.5811E−5	9.668E−5	1.2266E−4
0.8	0.0489923	0.00432643	0.0218834	0.0300975	1.99841E−5	6.761E−5	1.259E−4	1.7945E−4
0.9	0.0461399	0.00580079	0.0157611	0.0218232	2.2458E−5	7.8733E−5	1.537E−4	2.3396E−4
1.0	0.0407954	0.00797543	7.28187E−3	0.010615	2.47294E−5	8.9092E−5	1.799E−4	2.8567E−4

Table 3.4 Approximate solutions of fractional Fisher-type Eq. (3.46) using the Haar wavelet method and second-order OHAM at various points of x and t for $\alpha = 0.75$

x	$t = 0.2$		$t = 0.4$		$t = 0.6$		$t = 0.8$	
	u_{Haar}	u_{OHAM}	u_{Haar}	u_{OHAM}	u_{Haar}	u_{OHAM}	u_{Haar}	u_{OHAM}
0.1	0.529262	0.541972	0.550815	0.558464	0.57178	0.572871	0.58789	0.586061
0.2	0.54032	0.559441	0.567777	0.57575	0.592323	0.589947	0.610112	0.6029
0.3	0.551007	0.576764	0.583637	0.592852	0.611195	0.606805	0.630359	0.619494
0.4	0.561805	0.5939	0.598653	0.60973	0.628487	0.62341	0.648635	0.635808
0.5	0.577346	0.61081	0.619426	0.62635	0.652014	0.639728	0.673325	0.651811
0.6	0.589669	0.627458	0.63334	0.642676	0.666293	0.655727	0.687588	0.667476
0.7	0.603304	0.643809	0.646865	0.658676	0.679049	0.67138	0.699751	0.682775
0.8	0.618509	0.659832	0.659997	0.674324	0.690193	0.68666	0.709697	0.697687
0.9	0.635416	0.675498	0.672635	0.689592	0.699573	0.701546	0.717268	0.712192
1.0	0.653985	0.69078	0.684559	0.704459	0.706961	0.716016	0.722251	0.726273

Table 3.5 Approximate solutions of fractional Fisher-type Eq. (3.46) using the Haar wavelet method and three terms for second-order OHAM at various points of x and t for $\alpha = 0.5$

x	$t = 0.2$		$t = 0.4$		$t = 0.6$		$t = 0.8$	
	u_{Haar}	u_{OHAM}	u_{Haar}	u_{OHAM}	u_{Haar}	u_{OHAM}	u_{Haar}	u_{OHAM}
0.1	0.531396	0.55521	0.550389	0.570645	0.570167	0.582442	0.586081	0.592358
0.2	0.544463	0.572501	0.567129	0.587683	0.589396	0.599243	0.606722	0.608926
0.3	0.557098	0.589616	0.582811	0.604511	0.607055	0.615806	0.625465	0.625237
0.4	0.569581	0.606516	0.597627	0.621093	0.62327	0.6321	0.642398	0.64126
0.5	0.586931	0.623164	0.617982	0.637394	0.645433	0.648094	0.665485	0.656966
0.6	0.599906	0.639526	0.631544	0.653383	0.659045	0.663758	0.678972	0.672331
0.7	0.613502	0.655571	0.644668	0.669033	0.671439	0.679069	0.690761	0.68733
0.8	0.627951	0.671268	0.657436	0.684317	0.682619	0.694001	0.700823	0.701944
0.9	0.643461	0.686593	0.669891	0.699213	0.69255	0.708537	0.709084	0.716155
1.0	0.660213	0.701522	0.682031	0.713701	0.701145	0.722658	0.715421	0.729948

Table 3.6 Approximate solutions of fractional Fisher-type Eq. (8.1) using the Haar wavelet method and three terms for second-order OHAM at various points of x and t for $\alpha = 0.25$

x	$t = 0.2$		$t = 0.4$		$t = 0.6$		$t = 0.8$	
	u_{Haar}	u_{OHAM}	u_{Haar}	u_{OHAM}	u_{Haar}	u_{OHAM}	u_{Haar}	u_{OHAM}
0.1	0.532613	0.572089	0.549759	0.582288	0.56869	0.589109	0.584364	0.594376
0.2	0.546845	0.589079	0.566132	0.599061	0.586797	0.605718	0.603614	0.610849
0.3	0.560632	0.605856	0.581558	0.615598	0.603479	0.622078	0.62109	0.627063
0.4	0.574145	0.622383	0.596189	0.631866	0.618879	0.638157	0.63693	0.642985
0.5	0.592632	0.638629	0.6162	0.647836	0.639969	0.653925	0.658653	0.65859
0.6	0.60613	0.654561	0.62967	0.663478	0.653168	0.669358	0.671551	0.673851
0.7	0.6199	0.670153	0.642758	0.678767	0.665416	0.68443	0.683099	0.688748
0.8	0.634137	0.685379	0.655588	0.693681	0.67679	0.699122	0.693344	0.703261
0.9	0.649049	0.700217	0.668278	0.7082	0.687344	0.713415	0.702305	0.717372
1.0	0.664857	0.714648	0.680936	0.722306	0.697114	0.727293	0.709973	0.731069

Table 3.7 L_2 and L_∞ error norm for Fisher-type equation at different values of t

Time (s)	Haar wavelet method		Optimal homotopy asymptotic method (OHAM)	
	L_2	L_∞	L_2	L_∞
0.2	0.0377811	0.0489923	1.50470E−5	2.47294E−5
0.4	0.00380168	0.00797543	5.05627E−5	8.9092E−5
0.6	0.020685	0.0293499	9.97048E−5	1.799E−4
0.8	0.0281228	0.0394803	1.69576E−4	2.8567E−4

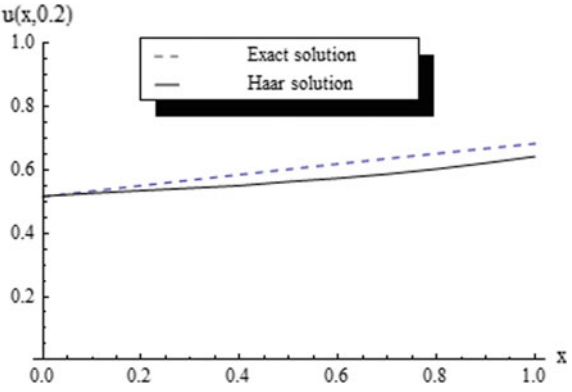

Fig. 3.4 Comparison of the numerical solution and exact solution of fractional Fisher-type equation when $t = 0.2$ and $\alpha = 1$

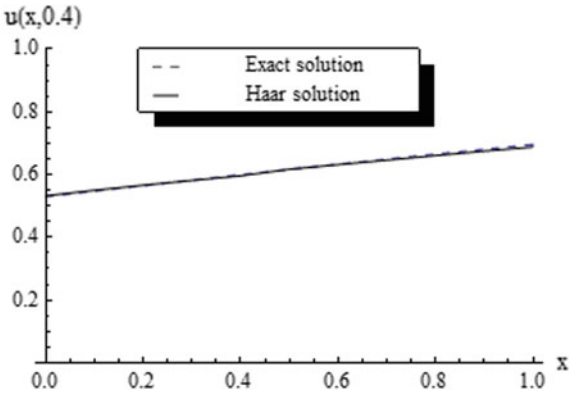

Fig. 3.5 Comparison of the numerical solution and exact solution of fractional Fisher-type equation when $t = 0.4$ and $\alpha = 1$

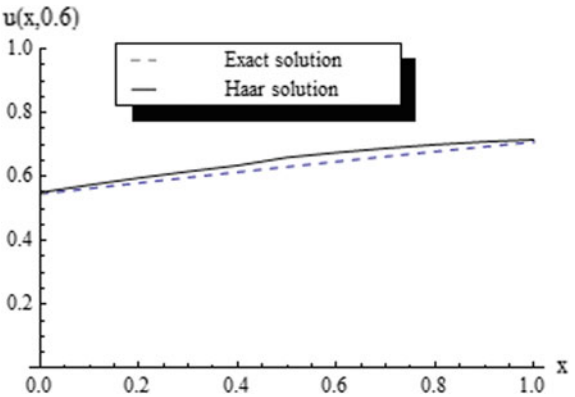

Fig. 3.6 Comparison of the numerical solution and exact solution of fractional Fisher-type equation when $t = 0.6$ and $\alpha = 1$

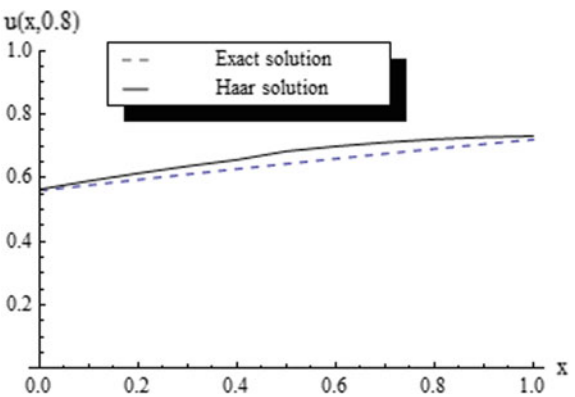

Fig. 3.7 Comparison of the numerical solution and exact solution of fractional Fisher-type equation when $t = 0.8$ and $\alpha = 1$

3.7 Conclusion

In the present chapter, a numerical method based on the Haar wavelet operational method is applied to solve the Bagley–Torvik equation. An attempt has been made to apply the Haar wavelet operational method for the numerical solution of the Bagley–Torvik equation.

We exhibit a numerical method for the fractional-order Bagley–Torvik equation based on Haar wavelet operational matrices of the general order of integration. In this regard, a general procedure of obtaining the Haar wavelet operational matrix Q^{α} of integration of the general order α is derived first time in this work. This operational matrix is the correct general order operational matrix confirmed after examined by the author.

The numerical solution is compared with the exact solution and the R.M.S. error is 0.204029. The error may be reduced if we take more number of collocation points. The advantage of this method is that it transforms the problem into algebraic matrix equation so that the computation is simple, and it is a computer-oriented method. It shows the simplicity and effectiveness of this method. It is based on the operational matrices of Haar wavelet functions. Moreover, wavelet operational method is much simpler than the conventional numerical method for fractional differential equations, and the result obtained is quite satisfactory. The admissible comparison of the results obtained by the present method justifies the applicability, accuracy, and efficiency of the proposed method.

Also, in this chapter, the fractional Fisher-type equation has been solved by using the Haar wavelet method. The obtained results are then compared with exact solutions as well as the optimal homotopy asymptotic method. These results have been presented in the tables and also graphically demonstrated in order to justify the accuracy and efficiency of the proposed schemes. The Haar wavelet technique provides quite satisfactory results for the fractional Fisher-type Eq. (3.46). The main advantages of this Haar wavelet method are it transfers the whole scheme into a system of algebraic equations for which the computation is easy and simple. OHAM allows fine-tuning of the convergence region and the rate of convergence by suitably identifying convergence control parameters $C_1, C_2, C_3, \ldots$. The results obtained by OHAM are more accurate as its convergence region can be easily adjusted and controlled. The main advantages of these schemes are their simplicity, applicability, and less computational errors. Although the obtained results indicate that the optimal homotopy asymptotic method provides more accurate value than Haar wavelet method, and however, the accuracy of the wavelet method may be improved with the increase in level of resolution.

References

1. Kilbas, A.A., Srivastava, H.M., Trujillo, J.J.: Theory and Applications of Fractional Differential Equations. Elsevier Science and Tech, Amsterdam, The Netherlands (2006)
2. Sabatier, J., Agrawal, O.P., Tenreiro Machado, J A.: Advances in Fractional Calculus: Theoretical Developments and Applications in Physics and Engineering. Springer, Dordrecht, The Netherlands (2007)
3. Gorenflo, R., Mainardi, F.: Fractional calculus: integral and differential equations of fractional order, In: Carpinteri, A., Mainardi, F. (eds.) Fractals and Fractional Calculus in Continuum Mechanics, pp. 223–276. Springer, Vienna (1997)
4. Podlubny, I.: Fractional Differential Equations. Academic Press, New York (1999)
5. Torvik, P.J., Bagley, R.L.: On the appearance of the fractional derivative in the behavior of real materials. ASME J. Appl. Mech. **51**, 294–298 (1984)
6. Trinks, C., Ruge, P.: Treatment of dynamic systems with fractional derivatives without evaluating memory-integrals. Comput. Mech. **29**(6), 471–476 (2002)
7. Saha Ray, S.: On Haar wavelet operational matrix of general order and its application for the numerical solution of fractional Bagley Torvik equation. Appl. Math. Comput. **218**, 5239–5248 (2012)
8. Chen, C.F., Hsiao, C.H.: Haar wavelet method for solving lumped and distributed parameter-systems. IEE Proc-Control Theory Appl. **144**(1), 87–94 (1997)
9. Kilicman, A., Zhour, Z.A.A.A.: Kronecker operational metrics for fractional calculus and some applications. Appl. Math. Comp. **187**, 250–265 (2007)
10. Li, Y., Zhao, W.: Haar wavelet operational matrix of fractional order integration and its applications in solving the fractional order differential equations. Appl. Math. Comp. **216**, 2276–2285 (2010)
11. Bouafoura, M.K., Braiek, N.B.: $PI^{\lambda}D^{\mu}$ controller design for integer and fractional plants using piecewise orthogonal functions. Comm. Nonlinear Sci. Numer. Simul. **15**, 1267–1278 (2010)
12. Wolfram, S.: Mathematica for Windows, Version 7.0. Wolfram Research (2008)
13. Wazwaz, A.M.: Partial Differential Equations and Solitary Waves Theory. Springer, Berlin, Heidelberg (2009)
14. Fisher, R.A.: The wave of advance of advantageous genes. Ann. Eugenics **7**(4), 355–369 (1937)
15. Wazwaz, A.M., Gorguis, A.: An analytic study of Fisher's equation by using Adomian decomposition method. Appl. Math. Comput. **154**(3), 609–620 (2004)
16. Liu, Y.: General solution of space fractional Fisher's nonlinear diffusion equation. J. Fractional Calc. Appl. **1**(2), 1–8 (2011)

Chapter 4
Numerical Solutions of Riesz Fractional Partial Differential Equations

4.1 Introduction

Nowadays, different applications of fractional differential equations in many areas, such as engineering, physics, chemistry, astrophysics, and many other sciences, are observed. Fractional kinetics systems are widely applied to describe anomalous diffusion or advection-dispersion processes [1]. Fractional differential equations are comprehensively used in examining physical phenomena in numerous disciplines of engineering and science. For this, we need reliable and efficient techniques for the solutions of fractional differential equations [2, 3]. The fractional-order models are more adequate than the previously used integer-order models because fractional-order derivatives and integrals enable the description of the memory and hereditary properties of different substances [4]. This is the most significant advantage of the fractional-order models in comparison with integer-order models, in which such effects are neglected. In the area of physics, fractional space derivatives are used to model anomalous diffusion or dispersion, where a particle spreads at a rate inconsistent with the classical Brownian motion model [5]. In particular, the Riesz fractional derivative includes a left Riemann–Liouville derivative and a right Riemann–Liouville derivative that allows the modeling of flow regime impacts from either side of the domain [6]. The fractional advection-dispersion equation (FADE) is used in groundwater hydrology to model the transport of passive tracers carried by fluid flow in a porous medium [7–9].

The Riesz fractional advection-dispersion equation (RFADE) with a symmetric fractional derivative, namely the Riesz fractional derivative, was derived from the kinetics of chaotic dynamics by Saichev and Zaslavsky [10] and summarized by Zaslavsky [6]. Ciesielski and Leszczynski [11] presented a numerical solution for the RFADE (without the advection term) based on the finite difference method. Shen et al. [12] presented explicit and implicit difference approximations for the space RFADE with initial and boundary conditions on a finite domain and derived the stability and convergence of their proposed numerical methods.

S. Saha Ray, *Nonlinear Differential Equations in Physics*,
https://doi.org/10.1007/978-981-15-1656-6_4

Fokker–Planck equation (FPE) was introduced by Adriaan Fokker and Max Planck, commonly used to describe the Brownian motion of particles [13]. The FPE describes the change of probability of a random function in space and time, so it is naturally used to describe solute transport. The FPE is involved with the conservation of probability that a particle will occupy a specific location. At any particular time, the sum of the probabilities at all locations must equal unity. So if the probability changes in one location from one moment to the next, the probability must also change in the vicinity to conserve probability. An ensemble of a large number of particles can fulfill the probabilities, and the FPE becomes an equation of the conservation of mass. Also, the nonlinear Fokker–Planck equation has important applications in various other fields. The fractional Fokker–Planck equations have been useful for the description of transport dynamics in complex systems that are governed by anomalous diffusion and nonexponential relaxation patterns [5]. Fractional derivatives play a key role in modeling particle transport in anomalous diffusion. For the description of anomalous transport in the presence of an external field, Metzler and Klafter [5] introduced a time fractional extension of the FPE, namely the time fractional Fokker–Planck equation (TFFPE).

There are some researchers who have investigated the FFPE. So and Liu [14] studied the subdiffusive fractional Fokker–Planck equation of bistable systems. Saha Ray and Gupta [15] established the numerical solutions of time and space fractional Fokker–Planck equations with the aid of two-dimensional Haar wavelets. Chen et al. [16] proposed three different implicit approximations for the TFFPE and proved these approximations are unconditionally stable and convergent. Zhuang et al. [17] presented an implicit numerical method for the TSFFPE and discussed its stability and convergence.

Numerous mathematical methods such as the Adomian decomposition method (ADM) [18], variational iteration method (VIM) [18], operational Tau method (OTM) [19], and homotopy perturbation method (HPM) [20] have been used in order to solve fractional Fokker–Planck equations. In Refs. [18–20], the fractional derivative is considered in Caputo sense. The aim of the present work is to implement shifted Grünwald approximation and fractional centered difference approximation to discretize the Riesz fractional diffusion equation and time and space Riesz fractional Fokker–Planck equation, respectively. The stability and convergence of the proposed finite difference schemes have been also analyzed rigorously.

The classical sine-Gordon equation (SGE) [21] is one of the basic equations of modern nonlinear wave theory, and it arises in many different areas of physics, such as nonlinear optics, Josephson junction theory, field theory, and the theory of lattices [22]. In these applications, the sine-Gordon equation provides the simplest nonlinear description of physical phenomena in different configurations. The theory, methods of solutions, and applications of the celebrated fractional sine-Gordon equation are discussed in great detail in two recent books [23, 24]. Special attention is also given to soliton, antisoliton solutions, and a remarkable new mode that propagates in a two-level atomic system. In order to further emphasis on the analysis of one-soliton and two-soliton solitary wave solutions, it may be referred to Ref. [25].

The more adequate modeling can be prevailed corresponding to the generalization of the classical sine-Gordon equation. In particular, taking into account of nonlocal effects, such as long-range interactions of particles, complex law of medium dispersion, or curvilinear geometry of the initial boundary problem, classical sine-Gordon equation results in the nonlocal generalization of SGE.

In this chapter, the nonlocal generalization of the sine-Gordon equation has been proposed in [26] as follows:

$$u_{tt} - {}^{R}D_{x}^{\alpha}u + \sin u = 0, \tag{4.1}$$

where the nonlocal operator ${}^{R}D_{x}^{\alpha}$ is the Riesz space fractional derivative, $1 \leq \alpha \leq 2$.

These similar types of evolution Eq. (4.2) arise in various interesting problems of nonlocal Josephson electrodynamics. These problems were introduced in [27–32]; among these, one of the basic model equation is

$$u_{tt} - H[u_x] + \sin u = 0, \tag{4.2}$$

where H is the Hilbert transform, given by

$$H[\phi] \equiv \frac{1}{\pi} v \cdot p \cdot \int_{-\infty}^{\infty} \frac{\phi(\xi)}{\xi - x} \mathrm{d}\xi, \tag{4.3}$$

and the integral is understood in the Cauchy principal value sense. The evolution Eq. (4.2) was an object of study in a series of papers [27, 28, 31, 33, 34] available in the open literature. Other nonlocal sine-Gordon equations were considered in [35, 36].

In this case, the derived approximate solutions are based on modified homotopy analysis method with Fourier transform. In this present chapter, we employ a new technique such as applying the Fourier transform followed by homotopy analysis method. This new technique enables derivation of the approximate solutions for the nonlocal fractional sine-Gordon Eq. (4.1). To the best possible information of the author, the present approximation technique has been proposed first time in this work for solving the nonlocal fractional sine-Gordon equation.

4.2 Outline of the Present Study

In this chapter, numerical solutions of fractional Fokker–Planck equations with Riesz space fractional derivatives have been developed. Here, the fractional Fokker–Planck equations have been considered in a finite domain. In order to deal with the Riesz fractional derivative operator, shifted Grünwald approximation and

fractional centered difference approaches have been used. The explicit finite difference method and Crank–Nicolson implicit method have been applied to obtain the numerical solutions of the fractional diffusion equation and fractional Fokker–Planck equations, respectively. Numerical results are presented to demonstrate the accuracy and effectiveness of the proposed numerical solution techniques.

Also, a novel approach comprising modified homotopy analysis method with Fourier transform has been implemented for the approximate solution of the fractional sine-Gordon equation

$$u_{tt} - {}^{R}D_{x}^{\alpha}u + \sin u = 0,$$

where ${}^{R}D_{x}^{\alpha}$ is the Riesz space fractional derivative, $1 \leq \alpha \leq 2$.

For $\alpha = 2$, it becomes a classical sine-Gordon equation

$$u_{tt} - u_{xx} + \sin u = 0,$$

and corresponding to $\alpha = 1$, it becomes nonlocal sine-Gordon equation

$$u_{tt} - Hu + \sin u = 0,$$

which arises in Josephson junction theory, where H is the Hilbert transform. The fractional sine-Gordon equation is considered as an interpolation between the classical sine-Gordon equation (corresponding to $\alpha = 2$) and nonlocal sine-Gordon equation (corresponding to $\alpha = 1$). Here the approximate solution of the fractional sine-Gordon equation is derived by using the modified homotopy analysis method with Fourier transform. Then, the obtained results have been analyzed by numerical simulations, which demonstrate the simplicity and effectiveness of the present method.

4.3 Numerical Approximation Techniques for Riesz Space Fractional Derivative

There are different approximation techniques for Riesz space fractional derivative [37–40]. In the present chapter, the emphasis has been focused on the shifted Grünwald formula to discretize the Riesz space fractional differential equation which, unlike the standard Grünwald formula, does not suffer from instability problems [41] and also on the fractional centered difference approximation technique, respectively.

Let us assume that the function $W(x,t)$ is $n-1$ times continuously differentiable in the interval $[0,L]$ and that $W^{(n)}(x,t)$ is integrable in $[0,L]$. Then for every $\alpha(0 \leq n-1 < \alpha \leq n, n \in \mathbf{N})$, the Riemann–Liouville fractional derivative exists and coincides with the Grünwald–Letnikov derivative. This relationship enables the use of the Grünwald–Letnikov derivative for obtaining the numerical solution [8, 42].

The fractional Grünwald–Letnikov derivative with order $1-\alpha$ is given by

$$\begin{aligned} {}_0D_t^{1-\alpha}W(x,t_k) &= \lim_{\tau\to 0}\tau^{\alpha-1}\sum_{r=0}^{k}(-1)^r\binom{1-\alpha}{r}W(x,t_k-r\tau) \\ &= \tau^{\alpha-1}\sum_{r=0}^{k}\omega_r^{1-\alpha}W(x,t_k-r\tau)+O(\tau^p), \end{aligned} \tag{4.4}$$

where $\tau = T/N$, $t_r = r\tau$, $\omega_0^{1-\alpha} = 1$, $\omega_r^{1-\alpha} = (-1)^r\frac{(1-\alpha)(-\alpha)\ldots(2-\alpha-r)}{r!}$, for $r = 1, 2\ldots, N$.

4.3.1 Shifted Grünwald Approximation Technique for the Riesz Space Fractional Derivative

The shifted Grünwald formula which was proposed by Meerschaert and Tadjeran [41] has been applied for discretizing the Riesz fractional derivative. In this problem, we discretize the Riesz space fractional derivative using the following shifted Grünwald approximation:

$$\frac{\partial^\alpha W(x_l,t)}{\partial|x|^\alpha} \approx -\frac{h^{-\alpha}}{2\cos\left(\frac{\alpha\pi}{2}\right)}\left[\sum_{j=0}^{l+1}\tilde{g}_j W_{l-j+1}+\sum_{j=0}^{m-l+1}\tilde{g}_j W_{l+j-1}\right], \tag{4.5}$$

where the coefficients are defined by

$$\tilde{g}_0 = 1, \tilde{g}_j = (-1)^j\frac{\alpha(\alpha-1)\ldots(\alpha-j+1)}{j!}, \quad j = 1,2,\ldots,m.$$

4.3.2 Fractional Centered Difference Approximation Technique for the Riesz Space Fractional Derivative

Recently, Çelik and Duman [43] derived the interesting result that if $f^*(x)$ be defined as follows

$$f^*(x) = \begin{cases} f(x), & x\in[a,b] \\ 0, & x\notin[a,b] \end{cases}$$

such that $f^*(x)\in C^5(\mathsf{R})$ and all derivatives up to order five belong to $L_1(\mathsf{R})$, then for the Riesz fractional derivative of order $\alpha(1<\alpha\le 2)$

$$\frac{\partial^{\alpha} f(x)}{\partial |x|^{\alpha}} = -h^{-\alpha} \sum_{j=-\frac{b-x}{h}}^{\frac{x-a}{h}} g_j f(x - jh) + O(h^2), \tag{4.6}$$

where $h = \frac{b-a}{m}$, and m is the number of partitions of the interval $[a, b]$ and

$$g_j = \frac{(-1)^j \Gamma(\alpha + 1)}{\Gamma(\alpha/2 - j + 1)\Gamma(\alpha/2 + j + 1)}.$$

Property 4.1 *The coefficients g_j of the fractional centered difference approximation have the following properties for $j = 0, \mp 1, \mp 2, \ldots$, and $\alpha > -1$:*

(i) $g_0 \geq 0$,
(ii) $g_{-j} = g_j \leq 0$ *for all* $|j| \geq 1$,
(iii) $g_{j+1} = \frac{j - \alpha/2}{\alpha/2 + j + 1} g_j$,
(iv) $g_j = O(j^{-\alpha - 1})$.

Proof For the proof of the above properties, it may be referred to Ref. [43].

Lemma 4.1 *Let $f \in C^5(\mathsf{R})$ and all derivatives up to order five belong to $L_1(\mathsf{R})$ and the fractional central derivative of f be*

$$\delta^{\alpha} f(x) = \sum_{j=-\infty}^{\infty} g_j f(x - jh),$$

where

$$g_j = \frac{(-1)^j \Gamma(\alpha + 1)}{\Gamma(\alpha/2 - j + 1)\Gamma(\alpha/2 + j + 1)},$$

then

$$\frac{\partial^{\alpha} f(x)}{\partial |x|^{\alpha}} = -h^{-\alpha} \sum_{j=-\infty}^{\infty} g_j f(x - jh) + O(h^2),$$

when $h \to 0$ and $\frac{\partial^{\alpha} f(x)}{\partial |x|^{\alpha}}$ is the Riesz fractional derivative for $1 < \alpha \leq 2$.

Proof For the proof also, it may be referred to Ref. [43].

4.3.3 Inhomogeneous Fractional Diffusion Equation with Riesz Space Fractional Derivative

Let us consider the following inhomogeneous Riesz fractional diffusion equation with source term in a finite domain associated with initial and Dirichlet boundary conditions [42, 43]

$$\frac{\partial W(x,t)}{\partial t} = K\frac{\partial^{\alpha} W(x,t)}{\partial |x|^{\alpha}} + f(x,t), a < x < b, \quad t \in [0,T], \tag{4.7}$$

$$W(x,0) = \phi(x), a \le x \le b,$$
$$W(a,t) = W(b,t) = 0, 0 \le t \le T,$$

where $K > 0$ is diffusion coefficient and $\phi(x)$ is a real-valued sufficiently smooth function. We consider a super-diffusion model, i.e., $1 < \alpha \le 2$. This type of super-diffusion problems largely arises in the modeling of fluid flow, finance, and other applications.

Explicit Finite Difference Method for Riesz Fractional Diffusion Equation

In this present analysis, numerical solution of Eq. (4.7) has been provided based on the explicit finite difference method (EFDM). Let us assume that the spatial domain is $[0, L]$, and it is partitioned into m subintervals. Thus, the mesh is of m equal subintervals of width $h = L/m$ and $x_l = lh$, for $l = 0, 1, 2, \ldots, m$. Let W_l^k denote the numerical approximation of $W(x_l, t_k)$ at (x_l, t_k).

Now we obtain the following explicit finite difference numerical discretization scheme for the Eq. (4.7).

$$W_l^{k+1} = W_l^k + \tau\left[-\frac{Kh^{-\alpha}}{2\cos\left(\frac{\alpha\pi}{2}\right)}\left(\sum_{j=0}^{l+1}\tilde{g}_j W_{l-j+1}^k + \sum_{j=0}^{m-l+1}\tilde{g}_j W_{l+j-1}^k\right) + f_l^k\right], \tag{4.8}$$

for $l = 1, 2, \ldots, m-1$, and $k = 0, 1, \ldots, N-1$.

The aforementioned Eq. (4.8) determines the numerical approximate value of the solution W_l^{k+1} at (x_l, t_{k+1}).

In matrix form, Eq. (4.8) can be written as

$$\boldsymbol{U}^{k+1} = \boldsymbol{A}\boldsymbol{U}^k + \tau \boldsymbol{F}^{k+1/2}, \tag{4.9}$$

where $\boldsymbol{U}^k = (W_1^k, W_2^k, \ldots, W_{m-1}^k)^T$,

$\boldsymbol{F}^k = \left[f_1^k, f_2^k, \ldots, f_{m-1}^k\right]^T$, and $\boldsymbol{A}_i$ is a symmetric $(m-1)\times(m-1)$ matrix of the following form

$$\boldsymbol{A} = \begin{pmatrix} 1 - \frac{K\tau h^{-\alpha}}{\cos\frac{\alpha\pi}{2}}\tilde{g}_1 & -\frac{K\tau h^{-\alpha}}{2\cos\frac{\alpha\pi}{2}}(\tilde{g}_0+\tilde{g}_2) & -\frac{K\tau h^{-\alpha}}{2\cos\frac{\alpha\pi}{2}}\tilde{g}_3 & \cdots & -\frac{K\tau h^{-\alpha}}{2\cos\frac{\alpha\pi}{2}}\tilde{g}_{m-1} \\ -\frac{K\tau h^{-\alpha}}{2\cos\frac{\alpha\pi}{2}}(\tilde{g}_0+\tilde{g}_2) & 1 - \frac{K\tau h^{-\alpha}}{\cos\frac{\alpha\pi}{2}}\tilde{g}_1 & -\frac{K\tau h^{-\alpha}}{2\cos\frac{\alpha\pi}{2}}(\tilde{g}_0+\tilde{g}_2) & \cdots & -\frac{K\tau h^{-\alpha}}{2\cos\frac{\alpha\pi}{2}}\tilde{g}_{m-2} \\ \cdots & \cdots & \cdots & \cdots & \\ -\frac{K\tau h^{-\alpha}}{2\cos\frac{\alpha\pi}{2}}\tilde{g}_{m-1} & -\frac{K\tau h^{-\alpha}}{2\cos\frac{\alpha\pi}{2}}\tilde{g}_{m-2} & -\frac{K\tau h^{-\alpha}}{2\cos\frac{\alpha\pi}{2}}\tilde{g}_{m-3} & \cdots & 1 - \frac{K\tau h^{-\alpha}}{\cos\frac{\alpha\pi}{2}}\tilde{g}_1 \end{pmatrix}. \tag{4.10}$$

4.3.4 Time and Space Fractional Fokker–Planck Equation with Riesz Fractional Operator

In this section, we consider the following time and space fractional Fokker–Planck equation which describes the anomalous transport in the presence of an external field [42]

$$\frac{\partial W(x,t)}{\partial t} = {}_0D_t^{1-\alpha}\left[\left(\frac{\partial}{\partial x}\frac{V'(x)}{m\eta_\alpha} + K_\alpha^\mu \frac{\partial^\mu}{\partial|x|^\mu}\right)W(x,t) + f(x,t)\right], a < x < b, \quad t \in [0,T], \tag{4.11}$$

subject to initial and homogeneous Dirichlet boundary conditions

$$W(x,0) = \phi(x), a \le x \le b,$$
$$W(a,t) = W(b,t) = 0, 0 \le t \le T,$$

where K_α^μ denotes the anomalous diffusion coefficient; m is the mass of the diffusing test particle; η_α is the generalized friction constant of dimension $[\eta_\alpha] = s^{\alpha-2}$; $\frac{V'(x)}{m\eta_\alpha}$ is known as the drift coefficient, and the force is related to the external potential through $F(x) = -\frac{\mathrm{d}V(x)}{\mathrm{d}x}$. ${}_0D_t^{1-\alpha}(.)$ denotes the Riemann–Liouville time fractional derivative of order $1-\alpha(0<\alpha<1)$ defined by [44–47]

$${}_0D_t^{1-\alpha}\psi(x,t) = \frac{1}{\Gamma(\alpha)}\frac{\partial}{\partial t}\int_0^t \frac{\psi(x,\zeta)}{(t-\zeta)^{1-\alpha}}\mathrm{d}\zeta. \tag{4.12}$$

For $\alpha \to 1$ and $\mu \to 2$, the standard Fokker–Planck equation [5] is recovered, and for $\alpha \to 1$ and $V(x) \equiv$ const., i.e., in the force-free limit, the inhomogeneous fractional diffusion Eq. (4.7) emerges.

The Riesz space fractional derivative of order $v(1<v<2)$ is defined by [48, 49]

$$\frac{\partial^v W(x_l,t)}{\partial|x|^v} = -\frac{1}{2\cos\left(\frac{\pi v}{2}\right)}\left({}_aD_x^v + {}_xD_b^v\right)W(x,t), \tag{4.13}$$

where ${}_aD_x^v$ and ${}_xD_b^v$ are the left and right Riemann–Liouville space fractional derivative operators of order v, which are, respectively, given by

$${}_aD_x^v W(x,t) = \frac{1}{\Gamma(2-v)}\frac{\partial^2}{\partial x^2}\int_a^x \frac{W(\xi,t)}{(x-\xi)^{v-1}}\mathrm{d}\xi,$$

$${}_xD_b^v W(x,t) = \frac{1}{\Gamma(2-v)}\frac{\partial^2}{\partial x^2}\int_x^b \frac{W(\xi,t)}{(\xi-x)^{v-1}}\mathrm{d}\xi.$$

Implicit Finite Difference Method for Time and Riesz Space Fractional Fokker–Planck Equation

In order to solve Eq. (4.11) with the drift coefficient $-v$, fractional centered difference approximation along with Grünwald–Letnikov derivative approximation has been used to discretize it.

From Taylor's theorem, we have

$$\frac{W_l^{k+1}-W_l^k}{\tau} = \left(\frac{\partial W}{\partial t}\right)_l^{k+1/2} + O(\tau^2), \tag{4.14}$$

where the central difference with step size $\tau/2$ has been used.

Thus, using Eq. (4.14) and Lemma 4.1, we obtain the following implicit finite difference discretization scheme

$$\begin{aligned}\frac{W_l^{k+1}-W_l^k}{\tau} = \frac{1}{2}\Bigg[&-v\tau^{\alpha-1}\sum_{j=0}^{k}\omega_j^{1-\alpha}\left(\frac{W_{l+1}^{k-j}-W_l^{k-j}}{h}\right)\\ &-K_\alpha^\mu\,\tau^{\alpha-1}\,h^{-\mu}\sum_{j=0}^{k}\omega_j^{1-\alpha}\sum_{i=l-m}^{l}g_i W_{l-i}^{k-j}+\tau^{\alpha-1}\sum_{j=0}^{k}\omega_j^{1-\alpha}f_l^{k-j}\\ &-v\tau^{\alpha-1}\sum_{j=0}^{k+1}\omega_j^{1-\alpha}\left(\frac{W_{l+1}^{k+1-j}-W_l^{k+1-j}}{h}\right)-K_\alpha^\mu\,\tau^{\alpha-1}\,h^{-\mu}\sum_{j=0}^{k+1}\omega_j^{1-\alpha}\sum_{i=l-m}^{l}g_i W_{l-i}^{k+1-j}\\ &+\tau^{\alpha-1}\sum_{j=0}^{k+1}\omega_j^{1-\alpha}f_l^{k+1-j}\Bigg]+TE_l^{k+1/2},\end{aligned} \tag{4.15}$$

for $l=1,2,\ldots,m-1$, and $k=0,1,\ldots,N-1$, where the local truncation error $TE_l^{k+1/2}\equiv O(\tau^2+h^2)$.

Now, omitting the local truncation error in Eq. (4.15), we obtain

$$
\begin{aligned}
&W_l^{k+1}+\frac{v\tau^\alpha}{2}\omega_0^{1-\alpha}\left(\frac{W_{l+1}^{k+1}-W_l^{k+1}}{h}\right)+K_\alpha^\mu\frac{\tau^\alpha}{2}h^{-\mu}\omega_0^{1-\alpha}\sum_{i=l-m}^{l}g_iW_{l-i}^{k+1}=W_l^k\\
&-\frac{v\tau^\alpha}{2}\sum_{r=0}^{k}\omega_r^{1-\alpha}\left(\frac{W_{l+1}^{k-r}-W_l^{k-r}}{h}\right)-K_\alpha^\mu\frac{\tau^\alpha}{2}h^{-\mu}\sum_{r=0}^{k}\omega_r^{1-\alpha}\sum_{i=l-m}^{l}g_iW_{l-i}^{k-r}\\
&+\frac{\tau^\alpha}{2}\left(\sum_{r=0}^{k}\omega_r^{1-\alpha}f_l^{k-r}+\sum_{r=0}^{k+1}\omega_r^{1-\alpha}f_l^{k+1-r}\right)-v\frac{\tau^\alpha}{2}\sum_{r=1}^{k+1}\omega_r^{1-\alpha}\left(\frac{W_{l+1}^{k+1-r}-W_l^{k+1-r}}{h}\right)\\
&-K_\alpha^\mu\frac{\tau^\alpha}{2}h^{-\mu}\sum_{r=1}^{k+1}\omega_r^{1-\alpha}\sum_{i=l-m}^{l}g_iW_{l-i}^{k+1-r}.
\end{aligned}
\tag{4.16}
$$

Further, Eq. (4.16) can be written into the following matrix form

$$
\begin{aligned}
(\boldsymbol{I}+\boldsymbol{A}_0)\boldsymbol{U}^{k+1}=&(\boldsymbol{I}-\boldsymbol{A}_0-\boldsymbol{A}_1)\boldsymbol{U}^k-(\boldsymbol{A}_1+\boldsymbol{A}_2)\boldsymbol{U}^{k-1}-(\boldsymbol{A}_2+\boldsymbol{A}_3)\boldsymbol{U}^{k-2}-\cdots\\
&-(\boldsymbol{A}_k+\boldsymbol{A}_{k+1})\boldsymbol{U}^0+\tau^\alpha\boldsymbol{F}^{k+1/2},
\end{aligned}
\tag{4.17}
$$

where $\boldsymbol{U}^k=(W_1^k,W_2^k,\ldots,W_{m-1}^k)^T$,

$$
\begin{aligned}
F^{k+1/2}=&\left[\frac{1}{2}\left(\sum_{r=0}^{k}\omega_r^{1-\alpha}f_1^{k-r}+\sum_{r=0}^{k+1}\omega_r^{1-\alpha}f_1^{k+1-r}\right),\frac{1}{2}\left(\sum_{r=0}^{k}\omega_r^{1-\alpha}f_2^{k-r}+\sum_{r=0}^{k+1}\omega_r^{1-\alpha}f_2^{k+1-r}\right),\right.\\
&\left.\ldots,\frac{\tau^\alpha}{2}\left(\sum_{r=0}^{k}\omega_r^{1-\alpha}f_{m-1}^{k-r}+\sum_{r=0}^{k+1}\omega_r^{1-\alpha}f_{m-1}^{k+1-r}\right)\right]^T,
\end{aligned}
$$

and $\boldsymbol{A}_i$ is an $(m-1)\times(m-1)$ matrix of the following form

$$
\boldsymbol{A}_i=\omega_i^{1-\alpha}\begin{pmatrix}
-\frac{v\tau^\alpha}{2h}+\frac{K_\alpha^\mu\tau^\alpha}{2}h^{-\mu}g_0 & \frac{v\tau^\alpha}{2h}+\frac{K_\alpha^\mu\tau^\alpha}{2}h^{-\mu}g_{-1} & \cdots & \frac{K_\alpha^\mu\tau^\alpha}{2}h^{-\mu}g_{2-m}\\
\frac{K_\alpha^\mu\tau^\alpha}{2}h^{-\mu}g_1 & -\frac{v\tau^\alpha}{2h}+\frac{K_\alpha^\mu\tau^\alpha}{2}h^{-\mu}g_0 & \cdots & \frac{K_\alpha^\mu\tau^\alpha}{2}h^{-\mu}g_{3-m}\\
\cdots & \cdots & \cdots & \cdots\\
\frac{K_\alpha^\mu\tau^\alpha}{2}h^{-\mu}g_{m-2} & \frac{K_\alpha^\mu\tau^\alpha}{2}h^{-\mu}g_{m-3} & \cdots & -\frac{v\tau^\alpha}{2h}+\frac{K_\alpha^\mu\tau^\alpha}{2}h^{-\mu}g_0
\end{pmatrix}.
\tag{4.18}
$$

Now, we define the function space as follows: $\Lambda(\Omega)=\left\{W(x,t)\middle|\frac{\partial^5W(x,t)}{\partial x^5},\frac{\partial^4W(x,t)}{\partial x^2\partial t^2}\in C(\Omega)\right\}$, where $\Omega\equiv[a,b]\times[0,T]$. In this work, we assume that the Problems (4.7) and (4.11) have a smooth exact solution $W(x,t)\in\Lambda(\Omega)$, and $f(x,t)$ and $\phi(x)$ are sufficiently smooth functions.

4.3.5 Numerical Results for Riesz Fractional Diffusion Equation and Riesz Fractional Fokker–Planck Equation

In the present section, the numerical examples for Riesz fractional diffusion Eq. (4.7) and time and Riesz space fractional Fokker–Planck Eq. (4.11) with the drift coefficient $-v$ have been presented to demonstrate the effectiveness of the above-discussed numerical schemes for solving Riesz fractional diffusion equation and time-space fractional Fokker–Planck equation with Riesz derivative operator.

Example 4.1 Let us consider the following Riesz fractional diffusion equation [42, 43] on the finite domain $[0, 1]$.

$$\frac{\partial W(x,t)}{\partial t} = K\frac{\partial^{\alpha} W(x,t)}{\partial |x|^{\alpha}} + f(x,t), 0 < x < 1, \quad t \in [0,T], \tag{4.19}$$

subject to initial and homogeneous Dirichlet boundary conditions

$$W(x,0) = x^2(1-x)^2, 0 \le x \le 1,$$
$$W(0,t) = W(1,t) = 0, 0 \le t \le T$$

and the nonhomogenous part is

$$f(x,t) = (1+t)^{-1+\alpha}(-1+x)^2x^2\alpha + \frac{1}{\Gamma(5-\alpha)}x^{-\alpha}\left[\left(\frac{1+t}{1-x}\right)^{\alpha}(-1+x)^2x^{\alpha}(12x^2 - 6x\alpha + (-1+\alpha)\alpha) + (1+t)^{\alpha}x^2\left[12(-1+x)^2 + (-7+6x)\alpha + \alpha^2\right]\right]\sec\left(\frac{\pi\alpha}{2}\right).$$

The exact solution is

$$W(x,t) = (1+t)^{\alpha}x^2(1-x)^2. \tag{4.20}$$

In this example, we take $K = 1$, $\tau = 0.001$, and $h = 0.05$. Figures 4.1, 4.2, and 4.3 show the comparison of the exact and numerical solutions when $\alpha = 1.5$ at $t = 1, 3, 5$, respectively. It can be easily observed that the numerical solutions are in good agreement with the exact solution.

Example 4.2 Let us consider the following time fractional Fokker–Planck equation with Riesz space fractional derivative operator [42]

$$\frac{\partial W(x,t)}{\partial t} = {}_0D_t^{1-\alpha}\left[\left(-v\frac{\partial}{\partial x} + K_{\alpha}^{\mu}\frac{\partial^{\mu}}{\partial |x|^{\mu}}\right)W(x,t) + f(x,t)\right], 0 < x < 1, \quad t \in [0,T], \tag{4.21}$$

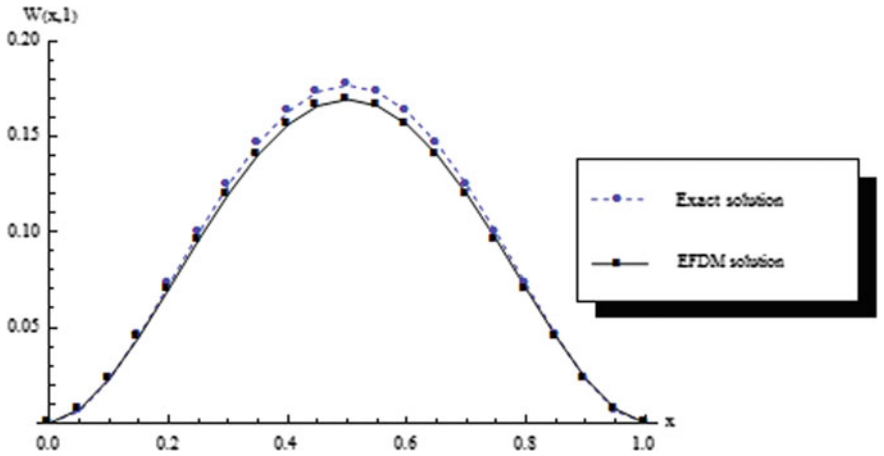

Fig. 4.1 Comparison of numerical solution of $W(x,t)$ with the exact solution at $t = 1$ for Example 4.1 with $\alpha = 1.5$, $h = 0.05$, and $\tau = 0.001$

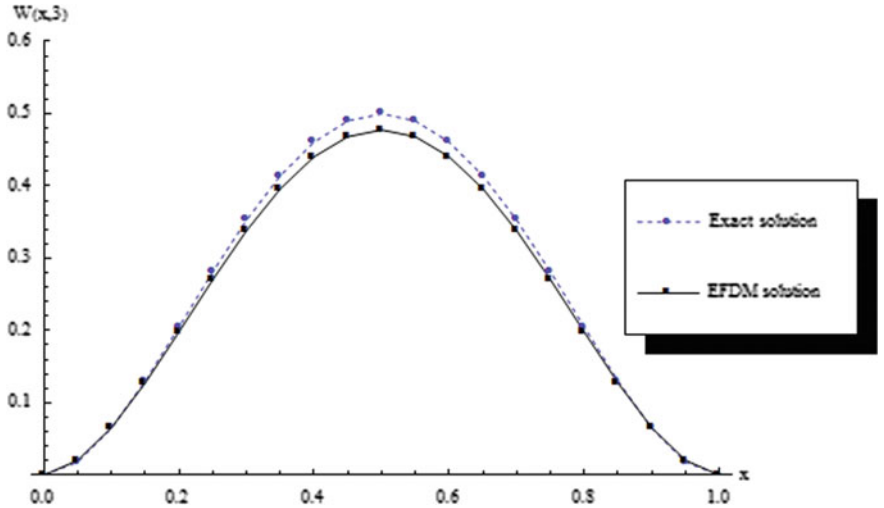

Fig. 4.2 Comparison of numerical solution of $W(x,t)$ with the exact solution at $t = 3$ for Example 4.1 with $\alpha = 1.5$, $h = 0.05$, and $\tau = 0.001$

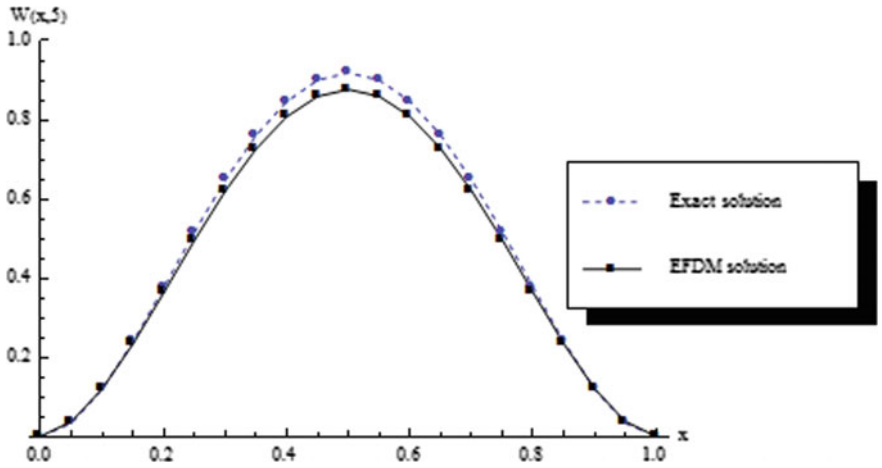

Fig. 4.3 Comparison of numerical solution of $W(x,t)$ with the exact solution at $t = 5$ for Example 4.1 with $\alpha = 1.5$, $h = 0.05$, and $\tau = 0.001$

subject to initial and homogeneous Dirichlet boundary conditions

$$W(x,0) = K_\alpha^\mu x^2(1-x)^2, 0 \le x \le 1,$$
$$W(0,t) = W(1,t) = 0, 0 \le t \le T,$$

The exact solution is

$$W(x,t) = (K_\alpha^\mu + vt^{1+\alpha})x^2(1-x)^2. \tag{4.22}$$

In this example, we take $K_\alpha^\mu = 25$, $\tau = 0.001$, $h = 0.05$, $\alpha = 0.8$, and $\mu = 1.9$. Figure 4.4 shows the comparison between the exact and numerical solutions at $t = 1$. In Fig. 4.5, comparison of numerical solution of $W(x,t)$ with the exact solution at $t = 3$ has been presented for Example 4.2 with $\alpha = 0.8$, $\mu = 1.9$, $h = 0.02$, and $\tau = 0.075$. Figure 4.6 explores the comparison of results for Example 4.2 with $\alpha = 0.8$, $\mu = 1.9$, $h = 0.02$, and $\tau = 0.1$. It can be clearly observed from the presented figures that the implicit finite difference solutions highly agree with the exact solutions.

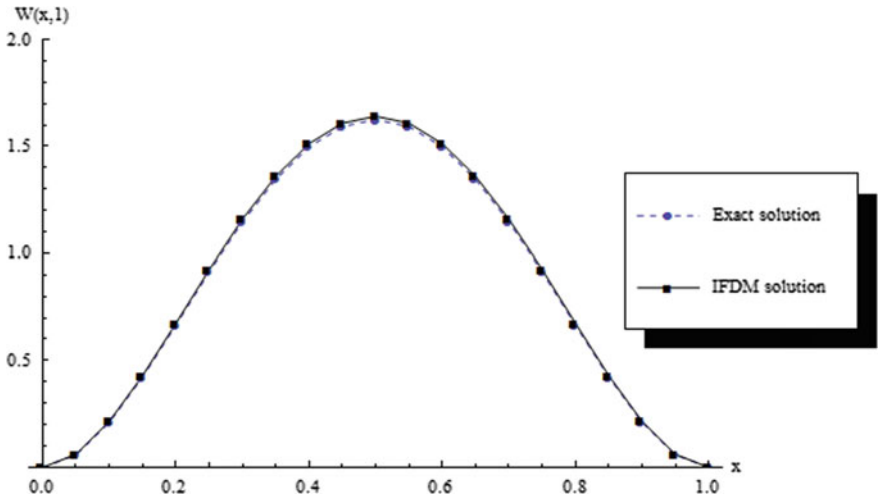

Fig. 4.4 Comparison of numerical solution of $W(x,t)$ with the exact solution at $t=1$ for Example 4.2 with $\alpha=0.8$, $\mu=1.9$, $h=0.05$, and $\tau=0.01$

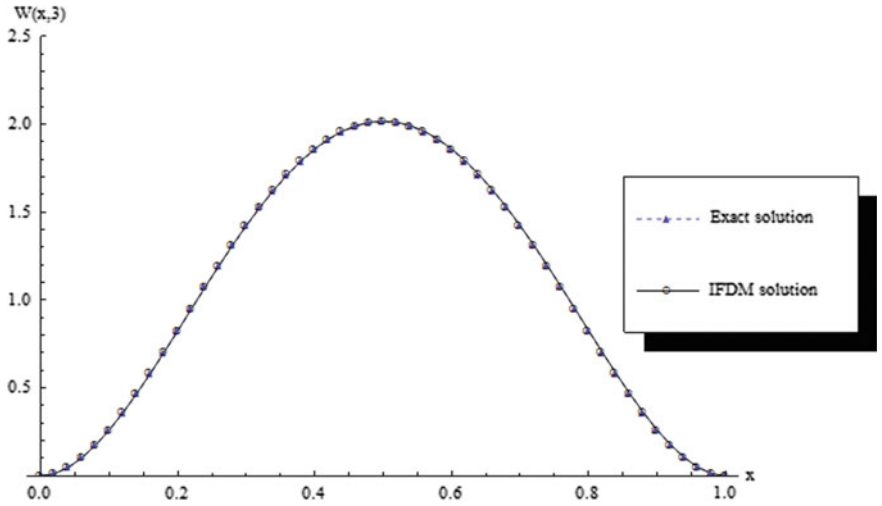

Fig. 4.5 Comparison of numerical solution of $W(x,t)$ with the exact solution at $t=3$ for Example 4.2 with $\alpha=0.8$, $\mu=1.9$, $h=0.02$, and $\tau=0.075$

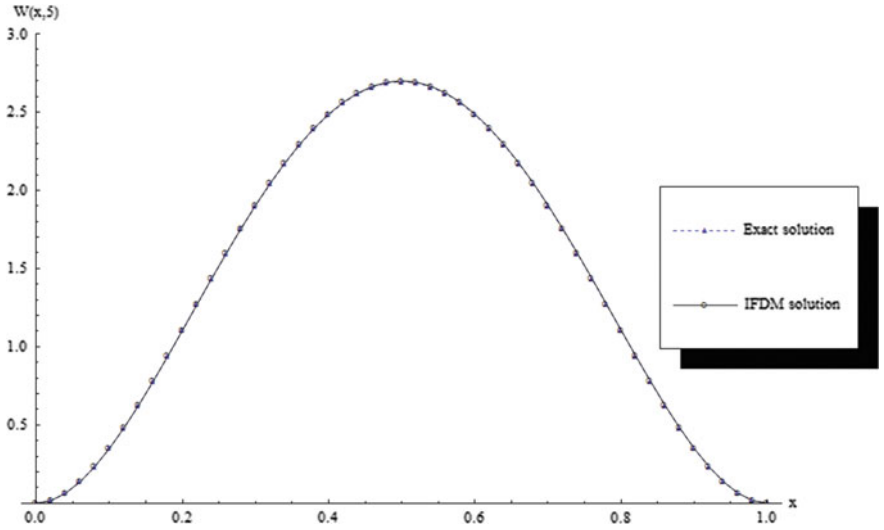

Fig. 4.6 Comparison of numerical solution of $W(x,t)$ with the exact solution at $t=5$ for Example 4.2 with $\alpha=0.8$, $\mu=1.9$, $h=0.02$, and $\tau=0.1$

4.3.6 *Stability and Convergence of the Proposed Finite Difference Schemes*

Theorem 4.1 *The numerical discretization scheme for the problem in* Eq. (4.19) *is stable, if*

$$r=\frac{\tau}{h^{\alpha}}\leq\frac{2\left|\cos\frac{\alpha\pi}{2}\right|}{K\left(\frac{\tilde{g}_1-(\tilde{g}_0+\tilde{g}_2)}{\operatorname{sgn}\left(\cos\frac{\alpha\pi}{2}\right)}+\tilde{g}_0\right)},\quad \text{for } 1<\alpha\leq 2.$$

Proof The matrix A in Eq. (4.10) can be written as

$$A=T+R, \tag{4.23}$$

where T is a tridiagonal $(m-1)\times(m-1)$ matrix of the following form

$$T=\begin{pmatrix} 1-\frac{K\tau h^{-\alpha}}{\cos\frac{\alpha\pi}{2}}\tilde{g}_1 & -\frac{K\tau h^{-\alpha}}{2\cos\frac{\alpha\pi}{2}}(\tilde{g}_0+\tilde{g}_2) & 0 & \dots & 0 \\ -\frac{K\tau h^{-\alpha}}{2\cos\frac{\alpha\pi}{2}}(\tilde{g}_0+\tilde{g}_2) & 1-\frac{K\tau h^{-\alpha}}{\cos\frac{\alpha\pi}{2}}\tilde{g}_1 & -\frac{K\tau h^{-\alpha}}{2\cos\frac{\alpha\pi}{2}}(\tilde{g}_0+\tilde{g}_2) & \dots & 0 \\ \dots & \dots & \dots & \dots & \dots \\ 0 & 0 & 0 & \dots & 1-\frac{K\tau h^{-\alpha}}{\cos\frac{\alpha\pi}{2}}\tilde{g}_1 \end{pmatrix}, \tag{4.24}$$

and R is a symmetric $(m-1)\times(m-1)$ matrix of the following form

$$R=\begin{pmatrix} 0 & 0 & -\frac{K\tau h^{-\alpha}}{2\cos\frac{\alpha\pi}{2}}\tilde{g}_3 & \cdots & -\frac{K\tau h^{-\alpha}}{2\cos\frac{\alpha\pi}{2}}\tilde{g}_{m-1} \\ 0 & 0 & 0 & \cdots & -\frac{K\tau h^{-\alpha}}{2\cos\frac{\alpha\pi}{2}}\tilde{g}_{m-2} \\ \cdots & \cdots & \cdots & \cdots & \cdots \\ -\frac{K\tau h^{-\alpha}}{2\cos\frac{\alpha\pi}{2}}\tilde{g}_{m-1} & -\frac{K\tau h^{-\alpha}}{2\cos\frac{\alpha\pi}{2}}\tilde{g}_{m-2} & -\frac{K\tau h^{-\alpha}}{2\cos\frac{\alpha\pi}{2}}\tilde{g}_{m-3} & \cdots & 0 \end{pmatrix}.$$

Now, let λ_i be the eigenvalue of the matrix R. Then, according to the Gerschgorin circle theorem [50], we have

$$|\lambda_i-0|\le\frac{K\tau h^{-\alpha}}{2\left|\cos\frac{\alpha\pi}{2}\right|}\sum_{k=3}^{m-1}|\tilde{g}_k|<\frac{K\tau h^{-\alpha}}{2\left|\cos\frac{\alpha\pi}{2}\right|}\sum_{k=3}^{\infty}\tilde{g}_k<\frac{K\tau h^{-\alpha}}{2\left|\cos\frac{\alpha\pi}{2}\right|}, \tag{4.25}$$

where $\sum_{k=3}^{\infty}\tilde{g}_k=-1+\alpha-\frac{\alpha(\alpha-1)}{2!}<1$.

This implies that

$$\|R\|_2=\rho(R)\le\frac{K\tau h^{-\alpha}}{2\left|\cos\frac{\alpha\pi}{2}\right|}, \tag{4.26}$$

since R is a real and symmetric matrix.

Now, the eigenvalues of the tridiagonal matrix T are given by [51]

$$\lambda_v=1-\frac{K\tau h^{-\alpha}}{\cos\frac{\alpha\pi}{2}}\tilde{g}_1-\frac{K\tau h^{-\alpha}}{\cos\frac{\alpha\pi}{2}}(\tilde{g}_0+\tilde{g}_2)\cos\frac{v\pi}{m},\quad v=1,2,\ldots,m-1. \tag{4.27}$$

Now, let assume that $\overline{W}_l^k$ be the computed value of W_l^k of the explicit finite difference numerical scheme in Eq. (4.8), let $\varepsilon_l^k=\bar{W}_l^k-W_l^k$ and $\boldsymbol{Y}^k=[\varepsilon_1^k,\varepsilon_2^k,\ldots,\varepsilon_{m-1}^k]^T$.

Then, the vector $\boldsymbol{Y}^k$ satisfies the following equation

$$\boldsymbol{Y}^{k+1}=A\boldsymbol{Y}^k. \tag{4.28}$$

Thus, the explicit finite difference numerical scheme in Eq. (4.8) is stable if

$$\|A\|_2=\rho(A)\le\|T\|_2+\|R\|_2\le 1$$

This implies that

$$\left|1-\frac{K\tau h^{-\alpha}}{\cos\frac{\alpha\pi}{2}}\tilde{g}_1-\frac{K\tau h^{-\alpha}}{\cos\frac{\alpha\pi}{2}}(\tilde{g}_0+\tilde{g}_2)\cos\frac{(m-1)\pi}{m}\right|+\left|\frac{rK}{2\cos\frac{\alpha\pi}{2}}\right|\le 1, \tag{4.29}$$

After simplifications, from Eq. (4.29), we obtain

$$r \leq \frac{2\left|\cos\frac{\alpha\pi}{2}\right|}{K\left(\frac{\tilde{g}_1-(\tilde{g}_0+\tilde{g}_2)}{\operatorname{sgn}\left(\cos\frac{\alpha\pi}{2}\right)}+\tilde{g}_0\right)}, \tag{4.30}$$

as $h \to 0$, $m \to \infty$.

This completes the proof. ■

Theorem 4.2 *The numerical discretization scheme for the problem in* Eq. (4.21) *is unconditionally stable.*

Proof The matrix $\boldsymbol{A}_i$ in Eq. (4.18) can be written as

$$\boldsymbol{A}_i = \omega_i^{1-\alpha}\left(P + \frac{\nu\tau^\alpha}{2h}J\right), \quad i = 0, 1, 2, \ldots, k+1, \tag{4.31}$$

where

$$P = \begin{pmatrix} \frac{K_\alpha^\mu\tau^\alpha}{2}h^{-\mu}g_0 & \frac{K_\alpha^\mu\tau^\alpha}{2}h^{-\mu}g_{-1} & \ldots & \frac{K_\alpha^\mu\tau^\alpha}{2}h^{-\mu}g_{2-m} \\ \frac{K_\alpha^\mu\tau^\alpha}{2}h^{-\mu}g_1 & \frac{K_\alpha^\mu\tau^\alpha}{2}h^{-\mu}g_0 & \ldots & \frac{K_\alpha^\mu\tau^\alpha}{2}h^{-\mu}g_{3-m} \\ \ldots & \ldots & \ldots & \ldots \\ \frac{K_\alpha^\mu\tau^\alpha}{2}h^{-\mu}g_{m-2} & \frac{K_\alpha^\mu\tau^\alpha}{2}h^{-\mu}g_{m-3} & \ldots & \frac{K_\alpha^\mu\tau^\alpha}{2}h^{-\mu}g_0 \end{pmatrix},$$

$$J = \begin{pmatrix} -1 & 1 & 0 & \ldots & 0 \\ 0 & -1 & 1 & \ldots & 0 \\ \ldots & \ldots & \ldots & \ldots & \ldots \\ 0 & 0 & 0 & \ldots & -1 \end{pmatrix}.$$

Since $g_{-j} = g_j$, P is a $(m-1) \times (m-1)$ symmetric matrix and J is a $(m-1)\times(m-1)$ Jordan block matrix with eigenvalue -1.

Now, let λ_j be the eigenvalue of the matrix P. Then, according to the Gerschgorin circle theorem [50], we have

$$\left|\lambda_j - \frac{K_\alpha^\mu\tau^\alpha}{2}h^{-\mu}g_0\right| \leq \frac{K_\alpha^\mu\tau^\alpha}{2}h^{-\mu}\sum_{\substack{k=1 \\ k\neq i}}^{m-1}|g_{i-k}| < \frac{K_\alpha^\mu\tau^\alpha}{2}h^{-\mu}g_0, \tag{4.32}$$

where $\sum_{\substack{k=-\infty \\ k\neq 0}}^{\infty}|g_k| = g_0$.

This implies that

$$0 < \lambda_j < K_\alpha^\mu \tau^\alpha h^{-\mu} g_0. \tag{4.33}$$

Thus, the eigenvalue of $\boldsymbol{A}_i$ satisfies the following range

$$-\omega_i^{1-\alpha} \frac{\nu\tau^\alpha}{h} < \lambda(\boldsymbol{A}_i) < \omega_i^{1-\alpha} K_\alpha^\mu \tau^\alpha h^{-\mu} g_0$$

Therefore, we obtain

$$\rho(\boldsymbol{A}_i) < \omega_i^{1-\alpha} K_\alpha^\mu \tau^\alpha h^{-\mu} g_0 + \omega_i^{1-\alpha} \frac{\nu\tau^\alpha}{2h}. \tag{4.34}$$

Now, let assume that $\bar{W}_l^k$ be the computed value of W_l^k of the second-order accurate implicit numerical scheme in Eq. (4.16), let $\varepsilon_l^k = \bar{W}_l^k - W_l^k$ and $\boldsymbol{Y}^k = [\varepsilon_1^k, \varepsilon_2^k, \ldots, \varepsilon_{m-1}^k]^T$.

Then, the vector $\boldsymbol{Y}^k$ satisfies the following equation

$$\begin{aligned} \boldsymbol{Y}^{k+1} = {} & (\boldsymbol{I}+\boldsymbol{A}_0)^{-1}(\boldsymbol{I}-\boldsymbol{A}_0-\boldsymbol{A}_1)\boldsymbol{Y}^k - (\boldsymbol{I}+\boldsymbol{A}_0)^{-1}(\boldsymbol{A}_1+\boldsymbol{A}_2)\boldsymbol{Y}^{k-1} \\ & - (\boldsymbol{I}+\boldsymbol{A}_0)^{-1}(\boldsymbol{A}_2+\boldsymbol{A}_3)\boldsymbol{Y}^{k-2} - \cdots - (\boldsymbol{I}+\boldsymbol{A}_0)^{-1}(\boldsymbol{A}_k+\boldsymbol{A}_{k+1})\boldsymbol{Y}^0. \end{aligned} \tag{4.35}$$

Therefore, we obtain

$$\begin{aligned} \left\|\boldsymbol{Y}^{k+1}\right\|_2 \le {} & \left\|(\boldsymbol{I}+\boldsymbol{A}_0)^{-1}(\boldsymbol{I}-\boldsymbol{A}_0-\boldsymbol{A}_1)\right\|_2 \left\|\boldsymbol{Y}^k\right\|_2 + \left\|(\boldsymbol{I}+\boldsymbol{A}_0)^{-1}(\boldsymbol{A}_1+\boldsymbol{A}_2)\right\|_2 \left\|\boldsymbol{Y}^{k-1}\right\|_2 \\ & + \left\|(\boldsymbol{I}+\boldsymbol{A}_0)^{-1}(\boldsymbol{A}_2+\boldsymbol{A}_3)\right\|_2 \left\|\boldsymbol{Y}^{k-2}\right\|_2 + \cdots + \left\|(\boldsymbol{I}+\boldsymbol{A}_0)^{-1}(\boldsymbol{A}_k+\boldsymbol{A}_{k+1})\right\|_2 \left\|\boldsymbol{Y}^0\right\|_2. \end{aligned} \tag{4.36}$$

Now, without loss of generality, there exists $\alpha_i \in \mathsf{R}^+$, $i = 0, 1, \ldots, k$ such that

$$\begin{aligned} & \left\|(\boldsymbol{I}+\boldsymbol{A}_0)^{-1}(\boldsymbol{I}-\boldsymbol{A}_0-\boldsymbol{A}_1)\right\|_2 = [\rho([(\boldsymbol{I}+\boldsymbol{A}_0)^{-1}(\boldsymbol{I}-\boldsymbol{A}_0-\boldsymbol{A}_1)]^T[(\boldsymbol{I}+\boldsymbol{A}_0)^{-1}(\boldsymbol{I}-\boldsymbol{A}_0-\boldsymbol{A}_1)])]^{1/2} \le \alpha_k, \\ & \left\|(\boldsymbol{I}+\boldsymbol{A}_0)^{-1}(\boldsymbol{A}_1+\boldsymbol{A}_2)\right\|_2 = [\rho([(\boldsymbol{I}+\boldsymbol{A}_0)^{-1}(\boldsymbol{A}_1+\boldsymbol{A}_2)]^T[(\boldsymbol{I}+\boldsymbol{A}_0)^{-1}(\boldsymbol{A}_1+\boldsymbol{A}_2)])]^{1/2} \le \alpha_{k-1}, \\ & \ldots, \\ & \left\|(\boldsymbol{I}+\boldsymbol{A}_0)^{-1}(\boldsymbol{A}_k+\boldsymbol{A}_{k+1})\right\|_2 = [\rho([(\boldsymbol{I}+\boldsymbol{A}_0)^{-1}(\boldsymbol{A}_k+\boldsymbol{A}_{k+1})]^T[(\boldsymbol{I}+\boldsymbol{A}_0)^{-1}(\boldsymbol{A}_k+\boldsymbol{A}_{k+1})])]^{1/2} \le \alpha_0. \end{aligned} \tag{4.37}$$

Consequently, we obtain

$$\left\|\boldsymbol{Y}^{k+1}\right\|_2 \le \alpha_k \left\|\boldsymbol{Y}^k\right\|_2 + \alpha_{k-1} \left\|\boldsymbol{Y}^{k-1}\right\|_2 + \alpha_{k-2} \left\|\boldsymbol{Y}^{k-2}\right\|_2 + \cdots + \alpha_0 \left\|\boldsymbol{Y}^0\right\|_2. \tag{4.38}$$

Hence, we conclude that

$$\left\|\boldsymbol{Y}^{k+1}\right\|_2 \leq \alpha_0(\alpha_1+1)(\alpha_2+1)\ldots(\alpha_k+1)\left\|\boldsymbol{Y}^0\right\|_2. \tag{4.39}$$

Thus, the second-order accurate implicit numerical scheme in Eq. (4.16) for the problem (4.21) is unconditionally stable. ■

Theorem 4.3 *Assuming that the problem in* Eq. (4.21) *has a smooth exact solution* $W_l^n = W(x_l, t_n) \in \Lambda(\Omega)$ *and* $\bar{W}_l^n$ *be the numerically computed solution of the second-order implicit numerical scheme in* Eq. (4.15). *Then, the numerical solution* $\bar{W}_l^n$ *unconditionally converges to* W_l^n *as* h *and* τ *tend to zero.*

Proof Let the error at the grid point (x_l, t_k) defined by $e_l^k = \bar{W}_l^k - W_l^k$ and $\boldsymbol{E}^k = (e_1^k, e_2^k, \ldots, e_{m-1}^k)^T$. Then, from Eqs. (4.15) and (4.16) for problem 4.2, we have

$$\begin{aligned}\frac{\mathrm{e}_l^{k+1}-\mathrm{e}_l^k}{\tau} &= -\frac{v}{2}\tau^{\alpha-1}\sum_{r=0}^{k}\omega_r^{1-\alpha}\left(\frac{\mathrm{e}_{l+1}^{k-r}-\mathrm{e}_l^{k-r}}{h}\right) - \frac{v}{2}\tau^{\alpha-1}\sum_{r=1}^{k+1}\omega_r^{1-\alpha}\left(\frac{\mathrm{e}_{l+1}^{k+1-r}-\mathrm{e}_l^{k+1-r}}{h}\right)\\ &\quad -\frac{K_\alpha^\mu\tau^{\alpha-1}}{2}h^{-\mu}\sum_{r=0}^{k}\omega_r^{1-\alpha}\sum_{i=l-m}^{l}g_i\mathrm{e}_{l-i}^{k-r}\\ &\quad -\frac{K_\alpha^\mu\tau^{\alpha-1}}{2}h^{-\mu}\sum_{r=0}^{k+1}\omega_r^{1-\alpha}\sum_{i=l-m}^{l}g_i\mathrm{e}_{l-i}^{k+1-r}+O(\tau^2+h^2).\end{aligned} \tag{4.40}$$

Now, Eq. (4.40) can be written in the following matrix form

$$\begin{aligned}(\boldsymbol{I}+\boldsymbol{A}_0)\boldsymbol{E}^{k+1} &= (\boldsymbol{I}-\boldsymbol{A}_0-\boldsymbol{A}_1)\boldsymbol{E}^k-(\boldsymbol{A}_1+\boldsymbol{A}_2)\boldsymbol{E}^{k-1}\\ &\quad -(\boldsymbol{A}_2+\boldsymbol{A}_3)\boldsymbol{E}^{k-2}-\cdots-(\boldsymbol{A}_k+\boldsymbol{A}_{k+1})\boldsymbol{E}^0+\boldsymbol{C}_1\tau(\tau^2+h^2)\boldsymbol{I}.\end{aligned} \tag{4.41}$$

Thus, we have

$$\begin{aligned}\boldsymbol{E}^{k+1} &= (\boldsymbol{I}+\boldsymbol{A}_0)^{-1}(\boldsymbol{I}-\boldsymbol{A}_0-\boldsymbol{A}_1)\boldsymbol{E}^k-(\boldsymbol{I}+\boldsymbol{A}_0)^{-1}(\boldsymbol{A}_1+\boldsymbol{A}_2)\boldsymbol{E}^{k-1}\\ &\quad -(\boldsymbol{I}+\boldsymbol{A}_0)^{-1}(\boldsymbol{A}_2+\boldsymbol{A}_3)\boldsymbol{E}^{k-2}-\cdots-(\boldsymbol{I}+\boldsymbol{A}_0)^{-1}(\boldsymbol{A}_k+\boldsymbol{A}_{k+1})\boldsymbol{E}^0\\ &\quad +\boldsymbol{C}_1\tau(\tau^2+h^2)(\boldsymbol{I}+\boldsymbol{A}_0)^{-1}.\end{aligned} \tag{4.42}$$

Hence, we obtain

$$\begin{aligned}\left\|\boldsymbol{E}^{k+1}\right\|_2 &\leq \left\|(\boldsymbol{I}+\boldsymbol{A}_0)^{-1}(\boldsymbol{I}-\boldsymbol{A}_0-\boldsymbol{A}_1)\right\|_2\left\|\boldsymbol{E}^k\right\|_2+\left\|(\boldsymbol{I}+\boldsymbol{A}_0)^{-1}(\boldsymbol{A}_1+\boldsymbol{A}_2)\right\|_2\left\|\boldsymbol{E}^{k-1}\right\|_2\\ &\quad +\left\|(\boldsymbol{I}+\boldsymbol{A}_0)^{-1}(\boldsymbol{A}_2+\boldsymbol{A}_3)\right\|_2\left\|\boldsymbol{E}^{k-2}\right\|_2+\cdots+\left\|(\boldsymbol{I}+\boldsymbol{A}_0)^{-1}(\boldsymbol{A}_k+\boldsymbol{A}_{k+1})\right\|_2\left\|\boldsymbol{E}^0\right\|_2\\ &\quad +C_1\tau(\tau^2+h^2)\left\|(\boldsymbol{I}+\boldsymbol{A}_0)^{-1}\right\|_2 \leq \alpha_0(\alpha_1+1)(\alpha_2+1)\ldots(\alpha_k+1)\left\|\boldsymbol{E}^0\right\|_2\\ &\quad +C_1\tau(\tau^2+h^2)\left\|(\boldsymbol{I}+\boldsymbol{A}_0)^{-1}\right\|_2 < \alpha_0(\alpha_1+1)(\alpha_2+1)\ldots(\alpha_k+1)\left\|\boldsymbol{E}^0\right\|_2\\ &\quad +\frac{C_1\tau(\tau^2+h^2)}{\left(1-\frac{v\tau^2}{h}\omega_0\right)} \leq CT(\tau^2+h^2).\end{aligned}$$

Consequently, $\left\|\boldsymbol{E}^{k+1}\right\|_2 \to 0$ as $\tau \to 0$, $h \to 0$. This completes the proof. ■

4.4 Soliton Solutions of a Nonlinear and Nonlocal Sine-Gordon Equation Involving Riesz Space Fractional Derivative

In the present section, a new semi-numerical technique MHAM-FT method has been proposed to obtain the approximate solution of nonlocal fractional sine-Gordon equation (SGE). The fractional SGE with nonlocal Riesz derivative operator has been first time solved by MHAM-FT method.

4.4.1 Basic Idea of Modified Homotopy Analysis Method with Fourier Transform

Let us focus a brief overview of modified homotopy analysis method with Fourier transform (MHAM-FT). Consider the following fractional differential equation

$$N[u(x,t)] = 0, \tag{4.43}$$

where N is a nonlinear differential operator containing Riesz fractional derivative defined in Eq. (1.18) of Chap. 1, x and t denote independent variables, and $u(x,t)$ is an unknown function.

Then, applying Fourier transform Eq. (4.43) has been reduced to the following Fourier transformed differential equation

$$N[\hat{u}(k,t)] = 0, \tag{4.44}$$

where $\hat{u}(k,t)$ is the Fourier transform of $u(x,t)$.

According to HAM, the zeroth-order deformation equation of Eq. (4.44) reads as

$$(1-p)L[\phi(k,t;p) - \hat{u}_0(k,t)] = p\hbar N[\phi(k,t;p)], \tag{4.45}$$

where L is an auxiliary linear operator, $\phi(k,t;p)$ is an unknown function, $\hat{u}_0(k,t)$ is an initial guess of $\hat{u}(k,t)$, $\hbar \neq 0$ is an auxiliary parameter, and $p \in [0,1]$ is the embedding parameter. In this proposed MHAM-FT, the nonlinear term appeared in expression for nonlinear operator form has been expanded using Adomian's type of polynomials as $\sum_{n=0}^{\infty} A_n p^n$ [52].

Obviously, when $p = 0$ and $p = 1$, we have

$$\phi(k,t;0) = \hat{u}_0(k,t), \phi(k,t;1) = \hat{u}(k,t), \tag{4.46}$$

respectively. Thus, as p increases from 0 to 1, the solution $\phi(k,t;p)$ varies from the initial guess $\hat{u}_0(k,t)$ to the solution $\hat{u}(k,t)$. Expanding $\phi(x,t;p)$ in Taylor series with respect to the embedding parameter p, we have

$$\phi(k,t;p) = \hat{u}_0(k,t) + \sum_{m=1}^{+\infty} p^m \hat{u}_m(k,t), \tag{4.47}$$

where $\hat{u}_m(k,t) = \frac{1}{m!}\frac{\partial^m}{\partial p^m}\phi(k,t;p)\Big|_{p=0}$.

The convergence of the series (4.47) depends upon the auxiliary parameter $\hbar$. If it is convergent at $p = 1$, we have

$$\hat{u}(k,t) = \hat{u}_0(k,t) + \sum_{m=1}^{+\infty} \hat{u}_m(k,t),$$

which must be one of the solutions of the original nonlinear equation.

Differentiating the zeroth-order deformation Eq. (4.45) m times with respect to p and then setting $p = 0$ and finally dividing them by $m!$, we obtain the following mth-order deformation equation

$$L[\hat{u}_m(k,t) - \chi_m \hat{u}_{m-1}(k,t)] = \hbar \Re_m(\hat{u}_0, \hat{u}_1, \ldots, \hat{u}_{m-1}), \tag{4.48}$$

where

$$\Re_m(\hat{u}_0, \hat{u}_1, \ldots, \hat{u}_{m-1}) = \frac{1}{(m-1)!}\frac{\partial^{m-1} N[\phi(k,t;p)]}{\partial p^{m-1}}\Big|_{p=0}$$

and

$$\chi_m = \begin{cases} 1, & m > 1 \\ 0, & m \leq 1 \end{cases}. \tag{4.49}$$

It should be noted that $\hat{u}_m(k,t)$ for $m \geq 1$ is governed by the linear Eq. (4.48) which can be solved by symbolic computational software. Then, by applying inverse Fourier transformation, we can get each component $u_m(x,t)$ of the approximate series solution

$$u(x,t) = \sum_{m=0}^{\infty} u_m(x,t).$$

In the present analysis, for reducing Riesz space fractional differential equation to ordinary differential equation, we applied here Fourier transform. In this modified homotopy analysis method, with Fourier transform (MHAM-FT), we applied the inverse Fourier transform for getting the solution of Riesz space fractional differential equation. This MHAM-FT technique has been first time proposed by the author.

4.4.2 Implementation of the MHAM-FT Method for Approximate Solution of Nonlocal Fractional SGE

In this section, we first consider two examples for the application of MHAM-FT for the solution of nonlocal fractional SGE Eq. (4.1).

Example 4.3 In this example, we shall find the approximate solution of the nonlocal fractional SGE Eq. (4.1) with given initial conditions [52–54]

$$u(x,0) = 0, u_t(x,0) = 4 \text{ sec } hx \tag{4.50}$$

Then, using Eq. (1.18) of Chap. 1 and applying Fourier transform on Eqs. (4.1) and (4.50), we get

$$\hat{u}_{tt}(k,t) + |k|^{\alpha}\hat{u}(k,t) + \mathsf{F}(\sin u) = 0, \tag{4.51}$$

with initial conditions

$$\hat{u}(k,0) = 0, \quad \hat{u}_t(k,0) = 2\sqrt{2\pi}\sec h\left(\frac{k\pi}{2}\right), \tag{4.52}$$

where F denotes the Fourier transform and k is called the transform parameter for Fourier transform.

Expanding $\phi(k,t;p)$ in Taylor series with respect to p, we have

$$\phi(k,t;p) = \hat{u}_0(k,t) + \sum_{m=1}^{+\infty} p^m \hat{u}_m(k,t), \tag{4.53}$$

where

$$\hat{u}_m(k,t) = \frac{1}{m!}\frac{\partial^m \phi(k,t;p)}{\partial p^m}\bigg|_{p=0}.$$

To obtain the approximate solution of the fractional SGE in Eq. (4.51), we choose the linear operator

$$L[\phi(k,t;p)] = \phi_{tt}(k,t;p). \tag{4.54}$$

From Eq. (4.44), we define a nonlinear operator as

$$N[\phi(k,t;p)] = \phi_{tt}(k,t;p) + |k|^{\alpha}\phi(k,t;p) + \mathsf{F}(\sin(\phi(k,t;p))), \tag{4.55}$$

where the nonlinear term $\sin(\phi(k,t;p))$ is expanded in terms of Adomian-like polynomials.

The nonlinear term $\sin(\phi(k,t;p))$ has been taken as

$$\sin(\phi(k,t;p)) = \sum_{n=0}^{\infty} p^n A_n,$$

where $A_n = \frac{1}{n!}\frac{\partial^n}{\partial p^n}\left(\sin\left(\hat{u}_0(k,t) + \sum_{m=1}^{+\infty} p^m \hat{u}_m(k,t)\right)\right)_{p=0}, n \geq 0.$

Using Eq. (4.45), we construct the so-called zeroth-order deformation equation

$$(1-p)L[\phi(k,t;p) - \hat{u}_0(k,t)] = p\hbar N[\phi(k,t;p)]. \tag{4.56}$$

Obviously, when $p = 0$ and $p = 1$, Eq. (4.56) yields

$$\phi(k,t;0) = \hat{u}_0(k,t); \phi(k,t;1) = \hat{u}(k,t).$$

Therefore, as the embedding parameter p increases from 0 to 1, $\phi(k,t;p)$ varies from the initial guess to the exact solution $\hat{u}(k,t)$.

If the auxiliary linear operator, the initial guess, and the auxiliary parameter $\hbar$ are so properly chosen, the above series in Eq. (4.53) converges at $p = 1$, and we obtain

$$\hat{u}(k,t) = \phi(k,t;1) = \hat{u}_0(k,t) + \sum_{m=1}^{+\infty} \hat{u}_m(k,t). \tag{4.57}$$

According to Eq. (4.48), we have the mth-order deformation equation

$$L[\hat{u}_m(k,t) - \chi_m \hat{u}_{m-1}(k,t)] = \hbar \Re_m(\hat{u}_0, \hat{u}_1, \ldots, \hat{u}_{m-1}), m \geq 1, \tag{4.58}$$

where

$$\begin{aligned} \Re_m(\hat{u}_0, \hat{u}_1, \ldots, \hat{u}_{m-1}) &= \frac{1}{(m-1)!}\frac{\partial^{m-1}}{\partial p^{m-1}} N[\phi(k,t;p)]\Big|_{p=0} \\ &= \frac{\partial^2 \hat{u}_{m-1}(k,t;p)}{\partial t^2} + |k|^{\alpha}\hat{u}_{m-1}(k,t;p) + \mathsf{F}(A_{m-1}). \end{aligned} \tag{4.59}$$

Now, the solution of the mth-order deformation Eq. (4.58) for $m \geq 1$ becomes

$$\hat{u}_m(k,t) = \chi_m \hat{u}_{m-1}(k,t) + \hbar L^{-1}[\Re_m(\hat{u}_0, \hat{u}_1, \ldots, \hat{u}_{m-1})]. \tag{4.60}$$

From Eq. (4.60), we have the following equations

$$\begin{aligned}
\hat{u}_0(k,t) &= \hat{u}(k,0) + t\hat{u}_t(k,0),\\
\hat{u}_1(k,t) &= \hbar L^{-1}\left(\frac{\partial^2 \hat{u}_0(k,t;p)}{\partial t^2} + |k|^{\alpha}\hat{u}_0(k,t;p) + \mathsf{F}(A_0)\right),\\
\hat{u}_2(k,t) &= \hat{u}_1(k,t) + \hbar L^{-1}\left(\frac{\partial^2 \hat{u}_1(k,t;p)}{\partial t^2} + |k|^{\alpha}\hat{u}_1(k,t;p) + \mathsf{F}(A_1)\right),\\
\hat{u}_3(k,t) &= \hat{u}_2(k,t) + \hbar L^{-1}\left(\frac{\partial^2 \hat{u}_2(k,t;p)}{\partial t^2} + |k|^{\alpha}\hat{u}_2(k,t;p) + \mathsf{F}(A_2)\right),
\end{aligned} \tag{4.61}$$

and so on.

But here for the sake of efficient computation for the nonlinear term, the above scheme in Eq. (4.61) has been modified in the following way

$$\begin{aligned}
\hat{u}_0(k,t) &= \hat{u}(k,0),\\
\hat{u}_1(k,t) &= t\hat{u}_t(k,0) + \hbar L^{-1}\left(\frac{\partial^2 \hat{u}_0(k,t;p)}{\partial t^2} + |k|^{\alpha}\hat{u}_0(k,t;p) + \mathsf{F}(A_0)\right),\\
\hat{u}_2(k,t) &= \hbar L^{-1}\left(\frac{\partial^2 \hat{u}_1(k,t;p)}{\partial t^2} + |k|^{\alpha}\hat{u}_1(k,t;p) + \mathsf{F}(A_1)\right),\\
\hat{u}_3(k,t) &= \hat{u}_2(k,t) + \hbar L^{-1}\left(\frac{\partial^2 \hat{u}_2(k,t;p)}{\partial t^2} + |k|^{\alpha}\hat{u}_2(k,t;p) + \mathsf{F}(A_2)\right),\\
\hat{u}_4(k,t) &= \hat{u}_3(k,t) + \hbar L^{-1}\left(\frac{\partial^2 \hat{u}_3(k,t;p)}{\partial t^2} + |k|^{\alpha}\hat{u}_3(k,t;p) + \mathsf{F}(A_3)\right),
\end{aligned} \tag{4.62}$$

and so on.

By putting the initial conditions in Eq. (4.52) into Eq. (4.62) and solving them, we now successively obtain

$$\hat{u}_0(k,t) = 0, \tag{4.63}$$

$$\hat{u}_1(k,t) = 2\sqrt{2\pi}t \sec h\left(\frac{k\pi}{2}\right), \tag{4.64}$$

$$\hat{u}_2(k,t) = \hbar\left(\frac{1}{3}\sqrt{2\pi}t^3 \sec h\left(\frac{k\pi}{2}\right) + \frac{1}{3}\sqrt{2\pi}t^3|k|^{\alpha}\sec h\left(\frac{k\pi}{2}\right)\right), \tag{4.65}$$

and so on.

Then, by applying the inverse Fourier transform of Eqs. (4.63)–(4.65), we determine

$$
\begin{aligned}
u_0(x,t) &= 0,\\
u_1(x,t) &= 4t\ \text{sec}\ hx,\\
u_2(x,t) &= \frac{1}{3}t^3\hbar\Big(2\ \text{sec}\ hx + 2^{-\alpha}\pi^{-1-\alpha}\Gamma(1+\alpha)\Big(\zeta\Big(1+\alpha,\frac{\pi-2ix}{4\pi}\Big)+\zeta\Big(1+\alpha,\frac{\pi+2ix}{4\pi}\Big)\\
&\quad -\zeta\Big(1+\alpha,\frac{3}{4}-\frac{ix}{2\pi}\Big)-\zeta\Big(1+\alpha,\frac{3}{4}+\frac{ix}{2\pi}\Big)\Big)\Big),
\end{aligned}
$$

and so on, where $\zeta(s,a)=\sum_{k=0}^{\infty}\frac{1}{(k+a)^s}$ is called Hurwitz zeta function which is a generalization of the Riemann zeta function $\zeta(s)$ and also known as the generalized zeta function.

In this manner, the other components of the homotopy series can be easily obtained by which $u(x,t)$ can be evaluated in a series form as

$$
\begin{aligned}
u(x,t) &= u_0(x,t)+u_1(x,t)+u_2(x,t)+\cdots\\
&= 4t\ \text{sec}\ hx+\frac{1}{3}t^3\hbar\Big(2\ \text{sec}\ hx+2^{-\alpha}\pi^{-1-\alpha}\Gamma(1+\alpha)\Big(\zeta\Big(1+\alpha,\frac{\pi-2ix}{4\pi}\Big)\\
&\quad +\zeta\Big(1+\alpha,\frac{\pi+2ix}{4\pi}\Big)-\zeta\Big(1+\alpha,\frac{3}{4}-\frac{ix}{2\pi}\Big)\\
&\quad -\zeta\Big(1+\alpha,\frac{3}{4}+\frac{ix}{2\pi}\Big)\Big)\Big)+\cdots.
\end{aligned}
\tag{4.66}
$$

Example 4.4 In this case, we shall find the approximate solution of the nonlocal fractional SGE Eq. (4.1) with given initial conditions [55–57]

$$
u(x,0)=\pi+\varepsilon\cos(\mu x),\quad u_t(x,0)=0. \tag{4.67}
$$

Then, using Eq. (1.18) of Chap. 1 and applying Fourier transform on Eqs. (4.1) and (4.67), we get

$$
\hat{u}_{tt}(k,t)+|k|^{\alpha}\hat{u}(k,t)+\mathsf{F}(\sin u)=0, \tag{4.68}
$$

with initial conditions

$$
\hat{u}(k,0)=\sqrt{2}\pi^{3/2}\delta(k)+\sqrt{\frac{\pi}{2}}\varepsilon\delta(k-\mu)+\sqrt{\frac{\pi}{2}}\varepsilon\delta(k+\mu),\quad \hat{u}_t(k,0)=0, \tag{4.69}
$$

where F denotes the Fourier transform, k is called the transform parameter for Fourier transform, and $\delta(.)$ denotes the Dirac delta function.

Analogous to arguments as discussed in Example 4.3, we may obtain the following equations

$$\begin{aligned}
\hat{u}_0(k,t) &= \sqrt{2}\pi^{3/2}\delta(k),\\
\hat{u}_1(k,t) &= \sqrt{\frac{\pi}{2}}\varepsilon\delta(k-\mu)+\sqrt{\frac{\pi}{2}}\varepsilon\delta(k+\mu)+\hbar L^{-1}\left(\frac{\partial^2\hat{u}_0(k,t;p)}{\partial t^2}+|k|^{\alpha}\hat{u}_0(k,t;p)+\mathsf{F}(A_0)\right),\\
\hat{u}_2(k,t) &= \hbar L^{-1}\left(\frac{\partial^2\hat{u}_1(k,t;p)}{\partial t^2}+|k|^{\alpha}\hat{u}_1(k,t;p)+\mathsf{F}(A_1)\right),\\
\hat{u}_3(k,t) &= \hat{u}_2(k,t)+\hbar L^{-1}\left(\frac{\partial^2\hat{u}_2(k,t;p)}{\partial t^2}+|k|^{\alpha}\hat{u}_2(k,t;p)+\mathsf{F}(A_1)\right),\\
\hat{u}_4(k,t) &= \hat{u}_3(k,t)+\hbar L^{-1}\left(\frac{\partial^2\hat{u}_3(k,t;p)}{\partial t^2}+|k|^{\alpha}\hat{u}_3(k,t;p)+\mathsf{F}(A_3)\right),
\end{aligned} \tag{4.70}$$

and so on.

Solving Eq. (4.70), we now successively obtain

$$\hat{u}_0(k,t) = \sqrt{2}\pi^{3/2}\delta(k), \tag{4.71}$$

$$\hat{u}_1(k,t) = \sqrt{\frac{\pi}{2}}\varepsilon\delta(k-\mu)+\sqrt{\frac{\pi}{2}}\varepsilon\delta(k+\mu), \tag{4.72}$$

$$\begin{aligned}
\hat{u}_2(k,t) = \hbar\Bigg(&-\frac{1}{2}\sqrt{\frac{\pi}{2}}t^2\varepsilon\delta(k-\mu)+\frac{1}{2}\sqrt{\frac{\pi}{2}}t^2\varepsilon|k|^{\alpha}\delta(k-\mu)-\frac{1}{2}\sqrt{\frac{\pi}{2}}t^2\varepsilon\delta(k+\mu)\\
&+\frac{1}{2}\sqrt{\frac{\pi}{2}}t^2\varepsilon|k|^{\alpha}\delta(k+\mu)\Bigg),
\end{aligned} \tag{4.73}$$

and so on.

Then, by applying the inverse Fourier transform of Eqs. (4.71)–(4.73), we have

$$\begin{aligned}
u_0(x,t) &= \pi,\\
u_1(x,t) &= \varepsilon\cos(\mu x),\\
u_2(x,t) &= \frac{1}{2}t^2\varepsilon\hbar(-1+\mu^{\alpha})\cos(\mu x),\\
u_3(x,t) &= \frac{1}{24}t^2\varepsilon\hbar(-1+\mu^{\alpha})\left(12-\left(-12+t^2\right)\hbar+t^2\hbar\mu^{\alpha}\right)\cos(\mu x),
\end{aligned}$$

and so on.

In this manner, the other components of the homotopy series can be easily obtained by which $u(x,t)$ can be evaluated in a series form as

$$u(x,t) = u_0(x,t) + u_1(x,t) + u_2(x,t) + \cdots$$
$$= \frac{1}{24}\left(24\pi + \varepsilon\left(24 + 12t^2\hbar(2+\hbar)(-1+\mu^\alpha) + t^4\hbar^2(-1+\mu^\alpha)^2\right)\cos(\mu x)\right) + \cdots. \tag{4.74}$$

The After-Treatment Technique

Padé approximation may be used to enable us in order to increase the radius of convergence of the series. This method can be used for analytic continuation of a series for extending the radius of convergence. A Padé approximant is the ratio of two polynomials constructed from the coefficients of the Maclaurin series expansion of a function. Given a function $f(t)$ expanded in a Maclaurin series $f(t) = \sum_{n=0}^{\infty} c_n t^n$, we can use the coefficients of the series to represent the function by a ratio of two polynomials denoted by $[L/M]$ and called the Padé approximant, i.e.,

$$\left[\frac{L}{M}\right] = \frac{P_L(t)}{Q_M(t)}, \tag{4.75}$$

where $P_L(t)$ is a polynomial of degree at most L and $Q_M(t)$ is a polynomial of degree at most M. The polynomials $P_L(t)$ and $Q_M(t)$ have no common factors. Such rational fractions are known to have remarkable properties of analytic continuation. Even though the series has a finite region of convergence, we can obtain the limit of the function as $t \to \infty$ if $L = M$.

In case of Example 4.4, $u(x,t)$ can be evaluated in a series form as

$$u(x,t) = \frac{1}{24}\left(24\pi + \varepsilon\left(24 + 12t^2\hbar(2+\hbar)(-1+\mu^\alpha) + t^4\hbar^2(-1+\mu^\alpha)^2\right)\cos(\mu x)\right). \tag{4.76}$$

Putting $x = 0.05, \hbar = -1, \varepsilon = 0.01, \mu = \frac{1}{\sqrt{2}}$ and $\alpha = 2$ and applying Padé approximant [5/5] to Eq. (4.76), we obtain

$$u(0.05,t) = \left(\frac{3.15158 - 0.066294\,t^2 + 0.00072717\,t^4}{1 - 0.021828\,t^2 + 0.00021501\,t^4}\right). \tag{4.77}$$

The $\hbar$-Curve and Numerical Simulations for MHAM-FT Method and Discussions

As pointed out by Liao [58] in general, by means of the so-called $\hbar$-curve, it is straightforward to choose a proper value of $\hbar$ which ensures that the solution series is convergent.

To investigate the influence of $\hbar$ on the solution series, we plot the so-called $\hbar$-curve of partial derivatives of $u(x,t)$ at $(0,0)$ obtained from the sixth-order MHAM-FT solutions as shown in Fig. 4.7. In this way, it is found that our series converges when $\hbar = -1$.

In this present numerical experiment, Eq. (4.66) obtained by MHAM-FT has been used to draw the graphs as shown in Fig. 4.8 for $\alpha = 1.75$. The numerical solutions of Riesz fractional SGE in Eq. (4.1) have been shown in Fig. 4.8 with the help of third-order approximation for the homotopy series solution of $u(x,t)$, when $\hbar = -1$.

In this present analysis, Eq. (4.74) obtained by MHAM-FT has been used to draw the graphs as shown in Fig. 4.9 for fractional-order value $\alpha = 1.75$. The numerical solutions of fractional SGE Eq. (4.1) have been shown in Fig. 4.9 with the help of sixth-order approximation for the homotopy series solution of $u(x,t)$, when $\hbar = -1$.

In order to examine the numerical results obtained by the proposed method, both Examples 4.3 and 4.4 have been solved by a numerical method involving Chebyshev polynomial. The comparison of the approximate solutions for fractional SGE Eq. (4.1) given in Examples 4.3 and 4.4 has been exhibited in Tables 4.1 and 4.4 which are constructed using the results obtained by MHAM and Chebyshev polynomial at different values of x and t taking $\alpha = 1.75$ and 1.5, respectively. Similarly, Tables 4.2 and 4.5 show the comparison of absolute errors for classical SGE given in Examples 4.3 and 4.4, respectively. To show the accuracy of the proposed MHAM over Chebyshev polynomials, L_2 and L_∞ error norms for classical order SGE given in Examples 4.3 and 4.4 have been presented in Tables 4.3 and 4.6, respectively. Agreement between present numerical results obtained by MHAM with Chebyshev polynomials and exact solutions appear very satisfactory through illustrations in Tables 4.1, 4.2, 4.3, 4.4, and 4.6. The following Fig. 4.10

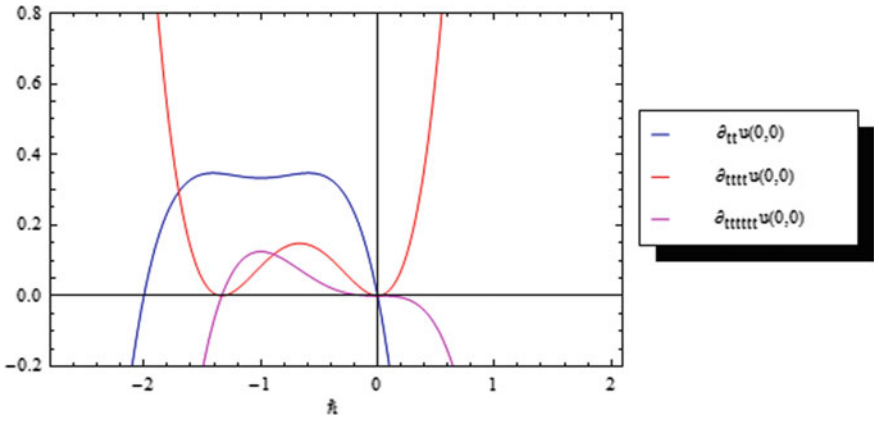

Fig. 4.7 $\hbar$-curve for partial derivatives of $u(x,t)$ at $(0,0)$ for the sixth-order MHAM-FT solution when $\alpha = 2$

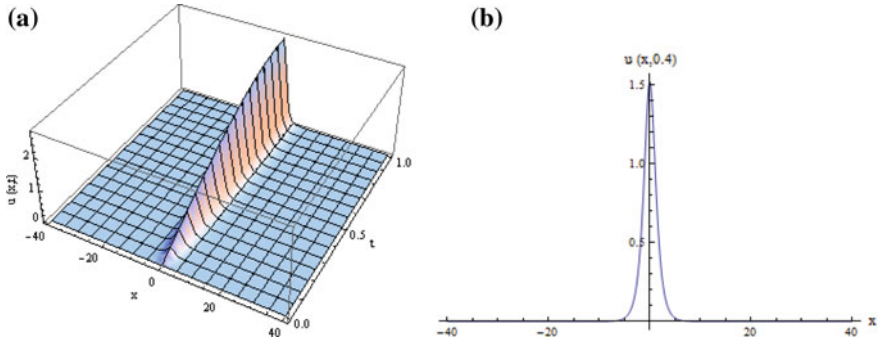

Fig. 4.8 **a** MHAM-FT method solution for $u(x,t)$ and **b** corresponding solution for $u(x,t)$ when $t = 0.4$

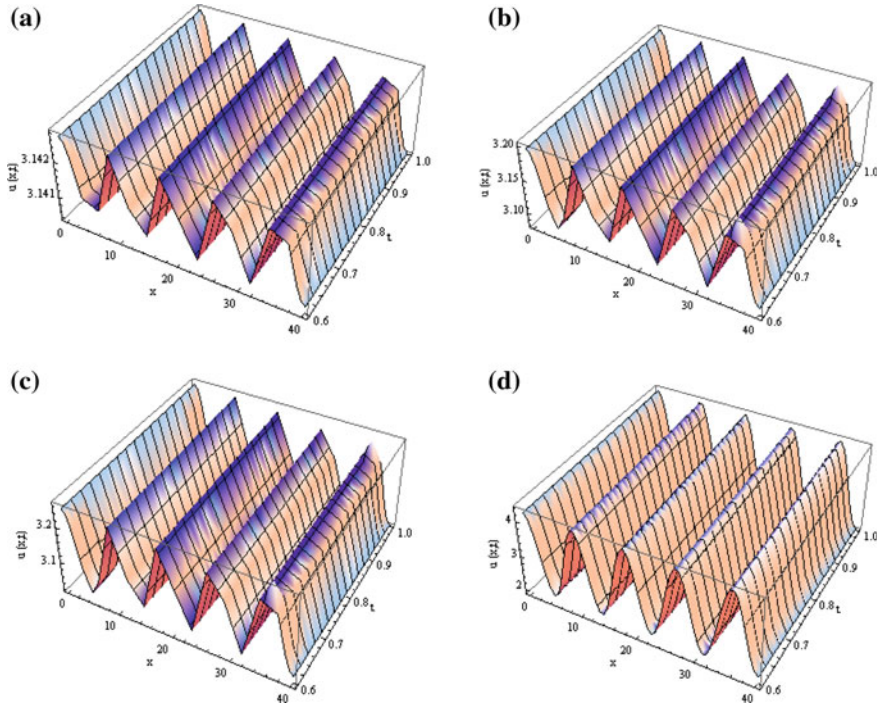

Fig. 4.9 Numerical results for $u(x,t)$ obtained by MHAM-FT for **a** $\varepsilon = 0.001$, **b** $\varepsilon = 0.05$, **c** $\varepsilon = 0.1$, and **d** $\varepsilon = 1.0$

demonstrates a graphical comparison of the numerical solutions for $u(0.05,t)$ obtained by MHAM-FT and Padé approximation with regard to the exact solution for Example 4.3.

Table 4.1 Comparison of approximate solutions obtained by modified homotopy analysis method and Chebyshev polynomial of second kind for fractional SGE Eq. (4.1) given in Example 4.3 at various points of x and t taking $\alpha = 1.75$ and 1.5 with $\hbar = -1$

x	$\alpha = 1.75$				$\alpha = 1.5$			
	$t = 0.01$		$t = 0.02$		$t = 0.01$		$t = 0.02$	
	$u_{\text{Chebyshev}}$	u_{MHAM}	$u_{\text{Chebyshev}}$	u_{MHAM}	$u_{\text{Chebyshev}}$	u_{MHAM}	$u_{\text{Chebyshev}}$	u_{MHAM}
0.01	0.033828	0.039996	0.0600056	0.079986	0.034480	0.039996	0.059515	0.079986
0.02	0.018271	0.039991	0.0571674	0.079974	0.033566	0.039991	0.062218	0.079974
0.03	0.010936	0.039981	0.0562336	0.079954	0.033364	0.039981	0.064389	0.079954
0.04	0.009624	0.039966	0.0566734	0.079926	0.033664	0.039966	0.066099	0.079926
0.05	0.012513	0.039948	0.0580476	0.079890	0.034294	0.039948	0.067413	0.079890
0.06	0.018109	0.039926	0.0599977	0.079846	0.035114	0.039926	0.068388	0.079846
0.07	0.025213	0.039901	0.0622362	0.079794	0.036014	0.039901	0.069075	0.079794
0.08	0.032879	0.039871	0.0645376	0.079734	0.036907	0.039871	0.069521	0.079735
0.09	0.040384	0.039837	0.0667305	0.079667	0.037728	0.039837	0.069766	0.079667
0.1	0.047194	0.039799	0.0686896	0.079592	0.038433	0.039799	0.069845	0.079592

Table 4.2 Comparison of absolute errors obtained by modified homotopy analysis method and Chebyshev polynomial of second kind for SGE equation given in Example 4.3 at various points of x and t taking $\alpha = 2$ and $\hbar = -1$

x	t	$\lvert u_{\text{Exact}} - u_{\text{Chebyshev}} \rvert$	$\lvert u_{\text{Exact}} - u_{\text{MHAM}} \rvert$
0.02	0.02	1.45347E−5	2.55671E−9
0.04	0.02	1.46767E−5	2.54906E−9
0.06	0.02	1.48475E−5	2.53636E−9
0.08	0.02	1.50368E−5	2.51869E−9
0.1	0.02	1.52361E−5	2.49619E−9
0.02	0.04	5.26987E−5	8.17448E−8
0.04	0.04	5.32093E−5	8.15001E−8
0.06	0.04	5.38216E−5	8.10941E−8
0.08	0.04	5.45030E−5	8.05296E−8
0.1	0.04	5.52250E−5	7.98104E−8
0.02	0.06	1.07843E−5	6.19865E−7
0.04	0.06	1.08860E−4	6.18011E−7
0.06	0.06	1.10091E−4	6.14935E−7
0.08	0.06	1.11471E−4	6.10656E−7
0.1	0.06	1.12943E−4	6.05206E−7
0.02	0.08	1.75050E−4	2.60691E−6
0.04	0.08	1.76623E−4	2.59912E−6
0.06	0.08	1.78561E−4	2.58619E−6
0.08	0.08	1.80758E−4	2.56821E−6
0.1	0.08	1.83120E−4	2.54531E−6
0.02	0.1	2.50768E−4	7.93538E−6
0.04	0.1	2.52867E−4	7.91169E−6

(continued)

Table 4.2 (continued)

x	t	$\lvert u_{\text{Exact}} - u_{\text{Chebyshev}} \rvert$	$\lvert u_{\text{Exact}} - u_{\text{MHAM}} \rvert$
0.06	0.1	2.55516E−4	7.87237E−6
0.08	0.1	2.58561E−4	7.81770E−6
0.1	0.1	2.61864E−4	7.74804E−6

Table 4.3 L_2 and L_∞ error norm for SGE Eq. (4.1) given in Example 4.3 at various points of x and t taking $\alpha = 2$

t	MHAM		Chebyshev polynomial	
	L_2	L_∞	L_2	L_∞
0.02	5.6606E−9	2.55671E−9	3.32469E−5	1.52361E−5
0.04	1.80985E−7	8.17448E−8	1.20522E−4	5.52250E−5
0.06	1.37240E−6	6.19865E−7	2.46541E−4	1.12943E−4
0.08	5.77184E−6	2.60691E−6	3.99911E−4	1.83120E−4
0.10	1.75695E−5	7.93538E−6	5.72312E−4	2.61864E−4

Table 4.4 Comparison of approximate solutions obtained by modified homotopy analysis method and Chebyshev polynomial of second kind for fractional SGE Eq. (4.1) given in Example 4.4 at various points of x and t taking $\alpha = 1.75$ and 1.5 with $\hbar = -1$

x	$\alpha = 1.75$				$\alpha = 1.5$			
	$t = 0.01$		$t = 0.02$		$t = 0.01$		$t = 0.02$	
	$u_{\text{Chebyshev}}$	u_{MHAM}	$u_{\text{Chebyshev}}$	u_{MHAM}	$u_{\text{Chebyshev}}$	u_{MHAM}	$u_{\text{Chebyshev}}$	u_{MHAM}
0.10	3.13459	3.151570	3.08713	3.1515800	3.15003	3.151567	3.14319	3.15156847
0.15	3.15900	3.151536	3.18638	3.1515373	3.16211	3.151540	3.19226	3.15153726
0.20	3.16542	3.15149	3.20162	3.1514930	3.16066	3.151492	3.18787	3.15149362
0.25	3.15980	3.15144	3.18315	3.1514377	3.15390	3.151438	3.16158	3.15143760
0.30	3.15161	3.15137	3.15421	3.1513693	3.14879	3.15136	3.14129	3.15136928
0.35	3.14675	3.15129	3.13604	3.1512888	3.14823	3.15128	3.13897	3.15128874
0.40	3.14623	3.15120	3.13282	3.1511961	3.15131	3.15119	3.15122	3.15119609
0.45	3.14781	3.15109	3.13733	3.1510915	3.15506	3.15108	3.16632	3.15109143
0.50	3.14867	3.15097	3.14015	3.1509749	3.15662	3.150970	3.17283	3.15097489

Table 4.5 Absolute errors obtained by modified homotopy analysis method and Chebyshev polynomial of second kind for classical SGE equation given in Example 4.4 at various points of x and t taking $\hbar = -1$

x	t	$\lvert u_{\text{Chebyshev}} - u_{\text{MHAM}} \rvert$
0.2	0.2	5.09463E−5
0.4	0.2	8.84127E−5
0.6	0.2	1.48843E−4
0.8	0.2	2.20924E−4

(continued)

Table 4.5 (continued)

x	t	$\lvert u_{\text{Chebyshev}} - u_{\text{MHAM}} \rvert$
1.0	0.2	2.85454E−4
0.2	0.4	2.00397E−5
0.4	0.4	1.11716E−4
0.6	0.4	3.30001E−4
0.8	0.4	5.79195E−4
1.0	0.4	8.02329E−4
0.2	0.6	4.93420E−4
0.4	0.6	2.19299E−4
0.6	0.6	2.24080E−4
0.8	0.6	7.26968E−4
1.0	0.6	1.19255E−4
0.2	0.8	1.56021E−3
0.4	0.8	1.09038E−3
0.6	0.8	3.68090E−4
0.8	0.8	4.64603E−4
1.0	0.8	1.30778E−3
0.2	1.0	3.30232E−3
0.4	1.0	2.56352E−3
0.6	1.0	1.50743E−3
0.8	1.0	2.41294E−4
1.0	1.0	1.22502E−3

Table 4.6 L_2 and L_∞ error norm obtained by MHAM and Chebyshev polynomial with regard to HAM for SGE Eq. (4.1) given in Example 4.4 at various points of x and t taking $\varepsilon = 1$ and $\alpha = 2$

t	MHAM		Chebyshev polynomial	
	L_2	L_∞	L_2	L_∞
0.02	3.61832E−6	1.62617E−6	3.16274E−6	1.98279E−6
0.04	1.44585E−5	6.49802E−6	2.02068E−5	9.70659E−6
0.06	3.24763E−5	1.45956E−5	4.76627E−5	2.21017E−5
0.08	5.75978E−5	2.58855E−5	8.09011E−5	3.87676E−5
0.10	8.97196E−5	5.92957E−5	1.30016E−4	5.85008E−5

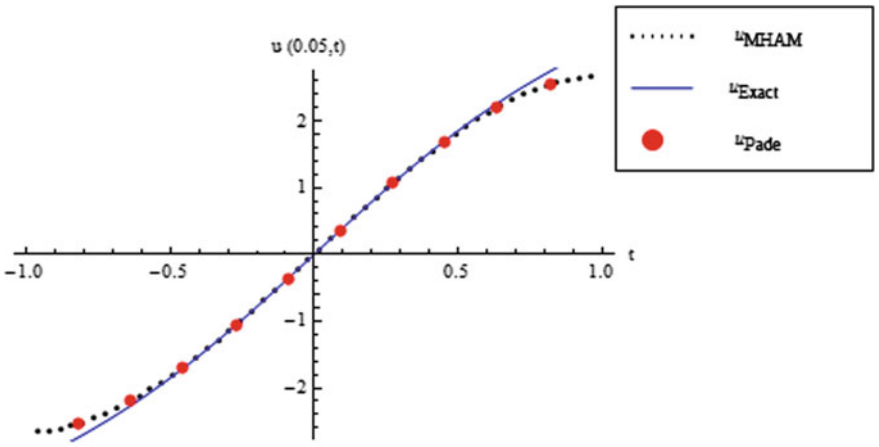

Fig. 4.10 Graphical comparison of the numerical solutions $u(0.05, t)$ obtained by MHAM-FT and Padé approximation with regard to the exact solution for Example 4.3

4.5 Conclusion

In the present chapter, shifted Grünwald approximation has been used in order to discretize the Riesz fractional diffusion equation. This equation has been solved by explicit finite difference method. The numerical solution of time and space Riesz fractional Fokker–Planck equation has been obtained from the discretization by fractional centered difference approximation of the Riesz space fractional derivative. The implicit finite difference method has been applied in order to solve the Riesz fractional Fokker–Planck equation. The above numerical schemes are quite accurate and efficient, and the numerical results demonstrated here exhibit the pretty good agreement with the exact solutions.

Moreover, in this chapter, a new semi-numerical technique MHAM-FT method has been proposed to obtain the approximate solution of nonlocal fractional SGE. The fractional SGE with nonlocal Riesz derivative operator has been first time solved by MHAM-FT method in order to justify the applicability of the proposed method. The approximate solutions obtained by MHAM-FT provide us with a convenient way to control the convergence of approximate series solution and solves the problem without any need for the discretization of the variables. To control the convergence of the solution, we can choose the proper values of $\hbar$; here we choose $\hbar = -1$. In order to examine the numerical results obtained by the proposed method, both Examples 4.3 and 4.4 have been solved by a numerical method involving Chebyshev polynomial. To show the accuracy of the proposed MHAM over Chebyshev polynomials, L_2 and L_∞ error norms for classical order SGE given in Examples 4.3 and 4.4 have been presented in Tables 4.3 and 4.6, respectively. Agreement between present numerical results obtained by MHAM with Chebyshev polynomials and exact solutions appears very satisfactory through

illustrations in Tables 4.1, 4.2, 4.3, 4.4, and 4.6. The proposed MHAM-FT method is very simple and efficient for solving the nonlinear fractional sine-Gordon equation with nonlocal Riesz derivative operator. Thus, the proposed MHAM-FT method can be elegantly applied for solving other Riesz fractional differential equations.

References

1. Wang, X., Liu, F., Chen, X.: Novel second-order accurate implicit numerical methods for the riesz space distributed-order advection-dispersion equations. Adv. Math. Phys. **2015**, 14 (2015). (Article ID 590435)
2. Saha Ray, S.: Exact solutions for time fractional diffusion method by decomposition method. Phys. Scr. **75**, 53–61 (2007)
3. Khan, Y., Diblík, J., Faraz, N., Šmarda, Z.: An efficient new perturbative Laplace method for space-time fractional telegraph equations. Adv. Differ. Equ. **2012** (2012). (Article number 204)
4. Podlubny, I.: Fractional Differential Equations. Academic Press, New York (1999)
5. Metzler, R., Klafter, J.: The random walk's guide to anomalous diffusion: a fractional dynamics approach. Phys. Rep. **339**(1), 1–77 (2000)
6. Zaslavsky, G.M.: Chaos, fractional kinetics, and anomalous transport. Phys. Rep. **371**(6), 461–580 (2002)
7. Meerschaert, M.M., Tadjeran, C.: Finite difference approximations for fractional advection–dispersion flow equations. J. Comp. Appl. Math. **172**, 65–77 (2004)
8. Liu, F., Anh, V., Turner, I.: Numerical solution of the space Fokker-Planck equation. J. Comput. Appl. Math. **166**, 209–219 (2004)
9. Yang, Q., Liu, F., Turner, I.: Numerical methods for fractional partial differential equations with Riesz space fractional derivatives. Appl. Math. Model. **34**, 200–218 (2010)
10. Saichev, A.I., Zaslavsky, G.M.: Fractional kinetic equations: solutions and applications. Chaos **7**(4), 753–764 (1997)
11. Ciesielski, M., Leszczynski, J.: Numerical solutions of a boundary value problem for the anomalous diffusion equation with the Riesz fractional derivative. In: Proceedings of the 16th International Conference on Computer Methods in Mechanics Czestochowa, Poland (2005)
12. Shen, S., Liu, F., Anh, V., Turner, I.: The fundamental solution and numerical solution of the Riesz fractional advection–dispersion equation. IMA J. Appl. Math. **73**(6), 850–872 (2008)
13. Risken, H.: The Fokker-Planck Equation: Methods of solution and Applications. Springer, Berlin (1989)
14. So, F., Liu, K.L.: A study of the subdiffusive fractional Fokker-Planck equation of bistable systems. Phys. A **331**(3–4), 378–390 (2004)
15. Saha Ray, S., Gupta, A.K.: A two-dimensional Haar wavelet approach for the numerical simulations of time and space fractional Fokker-Planck equations in modelling of anomalous diffusion systems. J. Math. Chem. **52**(8), 2277–2293 (2014)
16. Chen, S., Liu, F., Zhuang, P., Anh, V.: Finite difference approximations for the fractional Fokker-Planck equation. Appl. Math. Model. **33**, 256–273 (2009)
17. Zhuang, P., Liu, F., Turner, I., Anh, V.: Numerical treatment for the fractional Fokker-Plank equation. ANZIAM J. **48**, 759–774 (2007)
18. Odibat, Z., Momani, S.: Numerical solution of Fokker-Planck equation with space- and time-fractional derivatives. Phys. Lett. A **369**, 349–358 (2007)
19. Vanani, S.K., Aminataei, A.: A numerical algorithm for the space and time fractional Fokker-Planck equation. Int. J. Numer. Meth. Heat Fluid Flow **22**(8), 1037–1052 (2012)

20. Yildirm, A.: Analytical approach to Fokker-Planck equation with space- and time-fractional derivatives by means of the homotopy perturbation method. J. King Saud Univ. (Science) **22**, 257–264 (2010)
21. Wazwaz, A.M.: Partial Differential Equations and Solitary Waves Theory. Springer, Berlin, Heidelberg (2009)
22. Dodd, R.K., Eilbeck, J.C., Gibbon, J.D., Morris, H.C.: Solitons and Nonlinear Wave Solutions. Academic, London (1982)
23. Debnath, L.: Nonlinear Partial Differential Equations for Scientists and Engineers. Birkhäuser, Boston (2005)
24. Newell, A.C.: Nonlinear Optics. Addition-Wesley, New York (1992)
25. Saha Ray, S.: Numerical solutions and solitary wave solutions of fractional KDV equations using modified fractional reduced differential transform method. Comput. Math. Math. Phys. **53**(12), 1870–1881 (2013)
26. Alfimov, G., Pierantozzi, T., Vázquez, L.: Numerical study of a fractional sine-Gordon equation. In: Workshop Preprints/Proceedings of Fractional Differentiation and Its Applications, FDA 2004, pp. 153–162 (2004)
27. Ivanchenko, YuM, Soboleva, T.K.: Nonlocal interaction in Josephson junctions. Phys. Lett. A **147**, 65–69 (1990)
28. Gurevich, A.: Nonlocal Josephson electrodynamics and pinning in superconductors. Phys. Rev. B. **46**, 3187–3190 (1992)
29. Barone, A., Paterno, G.: Physics and applications of the Josephson effect. Wiley, New York (1982)
30. Aliev, Y.M., Silin, V.P.: Travelling 4π-kink in nonlocal Josephson electrodynamics. Phys. Lett A, **177**(3), 259–262 (1993)
31. Aliev, Y.M., Ovchinnikov, K.N., Silin V.P., Uryupin, S.A. Perturbations of stationary solutions in a nonlocal model of a josephson junction. J. Exp. Theor. Phys., **80**(551) (1995)
32. Alfimov, G.L., Silin, V.P.: On small perturbations of stationary states in a nonlinear nonlocal model of a Josephson junction. Phys. Lett. A **198**(2), 105–112 (1995)
33. Alfimov, G.L., Popkov, A.F.: Magnetic vortices in a distributed Josephson junction with electrodes of finite thickness. Phys. Rev. B: Condens. Matter **52**(6), 4503–4510 (1995)
34. Mintz, R.G., Snapiro, I.B.: Dynamics of Josephson pancakes in layered superconductors. Phys. Rev. B: Condens. Matter **49**(9), 6188–6192 (1994)
35. Cunha, M.D., Konotop, V.V., Vázquez, L.: Small-amplitude solitons in a nonlocal sine-Gordon model. Phys. Lett. A **221**(5), 317–322 (1996)
36. Vázquez, L., Evans, W.A., Rickayzen, G.: Numerical investigation of a non-local sine-Gordon model. Phys. Lett. A **189**(6), 454–459 (1994)
37. Wu, G., Baleanu, D., Deng, Z., Zeng, S.: Lattice fractional diffusion equation in terms of a Riesz-Caputo difference. Physica A-Stat. Mech. Appl. **438**, 335–339 (2015)
38. Rabei, E.M., Rawashdeh, I.M., Muslih, S., Baleanu, D.: Hamilton-Jacobi formulation for systems in terms of Riesz's fractional derivatives. Int. J. Theor. Phys. **50**(5), 1569–1576 (2011)
39. Fahd, J., Thabet, A., Baleanu, D.: On Riesz-caputo formulation for sequential fractional variational principles. Abstr. Appl, Anal. **2012**, 1–15 (2012). (Article Number: 890396)
40. Magin, R.L., Abdullah, O., Baleanu, D., Zhou, X.J.: Anomalous diffusion expressed through fractional order differential operators in the Bloch-Torrey equation. J. Magn. Reson. **190**(2), 255–270 (2008)
41. Meerschaert, M.M., Tadjeran, C.: Finite difference approximations for two-sided space-fractional partial differential equations. Appl. Numer. Math. **56**, 80–90 (2006)
42. Yang, Q., Liu, F., Turner, I.: Computationally efficient numerical methods for time- and space-fractional Fokker-Planck equations. Phys. Scr. **2009**, T136 (2009)
43. Çelik, C., Duman, M.: Crank–Nicolson method for the fractional diffusion equation with the Riesz fractional derivative. J. Comput. Phys. **231**, 1743–1750 (2012)
44. Debnath, L.: Integral Transforms and Their Applications. CRC Press, Boca Raton (1995)

45. Samko, S.G., Kilbas, A.A., Marichev, O.I.: Fractional Integrals and Derivatives: Theory and Applications. Taylor and Francis, London (1993)
46. Saha Ray, S.: Fractional Calculus with Applications for Nuclear Reactor Dynamics. CRC Press, Taylor and Francis Group, Boca Raton, New York (2015)
47. Tarasov, V.E.: Fractional dynamics: applications of fractional calculus to dynamics of particles, fields and media. Springer, Berlin, Heidelberg, New York (2011)
48. Herrmann, R.: Fractional Calculus: An Introduction for Physicists. World Scientific, Singapore (2011)
49. Gorenflo, R., Mainardi, F.: Random walk models for space-fractional diffusion processes. Fractional Calculus Appl. Anal. **1**(2), 167–191 (1998)
50. Saha Ray, S.: Numerical Analysis with Algorithms and Programming. CRC Press, Taylor and Francis Group, Boca Raton, New York (2016)
51. Smith, G.D.: Numerical Solution of Partial Differential Equations: Finite Difference Methods. Oxford University Press Inc., New York, USA (1985)
52. Adomian, G.: Solving Frontier Problems of Physics: The Decomposition Method. Kluwer Academic Publishers, Boston (1994)
53. Khan, Y., Taghipour, R., Falahian, M., Nikkar, A.: A new approach to modified regularized long wave equation. Neural Comput. Appl. **23**, 1335–1341
54. Jafari, H., Sayevand, K., Khan, Y., Nazari, M.: Davey-Stewartson equation with fractional coordinate derivatives. Sci World J **2013**, 8 pp (2013). (Article ID 941645)
55. Kaya, D.: A numerical solution of the Sine-Gordon equation using the modified decomposition method. Appl. Math. Comp. **143**, 309–317 (2003)
56. Wei, G.W.: Discrete singular convolution for the sine-Gordon equation. Physica D **137**, 247–259 (2000)
57. Batiha, B., Noorani, M.S.M., Hashim, I.: Numerical solution of sine-Gordon equation by variational iteration method. Phys. Lett. A **370**, 437–440 (2007)
58. Liao, S.: The proposed homotopy analysis techniques for the solution of nonlinear problems. Ph.D. Thesis, Shanghai Jiao Tong University, Shanghai (1992) (in English)

Chapter 5
New Exact Solutions of Fractional-Order Partial Differential Equations

5.1 Introduction

Fractional differential equations (FDEs) have been used nowadays frequently in various applications for modeling anomalous diffusion, heat transfer, seismic wave analysis, signal processing, sound wave propagation, and many other fractional dynamical systems [1–6]. The FDEs are used in modeling many problems in physics and engineering. The fractional derivatives introduced in physical models can describe sound attenuation in complex media. When introduced into the constitutive equations, they build a wave equation in which attenuation obeys a frequency power law characteristic of many media [7].

The last few decades have witnessed rapid development in novel diagnostic and therapeutic applications of ultrasound in biology and medicine. Nonlinear ultrasound modeling has become gradually important for accurate evaluation and simulation of ultrasound in a number of purposes. Ultrasound beams in the therapeutic modalities are finite amplitude in nature. Accurate nonlinear ultrasound models and their competent applications are required for accurate modeling and simulation of those models of ultrasound applications. Additionally, accurate and efficient exact solutions of nonlinear ultrasound models will significantly help us in order to understand the complicated physical phenomena of ultrasound and the associated bioeffects. The main motivation of this work is to develop the exact solutions of fractional-order nonlinear acoustic wave equations.

The study of numerous approximations to the Burgers–Hopf equations in (5.1) has a prominent history concerning the symbiotic interaction of mathematical model and scientific computing to gain insight into the topic.

The propagation of focused and intense ultrasound beams is accompanied by nonlinearity, diffraction, and absorption. For modeling of nonlinear propagation of ultrasound beams in soft tissue, among others, the combined effects of nonlinearity, absorption, and diffraction must be taken into consideration. The description of large amplitude ultrasonic beams requires an accurate representation of

S. Saha Ray, *Nonlinear Differential Equations in Physics*,
https://doi.org/10.1007/978-981-15-1656-6_5

nonlinearity, absorption, and diffraction. One of the extensively used nonlinear models for the propagation of diffractive ultrasound in dissipative media is the Khokhlov–Zabolotskaya–Kuznetsov (KZK) nonlinear acoustic wave equation [8, 9]. The Khokhlov–Zabolotskaya–Kuznetsov (KZK) equation is a nonlinear beam equation that has been used to model nonlinear wave propagation in therapeutic ultrasound.

Recently, a considerable number of research works have been rendered by the notable researchers to develop the solutions of fractional partial differential equations, fractional ordinary differential equations, and integral equations of physical interest. The fractional differential equations can be described best in discontinuous media, and the fractional order is equivalent to its fractional dimensions. Fractal media which are complex appear in different fields of engineering and physics. In this context, the local fractional calculus theory is very important for modeling problems for fractal mathematics and engineering on Cantorian space in fractal media. Several analytical and numerical methods have been proposed to attain exact and approximate solutions of fractional differential equations [10–22].

With the help of fractional complex transform via the local fractional derivatives, fractional differential equations can be converted into integer-order ordinary differential equations. The fractional complex transform is used to change fractal time-space to continuous time-space. The first integral method [23–27] can be devised to establish the exact solutions for some time fractional differential equations. The present work focuses on the first time the applicability and efficacy of the first integral method on fractional nonlinear acoustic wave equations. To the best information of the author, the exact analytical solutions for the above nonlinear fractional-order acoustic wave equations have been obtained first time ever in this chapter.

In recent years, fractional calculus has played a very important role in various applications for modeling anomalous diffusion, heat transfer, seismic wave analysis, signal processing, control theory, image processing, and many other fractional dynamical systems [1–6]. Fractional differential equations (FDEs) are the generalization of classical differential equations of integer order. The FDEs are inherently multidisciplinary with its application across diverse disciplines of applied science and engineering. Recently, FDEs have attracted great interest due to their applications in various real physical problems. The descriptions of properties of several physical phenomena are found to be best described by fractional differential equations. For this purpose, a reliable and efficient technique is essential for the solution of nonlinear fractional differential equations. In this connection, it is worthwhile to mention the recent notable works on the solutions of fractional differential equations, integral equations, and fractional partial differential equations of physical interest. Several analytical and numerical methods have been employed to develop approximate and exact solutions of fractional differential equations [10, 12–14, 16, 17, 19–22, 28, 29].

The sound propagation in a fluid is determined by nonlinearity, diffraction, absorption, and dispersion. For modeling of nonlinear sound propagation in fluid, the combined effects of nonlinearity, absorption, dispersion, and diffraction should

be taken into account. The description of sound propagation in fluid requires an accurate representation of nonlinearity, dispersion, absorption, and diffraction.

The KdV-Khokhlov–Zabolotskaya–Kuznetsov (KdV-KZK) equation describes all the basic physical mechanisms of sound propagation in fluids [30]. The KdV-KZK equation for fluids has profound applications in aerodynamics, acoustics, and also its extension to solids has applications in biomedical engineering and in nonlinear acoustical nondestructive testing.

Nonlinear FDEs can be transformed into integer-order nonlinear ordinary differential equations via fractional complex transform with the help of modified Riemann–Liouville fractional derivative and corresponding useful formulae. The present methods [31–36] under study can be devised to develop the exact analytical solutions for time fractional KdV-KZK equation. The main motivation of this work is to develop the exact solutions of the fractional-order KdV-KZK equation. To the best information of the author, the exact analytical solutions for the fractional KdV-KZK equation have been reported first time ever in this chapter.

In recent decades, FDEs have attracted increasing attention as they are widely used to describe various complex phenomena in many fields [1, 37–41], such as the fluid dynamics, acoustic dissipation, geophysics, relaxation, creep, viscoelasticity, rheology, chaos, control theory, economics, signal and image processing, systems identification, biology, and other areas. Most of the classical mechanic techniques have been used in studies of conservative systems, but most of the processes observed in the physical real world are nonconservative. If the Lagrangian of a conservative system is constructed using fractional derivatives, the resulting equations of motion can be nonconservative. In view of the fact that most physical phenomena may be considered as nonconservative, they can be described using fractional-order differential equations. Therefore, in many cases, the real physical processes could be modeled in a reliable manner using fractional-order differential equations rather than integer-order equations [39].

In particular, the fractional derivative is useful in describing the memory and hereditary properties of materials and processes. The fractional differential equations can be described best in discontinuous media, and the fractional order is equivalent to its fractional dimensions. Fractal media which are complex appear in different fields of engineering and physics. In this context, the local fractional calculus theory is very important for modeling problems for fractal mathematics and engineering on Cantorian space in fractal media. Among the investigations for fractional differential equations, finding numerical and exact solutions to fractional differential equations is a prior matter of concern. Many efficient methods have been proposed so far to obtain numerical solutions and exact solutions of fractional differential equations. Most nonlinear physical phenomena that appear in many areas of scientific fields, such as plasma physics, solid state physics, fluid dynamics, optical fibers, mathematical biology, and chemical kinetics, can be best modeled by nonlinear fractional partial differential equations.

With the help of fractional complex transform via the local fractional derivatives, fractional differential equations can be converted into integer-order ordinary differential equations. The fractional complex transform is used to change fractal time-space to continuous time-space.

In this chapter, we present the traveling wave solutions of the fractional (2 + 1)-dimensional Davey–Stewartson equation and doubly periodic solutions of new integrable Davey–Stewartson-type equation. We employ the mixed dn-sn method [42] approach via fractional complex transform in order to obtain exact solutions to the fractional (2 + 1)-dimensional Davey–Stewartson equation and the new integrable Davey–Stewartson-type equation.

5.2 Outline of the Present Study

In this chapter, new exact solutions of fractional nonlinear acoustic wave equations have been devised. The traveling periodic wave solutions of fractional Burgers–Hopf equation and Khokhlov–Zabolotskaya–Kuznetsov (KZK) equation have obtained by the first integral method. Nonlinear ultrasound modeling is found to have an increasing number of applications in both medical and industrial areas where due to high-pressure amplitudes the effects of nonlinear propagation are no longer negligible. Taking nonlinear effects into account, the ultrasound beam analysis makes more accurate in these applications. The Burgers–Hopf equation is one of the extensively studied models in mathematical physics. In addition, the KZK parabolic nonlinear wave equation is one of the most widely employed nonlinear models for the propagation of 3D diffraction sound beams in dissipative media. In the present chapter, these nonlinear equations have solved by the first integral method. As a result, new exact analytical solutions have been obtained first time ever for these fractional-order acoustic wave equations. The obtained results are presented graphically to demonstrate the efficiency of this proposed method.

Also in this chapter, new exact solutions of time fractional KdV-Khokhlov–Zabolotskaya–Kuznetsov (KdV-KZK) equation have been established by classical Kudryashov method and modified Kudryashov method, respectively. In this purpose, modified Riemann–Liouville derivative has been applied to convert nonlinear time fractional KdV-KZK equation into the nonlinear ordinary differential equation. In the present chapter, the classical Kudryashov method and modified Kudryashov method both have been applied successively to compute the analytical solutions of time fractional KdV-KZK equation. As a result, new exact solutions have been obtained first time ever involving symmetric Fibonacci function, hyperbolic function, and exponential function. The methods under consideration are reliable, efficient and can be used as an alternative to establish new exact solutions of different types of fractional differential equations arising in mathematical physics. The obtained results are exhibited graphically in order to demonstrate the efficiency and applicability of these proposed methods for solving nonlinear time fractional KdV-KZK equation.

Moreover, the Jacobi elliptic function method, viz. mixed dn-sn method, has been presented in this chapter for finding the traveling wave solutions of the Davey–Stewartson equations. As a result, some solitary wave solutions and doubly periodic solutions are obtained in terms of Jacobi elliptic functions. Furthermore, solitary wave solutions are obtained as simple limits of doubly periodic functions. These solutions can be useful to explain some physical phenomena, viz. evolution of a three-dimensional wave packet on the water of finite depth. The proposed Jacobi elliptic function method is efficient, powerful and can be used in order to establish more newly exact solutions for other kinds of nonlinear fractional partial differential equations arising in mathematical physics.

5.2.1 Time Fractional Nonlinear Acoustic Wave Equations

Let us consider the time fractional Burgers–Hopf equation [43]

$$\partial_z p = \gamma D_\tau^{2\alpha} p + \beta D_\tau^{\alpha} p^2 \tag{5.1}$$

and the (3 + 1)-dimensional time fractional Khokhlov–Zabolotskaya–Kuznetsov (KZK) equation [44–46]

$$\partial_z D_\tau^{\alpha} p = \frac{c_0}{2} \Delta_\perp p + \gamma D_\tau^{3\alpha} p + \beta D_\tau^{2\alpha} p^2 \tag{5.2}$$

where $0 < \alpha \leq 1$, $\gamma = \frac{D}{2c_0^3}$, and $\beta = \frac{\tilde{\beta}}{2\rho_0 c_0^2}$. Here, p is the acoustic pressure, z is the direction of propagation, $\tau = t - \frac{z}{c_0}$ is the retarded time variable, c_0 is the small signal speed of sound, D is the diffusivity parameter, and ρ_0 is the ambient fluid density.

The first term on the right-hand side of Eq. (5.2) represents diffraction. The second term accounts for thermoviscous attenuation as with Burgers' equation and nonlinearity is described in the third term. The coefficient of nonlinearity $\tilde{\beta}$ is defined by $\tilde{\beta} = 1 + B/2A$, where B/A is the nonlinearity parameter of the medium. The transverse Laplacian can be written in Cartesian coordinates as

$$\Delta_\perp p = \frac{\partial^2 p}{\partial x^2} + \frac{\partial^2 p}{\partial y^2} \tag{5.3}$$

The Khokhlov–Zabolotskaya–Kuznetsov (KZK) equation is an augmented type of Burgers' equation. In addition to absorption and nonlinearity, it is also involved with diffraction. This last term allows the KZK equation to describe

three-dimensional directional nonlinear sound beams; the form generated through the ultrasonic transducer. The nonlinear parabolic KZK wave equation describes the effects of diffraction, absorption, and nonlinearity.

5.2.2 Time Fractional KdV-Khokhlov–Zabolotskaya–Kuznetsov Equation

Let us consider the (3 + 1)-dimensional time fractional KdV-KZK equation

$$\partial_z D_\tau^\alpha p = \frac{c_0}{2}\Delta_\perp p + A_1 D_\tau^{3\alpha} p + A_2 D_\tau^{2\alpha} p^2 - \gamma D_\tau^{4\alpha} p \tag{5.4}$$

where $0 < \alpha \leq 1$, $A_1 = \frac{b}{2c_0^3\rho_0}$, and $A_2 = \frac{\varepsilon}{2\rho_0 c_0^3}$. Here, p is the acoustic pressure, z is the direction of sound propagation, $\tau = t - \frac{z}{c_0}$ is the retarded time variable, c_0 is the small signal speed of sound, ε is the parameter of nonlinearity, b is the diffusivity parameter, ρ_0 is the ambient fluid density, and γ is the adiabatic index defined by $\gamma = c_p/c_v$, where c_p and c_v are the specific heats at constant pressure and constant volume.

The first term on the right-hand side of Eq. (5.4) represents diffraction. The second term accounts for thermoviscous attenuation as with Burgers' equation and nonlinearity is described in the third term. In comparison to KdV–Burgers equation, the KdV-KZK equation has only one extra term. The diffusivity parameter b is defined by $b = \zeta + 4\eta/3$, where ζ and η are the bulk and shear viscosity. The transverse Laplacian can be written in Cartesian coordinates as

$$\Delta_\perp p = \frac{\partial^2 p}{\partial x^2} + \frac{\partial^2 p}{\partial y^2} \tag{5.5}$$

The KdV-KZK equation is an augmented form of the KdV–Burgers equation. In addition to absorption, dispersion, and nonlinearity, it also accounts for diffraction. The nonlinear parabolic KdV-KZK equation describes the combined effects of diffraction, absorption, dispersion, and nonlinearity.

5.2.3 Time Fractional (2 + 1)-Dimensional Davey–Stewartson Equations

Davey–Stewartson (DS) equations have been used for various applications in fluid dynamics. It was proposed initially for the evolution of weakly nonlinear pockets of water waves in the finite depth by Davey and Stewartson [47].

Time Fractional (2 + 1)-Dimensional Davey–Stewartson Equation (Type I)

Let us consider the fractional (2 + 1)-dimensional Davey–Stewartson equation [48]

$$iD_t^{\alpha}q + a(D_x^{2\beta}q + D_y^{2\gamma}q) + b|q|^{2n}q - \lambda qr = 0, \tag{5.6}$$

$$D_x^{2\beta}r + D_y^{2\gamma}r + \delta D_x^{2\beta}\left(|q|^{2n}\right) = 0, \tag{5.7}$$

where $0<\alpha,\beta,\gamma\leq 1$, $q\equiv q(x,y,t)$, and $r\equiv r(x,y,t)$. Also, a, b, λ, and δ are all constant coefficients. The exponent n is the power law parameter. It is necessary to have $n>0$. In Eqs. (5.6) and (5.7), $q(x,y,t)$ is a complex-valued function which stands for wave amplitude, while $r(x,y,t)$ is a real-valued function which stands for mean flow. This system of equations is completely integrable and is often used to describe the long-time evolution of a two-dimensional wave packet [49–51].

Time Fractional (2 + 1)-Dimensional New Integrable Davey–Stewartson-Type Equation (Type II)

Let us consider the fractional (2 + 1)-dimensional new integrable Davey–Stewartson-type equation

$$\begin{gathered} iD_{\tau}^{\alpha}\Psi + L_1\Psi + \Psi\Phi + \Psi\chi = 0, \\ L_2\chi = L_3|\Psi|^2, \\ D_{\xi}^{\beta}\Phi = D_{\eta}^{\gamma}\chi + \mu D_{\eta}^{\gamma}\left(|\Psi|^2\right), \quad \mu = \mp 1,\ 0<\alpha,\beta,\gamma\leq 1 \end{gathered} \tag{5.8}$$

where the linear differential operators are given by

$$\begin{gathered} L_1 \equiv \left(\tfrac{b^2-a^2}{4}\right)D_{\xi}^{2\beta} - aD_{\xi}^{\beta}D_{\eta}^{\gamma} - D_{\eta}^{2\gamma}, \\ L_2 \equiv \left(\tfrac{b^2+a^2}{4}\right)D_{\xi}^{2\beta} + aD_{\xi}^{\beta}D_{\eta}^{\gamma} + D_{\eta}^{2\gamma}, \\ L_3 \equiv \pm\tfrac{1}{4}\left(b^2+a^2+\tfrac{8b^2(a-1)}{(a-2)^2-b^2}\right)D_{\xi}^{2\beta} \pm \left(a+\tfrac{2b^2}{(a-2)^2-b^2}\right)D_{\xi}^{\beta}D_{\eta}^{\gamma} \pm D_{\eta}^{2\gamma}, \end{gathered}$$

where $\Psi\equiv\Psi(\xi,\eta,\tau)$ is complex, while $\Phi\equiv\Phi(\xi,\eta,\tau)$, $\chi\equiv\chi(\xi,\eta,\tau)$ are real and a, b are real parameters. The above equation in integer order was devised firstly by Maccari [52] from the Konopelchenko–Dubrovsky (KD) equation [53].

5.3 Algorithm of the First Integral Method with Fractional Complex Transform

In this section, we deal with the explicit solutions of Eqs. (5.1) and (5.2) by using the first integral method [54]. The main steps of this method are described as follows:

Step 1: Suppose that a nonlinear FPDE, say in four independent variables x, y, z, and t, is given by

$$P(u, u_x, u_{xx}, u_y, u_{yy}, u_z, u_t, D_t^{\alpha}u, D_t^{2\alpha}u, D_t^{3\alpha}u, \partial_z D_t^{\alpha}u, \ldots) = 0,\ 0 < \alpha \leq 1 \tag{5.9}$$

where $u = u(x, y, z, t)$ is an unknown function, P is a polynomial in u and its various partial derivatives in which the highest order derivatives and nonlinear terms are involved.

Step 2: By using the fractional complex transform [55–58]:

$$u(x, y, z, t) = \Phi(\xi),\ \xi = lx + my + kz + \frac{\lambda t^{\alpha}}{\Gamma(\alpha + 1)} \tag{5.10}$$

where l, m, k, and λ are constants.

By using the chain rule [55, 58], we have

$$\begin{aligned} D_t^{\alpha}u &= \sigma_t u_{\xi} D_t^{\alpha}\xi, \\ D_x^{\alpha}u &= \sigma_x u_{\xi} D_x^{\alpha}\xi, \\ D_y^{\alpha}u &= \sigma_y u_{\xi} D_y^{\alpha}\xi, \\ D_z^{\alpha}u &= \sigma_z u_{\xi} D_z^{\alpha}\xi, \end{aligned}$$

where σ_t, σ_x, σ_y, and σ_z are the fractal indexes [57, 58], without loss of generality we can take $\sigma_t = \sigma_x = \sigma_y = \sigma_z = \kappa$, where κ is a constant.

Thus, the FPDE (5.9) is transformed to the following ordinary differential equation (ODE) for $u(x, y, z, t) = \Phi(\xi)$:

$$P(\Phi, \lambda\Phi', \lambda^2\Phi'', \lambda^3\Phi''', l\Phi', l^2\Phi'', m\Phi', m^2\Phi'', \ldots, k\lambda\Phi'', \ldots) = 0, \tag{5.11}$$

where prime denotes the derivative with respect to ξ.

Step 3: We suppose that Eq. (5.11) has a solution in the form

$$\Phi(\xi) = X(\xi) \tag{5.12}$$

and introduce a new independent variable $Y(\xi) = \Phi_{\xi}(\xi)$, which leads to a system of ODEs of the form

$$\frac{\mathrm{d}X(\xi)}{\mathrm{d}\xi} = Y(\xi), \tag{5.13}$$

$$\frac{\mathrm{d}Y(\xi)}{\mathrm{d}\xi} = F(X(\xi), Y(\xi)).$$

In general, it is very difficult to solve a two-dimensional autonomous planar system of ODEs, such as Eq. (5.13).

Step 4: By using the qualitative theory of differential equations [59], if we can find the integrals to Eq. (5.13) under the same conditions, then the general solutions to Eq. (5.13) can be derived directly. With the aid of the division theorem for two variables in the complex domain **C** which is based on Hilbert's Nullstellensatz theorem [60], one first integral to Eq. (5.13) can be obtained. This first integral can reduce Eq. (5.11) to a first-order integrable ordinary differential equation. Then by solving this equation directly, the exact solution to Eq. (5.9) is obtained.

Now, let us recall the division theorem.

Theorem 5.1 (Division theorem)
Let $Q(x,y)$ and $R(x,y)$ are polynomials in $\boldsymbol{C}[[x,y]]$, and $Q(x,y)$ is irreducible in $\boldsymbol{C}[[x,y]]$. If $R(x,y)$ vanishes at all zero points of $Q(x,y)$, then there exists a polynomial $H(x,y)$ in $\boldsymbol{C}[[x,y]]$ such that

$$R(x,y) = Q(x,y)H(x,y). \tag{5.14}$$

5.4 Algorithm of the Kudryashov Methods Applied with Fractional Complex Transform

In this section, an algorithm has been presented for the analytical solutions of Eq. (5.4) by using both the classical Kudryashov method and modified Kudryashov method [31, 34, 35]. The main steps of this method are described as follows:

Step 1: Suppose that a nonlinear FPDE, say in four independent variables x, y, z, and t, is given by

$$P(u, u_x, u_{xx}, u_y, u_{yy}, u_z, u_t, D_t^{\alpha}u, D_t^{2\alpha}u, D_t^{3\alpha}u, \partial_z D_t^{\alpha}u, \ldots) = 0,\ 0 < \alpha \leq 1 \tag{5.15}$$

where $D_t^{\alpha}u$, $D_t^{2\alpha}u$ and $D_t^{3\alpha}u$ are modified Riemann–Liouville derivatives of u, where $u = u(x,y,z,t)$ is an unknown function, P is a polynomial in u, and its various partial derivatives in which the highest order derivatives and nonlinear terms are involved.

Step 2: By using the fractional complex transform [55, 56]:

$$u(x,y,z,t) = U(\xi) \quad \xi = lx + my + kz + \frac{\lambda t^{\alpha}}{\Gamma(\alpha+1)} \tag{5.16}$$

where l, m, k, and λ are constants.

By using the chain rule [55, 58], we have

$$\begin{aligned} D_t^{\alpha} u &= \sigma_t u_{\xi} D_t^{\alpha} \xi, \\ D_x^{\alpha} u &= \sigma_x u_{\xi} D_x^{\alpha} \xi, \\ D_y^{\alpha} u &= \sigma_y u_{\xi} D_y^{\alpha} \xi, \\ D_z^{\alpha} u &= \sigma_z u_{\xi} D_z^{\alpha} \xi, \end{aligned}$$

where σ_t, σ_x, σ_y, and σ_z are the fractal indexes [57, 58], without loss of generality we can take $\sigma_t = \sigma_x = \sigma_y = \sigma_z = \kappa$, where κ is a constant.

Thus, the FPDE (5.15) is reduced to the following nonlinear ordinary differential equation (ODE) for $u(x, y, z, t) = U(\xi)$:

$$P(U, \lambda U', \lambda^2 U'', \lambda^3 U''', lU', l^2 U'', mU', m^2 U'', \ldots, k\lambda U'', \ldots) = 0. \tag{5.17}$$

Step 3: We assume that the exact solution of Eq. (5.17) can be expressed in the following form

$$U(\xi) = \sum_{i=0}^{N} a_i Q^i(\xi), \tag{5.18}$$

where a_i $(i = 0, 1, 2, \ldots, N)$ are constants to be determined later, such that $a_N \neq 0$, while $Q(\xi)$ has the following form

I. **Classical Kudryashov method**

$$Q(\xi) = \frac{1}{1 + \exp(\xi)}. \tag{5.19}$$

This function $Q(\xi)$ satisfies the first-order differential equation

$$Q_{\xi}(\xi) = Q(\xi)(Q(\xi) - 1). \tag{5.20}$$

II. **Modified Kudryashov method**

$$Q(\xi) = \frac{1}{1 \pm a^{\xi}}. \tag{5.21}$$

This function satisfies the first-order differential equation

$$Q_{\xi}(\xi) = Q(\xi)(Q(\xi) - 1) \ln a. \tag{5.22}$$

Step 4: To determine the dominant term with the highest order of singularity, we substitute

$$U = \xi^{-p}, \tag{5.23}$$

to all terms of Eq. (5.17). Then, the degrees of all terms of Eq. (5.17) are compared, and consequently two or more terms with the lowest degree are chosen. The maximum value of p is the pole of Eq. (5.17), and it is equal to N. This method can be employed when N is integer. If N is noninteger, the equation under study needs to be transformed, and then, the above procedure to be repeated.

Step 5: The necessary number of derivatives of the function $U(\xi)$ with respect to ξ can be calculated using the computer algebra systems of any mathematical software.

Step 6: Substituting the derivatives of function $U(\xi)$ along with Eq. (5.18) in Eq. (5.17) in case of classical Kudryashov method or substituting the derivatives of function $U(\xi)$ along with Eq. (5.18) in Eq. (5.17) in case of modified Kudryashov method, Eq. (5.17) becomes the following form

$$\Phi[Q(\xi)] = 0, \tag{5.24}$$

where $\Phi[Q(\xi)]$ is a polynomial in $Q(\xi)$. Then, after collecting all terms with the same powers of $Q(\xi)$ and equating every coefficient of this polynomial to zero yield a set of algebraic equations for $a_i (i = 0,1,2,\ldots, N)$ and λ.

Step 7: Solving the algebraic equations system thus obtained in step 6 and subsequently substituting these values of the constants $a_i (i = 0, 1, 2,\ldots, N)$ and λ, we can obtain the explicit exact solutions of Eq. (5.4) instantly. The obtained solutions may involve in the symmetric hyperbolic Fibonacci functions [61, 62]. The symmetric Fibonacci sine, cosine, tangent, and cotangent functions are, respectively, defined as follows:

$$sFs(x) = \frac{a^x - a^{-x}}{\sqrt{5}}, \qquad cFs(x) = \frac{a^x + a^{-x}}{\sqrt{5}}$$

$$\tan Fs(x) = \frac{a^x - a^{-x}}{a^x + a^{-x}}, \qquad \cot Fs(x) = \frac{a^x + a^{-x}}{a^x - a^{-x}}.$$

5.5 Algorithm of the Mixed Dn-Sn Method with Fractional Complex Transform

In this present analysis, we deal with the determination of explicit solutions of fractional (2 + 1)-dimensional Davey–Stewartson equation by using the mixed dn-sn method. The main steps of this method are described as follows:

Step 1: Suppose that coupled nonlinear FPDEs, say in three independent variables x, y, and t, is given by

$$F(u, v, u_x, v_x, u_y, v_y, u_t, v_t, iD_t^{\alpha}u, D_t^{\alpha}v, D_x^{2\beta}u, D_x^{2\beta}v, D_y^{2\gamma}u, D_y^{2\gamma}v, \ldots) = 0,\ 0 < \alpha, \beta, \gamma \leq 1 \tag{5.25a}$$

$$G(u, v, u_x, v_x, u_y, v_y, u_t, v_t, D_t^{\alpha}u, D_t^{\alpha}v, D_x^{2\beta}u, D_x^{2\beta}v, D_y^{2\gamma}u, D_y^{2\gamma}v, \ldots) = 0,\ 0 < \alpha, \beta, \gamma \leq 1 \tag{5.25b}$$

where $u = u(x, y, t)$ and $v = v(x, y, t)$ are unknown functions, F and G are polynomials in u, v, and its various partial derivatives in which the highest order derivatives and nonlinear terms are involved.

Step 2: We use the fractional complex transform [55–58]:

$$u(x, y, t) = e^{i\theta}u(\xi), \quad v(x, y, t) = v(\xi),$$

$$\theta = \frac{\theta_1 x^{\beta}}{\Gamma(1+\beta)} + \frac{\theta_2 y^{\gamma}}{\Gamma(1+\gamma)} + \frac{\theta_3 t^{\alpha}}{\Gamma(1+\alpha)} \text{ and } \xi = \frac{\xi_1 x^{\beta}}{\Gamma(1+\beta)} + \frac{\xi_2 y^{\gamma}}{\Gamma(1+\gamma)} + \frac{\xi_3 t^{\alpha}}{\Gamma(1+\alpha)}, \tag{5.26}$$

where θ_1, θ_2, θ_3, ξ_1, ξ_2, and ξ_3 are real constants to be determined later.

By using the chain rule [55, 58], we have

$$\begin{aligned} D_t^{\alpha}u &= \sigma_t u_{\xi} D_t^{\alpha}\xi, \\ D_x^{\alpha}u &= \sigma_x u_{\xi} D_x^{\alpha}\xi, \\ D_y^{\alpha}u &= \sigma_y u_{\xi} D_y^{\alpha}\xi, \end{aligned}$$

where σ_t, σ_x, and σ_y are the fractal indexes [57, 58], without loss of generality we can take $\sigma_t = \sigma_x = \sigma_y = \kappa$, where κ is a constant.

Using fractional complex transform Eq. (5.26), the FPDE (5.25) can be converted to couple nonlinear ordinary differential equations (ODEs) involving $\Phi(\xi) = u(x, y, t)$ and $\Psi(\xi) = v(x, y, t)$. Then eliminating $\Psi(\xi)$ between the resultant coupled ODEs, the following ODE for $\Phi(\xi)$ is obtained

$$F(\Phi, \theta_3\Phi', \theta_3^2\Phi'', \theta_3^3\Phi''', \xi_3\Phi', \xi_3^2\Phi'', \xi_3^3\Phi, \ldots) = 0, \tag{5.27}$$

where prime denotes the derivative with respect to ξ.

Step 3: Let us assume that the exact solution of Eq. (5.27) is to be defined in the polynomial $\phi(\xi)$ of the following form:

$$\Phi(\xi) = \sum_{i=0}^{N} c_i \phi^i(\xi) + \sqrt{k^2 - \phi^2(\xi)} \sum_{i=0}^{N-1} d_i \phi^i(\xi), \tag{5.28}$$

where $\phi(\xi)$ satisfies the following elliptic equation:

$$\phi_{\xi} = \sqrt{(k^2 - \phi^2)(\phi^2 - k^2(1-m))}. \tag{5.29}$$

The solutions of Eq. (5.29) are given by

$$\phi(\xi) = kdn(k\xi|m),$$

$$\phi(\xi) = k\sqrt{1-m}nd(k\xi|m), \tag{5.30}$$

where $dn(k\xi|m)$ and $nd(k\xi|m) = \frac{1}{dn(k\xi|m)}$ are the Jacobi elliptic functions with modulus m $(0 < m < 1)$.

If $\phi(\xi) = kdn(k\xi|m)$, then Eq. (5.28) becomes

$$\Phi(\xi) = \sum_{i=0}^{N} c_i k^i dn^i(k\xi|m) + k\sqrt{m}sn(k\xi|m) \sum_{i=0}^{N-1} d_i k^i dn^i(k\xi|m),$$

while if $\phi(\xi) = k\sqrt{1-m}nd(k\xi|m)$, then Eq. (5.28) becomes

$$\Phi(\xi) = \sum_{i=0}^{N} c_i k^i (1-m)^{i/2} nd^i(k\xi|m) + k\sqrt{m}cd(k\xi|m) \sum_{i=0}^{N-1} d_i k^i (1-m)^{i/2} nd^i(k\xi|m),$$

where $cd(k\xi|m) = cn((k\xi|m)/dn(k\xi|m)$ and cn is the Jacobi cnoidal function. If $d_i = 0, i = 0, 1, 2, \ldots, N-1$, then Eq. (5.28) constitutes the dn (or nd) expansions.

Step 4: According to the proposed method, we substitute $\Phi(\xi) = \xi^{-p}$ in all terms of Eq. (5.27) for determining the highest order singularity. Then, the degree of all terms of Eq. (5.27) has been taken into the study, and consequently, the two or more terms of lower degree are chosen. The maximum value of p is known as the pole and it is denoted as "N." If "N" is an integer, then the method only can be implemented, and otherwise if "N" is a noninteger, the above Eq. (5.27) may be transferred and the above procedure is to be repeated.

Step 5: Substituting Eq. (5.28) into Eq. (5.27) yields the following algebraic equation

$$P(\phi) + \sqrt{k^2 - \phi^2} Q(\phi) = 0, \tag{5.31}$$

where $P(\phi)$ and $Q(\phi)$ are the polynomials in $\phi(\xi)$. Setting the coefficients of the various powers of ϕ in $P(\phi)$ and $Q(\phi)$ to zero will yield a system of algebraic equations in the unknowns c_i, d_i, k, and m. Solving this system, we can determine the value of these unknowns. Therefore, we can obtain several classes of exact solutions involving the Jacobi elliptic functions *sn*, *dn*, *nd,* and *cd* functions.

The Jacobi elliptic functions $sn(k\xi|m)$, $cn(k\xi|m)$, and $dn(k\xi|m)$ are double periodic and have the following properties:

$$sn^2(k\xi|m) + cn^2(k\xi|m) = 1,$$

$$dn^2(k\xi|m) + msn^2(k\xi|m) = 1.$$

Especially when $m \to 1$, the Jacobi elliptic functions degenerate to the hyperbolic functions, i.e.,

$$\begin{aligned} sn(k\xi|1) &\to \tanh(k\xi), \\ cn(k\xi|1) &\to \sec h(k\xi), \\ dn(k\xi|1) &\to \sec h(k\xi), \end{aligned}$$

and when $m \to 0$, the Jacobi elliptic functions degenerate to the trigonometric functions, i.e.,

$$\begin{aligned} sn(k\xi|0) &\to \sin(k\xi), \\ cn(k\xi|0) &\to \cos(k\xi), \\ dn(k\xi|0) &\to 1. \end{aligned}$$

Further explanations in detail about the Jacobi elliptic functions can be found in [63].

5.6 Implementation of the First Integral Method for Time Fractional Nonlinear Acoustic Wave Equations

In this section, the new exact analytical solutions of time fractional nonlinear acoustic wave equations have been obtained first time ever using the first integral method.

5.6.1 The Burgers–Hopf Equation

In the present analysis, we introduce the following fractional complex transform in Eq. (5.1):

$$p(z,\tau)=\Phi(\xi),\ \xi=kz+\frac{\lambda\tau^{\alpha}}{\Gamma(\alpha+1)} \tag{5.32}$$

where k and λ are constants.

By applying the fractional complex transform (5.32), Eq. (5.1) can be transformed to the following nonlinear ODE:

$$k\Phi'(\xi)=\gamma\lambda^2\Phi''(\xi)+2\lambda\beta\Phi(\xi)\Phi'(\xi). \tag{5.33}$$

Using Eqs. (5.12), (5.13), and (5.33) can be written as the following two-dimensional autonomous system

$$\frac{\mathrm{d}X(\xi)}{\mathrm{d}\xi}=Y(\xi), \tag{5.34}$$

$$\frac{\mathrm{d}Y(\xi)}{\mathrm{d}\xi}=\frac{k}{\lambda^2\gamma}Y(\xi)-\frac{2\beta}{\lambda\gamma}X(\xi)Y(\xi).$$

According to the first integral method, we assume that $X(\xi)$ and $Y(\xi)$ are the nontrivial solutions of Eq. (5.34) and

$$Q(X,Y)=\sum_{i=0}^{m}a_i(X)Y^i$$

is an irreducible polynomial in the complex domain $\boldsymbol{C}[X,Y]$ such that

$$Q[X(\xi),Y(\xi)]=\sum_{i=0}^{m}a_i(X(\xi))Y(\xi)^i=0, \tag{5.35}$$

where $a_i(X(\xi)),\ i=0,1,2,\ldots,m$ are polynomials in X and $a_m(X)\neq 0$. Equation (5.35) is called the first integral to Eq. (5.34). Applying the division theorem, there exists a polynomial $g(X)+h(X)Y$ in the complex domain $\boldsymbol{C}[X,Y]$ such that

$$\frac{\mathrm{d}Q}{\mathrm{d}\xi}=\frac{\partial Q}{\partial X}\frac{\mathrm{d}X}{\mathrm{d}\xi}+\frac{\partial Q}{\partial Y}\frac{\mathrm{d}Y}{\mathrm{d}\xi}=(g(X)+h(X)Y)\sum_{i=0}^{m}a_i(X)Y^i. \tag{5.36}$$

Let us suppose that $m=1$ in Eq. (5.35), and then by equating the coefficients of Y^i, $i=0,1$ on both sides of Eq. (5.36), we have

$$Y^0:\ a_0(X)g(X)=0 \tag{5.37}$$

$$Y^1 : \dot{a}_0(X) + a_1(X)\left(\frac{k}{\lambda^2\gamma} - \frac{2\beta X}{\lambda\gamma}\right) = a_0(X)h(X) + a_1(X)g(X) \tag{5.38}$$

$$Y^2 : \dot{a}_1(X) = a_1(X)h(X) \tag{5.39}$$

Since, $a_i(X)$, $i = 0, 1$ are polynomials in X, from Eq. (5.39) we infer that $a_1(X)$ is a constant and $h(X) = 0$. For simplicity, we take $a_1(X) = 1$. Then balancing the degrees of $g(X)$ and $a_0(X)$ in Eq. (5.38), we conclude that $\deg(g(X)) = 1$ only. Now suppose that

$$g(X) = b_1X + b_0,\ a_0(X) = \frac{A_2}{2}X^2 + A_1X + A_0, \quad (b_1 \neq 0, A_2 \neq 0) \tag{5.40}$$

where b_1, b_0, A_2, A_1, and A_0 are all constants to be determined. Using Eq. (5.38), we find that

$$b_0 = A_1 + \frac{k}{\lambda^2\gamma},$$
$$b_1 = A_2 - \frac{2\beta}{\lambda\gamma}.$$

Next, substituting $a_0(X)$ and $g(X)$ in Eq. (5.37) and consequently equating the coefficients of X^i, $i = 0, 1, 2, 3$ to zero, we obtain the following system of nonlinear algebraic equations:

$$X^0 : A_0\left(A_1 + \frac{k}{\lambda^2\gamma}\right) = 0 \tag{5.41}$$

$$X^1 : A_0\left(A_2 - \frac{2\beta}{\lambda\gamma}\right) + A_1\left(A_1 + \frac{k}{\lambda^2\gamma}\right) = 0, \tag{5.42}$$

$$X^2 : A_1\left(A_2 - \frac{2\beta}{\lambda\gamma}\right) + \frac{A_2}{2}\left(A_1 + \frac{k}{\lambda^2\gamma}\right) = 0, \tag{5.43}$$

$$X^3 : \frac{A_2}{2}\left(A_2 - \frac{2\beta}{\lambda\gamma}\right) = 0. \tag{5.44}$$

Solving the above system of Eqs. (5.41)–(5.44) simultaneously, we get the following nontrivial solution

$$A_0 = 0,\ A_1 = -\frac{k}{\lambda^2\gamma},\ A_2 = \frac{2\beta}{\lambda\gamma}, \tag{5.45}$$

Using Eqs. (5.45) into Eq. (5.35), we obtain

$$Y(\xi) = -\frac{\beta}{\lambda\gamma}X^2 + \frac{k}{\lambda^2\gamma}X. \tag{5.46}$$

Combining Eq. (5.46) with the system given by Eq. (5.34), the exact solution to Eq. (5.33) can be obtained as

$$p(z,\tau) = X(\xi) = \frac{k}{\beta\lambda + \cosh\left(\frac{k\xi}{\lambda^2\gamma} - kC_1\right) - \sinh\left(\frac{k\xi}{\lambda^2\gamma} - kC_1\right)}, \tag{5.47}$$

where C_1 is an arbitrary constant.

5.6.2 The Khokhlov–Zabolotskaya–Kuznetsov Equation

First, we introduce the following fractional complex transform in Eq. (5.2):

$$p(x,y,z,\tau) = \Phi(\xi),\ \xi = lx + my + kz + \frac{\lambda\tau^\alpha}{\Gamma(\alpha+1)} \tag{5.48}$$

where l, m, k, and λ are constants.

By applying the fractional complex transform (5.48), Eq. (5.2) can be transferred to the following nonlinear ODE:

$$k\lambda\Phi''(\xi) = \frac{c_0}{2}(l^2+m^2)\Phi''(\xi) + \gamma\lambda^3\Phi'''(\xi) + 2\lambda^2\beta(\Phi(\xi)\Phi''(\xi) + \Phi'(\xi)^2). \tag{5.49}$$

Then integrating Eq. (5.49) once, we obtain

$$\tilde{\xi}_0 + k\lambda\Phi'(\xi) = \frac{c_0}{2}(l^2+m^2)\Phi'(\xi) + \gamma\lambda^3\Phi''(\xi) + \lambda^2\beta(\Phi^2(\xi))', \tag{5.50}$$

where $\tilde{\xi}_0 = \lambda^3\gamma\xi_0$ is an integration constant.

Using Eqs. (5.12), (5.13), and (5.50) can be written as the following two-dimensional autonomous system

$$\frac{\mathrm{d}X(\xi)}{\mathrm{d}\xi} = Y(\xi), \tag{5.51}$$

$$\frac{\mathrm{d}Y(\xi)}{\mathrm{d}\xi} = \xi_0 + \frac{k}{\lambda^2\gamma}Y(\xi) - \frac{c_0}{2}\frac{(l^2+m^2)}{\lambda^3\gamma}Y(\xi) - \frac{2\beta}{\lambda\gamma}X(\xi)Y(\xi).$$

According to the first integral method, we suppose that $X(\xi)$ and $Y(\xi)$ are the nontrivial solutions of Eq. (5.51) and

$$Q(X,Y)=\sum_{i=0}^{m}a_i(X)Y^i$$

is an irreducible polynomial in the complex domain $\boldsymbol{C}[X,Y]$ such that

$$Q[X(\xi),Y(\xi)]=\sum_{i=0}^{m}a_i(X(\xi))Y(\xi)^i=0, \tag{5.52}$$

where $a_i(X(\xi))$, $i=0,1,2,\ldots,m$ are polynomials in X and $a_m(X)\neq 0$. Equation (5.52) is called the first integral to Eq. (5.51). Applying the division theorem, there exists a polynomial $g(X)+h(X)Y$ in the complex domain $\boldsymbol{C}[X,Y]$ such that

$$\frac{\mathrm{d}Q}{\mathrm{d}\xi}=\frac{\partial Q}{\partial X}\frac{\mathrm{d}X}{\mathrm{d}\xi}+\frac{\partial Q}{\partial Y}\frac{\mathrm{d}Y}{\mathrm{d}\xi}=(g(X)+h(X)Y)\sum_{i=0}^{m}a_i(X)Y^i. \tag{5.53}$$

Let us suppose that $m=1$ in Eq. (5.52), and then by equating the coefficients of Y^i, $i=0,1$ on both sides of Eq. (5.53), we have

$$Y^0:\ a_1(X)\xi_0=a_0(X)g(X), \tag{5.54}$$

$$Y^1:\ \dot{a}_0(X)=a_0(X)h(X)-a_1(X)\left(-\frac{c_0}{2}\frac{(l^2+m^2)}{\lambda^3\gamma}+\frac{k}{\lambda^2\gamma}-\frac{2\beta}{\lambda\gamma}X\right)+a_1(X)g(X), \tag{5.55}$$

$$Y^2:\ \dot{a}_1(X)=a_1(X)h(X), \tag{5.56}$$

Since $a_i(X)$, $i=0,1$ are polynomials in X, from Eq. (5.56) we infer that $a_1(X)$ is a constant and $h(X)=0$. For simplicity, we take $a_1(X)=1$. Then balancing the degrees of $a_0(X)$ and $g(X)$, Eq. (5.55) implies that $\deg(g(X))\leq\deg(a_0(X))$, and thus from Eq. (5.55), we infer that $\deg(g(X))=0$ or 1. If $\deg(g(X))=0$, suppose that $g(X)=A$, then from Eq. (5.55), we find

$$\dot{a}_0(X)=A+\frac{c_0}{2}\frac{(l^2+m^2)}{\lambda^3\gamma}-\frac{k}{\lambda^2\gamma}+\frac{2\beta}{\lambda\gamma}X. \tag{5.57}$$

Solving Eq. (5.57), we have

$$a_0(X) = AX + \frac{c_0}{2}\frac{(l^2+m^2)}{\lambda^3\gamma}X - \frac{k}{\lambda^2\gamma}X + \frac{\beta}{\lambda\gamma}X^2 + B, \tag{5.58}$$

where B is an arbitrary constant.

Next, replacing $a_0(X)$, $a_1(X)$, and $g(X)$ in Eq. (5.54) and consequently equating the coefficients of X^i, $i = 0, 1, 2$ to zero, we obtain the following system of nonlinear algebraic equations:

$$X^0 : AB = \xi_0 \tag{5.59}$$

$$X^1 : A^2 + \frac{c_0}{2}\frac{(l^2+m^2)}{\lambda^3\gamma}A - \frac{k}{\lambda^2\gamma}A = 0 \tag{5.60}$$

$$X^2 : \frac{\beta}{\lambda\gamma}A = 0 \tag{5.61}$$

Solving the above system of Eqs. (5.59)–(5.61) simultaneously, we get

$$A = 0. \tag{5.62}$$

Using Eqs. (5.62) into Eq. (5.52), we obtain

$$Y(\xi) = -\frac{c_0}{2}\frac{(l^2+m^2)}{\lambda^3\gamma}X + \frac{k}{\lambda^2\gamma}X - \frac{\beta}{\lambda\gamma}X^2 - B. \tag{5.63}$$

Combining Eq. (5.63) with the system given by Eq. (5.51), the exact solution to Eq. (5.50) can be obtained as

$$p(x,y,z,\tau) = X(\xi) = \frac{-1}{4\lambda^2\beta}\left(c_0(l^2+m^2) - 2k\lambda + \sqrt{\eta}\tan\left(\frac{\sqrt{\eta}}{4\lambda^3\gamma}\left(\xi - 2\lambda^3\gamma C_1\right)\right)\right), \tag{5.64}$$

where $\eta = -c_0^2(l^2+m^2)^2 + 4c_0k\lambda(l^2+m^2) - 4\lambda^2(k^2 - 4B\beta\gamma\lambda^3)$ and C_1 is an arbitrary constant.

The established solutions (5.63) and (5.64) have been checked by putting them into the original Eqs. (5.1) and (5.2). Thus, the new exact solutions (5.63) and (5.64) of fractional Burgers–Hopf and KZK equations, respectively, have been first time obtained in this present work.

5.6.3 *Numerical Results and Discussions for Nonlinear Fractional Acoustic Wave Equations*

In this present numerical experiment, two exact solutions of Eqs. (5.1) and (5.2) have been used to draw the graphs as shown in Figs. 5.1, 5.2, 5.3, and 5.4 for different fractional-order values of α.

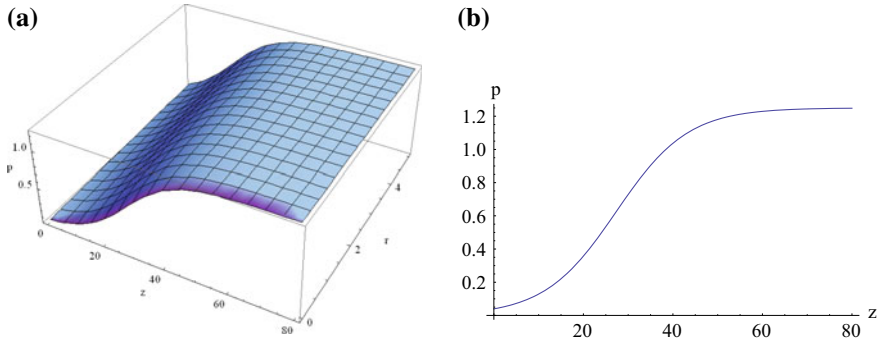

Fig. 5.1 **a** The periodic traveling wave solution for $p(z,\tau)$ appears in Eq. (5.47) of **Case I**, **b** corresponding solution for $p(z,\tau)$, when $\tau = 0$

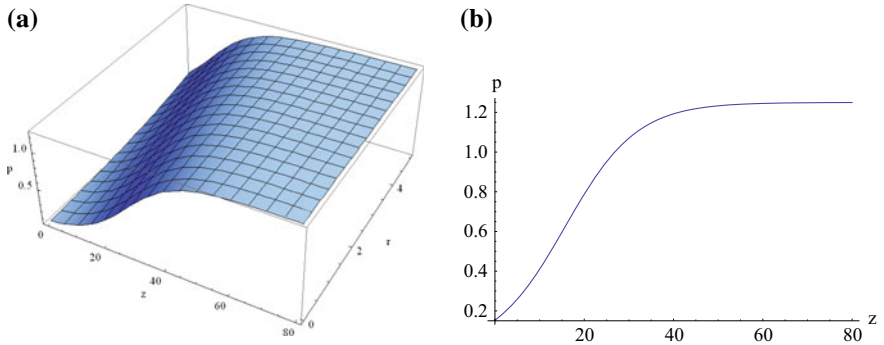

Fig. 5.2 **a** The periodic traveling wave solution for $p(z,\tau)$ appears in Eq. (5.47) of **Case II**, **b** corresponding solution for $p(z,\tau)$, when $\tau = 3$

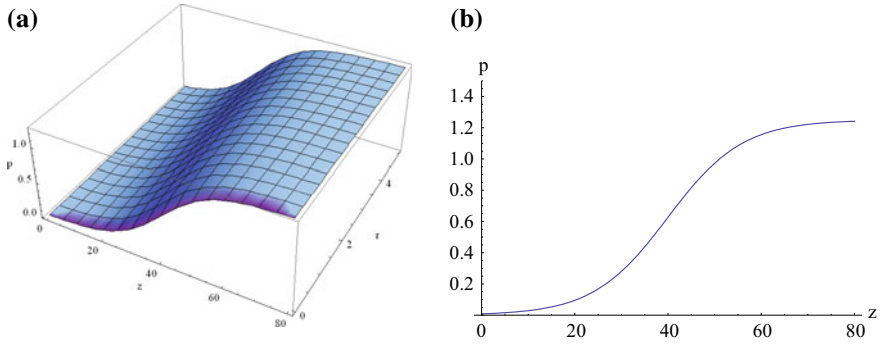

Fig. 5.3 **a** The periodic traveling wave solution for $p(x, y, z, \tau)$ obtained in Eq. (5.64) of **Case III**, **b** corresponding solution for $p(x, y, z, \tau)$, when $\tau = 0$

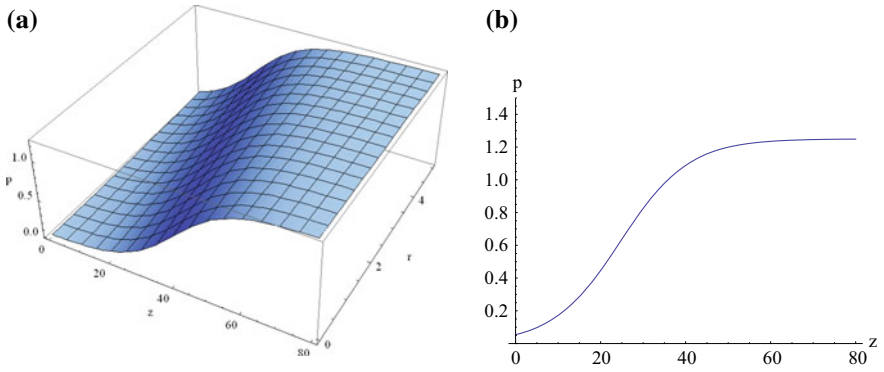

Fig. 5.4 **a** The periodic traveling wave solution for $p(x, y, z, \tau)$ obtained in Eq. (5.64) of **Case IV**, **b** corresponding solution for $p(x, y, z, \tau)$, when $\tau = 4$

Numerical Simulations for Fractional Burgers–Hopf Equation

Case I: For $\alpha = 0.5$ (Fractional order)

Case II: For $\alpha = 0.95$ (Fractional order)

Numerical Simulations for Fractional KZK Equation

Case III: For $\alpha = 0.5$ (Fractional order)

Case IV: For $\alpha = 0.95$ (Fractional order)

In the present numerical simulation, the traveling wave 3-D solutions surfaces and corresponding 2-D solution graphs have been drawn for the obtained exact solutions of Eqs. (5.1) and (5.2) in case of fractional-order time derivative. It can be observed that in all the above cases, the obtained exact solutions represent the kink-type traveling wave solutions with regard to various fractional-order solutions.

5.7 Exact Solutions of Time Fractional KdV-KZK Equation

In the present section, the new exact analytical solutions of time fractional KdV-KZK equation have been obtained first time ever using the Kudryashov method and modified Kudryashov method, respectively.

5.7.1 *Kudryashov Method for Time Fractional KdV-KZK Equation*

In the present analysis, we introduce the following fractional complex transform in Eq. (5.4):

$$p(x,y,z,\tau) = U(\xi),\ \xi = lx + my + kz + \frac{\lambda\tau^{\alpha}}{\Gamma(\alpha+1)}, \tag{5.65}$$

where k and λ are constants.

By applying the fractional complex transform (5.65), Eq. (5.4) can be transformed to the following nonlinear ODE:

$$k\lambda U_{\xi\xi} = \frac{c_0}{2}(l^2+m^2)U_{\xi\xi} + A_1\lambda^3 U_{\xi\xi\xi\xi} + 2A_2\lambda^2[UU_{\xi\xi} + (U_{\xi})^2] - \gamma\lambda^4 U_{\xi\xi\xi\xi\xi}. \tag{5.66}$$

Integrating Eq. (5.66) with respect to ξ once, we have

$$C_1 + k\lambda U'(\xi) = \frac{c_0}{2}(l^2+m^2)U'(\xi) + A_1\lambda^3 U''(\xi) + 2A_2\lambda^2 U(\xi)U'(\xi) - \gamma\lambda^4 U'''(\xi), \tag{5.67}$$

where C_1 is the integration constant.

The dominant terms with highest order of singularity are $\gamma\lambda^4 U'''(\xi)$ and $2A_2\lambda^2 U(\xi)U'(\xi)$. Thus, the pole order of Eq. (5.67) is $N = 2$.

Therefore, we sought for a solution in the form

$$U(\xi) = a_0 + a_1 Q(\xi) + a_2 Q(\xi)^2 \tag{5.68}$$

where a_0, a_1, and a_2 are constants to be determined later.

Substituting the derivatives of function $U(\xi)$ with respect to ξ and taking into account ansatz (5.68) in Eq. (5.67), we obtain a system of algebraic equations in the following form

$$
\begin{aligned}
Q^1 &: -\frac{1}{2}a_1c_0(l^2+m^2)\ln a + a_1k\lambda \ln a - 2a_0a_1A_2\lambda^2 \ln a \\
&\quad + a_1A_1\lambda^3(\ln a)^2 + a_1\gamma\lambda^4(\ln a)^3 = 0 \\
Q^2 &: \frac{1}{2}a_1c_0(l^2+m^2)\ln a - a_2c_0(l^2+m^2)\ln a - a_1k\lambda \ln a + 2a_2k\lambda \ln a \\
&\quad + 2a_0a_1A_2\lambda^2 \ln a - 2a_1^2A_2\lambda^2 \ln a - 4a_0a_2A_2\lambda^2 \ln a - 3a_1A_1\lambda^3(\ln a)^2 \\
&\quad + 4a_2A_1\lambda^3(\ln a)^2 - 7a_1\gamma\lambda^4(\ln a)^3 + 8a_2\gamma\lambda^4(\ln a)^3 = 0 \\
Q^3 &: a_2c_0(l^2+m^2)\ln a - 2a_2k\lambda \ln a + 2a_1^2A_2\lambda^2 \ln a + 4a_0a_2A_2\lambda^2 \ln a \\
&\quad - 6a_1a_2A_2\lambda^2 \ln a + 2a_1A_1\lambda^3(\ln a)^2 - 10A_1a_2\lambda^3(\ln a)^2 \\
&\quad + 12a_1\gamma\lambda^4(\ln a)^3 - 38a_2\gamma\lambda^4(\ln a)^3 = 0 \\
Q^4 &: 6a_1a_2A_2\lambda^2 \ln a - 4a_2^2A_2\lambda^2 \ln a + 6a_2A_1\lambda^3(\ln a)^2 \\
&\quad - 6a_1\gamma\lambda^4(\ln a)^3 + 54a_2\gamma\lambda^4(\ln a)^3 = 0 \\
Q^5 &: 4a_2^2A_2\lambda^2 \ln a - 24a_2\gamma\lambda^4(\ln a)^3 = 0
\end{aligned}
$$

Solving this system, we obtain the following family of solutions

Case I:

$$
\begin{aligned}
a_0 &= -\frac{12A_1^4 + 250A_1k\gamma^2 + 625c_0(l^2+m^2)\gamma^3}{100A_1^2A_2\gamma}, \\
a_1 &= 0, \\
a_2 &= \frac{6A_1^2}{25A_2\gamma}, \\
\lambda &= -\frac{A_1}{5\gamma}.
\end{aligned}
$$

Substituting the above parameter values in the ansatz given by Eq. (5.68), we obtain the following solution of Eq. (5.4)

$$
\begin{aligned}
p(x,y,z,\tau) &= U(\xi) \\
&= -\frac{125\gamma^2(2kA_1 + 5c_0(l^2+m^2)\gamma) + 6A_1^4 \sec h^2\left(\frac{\xi}{2}\right)(1+\sinh(\xi))}{100A_1^2A_2\gamma},
\end{aligned}
\tag{5.69}
$$

where $\xi = lx + my + kz + \frac{\lambda t^\alpha}{\Gamma(\alpha+1)}$ and $\lambda = -\frac{A_1}{5\gamma}$.

Case II:

$$\begin{aligned} a_0 &= \frac{12A_1^4+250A_1k\gamma^2-625c_0(l^2+m^2)\gamma^3}{100A_1^2A_2\gamma}, \\ a_1 &= -\frac{12A_1^2}{25A_2\gamma}, \\ a_2 &= \frac{6A_1^2}{25A_2\gamma}, \\ \lambda &= \frac{A_1}{5\gamma}. \end{aligned}$$

Substituting the above parameter values in the ansatz given by Eq. (5.68), we obtain the following solution of Eq. (5.4)

$$p(x,y,z,\tau) = U(\xi) = \frac{125\gamma^2(2kA_1 - 5c_0(l^2+m^2)\gamma) - 6A_1^4\text{sech}^2\left(\frac{\xi}{2}\right)(1-\sinh(\xi))}{100A_1^2A_2\gamma}, \tag{5.70}$$

where $\xi = lx + my + kz + \frac{\lambda t^{\alpha}}{\Gamma(\alpha+1)}$ and $\lambda = \frac{A_1}{5\gamma}$.

5.7.2 *Modified Kudryashov Method for Time Fractional KdV-KZK Equation*

Following the same preceding argument, Eq. (5.67) is to be acquired. Then substituting the derivatives of function $U(\xi)$ with respect to ξ into Eq. (5.67) and the ansatz given by Eq. (5.68) into the resulting Eq. (5.67), we obtain a system of algebraic equations in the following form

$$\begin{aligned} Q^1 &: -\tfrac{1}{2}a_1c_0(l^2+m^2)\ln a + a_1k\lambda\ln a - 2a_0a_1A_2\lambda^2\ln a + a_1A_1\lambda^3(\ln a)^2 + a_1\gamma\lambda^4(\ln a)^3 = 0, \\ Q^2 &: \tfrac{1}{2}a_1c_0(l^2+m^2)\ln a - a_2c_0(l^2+m^2)\ln a - a_1k\lambda\ln a + 2a_2k\lambda\ln a + 2a_0a_1A_2\lambda^2\ln a - 2a_1^2A_2\lambda^2\ln a \\ &\quad -4a_0a_2A_2\lambda^2\ln a - 3a_1A_1\lambda^3(\ln a)^2 + 4a_2A_1\lambda^3(\ln a)^2 - 7a_1\gamma\lambda^4(\ln a)^3 + 8a_2\gamma\lambda^4(\ln a)^3 = 0, \\ Q^3 &: a_2c_0(l^2+m^2)\ln a - 2a_2k\lambda\ln a + 2a_1^2A_2\lambda^2\ln a + 4a_0a_2A_2\lambda^2\ln a - 6a_1a_2A_2\lambda^2\ln a + 2a_1A_1\lambda^3(\ln a)^2 \\ &\quad -10A_1a_2\lambda^3(\ln a)^2 + 12a_1\gamma\lambda^4(\ln a)^3 - 38a_2\gamma\lambda^4(\ln a)^3 = 0, \\ Q^4 &: 6a_1a_2A_2\lambda^2\ln a - 4a_2^2A_2\lambda^2\ln a + 6a_2A_1\lambda^3(\ln a)^2 - 6a_1\gamma\lambda^4(\ln a)^3 + 54a_2\gamma\lambda^4(\ln a)^3 = 0, \\ Q^5 &: 4a_2^2A_2\lambda^2\ln a - 24a_2\gamma\lambda^4(\ln a)^3 = 0. \end{aligned}$$

Solving this system we obtain the following family of solutions

Case I:

$$a_0 = -\frac{12A_1^4 + 250A_1k\gamma^2 \ln a + 625c_0(l^2+m^2)\gamma^3(\ln a)^2}{100A_1^2A_2\gamma},$$
$$a_1 = 0,$$
$$a_2 = \frac{6A_1^2}{25A_2\gamma},$$
$$\lambda = -\frac{A_1}{5\gamma \ln a}.$$

Substituting the above parameter values in the ansatz given by Eq. (5.68), we obtain the following solutions of Eq. (5.4)

$$p_1(x,y,z,\tau) = -\frac{1}{100A_1^2A_2\gamma}\left[12\left(1-\frac{\left(1-\tan Fs\left(\frac{\xi}{2}\right)\right)^2}{2}\right)\right. \\ \left. A_1^4 + 250A_1k\gamma^2 \ln a + 625c_0(l^2+m^2)\gamma^3(\ln a)^2\right], \tag{5.71}$$

$$p_2(x,y,z,\tau) = -\frac{1}{100A_1^2A_2\gamma}\left[12\left(1-\frac{\left(1-\cot Fs\left(\frac{\xi}{2}\right)\right)^2}{2}\right)\right. \\ \left. A_1^4 + 250A_1k\gamma^2 \ln a + 625c_0(l^2+m^2)\gamma^3(\ln a)^2\right], \tag{5.72}$$

where $\xi = lx + my + kz + \frac{\lambda t^\alpha}{\Gamma(\alpha+1)}$ and $\lambda = -\frac{A_1}{5\gamma \ln a}$.

Case II:

$$a_0 = \frac{12A_1^4 + 250A_1k\gamma^2 \ln a - 625c_0(l^2+m^2)\gamma^3(\ln a)^2}{100A_1^2A_2\gamma},$$
$$a_1 = -\frac{12A_1^2}{25A_2\gamma},$$
$$a_2 = \frac{6A_1^2}{25A_2\gamma},$$
$$\lambda = \frac{A_1}{5\gamma \ln a}.$$

Substituting the above parameter values in the ansatz given by Eq. (5.68), we obtain the following solutions of Eq. (5.4)

$$p_1(x,y,z,\tau)=\frac{12(-1-2a^{\xi}+a^{2\xi})A_1^4+250(1+a^{\xi})^2A_1k\gamma^2\ln a-625(1+a^{\xi})^2c_0(l^2+m^2)\gamma^3(\ln a)^2}{100(1+a^{\xi})^2A_1^2A_2\gamma}, \tag{5.73}$$

$$p_2(x,y,z,\tau)=\frac{12(-1+2a^{\xi}+a^{2\xi})A_1^4+250(-1+a^{\xi})^2A_1k\gamma^2\ln a-625(-1+a^{\xi})^2c_0(l^2+m^2)\gamma^3(\ln a)^2}{100(-1+a^{\xi})^2A_1^2A_2\gamma}, \tag{5.74}$$

where $\xi=lx+my+kz+\frac{\lambda t^{\alpha}}{\Gamma(\alpha+1)}$ and $\lambda=\frac{A_1}{5\gamma\ln a}$.

5.7.3 Numerical Results and Discussions

In this section, the numerical simulations of time fractional KdV-KZK equation have been presented graphically. Here, the exact solutions (5.69) and (5.70) obtained by classical Kudryashov method and also the exact solutions (5.71)–(5.74) obtained by modified Kudryashov method have been used to draw the 3-D solution graphs.

Numerical Simulations for the Solutions Obtained by Classical Kudryashov Method

In the present analysis, Eqs. (5.69) and (5.70) have been used for drawing the solution graphs for time fractional KdV-KZK equation in case of both fractional and classical orders (Figs. 5.5, 5.6, 5.7, 5.8, 5.9, and 5.10).

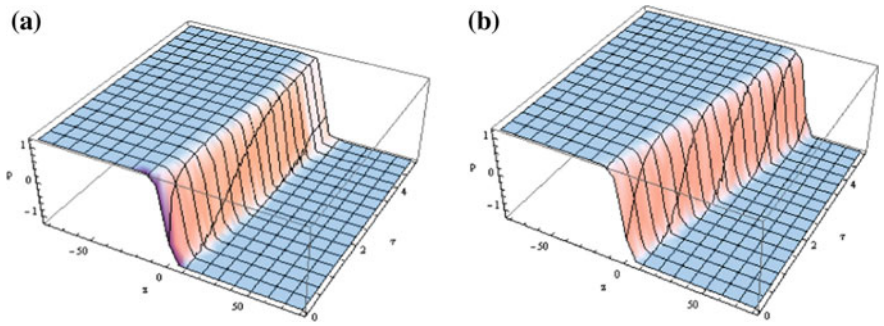

Fig. 5.5 Solitary wave solutions for Eq. (5.69) at $A_1=10$, $A_2=20$, $\gamma=0.5$, $k=l=m=0.5$, $c_0=1$, **a** when $\alpha=0.5$ and **b** when $\alpha=1$

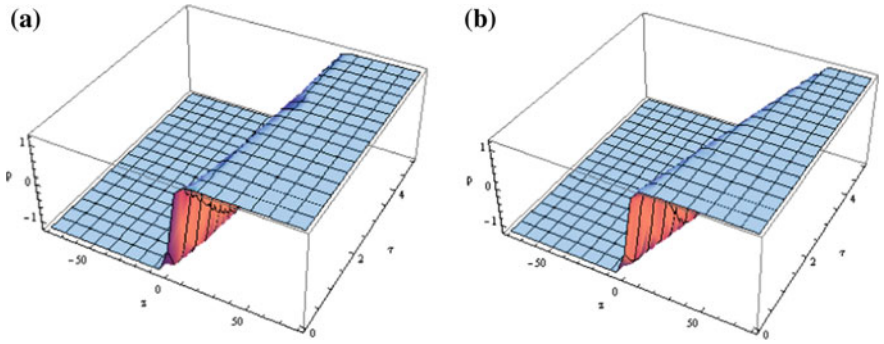

Fig. 5.6 Solitary wave solutions for Eq. (5.70) at $A_1 = 10$, $A_2 = 20$, $\gamma = 0.5$, $k = l = m = 0.5$, $c_0 = 1$, **a** when $\alpha = 0.5$ and **b** when $\alpha = 1$

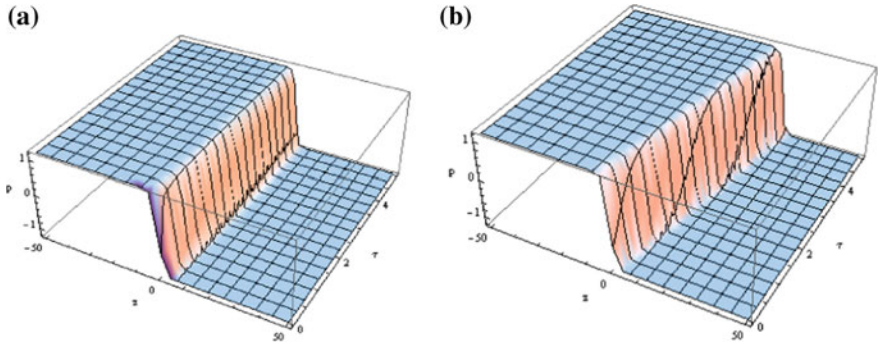

Fig. 5.7 Solitary wave solutions for Eq. (5.71) at $A_1 = 10$, $A_2 = 20$, $\gamma = 0.5$, $k = l = m = 0.5$, $c_0 = 1$, $a = 10$ **a** when $\alpha = 0.25$ and **b** when $\alpha = 1$

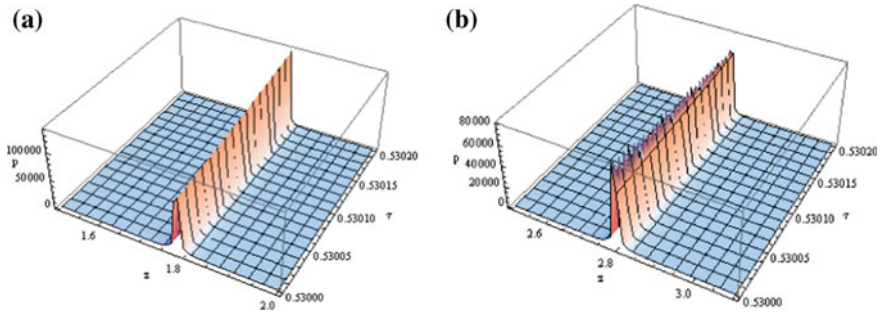

Fig. 5.8 Solitary wave solutions for Eq. (5.72) at $A_1 = 10$, $A_2 = 20$, $\gamma = 0.5$, $k = l = m = 0.5$, $c_0 = 1$, $a = 10$ **a** when $\alpha = 1$ and **b** when $\alpha = 0.5$

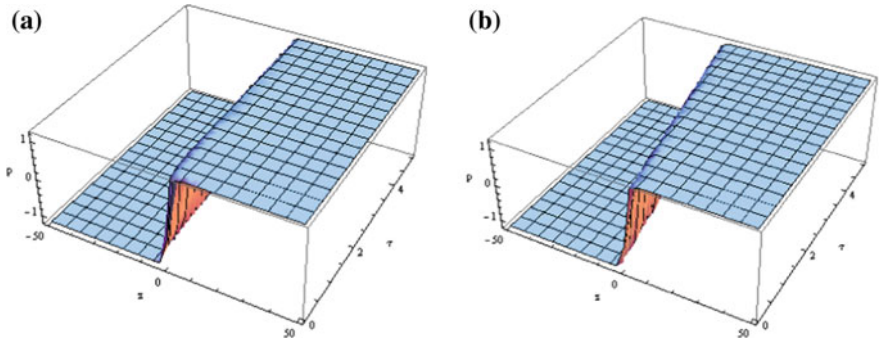

Fig. 5.9 Solitary wave solutions for Eq. (5.73) at $A_1 = 10$, $A_2 = 20$, $\gamma = 0.5$, $k = l = m = 0.5$, $c_0 = 1$, $a = 10$ **a** when $\alpha = 0.25$ and **b** when $\alpha = 1$

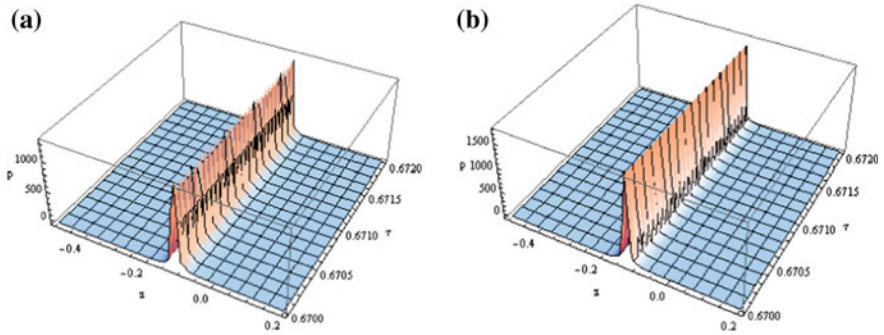

Fig. 5.10 Solitary wave solutions for Eq. (5.74) at $A_1 = A_2 = \gamma = k = l = m = c_0 = 1$, $a = 10$, **a** when $\alpha = 1$ and **b** when $\alpha = 0.75$

Numerical Simulations for the Solutions Obtained by the Modified Kudryashov Method

In the present analysis, Eqs. (5.71)–(5.74) have been used for drawing the solution graphs for time fractional KdV-KZK equation in case of both fractional and classical orders.

In the present numerical simulations, the solitary wave solutions for Eqs. (5.69)–(5.74) have been demonstrated in 3-D graphs. From the above figures, it may be observed that the solution surfaces obtained by classical Kudryashov for Eq. (5.69) are anti-kink solitary waves. On the other hand, the solution surfaces obtained by classical Kudryashov for Eq. (5.70) show the kink solitary waves. Similarly, the solution surfaces obtained by modified Kudryashov for Eqs. (5.71) and (5.73) show the anti-kink and kink solitary waves, respectively. However, in case of the solution surfaces obtained by modified Kudryashov for Eqs. (5.72) and (5.74), single soliton solitary waves of different shapes have been observed.

5.7.4 Physical Significance for the Solution of KdV-KZK Equation

The KdV-KZK equation covers all the four basic physical mechanisms of nonlinear acoustics, viz. diffraction, nonlinearity, dissipation, and dispersion. The solution of the KdV-KZK equation describes a shock wave as a transition between two constant velocity values. This transition can undergo oscillations due to the dispersion.

The obtained results are related to the physical phenomenon in Cantorian time-space. These results enrich the properties of the genuinely nonlinear phenomenon. To the best of the author information, the obtained solutions of this work have not been reported earlier in the open literature. The reported results have a potential application in observing the structure of KdV-KZK equation from micro-physical to macro-physical behavior of substance in the real world.

5.8 Implementation of the Jacobi Elliptic Function Method

In this section, the new exact analytical solutions of fractional (2 + 1)-dimensional Davey–Stewartson equation and new integrable Davey–Stewartson-type equation have been obtained using the mixed dn-sn method.

5.8.1 Exact Solutions of Fractional (2 + 1)-Dimensional Davey–Stewartson Equation

Let us consider the fractional (2 + 1)-dimensional Davey–Stewartson equation [48]

$$iD_t^{\alpha}q + a(D_x^{2\beta}q + D_y^{2\gamma}q) + b|q|^{2n}q - \lambda qr = 0, \tag{5.75}$$

$$D_x^{2\beta}r + D_y^{2\gamma}r + \delta D_x^{2\beta}\left(|q|^{2n}\right) = 0, \tag{5.76}$$

where $0 < \alpha, \beta, \gamma \leq 1$, $q \equiv q(x, y, t)$, and $r \equiv r(x, y, t)$. Also, a, b, λ, and δ are all constant coefficients. The exponent n is the power law parameter. It is necessary to have $n > 0$. In Eqs. (5.75) and (5.76), $q(x, y, t)$ is a complex-valued function which stands for wave amplitude, while $r(x, y, t)$ is a real-valued function which stands for mean flow. This system of equations is completely integrable and is often used to describe the long-time evolution of a two-dimensional wave packet [49–51].

We first transform the fractional (2 + 1)-dimensional Davey–Stewartson Eqs. (5.75) and (5.76) to a system of nonlinear ordinary differential equations in order to derive its exact solutions.

By applying the following fractional complex transform

$$q(x,y,t) = e^{i\theta}u(\xi),\ r(x,y,t) = v(\xi),$$

$$\theta = \frac{\theta_1 x^{\beta}}{\Gamma(1+\beta)} + \frac{\theta_2 y^{\gamma}}{\Gamma(1+\gamma)} + \frac{\theta_3 t^{\alpha}}{\Gamma(1+\alpha)} \text{ and } \xi = \frac{\xi_1 x^{\beta}}{\Gamma(1+\beta)} + \frac{\xi_2 y^{\gamma}}{\Gamma(1+\gamma)} + \frac{\xi_3 t^{\alpha}}{\Gamma(1+\alpha)},$$

Equations (5.75) and (5.76) can be reduced to the following couple nonlinear ODEs:

$$-(\theta_3 + a\theta_1^2 + a\theta_2^2)u + (a\xi_1^2 + a\xi_2^2)u_{\xi\xi} + bu^{2n+1} - \lambda uv = 0, \tag{5.77}$$

$$\xi_1^2 v_{\xi\xi} + \xi_2^2 v_{\xi\xi} + \delta\xi_1^2\left(u^{2n}\right)_{\xi\xi} = 0, \tag{5.78}$$

where ξ_3 has been set to $-2a\xi_1\theta_1 - 2a\xi_2\theta_2$. Equation (5.78) is then integrated term by term twice with respect to ξ where integration constants are considered zero. Thus, we obtain

$$v = -\frac{\delta\xi_1^2 u^{2n}}{\xi_1^2 + \xi_2^2}. \tag{5.79}$$

Substituting Eq. (5.79) into Eq. (5.77) yields

$$-(\theta_3 + a\theta_1^2 + a\theta_2^2)u + (a\xi_1^2 + a\xi_2^2)u_{\xi\xi} + bu^{2n+1} + \lambda\frac{\delta\xi_1^2 u^{2n+1}}{\xi_1^2 + \xi_2^2} = 0. \tag{5.80}$$

Using the transformation

$$u(\xi) = \Phi^{\frac{1}{n}}(\xi),$$

Equation (5.80) further reduces to

$$\begin{aligned} &-(\theta_3 + a\theta_1^2 + a\theta_2^2)n^2\Phi^2 + (a\xi_1^2 + a\xi_2^2)(1-n)\Phi_{\xi}^2 \\ &+(a\xi_1^2 \quad + a\xi_2^2)n\Phi_{\xi\xi} + bn^2\Phi^4 + \lambda\frac{\delta\xi_1^2 n^2\Phi^4}{\xi_1^2 + \xi_2^2} = 0 \end{aligned} \tag{5.81}$$

By balancing the terms $\Phi\Phi_{\xi\xi}$ and Φ^4 in Eq. (5.81), the value of N can be determined, which is $N = 1$ in this problem.

Therefore, the solution of Eq. (5.81) can be written in the following ansatz as

$$\Phi(\xi) = c_0 + c_1\phi(\xi) + d_0\sqrt{k^2 - \phi^2(\xi)}, \tag{5.82}$$

where c_0, c_1, and d_0 are constants to be determined later and $\phi(\xi)$ satisfies Eq. (5.29).

Now substituting Eq. (5.82) along with Eq. (5.29) into Eq. (5.81) and then equating each coefficient of $\phi^i(\xi)$, $i = 0,1,2,\ldots$ to zero, we can get a set of algebraic equations for c_0, c_1, d_0, θ_3, and m as follows:

$$
\begin{aligned}
&-(a\xi_1^2+a\xi_2^2)(-k^4(-1+m)(\xi_1^2+\xi_2^2)c_1^2+k^4(-1+m)n(\xi_1^2+\xi_2^2)(c_1^2+d_0^2)\\
&\quad+n^2(\theta_1^2+\theta_2^2)(c_0^2+k^2d_0^2))\\
&\quad+n^2(-\theta_3(\xi_1^2+\xi_2^2)(c_0^2+k^2d_0^2)+(\lambda\delta\xi_1^2+b(\xi_1^2+\xi_2^2))\\
&\quad(c_0^4+6k^2c_0^2d_0^2+k^4d_0^4))=0\\
&-nc_0c_1(a(\xi_1^2+\xi_2^2)(2n(\theta_1^2+\theta_2^2)+k^2(-2+m)(\xi_1^2+\xi_2^2))\\
&\quad-2n(-\theta_3(\xi_1^2+\xi_2^2)+2(\lambda\delta\xi_1^2+b(\xi_1^2+\xi_2^2))(c_0^2+3k^2d_0^2)))=0\\
&-(a\xi_1^2+a\xi_2^2)(2k^2n(\xi_1^2+\xi_2^2)d_0^2+n^2(\theta_1^2+\theta_2^2)(c_1^2+d_0^2)\\
&\quad+k^2(\xi_1^2+\xi_2^2)((-2+m))c_1^2-(-1+m)d_0^2))\\
&\quad-n^2(\theta_3(\xi_1^2+\xi_2^2)(c_1^2-d_0^2)-2(\lambda\delta\xi_1^2+b(\xi_1^2+\xi_2^2))(3c_0^2(c_1^2-d_0^2)\\
&\quad-k^2d_0^2(-3c_1^2+d_0^2)))=0\\
&-2nc_0c_1(a(\xi_1^2+\xi_2^2)^2-2n(\lambda\delta\xi_1^2+b(\xi_1^2+\xi_2^2))(c_1^2-3d_0^2))=0\\
&-a(1+n)(\xi_1^2+\xi_2^2)^2(c_1^2-d_0^2)+n^2(\lambda\delta\xi_1^2+b(\xi_1^2+\xi_2^2))(c_1^4-6c_1^2d_0^2+d_0^4)=0\\
&nc_0d_0(-a(\xi_1^2+\xi_2^2)(2n(\theta_1^2+\theta_2^2)+k^2(-1+m)(\xi_1^2+\xi_2^2))\\
&\quad+2n(-\theta_3(\xi_1^2+\xi_2^2)+2(\lambda\delta\xi_1^2+b(\xi_1^2+\xi_2^2))(c_0^2+k^2d_0^2)))=0\\
&c_1d_0(a(\xi_1^2+\xi_2^2)(-2n^2(\theta_1^2+\theta_2^2)-2k^2(-1+m)(\xi_1^2+\xi_2^2)\\
&\quad+k^2n(\xi_1^2+\xi_2^2))+2n^2(-\theta_3(\xi_1^2+\xi_2^2)\\
&\quad+2(\lambda\delta\xi_1^2+b(\xi_1^2+\xi_2^2))(3c_0^2+k^2d_0^2)))=0\\
&-2nc_0d_0(a(\xi_1^2+\xi_2^2)^2-2n(\lambda\delta\xi_1^2+b(\xi_1^2+\xi_2^2))(3c_1^2-d_0^2))=0\\
&-2c_1d_0(a(1+n)(\xi_1^2+\xi_2^2)^2-2n^2(\lambda\delta\xi_1^2+b(\xi_1^2+\xi_2^2))(c_1^2-d_0^2))=0
\end{aligned}
\tag{5.83}
$$

Solving the above algebraic Eqs. (5.83), we have the set of coefficients for the nontrivial solutions of Eq. (5.81) as given below:

Case 1:

$$
\begin{aligned}
c_0=0, c_1=&-\frac{i\sqrt{a}\sqrt{1+n}(\xi_1^2+\xi_2^2)}{\sqrt{-bn^2\xi_1^2-n^2\delta\lambda\xi_1^2-bn^2\xi_2^2}}, d_0=0, m=1, \theta_3\\
=&-\frac{a(n^2\theta_1^2+n^2\theta_2^2-k^2\xi_1^2-k^2\xi_2^2)}{n^2},
\end{aligned}
\tag{5.84}
$$

where $\xi_3 = -2a\xi_1\theta_1 - 2a\xi_2\theta_2$ and k is the free parameter.

Substituting Eqs. (5.84) into Eq. (5.28) and using special solutions (5.30) of Eq. (5.29), we obtain

$$\Phi(\xi) = -\frac{i\sqrt{a}\sqrt{1+n}(\xi_1^2+\xi_2^2)k \text{ sec } h(k\xi)}{\sqrt{-bn^2\xi_1^2 - n^2\delta\lambda\xi_1^2 - bn^2\xi_2^2}}$$

which yields the following solitary wave solutions of Eqs. (5.75) and (5.76):

$$u(x,y,t) = \Phi(\xi)^{\frac{1}{n}} = \left(-\frac{i\sqrt{a}\sqrt{1+n}(\xi_1^2+\xi_2^2)k \text{ sec } h(k\xi)}{\sqrt{-bn^2\xi_1^2 - n^2\delta\lambda\xi_1^2 - bn^2\xi_2^2}}\right)^{\frac{1}{n}}, \tag{5.85a}$$

$$v(x,y,t) = -\frac{a(1+n)\delta\xi_1^2(\xi_1^2+\xi_2^2)k \text{ sec } h^2(k\xi)}{(bn^2\xi_1^2 + n^2\delta\lambda\xi_1^2 + bn^2\xi_2^2)}. \tag{5.85b}$$

Case 2:

$$\begin{aligned} c_0 = 0, c_1 &= \frac{i\sqrt{a}\sqrt{1+n}(\xi_1^2+\xi_2^2)}{\sqrt{-bn^2\xi_1^2 - n^2\delta\lambda\xi_1^2 - bn^2\xi_2^2}}, d_0 = 0, m = 1, \theta_3 \\ &= -\frac{a(n^2\theta_1^2 + n^2\theta_2^2 - k^2\xi_1^2 - k^2\xi_2^2)}{n^2}, \end{aligned} \tag{5.86}$$

where $\xi_3 = -2a\xi_1\theta_1 - 2a\xi_2\theta_2$ and k is the free parameter.

Substituting Eqs. (5.86) into Eq. (5.28) and using special solutions (5.30) of Eq. (5.29), we obtain

$$\Phi(\xi) = \frac{i\sqrt{a}\sqrt{1+n}(\xi_1^2+\xi_2^2)k \text{ sec } h(k\xi)}{\sqrt{-bn^2\xi_1^2 - n^2\delta\lambda\xi_1^2 - bn^2\xi_2^2}}$$

which yields the following solitary wave solutions of Eqs. (5.75) and (5.76):

$$u(x,y,t) = \Phi(\xi)^{\frac{1}{n}} = \left(\frac{i\sqrt{a}\sqrt{1+n}(\xi_1^2+\xi_2^2)k \text{ sec } h(k\xi)}{\sqrt{-bn^2\xi_1^2 - n^2\delta\lambda\xi_1^2 - bn^2\xi_2^2}}\right)^{\frac{1}{n}}, \tag{5.87a}$$

$$v(x,y,t) = -\frac{a(1+n)\delta\xi_1^2(\xi_1^2+\xi_2^2)k \text{ sec } h^2(k\xi)}{(bn^2\xi_1^2 + n^2\delta\lambda\xi_1^2 + bn^2\xi_2^2)}. \tag{5.87b}$$

5.8.2 Exact Solutions of the Fractional (2 + 1)-Dimensional New Integrable Davey–Stewartson-Type Equation

Let us consider the fractional (2 + 1)-dimensional new integrable Davey–Stewartson-type equation

$$\begin{gathered} iD_\tau^\alpha \Psi + L_1\Psi + \Psi\,\Phi + \Psi\chi = 0, \\ L_2\chi = L_3|\Psi|^2, \\ D_\xi^\beta \Phi = D_\eta^\gamma \chi + \mu D_\eta^\gamma\left(|\Psi|^2\right), \quad \mu = \mp 1,\ 0<\alpha,\beta,\gamma\le 1 \end{gathered} \tag{5.88}$$

where the linear differential operators are given by

$$\begin{aligned} L_1 &\equiv \left(\frac{b^2-a^2}{4}\right)D_\xi^{2\beta} - aD_\xi^\beta D_\eta^\gamma - D_\eta^{2\gamma}, \\ L_2 &\equiv \left(\frac{b^2+a^2}{4}\right)D_\xi^{2\beta} + aD_\xi^\beta D_\eta^\gamma + D_\eta^{2\gamma}, \\ L_3 &\equiv \pm\frac{1}{4}\left(b^2+a^2+\frac{8b^2(a-1)}{(a-2)^2-b^2}\right)D_\xi^{2\beta} \pm \left(a+\frac{2b^2}{(a-2)^2-b^2}\right)D_\xi^\beta D_\eta^\gamma \pm D_\eta^{2\gamma}, \end{aligned}$$

where $\Psi \equiv \Psi(\xi,\eta,\tau)$ is complex while $\Phi \equiv \Phi(\xi,\eta,\tau)$, $\chi \equiv \chi(\xi,\eta,\tau)$ are real and a, b are real parameters. The above equation in integer order was devised firstly by Maccari [52] from the Konopelchenko–Dubrovsky (KD) equation [53].

In the present analysis, the Jacobi elliptic function method has been used to investigate for new types of doubly periodic exact solutions in terms of Jacobi elliptic functions.

According to the algorithm discussed in Sect. 5.5, let us consider the following fractional complex transform

$$\begin{gathered} \Psi(\xi,\eta,\tau) = \Psi(X)e^{i\theta},\ \Phi(\xi,\eta,\tau) = \Phi(X),\ \chi(\xi,\eta,\tau) = \chi(X), \\ X = k\left(\frac{\xi^\beta}{\Gamma(1+\beta)} + l\frac{\eta^\gamma}{\Gamma(1+\gamma)} + \lambda\frac{\tau^\alpha}{\Gamma(1+\alpha)}\right),\ \theta \\ = \frac{\theta_1\xi^\beta}{\Gamma(1+\beta)} + \frac{\theta_2\eta^\gamma}{\Gamma(1+\gamma)} + \frac{\theta_3\tau^\alpha}{\Gamma(1+\alpha)}, \end{gathered} \tag{5.89}$$

where k, l, λ, θ_1, θ_2, and θ_3 are constants.

By applying the fractional complex transform (5.89), Eq. (5.88) can be reduced to the following couple nonlinear ODEs:

$$k^2M_1\frac{\mathrm{d}^2\Psi(X)}{\mathrm{d}X^2}+M_0\Psi(X)+\Psi(X)\Phi(X)+\Psi(X)\chi(X)=0, \tag{5.90}$$

$$k^2M_2\frac{\mathrm{d}^2\chi(X)}{\mathrm{d}X^2}=k^2M_3\frac{\mathrm{d}^2\Psi^2(X)}{\mathrm{d}X^2}, \tag{5.91}$$

$$k\frac{\mathrm{d}\Phi(X)}{\mathrm{d}X}=kl\frac{\mathrm{d}\chi(X)}{\mathrm{d}X}+\mu kl\frac{\mathrm{d}\Psi^2(X)}{\mathrm{d}X}, \tag{5.92}$$

where λ has been set to $a(l\theta_1+\theta_2)+2l\theta_2-\frac{\theta_1(b^2-a^2)}{2}$.

Here,

$$\begin{aligned}
M_0&=-\theta_3-\frac{(b^2-a^2)}{4}\theta_1^2+a\theta_1\theta_2+\theta_2^2,\\
M_1&=-al-l^2+\frac{(b^2-a^2)}{4},\\
M_2&=al+l^2+\frac{(b^2+a^2)}{4},\\
M_3&=\pm l^2\pm\left(a+\frac{2b^2}{(a-2)^2-b^2}\right)l\pm\frac{1}{4}\left(b^2+a^2+\frac{8b^2(a-1)}{(a-2)^2-b^2}\right).
\end{aligned}$$

Now, Eqs. (5.92) and (5.91) are integrated once and twice term by term with respect to X where integration constants are considered zero. Thus, we obtain

$$\begin{aligned}
\chi(X)&=\frac{M_3}{M_2}\Psi^2(X),\\
\Phi(X)&=\left(l\frac{M_3}{M_2}+\mu l\right)\Psi^2(X).
\end{aligned} \tag{5.93}$$

Eliminating $\chi(X)$, $\Phi(X)$ from Eqs. (5.90) and (5.93), we arrive at

$$k^2M_1\frac{\mathrm{d}^2\Psi(X)}{\mathrm{d}X^2}+M_0\Psi(X)+\left(\frac{lM_3}{M_2}+\mu l+\frac{M_3}{M_2}\right)\Psi^3(X)=0 \tag{5.94}$$

By balancing the nonlinear term $\Psi^3(X)$ and highest order derivative term $\frac{\mathrm{d}^2\Psi(X)}{\mathrm{d}X^2}$ in Eq. (5.94), the value of N can be determined, which is $N=1$ in this problem.

Therefore, the solution of Eq. (5.94) can be written in the following ansatz as

$$\Psi(X) = c_0 + c_1\phi(X) + d_0\sqrt{p^2 - \phi^2(X)}, \tag{5.95}$$

where c_0, c_1, and d_0 are constants to be determined later, and $\phi(X)$ satisfies the elliptic equation:

$$\frac{\mathrm{d}\phi(X)}{\mathrm{d}X} = \sqrt{(p^2 - \phi^2(X))(\phi^2(X) - p^2(1-m))}, \tag{5.96}$$

whose solutions are given by

$$\begin{aligned}\phi(X) &= pdn(pX|m),\\ \phi(X) &= p\sqrt{1-m}nd(pX|m),\end{aligned} \tag{5.97}$$

Now substituting Eq. (5.95) along with Eq. (5.96) into Eq. (5.94) and then equating each coefficient of $\phi^i(X)$, i = 0,1,2,… to zero, we can get a set of algebraic equations for c_0, c_1, d_0, p, and m as follows:

$$\begin{gathered}c_0(M_0M_2 + (M_3 + lM_3 + lM_2\mu)(c_0^2 + 3p^2d_0^2)) = 0,\\ c_1(M_0M_2 - k^2(-2+m)M_1M_2p^2 + 3(M_3 + lM_3 + lM_2\mu)(c_0^2 + p^2d_0^2)) = 0,\\ 3(M_3 + lM_3 + lM_2\mu)c_0(c_1^2 - d_0^2)) = 0,\\ c_1(-2k^2M_1M_2 + (M_3 + lM_3 + lM_2\mu)(c_1^2 - 3d_0^2)) = 0,\\ d_0(M_0M_2 + k^2M_1M_2p^2 - k^2mM_1M_2p^2 + 3M_3c_0^2 + 3lM_3c_0^2 + 3lM_2\mu c_0^2\\ + M_3p^2d_0^2 + lM_3p^2d_0^2 + lM_2\mu p^2d_0^2) = 0,\\ 6(M_3 + lM_3 + lM_2\mu)c_0c_1d_0 = 0,\\ d_0(-2k^2M_1M_2 + (M_3 + lM_3 + lM_2\mu)(3c_1^2 - d_0^2)) = 0.\end{gathered} \tag{5.98}$$

Solving the above algebraic Eq. (5.98), we have the set of coefficients for the nontrivial traveling wave solutions of Eq. (5.94) as given below:

Case 1:

$$\begin{aligned}c_0 = 0, c_1 &= -\frac{k\sqrt{2M_1M_2}}{\sqrt{l\mu M_2 + (l+1)M_3}},\\ d_0 = 0, m &= \frac{M_0 + 2M_1k^2p^2}{M_1k^2p^2}.\\ \Psi_{11}(X) &= -\frac{kp\sqrt{2M_1M_2}}{\sqrt{l\mu M_2 + (l+1)M_3}}dn(pX|m),\\ \Phi_{11}(X) &= \left(l\frac{M_3}{M_2} + \mu l\right)\Psi_{11}^2(X),\end{aligned}$$

$$\chi_{11}(X) = \frac{M_3}{M_2}\Psi_{11}^2(X),$$
$$\Psi_{12}(X) = -\frac{kp\sqrt{2M_1M_2}\sqrt{1-m}}{\sqrt{l\mu M_2 + (l+1)M_3}} nd(pX|m),$$
$$\Phi_{12}(X) = \left(l\frac{M_3}{M_2} + \mu l\right)\Psi_{12}^2(X),$$
$$\chi_{12}(X) = \frac{M_3}{M_2}\Psi_{12}^2(X).$$

Case 2:

$$c_0 = 0, c_1 = \frac{k\sqrt{2M_1M_2}}{\sqrt{l\mu M_2 + (l+1)M_3}},$$

$$d_0 = 0, m = \frac{M_0 + 2M_1k^2p^2}{M_1k^2p^2}.$$

$$\Psi_{21}(X) = \frac{kp\sqrt{2M_1M_2}}{\sqrt{l\mu M_2 + (l+1)M_3}} dn(pX|m),$$

$$\Phi_{21}(X) = \left(l\frac{M_3}{M_2} + \mu l\right)\Psi_{21}^2(X),$$

$$\chi_{21}(X) = \frac{M_3}{M_2}\Psi_{21}^2(X),$$

$$\Psi_{22}(X) = \frac{kp\sqrt{2M_1M_2}\sqrt{1-m}}{\sqrt{l\mu M_2 + (l+1)M_3}} nd(pX|m),$$

$$\Phi_{22}(X) = \left(l\frac{M_3}{M_2} + \mu l\right)\Psi_{22}^2(X)$$

$$\chi_{22}(X) = \frac{M_3}{M_2}\Psi_{22}^2(X).$$

Case 3:

$$c_0 = 0, c_1 = -\frac{k\sqrt{M_1M_2}}{\sqrt{2l\mu M_2 + 2(l+1)M_3}},$$
$$d_0 = -\frac{k\sqrt{M_1M_2}}{\sqrt{-2l\mu M_2 - 2(l+1)M_3}}, m = \frac{2M_0 + M_1k^2p^2}{2M_1k^2p^2}.$$

$$\Psi_{31}(X) = -\frac{kp\sqrt{M_1M_2}}{\sqrt{2l\mu M_2 + 2(l+1)M_3}} dn(pX|m) - p\sqrt{m}sn(pX|m)\frac{k\sqrt{M_1M_2}}{\sqrt{-2l\mu M_2 - 2(l+1)M_3}},$$

$$\Phi_{31}(X) = \left(l\frac{M_3}{M_2} + \mu l\right)\Psi_{31}^2(X),$$

$$\chi_{31}(X) = \frac{M_3}{M_2}\Psi_{31}^2(X),$$

$$\Psi_{32}(X) = -\frac{kp\sqrt{M_1M_2}\sqrt{1-m}}{\sqrt{2l\mu M_2 + 2(l+1)M_3}} dn(pX|m) - p\sqrt{1-(1-m)nd^2(pX|m)}\frac{k\sqrt{M_1M_2}}{\sqrt{-2l\mu M_2 - 2(l+1)M_3}},$$

$$\Phi_{32}(X) = \left(l\frac{M_3}{M_2} + \mu l\right)\Psi_{32}^2(X),$$

$$\chi_{32}(X) = \frac{M_3}{M_2}\Psi_{32}^2(X).$$

Case 4:

$$c_0 = 0, c_1 = \frac{k\sqrt{M_1M_2}}{\sqrt{2l\mu M_2 + 2(l+1)M_3}},$$

$$d_0 = -\frac{k\sqrt{M_1M_2}}{\sqrt{-2l\mu M_2 - 2(l+1)M_3}}, m = \frac{2M_0 + M_1k^2p^2}{2M_1k^2p^2}.$$

$$\Psi_{41}(X) = \frac{kp\sqrt{M_1M_2}}{\sqrt{2l\mu M_2 + (l+2)M_3}} dn(pX|m) - \frac{k\sqrt{M_1M_2}}{\sqrt{-2l\mu M_2 - 2(l+1)M_3}},$$

$$\Phi_{41}(X) = \left(l\frac{M_3}{M_2} + \mu l\right)\Psi_{41}^2(X),$$

$$\chi_{41}(X) = \frac{M_3}{M_2}\Psi_{41}^2(X),$$

$$\Psi_{42}(X) = \frac{kp\sqrt{M_1M_2}\sqrt{1-m}}{\sqrt{2l\mu M_2 + (l+2)M_3}} nd(pX|m) - \frac{k\sqrt{M_1M_2}}{\sqrt{-2l\mu M_2 - 2(l+1)M_3}},$$

$$\Phi_{42}(X) = \left(l\frac{M_3}{M_2} + \mu l\right)\Psi_{42}^2(X),$$

$$\chi_{42}(X) = \frac{M_3}{M_2}\Psi_{42}^2(X).$$

Case 5:

$$c_0 = 0, c_1 = -\frac{k\sqrt{M_1M_2}}{\sqrt{2l\mu M_2 + 2(l+1)M_3}},$$

$$d_0 = \frac{k\sqrt{M_1M_2}}{\sqrt{-2l\mu M_2 - 2(l+1)M_3}}, m = \frac{2M_0 + M_1k^2p^2}{2M_1k^2p^2}.$$

$$\Psi_{51}(X) = -\frac{kp\sqrt{M_1M_2}}{\sqrt{2l\mu M_2 + 2(l+1)M_3}}dn(pX|m) + \frac{k\sqrt{M_1M_2}}{\sqrt{-2l\mu M_2 - 2(l+1)M_3}},$$

$$\Phi_{51}(X) = \left(l\frac{M_3}{M_2} + \mu l\right)\Psi_{51}^2(X),$$

$$\chi_{51}(X) = \frac{M_3}{M_2}\Psi_{51}^2(X),$$

$$\Psi_{52}(X) = -\frac{kp\sqrt{M_1M_2}\sqrt{1-m}}{\sqrt{2l\mu M_2 + 2(l+1)M_3}}nd(pX|m) + \frac{k\sqrt{M_1M_2}}{\sqrt{-2l\mu M_2 - 2(l+1)M_3}},$$

$$\Phi_{52}(X) = \left(l\frac{M_3}{M_2} + \mu l\right)\Psi_{52}^2(X),$$

$$\chi_{52}(X) = \frac{M_3}{M_2}\Psi_{52}^2(X).$$

Case 6:

$$c_0 = 0, c_1 = \frac{k\sqrt{M_1M_2}}{\sqrt{2l\mu M_2 + 2(l+1)M_3}},$$

$$d_0 = \frac{k\sqrt{M_1M_2}}{\sqrt{-2l\mu M_2 - 2(l+1)M_3}}, m = \frac{2M_0 + M_1k^2p^2}{2M_1k^2p^2}.$$

$$\Psi_{61}(X) = \frac{kp\sqrt{M_1M_2}}{\sqrt{2l\mu M_2 + 2(l+1)M_3}}dn(pX|m) + \frac{k\sqrt{M_1M_2}}{\sqrt{-2l\mu M_2 - 2(l+1)M_3}},$$

$$\Phi_{61}(X) = \left(l\frac{M_3}{M_2} + \mu l\right)\Psi_{61}^2(X),$$

$$\chi_{61}(X) = \frac{M_3}{M_2}\Psi_{61}^2(X),$$

$$\Psi_{62}(X) = \frac{kp\sqrt{M_1M_2}\sqrt{1-m}}{\sqrt{2l\mu M_2 + 2(l+1)M_3}}nd(pX|m) + \frac{k\sqrt{M_1M_2}}{\sqrt{-2l\mu M_2 - 2(l+1)M_3}},$$

$$\Phi_{62}(X) = \left(l\frac{M_3}{M_2} + \mu l\right)\Psi_{62}^2(X),$$

$$\chi_{62}(X) = \frac{M_3}{M_2}\Psi_{62}^2(X).$$

5.9 Conclusion

In this chapter, several traveling wave exact solutions of nonlinear fractional acoustic wave equations, namely the time fractional Burgers–Hopf and KZK equations have been successfully obtained by the first integral method with the help of fractional complex transform. The fractional complex transform can easily convert a fractional differential equation into its equivalent ordinary differential equation form. So, fractional complex transform has been efficiently used for solving fractional differential equations. Here, the fractional complex transform has been considered which is derived from the local fractional calculus defined on fractals.

The first integral method has been successfully employed to solve nonlinear fractional acoustic wave equations. The obtained solutions may be worthwhile for an explanation of some physical phenomena accurately. The present analysis indicates that the first integral method is effective and efficient for solving nonlinear fractional acoustic wave equations. The performance of this method is reliable, and it provides the exact traveling wave solutions. In this present analysis, the focused method clearly avoids linearization, discretization, and unrealistic assumptions, and therefore, it provides exact solutions efficiently and accurately.

Also, in this chapter, the new exact solutions of time fractional KdV-KZK equation have been obtained by classical Kudryashov and modified Kudryashov method, respectively, with the help of fractional complex transform. The fractional complex transform is employed in order to convert a fractional differential equation into its equivalent ordinary differential equation form. So, the fractional complex

transform facilitates solving fractional differential equations. Two methods are successfully applied to solve nonlinear time fractional KdV-KZK equation. The new obtained exact solutions may be useful for the explanation of some physical phenomena accurately. The present analysis indicates that the focused methods are effective and efficient for analytically solving the time fractional KdV-KZK equation. It also demonstrates that performances of these methods are substantially influential and absolutely reliable for finding new exact solutions in terms of symmetric hyperbolic Fibonacci function solutions. In this present analysis, the discussed methods clearly avoid linearization, discretization, and unrealistic assumptions, and therefore, these methods provide exact solutions efficiently and accurately. To the best information of the author, new exact analytical solutions of the time fractional KdV-KZK equation are obtained for the first time in this respect.

The Jacobi elliptic function method has been also used to determine the exact solutions of time fractional (2 + 1)-dimensional Davey–Stewartson equation and new integrable Davey–Stewartson-type equation. In both problems, with the help of fractional complex transform, the Davey–Stewartson system was first transformed into a system of nonlinear ordinary differential equations, which were then solved to obtain the exact solutions. Here also, the fractional complex transform has been considered which is derived from the local fractional calculus defined on fractals. The proposed method is more general than the dn-function method [64] and may be applied to other nonlinear evolution equations. Several classes of traveling wave solutions of the fractional Davey–Stewartson equation have been derived from the solitary wave solutions in Jacobi elliptic functions. Using this proposed method, some new solitary wave solutions and double-periodic solutions have been obtained. This method can also be used for many other nonlinear evolution equations or coupled ones. To the best information of the author, these solitary wave solutions of the fractional Davey–Stewartson equation are new exact solutions which are not reported earlier. Being concise and powerful, this current method can also be extended to solve many other fractional partial differential equations arising in mathematical physics.

References

1. Podlubny, I.: Fractional Differential Equations. Academic Press, New York (1999)
2. Debnath, L.: Integral transforms and their applications. CRC Press, Boca Raton (1995)
3. Sabatier, J., Agrawal, O.P., Tenreiro Machado, J.A.: Advances in Fractional Calculus: Theoretical Developments and Applications in Physics and Engineering. Springer, Dordrecht, The Netherlands (2007)
4. Hilfer, R.: Applications of Fractional Calculus in Physics. World Scientific, Singapore (2000)
5. Das, S.: Functional Fractional Calculus. Springer, New York (2011)
6. Ortigueira, M.D.: Fractional Calculus for Scientists and Engineers, Lecture Notes in Electrical Engineering, vol. 84. Springer, Netherlands (2011)
7. Prieur, F., Vilenskiy, G., Holm, S.: A more fundamental approach to the derivation of nonlinear acoustic wave equations with fractional loss operators (L). J. Acoust. Soc. Am. **132** (4), 2169–2172 (2012)

8. Zabolotskaya, E.A., Khokhlov, R.V.: Quasi-plane waves in the nonlinear acoustics of confined beams. Sov. Phys. Acoust. **15**, 35–40 (1969)
9. Kuznetsov, V.P.: Equations of nonlinear acoustics. Sov. Phys. Acoust. **16**, 467–470 (1971)
10. Saha Ray, S.: On Haar wavelet operational matrix of general order and its application for the numerical solution of fractional Bagley Torvik equation. Appl. Math. Comput. **218**, 5239–5248 (2012)
11. Saha Ray, S., Bera, R.K.: Analytical solution of a dynamic system containing fractional derivative of order one-half by Adomian decomposition method. Trans. ASME J. Appl. Mech. **72**(2), 290–295 (2005)
12. Diethelm, K., Ford, N.J., Freed, A.D.: A predictor-corrector approach for the numerical solution of fractional differential equations. Nonlinear Dyn. **29**(1–4), 3–22 (2002)
13. Liu, F., Anh, V., Turner, I.: Numerical solution of the space fractional Fokker-Planck equation. J. Comput. Appl. Math. **166**(1), 209–219 (2004)
14. Saha, Ray S.: A new approach for the application of adomian decomposition method for the solution of fractional space diffusion equation with insulated ends. Appl. Math. Comput. **202** (2), 544–549 (2008)
15. Ertürk, V.S., Momani, S., Odibat, Z.: Application of generalized differential transform method to multi-order fractional differential equations. Commun. Nonlinear Sci. Numer. Simul. **13**(8), 1642–1654 (2008)
16. Tong, B., He, Y., Wei, L., Zhang, X.: A generalized fractional sub-equation method for fractional differential equations with variable coefficients. Phys. Lett. A **376**(38–39), 2588–2590 (2012)
17. Liu, F., Zhuang, P., Burrage, K.: Numerical methods and analysis for a class of fractional advection-dispersion models. Comput. Math Appl. **64**(10), 2990–3007 (2012)
18. Zheng, B.: (G'/G)-expansion method for solving fractional partial differential equations in the theory of mathematical physics. Commun. Theor. Phys. **58**(5), 623–630 (2012)
19. Kadem, A., Kılıçman, A.: The approximate solution of fractional Fredholm integro-differential equations by variational iteration and homotopy perturbation methods. Abstr. Appl. Anal., Article ID 486193 (2012)
20. Gupta, A.K., Saha, Ray S.: Numerical treatment for the solution of fractional fifth order Sawada-Kotera equation using second kind Chebyshev wavelet method. Appl. Math. Model. **39**(17), 5121–5130 (2015)
21. Sahoo, S., Saha, Ray S.: New approach to find exact solutions of time-fractional Kuramoto-Sivashinsky equation. Physica A **434**, 240–245 (2015)
22. Saha, Ray S., Sahoo, S.: Improved fractional sub-equation method for (3 + 1)-dimensional generalized fractional KdV-Zakharov-Kuznetsov equations. Comput. Math Appl. **70**(2), 158–166 (2015)
23. Raslan, K.R.: The first integral method for solving some important nonlinear partial differential equations. Nonlinear Dynam. **53**, 281–286 (2008)
24. Abbasbandy, S., Shirzadi, A.: The first integral method for modified Benjamin–Bona–Mahony equation. Commun. Nonlinear Sci. Numer. Simul. **15**, 1759–1764 (2010)
25. Lu, B.: The first integral method for some time fractional differential equations. J. Math. Anal. Appl. **395**, 684–693 (2012)
26. Jafari, H., Soltani, R., Khalique, C.M., Baleanu, D.: Exact solutions of two nonlinear partial differential equations by using the first integral method. Bound. Value Probl. **2013**, 117 (2013)
27. Bekir, A., Güner, Ö., Ünsal, Ö.: The first integral method for exact solutions of nonlinear fractional differential equations. J. Comput. Nonlinear Dyn. **10**(021020), 1–5 (2015)
28. Saha Ray, S.: Exact solutions for time-fractional diffusion-wave equations by decomposition method. Phys. Scr. **75**(1), Article number 008, 53–61 (2007)
29. Ortigueira, M.D., Tenreiro Machado, J.A.: Fractional calculus applications in signals and systems. Sig. Process. **86**(10), 2503–2504 (2006)
30. Gan W.S.: Analytical Solutions of the KdV-KZK Equation. In: André M.P. (ed.), Acoustical Imaging, vol. 28, pp. 445–452 (2007)

31. Kudryashov, N.A.: On "new travelling wave solutions" of the KdV and the KdV–Burgers equations. Commun. Nonlinear Sci. Numer. Simul. **14**, 1891–1900 (2009)
32. Ryabov, P.N., Sinelshchikov, D.I., Kochanov, M.B.: Application of the Kudryashov method for finding exact solutions of the high order nonlinear evolution equations. Appl. Math. Comput. **218**, 3965–3972 (2011)
33. Kudryashov, N.A.: One method for finding exact solutions of nonlinear differential equations. Commun. Nonlinear Sci. Numer. Simul. **17**(6), 2248–2253 (2012)
34. Kabir, M.M., Khajeh, A., Aghdam, E.A., Koma, A.Y.: Modified Kudryashov method for finding exact solitary wave solutions of higher-order nonlinear equations. Math. Methods Appl. Sci. **34**, 244–246 (2011)
35. Ege, S.M., Misirli, E.: The modified Kudryashov method for solving some fractional-order nonlinear equations. Adv. Differ. Equ. **2014**, 135 (2014)
36. Taghizadeh, N., Mirzazadeh, M., Mahmoodirad, A.: Application of Kudryashov method for high-order nonlinear Schrödinger equation. Indian J. Phys. **87**(8), 781–785 (2013)
37. Miller, K.S., Ross, B.: An introduction to the fractional calculus and fractional differential equations. Wiley, New York (1993)
38. Tavazoei, M.S., Haeri, M.: Describing function based methods for predicting chaos in a class of fractional order differential equations. Nonlinear Dyn. **57**(3), 363–373 (2009)
39. Caputo, M.: Elasticità e dissipazione. Zanichelli, Bologna (1969)
40. Suarez, L.E., Shokooh, A.: "An eigenvector expansion method for the solution of motion containing fractional derivatives. ASME J. Appl. Mech. **64**, 629–635 (1997)
41. Torvik, P.J., Bagley, R.L.: On the appearance of the fractional derivative in the behavior of real materials. ASME J. Appl. Mech. **51**, 294–298 (1984)
42. Khater A.H., Hassan M.M.: Travelling and periodic wave solutions of some nonlinear wave equations. Z. Naturforsch., **59a**, 389–396 (2004)
43. Rozanova-Pierrat, A.: Mathematical analysis of Khokhlov-Zabolotskaya-Kuznetsov (KZK) equation, p. 6. Prepint of Laboratory Jaques-Louis Lions, Paris (2006)
44. Bakhvalov, N.S., Zhileikin, Y.M., Zabolotskaya, E.A.: Nonlinear theory of sound beams. American Institute of Physics, New York (1987)
45. Hamilton, M.F., Blackstock, D.T.: Nonlinear acoustics. Academic Press, San Diego (1997)
46. Pinton, G., Trahey, G.: Numerical solutions of the Khokhlov-Zabolotskaya-Kuznetsov (KZK) equation satisfying the Rankine-Hugoniot condition. J. Acoust. Soc. Am. **120**, 3109 (2006)
47. Davey, A., Stewartson, K.: On three-dimensional packets of surface waves. Proceeding R. Soc. Lond. A **338**, 101–110 (1974)
48. Shehata, A.R., Kamal, E.M., Kareem, H.A.: Solutions of the space-time fractional of some nonlinear systems of partial differential equations using modified kudryashov method. Int. J. Pure Appl. Math. **101**(4), 477–487 (2015)
49. El-Wakil, S.A., Abdou, M.A., Elhanbaly A.: New solitons and periodic wave solutions for nonlinear evolution equations. Phys. Lett. A, **353**(1), 40–47 (2006)
50. Fan, E., Zhang, J.: Applications of the Jacobi elliptic function method to special-type nonlinear equations. Phys. Lett. A **305**(6), 383–392 (2002)
51. Bekir, A., Cevikel, A.C.: New solitons and periodic solutions for nonlinear physical models in mathematical physics. Nonlinear Anal.: R. World Appl. **11**(4), 3275–3285 (2010)
52. Maccari, A.: A new integrable Davey–Stewartson-type equation. J. Math. Phys. **40**(8), 3971–3977 (1999)
53. Konopelchenko, B., Dubrovsky, V.: Some new integrable nonlinear evolution equations in 2 + 1 dimensions. Phys. Lett. A **102**(1–2), 15–17 (1984)
54. Feng, Z.S.: The first integral method to study the Burgers-KdV equation. J. Phys. A: Math. Gen. **35**, 343–349 (2002)
55. Su, W.H., Yang, X.J., Jafari, H., Baleanu, D.: Fractional complex transform method for wave equations on Cantor sets within local fractional differential operator. Adv. Differ. Equ. **97**, 1–8 (2013)

56. Yang, X.J., Baleanu, D., Srivastava, H.M.: Local Fractional Integral Transforms and Their Applications. Academic Press, Elsevier, London (2015)
57. He, J.H., Elagan, S.K., Li, Z.B.: Geometrical explanation of the fractional complex transform and derivative chain rule for fractional calculus. Phys. Lett. A **376**(4), 257–259 (2012)
58. Güner, O., Bekir, A., Cevikel, A.C.: A variety of exact solutions for the time fractional Cahn-Allen equation. Eur. Phys. J. Plus **130**, 146 (2015). https://doi.org/10.1140/epjp/i2015-15146-9
59. Ding, T.R., Li, C.Z.: Ordinary Differential Equations. Peking University Press, Peking (1996)
60. Bourbaki, N.: Commutative Algebra. Addison-Wesley, Paris (1972)
61. Stakhov, A., Rozin, B.: On a new class of hyperbolic functions. Chaos, Solitons Fractals **23**, 379–389 (2005)
62. Pandir, Y.: Symmetric fibonacci function solutions of some nonlinear partial differential equations. Appl. Math. Inf. Sci. **8**(5), 2237–2241 (2014)
63. Abramowitz, M., Stegun, I.A.: Handbook of Mathematical Functions. Dover, New York (1965)
64. Khater, A.H., Hassan, M.M., Temsah, R.S.: Cnoidal wave solutions for a class of fifth-order KdV equations. Math. Comput. Simulation **70**(4), 221–226 (2005)

Chapter 6
New Exact Traveling Wave Solutions of the Coupled Schrödinger–Boussinesq Equations and Tzitzéica-Type Evolution Equations

6.1 Introduction

In the recent years, the investigation of finding new exact solutions of nonlinear partial differential equations (NLPDEs) plays an important role in the study of nonlinear physical phenomena such as fluid mechanics, plasma physics, statistical physics, quantum physics, solid state physics, optics, and so on [1, 2]. NLPDEs are widely used to describe complex physical phenomena arising in the various fields of science and engineering. Several methods for finding the exact solutions to nonlinear equations in mathematical physics have been presented, such as the inverse scattering method [3], Bäcklund transformation [4, 5], the truncated Painlevé expansion method [6, 7], Hirota's bilinear method [8], tanh- function method [9, 10], exp-function method [11], (G'/G)-expansion method [12, 13], Jacobi elliptic function method [14–17], the first integral method [18–21], Riccati equation rational expansion method [22], Kudryashov method [23, 24], modified decomposition method [25, 26], and other methods [27–30].

It is commonly known that many problems in applied science and engineering are described by nonlinear partial differential equations (NLPDEs). One of the most significant advances of theoretical physics and nonlinear science has been the development of methods to determine the exact solutions for NLPDEs. When a NLPDE is analyzed, the main objective is the construction of the exact solutions for the equation.

Many powerful methods have been presented, such as the inverse scattering transform method [3] and the Hirota bilinear transform method [8] are known as impressive methods to find solutions of exactly solvable NLPDEs. The truncated Painlevé expansion method [6], Bäcklund transformation method [4], the homogeneous balance method [31], the tanh-function method [32–36], the modified extended tanh-function method [10, 37], the exp-function method [38], the (G'/G)-expansion method [12, 39], the auxiliary equation method [40], the extended auxiliary equation method [41, 42], the Jacobi elliptic function method [14, 43], the

S. Saha Ray, *Nonlinear Differential Equations in Physics*,
https://doi.org/10.1007/978-981-15-1656-6_6

simplest equation method [44], the extended simplest equation method [45], and the Weierstrass elliptic function method [46] are useful in many applications to find the exact solutions of NLPDEs.

There are many physical phenomena around us that are best described by nonlinear evolution equations. The Tzitzeica-type nonlinear evolution equations, including Tzitzeica, Dodd–Bullough–Mikhailov (DBM), and Tzitzéica–Dodd–Bullough (TDB) equations are a class of such equations which have gained significant attention during the last few decades. The objective of this work is to find the Jacobi elliptic function solutions, including the hyperbolic and trigonometric solutions for the DBM and TDB equations using a new extended auxiliary equation method. These two equations appear in problems varying from fluid flow to quantum field theory. The great deals of efforts have been devoted to solve these equations using a variety of methods that some of them are reviewed here. Abazari [47] used the (G'/G)-expansion method to find more general exact solutions of the Tzitzéica-type nonlinear evolution equations. Manafian and Lakestani [48] utilized the improved $\tan(\Phi(\xi)/2)$-expansion method and gained new and more general exact traveling wave solutions of the Tzitzéica-type nonlinear equations. In [49], Hosseini et al. employed first the Painlevé transformation and Lie symmetry method to convert the DBM and TDB equations into nonlinear ordinary differential equations and then, a modified version of improved $\tan(\Phi(\xi)/2)$-expansion method has been adopted to generate new exact solutions of the reduced equations. Wazwaz [36] exerted the tanh method to generate solitons and periodic solutions of the Tzitzéica-type nonlinear evolution equations, viz. DBM and TDB equations. Hosseini et al. [50] used the modified Kudryashov method and acquired new exact traveling wave solutions of the Tzitzéica-type equations.

6.2 Outline of the Present Study

In this present chapter, an improved algebraic method based on the generalized Jacobi elliptic function method with symbolic computation is used to construct more new exact solutions for coupled Schrödinger–Boussinesq equations. As a result, several families of new generalized Jacobi double periodic elliptic function wave solutions are obtained by using this method, some of them are degenerated to solitary wave solutions in the limiting cases. The present generalized method is efficient, powerful, straightforward, and concise, and it can be used in order to establish more entirely new exact solutions for other kinds of nonlinear partial differential equations arising in mathematical physics.

Also in this chapter, new types of Jacobi elliptic function solutions of Dodd–Bullough–Mikhailov (DBM) and Tzitzeica–Dodd–Bullough (TDB) equations have been obtained using a new extended auxiliary equation method. A new family of explicit traveling wave solutions is derived. The solitary wave solutions and periodic solutions for these equations are formally derived from the Jacobi elliptic function solutions. The proposed method has been efficiently applied to solve the DBM and TDB equations.

6.2.1 Coupled Schrödinger–Boussinesq Equations

The objective in this work is to use a generalized Jacobi elliptic function expansion method to construct the new exact solutions of the coupled Schrödinger–Boussinesq equations (CSBEs)

$$\mathrm{i}u_t + u_{xx} + \alpha u - uv = 0,\ x \in R, t > 0, \tag{6.1}$$

$$3v_{tt} - v_{xxxx} + 3\left(v^2\right)_{xx} + \beta v_{xx} = \left(|u|^2\right)_{xx},\ x \in R, t > 0, \tag{6.2}$$

where the complex-valued function $u(x,t)$ represents the short-wave amplitude, $v(x,t)$ represents the long-wave amplitude, and α and β are real parameters. Equations (6.1) and (6.2) were considered as a model of the interactions between short and intermediate long waves, and were originated in describing the dynamics of Langmuir soliton formation, the interaction in plasma [51, 52], the diatomic lattice system [53], etc.

6.2.2 Tzitzéica-Type Nonlinear Evolution Equations

A new extended auxiliary equation method is used to produce new exact traveling wave solutions of Dodd–Bullough–Mikhailov and Tzitzeica–Dodd–Bullough equations

The Dodd–Bullough–Mikhailov Equation

Let us consider the Dodd–Bullough–Mikhailov equation as follows

$$u_{xt} + \mathrm{e}^{u} + \mathrm{e}^{-2u} = 0. \tag{6.3}$$

In a traveling wave variable $\xi = kx + \omega t$, Eq. (6.3) reads in the form

$$k\omega f_{\xi\xi} + \mathrm{e}^{f} + \mathrm{e}^{-2f} = 0, \tag{6.4}$$

where $u(x,t) = f(\xi)$.

Using the Painlevé transformation $v = \mathrm{e}^{f}$ or $f = \ln v$, the Dodd–Bullough–Mikhailov Eq. (6.4) can be written as follows

$$k\omega v v_{\xi\xi} - k\omega(v_{\xi})^2 + v^3 + 1 = 0. \tag{6.5}$$

The Tzitzeica–Dodd–Bullough Equation

Now, we consider the Tzitzeica–Dodd–Bullough (TDB) equation as follows

$$u_{xt} = \mathrm{e}^{-u} + \mathrm{e}^{-2u}. \tag{6.6}$$

The traveling wave transformation $\xi = kx + \omega t$ reduces Eq. (6.6) to the following ODE

$$k\omega f_{\xi\xi} - \mathrm{e}^{-f} - \mathrm{e}^{-2f} = 0, \tag{6.7}$$

where $u(x,t) = f(\xi)$.

Using the Painlevé transformation $v = \mathrm{e}^{-f}$ or $f = -\ln v$, the Tzitzeica–Dodd–Bullough (6.7) can be written as follows

$$k\omega v v_{\xi\xi} - k\omega (v_{\xi})^2 + v^3 + v^4 = 0. \tag{6.8}$$

6.3 Algorithms for the Improved Generalized Jacobi Elliptic Function Method and the Extended Auxiliary Equation Method

In this section, algorithms for improved generalized Jacobi elliptic function method and extended auxiliary equation method have been presented.

6.3.1 Algorithm for the Improved Generalized Jacobi Elliptic Function Method

In this present analysis, the determination of exact solutions for coupled Schrödinger–Boussinesq equations have been described using the proposed method. The main steps of this present method are described as follows:

Step 1: Suppose that the coupled nonlinear NLPDEs in the class of coupled Schrödinger–Boussinesq equations, say in two independent variables x, and t are given by

$$F(u, v, u_x, v_x, iu_t, v_t, u_{xx}, v_{xx}, u_{xt}, v_{xt}, \ldots) = 0, \tag{6.9a}$$

$$G(u, v, u_x, v_x, u_t, v_t, u_{xx}, v_{xx}, u_{xt}, v_{xt}, \ldots) = 0, \tag{6.9b}$$

where $u = u(x,t)$ and $v = v(x,t)$ are unknown functions, F and G are polynomials in u, v and its various partial derivatives in which the highest order derivatives and nonlinear terms are involved.

Step 2: We introduce the following traveling wave transformations:

$$u(x,t) = U(\xi)\mathrm{e}^{\mathrm{i}(kx+ct+\zeta_0)}, \; v(x,t) = V(\xi), \tag{6.10}$$

$$\xi = x - 2kt + \eta_0 \tag{6.11}$$

where k, and c are real constants to be determined later; and ζ_0, and η_0 are arbitrary constants.

Using the above traveling wave transformations, the NLPDEs (6.9a and 6.9b) can be transformed to couple nonlinear ordinary differential equations (ODEs) involving $U(\xi)$ and $V(\xi)$. Then, the resultant coupled ODEs are obtained

$$P(U, V, kU, kV, cU, cV, U_\xi, V_\xi, kU_\xi, kV_\xi, cU_\xi, cV_\xi, U_{\xi\xi}, V_{\xi\xi}, \ldots) = 0, \tag{6.12}$$

$$Q(U, V, kU, kV, cU, cV, U_\xi, V_\xi, kU_\xi, kV_\xi, cU_\xi, cV_\xi, U_{\xi\xi}, V_{\xi\xi}, \ldots) = 0, \tag{6.13}$$

where the suffix denotes the derivative with respect to ξ.

Step 3: Let us assume that the exact solutions of Eqs. (6.12) and (6.13) are to be defined in the polynomial $\varphi(\xi)$ of the following forms:

$$U(\xi) = a_{10} + \sum_{i=1}^{M} \left[a_{1i}\phi^i(\xi) + b_{1i}\phi^{-i}(\xi) + c_{1i}\phi^{i-1}(\xi)\phi'(\xi) + d_{1i}\phi^{-i}(\xi)\phi'(\xi)\right], \tag{6.14}$$

$$V(\xi) = a_{20} + \sum_{j=1}^{N} \left[a_{2j}\phi^j(\xi) + b_{2j}\phi^{-j}(\xi) + c_{2j}\phi^{j-1}(\xi)\phi'(\xi) + d_{2j}\phi^{-j}(\xi)\phi'(\xi)\right], \tag{6.15}$$

where $\phi(\xi)$ satisfies the following Jacobi elliptic equation:

$$(\phi_\xi(\xi))^2 = p\phi^4(\xi) + q\phi^2(\xi) + r, \tag{6.16}$$

where p, q, r, a_{10}, a_{1i}, b_{1i}, c_{1i}, d_{1i} $(i = 1, 2, \ldots, M)$, a_{20}, a_{2j}, b_{2j}, c_{2j}, d_{2j} $(j = 1, 2, \ldots, N)$ are constants to be determined later.

Step 4: We determine the positive integers M, N in Eqs. (6.14) and (6.15) by balancing the highest order derivatives and the nonlinear terms in Eqs. (6.12) and (6.13), respectively.

Step 5: Substituting Eqs. (6.14) and (6.15) along with Eq.(6.16) into Eqs. (6.12) and (6.13) and collecting all the coefficients of $\varphi^l(\xi)$ $(l = 0, 1, 2, \ldots)$ and $\phi^m(\xi)\phi'(\xi)$ $(m = 0, 1, 2, \ldots)$, then equating these coefficients to zero, yield a set of algebraic equations, which can be solved by using the Mathematica or Maple to find the values of a_{10}, a_{1i}, b_{1i}, c_{1i}, d_{1i} $(i = 1, 2, \ldots, M)$, a_{20}, a_{2j}, b_{2j}, c_{2j}, d_{2j} $(j = 1, 2, \ldots, N)$, k, c.

Step 6: It may be referred to that Eq. (6.16) has families of Jacobi elliptic function solutions as follows [54].

It may be mentioned that there are other Jacobi elliptic function solutions of Eq. (6.16) which are excluded here for simplicity.

Step 7: Substituting the values of a_{10}, a_{1i}, b_{1i}, c_{1i}, d_{1i} $(i = 1, 2, \ldots, M)$, a_{20}, a_{2j}, b_{2j}, c_{2j}, d_{2j} $(j = 1, 2, \ldots, N)$, p, q, r as well as the solutions of Eq. (6.16) provided in Step 6, into Eqs. (6.14) and (6.15), we can obtain several classes of exact solutions for CSBEs involving the Jacobi elliptic functions *sn*, *cn*, *ns*, *nc*, *cs,* and *sc* functions.

In Table 6.1, $sn\xi = sn(\xi, m^2)$, $cn\xi = cn(\xi, m^2)$, $dn\xi = dn(\xi, m^2)$, $ns\xi = ns(\xi, m^2)$, $cs\xi = cs(\xi, m^2)$, $ds\xi = ds(\xi, m^2)$, $sc\xi = sc(\xi, m^2)$, $sd\xi = sd(\xi, m^2)$ are the Jacobi elliptic functions with modulus m, $0 < m < 1$.

The Jacobi elliptic functions $sn\xi$, $cn\xi$, and $dn\xi$ are double periodic and have the following properties:

$$sn^2\xi + cn^2\xi = 1,$$
$$dn^2\xi + m^2 sn^2\xi = 1.$$

In addition to these, these functions satisfy the followings:

$$(sn\xi)' = cn\xi dn\xi, \quad (cn\xi)' = -sn\xi dn\xi, \quad (dn\xi)' = -m^2 sn\xi cn\xi, \quad (ns\xi)' = -cs\xi ds\xi,$$
$$(cs\xi)' = -ns\xi ds\xi, \quad (ds\xi)' = -ns\xi cs\xi, \quad (sc\xi)' = nc\xi dc\xi, \quad (nc\xi)' = sc\xi dc\xi,$$
$$(dc\xi)' = (1 - m^2) nc\xi sc\xi, \quad (sd\xi)' = nd\xi cd\xi, \quad (cd\xi)' = (m^2 - 1) sd\xi nd\xi,$$
$$(nd\xi)' = m^2 cd\xi sd\xi.$$

Further explanations in details about the Jacobi elliptic functions can be found in [55].

Table 6.1 Jacobi elliptic function solutions of Eq. (6.16)

S. no.	p	q	r	$\phi(\xi)$
1.	m^2	$-(1+m^2)$	1	$sn\xi$
2.	1	$-(1+m^2)$	m^2	$ns\xi = (sn\xi)^{-1}$
3.	$-m^2$	$2m^2 - 1$	$1 - m^2$	$cn\xi$
4.	$1 - m^2$	$2m^2 - 1$	$-m^2$	$nc\xi = (cn\xi)^{-1}$
5.	$\frac{1}{4}$	$\frac{1-2m^2}{2}$	$\frac{1}{4}$	$ns\xi \pm cs\xi$
6.	$\frac{1-m^2}{4}$	$\frac{m^2+1}{2}$	$\frac{1-m^2}{4}$	$nc\xi \pm sc\xi$

6.3.2 Algorithm for the New Extended Auxiliary Equation Method

Let us consider the following nonlinear PDE

$$\Phi(u, u_x, u_t, u_{xx}, u_{tt}, \ldots) = 0, \tag{6.17}$$

where $u = u(x, t)$ is an unknown function, Φ is a polynomial in u and its partial derivatives in which the highest order derivatives and the nonlinear terms are involved. The main steps of the new extended auxiliary equation method [56] can be summarized as follows:

Step 1: The following traveling wave transformation

$$u(x, t) = U(\xi), \xi = kx + \omega t, \tag{6.18}$$

where k and ω are constants, has been considered to reduce Eq. (6.17) to the following nonlinear ordinary differential equation (ODE):

$$H(U, U', U'', \ldots) = 0, \tag{6.19}$$

where H is a polynomial in $U(\xi)$ and its total derivatives $U'(\xi)$, $U''(\xi)$, and so on.

Step 2: Let us assume that Eq. (6.19) has the formal solution

$$U(\xi) = \sum_{i=0}^{2N} a_i F^i(\xi), \tag{6.20}$$

where $F(\xi)$ satisfies the first-order ODE:

$$(F'(\xi))^2 = c_0 + c_2 F^2(\xi) + c_4 F^4(\xi) + c_6 F^6(\xi), \tag{6.21}$$

where $c_j (j = 0, 2, 4, 6)$ and $a_i (i = 0, \ldots, 2N)$ are arbitrary constants to be determined.

Step 3: By balancing the highest order nonlinear terms and the highest order derivatives of $U(\xi)$ in Eq. (6.19), the balance number N of Eq. (6.20) can be determined.

Step 4: Substituting Eq. (6.20) alongwith (6.21) into Eq. (6.19), collecting all the coefficients of $F^j(F')^l$ $(j = 0, 1, 2, \ldots)$ and $(l = 0, 1)$, and set them to zero, leads to a system of algebraic equations for $c_j (j = 0, 2, 4, 6)$, $a_i (i = 0, \ldots, 2N)$, k, and ω.

Step 5: The system of algebraic equations obtained in Step 4 is solved to find $c_j(j=0,2,4,6)$, $a_i(i=0,\ldots,2N)$, k, and ω.

Step 6: It is well familiar that Eq. (6.21) has the following solutions [56, 57]:

$$F(\xi)=\frac{1}{2}\left[-\frac{c_4}{c_6}(1\pm\phi_i(\xi))\right]^{1/2}, \tag{6.22}$$

where the function $\phi_i(\xi)$ $(i=1,2,\ldots,12)$ can be expressed through the Jacobi elliptic function $sn(\xi,m)$, $cn(\xi,m)$, $dn(\xi,m)$, and so on, where $0<m<1$ is the modulus of the Jacobi elliptic functions. When m approaches to 1 or 0, the Jacobi elliptic functions degenerate to hyperbolic functions and trigonometric functions, respectively. Further explanations in details about the Jacobi elliptic functions can be found in Ref. [55].

The function $\phi_i(\xi)$ in Eq. (6.22) has 12 forms as follows [41]:

Type I:

If $c_0=\frac{c_4^3(m^2-1)}{32c_6^2m^2}$, $c_2=\frac{c_4^2(5m^2-1)}{16c_6m^2}$, $c_6>0$, then $\phi_i(\xi)$ in Eq. (6.22) takes the form

$$\phi_1(\xi)=sn(\kappa\xi),\ \phi_2(\xi)=\frac{1}{msn(\kappa\xi)},\ \kappa=\frac{c_4}{2m}\frac{1}{\sqrt{c_6}}. \tag{6.23}$$

Type II:

If $c_0=\frac{c_4^3(1-m^2)}{32c_6^2}$, $c_2=\frac{c_4^2(5-m^2)}{16c_6}$, $c_6>0$, then $\phi_i(\xi)$ in Eq. (6.22) takes the form

$$\phi_3(\xi)=msn(\kappa\xi),\ \phi_4(\xi)=\frac{1}{sn(\kappa\xi)},\ \kappa=\frac{c_4}{2}\frac{1}{\sqrt{c_6}}. \tag{6.24}$$

Type III:

If $c_0=\frac{c_4^3}{32m^2c_6^2}$, $c_2=\frac{c_4^2(4m^2+1)}{16c_6m^2}$, $c_6<0$, then $\phi_i(\xi)$ in Eq. (6.22) takes the form

$$\phi_5(\xi)=cn(\kappa\xi),\ \phi_6(\xi)=\frac{\sqrt{1-m^2}sn(\kappa\xi)}{dn(\kappa\xi)},\ \kappa=\frac{c_4\sqrt{-c_6}}{2mc_6}. \tag{6.25}$$

Type IV:

If $c_0=\frac{c_4^3m^2}{32c_6^2(m^2-1)}$, $c_2=\frac{c_4^2(5m^2-4)}{16c_6(m^2-1)}$, $c_6<0$, then $\phi_i(\xi)$ in Eq. (6.22) takes the form

$$\phi_7(\xi)=\frac{\sqrt{1-m^2}dn(\kappa\xi)}{1-m^2},\ \phi_8(\xi)=\frac{1}{dn(\kappa\xi)},\ \kappa=\frac{c_4\sqrt{c_6(m^2-1)}}{2c_6(m^2-1)}. \tag{6.26}$$

Type V:

If $c_0 = \frac{c_4^3}{32c_6^2(1-m^2)}$, $c_2 = \frac{c_4^2(4m^2-5)}{16c_6(m^2-1)}$, $c_6 > 0$, then $\phi_i(\xi)$ in Eq. (6.22) takes the form

$$\phi_9(\xi) = \frac{1}{cn(\kappa\xi)}, \ \phi_{10}(\xi) = \frac{\sqrt{1-m^2}dn(\kappa\xi)}{(1-m^2)sn(\kappa\xi)}, \ \kappa = \frac{c_4\sqrt{c_6(1-m^2)}}{2c_6(1-m^2)}. \tag{6.27}$$

Type VI:

If $c_0 = \frac{m^2c_4^3}{32c_6^2}$, $c_2 = \frac{c_4^2(m^2+4)}{16c_6}$, $c_6 < 0$, then $\phi_i(\xi)$ in Eq. (6.22) takes the form

$$\phi_{11}(\xi) = dn(\kappa\xi), \ \phi_{12}(\xi) = \frac{\sqrt{1-m^2}}{dn(\kappa\xi)}, \ \kappa = \frac{c_4\sqrt{-c_6}}{2c_6}. \tag{6.28}$$

Step 7: Substituting Eq. (6.22) together with Eqs. (6.23–6.28) into Eq. (6.20), some new types of Jacobian elliptic function solutions of Eq. (6.17) can be obtained elegantly.

6.4 New Explicit Exact Solutions of Coupled Schrödinger–Boussinesq Equations

In this present analysis, an investigation has been made in searching the new generalized Jacobi elliptic function solutions for Eqs. (6.1) and (6.2) by using the proposed method discussed in Sect. 6.3.1. According to the technique discussed in the Algorithm of Sect. 6.3.1, we adopt the ansatz solutions of Eqs. (6.1) and (6.2) in the following forms

$$u(x,t) = U(x,t) = U(\xi)e^{i(kx+ct+\zeta_0)}, \tag{6.29}$$

and

$$v(x,t) = V(x,t) = V(\xi), \tag{6.30}$$

respectively. Here, $\xi = x - 2kt + \eta_0$, where k and c are real constants to be evaluated later; and ζ_0 and η_0 are arbitrary constants.

Now, plugging Eqs. (6.29) and (6.30) into Eqs. (6.1) and (6.2) and then, integrating the second Eq. (6.2) of the coupled Schrödinger–Boussinesq equations twice with respect to ξ, we have

$$U_{\xi\xi} - (k^2 + c - \alpha)U - UV = 0, \tag{6.31}$$

$$V_{\xi\xi} - 12k^2V - 3V^2 - \beta V + U^2 = 0, \tag{6.32}$$

Balancing the highest derivative term $U_{\xi\xi}$ with the nonlinear term UV in Eq. (6.31) and the highest derivative term $V_{\xi\xi}$ with the nonlinear term U^2 in Eq. (6.32) leads to $M = N = 2$. Thus, the exact solutions of Eqs. (6.1) and (6.2) have the following forms:

$$U(\xi) = a_{10} + \sum_{i=1}^{2} \left[a_{1i}\phi^i(\xi) + b_{1i}\phi^{-i}(\xi) + c_{1i}\phi^{i-1}(\xi)\phi'(\xi) + d_{1i}\phi^{-i}(\xi)\phi'(\xi)\right], \tag{6.33}$$

$$V(\xi) = a_{20} + \sum_{j=1}^{2} \left[a_{2j}\phi^j(\xi) + b_{2j}\phi^{-j}(\xi) + c_{2j}\phi^{j-1}(\xi)\phi'(\xi) + d_{2j}\phi^{-j}(\xi)\phi'(\xi)\right]. \tag{6.34}$$

Now, substituting Eqs. (6.33) and (6.34) alongwith Eq. (6.16) into Eqs. (6.31) and (6.32), and then collecting all the coefficients of $\phi^l(\xi)$ $(l = 0, 1, 2, \ldots)$ and $\phi^m(\xi)\phi'(\xi)$ $(m = 0, 1, 2, \ldots)$, then equating these coefficients to zero, yield a set of over-determined algebraic equations for a_{10}, a_{1i}, b_{1i}, c_{1i}, d_{1i} $(i = 1, 2)$, a_{20}, a_{2j}, b_{2j}, c_{2j}, d_{2j} $(j = 1, 2)$, k, c. Using the *Mathematica* and the *Wu's elimination methods*, the algebraic equations have been solved and thus, the following results have been obtained.

Result 1:

$$a_{10} = 0, a_{11} = 0, a_{12} = 0, b_{11} = 0, b_{12} = 0, c_{11} = 0, c_{12} = 0, d_{11} = -\frac{4\sqrt{pr}}{\sqrt{q}}, d_{12} = 0;$$
$$a_{20} = 0, a_{21} = 0, a_{22} = 2p, b_{21} = 0, b_{22} = 2r, c_{21} = 0, c_{22} = 0, d_{21} = 0, d_{22} = 0;$$
$$k = -\frac{\sqrt{4q^2 + 8pr - \beta q}}{2\sqrt{3}\sqrt{q}} \text{ and } c = \frac{-4q^2 - 8pr + 12\alpha q + \beta q}{12q}.$$

Result 2:

$$a_{10} = 0, a_{11} = 0, a_{12} = 0, b_{11} = 0, b_{12} = 0, c_{11} = 0, c_{12} = 0, d_{11} = \frac{4\sqrt{pr}}{\sqrt{q}}, d_{12} = 0;$$
$$a_{20} = 0, a_{21} = 0, a_{22} = 2p, b_{21} = 0, b_{22} = 2r, c_{21} = 0, c_{22} = 0, d_{21} = 0, d_{22} = 0;$$
$$k = \frac{\sqrt{4q^2 + 8pr - \beta q}}{2\sqrt{3}\sqrt{q}} \text{ and } c = \frac{-4q^2 - 8pr + 12\alpha q + \beta q}{12q}.$$

Result 3:

$$a_{10}=0, a_{11}=0, a_{12}=0, b_{11}=0, b_{12}=0, c_{11}=0, c_{12}=0, d_{11}=\frac{4\sqrt{pr}}{\sqrt{q}}, d_{12}=0;$$
$$a_{20}=0, a_{21}=0, a_{22}=2p, b_{21}=0, b_{22}=2r, c_{21}=0, c_{22}=0, d_{21}=0, d_{22}=0;$$
$$k=-\frac{\sqrt{4q^2+8pr-\beta q}}{2\sqrt{3}\sqrt{q}} \text{ and } c=\frac{-4q^2-8pr+12\alpha q+\beta q}{12q}.$$

Result 4:

$$a_{10}=0, a_{11}=0, a_{12}=0, b_{11}=0, b_{12}=0, c_{11}=0, c_{12}=0, d_{11}=-\frac{4\sqrt{pr}}{\sqrt{q}}, d_{12}=0;$$
$$a_{20}=0, a_{21}=0, a_{22}=2p, b_{21}=0, b_{22}=2r, c_{21}=0, c_{22}=0, d_{21}=0, d_{22}=0;$$
$$k=\frac{\sqrt{4q^2+8pr-\beta q}}{2\sqrt{3}\sqrt{q}} \text{ and } c=\frac{-4q^2-8pr+12\alpha q+\beta q}{12q}.$$

Substituting the results obtained above into Eqs. (6.33) and (6.34) alongwith the Jacobi elliptic function solutions provided in Table 6.1, we can obtain following families of exact solutions to Eqs. (6.1) and (6.2).

Set 1:

$$a_{10}=0, a_{11}=0, a_{12}=0, b_{11}=0, b_{12}=0, c_{11}=0, c_{12}=0, d_{11}=-\frac{4\sqrt{pr}}{\sqrt{q}}, d_{12}=0;$$
$$a_{20}=0, a_{21}=0, a_{22}=2p, b_{21}=0, b_{22}=2r, c_{21}=0, c_{22}=0, d_{21}=0, d_{22}=0;$$
$$k=-\frac{\sqrt{4q^2+8pr-\beta q}}{2\sqrt{3}\sqrt{q}} \text{ and } c=\frac{-4q^2-8pr+12\alpha q+\beta q}{12q}.$$

Case I: If $p=-m^2$, $q=2m^2-1$, $r=1-m^2$ and $\phi(\xi)=cn\xi$, then we get the following double periodic solutions in terms of Jacobi elliptic functions

$$u_{11}(x,t)=U(\xi)e^{i(kx+ct+\zeta_0)}=\frac{4\sqrt{m^2(m^2-1)}}{\sqrt{2m^2-1}}\frac{sn\xi dn\xi}{cn\xi}e^{i(kx+ct+\zeta_0)}, 1/2<m^2<1,$$
$$v_{11}(x,t)=V(\xi)=-2m^2cn^2\xi+2\left(1-m^2\right)nc^2\xi,$$

where

$$\xi = x - 2kt + \eta_0, k = -\frac{\sqrt{4 + 24m^4 + \beta - 2m^2(12 + \beta)}}{2\sqrt{-3 + 6m^2}}, \text{ and}$$
$$c = -\frac{4 + 24m^4 + 12\alpha + \beta - 2m^2(12 + 12\alpha + \beta)}{-12 + 24m^2}.$$

Case II: If $p = 1 - m^2$, $q = 2m^2 - 1$, $r = -m^2$ and $\phi(\xi) = nc\xi$, then we get the following double periodic solutions in terms of Jacobi elliptic functions

$$u_{12}(x,t) = U(\xi)e^{i(kx+ct+\zeta_0)} = -\frac{4\sqrt{m^2(m^2-1)}}{\sqrt{2m^2-1}}\frac{sc\xi dc\xi}{nc\xi}e^{i(kx+ct+\zeta_0)}, 1/2 < m^2 < 1,$$
$$v_{12}(x,t) = V(\xi) = 2\left(1 - m^2\right)nc^2\xi - 2m^2cn^2\xi,$$

where

$$\xi = x - 2kt + \eta_0, k = -\frac{\sqrt{4 + 24m^4 + \beta - 2m^2(12 + \beta)}}{2\sqrt{-3 + 6m^2}}, \text{ and}$$
$$c = -\frac{4 + 24m^4 + 12\alpha + \beta - 2m^2(12 + 12\alpha + \beta)}{-12 + 24m^2}.$$

Case III: If $p = \frac{1}{4}$, $q = \frac{1-2m^2}{2}$, $r = \frac{1}{4}$ and $\phi(\xi) = ns\xi \pm cs\xi$, then we get the following double periodic solutions

$$u_{13}(x,t) = U(\xi)e^{i(kx+ct+\zeta_0)} = \frac{2}{\sqrt{2-4m^2}}\frac{cs\xi ds\xi \pm ns\xi ds\xi}{ns\xi \pm cs\xi}e^{i(kx+ct+\zeta_0)}, m^2 < 1/2,$$
$$v_{13}(x,t) = V(\xi) = \frac{1}{2}(ns\xi \pm cs\xi)^2 + \frac{1}{2}(ns\xi \pm cs\xi)^{-2}$$

where

$$\xi = x - 2kt + \eta_0, k = -\frac{\sqrt{3 + 8m^4 + 2m^2(-4 + \beta) - \beta}}{2\sqrt{3 - 6m^2}}, \text{ and}$$
$$c = \frac{3 + 8m^4 - 12\alpha - \beta + 2m^2(-4 + 12\alpha + \beta)}{-12 + 24m^2}.$$

Case IV: If $p = \frac{1-m^2}{4}$, $q = \frac{1+m^2}{2}$, $r = \frac{1-m^2}{4}$ and $\phi(\xi) = nc\xi \pm sc\xi$, then we get the following Jacobi elliptic function solutions

$$u_{14}(x,t) = U(\xi)\mathrm{e}^{\mathrm{i}(kx+ct+\zeta_0)} = \mp\frac{\sqrt{2}(m^2-1)}{\sqrt{m^2+1}}dc\xi\ \mathrm{e}^{\mathrm{i}(kx+ct+\zeta_0)}, \quad 0<m<1,$$
$$v_{14}(x,t) = V(\xi) = \frac{1-m^2}{2}\left(\frac{cn\xi}{1\pm sn\xi}\right)^2 + \frac{1-m^2}{2}\left(\frac{cn\xi}{1\pm sn\xi}\right)^{-2},$$

where

$$\xi = x - 2kt + \eta_0, k = -\frac{\sqrt{3+3m^4-m^2(-2+\beta)-\beta}}{2\sqrt{3}\sqrt{1+m^2}}, \text{and}$$
$$c = \frac{-3-3m^4+12\alpha+\beta+m^2(-2+12\alpha+\beta)}{12(1+m^2)}.$$

Case V: If $p = m^2$, $q = -(1+m^2)$, $r = 1$ and $\phi(\xi) = sn\xi$, then we get the following Jacobi elliptic function solutions

$$u_{15}(x,t) = U(\xi)\mathrm{e}^{\mathrm{i}(kx+ct+\zeta_0)} = -\frac{4m}{\sqrt{-m^2-1}}\frac{cn\xi dn\xi}{sn\xi}\mathrm{e}^{\mathrm{i}(kx+ct+\zeta_0)}$$
$$v_{15}(x,t) = V(\xi) = 2m^2sn^2\xi + 2ns^2\xi,$$

where

$$\xi = x - 2kt + \eta_0, k = -\frac{\sqrt{4+24m^4+\beta-2m^2(12+\beta)}}{2\sqrt{-3+6m^2}}, \text{ and}$$
$$c = -\frac{4+24m^4+12\alpha+\beta-2m^2(12+12\alpha+\beta)}{-12+24m^2}.$$

Case VI: If $p = 1$, $q = -(1+m^2)$, $r = m^2$ and $\phi(\xi) = sn\xi$, then we get the following Jacobi elliptic function solutions

$$u_{16}(x,t) = U(\xi)\mathrm{e}^{\mathrm{i}(kx+ct+\zeta_0)} = \frac{4m}{\sqrt{-m^2-1}}\frac{cs\xi ds\xi}{ns\xi}\mathrm{e}^{\mathrm{i}(kx+ct+\zeta_0)},$$
$$v_{16}(x,t) = V(\xi) = 2ns^2\xi + 2m^2sn^2\xi,$$

where

$$\xi = x - 2kt + \eta_0, k = -\frac{\sqrt{4+24m^4+\beta-2m^2(12+\beta)}}{2\sqrt{-3+6m^2}} \text{ and}$$
$$c = -\frac{4+24m^4+12\alpha+\beta-2m^2(12+12\alpha+\beta)}{-12+24m^2}.$$

Set 2:

$$a_{10}=0, a_{11}=0, a_{12}=0, b_{11}=0, b_{12}=0, c_{11}=0, c_{12}=0, d_{11}=\frac{4\sqrt{pr}}{\sqrt{q}}, d_{12}=0;$$
$$a_{20}=0, a_{21}=0, a_{22}=2p, b_{21}=0, b_{22}=2r, c_{21}=0, c_{22}=0, d_{21}=0, d_{22}=0;$$
$$k=\frac{\sqrt{4q^2+8pr-\beta q}}{2\sqrt{3}\sqrt{q}} \text{ and } c=\frac{-4q^2-8pr+12\alpha q+\beta q}{12q}.$$

Case I: If $p=-m^2$, $q=2m^2-1$, $r=1-m^2$ and $\phi(\xi)=cn\xi$, then we get the following double periodic solutions in terms of Jacobi elliptic functions

$$u_{21}(x,t)=U(\xi)e^{i(kx+ct+\zeta_0)}=-\frac{4\sqrt{m^2(m^2-1)}}{\sqrt{2m^2-1}}\frac{sn\xi dn\xi}{cn\xi}e^{i(kx+ct+\zeta_0)}, 1/2<m^2<1,$$
$$v_{21}(x,t)=V(\xi)=-2m^2cn^2\xi+2(1-m^2)nc^2\xi,$$

where

$$\xi=x-2kt+\eta_0, k=\frac{\sqrt{4+24m^4+\beta-2m^2(12+\beta)}}{2\sqrt{-3+6m^2}}, \text{ and}$$
$$c=-\frac{4+24m^4+12\alpha+\beta-2m^2(12+12\alpha+\beta)}{-12+24m^2}.$$

Case II: If $p=1-m^2$, $q=2m^2-1$, $r=-m^2$ and $\phi(\xi)=nc\xi$, then we get the following double periodic solutions in terms of Jacobi elliptic functions

$$u_{22}(x,t)=U(\xi)e^{i(kx+ct+\zeta_0)}=\frac{4\sqrt{m^2(m^2-1)}}{\sqrt{2m^2-1}}\frac{sc\xi dc\xi}{nc\xi}e^{i(kx+ct+\zeta_0)}, 1/2<m^2<1,$$
$$v_{22}(x,t)=V(\xi)=2(1-m^2)nc^2\xi-2m^2cn^2\xi,$$

where

$$\xi=x-2kt+\eta_0, k=\frac{\sqrt{4+24m^4+\beta-2m^2(12+\beta)}}{2\sqrt{-3+6m^2}}, \text{ and}$$
$$c=-\frac{4+24m^4+12\alpha+\beta-2m^2(12+12\alpha+\beta)}{-12+24m^2}.$$

Case III: If $p=\frac{1}{4}$, $q=\frac{1-2m^2}{2}$, $r=\frac{1}{4}$ and $\phi(\xi)=ns\xi\pm cs\xi$, then we get the following double periodic solutions

$$u_{23}(x,t)=U(\xi)\mathrm{e}^{\mathrm{i}(kx+ct+\zeta_0)}=-\frac{2}{\sqrt{2-4m^2}}\frac{cs\xi ds\xi\pm ns\xi ds\xi}{ns\xi\pm cs\xi}\mathrm{e}^{\mathrm{i}(kx+ct+\zeta_0)}, m^2<1/2,$$
$$v_{23}(x,t)=V(\xi)=\frac{1}{2}(ns\xi\pm cs\xi)^2+\frac{1}{2}(ns\xi\pm cs\xi)^{-2},$$

where

$$\xi=x-2kt+\eta_0, k=\frac{\sqrt{3+8m^4+2m^2(-4+\beta)-\beta}}{2\sqrt{3-6m^2}},\ \text{and}$$
$$c=\frac{3+8m^4-12\alpha-\beta+2m^2(-4+12\alpha+\beta)}{-12+24m^2}.$$

Case IV: If $p=\frac{1-m^2}{4}$, $q=\frac{1+m^2}{2}$, $r=\frac{1-m^2}{4}$ and $\phi(\xi)=nc\xi\pm sc\xi$, then we get the following Jacobi elliptic function solutions

$$u_{24}(x,t)=U(\xi)\mathrm{e}^{\mathrm{i}(kx+ct+\zeta_0)}=\mp\frac{\sqrt{2}(m^2-1)}{\sqrt{m^2+1}}dc\xi\mathrm{e}^{\mathrm{i}(kx+ct+\zeta_0)}, 0<m<1,$$
$$v_{24}(x,t)=V(\xi)=\frac{1-m^2}{2}\left(\frac{cn\xi}{1\pm sn\xi}\right)^2+\frac{1-m^2}{2}\left(\frac{cn\xi}{1\pm sn\xi}\right)^{-2},$$

where

$$\xi=x-2kt+\eta_0, k=\frac{\sqrt{3+3m^4-m^2(-2+\beta)-\beta}}{2\sqrt{3}\sqrt{1+m^2}},\ \text{and}$$
$$c=\frac{-3-3m^4+12\alpha+\beta+m^2(-2+12\alpha+\beta)}{12(1+m^2)}.$$

Case V: If $p=m^2$, $q=-(1+m^2)$, $r=1$ and $\phi(\xi)=sn\xi$, then we get the following double periodic solutions in terms of Jacobi elliptic functions

$$u_{25}(x,t)=U(\xi)\mathrm{e}^{\mathrm{i}(kx+ct+\zeta_0)}=\frac{4m}{\sqrt{-m^2-1}}\frac{cn\xi dn\xi}{sn\xi}\mathrm{e}^{\mathrm{i}(kx+ct+\zeta_0)},$$
$$v_{25}(x,t)=V(\xi)=2m^2sn^2\xi+2ns^2\xi,$$

where

$$\xi = x - 2kt + \eta_0, k = \frac{\sqrt{4 + 4m^4 + \beta + m^2(16 + \beta)}}{2\sqrt{3}\sqrt{-1 - m^2}}, \text{ and}$$
$$c = \frac{4 + 4m^4 + 12\alpha + \beta + m^2(16 + 12\alpha + \beta)}{12(1 + m^2)}.$$

Case VI: If $p = 1$, $q = -(1 + m^2)$, $r = m^2$ and $\phi(\xi) = ns\xi$, then we get the following double periodic solutions

$$u_{26}(x,t) = U(\xi)e^{i(kx+ct+\zeta_0)} = -\frac{4m}{\sqrt{-m^2-1}}\frac{cs\xi ds\xi}{ns\xi}e^{i(kx+ct+\zeta_0)},$$
$$v_{26}(x,t) = V(\xi) = 2ns^2\xi + 2m^2sn^2\xi,$$

where

$$\xi = x - 2kt + \eta_0, k = \frac{\sqrt{4 + 4m^4 + \beta + m^2(16 + \beta)}}{2\sqrt{3}\sqrt{-1 - m^2}}, \text{ and}$$
$$c = \frac{4 + 4m^4 + 12\alpha + \beta + m^2(16 + 12\alpha + \beta)}{12(1 + m^2)}.$$

Similarly, as the established solutions for **Set 1 and Set 2**, we can construct corresponding exact solutions to Eqs. (6.1) and (6.2) for **Set 3 and Set 4**, which are omitted here.

6.4.1 *Numerical Simulations for the Solutions of Coupled Schrödinger–Boussinesq Equations*

In the present analysis, the first solutions of **Case IV** of **Set 1** have been used for drawing the solution graphs Figs. 6.1 and 6.2 for coupled Schrödinger–Boussinesq equations.

Again, the solutions of **Case V** of **Set 2** have been used for drawing the solution graphs Figs. 6.3 and 6.4 for coupled Schrödinger–Boussinesq equations.

In the present numerical simulations, the double periodic wave solutions for the first solutions of $u_{14}(x,t)$ and $v_{14}(x,t)$ have been demonstrated in 3D graphs of Figs. 6.1 and 6.2 with elliptic modulus $m = 0.5$. Also, the double periodic wave solutions for $u_{25}(x,t)$ and $v_{25}(x,t)$ have been demonstrated in 3D graphs of Figs. 6.3 and 6.4 with elliptic modulus $m = 0.5$.

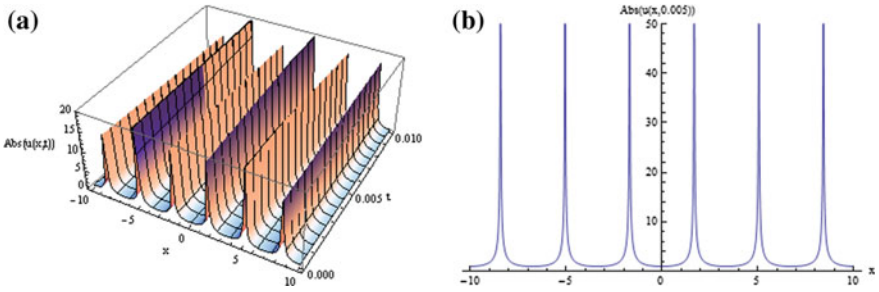

Fig. 6.1 **a** Double periodic wave solutions for the first solution of $u_{14}(x,t)$ when $\alpha = 1$, $\beta = -1$, $\zeta_0 = 0$, $\xi_0 = 0$, and $m = 0.5$, and **b** the corresponding 2D solution graph when $t = 0.005$

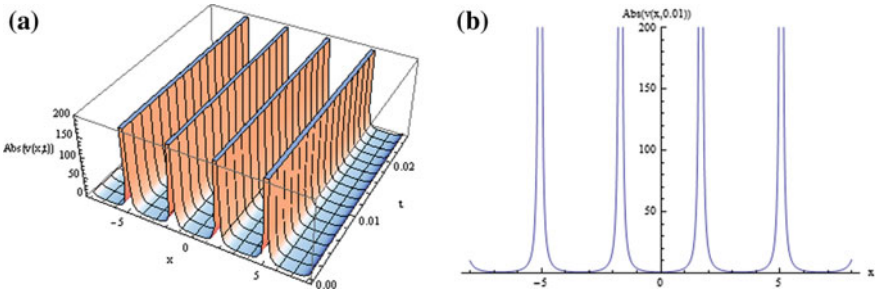

Fig. 6.2 **a** Double periodic wave solutions for the first solution of $v_{14}(x,t)$ when $\alpha = 1$, $\beta = -1$, $\zeta_0 = 0$, $\xi_0 = 0$, and $m = 0.5$, and **b** the corresponding 2D solution graph when $t = 0.01$

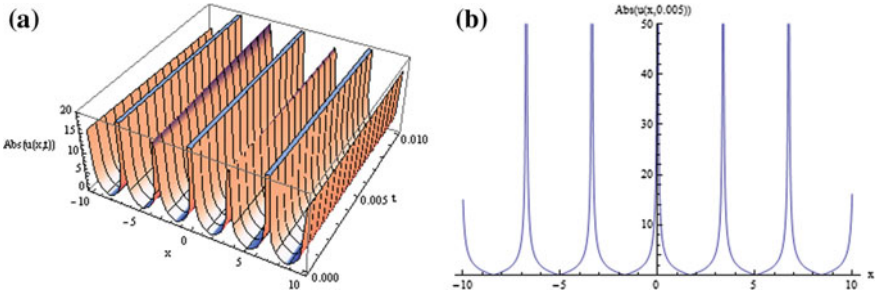

Fig. 6.3 **a** Double periodic wave solutions for $u_{25}(x,t)$ when $\alpha = 1$, $\beta = -1$, $\zeta_0 = 0$, $\xi_0 = 0$, and $m = 0.5$, and **b** the corresponding 2D solution graph when $t = 0.005$

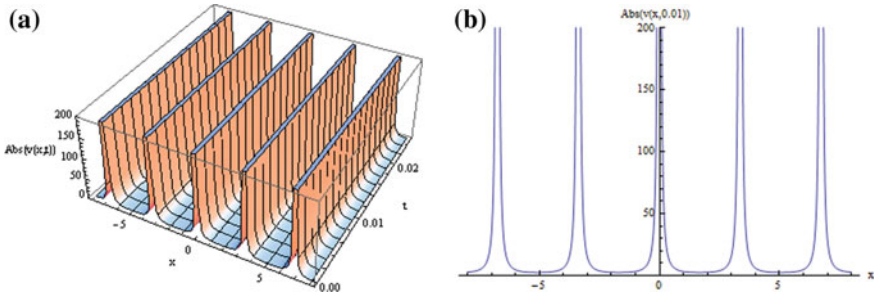

Fig. 6.4 **a** Double periodic wave solutions for $v_{25}(x,t)$ when $\alpha = 1$, $\beta = -1$, $\zeta_0 = 0$, $\xi_0 = 0$, and $m = 0.5$, and **b** the corresponding 2D solution graph when $t = 0.01$

6.5 Implementation of New Extended Auxiliary Equation Method to the Tzitzéica-Type Nonlinear Evolution Equations

In the present section, the Jacobi elliptic function solutions, including the hyperbolic and trigonometric solutions for the DBM and TDB equations have been obtained using a new extended auxiliary equation method.

6.5.1 New Exact Solutions of Dodd–Bullough–Mikhailov (DBM) Equation

In this part, we apply the new extended auxiliary equation method to determine the new exact solutions for Dodd–Bullough–Mikhailov Eq. (6.3).

Suppose the traveling wave solution of Eq. (6.5) can be expressed as

$$U(\xi) = v(\xi) = \sum_{i=0}^{2N} a_i F^i(\xi), \tag{6.35}$$

where $F(\xi)$ satisfies Eq. (6.21).

Balancing the highest order derivative term $vv_{\xi\xi}$ and the nonlinear term v^3 by using homogenous principle the following result could be obtained

$$N + N + 2 = 3N,$$

yielding

$$N = 2.$$

Therefore, the ansatz for the solution of Eq. (6.5) can be written as

$$U(\xi) = a_0 + a_1 F(\xi) + a_2 F^2(\xi) + a_3 F^3(\xi) + a_4 F^4(\xi), \tag{6.36}$$

where $F(\xi)$ satisfies

$$F(\xi) = \frac{1}{2}\left[-\frac{c_4}{c_6}(1 \pm \phi_i(\xi))\right]^{1/2}, \; i = 1, 2, \ldots, 12. \tag{6.37}$$

By substituting (6.36) and (6.21) into Eq. (6.5), the coefficients of each power of F^i, $i = 0, 1, 2\ldots$ are collected, which are then set to zero. Thus, it leads to a system of algebraic equations.

The derived system of algebraic equations has been solved by using mathematical software, yielding the following results:

$$a_0 = \frac{2^{1/3}3^{1/6} - 2^{1/3}3^{2/3}}{2}, a_2 = -22^{1/6}3^{1/12}\sqrt{a_4},$$
$$c_2 = \frac{2^{5/6}\sqrt{a_4}\left(96 \times 3^{5/12}c_0 + 11 \times 3^{11/12}c_0\right)}{156}, c_4 = -\frac{2}{13}\left(4 \times 2^{2/3}3^{1/3}a_4c_0 + 2^{2/3}3^{5/6}a_4c_0\right),$$
$$c_6 = \frac{1}{26}a_4^{3/2}\left(4\sqrt{2}3^{1/4}c_0 + \sqrt{2}3^{3/4}c_0\right), \omega = \frac{3\sqrt{2}3^{1/4} - 4\sqrt{2}3^{3/4}}{24kl^2},$$

where $l = a_4^{1/4}\sqrt{c_0}$.

Without loss of generality, let us assume $a_4 > 0$ and $c_0 > 0$, and hence $c_6 > 0$. Thus, $\phi(\xi)$ satisfies only the functions (6.23), (6.24), and (6.27).

Set I:

From Eqs. (6.23), (6.36), and (6.37), the Jacobi elliptic function solutions of Eq. (6.5) have been deduced as follows

$$U_{11}(\xi) = \frac{1}{2^{2/3}}(3^{1/6} - 3^{2/3}) - 2\left(2^{1/6}3^{1/12}\right)^2\left(1 \pm sn\left(\frac{2^{\frac{11}{12}}3^{\frac{5}{24}}l\sqrt{\frac{1}{13}(4+\sqrt{3})}}{m}\xi\right)\right)$$
$$+\left(2^{1/6}3^{1/12}\right)^2\left(1 \pm sn\left(\frac{2^{\frac{11}{12}}3^{\frac{5}{24}}l\sqrt{\frac{1}{13}(4+\sqrt{3})}}{m}\xi\right)\right)^2, \tag{6.38}$$

$$U_{12}(\xi)=\frac{1}{2^{2/3}}\left(3^{1/6}-3^{2/3}\right)-2\left(2^{1/6}3^{1/12}\right)^2\left(1\pm\frac{1}{msn\left(\frac{2^{\frac{11}{12}}3^{\frac{5}{24}}l\sqrt{\frac{1}{13}(4+\sqrt{3})}}{m}\xi\right)}\right)$$
$$+\left(2^{1/6}3^{1/12}\right)^2\left(1\pm\frac{1}{msn\left(\frac{2^{\frac{11}{12}}3^{\frac{5}{24}}l\sqrt{\frac{1}{13}(4+\sqrt{3})}}{m}\xi\right)}\right)^2, \tag{6.39}$$

where $\xi=kx+\frac{3\sqrt{2}3^{1/4}-4\sqrt{2}3^{3/4}}{24kl^2}t$ and $l=a_4^{1/4}\sqrt{c_0}$.

If $m\to 1$, then $sn(\xi)\to\tanh(\xi)$, and we have the hyperbolic function solutions of Eq. (6.5)

$$U_{13}(\xi)=\frac{1}{2^{2/3}}(3^{1/6}-3^{2/3})-2\left(2^{1/6}3^{1/12}\right)^2\left(1\pm\tanh\left(2^{\frac{11}{12}}3^{\frac{5}{24}}l\sqrt{\frac{1}{13}(4+\sqrt{3})}\xi\right)\right)$$
$$+\left(2^{1/6}3^{1/12}\right)^2\left(1\pm\tanh\left(2^{\frac{11}{12}}3^{\frac{5}{24}}l\sqrt{\frac{1}{13}(4+\sqrt{3})}\xi\right)\right)^2, \tag{6.40}$$

$$U_{14}(\xi)=\frac{1}{2^{2/3}}(3^{1/6}-3^{2/3})-2\left(2^{1/6}3^{1/12}\right)^2\left(1\pm\coth\left(2^{\frac{11}{12}}3^{\frac{5}{24}}l\sqrt{\frac{1}{13}(4+\sqrt{3})}\xi\right)\right)$$
$$+\left(2^{1/6}3^{1/12}\right)^2\left(1\pm\coth\left(2^{\frac{11}{12}}3^{\frac{5}{24}}l\sqrt{\frac{1}{13}(4+\sqrt{3})}\xi\right)\right)^2, \tag{6.41}$$

Set II:

From Eqs. (6.24), (6.36), and (6.37), the Jacobi elliptic function solutions of Eq. (6.5) have been obtained as follows

$$U_{21}(\xi)=\frac{1}{2^{2/3}}(3^{1/6}-3^{2/3})-2\left(2^{1/6}3^{1/12}\right)^2\left(1\pm msn\left(2^{\frac{11}{12}}3^{\frac{5}{24}}l\sqrt{\frac{1}{13}(4+\sqrt{3})}\xi\right)\right)$$
$$+\left(2^{1/6}3^{1/12}\right)^2\left(1\pm msn\left(2^{\frac{11}{12}}3^{\frac{5}{24}}l\sqrt{\frac{1}{13}(4+\sqrt{3})}\xi\right)\right)^2, \tag{6.42}$$

$$U_{22}(\xi) = \frac{1}{2^{2/3}}(3^{1/6} - 3^{2/3}) - 2\left(2^{1/6}3^{1/12}\right)^2 \left(1 \pm \frac{1}{sn\left(2^{\frac{11}{12}}3^{\frac{5}{24}} l \sqrt{\frac{1}{13}(4+\sqrt{3})}\xi\right)}\right) + \left(2^{1/6}3^{1/12}\right)^2 \left(1 \pm \frac{1}{sn\left(2^{\frac{11}{12}}3^{\frac{5}{24}} l \sqrt{\frac{1}{13}(4+\sqrt{3})}\xi\right)}\right)^2. \tag{6.43}$$

If $m \to 0$, then $sn(\xi) \to \sin(\xi)$, and we have the following trigonometric function solutions of Eq. (6.5)

$$U_{23}(\xi) = \frac{1}{2^{2/3}}(3^{1/6} - 3^{2/3}) - \left(2^{1/6}3^{1/12}\right)^2$$

$$U_{24}(\xi) = \frac{1}{2^{2/3}}(3^{1/6} - 3^{2/3}) - 2\left(2^{1/6}3^{1/12}\right)^2 \left(1 \pm \csc\left(2^{\frac{11}{12}}3^{\frac{5}{24}} l \sqrt{\frac{1}{13}(4+\sqrt{3})}\xi\right)\right) + \left(2^{1/6}3^{1/12}\right)^2 \left(1 \pm \csc\left(2^{\frac{11}{12}}3^{\frac{5}{24}} l \sqrt{\frac{1}{13}(4+\sqrt{3})}\xi\right)\right)^2. \tag{6.44}$$

If $m \to 1$, then we have the same hyperbolic function solutions (6.40) and (6.41).

Set III:

From Eqs. (6.27), (6.36) and (6.37), the Jacobi elliptic function solutions of Eq. (6.5) have been derived as follows

$$U_{31}(\xi) = \frac{1}{2^{2/3}}(3^{1/6} - 3^{2/3}) - 2\left(2^{1/6}3^{1/12}\right)^2 \left(1 \pm \frac{1}{cn\left(2^{\frac{11}{12}}3^{\frac{5}{24}} l \sqrt{\frac{1}{13(1-m^2)}(4+\sqrt{3})}\xi\right)}\right) + \left(2^{1/6}3^{1/12}\right)^2 \left(1 \pm \frac{1}{cn\left(2^{\frac{11}{12}}3^{\frac{5}{24}} l \sqrt{\frac{1}{13(1-m^2)}(4+\sqrt{3})}\xi\right)}\right)^2, \tag{6.45}$$

$$U_{32}(\xi)=\frac{1}{2^{2/3}}(3^{1/6}-3^{2/3})-2\left(2^{1/6}3^{1/12}\right)^2\left(1\pm\frac{dn\left(2^{\frac{11}{12}}3^{\frac{5}{24}}l\sqrt{\frac{1}{13(1-m^2)}(4+\sqrt{3})}\xi\right)}{\sqrt{1-m^2}sn\left(2^{\frac{11}{12}}3^{\frac{5}{24}}l\sqrt{\frac{1}{13(1-m^2)}(4+\sqrt{3})}\xi\right)}\right)$$
$$+\left(2^{1/6}3^{1/12}\right)^2\left(1\pm\frac{dn\left(2^{\frac{11}{12}}3^{\frac{5}{24}}l\sqrt{\frac{1}{13(1-m^2)}(4+\sqrt{3})}\xi\right)}{\sqrt{1-m^2}sn\left(2^{\frac{11}{12}}3^{\frac{5}{24}}l\sqrt{\frac{1}{13(1-m^2)}(4+\sqrt{3})}\xi\right)}\right)^2. \tag{6.46}$$

If $m\to 0$, then $dn(\xi)\to 1$, $sn(\xi)\to\sin(\xi)$, $cn(\xi)\to\cos(\xi)$, and hence, the following trigonometric solutions of Eq. (6.5) have been obtained

$$U_{33}(\xi)=\frac{1}{2^{2/3}}(3^{1/6}-3^{2/3})-2\left(2^{1/6}3^{1/12}\right)^2\left(1\pm\sec\left(2^{\frac{11}{12}}3^{\frac{5}{24}}l\sqrt{\frac{1}{13}(4+\sqrt{3})}\xi\right)\right)$$
$$+\left(2^{1/6}3^{1/12}\right)^2\left(1\pm\sec\left(2^{\frac{11}{12}}3^{\frac{5}{24}}l\sqrt{\frac{1}{13}(4+\sqrt{3})}\xi\right)\right)^2, \tag{6.47}$$

$$U_{34}(\xi)=\frac{1}{2^{2/3}}(3^{1/6}-3^{2/3})-2\left(2^{1/6}3^{1/12}\right)^2\left(1\pm\csc\left(2^{\frac{11}{12}}3^{\frac{5}{24}}l\sqrt{\frac{1}{13}(4+\sqrt{3})}\xi\right)\right)$$
$$+\left(2^{1/6}3^{1/12}\right)^2\left(1\pm\csc\left(2^{\frac{11}{12}}3^{\frac{5}{24}}l\sqrt{\frac{1}{13}(4+\sqrt{3})}\xi\right)\right)^2. \tag{6.48}$$

It may be noted that the solution (6.44) is in agreement with the solution (6.48).

6.5.2 *New Exact Solutions of Tzitzeica–Dodd–Bullough (TDB) Equation*

Suppose the traveling wave solution of Eq. (6.8) can be expressed as

$$\Psi(\xi)=v(\xi)=\sum_{i=0}^{2N}a_iF^i(\xi), \tag{6.49}$$

where $F(\xi)$ satisfies Eq. (6.21).

Balancing the highest order derivative term $vv_{\xi\xi}$ and the nonlinear term v^4 by using homogenous principle the following result could be obtained

$$N + N + 2 = 4N,$$

yielding

$$N = 1.$$

Therefore, the ansatz for the solution of Eq. (6.8) can be written as

$$\Psi(\xi) = a_0 + a_1 F(\xi) + a_2 F^2(\xi), \tag{6.50}$$

where $F(\xi)$ satisfies

$$F(\xi) = \frac{1}{2}\left[-\frac{c_4}{c_6}(1 \pm \phi_i(\xi))\right]^{1/2}, \; i = 1, 2, \ldots, 12. \tag{6.51}$$

Substituting (6.50) and (6.21) into Eq. (6.8) and collecting the coefficients of each power of F^i, $i = 0, 1, 2\ldots$ and set them to zero, we obtain a system of algebraic equations.

Solving this system of algebraic equations by using mathematical software, we obtain the following result:

$$c_2 = \frac{(4+5a_0)a_2c_0}{2a_0(1+a_0)}, c_4 = \frac{(1+2a_0)a_2^2c_0}{a_0^2(1+a_0)}, c_6 = \frac{a_2^3c_0}{2a_0^2(1+a_0)}, \omega = \frac{-a_0^2 - a_0^3}{2ka_2c_0}.$$

Without loss of generality, let us assume $a_0 > 0$, $a_2 > 0$ and $c_0 > 0$, and hence $c_6 > 0$. Thus, $\phi(\xi)$ satisfies only the functions (6.23), (6.24), and (6.27).

Set I:

From Eqs. (6.23), (6.50), and (6.51), the following Jacobi elliptic function solutions of Eq. (6.8) have been derived.

$$\Psi_{11}(\xi) = a_0 - \frac{(1+2a_0)}{2}\left(1 \pm sn\left(\sqrt{\frac{l(1+2a_0)^2}{2m^2a_0^2(1+a_0)}}\xi\right)\right), \tag{6.52}$$

$$\Psi_{12}(\xi) = a_0 - \frac{(1+2a_0)}{2}\left(1 \pm \frac{1}{msn\left(\sqrt{\frac{l(1+2a_0)^2}{2m^2a_0^2(1+a_0)}}\xi\right)}\right), \tag{6.53}$$

where $\xi = kx + \frac{-a_0^2-a_0^3}{2ka_2c_0}t$ and $l = a_2c_0$.

If $m \to 1$, then $sn(\xi) \to \tanh(\xi)$, and we have the hyperbolic function solutions of Eq. (6.8)

$$\Psi_{13}(\xi) = a_0 - \frac{(1+2a_0)}{2}\left(1 \pm \tanh\left(\sqrt{\frac{l(1+2a_0)^2}{2a_0^2(1+a_0)}}\xi\right)\right), \tag{6.54}$$

$$\Psi_{14}(\xi) = a_0 - \frac{(1+2a_0)}{2}\left(1 \pm \coth\left(\sqrt{\frac{l(1+2a_0)^2}{2a_0^2(1+a_0)}}\xi\right)\right). \tag{6.55}$$

Set II:

From Eqs. (6.24), (6.50) and (6.51), the following Jacobi elliptic function solutions of Eq. (6.8) have been obtained.

$$\Psi_{21}(\xi) = a_0 - \frac{(1+2a_0)}{2}\left(1 \pm msn\left(\sqrt{\frac{l(1+2a_0)^2}{2a_0^2(1+a_0)}}\xi\right)\right), \tag{6.56}$$

$$\Psi_{22}(\xi) = a_0 - \frac{(1+2a_0)}{2}\left(1 \pm \frac{1}{sn\left(\sqrt{\frac{l(1+2a_0)^2}{2a_0^2(1+a_0)}}\xi\right)}\right). \tag{6.57}$$

If $m \to 0$, then $sn(\xi) \to \sin(\xi)$, and we have the following solutions of Eq. (6.8)

$$\Psi_{23}(\xi) = -\frac{1}{2}, \tag{6.58}$$

$$\Psi_{24}(\xi) = a_0 - \frac{(1+2a_0)}{2}\left(1 \pm \csc\left(\sqrt{\frac{l(1+2a_0)^2}{2a_0^2(1+a_0)}}\xi\right)\right). \tag{6.59}$$

If $m \to 1$, then we can obtain the same hyperbolic function solutions (6.54) and (6.55).

Set III:

From Eqs. (6.27), (6.50), and (6.51), the following Jacobi elliptic function solutions of Eq. (6.8) have been derived.

$$\Psi_{31}(\xi) = a_0 - \frac{(1+2a_0)}{2}\left(1 \pm \frac{1}{cn\left(\sqrt{\frac{l(1+2a_0)^2}{2(1-m^2)a_0^2(1+a_0)}}\xi\right)}\right), \tag{6.60}$$

$$\Psi_{32}(\xi) = a_0 - \frac{(1+2a_0)}{2}\left(1 \pm \frac{dn\left(\sqrt{\frac{l(1+2a_0)^2}{2(1-m^2)a_0^2(1+a_0)}}\xi\right)}{\sqrt{1-m^2}sn\left(\sqrt{\frac{l(1+2a_0)^2}{2(1-m^2)a_0^2(1+a_0)}}\xi\right)}\right). \tag{6.61}$$

If $m \to 0$, then $dn(\xi) \to 1, sn(\xi) \to \sin(\xi)$, $cn(\xi) \to \cos(\xi)$, and hence, the following trigonometric solutions of Eq. (6.8) have been obtained

$$\Psi_{33}(\xi) = a_0 - \frac{(1+2a_0)}{2}\left(1 \pm \sec\left(\sqrt{\frac{l(1+2a_0)^2}{2a_0^2(1+a_0)}}\xi\right)\right), \tag{6.62}$$

$$\Psi_{34}(\xi) = a_0 - \frac{(1+2a_0)}{2}\left(1 \pm \csc\left(\sqrt{\frac{l(1+2a_0)^2}{2a_0^2(1+a_0)}}\xi\right)\right). \tag{6.63}$$

It may be noted that the solution (6.59) is in agreement with the solution (6.63).

6.5.3 *Physical Interpretations of the Solutions*

In the present analysis, three-dimensional and the corresponding two-dimensional graphs of the obtained solutions to the nonlinear evolution equations, viz. Dodd–Bullough–Mikhailov (DBM) and Tzitzeica–Dodd–Bullough (TDB) equations have been presented. To this aim, some special values of the parameters are selected. Here, the physical significance of the obtained solutions of the above equations has been discussed.

In Figs. 6.5, 6.6, 6.7, 6.8, 6.9, 6.10, 6.11 and 6.12, the 3D solution graphs of $U_{11}(\xi)$, $U_{13}(\xi)$, $U_{21}(\xi)$, $U_{34}(\xi)$, $\Psi_{11}(\xi)$, $\Psi_{13}(\xi)$, $\Psi_{21}(\xi)$, $\Psi_{34}(\xi)$, respectively, have been presented with appropriate selection of parameters. The three-dimensional

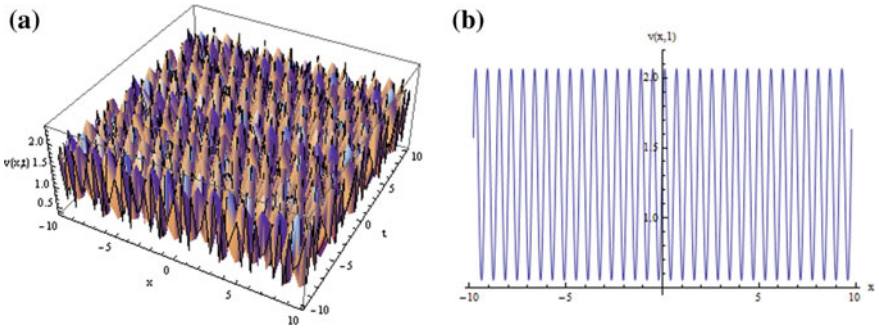

Fig. 6.5 **a** 3D double periodic solution surface for $v(x, t)$ appears in Eq. (6.38) as $U_{11}(\xi)$ in Set 1, when $k = 1$, $l = 1$, $\omega = 0.5$, $m = 0.3$, **b** the corresponding 2D graph for $v(x, t)$, when $t = 1$

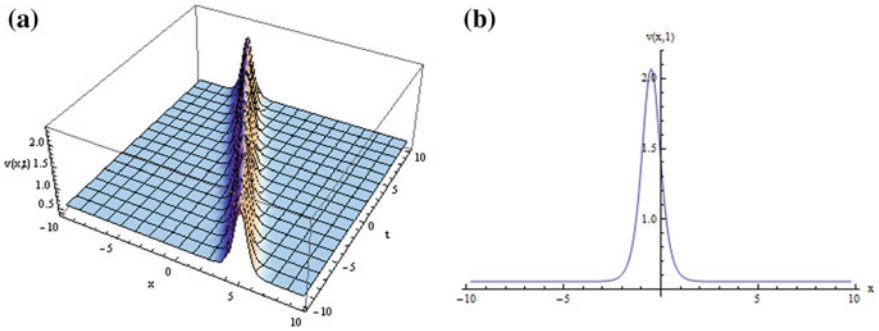

Fig. 6.6 **a** 3D soliton solution surface of $v(x, t)$ appears in Eq. (6.40) as $U_{13}(\xi)$ in Set 1, when $k = 1$, $l = 1$, $\omega = 0.5$, $m = 0.3$, **b** the corresponding 2D graph for $v(x, t)$, when $t = 1$

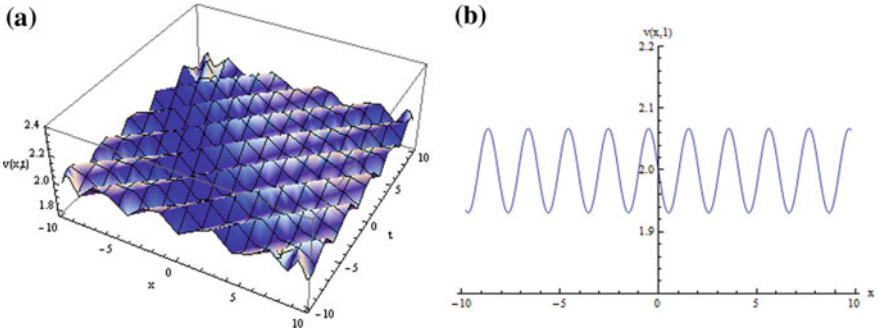

Fig. 6.7 **a** 3D double periodic solution surface of $v(x, t)$ appears in Eq. (6.42) as $U_{21}(\xi)$ in Set 2, when $k = 1$, $l = 1$, $\omega = 0.5$, $m = 0.3$, **b** the corresponding 2D graph for $v(x, t)$, when $t = 1$

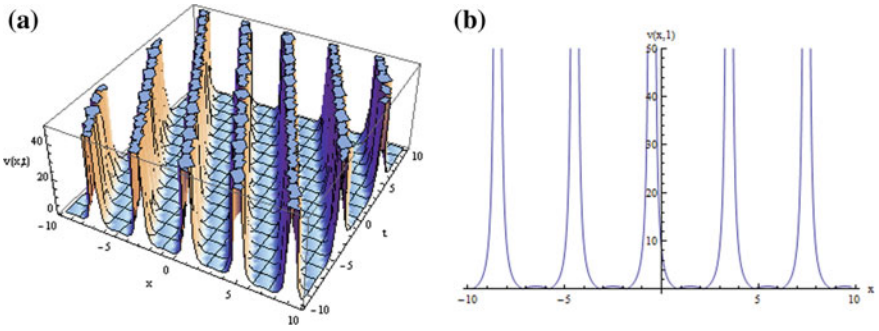

Fig. 6.8 **a** 3D periodic solution surface of $v(x, t)$ appears in Eq. (6.48) as $U_{34}(\xi)$ in Set 3, when $k = 1$, $l = 0.5$, $\omega = 0.5$, $m = 0.3$, **b** the corresponding 2D graph for $v(x, t)$, when $t = 1$

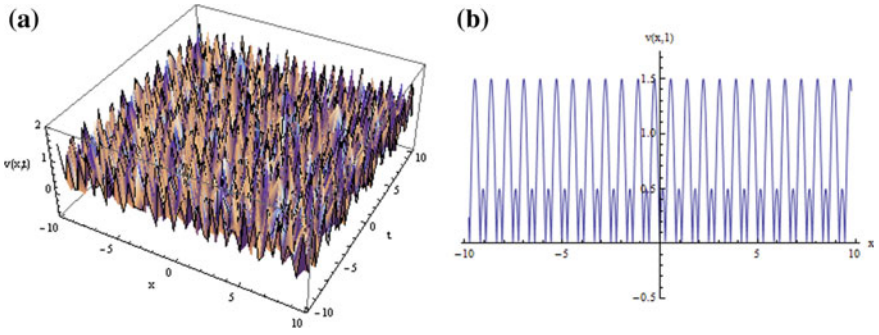

Fig. 6.9 **a** 3D double periodic solution surface of $v(x, t)$ appears in Eq. (6.52) as $\Psi_{11}(\xi)$ in Set I, when $k = 1$, $l = 1$, $\omega = 0.5$, $m = 0.3$, $a_0 = 0.5$, **b** the corresponding 2D graph for $v(x, t)$, when $t = 1$

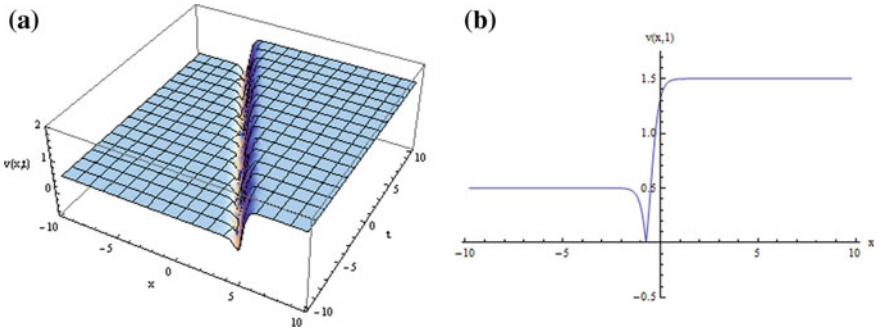

Fig. 6.10 **a** 3D soliton solution surface of $v(x, t)$ appears in Eq. (6.54) as $\Psi_{13}(\xi)$ in Set I, when $k = 1$, $l = 1$, $\omega = 0.5$, $a_0 = 0.5$, $m = 0.3$, **b** the corresponding 2D graph for $v(x, t)$, when $t = 1$

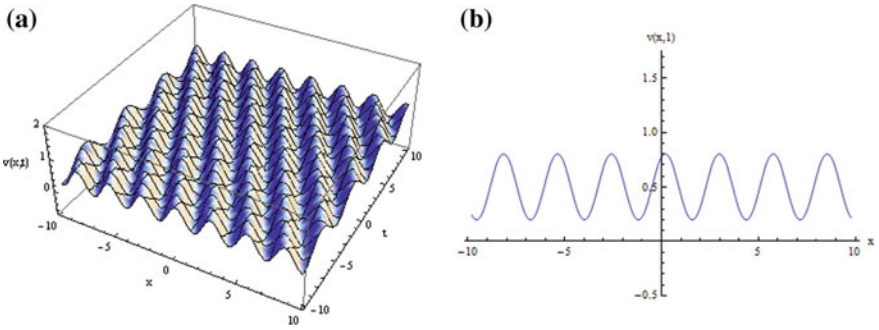

Fig. 6.11 **a** 3D double periodic solution surface of $v(x, t)$ appears in Eq. (6.56) as $\Psi_{21}(\xi)$ in Set II, when $k = 1$, $l = 1$, $\omega = 0.5$, $a_0 = 0.5$, $m = 0.3$, **b** the corresponding 2D graph for $v(x, t)$, when $t = 1$

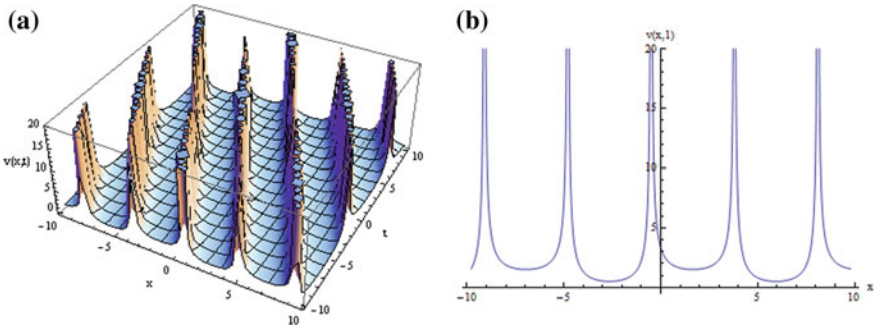

Fig. 6.12 **a** 3D periodic solution surface of $v(x, t)$ appears in Eq. (6.63) as $\Psi_{34}(\xi)$ in Set III, when $k = 1$, $l = 0.1$, $\omega = 0.5$, $a_0 = 0.5$, $m = 0.3$, **b** the corresponding 2D graph for $v(x, t)$, when $t = 1$

graphs of Figs. 6.5, 6.6, 6.7, 6.8, 6.9, 6.10, 6.11 and 6.12 have been depicted when $-10 \leq x \leq 10$, $-10 \leq t \leq 10$. To the best knowledge of information, these solutions have not been reported earlier in the open literature.

In Figs. 6.5 and 6.7, the double periodic solutions for U_{11} and U_{21} of DBM equation, have been displayed. Also, the double periodic solutions for Ψ_{11} and Ψ_{21} of TDB equation have been demonstrated in Figs. 6.9 and 6.11, respectively. Figures 6.6 and 6.10 show the solutions for U_{13} and Ψ_{13} representing the soliton wave solutions of DBM and TDB equations, respectively. Furthermore, the periodic traveling wave solutions for U_{34} and Ψ_{34} of DBM and TDB equations have been illustrated in Figs. 6.8 and 6.12, respectively.

6.6 Conclusion

In this chapter, an improved generalized Jacobi elliptic function method is successfully employed for acquiring new exact solutions of the coupled Schrödinger–Boussinesq equations. By using this present method, some new exact solutions of the coupled Schrödinger–Boussinesq equations are found. More importantly, the present method is more efficient and powerful to determine the new exact solutions to CSBEs. This proposed method can also be utilized for numerous other nonlinear evolution equations or coupled ones. To the best information of the author, these double periodic wave solutions of the CSBEs are new exact solutions which are not reported earlier. Being concise and powerful, this current method can also be extended to solve many other NLPDEs arising in mathematical physics.

Moreover, in the present chapter, a new extended auxiliary equation method is used to construct many new types of Jacobi elliptic function solutions of Dodd–Bullough–Mikhailov and Tzitzeica–Dodd–Bullough equations. Thus, as an achievement, a family of new exact traveling wave solutions of Dodd–Bullough–Mikhailov and Tzitzeica–Dodd–Bullough equations has been formally generated.

It clearly manifests that the employed approach is useful and efficient to find the various kinds of traveling wave solutions. Also, the physical interpretations of the obtained results for Tzitzéica-type nonlinear evolution equations have been surveyed as well. Therefore, the performance of the proposed method is effective and it can be applied to study many other nonlinear evolution equations which frequently arise in nonlinear optics, quantum theory, and other mathematical physics and engineering problems.

References

1. Debnath, L.: Nonlinear Partial Differential Equations for Scientists and Engineers. Birkhäuser, Boston (2005)
2. Wazwaz, A.M.: Partial Differential Equations and Solitary Waves Theory. Springer-Verlag, Berlin, Heidelberg (2009)
3. Ablowitz, M.J., Clarkson, P.A.: Solitons, Nonlinear Evolution Equations and Inverse Scattering. Cambridge University Press, Cambridge (1991)
4. Miura, M.R.: Bäcklund transformation. Springer, Berlin (1978)
5. Rogers, C., Shadwick, W.F.: Bäcklund transformations and their applications. Academic Press, New York (1982)
6. Weiss, J., Tabor, M., Carnevale, G.: The Painlevé property for partial differential equations. J. Math. Phys. **24**(1983), 522–526 (1983)
7. Li, B., Chen, Y.: A truncated Painlevé expansion and exact analytical solutions for the nonlinear Schrödinger equation with variable coefficients. Zeitschrift für Naturforschung A **60**, 768–774 (2005)
8. Hirota, R.: Exact solutions of the KdV equation for multiple collisions of solitons. Phys. Rev. Lett. **27**, 1192–1194 (1971)
9. Wazwaz, A.M.: The tanh method for traveling wave solutions of nonlinear equations. Appl. Math. Comput. **154**, 713–723 (2004)
10. Fan, E.G.: Extended tanh-function method and its applications to nonlinear equations. Phys. Lett. A **277**, 212–218 (2000)
11. He, J.H., Wu, X.H.: Exp-function method for nonlinear wave equations. Chaos, Solitons Fractals **30**, 700–708 (2006)
12. Wang, M.L., Li, X., Zhang, J.: The (G'/G)-expansion method and travel ling wave solutions of nonlinear evolution equations in mathematical physics. Phys. Lett. A **372**, 417–423 (2008)
13. Zayed, E.M.E.: New traveling wave solutions for higher dimensional nonlinear evolution equations using a generalized (G'/G)-expansion method. J. Phys. A: Math. Theor. **42**, 195202 (2009)
14. Liu, S., Fu, Z., Liu, S., Zhao, Q.: Jacobi elliptic function expansion method and periodic wave solutions of nonlinear wave equations. Phys. Lett. A **289**, 69–74 (2001)
15. Lü, D.: Jacobi elliptic function solutions for two variant Boussinesq equations. Chaos, Solitons Fractals **24**, 1373–1385 (2005)
16. Chen, Y., Wang, Q.: Extended Jacobi elliptic function rational expansion method and abundant families of Jacobi elliptic function solutions to (1+1)-dimensional dispersive long wave equation. Chaos, Solitons Fractals **24**, 745–757 (2005)
17. Huang, W., Liu, Y.: Jacobi elliptic function solutions of the Ablowitz-Ladik discrete nonlinear Schrödinger system. Chaos, Solitons Fractals **40**, 786–792 (2009)
18. Raslan, K.R.: The first integral method for solving some important nonlinear partial differential equations. Nonlinear Dyn. **53**, 281–286 (2008)

19. Abbasbandy, S., Shirzadi, A.: The first integral method for modified Benjamin–Bona–Mahony equation. Commun. Nonlinear Sci. Numer. Simul. **15**, 1759–1764 (2010)
20. Jafari, H., Soltani, R., Khalique, C.M., Baleanu, D.: Exact solutions of two nonlinear partial differential equations by using the first integral method. Bound. Value Probl. **2013**, 117 (2013)
21. Ray, S.S.: New exact solutions of nonlinear fractional acoustic wave equations in ultrasound. Comput. Math. Appl. **71**, 859–868 (2016)
22. Wang, Q., Chen, Y., Zhang, H.: A new Riccati equation rational expansion method and its application to (2+1)-dimensional Burgers equation. Chaos, Soliton Fractals **25**, 1019–1028 (2005)
23. Kudryashov, N.A.: One method for finding exact solutions of nonlinear differential equations. Commun. Nonlinear Sci. Numer. Simul. **17**(6), 2248–2253 (2012)
24. Ray, S.S.: New analytical exact solutions of time fractional KdV-KZK equation by Kudryashov methods. Chin. Phys. B **25**, 040204 (2016)
25. Saha Ray, S.: A numerical solution of the coupled Sine-Gordon equation using the modified decomposition method. Appl. Math. Comput. **175**(2), 1046–1054 (2006)
26. Ray, S.S.: An application of the modified decomposition method for the solution of the coupled klein-gordon schrödinger equation. Commun. Nonlinear Sci. Numer. Simul. **13**, 1311–1317 (2008)
27. Atangana, A.: Exact solution of the time-fractional groundwater flow equation within a leaky aquifer equation. JVC/J. Vib. Control **22**, 1749–1756 (2014)
28. Khan, Y., Faraz, N., Smarda, Z.: Difference kernel iterative method for linear and nonlinear partial differential equations. Neural Comput. Appl. **27**, 671–675 (2016)
29. Ghany, H.A., Elagan, S.K., Hyder, A.: Exact travelling wave solutions for stochastic fractional Hirota-Satsuma coupled KdV equations. Chin. J. Phys. **53**, 080705 (2015)
30. Choi, J.H., Kim, H.: Soliton solutions for the space-time nonlinear partial differential equations with fractional-orders. Chin. J. Phys. **55**, 556–565 (2017)
31. Fan, E., Hongqing, Z.: A note on the homogeneous balance method. Phys. Lett. A **246**, 403–406 (1998)
32. Wazwaz, A.M.: Partial Differential Equations: methods and Applications. Balkema, Lisse, The Netherlands (2002)
33. Parkes, E.J., Duffy, B.R.: An automated tanh-function method for finding solitary wave solutions to nonlinear evolution equations. Comput. Phys. Commun. **98**, 288–300 (1996)
34. Malfliet, W.: Solitary wave solutions of nonlinear wave equations. Am. J. Phys. **60**(7), 650–654 (1992)
35. Malfliet, W., Hereman, W.: The tanh-method: I. exact solutions of nonlinear evolution and wave equations. Phys. Scr. **54**, 563–568 (1996)
36. Wazwaz, A.M.: The tanh method: solitons and periodic solutions for the Dodd-Bullough-Mikhailov and the Tzitzeica-Dodd-Bullough equations. Chaos, Solitons Fractals **25**, 55–63 (2005)
37. Seadawy, A.R., Dianchen, L., Mostafa, M.A.K.: Bifurcations of travelling wave solutions for Dodd-Bullough-Mikhailov equation and coupled Higgs equation and their applications **55**, 1310–1318 (2017)
38. Bekir, A., Boz, A.: Application of He's exp-function method for nonlinear evolution equations **58**(11–12), 2286–2293 (2009)
39. Bekir, A., Aksoy, E.: Exact solutions of shallow water wave equations by using the (G'/G)-expansion method **22**(3), 317–331 (2012)
40. Sirendaoreji, S.: A new auxiliary equation and exact travelling wave solutions of nonlinear equations. Phys. Lett. A **356**, 124–130 (2006)
41. Xu, G.: Extended auxiliary equation method and its applications to three generalized NLS equations. Abstract and Applied Analysis, vol. 2014, 7, Article ID 541370
42. Seadawy, A.R.: Travelling-wave solutions of a weakly nonlinear two-dimensional higher-order Kadomtsev-Petviashvili dynamical equation for dispersive shallow-water waves. Eur. Phys. J. Plus **132**(1), Article number 29 (2017)

43. Fu, Z., Liu, S., Liu, S., Zhao, Q.: New Jacobi elliptic function expansion and new periodic solutions of nonlinear wave equations. Phys. Lett. A **290**, 72–76 (2001)
44. Kudryashov, N.A.: Simplest equation method to look for exact solutions of nonlinear differential equations. Chaos, Solitons Fractals **24**, 1217–1231 (2005)
45. Kudryashov, N.A., Loguinova, N.B.: Extended simplest equation method for nonlinear differential equations. Appl. Math. Comput. **205**, 396–402 (2008)
46. Kudryashov, N.A.: Exact solutions of the generalized Kuramoto-Sivashinsky equation. Phys. Lett. A **147**, 287–291 (1990)
47. Abazari, R.: The (G'/G)-expansion method for Tzitzéica Type nonlinear evolution equations. Math. Comput. Model. **52**, 1834–1845 (2010)
48. Manafian, J., Lakestani, M.: Dispersive dark optical soliton with Tzitzéica type nonlinear evolution equations arising in nonlinear optics. Opt. Quantum Electron **48**, 116 (32 P) (2016)
49. Hosseini, K., Ayati, Z., Ansari, R.: New exact solutions of the Tzitzéica type equations arising in nonlinear optics using a modified version of the improved $(\Phi(\xi)/2)$-expansion method. Opt. Quantum Electron **49**, **273** (14 P) (2017)
50. Hosseini, K., Bekir, A., Kaplan, M.: New exact traveling wave solutions of the Tzitzéica type nonlinear evolution equations arising in nonlinear optics. J. Mod. Opt. **64**, 1688–1692 (2017)
51. Makhankov, V.G.: On stationary solutions of the Schrödinger equation with a self-consistent potential satisfying Boussinesq's equation. Phys. Lett. A **50**, 42–44 (1974)
52. Zakharov, V.E.: Collapse of langmuir waves. Sov. Phys. JETP **35**(5), 908–914 (1972)
53. Yajima, N., Satsuma, J.: Soliton solutions in a diatomic lattice system. Prog. Theor. Phys. **62** (2), 370–378 (1979)
54. Ma, H., Zhang, Z.P., Deng, A.: A New periodic solution to Jacobi elliptic functions of MKdV equation and BBM equation. Acta. Math. Appl. Sin. **28**, 409–415 (2012). (in English)
55. Abramowitz, M., Stegun, I.A.: Handbook of Mathematical Functions. Dover, New York (1965)
56. Zayed, E.M.E., Alurrfi, K.A.E.: New extended auxiliary equation method and its applications to nonlinear Schrödinger-type equations. Optik **127**, 9131–9151 (2016)
57. Zayed, E.M.E., Alurrfi, K.A.E.: Extended auxiliary equation method and its applications for finding the exact solutions for a class of nonlinear Schrödinger-type equations. Appl. Math. Comput. **289**, 111–131 (2016)

Chapter 7
New Techniques on Fractional Reduced Differential Transform Method

7.1 Introduction

The fractional differential equations appear more and more frequently in different research areas and engineering applications. There is a long-standing interest in extending the classical calculus to noninteger orders because fractional differential equations are suitable models for many physical problems. Fractional calculus has been used to model physical and engineering processes which are found to be best described by fractional differential equations. In recent years, considerable interest in fractional differential equations has been stimulated due to their numerous applications in the areas of physics and engineering. Many important phenomena in electromagnetics, acoustics, viscoelasticity, electrochemistry, control theory, neutron point kinetics model, anomalous diffusion, vibration and control, continuous time random walk, Lévy statistics, Brownian motion, signal and image processing, relaxation, creep, chaos, fluid dynamics, and material science are well described by differential equations of fractional order [1–8]. The solution of differential equations of fractional order is much involved. Though many exact solutions for linear fractional differential equation had been found, in general, there is a scarcity of analytical method, available in the open literature, which yields an exact solution for nonlinear fractional differential equations.

In the past decades, both mathematicians and physicists have devoted considerable effort to the study of explicit and numerical solutions to nonlinear differential equations of integer order. Many methods have been presented [9–19]. Our main interest lies in determining an efficient and accurate method that provides an effective procedure for explicit and numerical solutions of a wide and general class of differential systems representing real physical problems. In this paper, we solve fractional KdV equations by the modified fractional reduced differential transform method (MFRDTM) which is presented with some modification of the reduced differential transformation method [20–22]. In this new approach, the nonlinear term is replaced by its Adomian polynomials. Thus, the nonlinear initial-value

S. Saha Ray, *Nonlinear Differential Equations in Physics*,
https://doi.org/10.1007/978-981-15-1656-6_7

problem can be easily solved with less computational effort. The main advantage of the method emphasizes the fact that it provides an explicit analytical approximate solution and also numerical solution elegantly. The merits of the new method are as follows: (1) no discretization required and (2) linearization or small perturbation also not required. Thus, it reduces the amount of numerical computation considerably. Application of this attractive new method may be taken into account for further research.

In the past decades, the fractional differential equations have been widely used in various fields of applied science and engineering. Many important phenomena in electromagnetics, acoustics, viscoelasticity, electrochemistry, control theory, neutron point kinetics model, anomalous diffusion, vibration and control, continuous time random walk, Levy statistics, Brownian motion, signal and image processing, relaxation, creep, chaos, fluid dynamics, and material science are well described by differential equations of fractional order [1–7, 12, 23–26]. Fractional calculus has been used to model physical and engineering processes that are found to be best described by fractional differential equations. For that reason, we need a reliable and efficient technique for the solution of fractional differential equations. An immense effort has been expended over the last many years to find robust and efficient numerical and analytical methods for solving such fractional differential equations. In the present analysis, a new approximate numerical technique, coupled fractional reduced differential transform method (CFRDTM), has been proposed which is applicable for coupled fractional differential equations. The proposed method is a very powerful solver for linear and nonlinear coupled fractional differential equations. It is relatively a new approach to provide the solution very efficiently and accurately.

In the field of engineering, physics, and other fields of applied sciences, many phenomena can be obtained very successfully by models using mathematical tools in the form of fractional calculus [1, 4, 12, 23–27]. In the past decades, the fractional differential equations have been widely used in various fields of applied science and engineering. Many important phenomena in electromagnetics, acoustics, viscoelasticity, electrochemistry, control theory, neutron point kinetics model, anomalous diffusion, vibration and control, continuous time random walk, Lévy statistics, Brownian motion, signal and image processing, relaxation, creep, chaos, fluid dynamics, and material science are well described by differential equations of fractional order. Fractional calculus has been used to model physical and engineering processes that are found to be best described by fractional differential equations. For that reason, we need a reliable and efficient technique for the solution of fractional differential equations. An immense effort has been expended over the last many years to find robust and efficient numerical and analytical methods for solving such fractional differential equations. In the present analysis, a new approximate numerical technique, coupled fractional reduced differential transform method (CFRDTM), has been applied which is applicable for coupled fractional differential equations. The new method is a very powerful solver for linear and nonlinear coupled fractional differential equations. It is relatively a new approach to provide the solution very efficiently and accurately.

In the field of engineering, physics, chemistry, and other sciences, many phenomena can be modeled very successfully by using mathematical tools in the form of fractional calculus, e.g., anomalous transport in disordered systems, some percolations in porous media, and the diffusion of biological populations [1, 25–28]. Fractional calculus has been used to model physical and engineering systems that are found to be more accurately described by fractional differential equations. Thus, we need a reliable and competent technique for the solution of fractional differential equations. In this paper, the predator–prey system [29] has been discussed in the form of the fractional coupled reaction-diffusion equation. In the present analysis, a new approximate numerical technique, coupled fractional reduced differential transform method (CFRDTM), has been presented which is appropriate for coupled fractional differential equations. The proposed method is an impressive solver for linear and nonlinear coupled fractional differential equations. It is comparatively a new approach to provide the solution very effectively and competently.

The significant advantage of the proposed method is the fact that it provides its user with an analytical approximation, in many instances an exact solution, in a rapidly convergent sequence with elegantly computed terms. This technique does not involve any linearization, discretization, or small perturbations, and therefore it reduces significantly the numerical computation. This method provides extraordinary accuracy for the approximate solutions when compared to the exact solutions, particularly in large-scale domain. It is not affected by computation round-off errors, and hence one does not face the need for large computer memory and time. The results reveal that the CFRDTM is very effective, convenient, and quite accurate to the system of nonlinear equations.

Several analytical as well as numerical methods have been implemented by various authors to solve fractional differential equations. Wei et al. [30] applied the homotopy method to determine the unknown parameters of solute transport with spatial fractional derivative advection-dispersion equation. Saha Ray and Gupta proposed numerical schemes based on the Haar wavelet method for finding numerical solutions of Burger–Huxley, Huxley, modified Burgers, and mKdV equations [31, 32]. An approximate analytical solution of the time fractional Cauchy reaction diffusion equation by using the fractional-order reduced differential transform method (FRDTM) has been proposed by Shukla et al. [33].

Nonlinear partial differential equations are useful in describing various phenomena. The solutions of the nonlinear evolution equations play an important role in the field of nonlinear wave phenomena. The exact solutions facilitate the verification of numerical methods when they exist. These equations arise in various areas of physics, mathematics, and engineering such as fluid dynamics, nonlinear optics, plasma physics, nuclear physics, mathematical biology, Brusselator model of the chemical reaction–diffusion, and many other areas.

In the past decades, the fractional differential equations have been widely used in various fields of applied science and engineering [1, 4, 23, 25, 27, 28, 34, 35]. Fractional calculus has been used to model physical and engineering processes that are found to be best described by fractional differential equations. An immense effort has been expended over the last many years to find robust and efficient

numerical and analytical methods for solving nonlinear fractional differential equations [12]. In the present analysis, a new approximate analytic technique, coupled fractional reduced differential transform method (CFRDTM) [34, 35], has been proposed which is applicable for coupled fractional linear and nonlinear differential equations. The proposed method originated from generalized Taylor's formula [36] is a very powerful solver for linear and nonlinear coupled fractional differential equations. It is relatively a new approach to provide the solution very efficiently and accurately.

Nonlinear partial differential equations are useful in describing various phenomena. These equations arise in various areas of physics, mathematics, and engineering such as fluid dynamics, nonlinear optics, plasma physics, nuclear physics, mathematical biology, Brusselator model of the chemical reaction–diffusion, and many other areas. In fluid dynamics, the nonlinear evolution equations show up in the context of shallow water waves. Some of the commonly studied equations are the Korteweg–de Vries (KdV) equation, modified KdV equation, Boussinesq equation, and Whitham–Broer–Kaup equation. In this paper, Whitham–Broer–Kaup equations have been solved by a new novel method revealed by Saha Ray [34, 35] and it is inherited from generalized Taylor's series.

The investigation of the traveling wave solutions to nonlinear partial differential equations (NLPDEs) plays an important role in the study of nonlinear physical phenomena.

In the past decades, the fractional differential equations have been widely used in various fields of applied science and engineering [1, 4, 23, 25, 27, 28, 34, 35]. Fractional calculus has been used to model physical and engineering processes that are found to be best described by fractional differential equations. An immense effort has been expended over the last many years to find robust and efficient numerical and analytical methods for solving nonlinear fractional differential equations [12]. In the present analysis, a new approximate analytic technique, coupled fractional reduced differential transform method (CFRDTM) [34, 35], has been proposed which is applicable for coupled fractional linear and nonlinear differential equations. The proposed method originated from generalized Taylor's formula [36] is a very powerful solver for linear and nonlinear coupled fractional differential equations. It is relatively a new approach to provide the solution very efficiently and accurately.

7.2 Outline of the Present Study

In this chapter, the modified fractional reduced differential transform method (MFRDTM) has been proposed and it is implemented for solving fractional Korteweg–de Vries (KdV) equations. The fractional derivatives are described in the Caputo sense. The reduced differential transform method is modified to be easily employed to solve wide kinds of nonlinear fractional differential equations. In this new approach, the nonlinear term is replaced by its Adomian polynomials. Thus,

the nonlinear initial-value problem can be easily solved with less computational effort. In order to show the power and effectiveness of the present modified method and to illustrate the pertinent features of the solutions, several fractional KdV equations with different types of nonlinearities are considered. The results reveal that the proposed method is very effective and simple for obtaining approximate solutions of fractional KdV equations.

A very new technique, coupled fractional reduced differential transform, has been implemented in this chapter to obtain the numerical approximate solution of coupled time fractional KdV equations. The fractional derivatives are described in the Caputo sense. By using the present method, we can solve many linear and nonlinear coupled fractional differential equations. The obtained results are compared with the exact solutions. Numerical solutions are presented graphically to show the reliability and efficiency of the method.

Newly proposed coupled fractional reduced differential transform has been implemented to obtain the soliton solutions of coupled time fractional modified KdV equations. This new method has been revealed by the author. The fractional derivatives are described in the Caputo sense. By using the present method, we can solve many linear and nonlinear coupled fractional differential equations. The results reveal that the proposed method is very effective and simple for obtaining approximate solutions of fractional coupled modified KdV equations. Numerical solutions are presented graphically to show the reliability and efficiency of the method. Solutions obtained by this new method have been also compared with Adomian decomposition method (ADM).

A relatively very new technique, viz. coupled fractional reduced differential transform, has been executed to attain the approximate numerical solution of the predator–prey dynamical system. The fractional derivatives are defined in the Caputo sense. Utilizing the present method, we can solve many linear and nonlinear coupled fractional differential equations. The results thus obtained are compared with those of other available methods. Numerical solutions are also presented graphically to show the simplicity and authenticity of the method for solving the fractional predator–prey dynamical system.

Also in this chapter, fractional coupled Schrödinger–Korteweg–de Vries (or Sch–KdV) equation with appropriate initial values has been solved by using a new novel method. The fractional derivatives are described in the Caputo sense. By using the present method, we can solve many linear and nonlinear coupled fractional differential equations. Basically, the present method originated from generalized Taylor's formula [36]. The results reveal that the proposed method is very effective and simple for obtaining approximate solutions of fractional coupled Schrödinger–KdV equation. Numerical solutions are presented graphically to show the reliability and efficiency of the method. The method does not need linearization, weak nonlinearity assumptions, or perturbation theory. The convergence of the method as applied to Sch–KdV is illustrated numerically as well as derived analytically. Moreover, the derived results are compared with those obtained by the Adomian decomposition method (ADM).

The analytical approximate traveling wave solutions of Whitham–Broer–Kaup (WBK) equations, which contain blow-up solutions and periodic solutions, have been obtained by using the coupled fractional reduced differential transform method [34, 35, 37–39]. By using this method, the solutions were calculated in the form of a generalized Taylor's series with easily computable components. The convergence of the method as applied to the Whitham–Broer–Kaup equations is illustrated numerically as well as analytically. By using the present method, we can solve many linear and nonlinear coupled fractional differential equations. The results justify that the proposed method is also very efficient, effective, and simple for obtaining approximate solutions of fractional coupled modified Boussinesq and fractional approximate long wave equations. Numerical solutions are presented graphically to show the reliability and efficiency of the method. Moreover, the results are compared with those obtained by the Adomian decomposition method (ADM) and variational iteration method (VIM) revealing that the present method is superior to others.

7.2.1 Fractional KdV Equation

The aim of this work is to directly apply the MFRDTM to determine the approximate solution of the nonlinear fractional KdV equation with time fractional derivative of the form

$$D_t^{\alpha} u + (u^m)_x + (u^n)_{xxx} = 0,\ m > 0,\ 1 \le n \le 3,\ t > 0,\ 0 < \alpha \le 1 \tag{7.1}$$

which is a generalization of the Korteweg–de Vries equation, denoted by $K(m, n)$ for the different values of m and n, respectively. These $K(m, n)$ equations have the property that for certain values of m and n, their solitary wave solutions have compact support which is known as compactons [40]. Here, the fractional derivative is considered in the Caputo sense [5, 6]. In the case of $\alpha = 1$, fractional Eq. (1.1) reduces to the classical nonlinear KdV equation [14, 16].

7.2.2 Time Fractional Coupled KdV Equations

For solving time fractional coupled KdV equations, two model equations have been considered in the present chapter.

I. Consider the following time fractional coupled KdV equations [41]

$$D_t^{\alpha} u = -\frac{\partial^3 u}{\partial x^3} - 6u\frac{\partial u}{\partial x} + 3v\frac{\partial v}{\partial x}, \tag{7.2}$$

$$D_t^{\beta} v = -\frac{\partial^3 v}{\partial x^3} - 3u\frac{\partial v}{\partial x}, \tag{7.3}$$

where $t > 0$, $0 < \alpha, \beta \leq 1$.

II. Consider the following time fractional coupled KdV equations [42]

$$D_t^{\alpha} u + 6uu_x - 6vv_x + u_{xxx} = 0, \tag{7.4}$$

$$D_t^{\beta} v + 3uv_x + v_{xxx} = 0, \tag{7.5}$$

where $t > 0$, $0 < \alpha, \beta \leq 1$.

7.2.3 Time Fractional Coupled Modified KdV Equations

In this case, for solving time fractional coupled modified KdV equations, again two model equations have been considered in the present chapter.

I. Consider the following time fractional coupled modified KdV equations [43]

$$D_t^{\alpha} u = \frac{1}{2}\frac{\partial^3 u}{\partial x^3} - 3u^2\frac{\partial u}{\partial x} + \frac{3}{2}\frac{\partial^2 v}{\partial x^2} + 3\frac{\partial (uv)}{\partial x} - 3\frac{\partial u}{\partial x}, \tag{7.6}$$

$$D_t^{\beta} v = -\frac{\partial^3 v}{\partial x^3} - 3v\frac{\partial v}{\partial x} - 3\frac{\partial u}{\partial x}\frac{\partial v}{\partial x} + 3u^2\frac{\partial v}{\partial x} + 3\frac{\partial v}{\partial x}, \tag{7.7}$$

where $t > 0$, $0 < \alpha, \beta \leq 1$.

II. Consider the following time fractional coupled modified KdV equations [44]

$$D_t^{\alpha} u = \frac{1}{2}\frac{\partial^3 u}{\partial x^3} - 3u^2\frac{\partial u}{\partial x} + \frac{3}{2}\frac{\partial^2 v}{\partial x^2} + 3\frac{\partial (uv)}{\partial x} + 3\frac{\partial u}{\partial x} \tag{7.8}$$

$$D_t^{\beta} v = -\frac{\partial^3 v}{\partial x^3} - 3v\frac{\partial v}{\partial x} - 3\frac{\partial u}{\partial x}\frac{\partial v}{\partial x} + 3u^2\frac{\partial v}{\partial x} - 3\frac{\partial v}{\partial x} \tag{7.9}$$

where $t > 0$, $0 < \alpha, \beta \leq 1$.

7.2.4 Time Fractional Predator–Prey Dynamical System

In the present chapter, a system of two species competitive models with prey population A and predator population B has been also studied. For prey population $A \rightarrow 2A$, at the rate a $(a > 0)$ expresses the natural birthrate. Similarly, for predator

population $B \to 2B$, at the rate c $(c > 0)$ represents the natural death rate. The interactive term between predator and prey population is $A + B \to 2B$, at rate b $(b > 0)$ where b denotes the competitive rate. According to the knowledge of fractional calculus and biological population, the time fractional dynamics of a predator–prey system can be described as

$$\frac{\partial^{\alpha} u}{\partial t^{\alpha}} = \frac{\partial^2 u}{\partial x^2} + \frac{\partial^2 u}{\partial y^2} + au - buv, \quad u(x, y, 0) = \varphi(x, y), \tag{7.10}$$

$$\frac{\partial^{\beta} v}{\partial t^{\beta}} = \frac{\partial^2 v}{\partial x^2} + \frac{\partial^2 v}{\partial y^2} + buv - cv, \quad v(x, y, 0) = \phi(x, y), \tag{7.11}$$

where $t > 0, x, y \in \mathcal{R}, a, b, c > 0, u(x, y, t)$ denotes the prey population density, and $v(x, y, t)$ represents the predator population density. Here, $\varphi(x, y)$ and $\phi(x, y)$ represent the initial conditions of the population system. The fractional derivatives are considered in Caputo sense. Caputo fractional derivative is used because of its advantage that it permits the initial and boundary conditions included in the formulation of the problem. Here, $u(x, y, t)$ and $v(x, y, t)$ are analytic functions. The physical interpretations of Eqs. (7.10) and (7.11) indicate that the prey–predator population system is analogous to the behavior of fractional-order model of anomalous biological diffusion.

7.2.5 *Fractional Coupled Schrödinger–KdV Equation*

Nonlinear phenomena play a crucial role in applied mathematics and physics. Calculating exact and numerical solutions, in particular, traveling wave solutions, of nonlinear equations in mathematical physics plays an important role in soliton theory [9, 45]. The investigation of the traveling wave solutions to nonlinear partial differential equations (NLPDEs) plays an important role in the study of nonlinear physical phenomena. Multiple traveling wave solutions of nonlinear evolution equations such as the coupled Schrödinger–KdV equation [46, 47] have been obtained by Fan [48]. The coupled Schrödinger–KdV equation is known to describe various processes in dusty plasma, such as Langmuir, dust-acoustic wave, and electromagnetic waves [48]. The model equation for the coupled fractional Schrödinger–KdV equation can be presented in the following form [48]

$$iD_t^{\alpha} u_t = u_{xx} + uv$$

$$D_t^{\beta} v_t = -6vv_x - v_{xxx} + (|u|^2)_x \tag{7.12}$$

where α, β $(0 < \alpha, \beta \leq 1)$ are the orders of the Caputo fractional time derivatives, respectively, $i = \sqrt{-1}$ and $t \geq 0$.

Recently, Fan [48] applied the unified algebraic method and Kaya et al. [49] applied Adomian's decomposition method for computing solutions to a (classical) integer-order Sch–KdV equation.

7.2.6 *Fractional Whitham–Broer–Kaup, Modified Boussinesq, and Approximate Long Wave Equations in Shallow Water*

In the present paper, coupled WBK equations introduced by Whitham, Broer, and Kaup [50–52] have been considered. The equations describe the propagation of shallow water waves with different dispersion relations. The fractional-order WBK equations are as follows

$$D_t^{\alpha}u + uu_x + v_x + bu_{xx} = 0, \tag{7.13a}$$

$$D_t^{\beta}v + (uv)_x + au_{xxx} - bv_{xx} = 0, \tag{7.13b}$$

where α, β $(0 < \alpha, \beta \leq 1)$ are the orders of the Caputo fractional time derivatives, respectively, and $t \geq 0$. In WBK equations (7.13a) and (7.13b), the field of horizontal velocity is represented by $u = u(x,t)$, $v = v(x,t)$ which is the height that deviates from the equilibrium position of liquid, and the constants a, b are represented in different diffusion powers [53].

If $a = 1$ and $b = 0$, the following fractional coupled modified Boussinesq equations (7.14a) and (7.14b)

$$D_t^{\alpha}u = -u\frac{\partial u}{\partial x} - \frac{\partial v}{\partial x} \tag{7.14a}$$

$$D_t^{\beta}v = -\frac{\partial (uv)}{\partial x} - \frac{\partial^3 u}{\partial x^3} \tag{7.14b}$$

where $t > 0$, $0 < \alpha, \beta \leq 1$, can be obtained as a special case of WBK equations (7.13a) and (7.13b).

If $a = 0$ and $b = 1/2$, the following fractional coupled approximate long wave equations (ALW) equations (7.15a) and (7.15b)

$$D_t^{\alpha}u = -u\frac{\partial u}{\partial x} - \frac{\partial v}{\partial x} - \frac{1}{2}\frac{\partial^2 u}{\partial x^2} \tag{7.15a}$$

$$D_t^{\beta}v = -\frac{\partial (uv)}{\partial x} + \frac{1}{2}\frac{\partial^2 v}{\partial x^2} \tag{7.15b}$$

where $t > 0$, $0 < \alpha, \beta \leq 1$, can be obtained as a special case of WBK equations (7.13a) and (7.13b).

7.3 Fractional Reduced Differential Transform Methods

In this section, proposed modified fractional reduced differential transform method (MFRDTM) and a newly developed technique, coupled fractional reduced differential transform method (CFRDTM), have been presented.

7.3.1 Modified Fractional Reduced Differential Transform Method

Consider a function of two variables $u(x,t)$ which can be represented as a product of two single-variable functions, i.e., $u(x,t) = f(x)g(t)$. Based on the properties of differential transform, the function $u(x,t)$ can be represented as

$$u(x,t) = \sum_{k=0}^{\infty} U_k(x) t^{\alpha k} \tag{7.16}$$

where t-dimensional spectrum function $U_k(x)$ is the transformed function of $u(x,t)$.

The basic definitions and operations of MFRDTM are as follows:

Definition 1 If the function $u(x,t)$ is analytic and differentiated continuously with respect to time t and space x in the domain of interest, then let

$$U_k(x) = \frac{1}{\Gamma(\alpha k + 1)} \left[\left(D_t^{\alpha} \right)^k u(x,t) \right]_{t=0}, \tag{7.17}$$

where $\left(D_t^{\alpha}\right)^k = D_t^{\alpha} \cdot D_t^{\alpha} \cdot D_t^{\alpha} \ldots D_t^{\alpha}$, the k times differentiable Caputo fractional derivative.

The differential inverse transform of $U_k(x)$ is defined as follows:

$$u(x,t) = \sum_{k=0}^{\infty} U_k(x) t^{\alpha k}. \tag{7.18}$$

Then combining Eqs. (7.17) and (7.18), we can write

$$u(x,t) = \sum_{k=0}^{\infty} \left(\frac{1}{\Gamma(\alpha k + 1)} \left[\left(D_t^{\alpha} \right)^k u(x,t) \right]_{t=0} \right) t^{\alpha k}. \tag{7.19}$$

Some basic properties of the reduced differential transform method are summarized in Table 7.1.

To illustrate the basic concepts for the application of MFRDTM, consider the following general nonlinear partial differential equation:

$$Lu(x,t) + Ru(x,t) + Nu(x,t) = g(x,t), \tag{7.20}$$

with initial condition

$$u(x,0) = f(x),$$

where $L \equiv D_t^{\alpha}$ is an easily invertible linear operator, R is the remaining part of the linear operator, $Nu(x,t)$ is a nonlinear term, and $g(x,t)$ is an inhomogeneous term.

We can look for the solution $u(x,t)$ of Eq. (7.20) in the form of the fractional power series:

$$u(x,t) = \sum_{k=0}^{\infty} U_k(x) t^{\alpha k}, \tag{7.21}$$

where t-dimensional spectrum function $U_k(x)$ is the transformed function of $u(x,t)$.

Now, let us write the nonlinear term

$$N(u,t) = \sum_{n=0}^{\infty} A_n(U_0(x), U_1(x), \ldots, U_n(x)) t^{n\alpha}, \tag{7.22}$$

where A_n is the appropriate Adomian's polynomials [13, 17]. In this specific nonlinearity, we use the general form of the formula for A_n Adomian polynomials as

$$A_n(U_0(x), U_1(x), \ldots, U_n(x)) = \frac{1}{n!} \frac{d^n}{d\lambda^n} \left[N\left(\sum_{i=0}^{\infty} \lambda^i U_i(x) \right) \right]_{\lambda=0}. \tag{7.23}$$

Table 7.1 Fundamental operations of MFRDTM

Properties	Function	Transformed function
1	$f(x,t) = au(x,t) \pm bv(x,t)$	$F_k(x) = aU_k(x) \pm bV_k(x)$
2	$f(x,t) = u(x,t)v(x,t)$	$F_k(x) = \sum_{l=0}^{k} U_l(x) V_{k-l}(x)$
3	$f(x,t) = \frac{\partial u(x,t)}{\partial x}$	$F_k(x) = \frac{\partial U_k(x)}{\partial x}$
4	$f(x,t) = D_t^{m\alpha} u(x,t)$, where $\alpha \in \mathcal{R}^+$ and $m \in \mathcal{N}$	$F_k(x) = \frac{\Gamma(\alpha(k+m)+1)}{\Gamma(\alpha k+1)} U_{k+m}(x)$

Now, applying Riemann–Liouville integral J^{α} on both sides of Eq. (7.20), we have

$$u(x,t) = \Phi + J^{\alpha} g(x,t) - J^{\alpha} Ru(x,t) - J^{\alpha} Nu(x,t), \tag{7.24}$$

where from the initial condition $\Phi = u(x,0) = f(x)$.

Substituting Eqs. (7.21) and (7.22), for $u(x,t)$ and $N(u,t)$, respectively, in Eq. (7.24) yields

$$\sum_{k=0}^{\infty} U_k(x) t^{\alpha k} = f(x) + J^{\alpha}\left(\sum_{k=0}^{\infty} G_k(x) t^{\alpha k}\right) - J^{\alpha}\left(R\left(\sum_{k=0}^{\infty} U_k(x) t^{\alpha k}\right)\right) - J^{\alpha}\left(\sum_{k=0}^{\infty} A_k(x) t^{\alpha k}\right),$$

where $g(x,t) = \left(\sum_{k=0}^{\infty} G_k(x) t^{\alpha k}\right)$, and $G_k(x)$ is the transformed function of $g(x,t)$.

After carrying out Riemann–Liouville integral J^{α}, we obtain

$$\sum_{k=0}^{\infty} U_k(x) t^{\alpha k} = f(x) + \left(\sum_{k=0}^{\infty} G_k(x) \frac{t^{\alpha(k+1)} \Gamma(\alpha k+1)}{\Gamma(\alpha(k+1)+1)}\right) - \left(R\left(\sum_{k=0}^{\infty} U_k(x) \frac{t^{\alpha(k+1)} \Gamma(\alpha k+1)}{\Gamma(\alpha(k+1)+1)}\right)\right) - \left(\sum_{k=0}^{\infty} A_k(x) \frac{t^{\alpha(k+1)} \Gamma(\alpha k+1)}{\Gamma(\alpha(k+1)+1)}\right).$$

Finally, equating coefficients of like powers of t, we derive the following recursive formula

$$U_0(x) = f(x),$$

and

$$U_{k+1}(x) = G_k(x) \frac{\Gamma(\alpha k+1)}{\Gamma(\alpha(k+1)+1)} - R\left(U_k(x) \frac{\Gamma(\alpha k+1)}{\Gamma(\alpha(k+1)+1)}\right) - A_k(x) \frac{\Gamma(\alpha k+1)}{\Gamma(\alpha(k+1)+1)}, k \geq 0. \tag{7.25}$$

Using the known $U_0(x)$, all components $U_1(x), U_2(x), \ldots, U_n(x), \ldots,$, etc., are determinable by using Eq. (7.25).

Substituting these $U_0(x), U_1(x), U_2(x), \cdots, U_n(x), \cdots,$, etc., in Eq. (7.21), the approximate solution can be obtained as

$$\tilde{u}_p(x,t) = \sum_{m=0}^{p} U_m(x) t^{m\alpha}, \tag{7.26}$$

where p is the order of approximate solution.

Therefore, the corresponding exact solution is given by

$$u(x,t) = \lim_{p\to\infty} \tilde{u}_p(x,t) \tag{7.27}$$

7.3.2 Coupled Fractional Reduced Differential Transform Method

In order to introduce coupled fractional reduced differential transform, two cases are considered.

For functions with two independent variables

In this case, $U(h,k-h)$ is considered as the coupled fractional reduced differential transform of $u(x,t)$. If the function $u(x,t)$ is analytic and differentiated continuously with respect to time t, then we define the fractional coupled reduced differential transform of $u(x,t)$ as

$$U(h,k-h) = \frac{1}{\Gamma(h\alpha+(k-h)\beta+1)}\left[D_t^{(h\alpha+(k-h)\beta)} u(x,t)\right]_{t=0}, \tag{7.28}$$

whereas the inverse transform of $U(h,k-h)$ is

$$u(x,t) = \sum_{k=0}^{\infty}\sum_{h=0}^{k} U(h,k-h) t^{h\alpha+(k-h)\beta}, \tag{7.29}$$

which is one of the solutions of coupled fractional differential equations.

Theorem 7.1 *Suppose that $U(h,k-h)$ and $V(h,k-h)$ are coupled fractional reduced differential transform of functions $u(x,t)$ and $v(x,t)$, respectively.*

i. If $u(x,t) = f(x,t) \pm g(x,t)$, then $U(h,k-h) = F(h,k-h) \pm G(h,k-h)$.
ii. If $u(x,t) = af(x,t)$, where $a \in \mathcal{R}$, then $U(h,k-h) = aF(h,k-h)$.
iii. If $f(x,t) = u(x,t)v(x,t)$, then $F(h,k-h) = \sum_{l=0}^{h}\sum_{s=0}^{k-h} U(h-l,s)V(l,k-h-s)$.
iv. If $f(x,t) = D_t^{\alpha} u(x,t)$, then

$$F(h,k-h) = \frac{\Gamma((h+1)\alpha+(k-h)\beta+1)}{\Gamma(h\alpha+(k-h)\beta+1)} U(h+1,k-h).$$

v. If $f(x,t) = D_t^{\beta} v(x,t)$, then

$$F(h,k-h) = \frac{\Gamma(h\alpha + (k-h+1)\beta + 1)}{\Gamma(h\alpha + (k-h)\beta + 1)} V(h,k-h+1).$$

For functions with three independent variables

In this case, $U(h,k-h)$ is considered as the coupled fractional reduced differential transform of $u(x,y,t)$. If the function $u(x,y,t)$ is analytic and differentiated continuously with respect to time t, then we define the fractional coupled reduced differential transform of $u(x,y,t)$ as

$$U(h,k-h) = \frac{1}{\Gamma(h\alpha + (k-h)\beta + 1)} \left[D_t^{(h\alpha + (k-h)\beta)} u(x,y,t) \right]_{t=0}, \tag{7.30}$$

whereas the inverse transform of $U(h,k-h)$ is

$$u(x,y,t) = \sum_{k=0}^{\infty} \sum_{h=0}^{k} U(h,k-h) t^{h\alpha + (k-h)\beta}, \tag{7.31}$$

which is one of the solutions of coupled fractional differential equations.

Theorem 7.2 *Suppose that $U(h,k-h)$ and $V(h,k-h)$ are coupled fractional reduced differential transform of functions $u(x,y,t)$ and $v(x,y,t)$, respectively.*

i. If $u(x,y,t) = f(x,y,t) \pm g(x,y,t)$, then $U(h,k-h) = F(h,k-h) \pm G(h,k-h)$.
ii. If $u(x,y,t) = af(x,y,t)$, where $a \in \mathcal{R}$, then $U(h,k-h) = aF(h,k-h)$.
iii. If $f(x,y,t) = u(x,y,t)v(x,y,t)$, then $F(h,k-h) = \sum_{l=0}^{h} \sum_{s=0}^{k-h} U(h-l,s) V(l,k-h-s)$.
iv. If $f(x,y,t) = D_t^{\alpha} u(x,y,t)$, then

$$F(h,k-h) = \frac{\Gamma((h+1)\alpha + (k-h)\beta + 1)}{\Gamma(h\alpha + (k-h)\beta + 1)} U(h+1,k-h).$$

v. If $f(x,y,t) = D_t^{\beta} v(x,y,t)$, then

$$F(h,k-h) = \frac{\Gamma(h\alpha + (k-h+1)\beta + 1)}{\Gamma(h\alpha + (k-h)\beta + 1)} V(h,k-h+1).$$

7.4 Application of MFRDTM for the Solution of Fractional KdV Equations

We consider the generalized fractional KdV equation of the form

$$D_t^{\alpha} u + (u^m)_x + (u^n)_{xxx} = 0, \quad m > 0,\ 1 \le n \le 3,\ t > 0,\ 0 < \alpha \le 1 \tag{7.32}$$

with initial condition

$$u(x, 0) = f(x). \tag{7.33}$$

Applying MFRDTM to Eq. (7.32) and using basic properties of Table 7.1, we can obtain

$$\frac{\Gamma(\alpha(k+1)+1)}{\Gamma(\alpha k+1)} U_{k+1}(x) + \frac{\partial A_k(x)}{\partial x} + \frac{\partial^3 \bar{A}_k(x)}{\partial x^3} = 0, k \ge 0 \tag{7.34}$$

where $U_k(x)$ is the transformed function of $u(x, t)$, and the nonlinear terms u^m and u^n have been considered as Adomian polynomials $\sum_{k=0}^{\infty} A_k(U_0(x), U_1(x), \ldots, U_k(x))$ and $\sum_{k=0}^{\infty} \bar{A}_k(U_0(x), U_1(x), \ldots, U_k(x))$, respectively.

From the initial condition (7.33), we have

$$U_0(x) = f(x). \tag{7.35}$$

Substituting (7.35) into (7.34), we obtain the values of $U_k(x)$ successively.

Then, the approximate solution can be obtained as

$$\tilde{u}_p(x, t) = \sum_{m=0}^{p} U_m(x) t^{m\alpha}, \tag{7.36}$$

where p is the order of approximate solution.

7.4.1 Numerical Solutions of Variant Types of Time Fractional KdV Equations

In order to assess the advantages and the accuracy of the modified fractional reduced differential transform method (MFRDTM) for solving nonlinear fractional KdV equation, this method has been applied to solve the following four examples. In the first two examples, we consider quasi-linear time fractional KdV equations, while in the last two examples, we consider a nonlinear time fractional dispersive $K(2, 2)$ equation. All the results are calculated by using the symbolic calculus software Mathematica.

Example 7.1

(a) (One-soliton solution)

Consider the following time fractional KdV equation

$$D_t^{\alpha} u + 6uu_x + u_{xxx} = 0, t > 0, 0 < \alpha \leq 1 \tag{7.37}$$

with initial condition

$$u(x,0) = \frac{1}{2}\operatorname{sech}^2\left(\frac{x}{2}\right). \tag{7.38}$$

After applying MFRDTM, according to Eq. (7.34), we can obtain the recursive formula

$$U_{k+1}(x) = \left(\frac{-\Gamma(\alpha k+1)}{\Gamma(\alpha(k+1)+1)}\right)\left(6\sum_{r=0}^{k} U_{k-r}(x)\frac{\partial U_r(x)}{\partial x} + \frac{\partial^3 U_k(x)}{\partial x^3}\right), k \geq 0 \tag{7.39}$$

where $U_k(x)$ is the transformed function of $u(x,t)$.

From the initial condition (7.38), we have

$$U_0(x) = \frac{1}{2}\operatorname{sech}^2\left(\frac{x}{2}\right). \tag{7.40}$$

Substituting (7.40) into (7.39), we obtain the values of $U_k(x)$ for $k = 1, 2, 3, \ldots$ successively.

Then, using Mathematica, the third-order approximate solution can be obtained as

$$u(x,t) = \frac{1}{2}\operatorname{sech}^2\left(\frac{x}{2}\right) + \frac{t^{2\alpha}(-2+\cosh(x))\operatorname{sech}^4\left(\frac{x}{2}\right)}{4\Gamma(1+2\alpha)} + \frac{4t^{\alpha}\operatorname{cosech}^3(x)\sinh^4\left(\frac{x}{2}\right)}{\Gamma(1+\alpha)} + \frac{t^{3\alpha}((39-32\cosh(x)+\cosh(2x))\Gamma(1+\alpha)^2 + 12(-2+\cosh(x))\Gamma(1+2\alpha))\operatorname{sech}^6\left(\frac{x}{2}\right)\tanh\left(\frac{x}{2}\right)}{16\Gamma(1+\alpha)^2\Gamma(1+3\alpha)}. \tag{7.41}$$

If $\alpha = 1$, the solution in Eq. (7.41), which becomes the single soliton solution, is given by

$$u(x,t) = \frac{1}{2}\operatorname{sech}^2\left(\frac{x-t}{2}\right). \tag{7.42}$$

For special case $\alpha = 1$, i.e., for classical integer order, the obtained results for the exact solution (7.42) and the approximate solution in Eq. (7.41) obtained by MFRDTM are shown in Figs. 7.1 and 7.2. It is very much graceful that the

approximate solution obtained by the present method and the exact solution are very much identical.

Figures 7.3, 7.4, 7.5, and 7.6 demonstrate the approximate solutions for $\alpha = 0.25$, $\alpha = 0.35$, $\alpha = 0.5$, and $\alpha = 0.75$, respectively.

(b) (Two-soliton solution)

Consider the following time fractional KdV equation

$$D_t^{\alpha} u + 6uu_x + u_{xxx} = 0, t > 0, 0 < \alpha \leq 1 \tag{7.43}$$

with initial condition

$$u(x, 0) = 6\text{sech}^2 x. \tag{7.44}$$

After applying MFRDTM, according to Eq. (7.34), we can obtain the recursive formula

$$U_{k+1}(x) = \left(\frac{-\Gamma(\alpha k + 1)}{\Gamma(\alpha(k+1)+1)}\right)\left(3\frac{\partial A_k(x)}{\partial x} + \frac{\partial^3 U_k(x)}{\partial x^3}\right), k \geq 0 \tag{7.45}$$

where $U_k(x)$ is the transformed function of $u(x, t)$, and the nonlinear term u^2 has been considered as Adomian polynomials $\sum_{k=0}^{\infty} A_k(U_0(x), U_1(x), \ldots, U_k(x))$.

From the initial condition (7.44), we have

$$U_0(x) = 6\text{sech}^2 x. \tag{7.46}$$

Substituting Eq. (7.46) into Eq. (7.45), we obtain the values of $U_k(x)$ for $k = 1, 2, 3, \ldots$ successively.

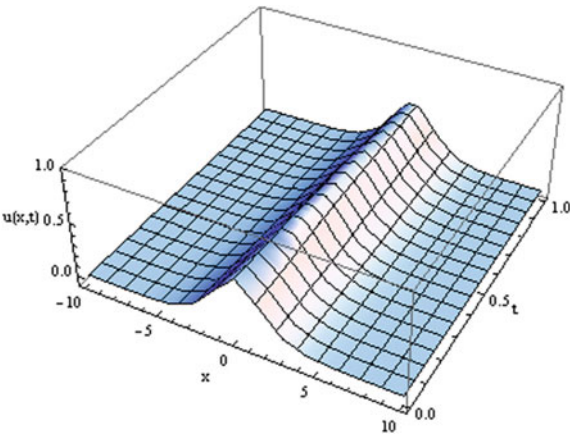

Fig. 7.1 Exact solution $u(x, t)$ for Eq. (7.37)

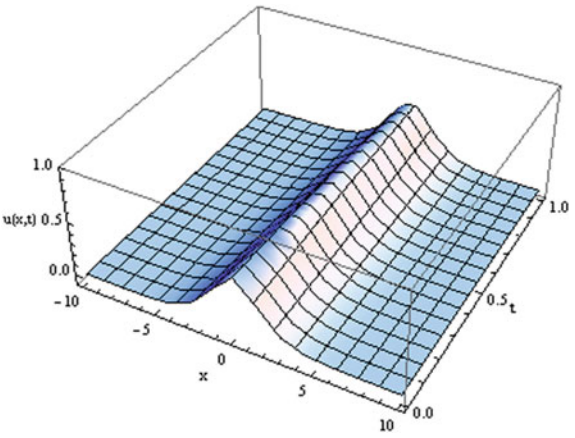

Fig. 7.2 Approximate solution $u(x,t)$ obtained by MFRDTM for Eq. (7.37)

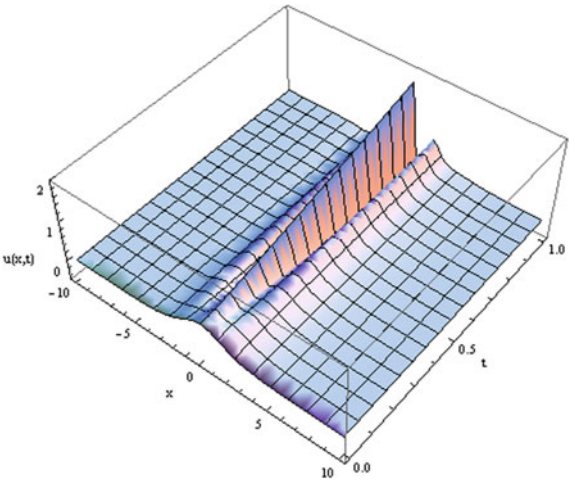

Fig. 7.3 Approximate solution $u(x,t)$ obtained by MFRDTM for Eq. (7.37) when $\alpha = 0.25$

Then, using Mathematica, the second-order approximate solution can be obtained as

$$u(x,t) = 6\text{sech}^2 x + \frac{12t^{2\alpha}(-1064 + 183\cosh(2x) + 240\cosh(4x) + \cosh(6x))\text{sech}^8 x}{\Gamma(1+2\alpha)} + \frac{12t^{\alpha}\text{sech}^5(x)(25\sinh(x) + \sinh(3x))}{\Gamma(1+\alpha)} + O(t^{3\alpha}). \tag{7.47}$$

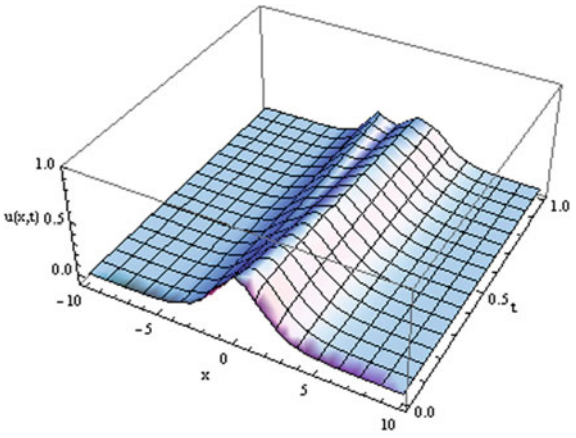

Fig. 7.4 Approximate solution $u(x,t)$ obtained by MFRDTM for Eq. (7.37) when $\alpha = 0.35$

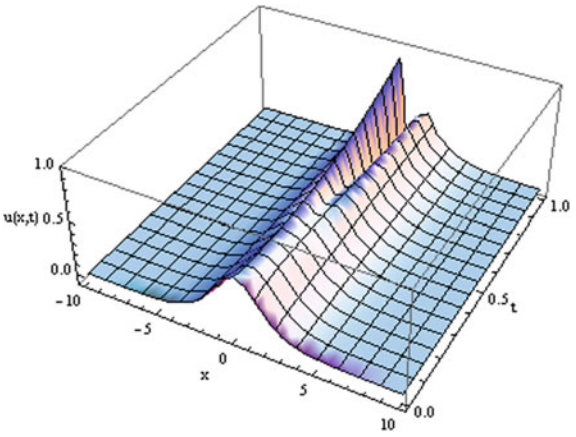

Fig. 7.5 Approximate solution $u(x,t)$ obtained by MFRDTM for Eq. (7.37) when $\alpha = 0.5$

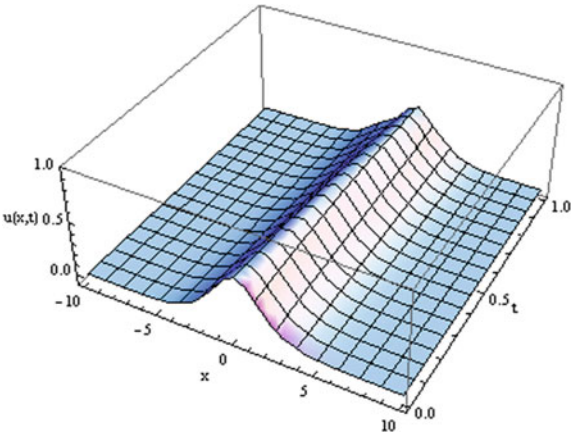

Fig. 7.6 Approximate solution $u(x,t)$ obtained by MFRDTM for Eq. (7.37) when $\alpha = 0.75$

If $\alpha = 1$, the solution in Eq. (7.47), which becomes the two-soliton solution, is given by

$$u(x,t) = \frac{24(4\cosh(x-4t)^2 + \sinh(2x-32t)^2)}{(\cosh(3x-36t) + 3\cosh(x-28t))^2}. \tag{7.48}$$

Figures 7.7, 7.8, and 7.9 exhibit the two-soliton approximate solutions of the KdV equation (7.43) for $\alpha = 0.5$, $\alpha = 0.75$, and $\alpha = 1$, respectively.

Example 7.2 Consider the following time fractional KdV equation

$$D_t^{\alpha} u - 3(u^2)_x + u_{xxx} = 0, t > 0, 0 < \alpha \leq 1 \tag{7.49}$$

with initial condition

$$u(x,0) = 6x. \tag{7.50}$$

After applying MFRDTM, according to Eq. (7.34), we can obtain the recursive formula

$$U_{k+1}(x) = \left(\frac{\Gamma(\alpha k+1)}{\Gamma(\alpha(k+1)+1)}\right)\left(3\frac{\partial A_k(x)}{\partial x} - \frac{\partial^3 U_k(x)}{\partial x^3}\right), k \geq 0 \tag{7.51}$$

where $U_k(x)$ is the transformed function of $u(x,t)$, and the nonlinear term u^2 has been considered as Adomian polynomials $\sum_{k=0}^{\infty} A_k(U_0(x), U_1(x), \ldots, U_k(x))$.

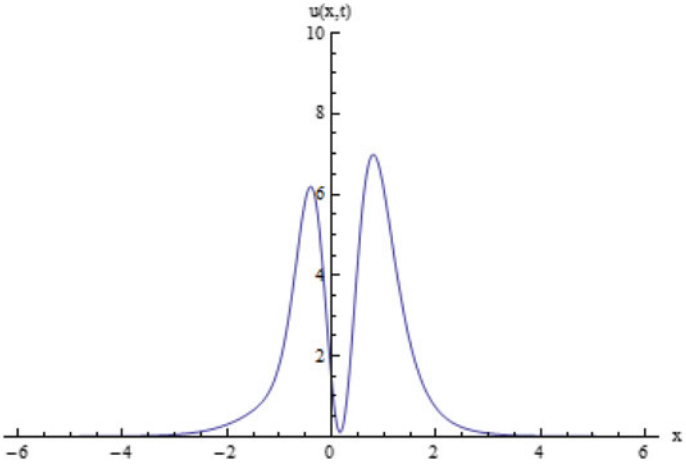

Fig. 7.7 Two-soliton approximate solution $u(x,t)$ of the KdV equation obtained by using Eq. (7.47) for $\alpha = 0.5$, $t = 0.0006$, and $-6 \leq x \leq 6$

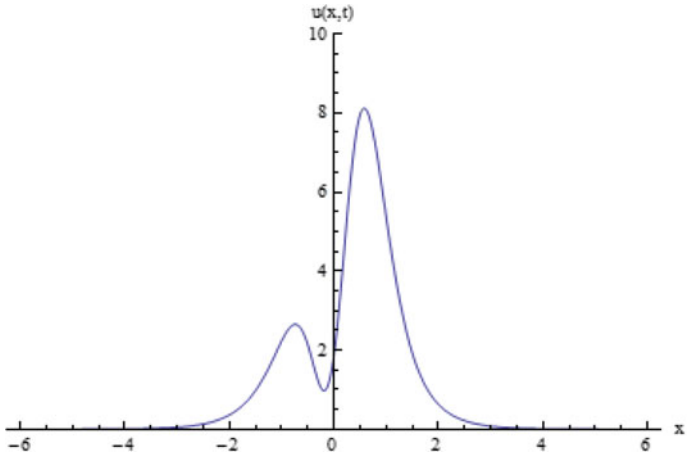

Fig. 7.8 Two-soliton approximate solution $u(x,t)$ of the KdV equation obtained by using Eq. (7.47) for $\alpha = 0.75$, $t = 0.008$, and $-6 \le x \le 6$

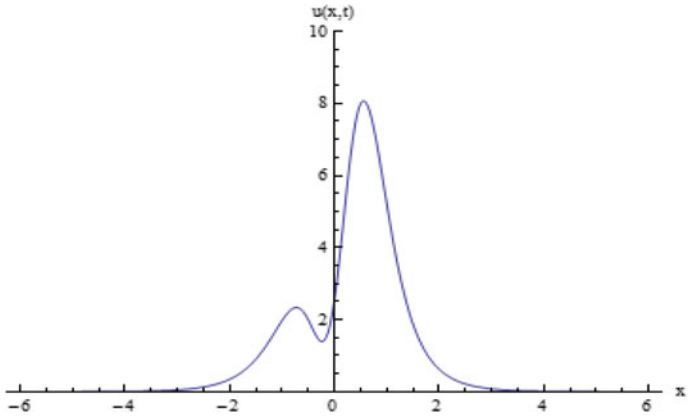

Fig. 7.9 Two-soliton approximate solution $u(x,t)$ of the KdV equation obtained by using Eq. (7.47) for $\alpha = 1$, $t = 0.03$, and $-6 \le x \le 6$

From the initial condition Eq. (7.50), we have

$$U_0(x) = 6x. \tag{7.52}$$

Substituting (7.52) into (7.51), we obtain the values of $U_k(x)$ for $k = 1, 2, 3, \ldots$ successively.

Then, using Mathematica, the fourth-order approximate solution can be obtained as

$$u(x,t) = 6x + \frac{216t^{\alpha}x}{\Gamma(1+\alpha)} + \frac{15552t^{2\alpha}x}{\Gamma(1+2\alpha)} + \frac{279936t^{3\alpha}x\left(\frac{1}{\Gamma(1+\alpha)^2} + \frac{4}{\Gamma(1+2\alpha)}\right)\Gamma(1+2\alpha)}{\Gamma(1+3\alpha)} + \frac{20155392t^{4\alpha}x(4\Gamma(1+\alpha)^2\Gamma(1+2\alpha) + \Gamma(1+2\alpha)^2 + 2\Gamma(1+\alpha)\Gamma(1+3\alpha))}{\Gamma(1+\alpha)^2\Gamma(1+2\alpha)\Gamma(1+4\alpha)}. \tag{7.53}$$

For the special case $\alpha = 1$, the solution in Eq. (7.53), which becomes the exact solitary wave solution, is given by

$$\begin{aligned} u(x,t) &= 6x + 216tx + 7776t^2x + 279936t^3x + 10077696t^4x + \cdots \\ &= \frac{6x}{1-36t}. \end{aligned} \tag{7.54}$$

Example 7.3 Consider the following time fractional dispersive $K(2,2)$ equation

$$D_t^{\alpha}u + (u^2)_x + (u^2)_{xxx} = 0, t > 0, 0 < \alpha \leq 1, \tag{7.55}$$

with initial condition

$$u(x,0) = x. \tag{7.56}$$

After applying MFRDTM, according to Eq. (7.34), we can obtain the recursive formula

$$U_{k+1}(x) = \left(\frac{-\Gamma(\alpha k+1)}{\Gamma(\alpha(k+1)+1)}\right)\left(\frac{\partial A_k(x)}{\partial x} + \frac{\partial^3 U_k(x)}{\partial x^3}\right), k \geq 0, \tag{7.57}$$

where $U_k(x)$ is the transformed function of $u(x,t)$, and the nonlinear term u^2 has been considered as Adomian polynomials $\sum_{k=0}^{\infty} A_k(U_0(x), U_1(x), \ldots, U_k(x))$.

From the initial condition (7.56), we have

$$U_0(x) = x. \tag{7.58}$$

Substituting (7.58) into (7.57), we obtain the values of $U_k(x)$ for $k = 1, 2, 3, \ldots$ successively.

Then, using Mathematica, the fifth-order approximate solution can be obtained as

$$u(x,t) = x - \frac{2t^{\alpha}x}{\Gamma(1+\alpha)} + \frac{8t^{2\alpha}x}{\Gamma(1+2\alpha)} - \frac{8t^{3\alpha}x\left(\frac{1}{\Gamma(1+\alpha)^2} + \frac{4}{\Gamma(1+2\alpha)}\right)\Gamma(1+2\alpha)}{\Gamma(1+3\alpha)} + \frac{32t^{4\alpha}x\left(4\Gamma(1+\alpha)^2\Gamma(1+2\alpha) + \Gamma(1+2\alpha)^2 + 2\Gamma(1+\alpha)\Gamma(1+3\alpha)\right)}{\Gamma(1+\alpha)^2\Gamma(1+2\alpha)\Gamma(1+4\alpha)}$$

$$-\frac{64t^{5\alpha}x\left(2+\frac{\Gamma(1+2\alpha)^2(4\Gamma(1+\alpha)^2+\Gamma(1+2\alpha))}{\Gamma(1+\alpha)^3\Gamma(1+3\alpha)}\right)\Gamma(1+4\alpha)}{\Gamma(1+2\alpha)^2\Gamma(1+5\alpha)}$$
$$+\frac{64t^{5\alpha}x\left(\frac{2\Gamma(1+2\alpha)\left(4\Gamma(1+\alpha)^2\Gamma(1+2\alpha)+\Gamma(1+2\alpha)^2+2\Gamma(1+\alpha)\Gamma(1+3\alpha)\right)}{\Gamma(1+\alpha)^2\Gamma(1+4\alpha)}\right)\Gamma(1+4\alpha)}{\Gamma(1+2\alpha)^2\Gamma(1+5\alpha)}. \tag{7.59}$$

For the special case $\alpha = 1$, the solution in Eq. (7.59), which becomes the exact solitary wave solution, is given by

$$u(x,t) = x - 2tx + 4t^2x - 8t^3x + 16t^4x - 32t^5x + \cdots = \frac{x}{1+2t}. \tag{7.60}$$

Example 7.4 Consider the following time fractional dispersive $K(2,2)$ equation

$$D_t^{\alpha}u + (u^2)_x + (u^2)_{xxx} = 0,\ t > 0,\ 0 < \alpha \leq 1 \tag{7.61}$$

with initial condition

$$u(x,0) = \frac{4c}{3}\cos^2\left(\frac{x}{4}\right). \tag{7.62}$$

Taking modified fractional reduced differential transform, we can obtain the same recursive formula as in Eq. (7.57).

From the initial condition (5.1.20), here in this case, we have

$$U_0(x) = \frac{4c}{3}\cos^2\left(\frac{x}{4}\right). \tag{7.63}$$

Substituting Eq. (7.63) into Eq. (7.57), we obtain the values of $U_k(x)$ for $k = 1, 2, 3, \ldots$ successively.

Then, using Mathematica, the third-order approximate solution can be obtained as

$$u(x,t) = \frac{4}{3}c\cos^2\left(\frac{x}{4}\right) + \frac{c^2t^{\alpha}\sin\left(\frac{x}{2}\right)}{3\Gamma(1+\alpha)} - \frac{c^3t^{2\alpha}\cos\left(\frac{x}{2}\right)}{6\Gamma(1+2\alpha)} - \frac{c^4t^{3\alpha}\sin\left(\frac{x}{2}\right)}{12\Gamma(1+3\alpha)}. \tag{7.64}$$

For the special case $\alpha = 1$, the solution in Eq. (7.64), which becomes the exact solitary wave solution, is given by

$$\begin{aligned} u(x,t) = {} & \frac{4}{3}c\cos^2\left(\frac{x}{4}\right) + \frac{1}{3}c^2t\sin\left(\frac{x}{2}\right) - \frac{1}{12}c^3t^2\cos\left(\frac{x}{2}\right) \\ & - \frac{1}{72}c^4t^3\sin\left(\frac{x}{2}\right) + \frac{1}{576}c^5t^4\cos\left(\frac{x}{2}\right) + \cdots. \end{aligned} \tag{7.65}$$

Using Taylor series into Eq. (7.65), we can find the closed-form solitary wave solution with compact support, i.e., compacton solution

$$u(x,t)=\begin{cases}\frac{4c}{3}\cos^2\left(\frac{x-ct}{4}\right), & |x-ct|\le 2\pi,\\ 0, & \text{otherwise.}\end{cases}.$$

7.4.2 Convergence Analysis and Error Estimate

Theorem 7.3 *Suppose that,* $D_t^{k\alpha}u(x,t)\in C([0,L]\times[0,T])$ *for* $k=0,1,2,\ldots,N+1$, *where* $0<\alpha<1$, *then*

$$u(x,t)\cong\sum_{m=0}^{N}U_m(x)t^{m\alpha}.$$

Moreover, there exists a value ξ, *where* $0\le\xi\le t$ *so that the error term* $E_N(x,t)$ *has the form*

$$|E_N(x,t)|=\underset{t\in[0,T]}{Sup}\left|\frac{D^{(N+1)\alpha}u(x,\xi)t^{(N+1)\alpha}}{\Gamma((N+1)\alpha+1)}\right|.$$

Proof For $0<\alpha<1$,

$$\begin{aligned}&J^{m\alpha}D^{m\alpha}u(x,t)-J^{(m+1)\alpha}D^{(m+1)\alpha}u(x,t)\\&\quad=J^{m\alpha}(D^{m\alpha}u(x,t)-J^{\alpha}D^{\alpha}(D^{m\alpha}u(x,t)))\\&=J^{m\alpha}(D^{m\alpha}u(x,0))\,\text{using Eq. (2.3.2)}\\&=\frac{D^{m\alpha}u(x,0)t^{m\alpha}}{\Gamma(m\alpha+1)}\\&=U_m(x)t^{m\alpha},\,\text{using Eq. (7.17)};\end{aligned}$$

Now, the *N*th order approximation for $u(x,t)$ is

$$\begin{aligned}\sum_{m=0}^{N}U_m(x)t^{m\alpha}&=\sum_{m=0}^{N}\left(J^{m\alpha}D^{m\alpha}u(x,t)-J^{(m+1)\alpha}D^{(m+1)\alpha}u(x,t)\right)\\&=u(x,t)-J^{(N+1)\alpha}D^{(N+1)\alpha}u(x,t)\\&=u(x,t)-\frac{1}{\Gamma((N+1)\alpha)}\int_0^t\frac{D^{(N+1)\alpha}u(x,\tau)}{(t-\tau)^{1-(N+1)\alpha}}\mathrm{d}\tau\end{aligned}$$

$$
\begin{aligned}
&= u(x,t) - \frac{D^{(N+1)\alpha}u(x,\xi)}{\Gamma((N+1)\alpha)} \int_0^t \frac{\mathrm{d}\tau}{(t-\tau)^{1-(N+1)\alpha}}, \\
&\quad \text{applying integral mean value theorem} \\
&= u(x,t) - \frac{D^{(N+1)\alpha}u(x,\xi)t^{(N+1)\alpha}}{\Gamma((N+1)\alpha+1)}
\end{aligned} \tag{7.66}
$$

Therefore,

$$
u(x,t) = \sum_{m=0}^{N} U_m(x)t^{m\alpha} + \frac{D^{(N+1)\alpha}u(x,\xi)t^{(N+1)\alpha}}{\Gamma((N+1)\alpha+1)}. \tag{7.67}
$$

Consequently, the error term

$$
|E_N(x,t)| = \left| u(x,t) - \sum_{m=0}^{N} U_m(x)t^{m\alpha} \right| = \left| \frac{D^{(N+1)\alpha}u(x,\xi)t^{(N+1)\alpha}}{\Gamma((N+1)\alpha+1)} \right|. \tag{7.68}
$$

This implies

$$
|E_N(x,t)| = \operatorname*{Sup}_{t\in[0,T]} \left| \frac{D^{(N+1)\alpha}u(x,\xi)t^{(N+1)\alpha}}{\Gamma((N+1)\alpha+1)} \right|. \tag{7.69}
$$

As $N \to \infty$, $|E_N| \to 0$.
Hence, $u(x,t)$ can be approximated as

$$
u(x,t) = \sum_{m=0}^{\infty} U_m(x)t^{m\alpha} \cong \sum_{m=0}^{N} U_m(x)t^{m\alpha}.
$$

with the error term given in Eq. (7.69).

7.5 Application of CFRDTM for the Solutions of Time Fractional Coupled KdV Equations

In the present section, CFRDTM has been applied to determine the approximate solutions for the coupled time fractional KdV equations.

7.5.1 Numerical Solutions of Time Fractional Coupled KdV Equations

In order to examine the efficiency and applicability of the proposed coupled fractional reduced differential transform method (CFRDTM) for solving time fractional coupled KdV equations, this method has been employed to solve the following two examples.

Example 7.5 Consider the following time fractional coupled KdV equations [41]

$$D_t^{\alpha} u = -\frac{\partial^3 u}{\partial x^3} - 6u\frac{\partial u}{\partial x} + 3v\frac{\partial v}{\partial x}, \tag{7.70a}$$

$$D_t^{\beta} v = -\frac{\partial^3 v}{\partial x^3} - 3u\frac{\partial v}{\partial x}, \tag{7.70b}$$

where $t > 0$, $0 < \alpha, \beta \leq 1$,

subject to the initial conditions

$$u(x,0) = \frac{4c^2 \exp(cx)}{(1+\exp(cx))^2}, \tag{7.70c}$$

$$v(x,0) = \frac{4c^2 \exp(cx)}{(1+\exp(cx))^2}. \tag{7.70d}$$

The exact solutions of Eqs. (7.70a) and (7.70b), for the special case where $\alpha = \beta = 1$, are given by

$$u(x,t) = v(x,t) = \frac{4c^2 \exp(c(x-c^2t))}{(1+\exp(c(x-c^2t)))^2}. \tag{7.71}$$

In order to assess the advantages and the accuracy of the CFRDTM, we consider the (2 + 1)-dimensional time fractional coupled Burgers equations. Firstly, we derive the recursive formula from Eqs. (7.70a) and (7.70b). Now, $U(h,k-h)$ and $V(h,k-h)$ are considered as the coupled fractional reduced differential transform of $u(x,t)$ and $v(x,t)$, respectively, where $u(x,t)$ and $v(x,t)$ are the solutions of coupled fractional differential equations. Here, $U(0,0) = u(x,0)$, $V(0,0) = v(x,0)$ are the given initial conditions. Without loss of generality, the following assumptions have taken

$$U(0,j) = 0, \quad j = 1,2,3,\ldots \text{ and } V(i,0) = 0, \quad i = 1,2,3,\ldots.$$

Applying CFRDTM to Eq. (7.70a), we obtain the following recursive formula

$$\frac{\Gamma((h+1)\alpha+(k-h)\beta+1)}{\Gamma(h\alpha+(k-h)\beta+1)}U(h+1,k-h) = -\frac{\partial^3}{\partial x^3}U(h,k-h) - 6\left(\sum_{l=0}^{h}\sum_{s=0}^{k-h}U(h-l,s)\frac{\partial}{\partial x}U(l,k-h-s)\right) + 3\left(\sum_{l=0}^{h}\sum_{s=0}^{k-h}V(h-l,s)\frac{\partial}{\partial x}V(l,k-h-s)\right). \tag{7.72}$$

From the initial condition of Eq. (7.70c), we have

$$U(0,0) = u(x,0). \tag{7.73}$$

In the same manner, we can obtain the following recursive formula from Eq. (7.70b)

$$\frac{\Gamma(h\alpha+(k-h+1)\beta+1)}{\Gamma(h\alpha+(k-h)\beta+1)}V(h,k-h+1) = -\frac{\partial^3}{\partial x^3}V(h,k-h) - 3\left(\sum_{l=0}^{h}\sum_{s=0}^{k-h}U(l,k-h-s)\frac{\partial}{\partial x}V(h-l,s)\right). \tag{7.74}$$

From the initial condition of Eq. (7.70d), we have

$$V(0,0) = v(x,0) \tag{7.75}$$

According to CFRDTM, using recursive Eq. (7.72) with initial condition Eq. (7.73) and also using recursive scheme Eq. (7.74) with initial condition Eq. (7.75) simultaneously, we obtain

$$U(1,0) = \frac{4c^5\exp(cx)(-1+\exp(cx))}{(1+\exp(cx))^3\Gamma(1+\alpha)},$$

$$V(0,1) = \frac{4c^5\exp(cx)(-1+\exp(cx))}{(1+\exp(cx))^3\Gamma(1+\beta)},$$

$$U(1,1) = -\frac{96c^8\exp(2cx)(1-3\exp(cx)+\exp(2cx))}{(1+\exp(cx))^6\Gamma(1+\alpha+\beta)},$$

$$V(0,2) = \frac{4c^8\exp(cx)(1-14\exp(cx)+18\exp(2cx)-14\exp(3cx)+\exp(4cx))}{(1+\exp(cx))^6\Gamma(1+2\beta)},$$

$$U(2,0)=\frac{4c^8\exp(cx)(1+22\exp(cx)-78\exp(2cx)+22\exp(3cx)+\exp(4cx))}{(1+\exp(cx))^6\Gamma(1+2\alpha)},$$

$$V(1,1)=\frac{48c^8\exp(2cx)(-1+\exp(cx))^2}{(1+\exp(cx))^6\Gamma(1+\alpha+\beta)},$$

$$U(2,1)=-\frac{96c^{11}\mathrm{e}^{2cx}(-8+81\mathrm{e}^{cx}-175\mathrm{e}^{2cx}+175\mathrm{e}^{3cx}-81\mathrm{e}^{4cx}+8\mathrm{e}^{5cx})}{(1+\mathrm{e}^{cx})^9\Gamma(1+2\alpha+\beta)},$$

$$V(2,1)=\frac{48c^{11}\mathrm{e}^{2cx}(-1+\mathrm{e}^{cx})(1+22\mathrm{e}^{cx}-78\mathrm{e}^{2cx}+22\mathrm{e}^{3cx}+\mathrm{e}^{4cx})}{(1+\mathrm{e}^{cx})^9\Gamma(1+2\alpha+\beta)},$$

and so on.

The approximate solutions, obtained in the series form, are given by

$$\begin{aligned}u(x,t)&=\sum_{k=0}^{\infty}\sum_{h=0}^{k}U(h,k-h)t^{(h\alpha+(k-h)\beta)}\\&=U(0,0)+\sum_{k=1}^{\infty}\sum_{h=1}^{k}U(h,k-h)t^{(h\alpha+(k-h)\beta)}\\&=\frac{4c^2\mathrm{e}^{cx}}{(1+\mathrm{e}^{cx})^2}+\frac{4c^5\mathrm{e}^{cx}(-1+\mathrm{e}^{cx})t^{\alpha}}{(1+\mathrm{e}^{cx})^3\Gamma(1+\alpha)}\\&\quad+\frac{4c^8\mathrm{e}^{cx}(1+22\mathrm{e}^{cx}-78\mathrm{e}^{2cx}+22\mathrm{e}^{3cx}+\mathrm{e}^{4cx})t^{2\alpha}}{(1+\mathrm{e}^{cx})^6\Gamma(1+2\alpha)}\\&\quad-\frac{96c^{11}\mathrm{e}^{2cx}(-8+81\mathrm{e}^{cx}-175\mathrm{e}^{2cx}+175\mathrm{e}^{3cx}-81\mathrm{e}^{4cx}+8\mathrm{e}^{5cx})t^{2\alpha+\beta}}{(1+\mathrm{e}^{cx})^9\Gamma(1+2\alpha+\beta)}\cdots\end{aligned}\tag{7.76}$$

$$\begin{aligned}v(x,t)&=\sum_{k=0}^{\infty}\sum_{h=0}^{k}V(h,k-h)t^{(h\alpha+(k-h)\beta)}\\&=V(0,0)+\sum_{k=1}^{\infty}\sum_{h=0}^{k}V(h,k-h)t^{(h\alpha+(k-h)\beta)}\\&=\frac{4c^2\mathrm{e}^{cx}}{(1+\mathrm{e}^{cx})^2}+\frac{4c^5\mathrm{e}^{cx}(-1+\mathrm{e}^{cx})t^{\beta}}{(1+\mathrm{e}^{cx})^3\Gamma(1+\beta)}\\&\quad+\frac{4c^8\mathrm{e}^{cx}(1-14\mathrm{e}^{cx}+18\mathrm{e}^{2cx}-14\mathrm{e}^{3cx}+\mathrm{e}^{4cx})t^{2\beta}}{(1+\exp(cx))^6\Gamma(1+2\beta)}\\&\quad+\frac{48c^{11}\mathrm{e}^{2cx}(-1+\mathrm{e}^{cx})(1+22\mathrm{e}^{cx}-78\mathrm{e}^{2cx}+22\mathrm{e}^{3cx}+\mathrm{e}^{4cx})t^{2\alpha+\beta}}{(1+\mathrm{e}^{cx})^9\Gamma(1+2\alpha+\beta)}\cdots\end{aligned}\tag{7.77}$$

When $\alpha = 1$ and $\beta = 1$, the solution in Eq. (7.76) becomes

$$u(x,t) = \frac{4c^2 e^{cx}}{(1+e^{cx})^2} + \frac{4c^5 e^{cx}(-1+e^{cx})t}{(1+e^{cx})^3} + \frac{2c^8 e^{cx}(1-4e^{cx}+e^{2cx})t^2}{(1+e^{cx})^4} + \ldots. \tag{7.78}$$

When $\alpha = 1$ and $\beta = 1$, the solution in Eq. (7.77) becomes

$$v(x,t) = \frac{4c^2 e^{cx}}{(1+e^{cx})^2} + \frac{4c^5 e^{cx}(-1+e^{cx})t}{(1+e^{cx})^3} + \frac{2c^8 e^{cx}(1-4e^{cx}+e^{2cx})t^2}{(1+e^{cx})^4} + \ldots. \tag{7.79}$$

The solutions in Eqs. (7.78) and (7.79) are exactly the same as the Taylor series expansion of the exact solution

$$u(x,t) = v(x,t) = \frac{4c^2 e^{cx}}{(1+e^{cx})^2} + \frac{4c^5 e^{cx}(-1+e^{cx})t}{(1+e^{cx})^3} + \frac{2c^8 e^{cx}(1-4e^{cx}+e^{2cx})t^2}{(1+e^{cx})^4} + \ldots. \tag{7.80}$$

In order to verify the efficiency and accuracy of the proposed method for the time fractional coupled KdV equations, the graphs have been drawn in Figs. 7.10, 7.11, and 7.12. The numerical solutions for Eqs. (7.76) and (7.77) for the special case where $\alpha = 1$ and $\beta = 1$ are shown in Fig. 7.10. It can be observed from Fig. 7.10 that the solutions obtained by the proposed method coincide with the exact solution. Figure 7.11 shows the numerical solutions of Eqs. (7.76) and (7.77) when $\alpha = 1/3$ and $\beta = 1/5$. Again, Fig. 7.12 cites the numerical solutions when $\alpha = 0.005$ and $\beta = 0.002$. From Figs. 7.11 and 7.12, it can be observed that the solutions for $u(x,t)$ and $v(x,t)$ bifurcate into waves as the time fractional derivatives α and β decrease.

Example 7.6 Consider the following time fractional coupled KdV equations [42]

$$D_t^{\alpha} u + 6uu_x - 6vv_x + u_{xxx} = 0, \tag{7.81a}$$

$$D_t^{\beta} v + 3uv_x + v_{xxx} = 0, \tag{7.81b}$$

where $t > 0$, $0 < \alpha, \beta \leq 1$, subject to the initial conditions

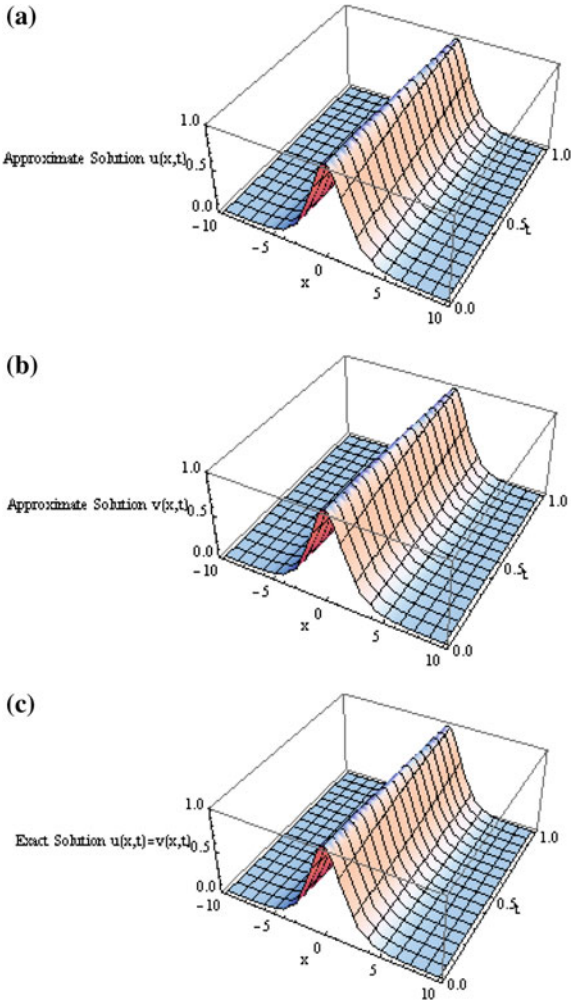

Fig. 7.10 Surfaces show **a** the numerical approximate solution of $u(x,t)$, **b** the numerical approximate solution of $v(x,t)$, and **c** the exact solution of $u(x,t) = v(x,t)$ when $\alpha = 1$ and $\beta = 1$

$$u(x,0) = \lambda \operatorname{sech}^2\left(\frac{\sqrt{\lambda}x}{2}\right), \tag{7.82}$$

$$v(x,0) = \frac{\lambda}{\sqrt{2}} \operatorname{sech}^2\left(\frac{\sqrt{\lambda}x}{2}\right). \tag{7.83}$$

First, we derive the recursive formula from Eqs. (7.81a) and (7.81b). Now, $U(h,k-h)$ and $V(h,k-h)$ are considered as the coupled fractional reduced differential transform of $u(x,t)$ and $v(x,t)$, respectively, where $u(x,t)$ and $v(x,t)$ are the solutions of coupled fractional differential equations. Here, $U(0,0) = u(x,0)$,

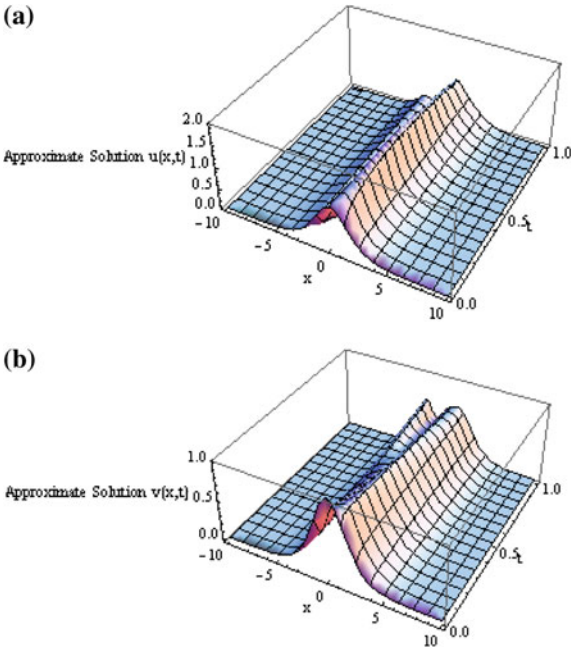

Fig. 7.11 Surfaces show **a** the numerical approximate solution of $u(x,t)$ and **b** the numerical approximate solution of $v(x,t)$ when $\alpha = 1/3$ and $\beta = 1/5$

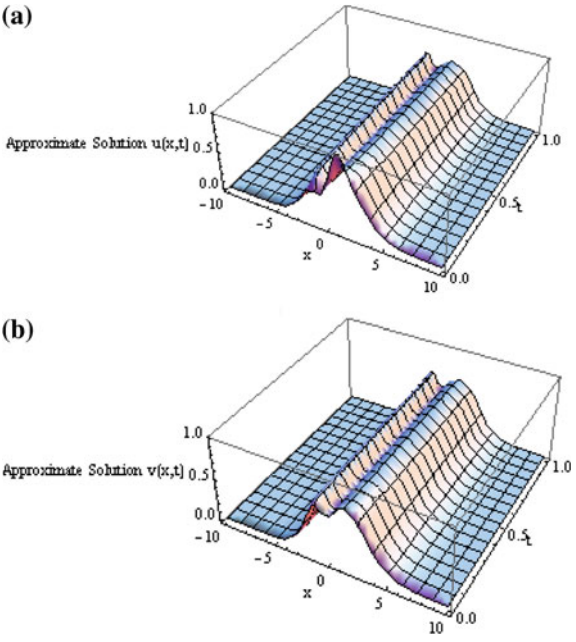

Fig. 7.12 Surfaces show **a** the numerical approximate solution of $u(x,t)$ and **b** the numerical approximate solution of $v(x,t)$ when $\alpha = 0.005$ and $\beta = 0.002$

$V(0,0) = v(x,0)$ are the given initial conditions. Without loss of generality, the following assumptions have taken

$$U(0,j) = 0, \quad j = 1,2,3,\ldots \quad \text{and} \quad V(i,0) = 0, \quad i = 1,2,3,\ldots.$$

Applying CFRDTM to Eq. (7.81a), we obtain the following recursive formula

$$\begin{aligned}\frac{\Gamma((h+1)\alpha+(k-h)\beta+1)}{\Gamma(h\alpha+(k-h)\beta+1)}U(h+1,k-h) = &-\frac{\partial^3}{\partial x^3}U(h,k-h)\\ &-6\left(\sum_{l=0}^{h}\sum_{s=0}^{k-h}U(h-l,s)\frac{\partial}{\partial x}U(l,k-h-s)\right)\\ &+6\left(\sum_{l=0}^{h}\sum_{s=0}^{k-h}V(h-l,s)\frac{\partial}{\partial x}V(l,k-h-s)\right)\end{aligned} \tag{7.84}$$

From the initial condition of Eq. (7.82), we have

$$U(0,0) = u(x,0) \tag{7.85}$$

In the same manner, we can obtain the following recursive formula from Eq. (7.81b)

$$\begin{aligned}\frac{\Gamma(h\alpha+(k-h+1)\beta+1)}{\Gamma(h\alpha+(k-h)\beta+1)}V(h,k-h+1) = &-\frac{\partial^3}{\partial x^3}V(h,k-h)\\ &-3\left(\sum_{l=0}^{h}\sum_{s=0}^{k-h}U(l,k-h-s)\frac{\partial}{\partial x}V(h-l,s)\right)\end{aligned} \tag{7.86}$$

From the initial condition of Eq. (7.83), we have

$$V(0,0) = v(x,0) \tag{7.87}$$

According to CFRDTM, using recursive Eq. (7.84) with initial condition Eq. (7.85) and also using recursive scheme Eq. (7.86) with initial condition Eq. (7.87) simultaneously, we obtain successively

$$U(1,0) = \frac{\lambda^{5/2}\operatorname{sech}^2\left(\frac{\sqrt{\lambda}x}{2}\right)\tanh\left(\frac{\sqrt{\lambda}x}{2}\right)}{\Gamma(1+\alpha)},$$

$$V(0,1) = \frac{4\sqrt{2}\lambda^{5/2}\operatorname{cosech}^3\left(x\sqrt{\lambda}\right)\sinh^4\left(\frac{\sqrt{\lambda}x}{2}\right)}{\Gamma(1+\beta)},$$

$$U(1,1) = -\frac{3\lambda^4\left(-3+2\cosh\left(x\sqrt{\lambda}\right)\right)\operatorname{sech}^6\left(\frac{\sqrt{\lambda}x}{2}\right)}{2\Gamma(1+\alpha+\beta)},$$

$$V(0,2) = \frac{\lambda^4\left(9-14\cosh\left(x\sqrt{\lambda}\right)+\cosh\left(2x\sqrt{\lambda}\right)\right)\operatorname{sech}^6\left(\frac{\sqrt{\lambda}x}{2}\right)}{8\sqrt{2}\Gamma(1+2\beta)},$$

$$U(2,0) = \frac{\lambda^4\left(-39+22\cosh\left(x\sqrt{\lambda}\right)+\cosh\left(2x\sqrt{\lambda}\right)\right)\operatorname{sech}^6\left(\frac{\sqrt{\lambda}x}{2}\right)}{8\Gamma(1+2\alpha)},$$

$$V(1,1) = \frac{96\sqrt{2}\lambda^4\operatorname{cosech}^6\left(x\sqrt{\lambda}\right)\sinh^8\left(\frac{\sqrt{\lambda}x}{2}\right)}{\Gamma(1+\alpha+\beta)},$$

and so on.

The approximate solutions, obtained in the series form, are given by

$$\begin{aligned}
u(x,t) &= \sum_{k=0}^{\infty}\sum_{h=0}^{k} U(h,k-h)t^{(h\alpha+(k-h)\beta)} \\
&= U(0,0) + \sum_{k=1}^{\infty}\sum_{h=1}^{k} U(h,k-h)t^{(h\alpha+(k-h)\beta)} \\
&= \lambda\operatorname{sech}^2\left(\frac{\sqrt{\lambda}x}{2}\right) + \frac{t^\alpha\lambda^{5/2}\operatorname{sech}^2\left(\frac{\sqrt{\lambda}x}{2}\right)\tanh\left(\frac{\sqrt{\lambda}x}{2}\right)}{\Gamma(1+\alpha)} \\
&\quad + \frac{t^{2\alpha}\lambda^4\left(-39+22\cosh\left(x\sqrt{\lambda}\right)+\cosh\left(2x\sqrt{\lambda}\right)\right)\operatorname{sech}^6\left(\frac{\sqrt{\lambda}x}{2}\right)}{8\Gamma(1+2\alpha)} \\
&\quad - \frac{3t^{\alpha+\beta}\lambda^4\left(-3+2\cosh\left(x\sqrt{\lambda}\right)\right)\operatorname{sech}^6\left(\frac{\sqrt{\lambda}x}{2}\right)}{2\Gamma(1+\alpha+\beta)} + \cdots
\end{aligned} \tag{7.88}$$

$$\begin{aligned}
v(x,t) &= \sum_{k=0}^{\infty}\sum_{h=0}^{k} V(h,k-h)t^{(h\alpha+(k-h)\beta)} \\
&= V(0,0) + \sum_{k=1}^{\infty}\sum_{h=0}^{k} V(h,k-h)t^{(h\alpha+(k-h)\beta)} \\
&= \frac{\lambda}{\sqrt{2}}\operatorname{sech}^2\left(\frac{\sqrt{\lambda}x}{2}\right) + \frac{4\sqrt{2}t^\beta\lambda^{5/2}\operatorname{cosech}^3\left(x\sqrt{\lambda}\right)\sinh^4\left(\frac{\sqrt{\lambda}x}{2}\right)}{\Gamma(1+\beta)}
\end{aligned}$$

$$+\frac{t^{2\beta}\lambda^4\left(9-14\cosh\left(x\sqrt{\lambda}\right)+\cosh\left(2x\sqrt{\lambda}\right)\right)\operatorname{sech}^6\left(\frac{\sqrt{\lambda}x}{2}\right)}{8\sqrt{2}\Gamma(1+2\beta)}$$
$$+\frac{96\sqrt{2}t^{\alpha+\beta}\lambda^4\operatorname{cosech}^6\left(x\sqrt{\lambda}\right)\sinh^8\left(\frac{\sqrt{\lambda}x}{2}\right)}{\Gamma(1+\alpha+\beta)}+\cdots \tag{7.89}$$

When $\alpha=1$ and $\beta=1$, the solution in Eq. (7.88) becomes

$$u(x,t)=\lambda\operatorname{sech}^2\left(\frac{\sqrt{\lambda}x}{2}\right)+\lambda^{5/2}\operatorname{sech}^2\left(\frac{\sqrt{\lambda}x}{2}\right)\tanh\left(\frac{\sqrt{\lambda}x}{2}\right)t$$
$$+\frac{\lambda^4}{4}\left(-2+\cosh\left(x\sqrt{\lambda}\right)\right)\operatorname{sech}^4\left(\frac{\sqrt{\lambda}x}{2}\right)t^2 \tag{7.90}$$
$$+\frac{\lambda^{11/2}}{24}\left(-11\sinh\left(\frac{x\sqrt{\lambda}}{2}\right)+\sinh\left(\frac{3x\sqrt{\lambda}}{2}\right)\right)\operatorname{sech}^5\left(\frac{\sqrt{\lambda}x}{2}\right)t^3+\cdots$$

When $\alpha=1$ and $\beta=1$, the solution in Eq. (7.89) becomes

$$v(x,t)=\frac{\lambda}{\sqrt{2}}\operatorname{sech}^2\left(\frac{\sqrt{\lambda}x}{2}\right)+4\sqrt{2}\lambda^{5/2}\operatorname{cosech}^3\left(x\sqrt{\lambda}\right)\sinh^4\left(\frac{\sqrt{\lambda}x}{2}\right)t$$
$$+\frac{\lambda^4\left(-2+\cosh\left(x\sqrt{\lambda}\right)\right)\operatorname{sech}^4\left(\frac{\sqrt{\lambda}x}{2}\right)t^2}{4\sqrt{2}} \tag{7.91}$$
$$+\frac{\lambda^{11/2}\left(-11\sinh\left(\frac{\sqrt{\lambda}x}{2}\right)+\sinh\left(\frac{3x\sqrt{\lambda}}{2}\right)\right)\operatorname{sech}^5\left(\frac{x\sqrt{\lambda}}{2}\right)t^3}{24\sqrt{2}}+\cdots$$

The solutions in Eqs. (7.90) and (7.91) are exactly the same as the Taylor series expansions of the exact solutions

$$u(x,t)=\lambda\operatorname{sech}^2\left(\frac{\sqrt{\lambda}(x-\lambda t)}{2}\right)$$
$$=\lambda\operatorname{sech}^2\left(\frac{\sqrt{\lambda}x}{2}\right)+\lambda^{5/2}\operatorname{sech}^2\left(\frac{\sqrt{\lambda}x}{2}\right)\tanh\left(\frac{\sqrt{\lambda}x}{2}\right)t$$
$$+\frac{\lambda^4}{4}\left(-2+\cosh\left(x\sqrt{\lambda}\right)\right)\operatorname{sech}^4\left(\frac{\sqrt{\lambda}x}{2}\right)t^2 \tag{7.92}$$
$$+\frac{\lambda^{11/2}}{24}\left(-11\sinh\left(\frac{x\sqrt{\lambda}}{2}\right)+\sinh\left(\frac{3x\sqrt{\lambda}}{2}\right)\right)\operatorname{sech}^5\left(\frac{\sqrt{\lambda}x}{2}\right)t^3+\cdots$$

$$\begin{aligned} v(x,t) &= \frac{\lambda}{\sqrt{2}}\operatorname{sech}^2\left(\frac{\sqrt{\lambda}(x-\lambda t)}{2}\right) \\ &= \frac{\lambda}{\sqrt{2}}\operatorname{sech}^2\left(\frac{\sqrt{\lambda}x}{2}\right) + 4\sqrt{2}\lambda^{5/2}\operatorname{cosech}^3\left(x\sqrt{\lambda}\right)\sinh^4\left(\frac{\sqrt{\lambda}x}{2}\right)t \\ &\quad + \frac{\lambda^4\left(-2+\cosh\left(x\sqrt{\lambda}\right)\right)\operatorname{sech}^4\left(\frac{\sqrt{\lambda}x}{2}\right)t^2}{4\sqrt{2}} \\ &\quad + \frac{\lambda^{11/2}\left(-11\sinh\left(\frac{\sqrt{\lambda}x}{2}\right)+\sinh\left(\frac{3x\sqrt{\lambda}}{2}\right)\right)\operatorname{sech}^5\left(\frac{x\sqrt{\lambda}}{2}\right)t^3}{24\sqrt{2}} + \cdots \end{aligned} \tag{7.93}$$

Again, in order to verify the efficiency and accuracy of the proposed method for the time fractional coupled KdV equations, the graphs have been drawn in Figs. 7.13, 7.14, and 7.15. The numerical solutions for Eqs. (7.90) and (7.91) for the special case where $\alpha = 1$ and $\beta = 1$ are shown in Fig. 7.13. It can be observed from Fig. 7.10 that the solutions obtained by the proposed method are exactly identical with the exact solutions. Figure 7.14 shows the numerical solutions of Eqs. (7.88) and (7.89) when $\alpha = 0.4$ and $\beta = 0.25$. Again, Fig. 7.15 cites the numerical solutions when $\alpha = 0.005$ and $\beta = 0.002$. From Figs. 7.14 and 7.15, it can be observed that the solutions for $u(x,t)$ and $v(x,t)$ bifurcate into two waves as the time fractional derivatives α and β decrease.

7.5.2 *Soliton Solutions for Time Fractional Coupled Modified KdV Equations*

In the present section, CFRDTM has been successfully implemented to determine the approximate solutions for the following coupled time fractional modified KdV equations.

Example 7.7 Consider the following time fractional coupled modified KdV equations [43]

$$D_t^{\alpha}u = \frac{1}{2}\frac{\partial^3 u}{\partial x^3} - 3u^2\frac{\partial u}{\partial x} + \frac{3}{2}\frac{\partial^2 v}{\partial x^2} + 3\frac{\partial(uv)}{\partial x} - 3\frac{\partial u}{\partial x}, \tag{7.94a}$$

$$D_t^{\beta}v = -\frac{\partial^3 v}{\partial x^3} - 3v\frac{\partial v}{\partial x} - 3\frac{\partial u}{\partial x}\frac{\partial v}{\partial x} + 3u^2\frac{\partial v}{\partial x} + 3\frac{\partial v}{\partial x}, \tag{7.94b}$$

where $t > 0$, $0 < \alpha, \beta \leq 1$, subject to the initial conditions

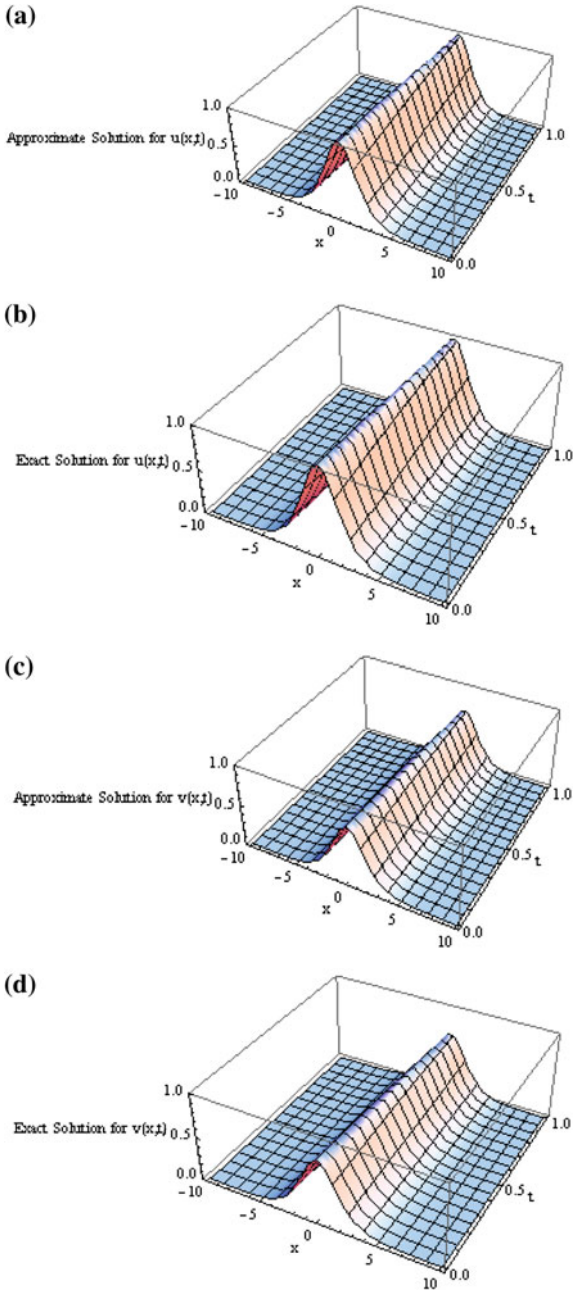

Fig. 7.13 Surfaces show **a** the numerical approximate solution of $u(x,t)$, **b** the exact solution of $u(x,t)$, **c** the numerical approximate solution of $v(x,t)$, and **d** the exact solution of $v(x,t)$ when $\alpha = 1$ and $\beta = 1$

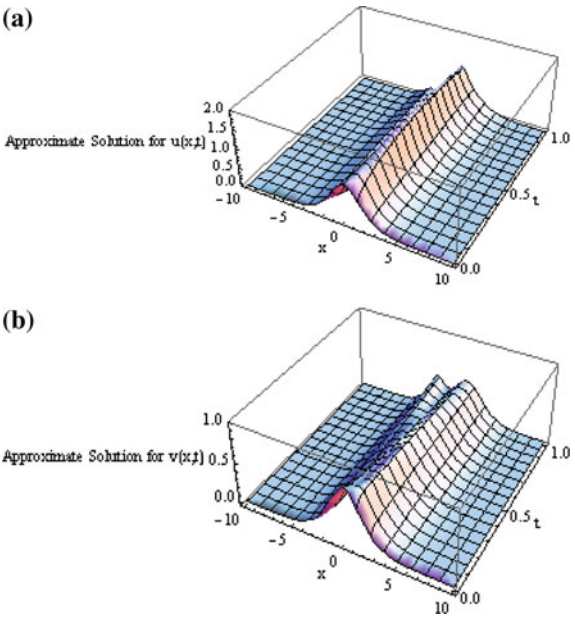

Fig. 7.14 Surfaces show **a** the numerical approximate solution of $u(x,t)$ and **b** the numerical approximate solution of $v(x,t)$ when $\alpha = 0.4$ and $\beta = 0.25$

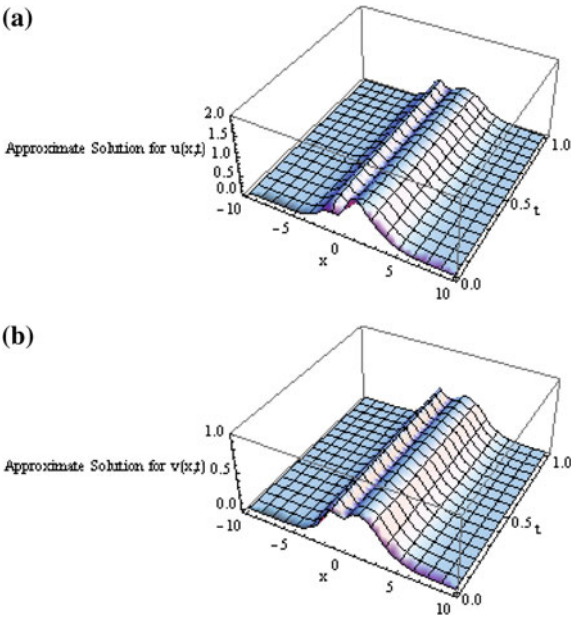

Fig. 7.15 Surfaces show **a** the numerical approximate solution of $u(x,t)$ and **b** the numerical approximate solution of $v(x,t)$ when $\alpha = 0.005$ and $\beta = 0.002$

$$u(x,0) = \frac{1}{2} + \tanh(x), \tag{7.94c}$$

$$v(x,0) = 1 + \tanh(x). \tag{7.94d}$$

The exact solutions of Eqs. (7.94a) and (7.94b), for the special case where $\alpha = \beta = 1$, are given by

$$u(x,t) = \frac{1}{2} + \tanh(x+ct), \tag{7.95a}$$

$$v(x,t) = 1 + \tanh(x+ct). \tag{7.95b}$$

In order to assess the advantages and the accuracy of the CFRDTM for solving time fractional coupled modified KdV equations. Firstly, we derive the recursive formula from Eqs. (7.94a), (7.94b). Now, $U(h,k-h)$ and $V(h,k-h)$ are considered as the coupled fractional reduced differential transform of $u(x,t)$ and $v(x,t)$, respectively, where $u(x,t)$ and $v(x,t)$ are the solutions of coupled fractional differential equations. Here, $U(0,0) = u(x,0)$, $V(0,0) = v(x,0)$ are the given initial conditions.

Without loss of generality, the following assumptions have been taken

$$U(0,j) = 0, \quad j = 1,2,3,\ldots \text{ and } V(i,0) = 0, \quad i = 1,2,3,\ldots.$$

Applying CFRDTM to Eq. (7.94a), we obtain the following recursive formula

$$\begin{aligned}\frac{\Gamma((h+1)\alpha+(k-h)\beta+1)}{\Gamma(h\alpha+(k-h)\beta+1)}U(h+1,k-h) &= \frac{1}{2}\frac{\partial^3}{\partial x^3}U(h,k-h)\\ &+ \frac{3}{2}\frac{\partial^2}{\partial x^2}V(h,k-h) - 3\frac{\partial}{\partial x}U(h,k-h)\\ &+ 3\frac{\partial}{\partial x}\left(\sum_{l=0}^{h}\sum_{s=0}^{k-h}U(h-l,s)V(l,k-h-s)\right)\\ &- 3\left(\sum_{r=0}^{h}\sum_{l=0}^{h-r}\sum_{s=0}^{k-h}\sum_{p=0}^{k-h-s}U(r,k-h-s-p)\right.\\ &\left.\times U(l,s)\frac{\partial}{\partial x}U(h-r-l,p)\right)\end{aligned} \tag{7.96}$$

From the initial condition of Eq. (7.94c), we have

$$U(0,0) = u(x,0) \tag{7.97}$$

In the same manner, we can obtain the following recursive formula from Eq. (7.94b)

$$\frac{\Gamma(h\alpha+(k-h+1)\beta+1)}{\Gamma(h\alpha+(k-h)\beta+1)}V(h,k-h+1) = -\frac{\partial^3}{\partial x^3}V(h,k-h)+3\frac{\partial}{\partial x}V(h,k-h) - 3\left(\sum_{l=0}^{h}\sum_{s=0}^{k-h}\frac{\partial}{\partial x}U(l,k-h-s)\frac{\partial}{\partial x}V(h-l,s)\right) - 3\left(\sum_{l=0}^{h}\sum_{s=0}^{k-h}V(l,k-h-s)\frac{\partial}{\partial x}V(h-l,s)\right) + 3\left(\sum_{r=0}^{h}\sum_{l=0}^{h-r}\sum_{s=0}^{k-h}\sum_{p=0}^{k-h-s}U(r,k-h-s-p) \times U(l,s)\frac{\partial}{\partial x}U(h-r-l,p)\right) \tag{7.98}$$

From the initial condition of Eq. (7.94d), we have

$$V(0,0) = v(x,0) \tag{7.99}$$

According to CFRDTM, using recursive Eq. (7.96) with initial condition Eq. (7.97) and also using recursive scheme Eq. (7.98) with initial condition Eq. (7.99) simultaneously, we obtain

$$U(1,0) = -\frac{\operatorname{sech}^2(x)}{4\Gamma(1+\alpha)},$$

$$V(0,1) = -\frac{\operatorname{sech}^2(x)}{4\Gamma(1+\beta)},$$

$$U(1,1) = \frac{3\operatorname{sech}^2(x)\tanh(x)}{4\Gamma(1+\alpha+\beta)},$$

$$V(0,2) = \frac{\operatorname{sech}^5(x)(9\cosh(x)-3\cosh(3x)+32\sinh(x)-4\sinh(3x))}{8\Gamma(1+2\beta)},$$

$$U(2,0) = -\frac{7\operatorname{sech}^2(x)\tanh(x)}{8\Gamma(1+2\alpha)},$$

$$V(1,1) = \frac{3\operatorname{sech}^5(x)(-12\cosh(x)+4\cosh(3x)-43\sinh(x)+5\sinh(3x))}{32\Gamma(1+\alpha+\beta)},$$

and so on.

The approximate solutions, obtained in the series form, are given by

$$\begin{aligned} u(x,t) &= \sum_{k=0}^{\infty}\sum_{h=0}^{k} U(h,k-h)t^{(h\alpha+(k-h)\beta)} \\ &= U(0,0) + \sum_{k=1}^{\infty}\sum_{h=1}^{k} U(h,k-h)t^{(h\alpha+(k-h)\beta)} \\ &= \frac{1}{2} + \tanh(x) - \frac{t^{\alpha}\operatorname{sech}^2(x)}{4\Gamma(1+\alpha)} - \frac{7t^{2\alpha}\operatorname{sech}^2(x)\tanh(x)}{8\Gamma(1+2\alpha)} \\ &\quad + \frac{3t^{\alpha+\beta}\operatorname{sech}^2(x)\tanh(x)}{4\Gamma(1+\alpha+\beta)} + \cdots \end{aligned} \tag{7.100}$$

$$\begin{aligned} v(x,t) &= \sum_{k=0}^{\infty}\sum_{h=0}^{k} V(h,k-h)t^{(h\alpha+(k-h)\beta)} \\ &= V(0,0) + \sum_{k=1}^{\infty}\sum_{h=0}^{k} V(h,k-h)t^{(h\alpha+(k-h)\beta)} \\ &= 1 + \tanh(x) - \frac{t^{\beta}\operatorname{sech}^2(x)}{4\Gamma(1+\beta)} \\ &\quad + \frac{t^{2\beta}\operatorname{sech}^5(x)(9\cosh(x) - 3\cosh(3x) + 32\sinh(x) - 4\sinh(3x))}{8\Gamma(1+2\beta)} \\ &\quad + \frac{3t^{\alpha+\beta}\operatorname{sech}^5(x)(-12\cosh(x) + 4\cosh(3x) - 43\sinh(x) + 5\sinh(3x))}{32\Gamma(1+\alpha+\beta)} + \ldots \end{aligned} \tag{7.101}$$

When $\alpha = 1$ and $\beta = 1$, the solution in Eq. (7.100) becomes

$$\begin{aligned} u(x,t) &= \frac{1}{2} + \tanh(x) - \frac{t\operatorname{sech}^2(x)}{4} - \frac{t^2\operatorname{sech}^2(x)\tanh(x)}{16} \\ &\quad - \frac{t^3\operatorname{sech}^4(x)(-2+\cosh(2x))}{192} + \cdots \end{aligned} \tag{7.102}$$

When $\alpha = 1$ and $\beta = 1$, the solution in Eq. (7.101) becomes

$$\begin{aligned} v(x,t) &= 1 + \tanh(x) - \frac{t\operatorname{sech}^2(x)}{4} - \frac{t^2\operatorname{sech}^2(x)\tanh(x)}{16} \\ &\quad - \frac{t^3\operatorname{sech}^4(x)(-2+\cosh(2x))}{192} + \ldots \end{aligned} \tag{7.103}$$

The solutions in Eqs. (7.102) and (7.103) are exactly the same as the Taylor series expansions of the exact solutions

$$\begin{aligned} u(x,t) &= \frac{1}{2} + \tanh\left(x - \frac{t}{4}\right) \\ &= \frac{1}{2} + \tanh(x) - \frac{t\operatorname{sech}^2(x)}{4} - \frac{t^2\operatorname{sech}^2(x)\tanh(x)}{16} \\ &\quad - \frac{t^3\operatorname{sech}^4(x)(-2+\cosh(2x))}{192} + \cdots \end{aligned} \tag{7.104}$$

$$\begin{aligned} v(x,t) &= 1 + \tanh\left(x - \frac{t}{4}\right) \\ &= 1 + \tanh(x) - \frac{t\operatorname{sech}^2(x)}{4} - \frac{t^2\operatorname{sech}^2(x)\tanh(x)}{16} \\ &\quad - \frac{t^3\operatorname{sech}^4(x)(-2+\cosh(2x))}{192} + \cdots \end{aligned} \tag{7.105}$$

In order to explore the efficiency and accuracy of the proposed method for the time fractional coupled modified KdV equations, the graphs have been drawn in Fig. 7.16a–d. The numerical solutions for Eqs. (7.102) and (7.103) for the special case where $\alpha = 1$ and $\beta = 1$ are shown in Fig. 7.16a, b. It can be observed from Fig. 7.16a–d that the solutions obtained by the proposed method coincide with the exact solution. In this case, we see that the soliton solutions are kink types for both $u(x,t)$ and $v(x,t)$.

Example 7.8 Consider the following time fractional coupled modified KdV equations [44]

$$D_t^{\alpha} u = \frac{1}{2}\frac{\partial^3 u}{\partial x^3} - 3u^2\frac{\partial u}{\partial x} + \frac{3}{2}\frac{\partial^2 v}{\partial x^2} + 3\frac{\partial(uv)}{\partial x} + 3\frac{\partial u}{\partial x}, \tag{7.106a}$$

$$D_t^{\beta} v = -\frac{\partial^3 v}{\partial x^3} - 3v\frac{\partial v}{\partial x} - 3\frac{\partial u}{\partial x}\frac{\partial v}{\partial x} + 3u^2\frac{\partial v}{\partial x} - 3\frac{\partial v}{\partial x}, \tag{7.106b}$$

where $t > 0$, $0 < \alpha, \beta \leq 1$, subject to the initial conditions

$$u(x,0) = \tanh(x), \tag{7.106c}$$

$$v(x,0) = 1 - 2\tanh^2(x). \tag{7.106d}$$

The exact solutions of Eqs. (7.106a) and (7.106b) obtained by Adomian decomposition method, for the special case where $\alpha = \beta = 1$, are given by

$$u(x,t) = \tanh(x - t), \tag{7.107a}$$

$$v(x,t) = 1 - 2\tanh^2(x - t). \tag{7.107b}$$

In order to assess the advantages and the accuracy of the CFRDTM for solving time fractional coupled modified KdV equations, firstly we derive the recursive formula

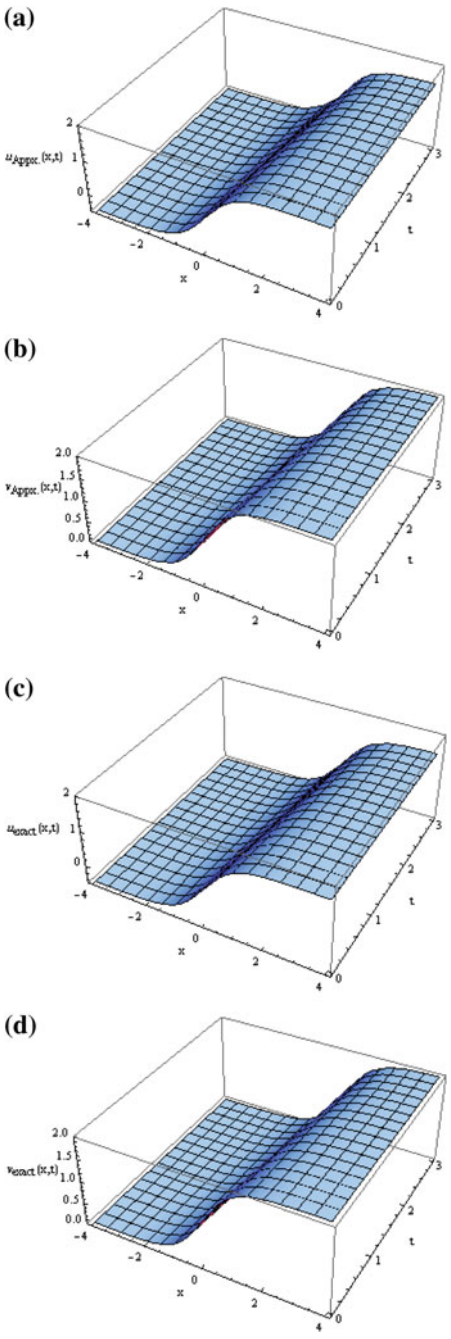

Fig. 7.16 Surfaces show **a** the numerical approximate solution of $u(x,t)$, **b** the numerical approximate solution of $v(x,t)$, **c** the exact solution of $u(x,t)$, and **d** the exact solution of $v(x,t)$ when $\alpha = 1$ and $\beta = 1$

from Eqs. (7.106a), (7.106b). Now, $U(h,k-h)$ and $V(h,k-h)$ are considered as the coupled fractional reduced differential transform of $u(x,t)$ and $v(x,t)$, respectively, where $u(x,t)$ and $v(x,t)$ are the solutions of coupled fractional differential equations. Here, $U(0,0)=u(x,0)$, $V(0,0)=v(x,0)$ are the given initial conditions.

Without loss of generality, the following assumptions have been taken

$$U(0,j)=0,\ \ j=1,2,3,\ldots \text{ and } V(i,0)=0,\ \ i=1,2,3,\ldots.$$

Applying CFRDTM to Eq. (7.106a), we obtain the following recursive formula

$$\begin{aligned}\frac{\Gamma((h+1)\alpha+(k-h)\beta+1)}{\Gamma(h\alpha+(k-h)\beta+1)}U(h+1,k-h) &= \frac{1}{2}\frac{\partial^3}{\partial x^3}U(h,k-h)\\ &+\frac{3}{2}\frac{\partial^2}{\partial x^2}V(h,k-h)+3\frac{\partial}{\partial x}U(h,k-h)\\ &+3\frac{\partial}{\partial x}\left(\sum_{l=0}^{h}\sum_{s=0}^{k-h}U(h-l,s)V(l,k-h-s)\right)\\ &-3\left(\sum_{r=0}^{h}\sum_{l=0}^{h-r}\sum_{s=0}^{k-h}\sum_{p=0}^{k-h-s}U(r,k-h-s-p)\right.\\ &\left.\times U(l,s)\frac{\partial}{\partial x}U(h-r-l,p)\right)\end{aligned} \tag{7.108}$$

From the initial condition of Eq. (7.106c), we have

$$U(0,0)=u(x,0) \tag{7.109}$$

In the same manner, we can obtain the following recursive formula from Eq. (7.106b)

$$\begin{aligned}\frac{\Gamma(h\alpha+(k-h+1)\beta+1)}{\Gamma(h\alpha+(k-h)\beta+1)}V(h,k-h+1) &= -\frac{\partial^3}{\partial x^3}V(h,k-h)-3\frac{\partial}{\partial x}V(h,k-h)\\ &-3\left(\sum_{l=0}^{h}\sum_{s=0}^{k-h}\frac{\partial}{\partial x}U(l,k-h-s)\frac{\partial}{\partial x}V(h-l,s)\right)\\ &-3\left(\sum_{l=0}^{h}\sum_{s=0}^{k-h}V(l,k-h-s)\frac{\partial}{\partial x}V(h-l,s)\right)\\ &+3\left(\sum_{r=0}^{h}\sum_{l=0}^{h-r}\sum_{s=0}^{k-h}\sum_{p=0}^{k-h-s}U(r,k-h-s-p)\right.\\ &\left.\times U(l,s)\frac{\partial}{\partial x}U(h-r-l,p)\right)\end{aligned} \tag{7.110}$$

From the initial condition of Eq. (7.106d), we have

$$V(0,0) = v(x,0) \tag{7.111}$$

According to CFRDTM, using recursive Eq. (7.108) with initial condition Eq. (7.109) and also using recursive scheme Eq. (7.110) with initial condition Eq. (7.111) simultaneously, we obtain

$$U(1,0) = -\frac{\operatorname{sech}^2(x)}{\Gamma(1+\alpha)}$$

$$V(0,1) = \frac{4\operatorname{sech}^2(x)\tanh(x)}{\Gamma(1+\beta)}$$

$$U(1,1) = -\frac{24\operatorname{sech}^4(x)\tanh(x)}{\Gamma(1+\alpha+\beta)}$$

$$V(0,2) = \frac{\operatorname{sech}^6(x)(21 - 26\cosh(2x) + \cosh(4x))}{\Gamma(1+2\beta)}$$

$$U(2,0) = -\frac{(-23 + \cosh(2x))\operatorname{sech}^4(x)\tanh(x)}{\Gamma(1+2\alpha)}$$

$$V(1,1) = \frac{48\operatorname{sech}^4(x)\tanh^2(x)}{\Gamma(1+\alpha+\beta)},$$

and so on.

The approximate solutions, obtained in the series form, are given by

$$\begin{aligned} u(x,t) &= \sum_{k=0}^{\infty}\sum_{h=0}^{k} U(h,k-h)t^{(h\alpha+(k-h)\beta)} \\ &= U(0,0) + \sum_{k=1}^{\infty}\sum_{h=1}^{k} U(h,k-h)t^{(h\alpha+(k-h)\beta)} \\ &= \tanh(x) - \frac{t^{\alpha}\operatorname{sech}^2(x)}{\Gamma(1+\alpha)} - \frac{t^{2\alpha}(-23+\cosh(2x))\operatorname{sech}^4(x)\tanh(x)}{\Gamma(1+2\alpha)} \\ &\quad - \frac{24t^{\alpha+\beta}\operatorname{sech}^4(x)\tanh(x)}{\Gamma(1+\alpha+\beta)} + \cdots \end{aligned} \tag{7.112}$$

$$\begin{aligned} v(x,t) &= \sum_{k=0}^{\infty}\sum_{h=0}^{k} V(h,k-h)t^{(h\alpha+(k-h)\beta)} \\ &= V(0,0) + \sum_{k=1}^{\infty}\sum_{h=0}^{k} V(h,k-h)t^{(h\alpha+(k-h)\beta)} \\ &= 1 - 2\tanh^2(x) + \frac{4t^{\beta}\operatorname{sech}^2(x)\tanh(x)}{\Gamma(1+\beta)} \\ &\quad + \frac{t^{2\beta}\operatorname{sech}^6(x)(21 - 26\cosh(2x) + \cosh(4x))}{\Gamma(1+2\beta)} \\ &\quad + \frac{48t^{\alpha+\beta}\operatorname{sech}^4(x)\tanh^2(x)}{\Gamma(1+\alpha+\beta)} + \cdots \end{aligned} \tag{7.113}$$

When $\alpha = 1$ and $\beta = 1$, the solution in Eq. (7.112) becomes

$$\begin{aligned} u(x,t) &= \tanh(x) - t\operatorname{sech}^2(x) - t^2\operatorname{sech}^2(x)\tanh(x) \\ &\quad - \frac{t^3\operatorname{sech}^4(x)(-2+\cosh(2x))}{3} + \cdots \end{aligned} \tag{7.114}$$

When $\alpha = 1$ and $\beta = 1$, the solution in Eq. (7.113) becomes

$$\begin{aligned} v(x,t) &= 1 - 2\tanh^2(x) + 4t\operatorname{sech}^2(x)\tanh(x) + 2t^2\operatorname{sech}^4(x)(-2+\cosh(2x)) \\ &\quad + \frac{2t^3\operatorname{sech}^5(x)(-11\sinh(x) + \sinh(3x))}{3} + \cdots \end{aligned} \tag{7.115}$$

The solutions in Eqs. (7.114) and (7.115) are exactly the same as the Taylor series expansions of the exact solutions

$$\begin{aligned} u(x,t) &= \tanh(x-t) \\ &= \tanh(x) - t\operatorname{sech}^2(x) - t^2\operatorname{sech}^2(x)\tanh(x) \\ &\quad - \frac{t^3\operatorname{sech}^4(x)(-2+\cosh(2x))}{3} + \cdots \end{aligned} \tag{7.116}$$

$$\begin{aligned} v(x,t) &= 1 - 2\tanh^2(x-t) \\ &= 1 - 2\tanh^2(x) + 4t\operatorname{sech}^2(x)\tanh(x) \\ &\quad + 2t^2\operatorname{sech}^4(x)(-2+\cosh(2x) \\ &\quad + \frac{2t^3\operatorname{sech}^5(x)(-11\sinh(x) + \sinh(3x))}{3} + \cdots \end{aligned} \tag{7.117}$$

Again, in order to verify the efficiency and reliability of the proposed method for the time fractional coupled modified KdV equations, the graphs have been drawn in Fig. 7.17a–d. The numerical solutions for Eqs. (7.114) and (7.115) for the special

case where $\alpha = 1$ and $\beta = 1$ are shown in Fig. 7.17a–d. It can be observed from Fig. 7.17a–d that the soliton solutions obtained by the proposed method are exactly identical with the exact solutions. In this case, we see that the soliton solutions are kink type for $u(x,t)$ and bell type for $v(x,t)$.

Verification of Classical Integer-Order Solutions by ADM

In case of $\alpha = 1$ and $\beta = 1$, to solve Eqs. (7.106a) and (7.106b) by means of Adomian decomposition method (ADM), we rewrite Eqs. (7.106a) and (7.106b) in an operator form

$$L_t u = \frac{1}{2}\frac{\partial^3 u}{\partial x^3} - 3A(u) + \frac{3}{2}\frac{\partial^2 v}{\partial x^2} + 3B(u,v) + 3\frac{\partial u}{\partial x}, \tag{7.118}$$

$$L_t v = -\frac{\partial^3 v}{\partial x^3} - 3C(v) - 3G(u,v) + 3H(u,v) - 3\frac{\partial v}{\partial x}, \tag{7.119}$$

where $L_t \equiv \frac{\partial}{\partial t}$ is the easily invertible linear differential operator with its inverse operator $L_t^{-1}(.) \equiv \int_0^t (.)\mathrm{d}\tau$. Here, the functions $A(u) = u^2\frac{\partial u}{\partial x}$, $B(u,v) = \frac{\partial (uv)}{\partial x}$, $C(v) = v\frac{\partial v}{\partial x}$, $G(u,v) = \frac{\partial u}{\partial x}\frac{\partial v}{\partial x}$, and $H(u,v) = u^2\frac{\partial v}{\partial x}$ are related to the nonlinear terms and they can be expressed in terms of the Adomian polynomials as follows:

$A(u) = \sum_{n=0}^{\infty} A_n$, $B(u,v) = \sum_{n=0}^{\infty} B_n$, $C(v) = \sum_{n=0}^{\infty} C_n$, $G(u,v) = \sum_{n=0}^{\infty} G_n$, and $H(u,v) = \sum_{n=0}^{\infty} H_n$. In particular, for nonlinear operators $A(u)$ and $B(u,v)$, the Adomian polynomials are defined by

$$A_n = \frac{1}{n!}\frac{d^n}{d\lambda^n}\left[A\left(\sum_{k=0}^{\infty}\lambda^k u_k\right)\right]\Bigg|_{\lambda=0}, \quad n \geq 0$$

$$B_n = \frac{1}{n!}\frac{d^n}{d\lambda^n}\left[B\left(\sum_{k=0}^{\infty}\lambda^k u_k, \sum_{k=0}^{\infty}\lambda^k v_k\right)\right]\Bigg|_{\lambda=0}, \quad n \geq 0$$

The first few components of $A(u)$, $B(u,v)$, $C(v)$, $G(u,v)$, and $H(u,v)$ are, respectively, given by

$$A_0 = u_0^2 u_{0x},$$

$$A_1 = u_0^2 u_{1x} + 2u_0 u_1 u_{0x},$$

$$A_2 = u_{0x}(2u_0 u_2 + u_1^2) + u_0^2 u_{2x} + 2u_0 u_1 u_{1x}$$

$$\ldots,$$

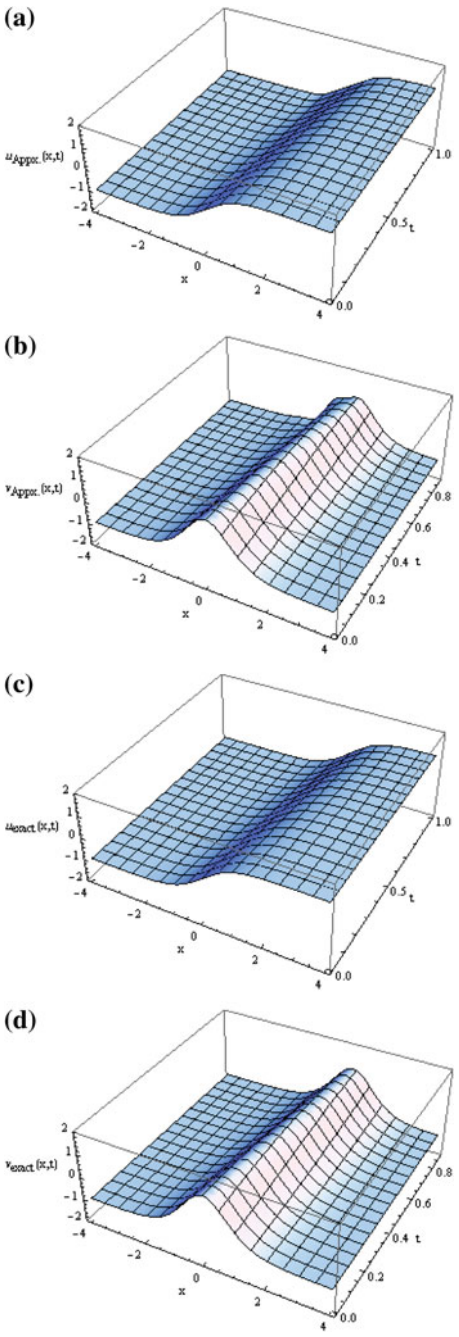

Fig. 7.17 Surfaces show **a** the numerical approximate solution of $u(x,t)$, **b** the numerical approximate solution of $v(x,t)$, **c** the exact solution of $u(x,t)$, and **d** the exact solution of $v(x,t)$ when $\alpha = 1$ and $\beta = 1$

$$B_0 = u_0 v_{0x} + v_0 u_{0x},$$

$$B_1 = u_0 v_{1x} + v_1 u_{0x} + u_1 v_{0x} + v_0 u_{1x},$$

$$B_2 = u_0 v_{2x} + v_2 u_{0x} + u_1 v_{1x} + v_1 u_{1x} + u_2 v_{0x} + v_0 u_{2x},$$

$$\ldots,$$

$$C_0 = v_0 v_{0x},$$

$$C_1 = v_0 v_{1x} + v_1 v_{0x},$$

$$C_2 = v_1 v_{1x} + v_0 v_{2x} + v_2 v_{0x},$$

$$\ldots,$$

$$G_0 = u_{0x} v_{0x},$$

$$G_1 = u_{0x} v_{1x} + v_{0x} u_{1x},$$

$$G_2 = u_{1x} v_{1x} + v_{0x} u_{2x} + u_{0x} v_{2x},$$

$$\ldots,$$

$$H_0 = u_0^2 v_{0x},$$

$$H_1 = u_0^2 v_{1x} + 2u_0 u_1 v_{0x},$$

$$H_2 = v_{0x}(2u_0 u_2 + u_1^2) + u_0^2 v_{2x} + 2u_0 u_1 v_{1x},$$

$$\ldots,$$

and so on, and the rest of the polynomials can be constructed in a similar manner.

Now, operating with L_t^{-1} on the both sides of Eqs. (7.118) and (7.119), yields

$$u(x,t) = u(x,0) + L_t^{-1}\left(\frac{1}{2}\frac{\partial^3 u}{\partial x^3} - 3A(u) + \frac{3}{2}\frac{\partial^2 v}{\partial x^2} + 3B(u,v) + 3\frac{\partial u}{\partial x}\right), \quad (7.120)$$

$$v(x,t) = v(x,0) + L_t^{-1}\left(-\frac{\partial^3 v}{\partial x^3} - 3C(v) - 3G(u,v) + 3H(u,v) - 3\frac{\partial v}{\partial x}\right). \quad (7.121)$$

The ADM assumes that the two unknown functions $u(x,t)$ and $v(x,t)$ can be expressed by infinite series in the following forms

$$u(x,t) = \sum_{n=0}^{\infty} u_n(x,t), \tag{7.122}$$

$$v(x,t) = \sum_{n=0}^{\infty} v_n(x,t). \tag{7.123}$$

Substituting Eqs. (7.122) and (7.123) into Eqs. (7.120) and (7.121) yields

$$u_0(x,t) = u(x,0),$$

$$u_{n+1}(x,t) = L_t^{-1}\left(\frac{1}{2}\frac{\partial^3 u_n(x,t)}{\partial x^3} - 3A_n + \frac{3}{2}\frac{\partial^2 v_n(x,t)}{\partial x^2} + 3B_n + 3\frac{\partial u_n(x,t)}{\partial x}\right), \quad n \geq 0. \tag{7.124}$$

$$v_0(x,t) = v(x,0),$$

$$v_{n+1}(x,t) = L_t^{-1}\left(-\frac{\partial^3 v_n(x,t)}{\partial x^3} - 3C_n - 3G_n + 3H_n - 3\frac{\partial v_n(x,t)}{\partial x}\right), \quad n \geq 0. \tag{7.125}$$

Using known $u_0(x,t)$ and $v_0(x,t)$, all the remaining components $u_n(x,t)$ and $v_n(x,t)$, $n > 0$ can be completely determined such that each term is determined by using the previous term. From Eqs. (7.124) and (7.125) with Eqs. (7.106c) and (7.106d), we determine the individual components of the decomposition series as

$$u_0 = \tanh(x),$$

$$v_0 = 1 - 2\tanh^2(x),$$

$$u_1 = -t\,\mathrm{sech}^2(x),$$

$$v_1 = 4t\,\mathrm{sech}^2(x)\tanh(x),$$

$$u_2 = -t^2\,\mathrm{sech}^2(x)\tanh(x),$$

$$v_2 = 2t^2(-2 + \cosh(2x))\mathrm{sech}^4(x),$$

$$u_3 = -\frac{1}{3}t^3(-2 + \cosh(2x))\mathrm{sech}^4(x),$$

$$v_3 = \frac{2}{3}t^3\,\mathrm{sech}^5(x)(-11\sinh(x) + \sinh(3x)),$$

and so on, and the other components of the decomposition series (7.122) and (7.123) can be determined in a similar way.

Substituting these $u_0, u_1, u_2, \ldots$ and $v_0, v_1, v_2, \ldots$ in Eqs. (7.122) and (7.123), respectively, gives the ADM solutions for $u(x,t)$ and $v(x,t)$ in a series form

$$\begin{aligned} u(x,t) = {} & \tanh(x) - t\operatorname{sech}^2(x) - t^2\operatorname{sech}^2(x)\tanh(x) \\ & - \frac{1}{3}t^3(-2+\cosh(2x))\operatorname{sech}^4(x) + \cdots, \end{aligned} \tag{7.126}$$

$$\begin{aligned} v(x,t) = {} & 1 - 2\tanh^2(x) + 4t\operatorname{sech}^2(x)\tanh(x) \\ & + 2t^2(-2+\cosh(2x))\operatorname{sech}^4(x) \\ & + \frac{2}{3}t^3\operatorname{sech}^5(x)(-11\sinh(x) + \sinh(3x)) + \cdots. \end{aligned} \tag{7.127}$$

Using Taylor series, we obtain the closed-form solutions

$$u(x,t) = \tanh(x-t), \tag{7.128}$$

$$v(x,t) = 1 - 2\tanh^2(x-t). \tag{7.129}$$

With initial conditions (7.106c) and (7.106d), the solitary wave solutions of Eqs. (7.118) and (7.119) are of kink type for $u(x,t)$ and bell type for $v(x,t)$ which agree to some extent with the results constructed by Fan [44]. According to the learned author Fan [44], the solitary wave solutions of Eqs. (7.118) and (7.119) are kink type for $u(x,t) = \tanh\left(x + \frac{t}{2}\right)$ and bell type for $v(x,t) = \frac{3}{2} - 2\tanh^2\left(x + \frac{t}{2}\right)$, where $k = 1$ and $\lambda = -1$. There is definitely a mistake to be reckoned with and should be taken into account for further study. Since using the same parameters $k = 1$ and $\lambda = -1$, the solitary wave solutions of Eqs. (7.118) and (7.119) have been obtained as in Eqs. (7.128) and (7.129).

In the present analysis, the two methods coupled fractional reduced differential transform and Adomian decomposition method confirm the justification and correctness of the solutions obtained in Eqs. (7.128) and (7.129).

7.5.3 *Approximate Solution for Fractional Predator–Prey Equation*

In order to assess the advantages and the accuracy of the CFRDTM, we consider three cases with different initial conditions of the predator–prey system [54]. Firstly, we derive the recursive formula obtained from predator–prey system of Eqs. (7.10)–(7.11). Now, $U(h, k-h)$ and $V(h, k-h)$ are considered as the coupled fractional reduced differential transform of $u(x,y,t)$ and $v(x,y,t)$, respectively, where $u(x,y,t)$ and $v(x,y,t)$ are the solutions of coupled fractional differential

equations. Here, $U(0,0) = u(x,y,0)$, $V(0,0) = v(x,y,0)$ are the given initial conditions. Without loss of generality, the following assumptions have taken

$$U(0,j) = 0, \quad j = 1,2,3,\ldots \text{ and } V(i,0) = 0, \quad i = 1,2,3,\ldots.$$

Applying CFRDTM to Eq. (7.10), we obtain the following recursive formula

$$\frac{\Gamma((h+1)\alpha+(k-h)\beta+1)}{\Gamma(h\alpha+(k-h)\beta+1)}U(h+1,k-h) = \frac{\partial^2}{\partial x^2}U(h,k-h) + \frac{\partial^2}{\partial y^2}U(h,k-h) + aU(h,k-h) - b\left(\sum_{l=0}^{h}\sum_{s=0}^{k-h}U(h-l,s)V(l,k-h-s)\right). \tag{7.130}$$

From the initial condition of Eq. (7.10), we have

$$U(0,0) = u(x,y,0). \tag{7.131}$$

In the same manner, we can obtain the following recursive formula from Eq. (7.11)

$$\frac{\Gamma(h\alpha+(k-h+1)\beta+1)}{\Gamma(h\alpha+(k-h)\beta+1)}V(h,k-h+1) = \frac{\partial^2}{\partial x^2}V(h,k-h) + \frac{\partial^2}{\partial y^2}V(h,k-h) + b\left(\sum_{l=0}^{h}\sum_{s=0}^{k-h}U(l,k-h-s)V(h-l,s)\right) - cV(h,k-h). \tag{7.132}$$

From the initial condition of Eq. (7.11), we have

$$V(0,0) = v(x,y,0). \tag{7.133}$$

Applications and Results

Now, let us consider the three cases of the predator–prey system.

Case 1: Here, we consider the fractional predator–prey equation with constant initial condition

$$u(x,y,0) = u_0, \quad v(x,y,0) = v_0 \tag{7.134}$$

According to CFRDTM, using recursive scheme Eq. (7.130) with initial condition Eq. (7.131) and also using recursive scheme Eq. (7.132) with initial condition Eq. (7.133) simultaneously, we obtain

$$U[0,0] = u(x,y,0) = u_0, \quad V[0,0] = v(x,y,0) = v_0,$$

$$U[1,0] = \frac{u_0(a - bv_0)}{\Gamma(1+\alpha)}, \quad V[0,1] = \frac{(bu_0v_0 - cv_0)}{\Gamma(1+\beta)},$$

$$U[2,0] = \frac{u_0(a - bv_0)^2}{\Gamma(1+2\alpha)},$$

$$V[0,2] = \frac{v_0(c - bu_0)^2}{\Gamma(1+2\beta)},$$

$$U[1,1] = -\frac{bu_0(-cv_0 + bu_0v_0)}{\Gamma(1+\alpha+\beta)},$$

$$V[1,1] = \frac{bu_0v_0(a - bv_0)}{\Gamma(1+\alpha+\beta)},$$

$$U[1,2] = -\frac{b(c - bu_0)^2u_0v_0}{\Gamma(1+\alpha+2\beta)},$$

$$V[1,2] = \frac{bu_0(c - bu_0)v_0(-(a - 2bv_0)\Gamma(1+\alpha)\Gamma(1+\beta) + (-a + bv_0)\Gamma(1+\alpha+\beta))}{\Gamma(1+\alpha+2\beta)\Gamma(1+\alpha)\Gamma(1+\beta)},$$

$$U[2,1] = \frac{bu_0v_0(a - bv_0)((c - 2bu_0)\Gamma(1+\alpha)\Gamma(1+\beta) + (c - bu_0)\Gamma(1+\alpha+\beta))}{\Gamma(1+2\alpha+\beta)\Gamma(1+\alpha)\Gamma(1+\beta)},$$

$$V[2,1] = \frac{bu_0v_0(a - bv_0)^2}{\Gamma(1+2\alpha+\beta)},$$

$$U[3,0] = \frac{u_0(a - bv_0)^3}{\Gamma(1+3\alpha)},$$

$$V[0,3] = -\frac{v_0(c - bu_0)^3}{\Gamma(1+3\beta)},$$

and so on.

The approximate solutions, obtained in the series form, are given by

$$\begin{aligned} u(x,y,t) &= U(0,0) + \sum_{k=1}^{\infty}\sum_{h=1}^{k} U(h,k-h)t^{(h\alpha+(k-h)\beta)} \\ &= u_0 + \frac{u_0(a-bv_0)t^{\alpha}}{\Gamma(1+\alpha)} + \frac{u_0(a-bv_0)^2t^{2\alpha}}{\Gamma(1+2\alpha)} \\ &\quad + \frac{u_0(a-bv_0)^3t^{3\alpha}}{\Gamma(1+3\alpha)} - \frac{bu_0(-cv_0+bu_0v_0)t^{\alpha+\beta}}{\Gamma(1+\alpha+\beta)} + \cdots \end{aligned} \tag{7.135}$$

$$\begin{aligned} v(x,y,t) &= V(0,0) + \sum_{k=1}^{\infty}\sum_{h=0}^{k} V(h,k-h)t^{(h\alpha+(k-h)\beta)} \\ &= v_0 + \frac{(bu_0v_0-cv_0)t^{\beta}}{\Gamma(1+\beta)} + \frac{bu_0v_0(a-bv_0)t^{\alpha+\beta}}{\Gamma(1+\alpha+\beta)} \\ &\quad + \frac{bu_0v_0(a-bv_0)^2t^{2\alpha+\beta}}{\Gamma(1+2\alpha+\beta)}\cdots. \end{aligned} \tag{7.136}$$

Figure 7.18 cites the numerical solutions for Eqs. (7.10)–(7.11) obtained by the proposed CFRDTM method for the constant initial conditions $u_0 = 100$, $v_0 = 10$, $a = 0.05$, $b = 0.03$, and $c = 0.01$. Figure 7.19 shows the time evolution of population of $u(x,y,t)$ and $v(x,y,t)$ obtained from Eqs. (5.2) to (5.3) for different values of α and β. In the present numerical analysis, Table 7.2 shows the comparison of the numerical solutions with the proposed method with homotopy perturbation method and variational iteration method, when $a = 0.05$, $b = 0.03$, and $c = 0.01$. From Table 7.2, it is evidently clear that CFRDTM used in this paper has high accuracy. The numerical results obtained in this proposed method coincide precisely with values obtained in the homotopy perturbation method.

Case 2: In this case, the initial conditions of Eqs. (7.10)–(7.11) are given by

$$u(x,y,0) = \mathrm{e}^{x+y}, v(x,y,0) = \mathrm{e}^{x+y}. \tag{7.137}$$

By using Eqs. (7.130) to (7.133), we can successively obtain

$$U[0,0] = u(x,y,0) = \mathrm{e}^{x+y}, V[0,0] = v(x,y,0) = \mathrm{e}^{x+y},$$

$$U[1,0] = \frac{2\mathrm{e}^{x+y} + a\mathrm{e}^{x+y} - b\mathrm{e}^{2x+2y}}{\Gamma(1+\alpha)},$$

$$V[0,1] = \frac{2\mathrm{e}^{x+y} - c\mathrm{e}^{x+y} + b\mathrm{e}^{2x+2y}}{\Gamma(1+\beta)},$$

$$U[1,1]=\frac{be^{2(x+y)}(2-c+be^{x+y})}{\Gamma(1+\alpha+\beta)},$$

$$V[1,1]=-\frac{be^{2(x+y)}(-2-a+be^{x+y})}{\Gamma(1+\alpha+\beta)},$$

$$U[2,0]=\frac{e^{x+y}(4+a^2-10be^{x+y}+b^2e^{2(x+y)}+a(4-2be^{x+y}))}{\Gamma(1+2\alpha)},$$

$$V[0,2]=\frac{e^{x+y}(4+c^2+10be^{x+y}+b^2e^{2(x+y)}-2c(2+be^{x+y}))}{\Gamma(1+2\beta)},$$

$$U[1,2]=-\frac{be^{2(x+y)}(4+c^2+10be^{x+y}+b^2e^{2(x+y)}-2c(2+be^{x+y}))}{\Gamma(1+\alpha+\beta)},$$

$$\begin{aligned}V[1,2]=&(be^{2(x+y)}(-(a(-8+c-be^{x+y})+2(-8+c+9be^{x+y}\\&-bce^{x+y}+b^2e^{2(x+y)}))\Gamma(1+\alpha)\Gamma(1+\beta)\\&+(2+a-be^{x+y})(2-c+be^{x+y})\\&\times\Gamma(1+\alpha+\beta))/(\Gamma(1+\alpha)\Gamma(1+\beta)\Gamma(1+\alpha+2\beta)),\end{aligned}$$

$$U[3,0]=\frac{e^{x+y}(8+a^3-84be^{x+y}+28b^2e^{2(x+y)}-b^3e^{3(x+y)}+a^2(6-3be^{x+y})+3a(4-10be^{x+y}+b^2e^{2(x+y)}))}{\Gamma(1+3\alpha)},$$

$$V[0,3]=\frac{e^{x+y}(8-c^3+84be^{x+y}+28b^2e^{2(x+y)}+b^3e^{3(x+y)}+3c^2(2+be^{x+y})-3c(4+10be^{x+y}+b^2e^{2(x+y)}))}{\Gamma(1+3\beta)},$$

and so on.

The explicit approximate solution is

$$\begin{aligned}u(x,y,t)=&e^{x+y}+\frac{(2e^{x+y}+ae^{x+y}-be^{2x+2y})t^{\alpha}}{\Gamma(1+\alpha)}\\&+\frac{e^{x+y}(4+a^2-10be^{x+y}+b^2e^{2(x+y)}+a(4-2be^{x+y}))t^{2\alpha}}{\Gamma(1+2\alpha)}+\cdots,\end{aligned}\tag{7.138}$$

and

$$\begin{aligned}v(x,y,t)=&e^{x+y}+\frac{(2e^{x+y}-ce^{x+y}+be^{2x+2y})t^{\beta}}{\Gamma(1+\beta)}\\&-\frac{be^{2(x+y)}(-2-a+be^{x+y})t^{\alpha+\beta}}{\Gamma(1+\alpha+\beta)}+\cdots,\end{aligned}\tag{7.139}$$

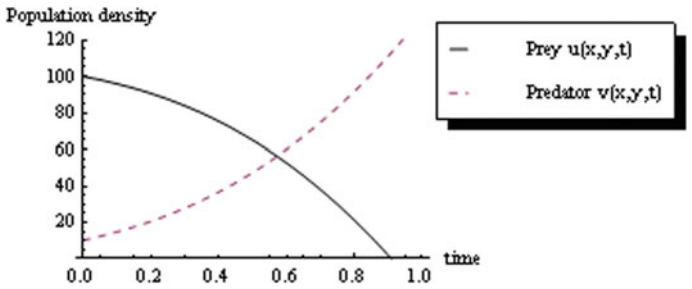

Fig. 7.18 Time evolution of the population for $u(x, y, t)$ and $v(x, y, t)$ obtained from Eqs. (7.135) and (7.136), when $\alpha = 1,\ \beta = 1$

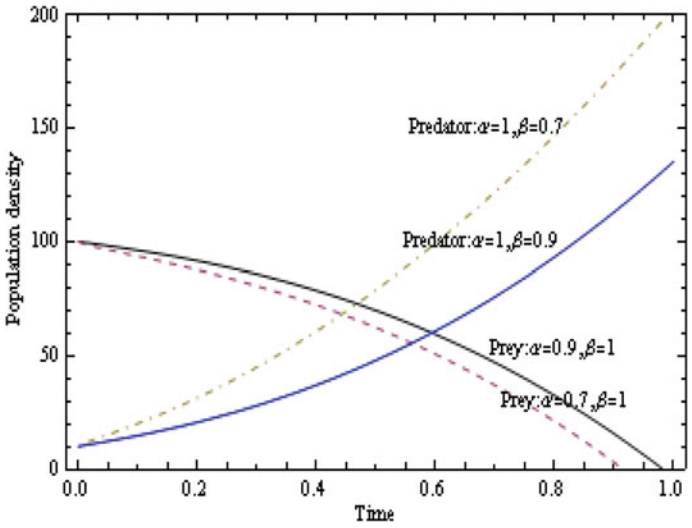

Fig. 7.19 Time evolution of the population for $u(x, y, t)$ and $v(x, y, t)$ obtained from Eqs. (7.135) and (7.136) for different values of α and β

Table 7.2 Comparison of the numerical solutions of the proposed method with homotopy perturbation method and variational iteration method

T	$\alpha = \beta$	Numerical value (u, v) by HPM	Numerical value (u, v) by VIM	Numerical value (u, v) by CFRDTM
0.02	1 0.9	(99.4831, 10.6146) (99.1865, 10.9633)	(99. 4834, 10.6323) (99.3065, 10. 8375)	(99.4831, 10.6146) (99.1865, 10.9633)
0.2	1 0.9	(93.0910, 17.8514) (90.5735, 20.5567)	(93. 3908, 17.7382) (92.4584, 18.8198)	(93.0910, 17.8514) (90.5735, 20.5567)
0.3	1 0.9	(87.9348, 23.4430) (83.7993, 27.7785)	(88. 9466, 22. 7237) (87. 8005, 24.0532)	(87.9348, 23.4430) (83.7993, 27.7785)

Figures 7.20 and 7.21 cite the numerical approximate solutions for the predator–prey system with the appropriate parameter. The obtained results of predator–prey population system indicate that this model exhibits the same behavior observed in the anomalous biological diffusion fractional model.

Figures 7.22 and 7.23 show the numerical solutions for prey population density for different values of parameters a, b, i.e., the natural birthrate of prey population and competitive rate between predator and prey populations. The results depicted in graphs agree with the realistic data.

Case 3: In this case, we consider the initial condition of fractional predator–prey Eqs. (7.10)–(7.11)

$$U[0,0] = u(x,y,0) = \sqrt{xy}, \quad V[0,0] = v(x,y,0) = \mathrm{e}^{x+y}, \tag{7.140}$$

$$U[1,0] = \frac{-\frac{x^2}{4(xy)^{3/2}} - \frac{y^2}{4(xy)^{3/2}} + a\sqrt{xy} - b\mathrm{e}^{x+y}\sqrt{xy}}{\Gamma(1+\alpha)},$$

$$V[0,1] = \frac{2\mathrm{e}^{x+y} - c\mathrm{e}^{x+y} + b\mathrm{e}^{x+y}\sqrt{xy}}{\Gamma(1+\beta)},$$

$$U[1,1] = \frac{b\mathrm{e}^{x+y}\sqrt{xy}(2-c+b\sqrt{xy})}{\Gamma(1+\alpha+\beta)},$$

$$V[1,1] = \frac{-b\mathrm{e}^{x+y}(y^2+x^2(1-4ay^2+4b\mathrm{e}^{x+y}y^2))}{4(xy)^{3/2}\Gamma(1+\alpha+\beta)},$$

$$\begin{aligned} U[2,0] = {} & \frac{1}{16x^4y^4\Gamma(1+2\alpha)}\sqrt{xy}\big(-15y^4 - 16b\mathrm{e}^{x+y}x^3y^4 + x^2(2y^2 - 8(a - b\mathrm{e}^{x+y})y^4\big) \\ & + x^4(-15 + 16a^2y^4 + 16b^2\mathrm{e}^{2(x+y)}y^4 \\ & - 8b\mathrm{e}^{x+y}y^2(-1+2y+4y^2) - 8ay^2(1+4b\mathrm{e}^{x+y}y^2))), \end{aligned}$$

$$V[0,2] = \frac{\mathrm{e}^{x+y}(4(-2+c)^2(xy)^{3/2} + 4b^2(xy)^{5/2} - b(y^2 - 4xy^2 + x^2(1-4y+8(-2+c)y^2)))}{4(xy)^{3/2}\Gamma(1+2\beta)},$$

and so on.

The solution becomes

$$u(x,y,t) = \sqrt{xy} + \frac{\left(-\frac{x^2}{4(xy)^{3/2}} - \frac{y^2}{4(xy)^{3/2}} + a\sqrt{xy} - b\mathrm{e}^{x+y}\sqrt{xy}\right)t^{\alpha}}{\Gamma(1+\alpha)} + \cdots, \tag{7.141}$$

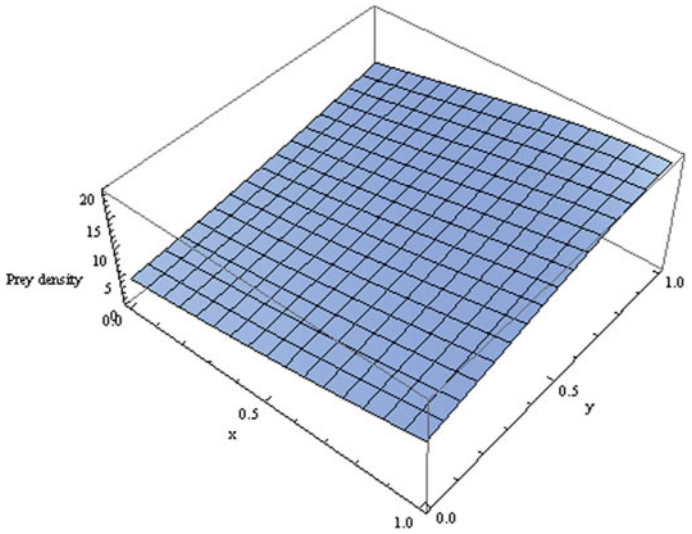

Fig. 7.20 Surface shows the numerical approximate solution of $u(x, y, t)$ when $\alpha = 0.88$, $\beta = 0.54$, $a = 0.7$, $b = 0.03$, $c = 0.3$, and $t = 0.53$

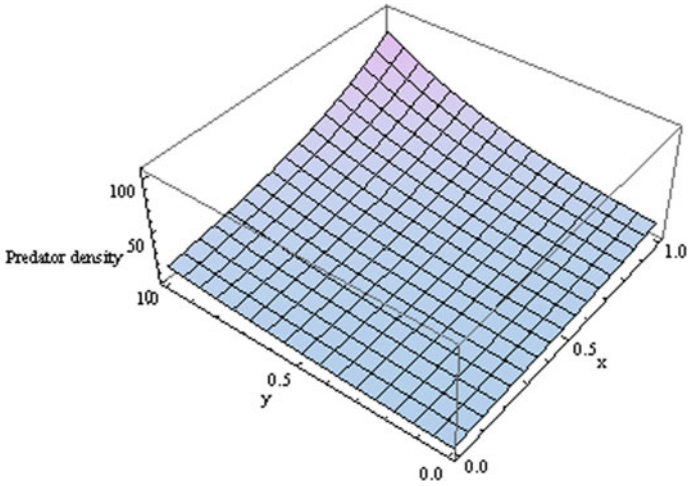

Fig. 7.21 Surface shows the numerical approximate solution of $v(x, y, t)$ when $\alpha = 0.88$, $\beta = 0.54$, $a = 0.7$, $b = 0.03$, $c = 0.9$, and $t = 0.6$

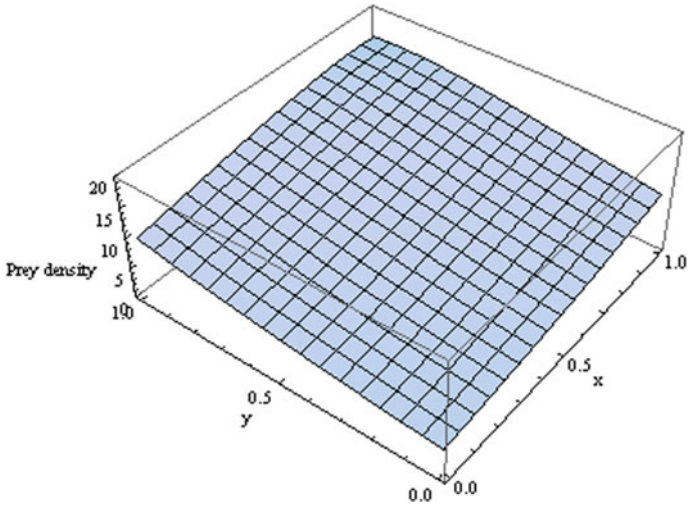

Fig. 7.22 Surface shows the numerical approximate solution of $u(x, y, t)$ when $\alpha = 0.88$, $\beta = 0.54$, $a = 0.5$, $b = 0.03$, $c = 0.3$, and $t = 0.53$

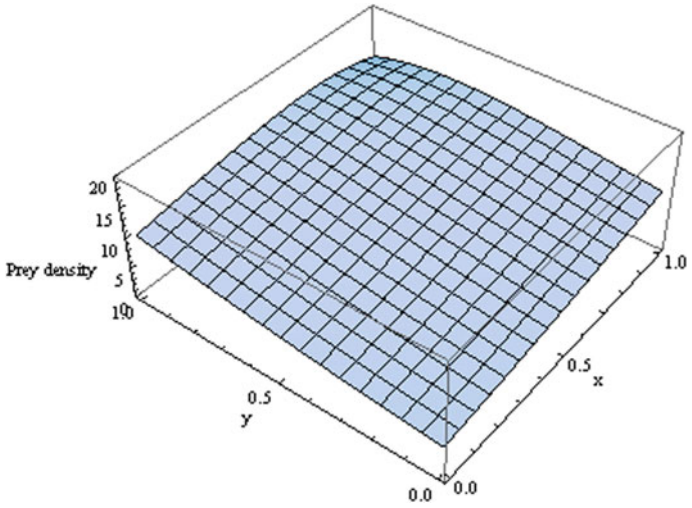

Fig. 7.23 Surface shows the numerical approximate solution of $u(x, y, t)$ when $\alpha = 0.88$, $\beta = 0.54$, $a = 0.7$, $b = 0.04$, $c = 0.3$, and $t = 0.53$

and

$$v(x,y,t) = \mathrm{e}^{x+y} + \frac{(2\mathrm{e}^{x+y} - c\mathrm{e}^{x+y} + b\mathrm{e}^{x+y}\sqrt{xy})t^{\beta}}{\Gamma(1+\beta)} + \frac{(-b\mathrm{e}^{x+y}(y^2 + x^2(1-4ay^2 + 4b\mathrm{e}^{x+y}y^2))t^{\alpha+\beta}}{4(xy)^{3/2}\Gamma(1+\alpha+\beta)} + \ldots, \tag{7.142}$$

7.5.4 Solutions for Time Fractional Coupled Schrödinger–KdV Equation

In the present analysis, fractional coupled Schrödinger–KdV equations with appropriate initial conditions have been solved by using the novel method, viz. CFRDTM.

Example 7.9 Consider the following time fractional coupled Schrödinger–KdV equation

$$iD_t^{\alpha} u_t = u_{xx} + uv, \tag{7.143a}$$

$$D_t^{\beta} v_t = -6vv_x - v_{xxx} + (|u|^2)_x, \tag{7.143b}$$

where $t > 0$, $0 < \alpha, \beta \leq 1$, subject to the initial conditions

$$u(x,0) = 6\sqrt{2}\mathrm{e}^{ipx}k^2\mathrm{sech}^2(kx), \tag{7.143c}$$

$$v(x,0) = \frac{p + 16k^2}{3} - 6k^2\tanh^2(kx). \tag{7.143d}$$

The exact solutions of Eqs. (7.143a) and (7.143b), for the special case where $\alpha = \beta = 1$, are given by [55]

$$u(x,t) = 6\sqrt{2}\mathrm{e}^{i\theta x}k^2\mathrm{sech}^2(k\xi), \tag{7.144a}$$

$$v(x,t) = \frac{p + 16k^2}{3} - 6k^2\tanh^2(k\xi), \tag{7.144b}$$

where

$$\theta = \left(\frac{pt}{3} + p^2t - \frac{10k^2t}{3} + px\right), \xi = x + 2pt,$$

and p, k are arbitrary constants.

In order to assess the advantages and the accuracy of the CFRDTM for solving time fractional coupled Schrödinger–KdV equation, firstly we derive the recursive formula from Eqs. (7.143a), (7.143b). Now, $U(h,k-h)$ and $V(h,k-h)$ are considered as the coupled fractional reduced differential transform of $u(x,t)$ and $v(x,t)$, respectively, where $u(x,t)$ and $v(x,t)$ are the solutions of coupled fractional differential equations. Here, $U(0,0)=u(x,0)$, $V(0,0)=v(x,0)$ are the given initial conditions. Without loss of generality, the following assumptions have taken

$$U(0,j)=0,\ \ j=1,2,3,\ldots \text{ and } V(i,0)=0,\ \ i=1,2,3,\ldots.$$

Applying CFRDTM to Eq. (7.143a), we obtain the following recursive formula

$$\frac{\Gamma((h+1)\alpha+(k-h)\beta+1)}{\Gamma(h\alpha+(k-h)\beta+1)}U(h+1,k-h)=-i\frac{\partial^2}{\partial x^2}U(h,k-h) - i\sum_{l=0}^{h}\sum_{s=0}^{k-h}U(h-l,s)V(l,k-h-s). \tag{7.145}$$

From the initial condition of Eq. (7.143c), we have

$$U(0,0)=u(x,0). \tag{7.146}$$

In the same manner, we can obtain the following recursive formula from Eq. (7.143b)

$$\frac{\Gamma(h\alpha+(k-h+1)\beta+1)}{\Gamma(h\alpha+(k-h)\beta+1)}V(h,k-h+1)=\frac{\partial}{\partial x}\left(\sum_{l=0}^{h}\sum_{s=0}^{k-h}U(l,k-h-s)\overline{U}(h-l,s)\right) - 6\left(\sum_{l=0}^{h}\sum_{s=0}^{k-h}V(l,k-h-s)\frac{\partial}{\partial x}V(h-l,s)\right) - \frac{\partial^3}{\partial x^3}V(h,k-h) \tag{7.147}$$

From the initial condition of Eq. (7.143d), we have

$$V(0,0)=v(x,0). \tag{7.148}$$

According to CFRDTM, using recursive equation (7.149) with initial condition Eq. (7.146) and also using recursive scheme Eq. (7.147) with initial condition Eq. (7.148) simultaneously, we obtain

$$U[1,0] = \frac{2\sqrt{2}k^2\operatorname{sech}^2(kx)(-i\cos(px) + \sin(px))(p - 3p^2 + 10k^2 - 12ipk\tanh(kx))}{\Gamma(1+\alpha)},$$

$$V[0,1] = \frac{24pk^3\operatorname{sech}^2(kx)\tanh(kx)}{\Gamma(1+\beta)},$$

$$U[1,1] = \frac{72\sqrt{2}pk^5\operatorname{sech}^6(kx)(-i\cos(px) + \sin(px))\sinh(2kx)}{\Gamma(1+\alpha+\beta)},$$

$$V[0,2] = \frac{12pk^4(-3(p+48k^2) - 2(p-48k^2)\cosh(2kx) + p\cosh(4kx))\operatorname{sech}^6(kx)}{\Gamma(1+2\beta)},$$

$$V[1,1] = \frac{576pk^6(-3+2\cosh(2kx))\operatorname{sech}^6(kx)}{\Gamma(1+\alpha+\beta)},$$

and so on.

The approximate solutions, obtained in the series form, are given by

$$\begin{aligned} u(x,t) &= \sum_{k'=0}^{\infty}\sum_{h=0}^{k'} U(h,k'-h)t^{(h\alpha+(k'-h)\beta)} \\ &= U(0,0) + \sum_{k'=1}^{\infty}\sum_{h=1}^{k'} U(h,k'-h)t^{(h\alpha+(k'-h)\beta)} + \cdots \\ &= 6\sqrt{2}k^2\operatorname{sech}^2(kx)e^{ipx} \\ &\quad + \frac{72\sqrt{2}pk^5t^{\alpha+\beta}\operatorname{sech}^6(kx)(-i\cos(px) + \sin(px))\sinh(2kx)}{\Gamma(1+\alpha+\beta)} + \cdots \end{aligned} \tag{7.149}$$

$$\begin{aligned} v(x,t) &= \sum_{k'=0}^{\infty}\sum_{h=0}^{k'} V(h,k'-h)t^{(h\alpha+(k'-h)\beta)} \\ &= V(0,0) + \sum_{k'=1}^{\infty}\sum_{h=0}^{k'} V(h,k'-h)t^{(h\alpha+(k'-h)\beta)} + \ldots \\ &= \frac{p+16k^2}{3} - 6k^2\tanh^2(kx) + \frac{24pk^3t^{\beta}\operatorname{sech}^2(kx)\tanh(kx)}{\Gamma(1+\beta)} \\ &\quad + \frac{576pk^6t^{\alpha+\beta}(-3+2\cosh(2kx))\operatorname{sech}^6(kx)}{\Gamma(1+\alpha+\beta)} + \ldots \end{aligned} \tag{7.150}$$

When $\alpha = 1$ and $\beta = 1$, the solutions in Eqs. (7.149) and (7.150) are exactly same as the Taylor series expansions of the exact solutions

$$u(x,t) = 6\sqrt{2}e^{i\theta x}k^2\operatorname{sech}^2(k\xi), \tag{7.151}$$

$$v(x,t) = \frac{p+16k^2}{3} - 6k^2\tanh^2(k\xi). \tag{7.152}$$

In the present numerical experiment, Eqs. (7.149) and (7.150) have been used to draw the graphs as shown in Figs. 7.24, 7.25, 7.26, and 7.27, respectively. The numerical solutions of the coupled Sch–KdV equation (7.143) have been shown in Figs. 7.24, 7.25, 7.26, and 7.27 with the help of third-order approximations for the series solutions of $u(x,t)$ and $v(x,t)$, respectively. In the present numerical computation, we have assumed $p = 0.05$ and $k = 0.05$. Figure 7.28 confirms that exact solution and approximate solutions coincide reasonably well with each other and consequently there is a good agreement of results between these two solutions when $\alpha = 1$ and $\beta = 1$. Figures 7.24, 7.25, 7.26, 7.27, and 7.28 show one-soliton solutions for coupled Sch–KdV equation (7.143). Table 7.3 explores the comparison between CFRDTM and Adomian decomposition method (ADM) results for $\mathrm{Re}(u(x,t))$ and $v(x,t)$ when $\alpha = 1$ and $\beta = 1$. It manifests that CFRDTM solutions are in good agreement with ADM solutions cited in [49].

Figures 7.29, 7.30, and 7.31 exhibit the numerical solutions of the coupled Sch–KdV equations (7.143) when $\alpha = 0.25$ and $\beta = 0.75$.

Example 7.10 Consider the time fractional coupled Schrödinger–KdV equations (7.143a)–(7.143b) with the following initial conditions

$$u(x,0) = \tanh(x)e^{ix}, \tag{7.153a}$$

$$v(x,0) = \frac{11}{12} - 2\tanh^2(x). \tag{7.153b}$$

The exact solutions of Eqs. (7.143a) and (7.143b), for the special case where $\alpha = \beta = 1$, are given by

$$u(x,t) = \tanh(x+2t)e^{i\left(x+\frac{25}{12}t\right)}, \tag{7.154a}$$

$$v(x,t) = \frac{11}{12} - 2\tanh^2(x+2t) \tag{7.154b}$$

Proceeding in a similar manner, using Eqs. (7.149) and (7.147), we can obtain

$$U[1,0] = \frac{(\cos(x)+i\sin(x))(24\operatorname{sech}^2(x)+25i\tanh(x))}{12\Gamma(1+\alpha)},$$

$$V[0,1] = -\frac{8\operatorname{sech}^2(x)\tanh(x)}{\Gamma(1+\beta)},$$

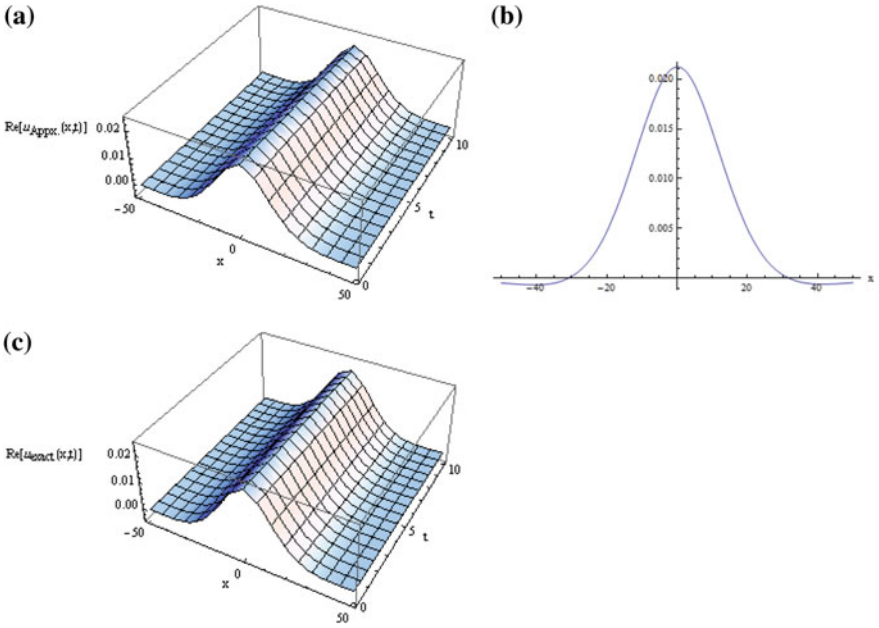

Fig. 7.24 **a** Approximate solution for $\mathrm{Re}(u(x,t))$ when $\alpha = 1$ and $\beta = 1$, **b** corresponding solution for $\mathrm{Re}(u(x,t))$ when $t = 1$, and **c** the exact solution for $\mathrm{Re}(u(x,t))$ when $\alpha = 1$ and $\beta = 1$

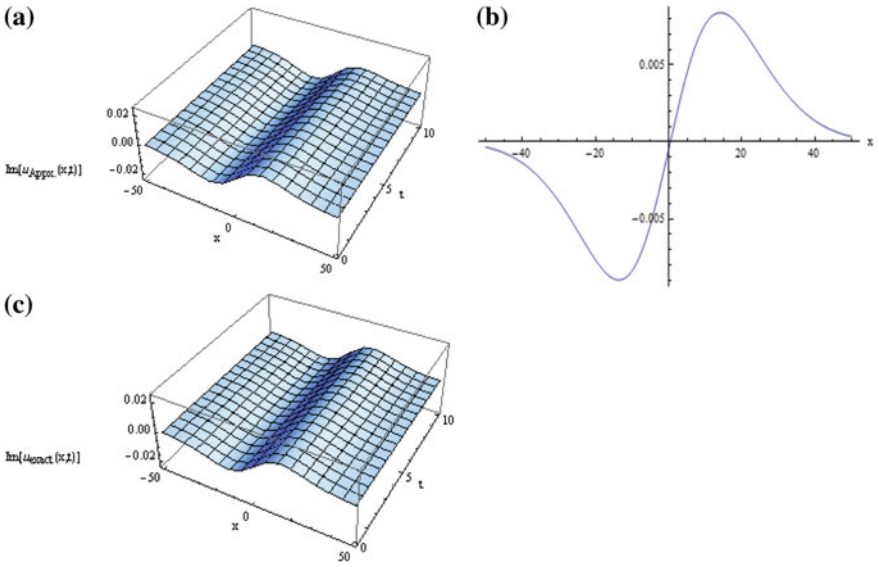

Fig. 7.25 **a** Approximate solution for $\mathrm{Im}(u(x,t))$ when $\alpha = 1$ and $\beta = 1$, **b** corresponding solution for $\mathrm{Im}(u(x,t))$ when $t = 1$, and **c** the exact solution for $\mathrm{Im}(u(x,t))$ when $\alpha = 1$ and $\beta = 1$

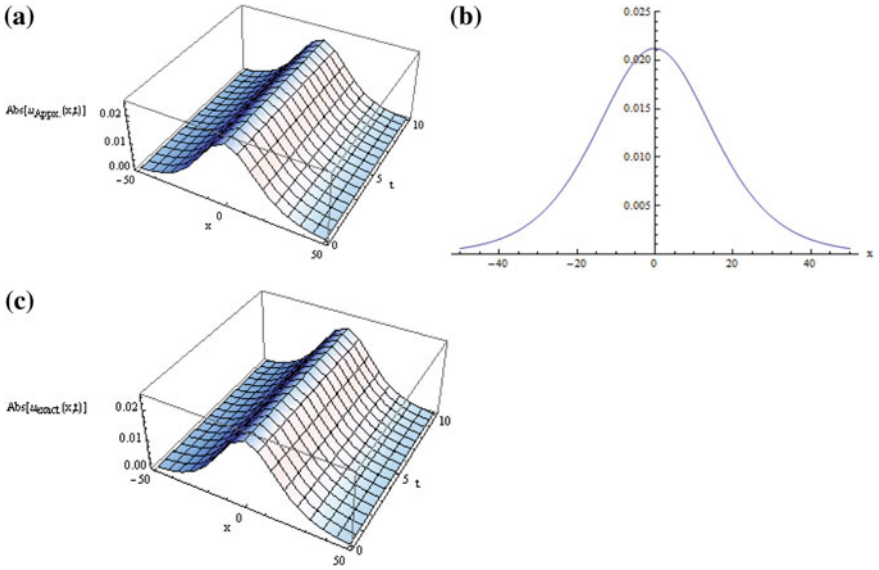

Fig. 7.26 **a** Approximate solution for $\text{Abs}(u(x,t))$ when $\alpha = 1$ and $\beta = 1$, **b** corresponding solution for $\text{Abs}(u(x,t))$ when $t = 1$, and **c** the exact solution for $\text{Abs}(u(x,t))$ when $\alpha = 1$ and $\beta = 1$

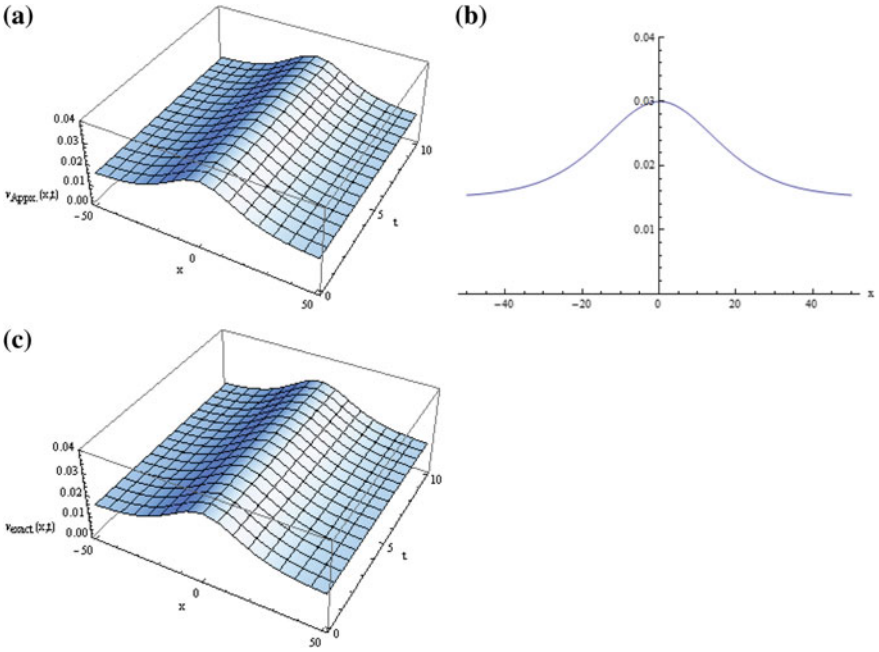

Fig. 7.27 **a** Approximate solution for $v(x,t)$ when $\alpha = 1$ and $\beta = 1$, **b** corresponding solution for $v(x,t)$ when $t = 1$, and **c** the exact solution for $v(x,t)$ when $\alpha = 1$ and $\beta = 1$

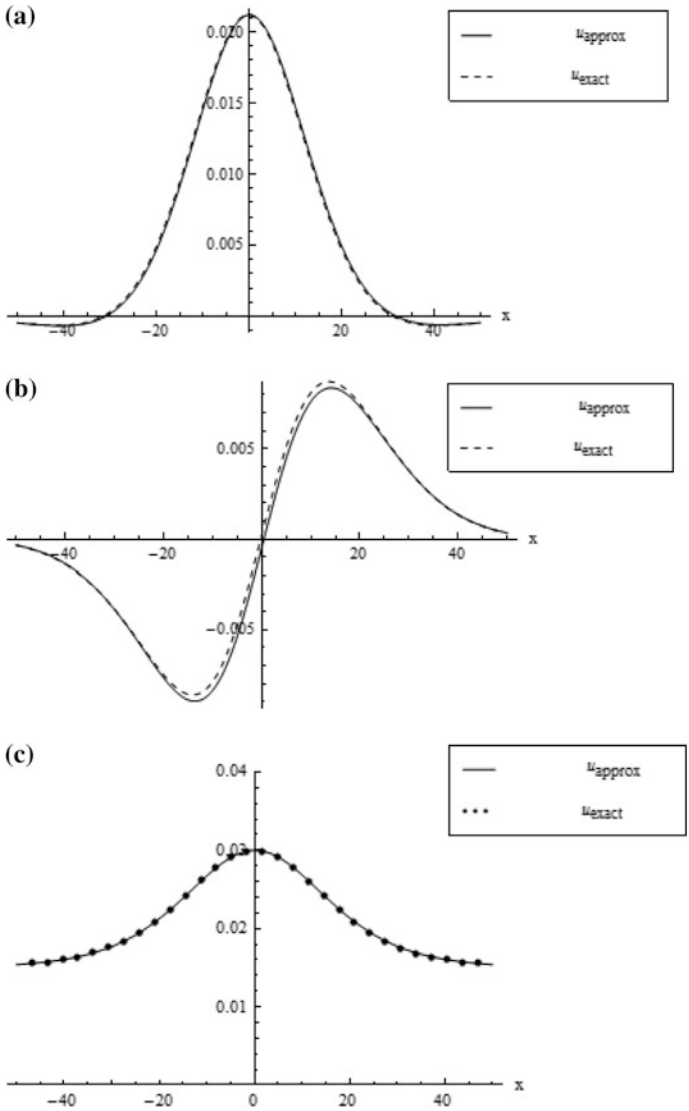

Fig. 7.28 **a** Exact and approximate solutions for $\mathrm{Re}(u(x,t))$, **b** the exact and approximate solutions for $\mathrm{Im}(u(x,t))$, and **c** the exact and approximate solutions for $v(x,t)$ when $t = 1$

Table 7.3 Comparison between CFRDTM and ADM results for $\mathrm{Re}(u(x,t))$ and $v(x,t)$ when $p = 0.05, k = 0.05$ for the approximate solution of Eq. (7.143)

(x,t)	$\lvert\mathrm{Re}(u_{\mathrm{Exact}}) - \mathrm{Re}(u_{\mathrm{CRFDTM}})\rvert$	$\lvert\mathrm{Re}(u_{\mathrm{Exact}}) - \mathrm{Re}(u_{\mathrm{ADM}})\rvert$	$\lvert v_{\mathrm{Exact}} - v_{\mathrm{CRFDTM}}\rvert$	$\lvert v_{\mathrm{Exact}} - v_{\mathrm{ADM}}\rvert$
(0.1, 0.1)	3.12296E−7	2.38712E−7	1.45496E−7	7.87471E−8
(0.1, 0.2)	5.42096E−7	5.12923E−7	2.81993E−7	1.64993E−7
(0.1, 0.3)	6.89399E−7	8.22631E−7	4.09489E−7	2.58738 E−7
(0.1, 0.4)	7.54204E−7	1.16783E−6	5.27985E−7	3.59982E−7
(0.1, 0.5)	7.36511E−7	1.54853E−6	6.3748E−7	4.68725E−7
(0.2, 0.1)	6.65778E−7	4.59621E−7	2.95463E−7	1.53728E−7
(0.2, 0.2)	1.24906E−6	9.54729E−7	5.81931E−7	3.14954E−7
(0.2, 0.3)	1.74985E−6	1.48532E−6	8.59402E−7	4.83675E−7
(0.2, 0.4)	2.16815E−6	2.0514E−6	1.12788E−6	6.59893E−7
(0.2, 0.5)	2.50394E−6	2.65296E−6	1.38735E−6	8.43606E−7
(0.3, 0.1)	1.01914E−6	6.80427E−7	4.45372E−7	2.28679E−7
(0.3, 0.2)	1.95579E−6	1.39632E−6	8.81756E−7	4.64851E−7
(0.3, 0.3)	2.80995E−6	2.14769E−6	1.30915E−6	7.08515E−7
(0.3, 0.4)	3.58161E−6	2.93452E−6	1.72755E−6	9.59671E−7
(0.3, 0.5)	4.27078E−6	3.75681E−6	2.13696E−6	1.21832E−6
(0.4, 0.1)	1.37231E−6	9.01083E−7	5.95192E−7	3.03584E−7
(0.4, 0.2)	2.66215E−6	1.83761E−6	1.18141E−6	6.14655E−7
(0.4, 0.3)	3.8695E−6	2.80958E−6	1.75864E−6	9.33213E−7
(0.4, 0.4)	4.99436E−6	3.81699E−6	2.32689E−6	1.25926E−6
(0.4, 0.5)	6.03672E−6	4.85984E−6	2.88616E−6	1.59279E−6
(0.5, 0.1)	1.72524E−6	1.12154E−6	7.44894E−7	3.78428E−7
(0.5, 0.2)	3.36802E−6	2.27849E−6	1.48082E−6	7.64337E−7
(0.5, 0.3)	4.92831E−6	3.47086E−6	2.20779E−6	1.15773E−6
(0.5, 0.4)	6.40613E−6	4.69863E−6	2.92578E−6	1.55859E−6
(0.5, 0.5)	7.80146E−6	5.96181E−6	3.6348E−6	1.96694E−6

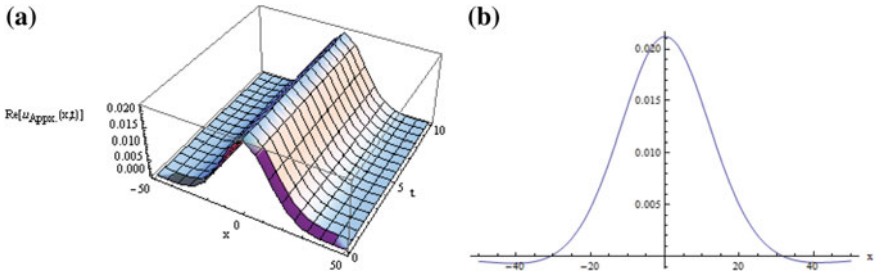

Fig. 7.29 **a** Approximate solution for $\mathrm{Re}(u(x,t))$ when $\alpha = 0.25$ and $\beta = 0.75$, and **b** corresponding solution for $\mathrm{Re}(u(x,t))$ when $t = 1$

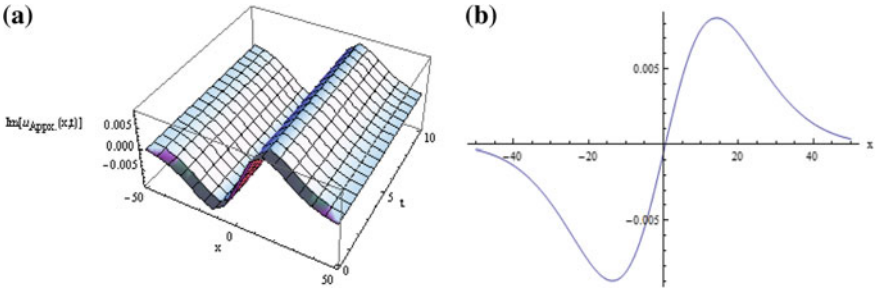

Fig. 7.30 **a** Approximate solution for $\mathrm{Im}(u(x,t))$ when $\alpha = 0.25$ and $\beta = 0.75$, and **b** corresponding solution for $\mathrm{Im}(u(x,t))$ when $t = 1$

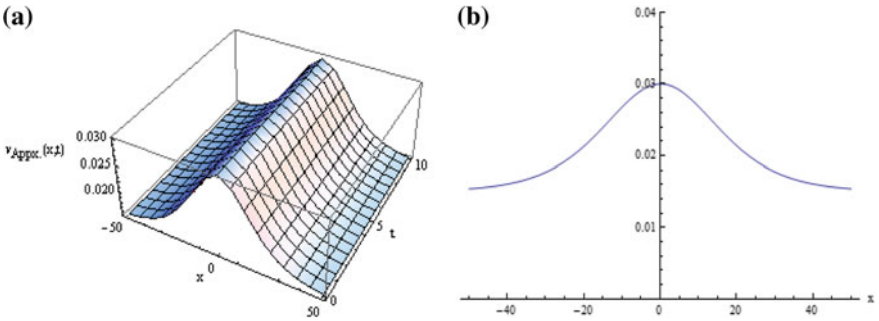

Fig. 7.31 **a** Approximate solution for $v(x,t)$ when $\alpha = 0.25$ and $\beta = 0.75$, and **b** corresponding solution for $v(x,t)$ when $t = 1$

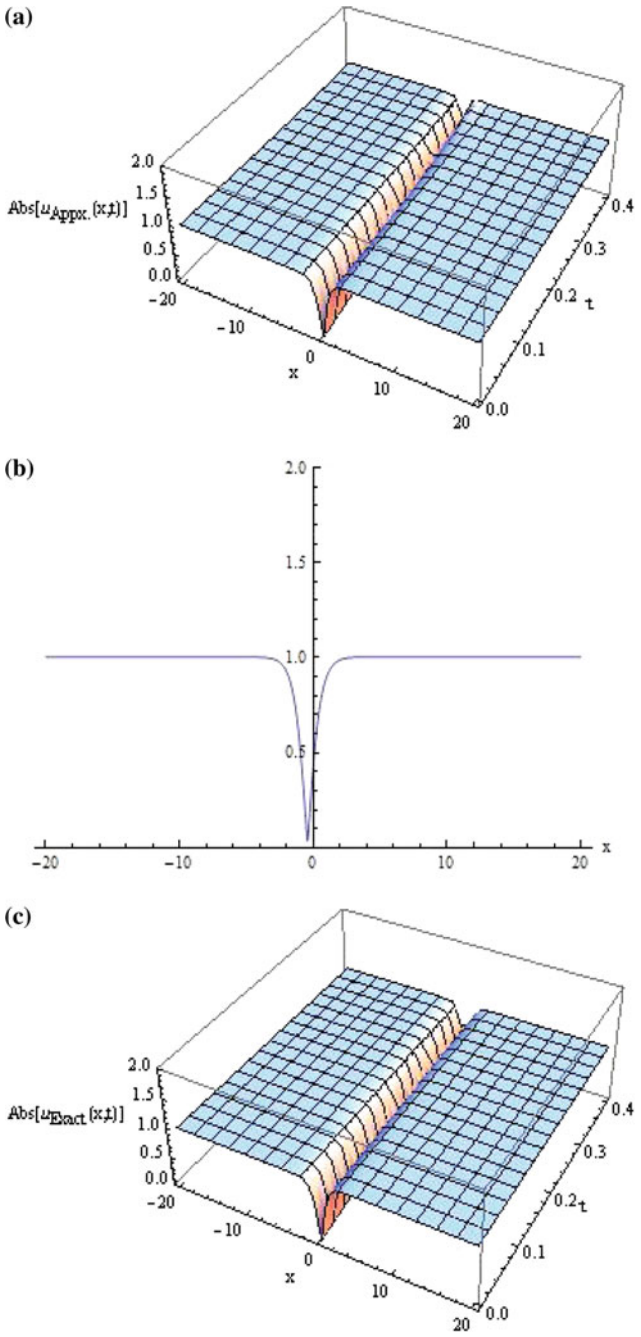

Fig. 7.32 **a** Approximate solution for $\text{Abs}(u(x,t))$ when $\alpha = 1$ and $\beta = 1$, **b** corresponding solution for $\text{Abs}(u(x,t))$ when $t = 0.2$, and **c** the exact solution for $Abs(u(x,t))$ when $\alpha = 1$ and $\beta = 1$

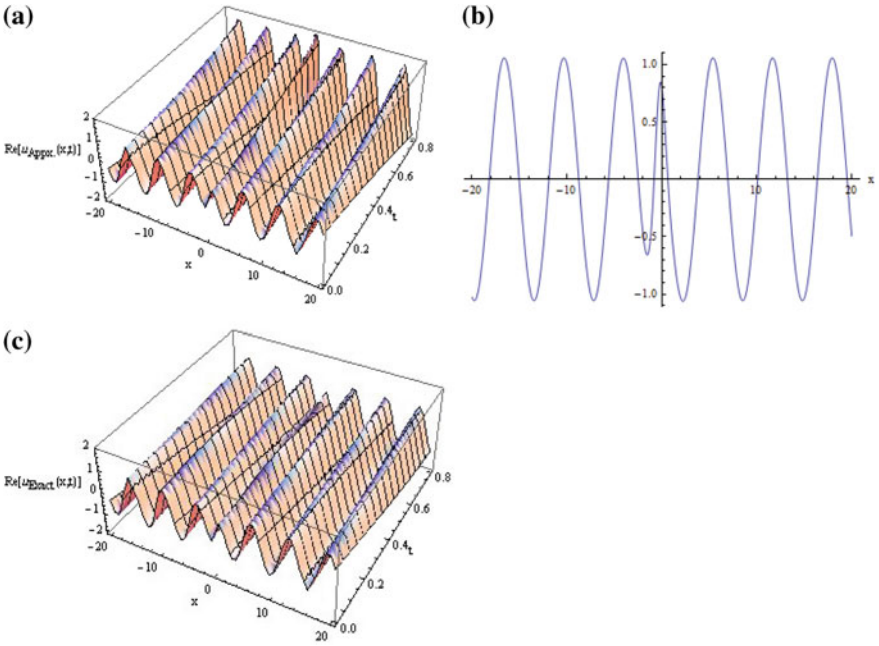

Fig. 7.33 **a** Approximate solution for $\mathrm{Re}(u(x,t))$ when $\alpha = 1$ and $\beta = 1$, **b** corresponding solution for $\mathrm{Re}(u(x,t))$ when $t = 0.4$, and **c** the exact solution for $\mathrm{Re}(u(x,t))$ when $\alpha = 1$ and $\beta = 1$

$$U[1,1] = \frac{8i\,\mathrm{sech}^2(x)(\cos(x) + i\sin(x))\tanh^2(x)}{\Gamma(1+\alpha+\beta)},$$

$$V[0,2] = \frac{20(-2+\cosh(2x))\mathrm{sech}^4(x)}{\Gamma(1+2\beta)},$$

$$U[2,0] = \frac{i\mathrm{sech}^4(x)\mathrm{e}^{ix}(9408 + 192\cosh(2x) + 5858i\sinh(2x) + 625i\sinh(4x))}{1152\Gamma(1+2\alpha)},$$

$$V[1,1] = -\frac{4(-2+\cosh(2x))\mathrm{sech}^4(x)}{\Gamma(1+\alpha+\beta)},$$

and so on.

The approximate solutions can be obtained by Eq. (7.29).

Figure 7.35 confirms that exact solution and approximate solutions coincide reasonably well with each other and consequently there is a good agreement of results between these two solutions when $\alpha = 1$ and $\beta = 1$.

Figures 7.32, 7.33, 7.34, 7.35, 7.37, 7.38, 7.39, and 7.40 exhibit the numerical solutions of the coupled Sch–KdV equations (7.143a)–(7.143b) with initial conditions (7.153a)–(7.153b) when $\alpha = 1$, $\beta = 1$ and $\alpha = 0.5$, $\beta = 0.5$, respectively (Fig. 7.36).

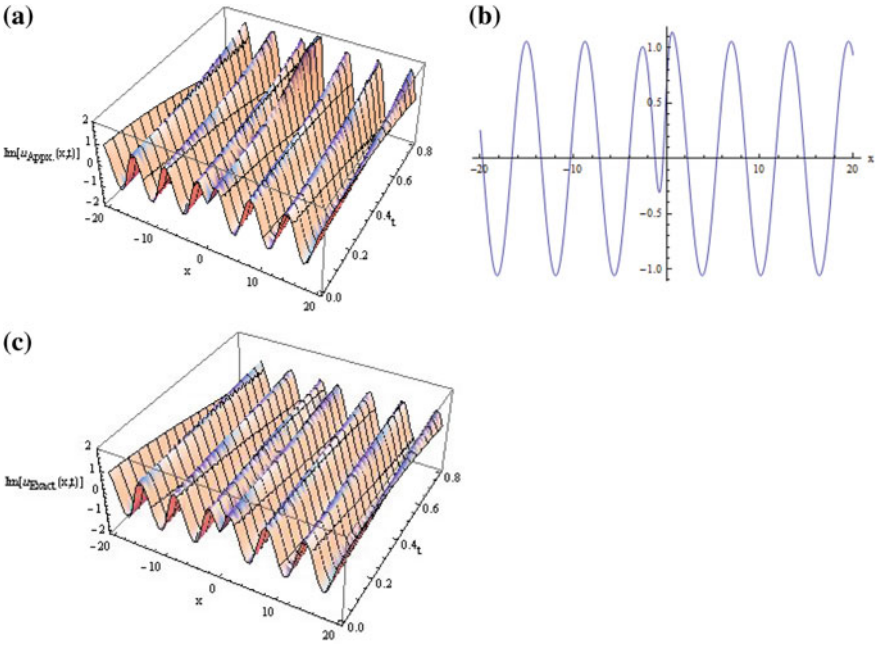

Fig. 7.34 **a** Approximate solution for $\mathrm{Im}(u(x,t))$ when $\alpha = 1$ and $\beta = 1$, **b** corresponding solution for $\mathrm{Im}(u(x,t))$ when $t = 0.4$, and **c** the exact solution for $\mathrm{Im}(u(x,t))$ when $\alpha = 1$ and $\beta = 1$

Example 7.11 Consider the time fractional coupled Schrödinger–KdV equations (7.143a)–(7.143b) with the following initial conditions

$$u(x,0) = \cos(x) + i\sin(x), \tag{7.155a}$$

$$v(x,0) = \frac{3}{4}. \tag{7.155b}$$

The exact solutions of Eqs. (7.143a) and (7.143b) with initial conditions (7.155), for the special case when $\alpha = \beta = 1$, are given by

$$u(x,t) = \cos\left(x + \frac{t}{4}\right) + i\sin\left(x + \frac{t}{4}\right), \tag{7.156a}$$

$$v(x,t) = \frac{3}{4}. \tag{7.156b}$$

The Jacobi periodic solutions [56] to coupled Sch–KdV equations (7.143a) and (7.143b) are given by

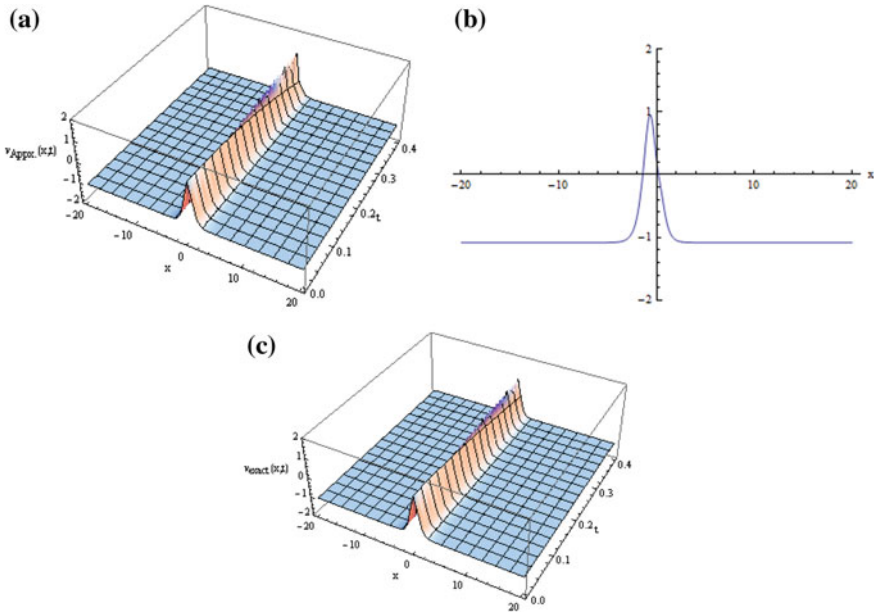

Fig. 7.35 **a** Approximate solution for $v(x,t)$ when $\alpha = 1$ and $\beta = 1$, **b** corresponding solution for $v(x,t)$ when $t = 0.3$, and **c** the exact solution for $\mathrm{Re}(u(x,t))$ when $\alpha = 1$ and $\beta = 1$

$$u(x,t) = \sqrt{\frac{2}{2-m^2}}\mathrm{e}^{i\theta} dn\left(\frac{1}{\sqrt{2-m^2}}\xi\right), \tag{7.157a}$$

$$v(x,t) = \frac{7}{4} - \frac{2}{2-m^2} dn^2\left(\frac{1}{\sqrt{2-m^2}}\xi\right). \tag{7.157b}$$

where $\theta = \left(x + \frac{t}{4}\right)$ and $\xi = x + 2t$.

For $m = 0$, Eq. (7.157a–b) reduces to Eq. (7.156a–b).

Proceeding in a similar manner, using Eqs. (7.149) and (7.147), we can obtain

$$U[1,0] = \frac{i(\cos(x) + i\sin(x))}{4\Gamma(1+\alpha)},$$

$$V[0,1] = 0,$$

$$U[1,1] = 0,$$

$$V[0,2] = 0,$$

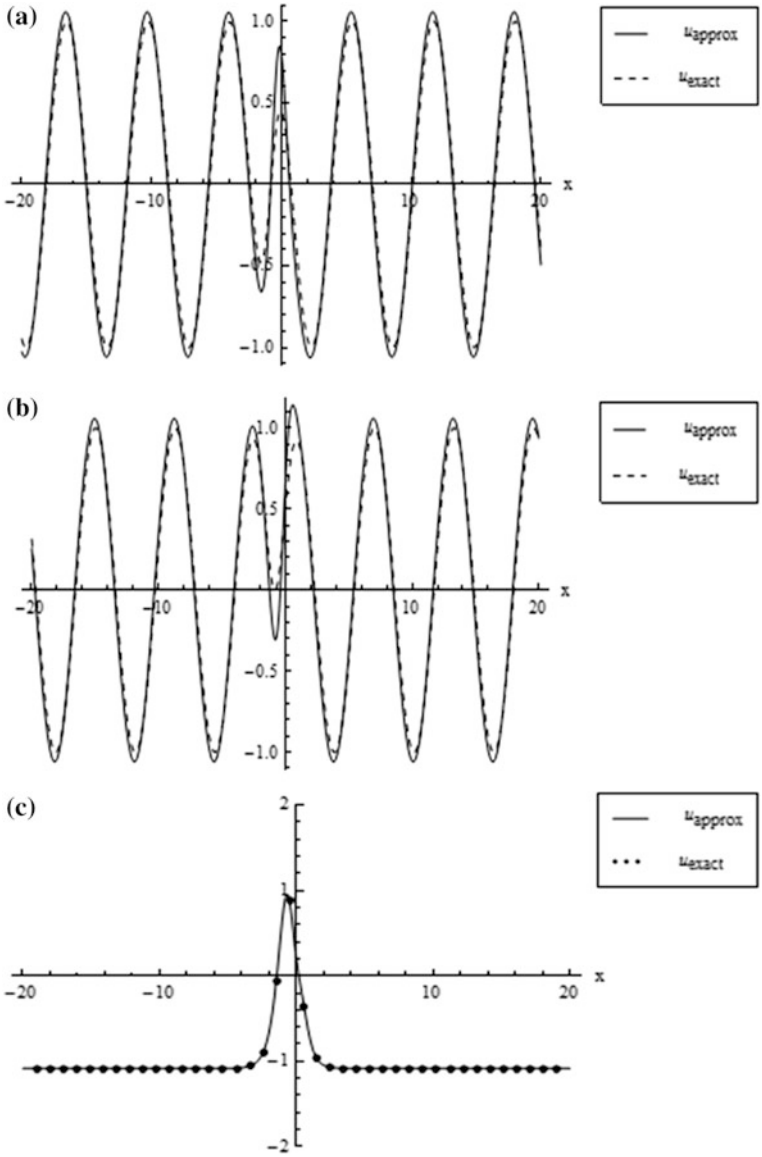

Fig. 7.36 **a** Exact and approximate solutions for $\mathrm{Re}(u(x,t))$ when $t = 0.4$, **b** the exact and approximate solutions for $\mathrm{Im}(u(x,t))$ when $t = 0.4$, and **c** the exact and approximate solutions for $v(x,t)$ when $t = 0.3$

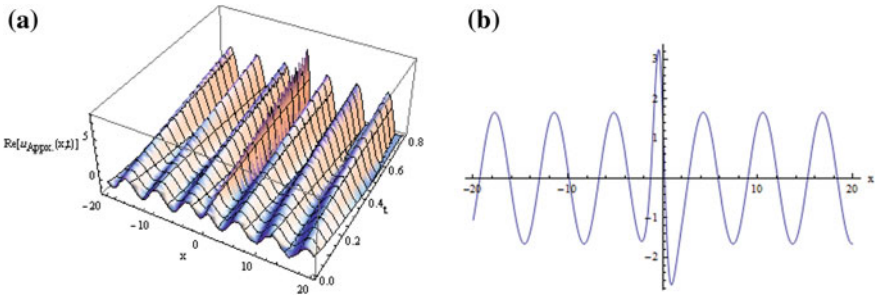

Fig. 7.37 **a** Approximate solution for $\mathrm{Re}(u(x,t))$ when $\alpha = 0.5$ and $\beta = 0.5$, and **b** corresponding solution for $\mathrm{Re}(u(x,t))$ when $t = 0.4$

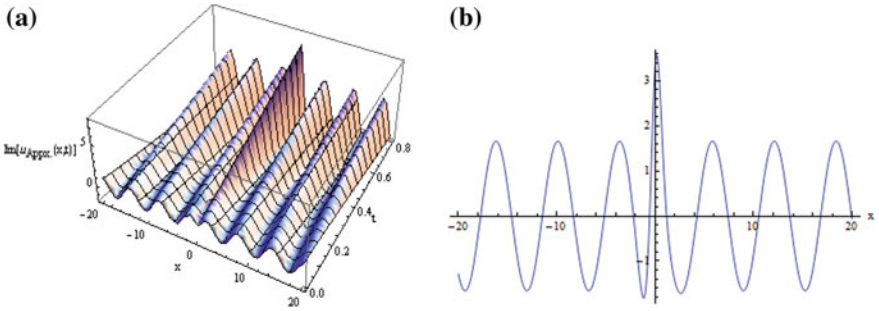

Fig. 7.38 **a** Approximate solution for $\mathrm{Im}(u(x,t))$ when $\alpha = 0.5$ and $\beta = 0.5$, and **b** corresponding solution for $\mathrm{Im}(u(x,t))$ when $t = 0.4$

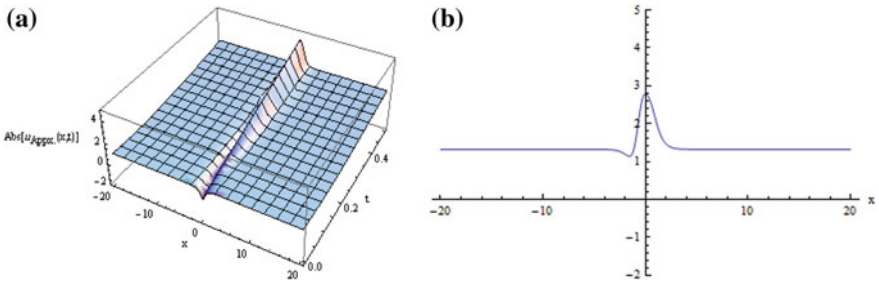

Fig. 7.39 **a** Approximate solution for $\mathrm{Abs}(u(x,t))$ when $\alpha = 0.5$ and $\beta = 0.5$, and **b** corresponding solution for $\mathrm{Abs}(u(x,t))$ when $t = 0.3$

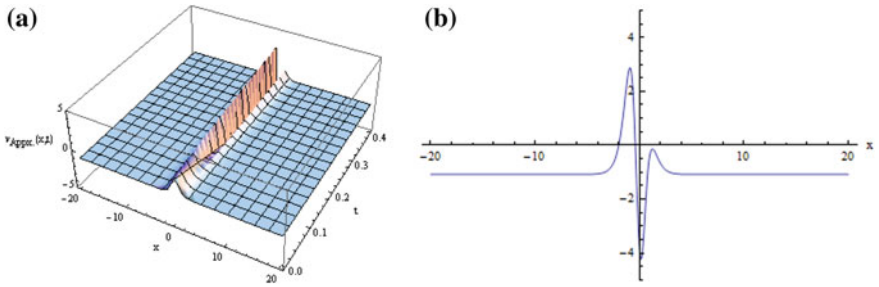

Fig. 7.40 **a** Approximate solution for $v(x,t)$ when $\alpha = 0.5$ and $\beta = 0.5$, and **b** corresponding solution for $v(x,t)$ when $t = 0.3$

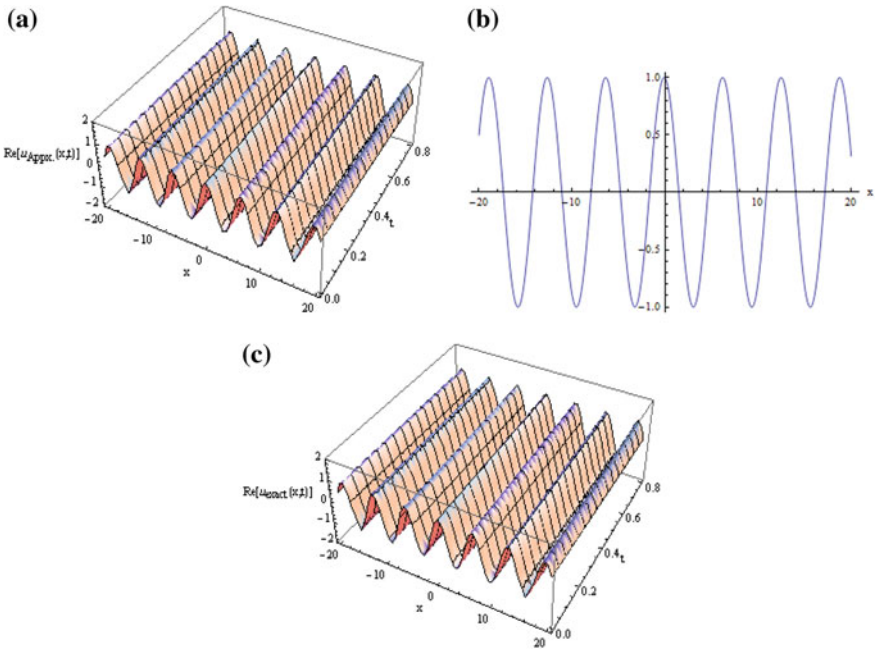

Fig. 7.41 **a** Approximate solution for $\mathrm{Re}(u(x,t))$ when $\alpha = 1$ and $\beta = 1$, **b** corresponding solution for $\mathrm{Re}(u(x,t))$ when $t = 0.4$, and **c** the exact solution for $\mathrm{Re}(u(x,t))$ when $\alpha = 1$ and $\beta = 1$

$$U[2,0] = -\frac{e^{ix}}{16\Gamma(1+2\alpha)},$$

$$V[1,1] = 0,$$

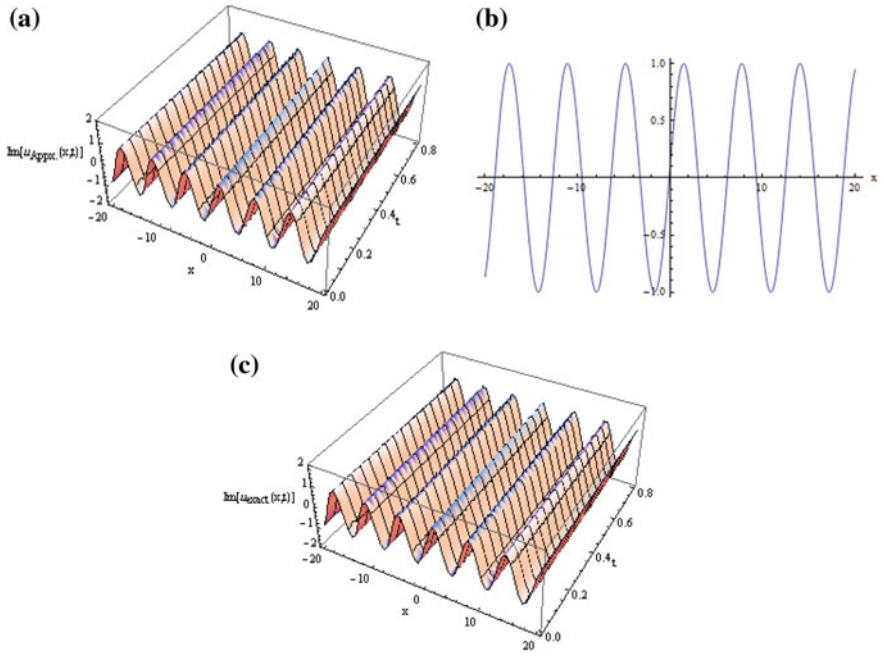

Fig. 7.42 **a** Approximate solution for $\mathrm{Im}(u(x,t))$ when $\alpha = 1$ and $\beta = 1$, **b** corresponding solution for $\mathrm{Im}(u(x,t))$ when $t = 0.4$, and **c** the exact solution for $\mathrm{Im}(u(x,t))$ when $\alpha = 1$ and $\beta = 1$

$$U[3,0] = \frac{-i\cos(x) + \sin(x)}{64\Gamma(1+3\alpha)},$$

and so on.

The approximate solutions can be obtained by Eq. (7.29).

Figures 7.41 and 7.42 show the exact and approximate solutions for $\mathrm{Re}(u(x,t))$ and $\mathrm{Im}(u(x,t))$ when $\alpha = 1$ and $\beta = 1$, respectively. Since the obtained approximate solution $v(x,t)$ is exact, it is not drawn.

Figure 7.43 confirms that exact solution and approximate solutions coincide reasonably well with each other and consequently there is a good agreement of results between these two solutions when $\alpha = 1$ and $\beta = 1$.

Figures 7.44 and 7.45 exhibit the numerical solutions of the coupled Sch–KdV equations (7.143a)–(7.143b) with initial conditions (7.155) when $\alpha = 0.5$ and $\beta = 0.5$.

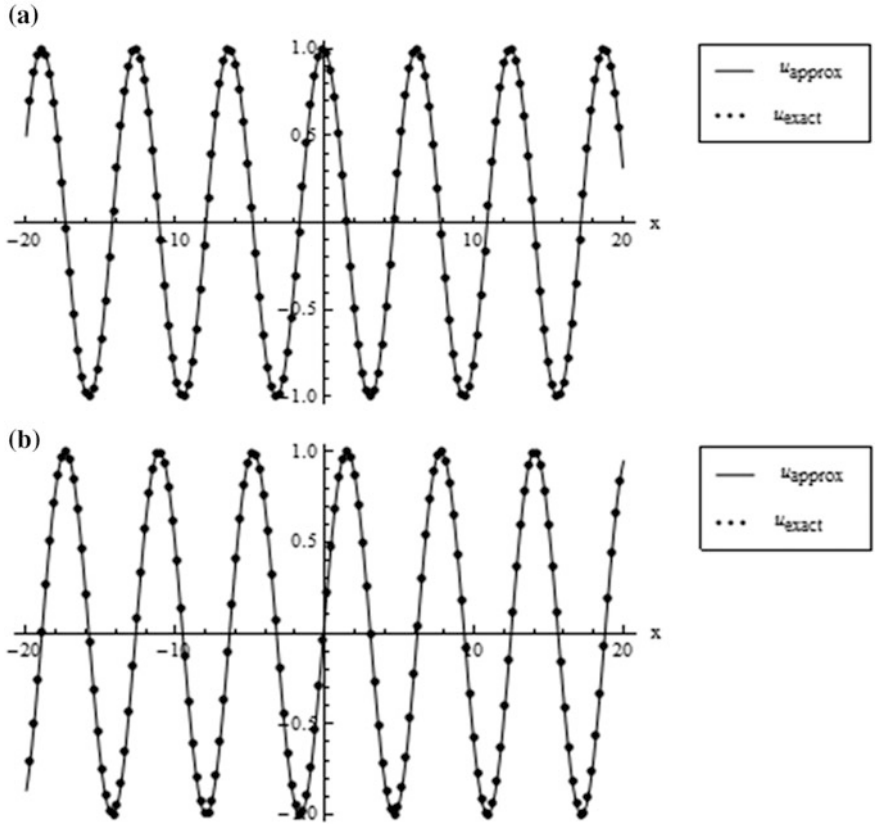

Fig. 7.43 **a** Exact and approximate solutions for $\mathrm{Re}(u(x,t))$ when $t = 0.4$ and **b** the exact and approximate solutions for $\mathrm{Im}(u(x,t))$ when $t = 0.4$

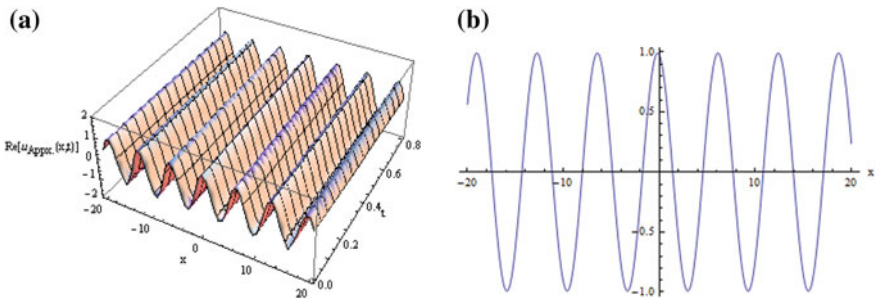

Fig. 7.44 **a** Approximate solution for $\mathrm{Re}(u(x,t))$ when $\alpha = 0.5$ and $\beta = 0.5$, and **b** corresponding solution for $\mathrm{Re}(u(x,t))$ when $t = 0.4$

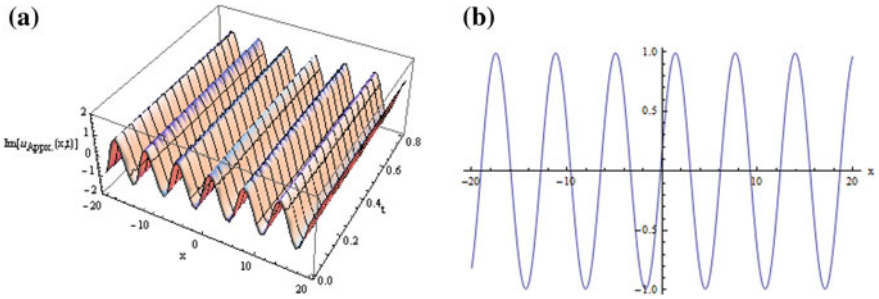

Fig. 7.45 **a** Approximate solution for $\mathrm{Im}(u(x,t))$ when $\alpha = 0.5$ and $\beta = 0.5$, and **b** corresponding solution for $\mathrm{Im}(u(x,t))$ when $t = 0.4$

7.5.5 *Traveling Wave Solutions for the Variant of Time Fractional Coupled WBK Equations*

In this section, the new proposed CFRDTM [34, 35] is very successfully employed for obtaining approximate traveling wave solutions of fractional coupled Whitham–Broer–Kaup (WBK) equations, fractional coupled modified Boussinesq equations, and fractional approximate long wave equations. By using this proposed method, the solutions were calculated in the form of a generalized Taylor's series with easily computable components. The obtained results justify that the proposed method is also very efficient, effective, and simple for obtaining approximate solutions of fractional coupled evolution equations.

Example 7.12 Consider the following time fractional coupled WBK equations [57–59]

$$D_t^{\alpha} u = -u\frac{\partial u}{\partial x} - \frac{\partial v}{\partial x} - b\frac{\partial^2 u}{\partial x^2}, \tag{7.158a}$$

$$D_t^{\beta} v = -\frac{\partial (uv)}{\partial x} - a\frac{\partial^3 u}{\partial x^3} + b\frac{\partial^2 v}{\partial x^2}, \tag{7.158b}$$

where $t > 0$, $0 < \alpha, \beta \leq 1$, subject to the initial conditions

$$u(x,0) = \lambda - 2Bk\coth(k\xi), \tag{7.158c}$$

$$v(x,0) = -2B(B+b)k^2\mathrm{csch}^2(k\xi), \tag{7.158d}$$

where $B = \sqrt{a+b^2}$, $\xi = x + c$, and c, k, λ are arbitrary constants.

The exact solutions [57, 60] of Eqs. (7.158a) and (7.158b), for the special case where $\alpha = \beta = 1$, are given by

$$u(x,t) = \lambda - 2Bk\coth(k(\xi - \lambda t)), \tag{7.159a}$$

$$v(x,t) = -2B(B+b)k^2\mathrm{csch}^2(k(\xi - \lambda t)), \tag{7.159b}$$

In order to assess the advantages and the accuracy of the proposed method, CFRDTM has been applied for solving time fractional coupled WBK equations. First, we derive the recursive formula from Eqs. (7.158a) and (7.158b), respectively. Now, $U(h,k-h)$ and $V(h,k-h)$ are considered as the coupled fractional reduced differential transform of $u(x,t)$ and $v(x,t)$, respectively, where $u(x,t)$ and $v(x,t)$ are the solutions of coupled fractional differential equations. Here, $U(0,0) = u(x,0)$, $V(0,0) = v(x,0)$ are the given initial conditions.

Without loss of generality, the following assumptions have been taken

$$U(0,j) = 0, \quad j = 1,2,3,\ldots \text{ and } V(i,0) = 0, \quad i = 1,2,3,\ldots.$$

Applying CFRDTM to Eq. (7.158a), we obtain the following recursive formula

$$\frac{\Gamma((h+1)\alpha + (k-h)\beta + 1)}{\Gamma(h\alpha + (k-h)\beta + 1)}U(h+1,k-h) = -\left(\sum_{l=0}^{h}\sum_{s=0}^{k-h} U(h-l,s)\frac{\partial}{\partial x}U(l,k-h-s)\right) - \frac{\partial}{\partial x}V(h,k-h) - b\frac{\partial^2}{\partial x^2}U(h,k-h). \tag{7.160}$$

From the initial condition of Eq. (7.158c), we have

$$U(0,0) = u(x,0). \tag{7.161}$$

In the same manner, we can obtain the following recursive formula from Eq. (7.158b)

$$\frac{\Gamma(h\alpha + (k-h+1)\beta + 1)}{\Gamma(h\alpha + (k-h)\beta + 1)}V(h,k-h+1) = -\frac{\partial}{\partial x}\left(\sum_{l=0}^{h}\sum_{s=0}^{k-h} U(l,k-h-s)V(h-l,s)\right) - a\frac{\partial^3}{\partial x^3}U(h,k-h) + b\frac{\partial^2}{\partial x^2}V(h,k-h). \tag{7.162}$$

From the initial condition of Eq. (7.158d), we have

$$V(0,0) = v(x,0). \tag{7.163}$$

According to CFRDTM, using recursive Eq. (7.160) with initial condition Eq. (7.161) and also using recursive scheme Eq. (7.162) with initial condition Eq. (7.163) simultaneously, we obtain

$$U(1,0) = -\frac{2Bk^2\lambda \operatorname{csch}^2(k\xi)}{\Gamma(1+\alpha)},$$

$$V(0,1) = -\frac{4(a+b(b+B))k^3\lambda \coth(k\xi)\operatorname{csch}^2(k\xi)}{\Gamma(1+\beta)},$$

$$U(1,1) = -\frac{4(a+b(b+B))k^4\lambda(2+\cosh(2k\xi))\operatorname{csch}^4(k\xi)}{\Gamma(1+\alpha+\beta)},$$

$$V(1,1) = -\frac{8k^5\lambda(-2b^2(b+B)+a(-2b+3B)+aB\cosh(2k\xi))\coth(k\xi)\operatorname{csch}^4(k\xi)}{\Gamma(1+\alpha+\beta)},$$

and so on.

The approximate solutions, obtained in the series form, are given by

$$\begin{aligned} u(x,t) &= \sum_{k=0}^{\infty}\sum_{h=0}^{k} U(h,k-h)t^{(h\alpha+(k-h)\beta)} \\ &= U(0,0) + \sum_{k=1}^{\infty}\sum_{h=1}^{k} U(h,k-h)t^{(h\alpha+(k-h)\beta)} \\ &= \lambda - 2Bk\coth(k\xi) - \frac{2Bk^2\lambda\operatorname{csch}^2(k\xi)t^{\alpha}}{\Gamma(1+\alpha)} \\ &\quad - \frac{4(a+b(b+B))k^4\lambda(2+\cosh(2k\xi))\operatorname{csch}^4(k\xi)t^{\alpha+\beta}}{\Gamma(1+\alpha+\beta)} + \cdots \end{aligned} \tag{7.164}$$

$$\begin{aligned} v(x,t) &= \sum_{k=0}^{\infty}\sum_{h=0}^{k} V(h,k-h)t^{(h\alpha+(k-h)\beta)} \\ &= V(0,0) + \sum_{k=1}^{\infty}\sum_{h=0}^{k} V(h,k-h)t^{(h\alpha+(k-h)\beta)} \\ &= -2B(b+B)k^2\operatorname{csch}^2(k\xi) \\ &\quad - \frac{4(a+b(b+B))k^3\lambda\coth(k\xi)\operatorname{csch}^2(k\xi)t^{\beta}}{\Gamma(1+\beta)} - \cdots. \end{aligned} \tag{7.165}$$

When $\alpha = 1$ and $\beta = 1$, the solution in Eq. (7.164) becomes

$$\begin{aligned} u(x,t) &= \lambda - 2Bk\coth(k\xi) - 2Bk^2\lambda\mathrm{csch}^2(k\xi)t \\ &\quad - 2Bk^3\lambda^2\coth(k\xi)\mathrm{csch}^2(k\xi)t^2 + \cdots. \end{aligned} \tag{7.166}$$

When $\alpha = 1$ and $\beta = 1$, the solution in Eq. (7.165) becomes

$$\begin{aligned} v(x,t) &= -2B(B+b)k^2\mathrm{csch}^2(k(\xi-\lambda t)) \\ &= -2(B(b+B)k^2\mathrm{csch}^2(k\xi)) - 4(B(b+B)k^3\lambda\coth(k\xi)\mathrm{csch}^2(k\xi))t \\ &\quad - 2(B(b+B)k^4\lambda^2(2+\cosh(2k\xi))\mathrm{csch}^4(k\xi))t^2 - \cdots. \end{aligned} \tag{7.167}$$

The solutions in Eqs. (7.166) and (7.167) are exactly the same as the Taylor series expansions of the exact solutions

$$\begin{aligned} u(x,t) &= \lambda - 2Bk\coth(k(\xi-\lambda t)) \\ &= \lambda - 2Bk\coth(k\xi) - 2Bk^2\lambda\mathrm{csch}^2(k\xi)t \\ &\quad - 2Bk^3\lambda^2\coth(k\xi)\mathrm{csch}^2(k\xi)t^2 + \cdots \end{aligned} \tag{7.168}$$

$$\begin{aligned} v(x,t) &= -2B(B+b)k^2\mathrm{csch}^2(k(\xi-\lambda t)) \\ &= -2(B(b+B)k^2\mathrm{csch}^2(k\xi)) - 4(B(b+B)k^3\lambda\coth(k\xi)\mathrm{csch}^2(k\xi))t \\ &\quad - 2(B(b+B)k^4\lambda^2(2+\cosh(2k\xi))\mathrm{csch}^4(k\xi))t^2 - \cdots \end{aligned} \tag{7.169}$$

Example 7.13 Consider the following time fractional coupled modified Boussinesq (MB) equations [57, 58, 60]

$$D_t^{\alpha}u = -u\frac{\partial u}{\partial x} - \frac{\partial v}{\partial x}, \tag{7.170a}$$

$$D_t^{\beta}v = -\frac{\partial(uv)}{\partial x} - \frac{\partial^3 u}{\partial x^3}, \tag{7.170b}$$

where $t > 0$, $0 < \alpha, \beta \leq 1$, subject to the initial conditions

$$u(x,0) = \lambda - 2k\coth(k\xi), \tag{7.170c}$$

$$v(x,0) = -2k^2\mathrm{csch}^2(k\xi). \tag{7.170d}$$

As already mentioned earlier, if $a = 1$ and $b = 0$, the above fractional coupled modified Boussinesq equations (7.170a) and (7.170b) can be obtained as a special case of WBK equations (7.158a) and (7.158b).

The exact solutions [57, 60] of Eqs. (7.170a) and (7.170b), for the special case where $\alpha = \beta = 1$, are given by

$$u(x,t) = \lambda - 2k\coth(k(\xi - \lambda t)), \tag{7.171a}$$

$$v(x,t) = -2k^2\mathrm{csch}^2(k(\xi - \lambda t)). \tag{7.171b}$$

Proceeding in a similar manner as in Example 7.12, after applying CFRDTM to Eq. (7.170a), we obtain the following recursive formula

$$\frac{\Gamma((h+1)\alpha + (k-h)\beta + 1)}{\Gamma(h\alpha + (k-h)\beta + 1)} U(h+1, k-h) = -\left(\sum_{l=0}^{h}\sum_{s=0}^{k-h} U(h-l,s)\frac{\partial}{\partial x}U(l,k-h-s)\right) - \frac{\partial}{\partial x}V(h,k-h). \tag{7.172}$$

From the initial condition of Eq. (7.170c), we have

$$U(0,0) = u(x,0). \tag{7.173}$$

In the same manner, we can obtain the following recursive formula from Eq. (7.170b)

$$\frac{\Gamma(h\alpha + (k-h+1)\beta + 1)}{\Gamma(h\alpha + (k-h)\beta + 1)} V(h, k-h+1) = -\frac{\partial}{\partial x}\left(\sum_{l=0}^{h}\sum_{s=0}^{k-h} U(l,k-h-s)V(h-l,s)\right) - \frac{\partial^3}{\partial x^3}U(h,k-h). \tag{7.174}$$

From the initial condition of Eq. (7.170d), we have

$$V(0,0) = v(x,0). \tag{7.175}$$

According to CFRDTM, using recursive formulae (7.172) and (7.174) along with initial conditions in Eqs. (7.173) and (7.175) simultaneously, we obtain the approximate solutions in the series forms as

$$\begin{aligned} u(x,t) &= \sum_{k=0}^{\infty}\sum_{h=0}^{k} U(h,k-h)t^{(h\alpha+(k-h)\beta)} \\ &= U(0,0) + \sum_{k=1}^{\infty}\sum_{h=1}^{k} U(h,k-h)t^{(h\alpha+(k-h)\beta)} \\ &= \lambda - 2k\coth(k\xi) - \frac{2k^2\lambda\,\mathrm{csch}^2(k\xi)t^{\alpha}}{\Gamma(1+\alpha)} \\ &\quad - \frac{4k^4\lambda(2+\cosh(2k\xi))\mathrm{csch}^4(k\xi)t^{\alpha+\beta}}{\Gamma(1+\alpha+\beta)} + \cdots. \end{aligned} \tag{7.176}$$

$$\begin{aligned} v(x,t) &= \sum_{k=0}^{\infty}\sum_{h=0}^{k} V(h,k-h)t^{(h\alpha+(k-h)\beta)} \\ &= V(0,0) + \sum_{k=1}^{\infty}\sum_{h=0}^{k} V(h,k-h)t^{(h\alpha+(k-h)\beta)} \\ &= -2k^2\mathrm{csch}^2(k\xi) - \frac{4k^3\lambda\coth(k\xi)\mathrm{csch}^2(k\xi)t^{\beta}}{\Gamma(1+\beta)} - \cdots. \end{aligned} \tag{7.177}$$

When $\alpha = 1$ and $\beta = 1$, the solutions in Eqs. (7.176) and (7.177) are exactly the same as the Taylor series expansions of the exact solutions

$$u(x,t) = \lambda - 2k\coth(k(\xi - \lambda t)), \tag{7.178}$$

$$v(x,t) = -2k^2\mathrm{csch}^2(k(\xi - \lambda t)). \tag{7.179}$$

Example 7.14 Consider the following time fractional coupled approximate long wave (ALW) equations [57, 58, 60]

$$D_t^{\alpha}u = -u\frac{\partial u}{\partial x} - \frac{\partial v}{\partial x} - \frac{1}{2}\frac{\partial^2 u}{\partial x^2}, \tag{7.180a}$$

$$D_t^{\beta}v = -\frac{\partial(uv)}{\partial x} + \frac{1}{2}\frac{\partial^2 v}{\partial x^2}, \tag{7.180b}$$

where $t > 0$, $0 < \alpha, \beta \leq 1$, subject to the initial conditions

$$u(x,0) = \lambda - k\coth(k\xi), \tag{7.180c}$$

$$v(x,0) = -k^2\mathrm{csch}^2(k\xi) \tag{7.180d}$$

As already mentioned earlier, if $a = 0$ and $b = 1/2$, the above fractional coupled ALW equations (7.180a) and (7.180b) can be obtained as a special case of WBK equations (7.158a) and (7.158b).

The exact solutions [57, 60] of Eqs. (7.180a) and (7.180b), for the special case where $\alpha = \beta = 1$, are given by

$$u(x,t) = \lambda - k\coth(k(\xi - \lambda t)), \tag{7.181a}$$

$$v(x,t) = -k^2\mathrm{csch}^2(k(\xi - \lambda t)). \tag{7.181b}$$

Proceeding in a similar manner as in Example 7.12, after applying CFRDTM to Eq. (7.180a), we obtain the following recursive formula

$$\frac{\Gamma((h+1)\alpha+(k-h)\beta+1)}{\Gamma(h\alpha+(k-h)\beta+1)}U(h+1,k-h)=-\left(\sum_{l=0}^{h}\sum_{s=0}^{k-h}U(h-l,s)\frac{\partial}{\partial x}U(l,k-h-s)\right)-\frac{\partial}{\partial x}V(h,k-h)-\frac{1}{2}\frac{\partial^2}{\partial x^2}U(h,k-h). \tag{7.182}$$

From the initial condition of Eq. (7.180c), we have

$$U(0,0)=u(x,0). \tag{7.183}$$

In the same manner, we can obtain the following recursive formula from Eq. (7.180b)

$$\frac{\Gamma(h\alpha+(k-h+1)\beta+1)}{\Gamma(h\alpha+(k-h)\beta+1)}V(h,k-h+1)=-\frac{\partial}{\partial x}\left(\sum_{l=0}^{h}\sum_{s=0}^{k-h}U(l,k-h-s)V(h-l,s)\right)+\frac{1}{2}\frac{\partial^2}{\partial x^2}V(h,k-h). \tag{7.184}$$

From the initial condition of Eq. (7.180d), we have

$$V(0,0)=v(x,0). \tag{7.185}$$

According to CFRDTM, using recursive formulae (7.182) and (7.184) along with initial condition Eqs. (7.183) and (7.185) simultaneously, we obtain the approximate solutions in the series forms as

$$\begin{aligned}u(x,t)&=\sum_{k=0}^{\infty}\sum_{h=0}^{k}U(h,k-h)t^{(h\alpha+(k-h)\beta)}\\&=U(0,0)+\sum_{k=1}^{\infty}\sum_{h=1}^{k}U(h,k-h)t^{(h\alpha+(k-h)\beta)}\\&=\lambda-k\coth(k\xi)-\frac{k^2\lambda\operatorname{csch}^2(k\xi)t^{\alpha}}{\Gamma(1+\alpha)}\\&\quad-\frac{2k^4\lambda(2+\cosh(2k\xi))\operatorname{csch}^4(k\xi)t^{\alpha+\beta}}{\Gamma(1+\alpha+\beta)}+\cdots.\end{aligned} \tag{7.186}$$

$$\begin{aligned} v(x,t) &= \sum_{k=0}^{\infty}\sum_{h=0}^{k} V(h,k-h)t^{(h\alpha+(k-h)\beta)} \\ &= V(0,0) + \sum_{k=1}^{\infty}\sum_{h=0}^{k} V(h,k-h)t^{(h\alpha+(k-h)\beta)} \\ &= -k^2\mathrm{csch}^2(k\xi) - \frac{2k^3\lambda\coth(k\xi)\mathrm{csch}^2(k\xi)t^{\beta}}{\Gamma(1+\beta)} - \cdots. \end{aligned} \tag{7.187}$$

When $\alpha = 1$ and $\beta = 1$, the solutions in Eqs. (7.186) and (7.187) are exactly the same as the Taylor series expansions of the exact solutions

$$u(x,t) = \lambda - k\coth(k(\xi - \lambda t)), \tag{7.188}$$

$$v(x,t) = -k^2\mathrm{csch}^2(k(\xi - \lambda t)). \tag{7.189}$$

Tables 7.4, 7.5, and 7.6 cite the comparison between CFRDTM, Adomian decomposition method (ADM) and variational iteration method (VIM) results for $u(x,t)$ and $v(x,t)$ of WBK equation (7.158), MB equation (7.170), and ALW equation (7.180) when $\alpha = 1$ and $\beta = 1$. It reveals that very good approximations have been obtained.

The comparison results between the proposed method CFRDTM with the other methods ADM and VIM presented in Tables 7.4, 7.5, and 7.6 demonstrate that the proposed method is more accurate and better than ADM and VIM. Therefore, the pertinent feature of the proposed method is that it provides more accurate solution than the existing methods ADM and VIM. Hence, the proposed methodology leads to high accuracy. Moreover, the present approximations show excellent accuracy and sufficiently justify the superiority over other methods.

Figures 7.46, 7.47, and 7.48 explore the numerical approximate solutions obtained by the present method and exact solutions of $u(x,t)$ and $v(x,t)$ for WBK equation (7.158), MB equation (7.170), and ALW equation (7.180) when $\alpha = 1$ and $\beta = 1$.

Figures 7.49, 7.50, and 7.51 exhibit the numerical approximate solutions of $u(x,t)$ and $v(x,t)$ for WBK equation (7.158), MB equation (7.170), and ALW equation (7.180) with regard to different values of α and β.

The comparison of approximate solutions $u(x,t)$ and $v(x,t)$ with regard to exact solutions for WBK equation (7.158), MB equation (7.170), and ALW equation (7.180) has been shown in Figs. 7.52, 7.53, and 7.54 at time instance $t = 5$ for $\alpha = 1$ and $\beta = 1$.

7.5.6 *Convergence and Error Analysis of CFRDTM*

In the present section, the error analysis of CFRDTM has been carried out through the following theorem.

Table 7.4 Comparison between CFRDTM, ADM, and VIM results for $u(x,t)$ and $v(x,t)$ when $k = 0.1$, $\lambda = 0.005$, $a = 1.5$, $b = 1.5$, and $c = 10$, for the approximate solutions of WKB equations (7.158a) and (7.158b)

(x, t)	$\lvert u_{\text{Exact}} - u_{\text{ADM}}\rvert$	$\lvert u_{\text{Exact}} - u_{\text{VIM}}\rvert$	$\lvert v_{\text{Exact}} - v_{\text{ADM}}\rvert$	$\lvert v_{\text{Exact}} - v_{\text{VIM}}\rvert$	$\lvert u_{\text{Exact}} - u_{\text{CRFDTM}}\rvert$	$\lvert v_{\text{Exact}} - v_{\text{CRFDTM}}\rvert(0.1,0.1)$
(0.1, 0.1)	1.04892E−04	1.23033E−04	6.41419E−03	1.10430E−04	1.11022E−16	2.77556E−17
(0.1, 0.3)	9.64474E−05	3.69597E−04	5.99783E−03	3.31865E−04	1.11022E−16	3.60822E−16
(0.1, 0.5)	8.88312E−05	6.16873E−04	5.61507E−03	5.54071E−04	1.33227E−15	2.40086E−15
(0.2, 0.1)	4.25408E−04	1.19869E−04	1.33181E−02	1.07016E−04	2.22045E−16	4.16334E−17
(0.2, 0.3)	3.91098E−04	3.60098E−04	1.24441E−02	3.21601E−04	1.66533E−16	3.05311E−16
(0.2, 0.5)	3.60161E−04	6.01006E−04	1.16416E−02	5.36927E−04	1.4988E−15	2.31759E−15
(0.3, 0.1)	9.71922E−04	1.16789E−04	2.07641E−02	1.03737E−04	0	5.55112E−17
(0.3, 0.3)	8.93309E−04	3.50866E−04	1.93852E−02	3.11737E−04	2.77556E−16	2.63678E−16
(0.3, 0.5)	8.22452E−04	5.85610E−04	1.81209E−02	5.20447E−04	1.27676E−15	2.15106E−15
(0.4, 0.1)	1.75596E−03	1.13829E−04	2.88100E−02	1.00579E−04	5.55112E−17	2.77556E−17
(0.4, 0.3)	1.61430E−03	3.41948E−04	2.68724E−02	3.02245E−04	1.66533E−16	2.498E−16
(0.4, 0.5)	1.48578E−03	5.70710E−04	2.50985E−02	5.04593E−04	1.27676E−15	2.04003E−15
(0.5, 0.1)	2.79519E−03	1.10936E−04	3.75193E−02	9.75385E−05	0	0
(0.5, 0.3)	2.56714E−03	3.33274E−04	3.49617E−02	2.93107E−04	2.22045E−16	2.63678E−16
(0.5, 0.5)	2.36184E−03	5.56235E−04	3.26239E−02	4.89335E−04	1.22125E−15	1.90126E−15

Table 7.5 Comparison between CFRDTM, ADM, and VIM results for $u(x,t)$ and $v(x,t)$ when $k = 0.1$, $\lambda = 0.005$, $a = 1$, $b = 0$, and $c = 10$, for the approximate solutions of MB equations (7.170a) and (7.170b)

(x, t)	$\lvert u_{\text{Exact}} - u_{\text{ADM}}\rvert$	$\lvert u_{\text{Exact}} - u_{\text{VIM}}\rvert$	$\lvert v_{\text{Exact}} - v_{\text{ADM}}\rvert$	$\lvert v_{\text{Exact}} - v_{\text{VIM}}\rvert$	$\lvert u_{\text{Exact}} - u_{\text{CRFDTM}}\rvert$	$\lvert v_{\text{Exact}} - v_{\text{CRFDTM}}\rvert$
(0.1, 0.1)	8.16297E−07	6.35269E−05	5.88676E−05	1.65942E−05	5.55112E−17	3.46945E−18
(0.1, 0.3)	7.64245E−07	1.90854E−04	5.56914E−05	4.98691E−05	5.55112E−17	5.20417E−17
(0.1, 0.5)	7.16083E−07	3.18549E−04	5.27169E−05	8.32598E−05	6.66134E−16	3.60822E−16
(0.2, 0.1)	3.26243E−06	6.18930E−05	1.18213E−04	1.60813E−05	1.11022E−16	6.93889E−18
(0.2, 0.3)	3.05458E−06	1.85945E−04	1.11833E−04	4.83269E−05	1.11022E−16	4.68375E−17
(0.2, 0.5)	2.86226E−06	3.10352E−04	1.05858E−04	8.06837E−05	7.77156E−16	3.46945E−16
(0.3, 0.1)	7.33445E−06	6.03095E−05	1.78041E−04	1.55880E−05	0	6.93889E−18
(0.3, 0.3)	6.86758E−06	1.81187E−04	1.68429E−04	4.68440E−05	1.66533E−16	3.98986E−17
(0.3, 0.5)	6.43557E−06	3.02408E−04	1.59428E−04	7.82068E−05	6.66134E−16	3.22659E−16
(0.4, 0.1)	1.30286E−05	5.87746E−05	2.38356E−04	1.51135E−05	5.55112E−17	5.20417E−18
(0.4, 0.3)	1.22000E−05	1.76574E−04	2.25483E−04	4.54174E−05	5.55112E−17	3.46945E−17
(0.4, 0.5)	1.14333E−05	2.94707E−04	2.13430E−04	7.58243E−05	6.66134E−16	3.05311E−16
(0.5, 0.1)	2.03415E−05	5.72867E−05	2.99162E−04	1.46569E−05	0	1.73472E−18
(0.5, 0.3)	1.90489E−05	1.72102E−04	2.83001E−04	4.40448E−05	1.11022E−16	4.16334E−17
(0.5, 0.5)	1.78528E−05	2.87241E−04	2.67868E−04	7.35317E−05	6.10623E−16	2.87964E−16

Table 7.6 Comparison between CFRDTM, ADM, and VIM results for $u(x,t)$ and $v(x,t)$ when $\alpha = 1$ and $\beta = 1$, $k = 0.1$, $\lambda = 0.005$, $a = 0$, $b = 0.5$, and $c = 10$, for the approximate solutions of ALW equations (7.180a) and (7.180b)

(x, t)	$\lvert u_{\text{Exact}} - u_{\text{ADM}}\rvert$	$\lvert u_{\text{Exact}} - u_{\text{VIM}}\rvert$	$\lvert v_{\text{Exact}} - v_{\text{ADM}}\rvert$	$\lvert v_{\text{Exact}} - v_{\text{VIM}}\rvert$	$\lvert u_{\text{Exact}} - u_{\text{CRFDTM}}\rvert$	$\lvert v_{\text{Exact}} - v_{\text{CRFDTM}}\rvert$
(0.1, 0.1)	8.02989E−06	3.17634E−05	4.81902E−04	8.29712E−06	2.77556E−17	1.73472E−18
(0.1, 0.3)	7.38281E−06	9.54273E−05	4.50818E−04	2.49346E−05	2.77556E−17	2.60209E−17
(0.1, 0.5)	6.79923E−06	1.59274E−04	4.22221E−04	4.16299E−05	3.33067E−16	1.80411E−16
(0.2, 0.1)	3.23228E−05	3.09466E−05	9.76644E−04	8.04063E−06	2.77556E−17	3.46945E−18
(0.2, 0.3)	2.97172E−05	9.29725E−05	9.13502E−04	2.41634E−05	4.16334E−17	2.34188E−17
(0.2, 0.5)	2.73673E−05	1.55176E−04	8.55426E−04	4.03419E−05	3.60822E−16	1.73472E−16
(0.3, 0.1)	7.32051E−05	3.01549E−05	1.48482E−03	7.79401E−06	1.38778E−17	3.46945E−18
(0.3, 0.3)	6.73006E−05	9.05935E−05	1.38858E−03	2.34220E−05	5.55112E−17	1.99493E−17
(0.3, 0.5)	6.19760E−05	1.51204E−04	1.30009E−03	3.91034E−05	3.19189E−16	1.61329E−16
(0.4, 0.1)	1.31032E−04	2.93874E−05	2.00705E−03	7.55675E−06	1.38778E−17	2.60209E−18
(0.4, 0.3)	1.20455E−04	8.82871E−05	1.87661E−03	2.27087E−05	2.77556E−17	1.73472E−17
(0.4, 0.5)	1.10919E−04	1.47354E−04	1.75670E−03	3.79121E−05	3.19189E−16	1.52656E−16
(0.5, 0.1)	2.06186E−04	2.86433E−05	2.54396E−03	7.32847E−06	0	8.67362E−19
(0.5, 0.3)	1.89528E−04	8.60509E−05	2.37815E−03	2.20224E−05	5.55112E−17	2.08167E−17
(0.5, 0.5)	1.74510E−04	1.43620E−04	2.22578E−03	3.67658E−05	3.19189E−16	1.43982E−16

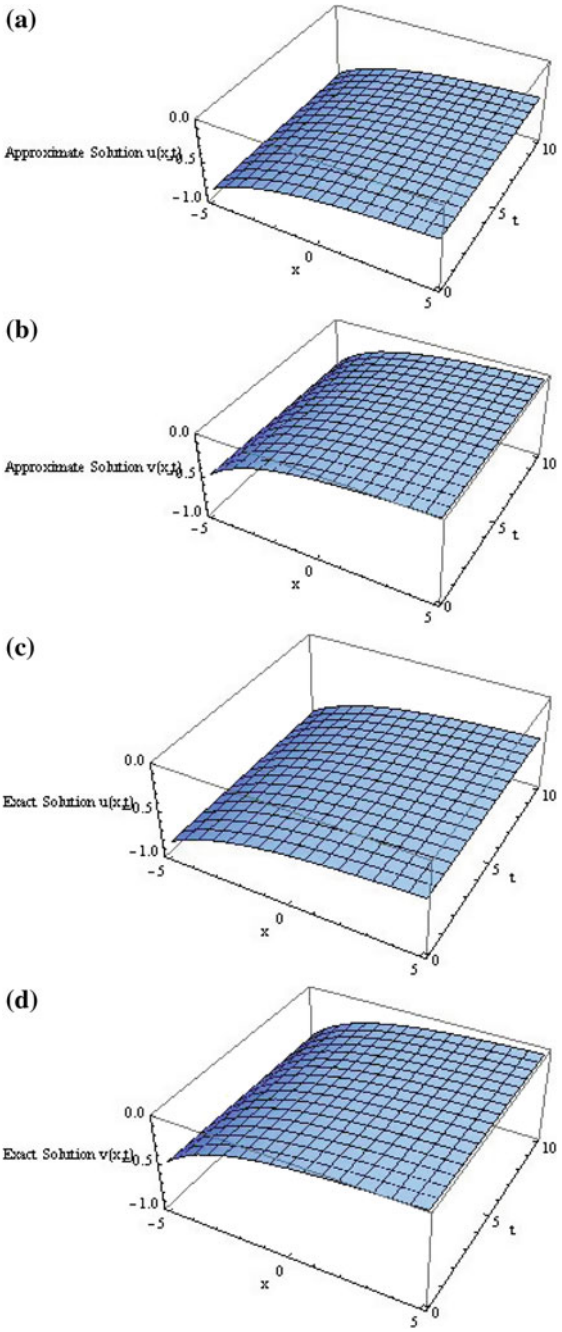

Fig. 7.46 Surfaces show **a** the numerical approximate solution of $u(x,t)$, **b** the numerical approximate solution of $v(x,t)$, **c** the exact solution of $u(x,t)$, and **d** the exact solution of $v(x,t)$ when $\alpha = 1$ and $\beta = 1$

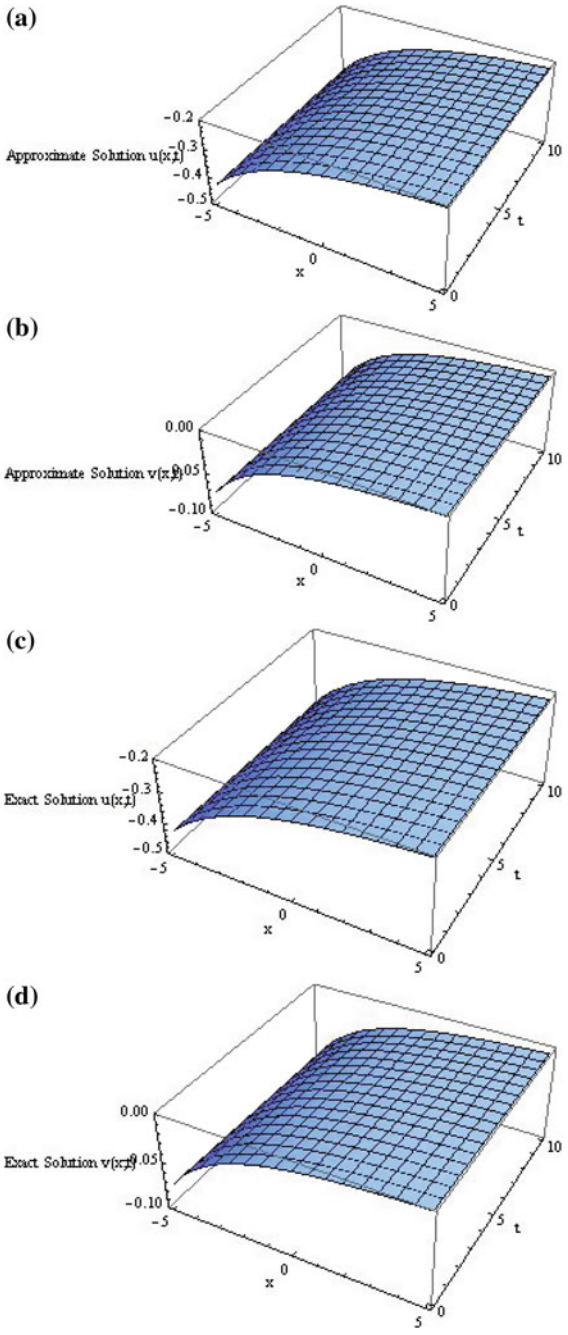

Fig. 7.47 Surfaces show **a** the numerical approximate solution of $u(x,t)$, **b** the numerical approximate solution of $v(x,t)$, **c** the exact solution of $u(x,t)$, and **d** the exact solution of $v(x,t)$ when $\alpha = 1$ and $\beta = 1$

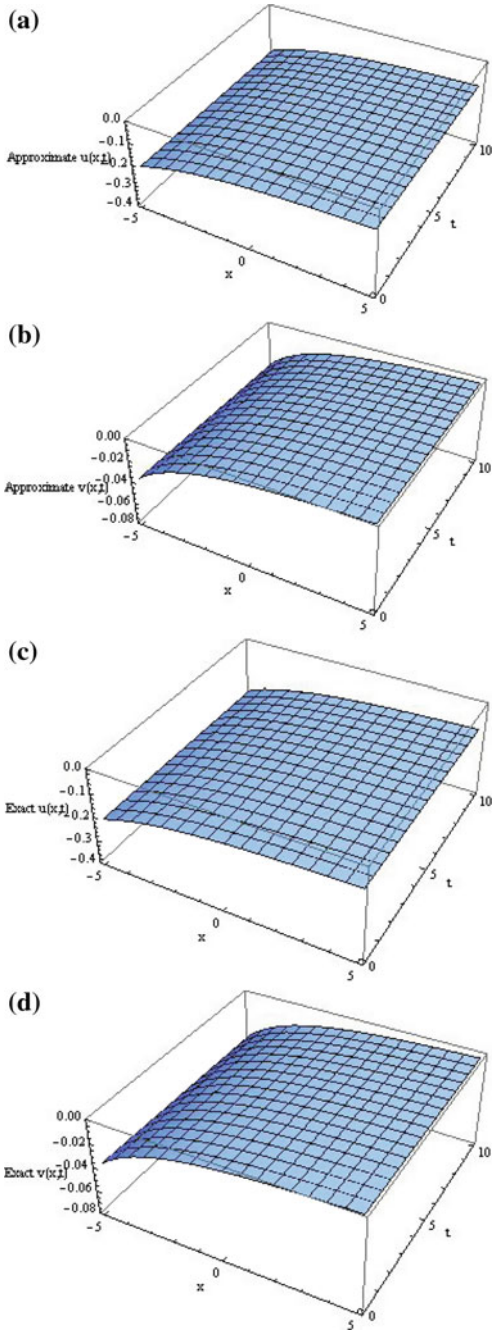

Fig. 7.48 Surfaces show **a** the numerical approximate solution of $u(x,t)$, **b** the numerical approximate solution of $v(x,t)$, **c** the exact solution of $u(x,t)$, and **d** the exact solution of $v(x,t)$ when $\alpha = 1$ and $\beta = 1$

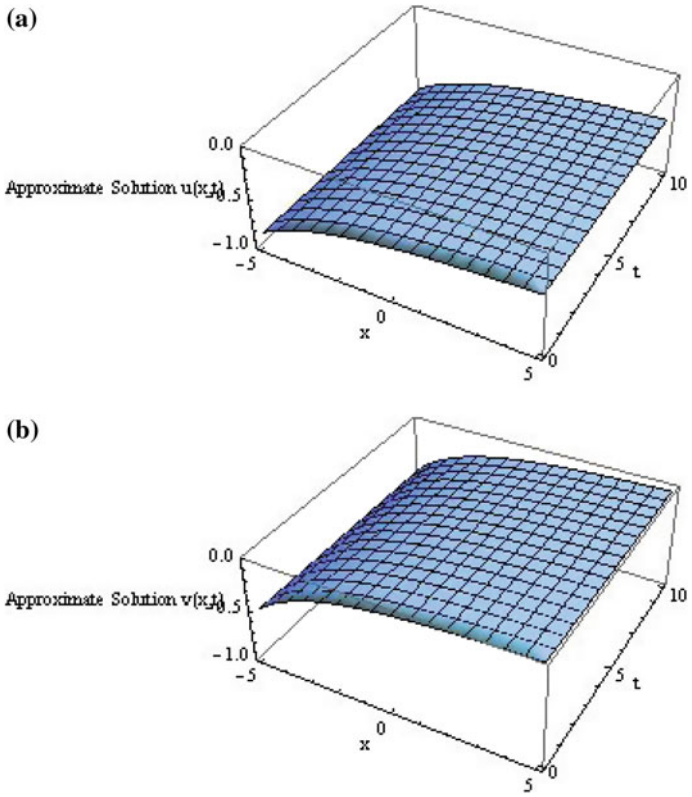

Fig. 7.49 Surfaces show **a** the numerical approximate solution of $u(x,t)$ and **b** the numerical approximate solution of $v(x,t)$ for WBK equations (7.158a) and (7.158b) when $\alpha = 1/8$ and $\beta = 1/4$

Theorem 7.4 *Let* $D_t^{\alpha} u = \mathcal{F}(u, v, u_x, v_x, u_{xx}, v_{xx}, u_{xxx}, v_{xxx}, \ldots)$ *and* $D_t^{\beta} v = \mathcal{H}(u, v, u_x, v_x, u_{xx}, v_{xx}, u_{xxx}, v_{xxx}, \ldots)$ *be the general coupled fractional differential equations, and let the Caputo derivatives* $D_t^{k\alpha} u(x,t)$ *and* $D_t^{k\beta} v(x,t)$ *be continuous functions on* $[0, L] \times [0, T]$, i.e.,

$$D_t^{k\alpha} u(x,t) \in C([0,L] \times [0,T]) \text{ and } D_t^{k\beta} v(x,t) \in C([0,L] \times [0,T]),$$

for $k = 0, 1, 2, \ldots, n+1$, where $0 < \alpha, \beta < 1$, then the approximate solutions $\tilde{u}(x,t)$ and $\tilde{v}(x,t)$ of the preceding general coupled fractional differential equations are

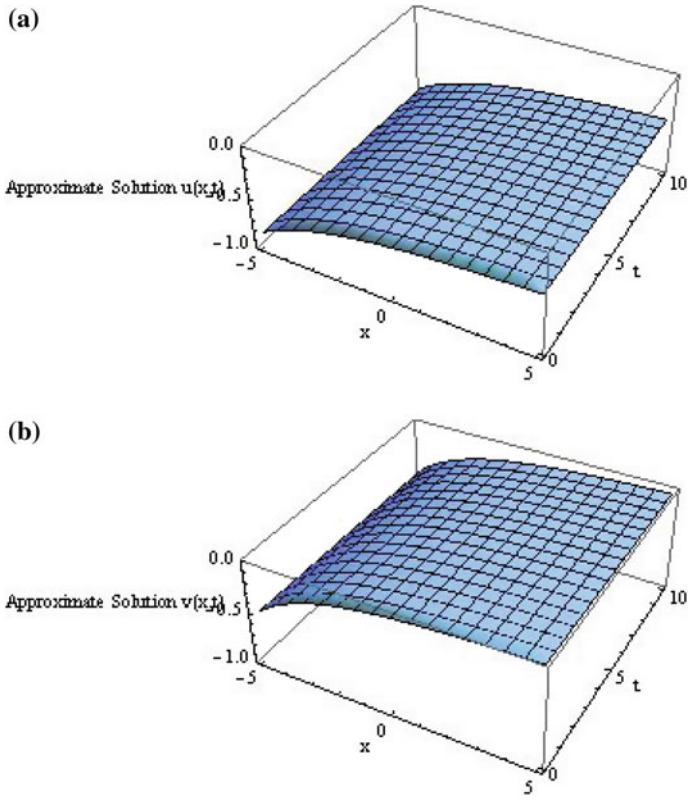

Fig. 7.50 Surfaces show **a** the numerical approximate solution of $u(x,t)$ and **b** the numerical approximate solution of $v(x,t)$ for MB equations (7.170a) and (7.170b) when $\alpha = 1/4$ and $\beta = 0.88$

$$\tilde{u}(x,t) \cong \sum_{k=0}^{n} \sum_{h=0}^{k} U(h,k-h) t^{h\alpha+(k-h)\beta},$$

and

$$\tilde{v}(x,t) \cong \sum_{k=0}^{n} \sum_{h=0}^{k} V(h,k-h) t^{h\alpha+(k-h)\beta},$$

where $U(h,k-h)$ and $V(h,k-h)$ are coupled fractional reduced differential transforms of $u(x,t)$ and $v(x,t)$, respectively.

Moreover, there exist values $\xi_1,\ \xi_2$ where $0 \leq \xi_1,\ \xi_2 \leq t$ so that the error $E_n(x,t)$ for the approximate solution $\tilde{u}(x,t)$ has the form

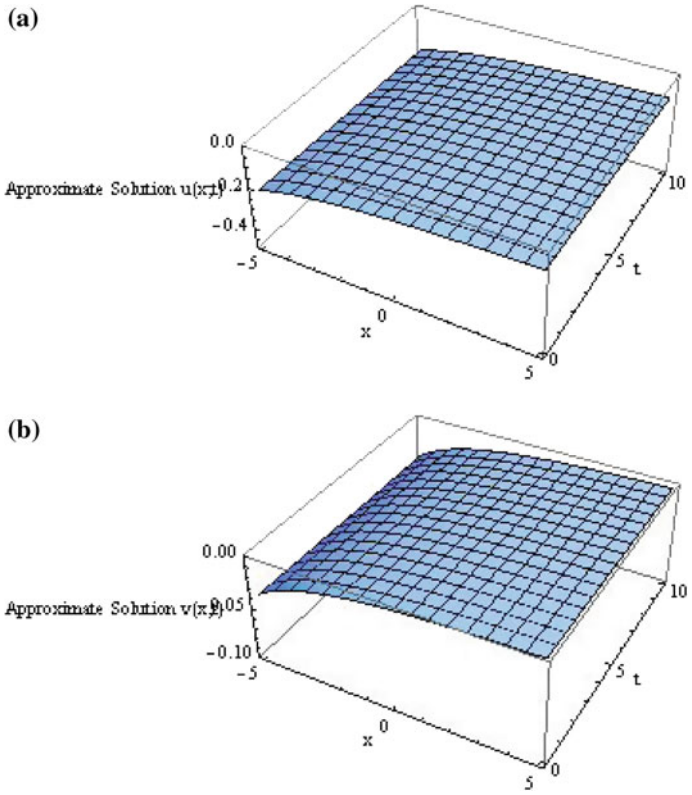

Fig. 7.51 Surfaces show **a** the numerical approximate solution of $u(x,t)$ and **b** the numerical approximate solution of $v(x,t)$ for ALW equations (7.180a) and (7.180b) when $\alpha = 1/2$ and $\beta = 1/2$

$$\|E_n(x,t)\| = \sup_{\substack{0 \le x \le L \\ 0 \le t \le T}} \left| \frac{D^{(n+1)\beta} u(x,0+)}{\Gamma((n+1)\beta+1)} t^{(n+1)\beta} \right|,$$

if $\xi_1,\ \xi_2 \to 0+$.

Proof From Lemma 1 of Chap. 1, we have

$$J^{\alpha} D^{\alpha} f(t) = f(t) - \sum_{k=0}^{m-1} \frac{t^k}{\Gamma(k+1)} f^{(k)}(0+), \quad m-1 < \alpha < m$$

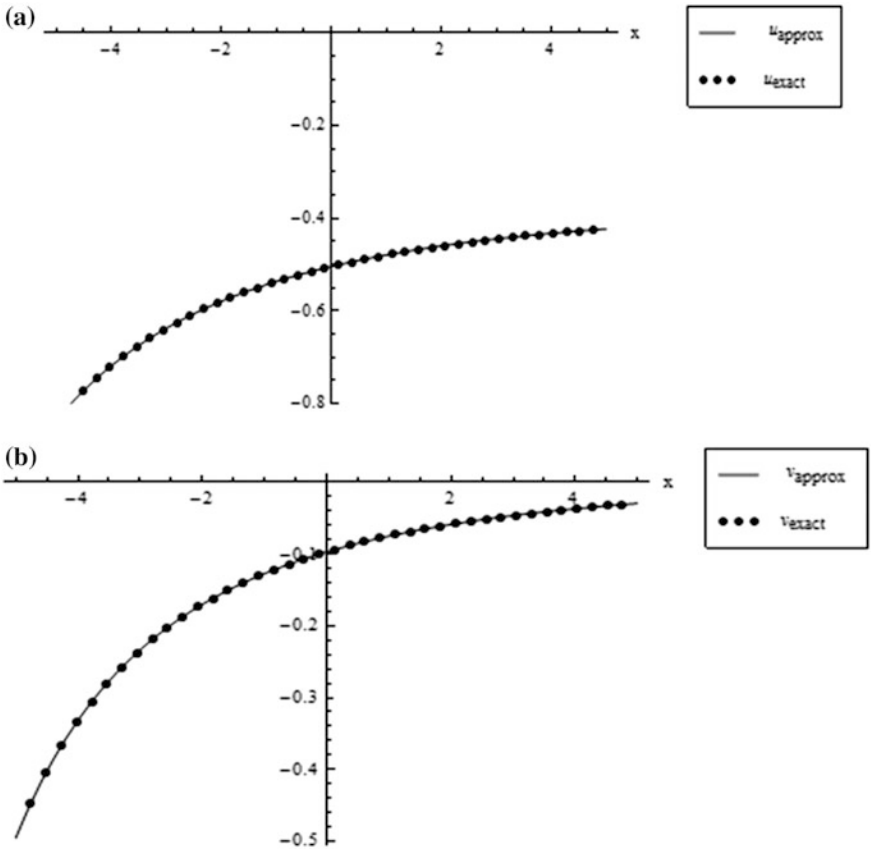

Fig. 7.52 Comparison of approximate solutions **a** $u(x,t)$ and **b** $v(x,t)$ with regard to exact solutions of WBK equation (7.158) at time instance $t = 5$

The error term

$$E_n(x,t) = u(x,t) - \tilde{u}(x,t),$$

where

$$u(x,t) = \sum_{k=0}^{\infty} \sum_{h=0}^{k} \frac{D^{h\alpha+\beta(k-h)} u(x,0)}{\Gamma(h\alpha+\beta(k-h)+1)} t^{h\alpha+\beta(k-h)},$$

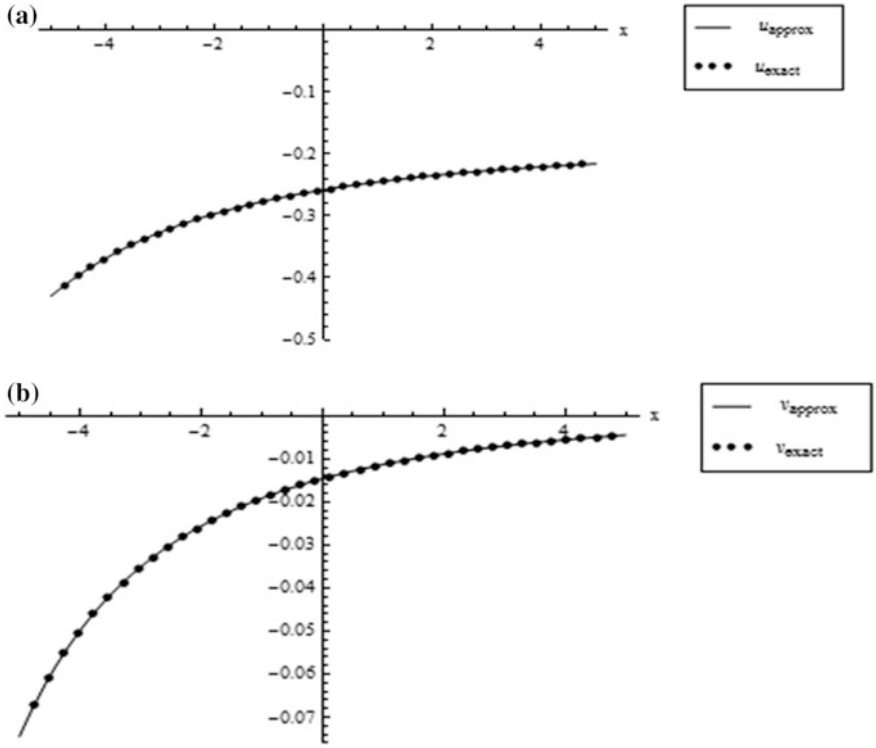

Fig. 7.53 Comparison of approximate solutions **a** $u(x,t)$ and **b** $v(x,t)$ with regard to exact solutions of MB equation (7.170) at time instance $t = 5$

and

$$\tilde{u}(x,t) = \sum_{k=0}^{n} \sum_{h=0}^{k} \frac{D^{h\alpha+\beta(k-h)} u(x,0)}{\Gamma(h\alpha+\beta(k-h)+1)} t^{h\alpha+\beta(k-h)}.$$

Now, for $0<\alpha<1$,

$$\begin{aligned} & J^{h\alpha+\beta(k-h)} D^{h\alpha+\beta(k-h)} u(x,t) - J^{(h+1)\alpha+\beta(k-h)} D^{(h+1)\alpha+\beta(k-h)} u(x,t) \\ &= J^{h\alpha+\beta(k-h)} \left(D^{h\alpha+\beta(k-h)} u(x,t) - J^{\alpha} D^{\alpha} \left(D^{h\alpha+\beta(k-h)} u(x,t) \right) \right) \\ &= J^{h\alpha+\beta(k-h)} D^{h\alpha+\beta(k-h)} u(x,0), \end{aligned}$$

since $0<\alpha<1$, using Eq. (1.14)

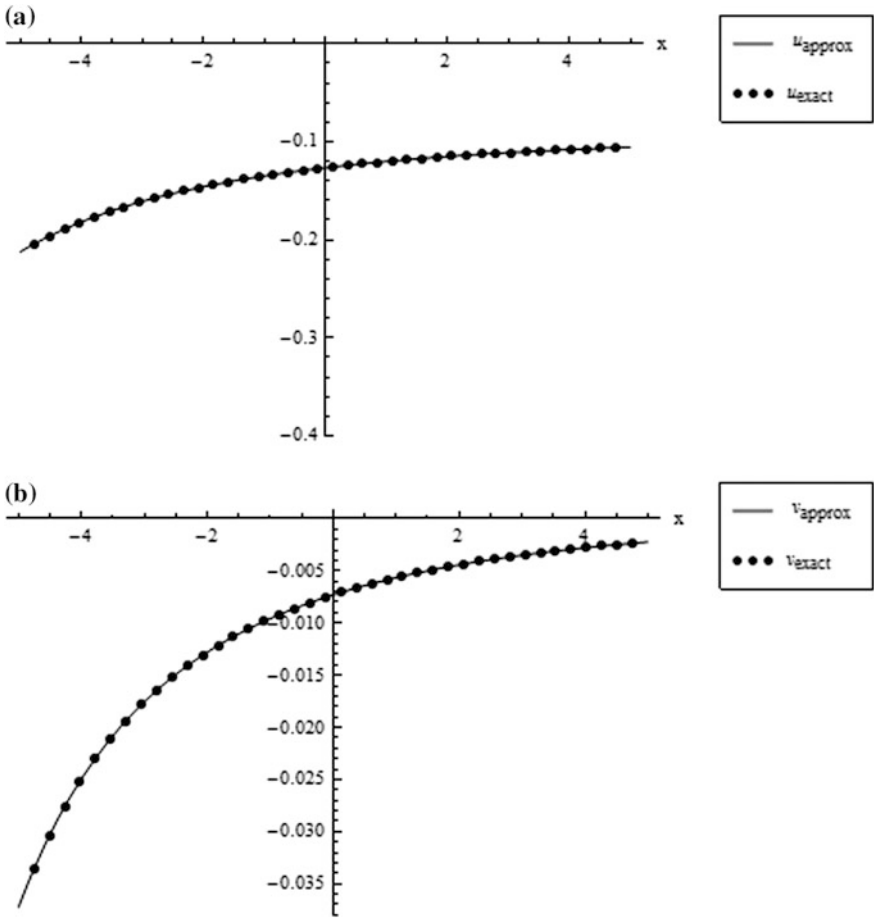

Fig. 7.54 Comparison of approximate solutions **a** $u(x,t)$ and **b** $v(x,t)$ with regard to exact solutions of ALW equation (7.180) at time instance $t = 5$

$$= \frac{D^{h\alpha+\beta(k-h)}u(x,0)}{\Gamma(h\alpha+\beta(k-h)+1)}t^{h\alpha+\beta(k-h)} \tag{7.190}$$

The nth order approximation for $u(x,t)$ is

$$\tilde{u}(x,t) = \sum_{k=0}^{n}\sum_{h=0}^{k}\frac{D^{h\alpha+\beta(k-h)}u(x,0)}{\Gamma(h\alpha+\beta(k-h)+1)}t^{h\alpha+\beta(k-h)}$$
$$= \sum_{k=0}^{n}\sum_{h=0}^{k}\left(J^{h\alpha+\beta(k-h)}D^{h\alpha+\beta(k-h)}u(x,t) - J^{(h+1)\alpha+\beta(k-h)}D^{(h+1)\alpha+\beta(k-h)}u(x,t)\right),$$

using Eq. (7.190)

$$= \sum_{k=0}^{n} J^{k\beta} D^{k\beta} u(x,t) - \sum_{h=0}^{n} J^{(h+1)\alpha+\beta(n-h)} D^{(h+1)\alpha+\beta(n-h)} u(x,t)$$
$$= u(x,t) + \sum_{k=0}^{n-1} J^{(k+1)\beta} D^{(k+1)\beta} u(x,t) - \sum_{h=0}^{n} J^{(h+1)\alpha+\beta(n-h)} D^{(h+1)\alpha+\beta(n-h)} u(x,t) \tag{7.191}$$

Therefore, from Eq. (7.191), the error term becomes

$$\begin{aligned} E_n(x,t) &= u(x,t) - \tilde{u}(x,t) \\ &= \sum_{h=0}^{n} J^{(h+1)\alpha+\beta(n-h)} D^{(h+1)\alpha+\beta(n-h)} u(x,t) - \sum_{k=0}^{n-1} J^{(k+1)\beta} D^{(k+1)\beta} u(x,t) \\ &= \sum_{i=0}^{n} J^{(i+1)\alpha+\beta(n-i)} D^{(i+1)\alpha+\beta(n-i)} u(x,t) - \sum_{i=0}^{n-1} J^{(i+1)\beta} D^{(i+1)\beta} u(x,t) \\ &= \sum_{i=0}^{n} \frac{1}{\Gamma((i+1)\alpha+\beta(n-i))} \int_0^t (t-\tau)^{(i+1)\alpha+\beta(n-i)-1} D^{(i+1)\alpha+\beta(n-i)} u(x,\tau) \mathrm{d}\tau \\ &\quad - \sum_{i=0}^{n-1} \frac{1}{\Gamma((i+1)\beta)} \int_0^t (t-\tau)^{(i+1)\beta-1} D^{(i+1)\beta} u(x,\tau) \mathrm{d}\tau \end{aligned}$$

Whence applying integral mean value theorem yielding

$$\begin{aligned} E_n(x,t) = &\sum_{i=0}^{n} \frac{D^{(i+1)\alpha+\beta(n-i)} u(x,\xi_1)}{\Gamma((i+1)\alpha+\beta(n-i)+1)} t^{(i+1)\alpha+\beta(n-i)} \\ &- \sum_{i=0}^{n-1} \frac{D^{(i+1)\beta} u(x,\xi_2)}{\Gamma((i+1)\beta+1)} t^{(i+1)\beta}, \end{aligned}$$

where $0 \le \xi_1,\ \xi_2 \le t$.

This implies

$$\begin{aligned}E_n(x,t) &= u(x,t) - \tilde{u}(x,t)\\ &= \sum_{i=0}^{n-1} \frac{D^{(i+1)\alpha+\beta(n-i)}u(x,\xi_1)}{\Gamma((i+1)\alpha+\beta(n-i)+1)} t^{(i+1)\alpha+\beta(n-i)}\\ &\quad + \frac{D^{(n+1)\alpha}u(x,\xi_1)}{\Gamma((n+1)\alpha+1)} t^{(n+1)\alpha} - \sum_{i=0}^{n-1} \frac{D^{(i+1)\beta}u(x,\xi_2)}{\Gamma((i+1)\beta+1)} t^{(i+1)\beta}\\ &= \sum_{i=0}^{n-1} \left[\frac{D^{(i+1)\alpha+\beta(n-i)}u(x,\xi_1)}{\Gamma((i+1)\alpha+\beta(n-i)+1)} t^{(i+1)\alpha+\beta(n-i)} - \frac{D^{(i+1)\beta}u(x,\xi_2)}{\Gamma((i+1)\beta+1)} t^{(i+1)\beta}\right]\\ &\quad + \frac{D^{(n+1)\alpha}u(x,\xi_1)}{\Gamma((n+1)\alpha+1)} t^{(n+1)\alpha}\end{aligned} \tag{7.192}$$

Using generalized Taylor's series formula, Eq. (7.192) becomes

$$\begin{aligned}E_n(x,t) &= u(x,t) - \frac{D^{(n+1)\alpha}u(x,\zeta_1)}{\Gamma((n+1)\alpha+1)} t^{(n+1)\alpha} - u(x,t)\\ &\quad + \frac{D^{(n+1)\beta}u(x,\zeta_2)}{\Gamma((n+1)\beta+1)} t^{(n+1)\beta} + \frac{D^{(n+1)\alpha}u(x,\xi_1)}{\Gamma((n+1)\alpha+1)} t^{(n+1)\alpha},\end{aligned}$$

where $0 \le \zeta_1,\ \zeta_2 \le \max\{\xi_1,\ \xi_2\}$ and $\xi_1,\ \xi_2 \to 0+$.

This implies

$$\begin{aligned}\|E_n\| &= \|u(x,t) - \tilde{u}(x,t)\|\\ &= \sup_{\substack{0\le x\le L\\ 0\le t\le T}} \left|\frac{D^{(n+1)\beta}u(x,\zeta_2)}{\Gamma((n+1)\beta+1)} t^{(n+1)\beta} - \frac{D^{(n+1)\alpha}u(x,\zeta_1)}{\Gamma((n+1)\alpha+1)} t^{(n+1)\alpha} + \frac{D^{(n+1)\alpha}u(x,\xi_1)}{\Gamma((n+1)\alpha+1)} t^{(n+1)\alpha}\right| < \infty\\ &= \sup_{\substack{0\le x\le L\\ 0\le t\le T}} \left|\frac{D^{(n+1)\beta}u(x,0+)}{\Gamma((n+1)\beta+1)} t^{(n+1)\beta}\right|, \text{since } \xi_1, \xi_2 \to 0+.\end{aligned} \tag{7.193}$$

As $n \to \infty$, from Eq. (7.193)

$$\|E_n\| \to 0.$$

Hence, $u(x,t)$ can be approximated as

$$u(x,t) = \sum_{k=0}^{\infty}\sum_{h=0}^{k} U(h,k-h)t^{h\alpha+(k-h)\beta} \cong \sum_{k=0}^{n}\sum_{h=0}^{k} U(h,k-h)t^{h\alpha+(k-h)\beta} = \tilde{u}(x,t),$$

with the error term given in Eq. (7.193).

Following a similar argument, we may also find the error $\left\|\hat{E}_n\right\| = \|v(x,t) - \tilde{v}(x,t)\|$ for the approximate solution $\tilde{v}(x,t)$. ■

7.6 Conclusion

In this chapter, the MFRDTM has been proposed and it is directly applied to obtain explicit and numerical solitary wave solutions of the fractional KdV like $K(m,n)$ equations with initial conditions. In this regard, the reduced differential transform method is modified to be easily employed to solve wide kinds of nonlinear fractional differential equations. In this new approach, the nonlinear term is replaced by its Adomian polynomials. As a result, we obtain the approximate solutions of fractional KdV equation with high accuracy. The obtained results demonstrate the reliability of the proposed algorithm and its wider applicability to fractional nonlinear evolution equations. It also exhibits that the proposed method is a very efficient and powerful technique in finding the solutions of the nonlinear fractional differential equations. The main advantage of the method is the fact that it provides an analytical approximate solution, in many cases an exact solution, in a rapidly convergent series with elegantly computed terms. It requires less amount of computational overhead in comparison with other numerical methods and consequently introduces a significant improvement in solving fractional nonlinear equations over existing methods available in the open literature.

A new approximate numerical technique, coupled fractional reduced differential transform, has been proposed in this chapter for solving nonlinear fractional partial differential equations. The proposed method is only well suited for coupled fractional linear and nonlinear differential equations. In comparison with other analytical methods, the present method is an efficient and simple tool to determine the approximate solution of nonlinear coupled fractional partial differential equations. The obtained results demonstrate the reliability of the proposed algorithm and its applicability to nonlinear coupled fractional evolution equations. It also exhibits that the proposed method is a very efficient and powerful technique in finding the solutions of the nonlinear coupled time fractional differential equations. The main advantage of the proposed method is that it requires less amount of computational overhead in comparison with other numerical and analytical approximate methods and consequently introduces a significant improvement in solving coupled fractional nonlinear equations over existing methods available in the open literature. The application of the proposed method for the solutions of time fractional coupled KdV equations satisfactorily justifies its simplicity and efficiency.

In this chapter, new CFRDTM has been successfully implemented to obtain the soliton solutions of coupled time fractional modified KdV equations. This new method has been revealed by the author. The application of the proposed method for the solutions of time fractional coupled modified KdV equations satisfactorily justifies its simplicity and efficiency. Moreover, in case of integer-order coupled

modified KdV equations, the obtained results have been verified by the Adomian decomposition method. This investigation leads to the conclusion that soliton solutions for integer-order coupled modified KdV equations have been wrongly reported by the reverend author Fan [44].

Also in this chapter, the new approximate numerical technique CFRDTM [34, 35] has been proposed for solving nonlinear fractional partial differential equations arising in predator–prey biological population dynamical system. The results thus obtained validate the reliability of the proposed algorithm. It additionally displays that the proposed process is an extraordinarily efficient and strong technique. The main advantage of the proposed method is that it necessitates less amount of computational effort. In a later study, it has been planned to use the proposed process for the solution of the fractional epidemic model, coupled fractional neutron diffusion equations with delayed neutrons, and other physical models with the intention to show the efficiency and wide applicability of the newly proposed method.

In view of the author [61], there is no difference between differential transform method (DTM) and Taylor series method (TSM) both of which (normally) are provided with an analytical continuation via a stepwise procedure, since it is essential to transform the formal series into an approximate solution of the problem (via analytical continuation). The author also wrote in [61] that one may then rightly remember the approach as being "*an extended Taylor series method.*" Thus, the DTM could, eventually, be named as the generalized Taylor series method (GTSM). In the belief of the learned author, "DTM could deserve its name (as a technique) when it extends the Taylor series method to new kinds of expansion (different from a Taylor series expansion)." He, additionally, acknowledges that the DTM has allowed an easy generalization of the Taylor series method to various derivation procedures. "For example, fractional differential equations have been considered using the DTM extended to the fractional derivative procedure via a modified version of the Taylor series." Despite the fact that there is a controversy in the name of DTM, the author of [61] admits that major contribution of the DTM is in the easy generalization of the Taylor series method to problems involving fractional derivatives.

Furthermore, it may be stated that the Taylor series method is used invariably in many mathematical analyses and derivations for the problems of applied science and engineering. Taylor series method of order one is commonly known as the Euler method. However, the Euler method has its independent existence. Like that, DTM is also self-contained for at least in the application of fractional-order calculus and has its own right for its existence.

Also, in this chapter, fractional coupled Schrödinger–Korteweg–de Vries equations with appropriate initial values have been solved by using the novel method, viz. CFRDTM. The applications of the proposed method for the solutions of time fractional coupled Sch–KdV equations reasonably well justify its simplicity, plausibility, and efficiency.

In this chapter, solutions of nonlinear coupled fractional partial differential equations have been proposed by CFRDTM which is only well suited for coupled

fractional linear and nonlinear differential equations. The present method is an efficient and simple tool in comparison with other analytical methods. The obtained results quite justify that the proposed method is very well suited and is an efficient and powerful technique in finding the solutions of the nonlinear coupled time fractional differential equations. One of the main advantages of the proposed method is that it requires less amount of computational overhead and consequently introduces a significant achievement in solving coupled fractional nonlinear equations over existing methods available in the open literature. Furthermore, the applications of the proposed method for the solutions of variant types of time fractional coupled WBK equations satisfactorily justify its simplicity and efficiency. The proposed method determines the analytical approximate solutions as well as numerical solutions. This proposed method can be efficiently applied to coupled fractional differential equations more accurately and easily than its comparable methods ADM and VIM. So, this proposed method can be a better substitute than its competitive methods ADM and VIM.

References

1. Podlubny, I.: Fractional Differential Equations. Academic Press, New York (1999)
2. Miller, K.S., Ross, B.: An Introduction to the Fractional Calculus and Fractional Differential Equations. Wiley, New York (1993)
3. Samko, S.G., Kilbas, A.A., Marichev, O.I.: Fractional Integrals and Derivatives: Theory and Applications. Taylor and Francis, London (1993)
4. Saha Ray, S., Bera, R.K.: Analytical solution of a dynamic system containing fractional derivative of order one-half by Adomian decomposition method. Trans. ASME J. Appl. Mech. **72**(2), 290–295 (2005)
5. Caputo, M.: Elasticità e Dissipazione. Zanichelli, Bologna (1969)
6. Caputo, M.: Linear models of dissipation whose Q is almost frequency independent, Part II. J. Roy. Astr. Soc. **13**(5), 529–539 (1967)
7. Saha Ray, S., Patra, A.: An explicit finite difference scheme for numerical solution of fractional neutron point kinetic equation. Ann. Nucl. Energy **41**, 61–66 (2012)
8. Wang, Q.: Homotopy perturbation method for fractional KdV equation. Appl. Math. Comput. **190**(2), 1795–1802 (2007)
9. Wazwaz, A.M.: Partial Differential Equations: methods and Applications. Balkema, Lisse, The Netherlands (2002)
10. Adomian, G.: Solving Frontier Problems of Physics: The Decomposition Method. Kluwer Academic Publishers, Boston (1994)
11. Liao, S.: Beyond Perturbation: Introduction to the Modified Homotopy Analysis Method. Chapman and Hall/CRC Press, Boca Raton (2003)
12. Saha Ray, S., Bera, R.K.: An approximate solution of a nonlinear fractional differential equation by Adomian decomposition method. Appl. Math. Comput. **167**(1), 561–571 (2005)
13. Saha Ray, S.: A numerical solution of the coupled Sine-Gordon equation using the modified decomposition method. Appl. Math. Comput. **175**(2), 1046–1054 (2006)
14. Ablowitz, M.J., Clarkson, P.A.: Solitons, Nonlinear Evolution Equations and Inverse Scattering. Cambridge University Press, Cambridge (1991)
15. Fan, E.G.: Extended tanh-function method and its applications to nonlinear equations. Phys. Lett. A **277**, 212–218 (2000)

16. Taha, T.R., Ablowitz, M.J.: Analytical and numerical aspects of certain nonlinear evolution equations. III. Numerical Korteweg-de Vries equation. J. Comput. Phys. **55**(2), 231 (1984)
17. Saha Ray, S.: An application of the modified decomposition method for the solution of the coupled Klein–Gordon–Schrödinger equation. Commun. Nonlinear Sci. Numer. Simul. **13**, 1311–1317 (2008)
18. He, J.H.: Variational principles for some nonlinear partial differential equations with variable coefficients. Chaos Solitons Fract. **19**(4), 847–851 (2004)
19. He, J.H.: Perturbation Methods: Basic and Beyond. Elsevier, Amsterdam (2006)
20. Keskin, Y., Oturanc, G.: Reduced differential transform method for partial differential equations. Int. J. Nonlinear Sci. Numer. Simul. **10**(6), 741–749 (2009)
21. Keskin, Y., Oturanc, G.: Reduced differential transform method for generalized KDV equations. Math. Comput. Appl. **15**(3), 382–393 (2010)
22. Keskin, Y., Oturanc, G.: Reduced differential transform method for fractional partial differential equations. Nonlinear Sci. Lett. A **2**, 207–217 (2010)
23. Saha Ray, S.: On Haar wavelet operational matrix of general order and its application for the numerical solution of fractional Bagley Torvik equation. Appl. Math. Comput. **218**, 5239–5248 (2012)
24. Saha Ray, S., Bera, R.K.: Analytical solution of the Bagley Torvik equation by Adomian decomposition method. Appl. Math. Comput. **168**(1), 398–410 (2005)
25. Saha Ray, S.: Exact solutions for time-fractional diffusion-wave equations by decomposition method. Phys. Scr. **75**(1), 53–61 (2007). (Article number 008)
26. Saha Ray, S., Bera, R.K.: Analytical solution of a fractional diffusion equation by Adomian decomposition method. Appl. Math. Comput. **174**(1), 329–336 (2006)
27. Saha Ray, S.: A new approach for the application of Adomian decomposition method for the solution of fractional space diffusion equation with insulated ends. Appl. Math. Comput. **202** (2), 544–549 (2008)
28. Hilfer, R.: Applications of Fractional Calculus in Physics. World Scientific, Singapore (2000)
29. Petrovskii, S., Malchow, H., Li, B.L.: An exact solution of a diffusive predator-prey system. Proc. R. Soc. Londn. A **461**(2056), 1029–1053 (2005)
30. Wei, H., Chen, W., Sun, H.: Homotopy method for parameter determination of solute transport with fractional advection-dispersion equation. CMES: Comput. Model. Eng. Sci. **100**(2), 85–103 (2014)
31. Saha Ray, S., Gupta, A.K.: On the solution of Burgers-Huxley and Huxley equation using Wavelet collocation method. CMES: Comput. Model. Eng. Sci. **91**(6), 409–424 (2013)
32. Saha Ray, S., Gupta, A.K.: An approach with Haar wavelet collocation method for numerical simulation of modified KdV and modified Burgers equations. CMES: Comput. Model. Eng. Sci. **103**(5), 315–341 (2014)
33. Shukla, H.S., Tamsir, M., Srivastava, V.K., Kumar, J.: Approximate analytical solution of time-fractional order Cauchy-reaction diffusion equation. CMES: Comput. Model. Eng. Sci. **103**(1), 1–17 (2014)
34. Saha Ray, S.: Numerical solutions of (1+1) dimensional time fractional coupled Burger equations using new coupled fractional reduced differential transform method. Int. J. Comput. Sci. Math. **4**(1), 1–15 (2013)
35. Saha Ray, S.: Soliton solutions for time fractional coupled modified KdV equations using new coupled fractional reduced differential transform method. J. Math. Chem. **51**(8), 2214–2229 (2013)
36. Odibat, Z.M., Shawagfeh, N.T.: Generalized Taylor's formula. Appl. Math. Comput. **186**(1), 286–293 (2007)
37. Saha Ray, S.: A new coupled fractional reduced differential transform method for solving time fractional coupled KdV equations. Int. J. Nonlinear Sci. Numer. Simul. **14**(7–8), 501–511 (2013)
38. Saha Ray, S.: On the Soliton solution and Jacobi doubly periodic solution of the fractional coupled Schrödinger–KdV equation by a novel approach. Int. J. Nonlinear Sci. Numer. Simul. **16**(2), 79–95 (2015)

39. Saha Ray, S.: A novel method for travelling wave solutions of fractional Whitham-Broer-Kaup, fractional modified Boussinesq and fractional approximate long wave equations in shallow water. Math. Methods Appl. Sci. **38**(7), 1352–1368 (2015)
40. Rosenau, P., Hyman, J.M.: Compactons: Solitons with finite wavelength. Phys. Rev. Lett. **70**, 564–567 (1993)
41. Cun, L.J., Lin, H.G.: New approximate solution for time-fractional coupled KdV equations by generalized differential transform method. Chin. Phys. B **19**(11), 110203 (2010)
42. Hirota, R., Satsuma, J.: Solitons solutions of a coupled Korteweg-de Vries equation. Phys. Lett. A **85**(8–9), 407–408 (1981)
43. Soliman, A.A., Abdou, M.A.: The decomposition method for solving the coupled modified KdV equations. Math. Comput. Model. **47**(9–10), 1035–1041 (2008)
44. Fan, E.: Soliton solutions for a generalized Hirota-Satsuma coupled KdV equation and a coupled MKdV equation. Phys. Lett. A **282**(1–2), 18–22 (2001)
45. Debnath, L.: Nonlinear Partial Differential Equations for Scientists and Engineers. Birkhäuser, Boston (2005)
46. Rao, N.N.: Nonlinear wave modulations in plasmas. Pramana J. Phys. **49**(1), 109–127 (1997)
47. Singh, S.V., Rao, N.N., Shukla, P.K.: Nonlinearly coupled Langmuir and dust-acoustic waves in a dusty plasma. J. Plasma Phys. **60**(3), 551–567 (1998)
48. Fan, E.: Multiple traveling wave solutions of nonlinear evolution equations using a unified algebraic method. J. Phys. A **35**(32), 6853–6872 (2002)
49. Kaya, D., El-Sayed, S.M.: On the solution of the coupled Schrödinger–KdV equation by the decomposition method. Phys. Lett. A **313**(1–2), 82–88 (2003)
50. Whitham, G.B.: Variational methods and applications to water waves. Proc. R. Soc. Lond. Ser. A **299**, 6–25 (1967)
51. Broer, L.J.F.: Approximate equations for long water waves. Appl. Sci. Res. **31**(5), 377–395 (1975)
52. Kaup, D.J.: A higher-order water-wave equation and the method for solving it. Prog. Theor. Phys. **54**(2), 396–408 (1975)
53. Kupershmidt, B.A.: Mathematics of dispersive water waves. Commun. Math. Phys. **99**, 51–73 (1985)
54. Liu, Y., Xin, B.: Numerical solutions of a fractional predator-prey system. In: Advances in Difference Equations, 14 pages (2011) (Article ID 190475)
55. Debnath, L.: Integral Transforms and Their Applications. CRC Press, Boca Raton (1995)
56. Küçükarslan, S.: Homotopy perturbation method for coupled Schrödinger–KdV equation. Nonlinear Anal. Real World Appl. **10**, 2264–2271 (2009)
57. El-Sayed, S.M., Kaya, D.: Exact and numerical traveling wave solutions of Whitham–Broer–Kaup equations. Appl. Math. Comput. **167**, 1339–1349 (2005)
58. Rafei, M., Daniali, H.: Application of the variational iteration method to the Whitham–Broer–Kaup equations. Comput. Math Appl. **54**, 1079–1085 (2007)
59. Xu, G., Li, Z.: Exact travelling wave solutions of the Whitham–Broer–Kaup and Broer–Kaup–Kupershmidt equations. Chaos Solitons Fractals **24**, 549–556 (2005)
60. Xie, F., Yan, Z., Zhang, H.Q.: Explicit and exact traveling wave solutions of Whitham–Broer–Kaup shallow water equations. Phys. Lett. A **285**, 76–80 (2001)
61. Bervillier, C.: Status of the differential transformation method. Appl. Math. Comput. **218**(20), 10158–10170 (2012)

Chapter 8
A Novel Approach with Time-Splitting Fourier Spectral Method for Riesz Fractional Differential Equations

8.1 Introduction

Nonlinear partial differential equations are useful in describing various physical phenomena. The solutions of the nonlinear evolution equations play a crucial role in the field of nonlinear wave phenomena. It is to be noticed that the nonlinear Schrödinger (NLS) equation is one of the most generic soliton equations. It appears in a wide variety of fields, such as nonlinear optics, quantum field theory, weakly nonlinear dispersive water waves, and hydrodynamics [1–4]. Nonlinear phenomena act as a significant role in a variety of scientific fields, especially in solid-state physics, fluid mechanics, plasma waves, plasma physics, and chemical physics [5, 6]. Determination of exact solutions, in particular, traveling wave solutions, of nonlinear equations in mathematical physics plays an important role in soliton theory [7, 8].

As a field of applied mathematics, fractional calculus is a generalization of the differentiation and integration of integer order to arbitrary order (real or complex order). The usefulness of fractional calculus has been found in various areas of science and engineering. Its application has been seen in many research areas such as transport processes, fluid dynamics, electrochemical processes, bioengineering, signal processing, control theory, fractal theory, porous media, viscoelastic materials, electrical circuits, plasma physics, and nuclear reactor kinetics [9–15]. Many physical and engineering phenomena which are analyzed by fractional calculus are considered to be best modeled by fractional differential equations (FDEs). During the past few decades, the intensive research pursuits in the development of the theory of FDEs have been experienced due to its capability to the accurate elucidation of many real-life problems as nature manifests in a fractional-order dynamical manner. Up to now, a great deal of effort has been devoted to solving the FDEs by various analytical and numerical methods. These methods include finite difference method [16], operational matrix method [17], (G'/G)-expansion method [18–21], Adomian decomposition method [22, 23], differential transform method [24, 25], first integral method [26, 27], and fractional subequation method [28, 29], etc.

S. Saha Ray, *Nonlinear Differential Equations in Physics*,
https://doi.org/10.1007/978-981-15-1656-6_8

Derivative nonlinear Schrödinger (DNLS)-type equations are significant nonlinear models that have many implementations in nonlinear optics fibers and plasma physics [30–33]. In nonlinear optics, nonlinear effects are studied comprehensively. To describe the nonlinear effects in optical fibers without the inclusion of loss and gain, the nonlinear Schrödinger (NLS) equation is utilized [30]. The employed NLS equation is a lowest order approximate model describing the nonlinear effects in optical fibers. Nowadays, higher-order nonlinear effects are inevitable in many optical systems due to the recent advancement of technologies in ultra-high-bit-rate optical fiber communication and laser. Thus, it is essential to be familiar with higher-order nonlinearity in order to have a highly satisfactory apprehension of the higher-order nonlinear effects.

8.2 Overview of the Present Study

In this chapter, Riesz fractional coupled Schrödinger–KdV equations have been solved by implementing a new approach, viz. time-splitting spectral method. In order to verify the results, it has been also solved by an implicit finite difference method by using fractional centered difference approximation for Riesz fractional derivative. The obtained results manifest that the proposed time-splitting spectral method is very effective and simple for obtaining approximate solutions of Riesz fractional coupled Schrödinger–KdV equations. In order to show the reliability and efficiency of the proposed methods, numerical solutions obtained by these methods have been presented graphically.

Also, time-splitting spectral approximation technique has been proposed for Chen–Lee–Liu (CLL) equation involving Riesz fractional derivative. The proposed numerical technique is efficient, unconditionally stable, and second-order accuracy in time and spectral accuracy in space. Moreover, it conserves the total density in the discretized level. In order to examine the results, with the aid of weighted shifted Grünwald–Letnikov formula for approximating Riesz fractional derivative, Crank–Nicolson weighted and shifted Grünwald difference (CN-WSGD) method has been applied for Riesz fractional CLL equation. The comparison of results reveals that the proposed time-splitting spectral method is very effective and simple for obtaining single-soliton numerical solution of Riesz fractional CLL equation.

8.2.1 Riesz Fractional Coupled Schrödinger–KdV Equations

In a nonlinear interaction between long and short waves, under the assumption of weak nonlinearity, two typical types of interaction equations can be unified as the following normalized form, namely coupled Schrödinger–KdV(S-K) equations. The coupled Schrödinger–KdV equations [6, 34, 35]

$$iu_t - u_{xx} - uv = 0, \tag{8.1}$$

$$v_t + 6vv_x + v_{xxx} - (|u|^2)_x = 0, \tag{8.2}$$

have been used extensively to model nonlinear dynamics of one-dimensional Langmuir and ion-acoustic waves in a system of coordinates moving at the ion-acoustic speed. Here, u is a complex function describing the electric field of Langmuir oscillations and v is real function describing low-frequency density perturbation. The coupled Schrödinger–KdV equations are known to describe various processes in dusty plasma, such as Langmuir, dust-acoustic wave, and electromagnetic waves [36]. Recently, Fan [36] devised unified algebraic method, Kaya et al. [34] used Adomian's decomposition method, Saha Ray [37] proposed a new technique coupled fractional reduced differential transform, and Küçükarslan [38] utilized homotopy perturbation method for computing solutions to coupled S-K equations. (8.1)–(8.2). Many important equations of mathematical physics are rewritten in the Hirota bilinear form through dependent variable transformations [39]. By using a transformation method, the Schrödinger–KdV equation is written as bilinear ordinary differential equations and two solutions to describing nonlinear interaction of traveling waves are generated. As a result of that, multiple traveling wave solutions of the coupled Schrödinger–KdV equations are obtained in Ref. [40].

The objective of the present work is to determine the numerical solutions of the coupled S-K equations with the Riesz space fractional derivative $(1 < \alpha \leq 2)$. The model equations for the fractional coupled Schrödinger–KdV equations can be presented in the following form

$$iu_t - \frac{\partial^\alpha u}{\partial |x|^\alpha} - uv = 0, \quad a < x < b, 0 \leq t \leq T \tag{8.3}$$

$$v_t + 6vv_x + v_{xxx} - (|u|^2)_x = 0, \quad a < x < b, 0 \leq t \leq T \tag{8.4}$$

with initial conditions

$$u(x,0) = u_0(x), \quad v(x,0) = v_0(x) \tag{8.5}$$

and the Dirichlet boundary conditions

$$u(a,t) = u(b,t) = 0, \quad v(a,t) = v(b,t) = 0. \tag{8.6}$$

The Riesz space fractional derivative of order $\alpha(1 < \alpha \leq 2)$ is defined as

$$\frac{\partial^\alpha}{\partial |x|^\alpha} f(x,t) = -(-\Delta)^{\alpha/2} f(x,t) = -\frac{1}{2\cos\frac{\pi\alpha}{2}} \left[{}_{-\infty}D_x^\alpha f(x,t) + {}_xD_\infty^\alpha f(x,t) \right], \tag{8.7}$$

where the left and right Riemann–Liouville fractional derivatives of order $\alpha(n-1<\alpha<n)$ on an infinite domain are defined as

$$-\infty D_x^{\alpha} f(x,t) = \frac{1}{\Gamma(n-\alpha)} \frac{\partial^n}{\partial x^n} \int_{-\infty}^{x} (x-\xi)^{n-1-\alpha} f(\xi,t) \mathrm{d}\xi, \tag{8.8}$$

$${}_x D_{+\infty}^{\alpha} f(x,t) = \frac{(-1)^n}{\Gamma(n-\alpha)} \frac{\partial^n}{\partial x^n} \int_{x}^{+\infty} (\xi-x)^{n-1-\alpha} f(\xi,t) \mathrm{d}\xi. \tag{8.9}$$

The Riesz fractional derivative can also be characterized as

$$-(-\Delta)^{\alpha/2} f(x,t) = -\mathsf{F}^{-1}(|\mu_k|^{\alpha} \hat{f}(\mu_k,t)), \tag{8.10}$$

where F is the Fourier transform.

If $f(x,t)$ is defined on the finite interval $[a,b]$ and satisfies the boundary conditions $f(a,t)=f(b,t)=0$, we can extend the function by taking $f(x,t)\equiv 0$ for $x\le a$ and $x\ge b$. Furthermore, if $f(x,t)$ satisfies that $u'(a,t)=u'(b,t)=0$, by the Fourier transform (8.10), it is shown in [41, 42] that the Riesz fractional derivative on the finite interval $[a,b]$ can be defined as

$$\frac{\partial^{\alpha}}{\partial |x|^{\alpha}} f(x,t) = -(-\Delta)^{\alpha/2} f(x,t) = -\frac{1}{2\cos\frac{\pi\alpha}{2}} \left[{}_a D_x^{\alpha} f(x,t) + {}_x D_b^{\alpha} f(x,t) \right], \quad 1<\alpha\le 2 \tag{8.11}$$

where

$${}_a D_x^{\alpha} f(x,t) = \frac{1}{\Gamma(n-\alpha)} \frac{\partial^n}{\partial x^n} \int_{a}^{x} (x-\xi)^{n-1-\alpha} f(\xi,t) \mathrm{d}\xi, \tag{8.12a}$$

$${}_x D_b^{\alpha} f(x,t) = \frac{(-1)^n}{\Gamma(n-\alpha)} \frac{\partial^n}{\partial x^n} \int_{x}^{b} (\xi-x)^{n-1-\alpha} f(\xi,t) \mathrm{d}\xi. \tag{8.12b}$$

8.2.2 *Riesz Fractional Chen–Lee–Liu Equation*

In the theories of plasma physics, fluid dynamics, and nonlinear optics, there persist several analogs of the NLS equation in which the appearance of second-order dispersion and cubic nonlinearity persist. The second-type derivative nonlinear Schrödinger (DNLSII) equation is one of these analogs of the NLS equation introduced in 1979 [43], given by

$$iq_t + q_{xx} + i|q|^2 q_x = 0, \tag{8.13}$$

which is also known as the Chen–Lee–Liu (CLL) equation. Without self-phase modulation, Moses et al. proved optical pulse propagation involving self-steepening in 2007 [44]. This experiment well establishes the first experimental manifestation of the DNLSII equation [30]. Alike the NLS equation, DNLSII equation is also a real physical model in optics.

In the present chapter, numerical solutions of the CLL equation with Riesz derivative of order α $(1 < \alpha \leq 2)$ have been also determined by a new approach. The proposed time-splitting spectral method (TSSM) is intended to discretize the CLL equation with Riesz fractional derivative.

The model problem for pulse propagation in a single-mode optical fiber can be described by the CLL equation involving Riesz derivative of the form:

$$iq_t + \frac{\partial^\alpha q}{\partial |x|^\alpha} + i|q|^2 q_x = 0, \quad a < x < b, 0 \leq t \leq T \tag{8.14}$$

with initial condition

$$q(x, 0) = \gamma_0(x), \quad a \leq x \leq b, \tag{8.15}$$

and the boundary conditions

$$q(a, t) = q(b, t), \quad q_x(a, t) = q_x(b, t), \quad t > 0. \tag{8.16}$$

Here, $q = q(x, t)$ is the complex wave function. In the optical fiber setting, the cubic nonlinear term is associated with the self-steepening phenomena, while the fractional-order term is related to dispersion.

The Riesz space fractional derivative [41] of order $\alpha(1 < \alpha \leq 2)$ is defined as

$$\frac{\partial^\alpha}{\partial |x|^\alpha} u(x, t) = -(-\Delta)^{\alpha/2} u(x, t) = -\frac{1}{2\cos\frac{\pi\alpha}{2}} \left[{}_{-\infty}D_x^\alpha u(x, t) + {}_xD_\infty^\alpha u(x, t) \right], \tag{8.17}$$

where the left and right Riemann–Liouville fractional derivatives of order $\alpha(n - 1 < \alpha < n)$ on an infinite domain are defined as

$${}_{-\infty}D_x^\alpha u(x, t) = \frac{1}{\Gamma(n - \alpha)} \frac{\partial^n}{\partial x^n} \int_{-\infty}^{x} (x - \zeta)^{n-1-\alpha} u(\zeta, t) \mathrm{d}\zeta, \tag{8.18}$$

$${}_xD_{+\infty}^\alpha u(x, t) = \frac{(-1)^n}{\Gamma(n - \alpha)} \frac{\partial^n}{\partial x^n} \int_{x}^{+\infty} (\zeta - x)^{n-1-\alpha} u(\zeta, t) \mathrm{d}\zeta. \tag{8.19}$$

The Riesz fractional derivative can also be characterized as [16]

$$-(-\Delta)^{\alpha/2}u(x,t) = -\mathsf{F}^{-1}(|\mu_k|^{\alpha}\hat{u}(\mu_k,t)), \tag{8.20}$$

where F is the Fourier transform.

If $u(x,t)$ is defined on the finite interval $[a,b]$ and satisfies the boundary conditions $u(a,t) = u(b,t) = 0$, the function can be extended by taking $u(x,t) \equiv 0$ for $x \le a$ and $x \ge b$. Additionally, if $u(x,t)$ satisfies that $u_x(a,t) = u_x(b,t) = 0$, by the Fourier transform (8.20), it is proven in [41, 42] that the Riesz fractional derivative on the finite interval $[a,b]$ can be defined as

$$\frac{\partial^{\alpha}}{\partial|x|^{\alpha}}u(x,t) = -(-\Delta)^{\alpha/2}u(x,t) = -\frac{1}{2\cos\frac{\pi\alpha}{2}}\left[{}_aD_x^{\alpha}u(x,t) + {}_xD_b^{\alpha}u(x,t)\right], \quad 1<\alpha\le 2 \tag{8.21}$$

where

$${}_aD_x^{\alpha}u(x,t) = \frac{1}{\Gamma(n-\alpha)}\frac{\partial^n}{\partial x^n}\int_a^x (x-\zeta)^{n-1-\alpha}u(\zeta,t)\mathrm{d}\zeta, \tag{8.22}$$

$${}_xD_b^{\alpha}u(x,t) = \frac{(-1)^n}{\Gamma(n-\alpha)}\frac{\partial^n}{\partial x^n}\int_x^b (\zeta-x)^{n-1-\alpha}u(\zeta,t)\mathrm{d}\zeta. \tag{8.23}$$

8.3 The Proposed Numerical Technique for Riesz Fractional Coupled Schrödinger–KdV Equations

In the present study, Riesz fractional coupled S-K equations (8.3)–(8.6) have been taken into consideration.

We choose the spatial mesh size $h = \Delta x > 0$ with $h = (b-a)/m$ for m being an even positive integer and the time step $\tau = \Delta t > 0$. We take the grid points and time steps as

$$x_j = a + jh, j = 0,1,\ldots,m;\ t_n = n\tau, n = 0,1,2,\ldots.$$

Let u_j^n and v_j^n be the approximation of $u(x_j,t_n)$ and $v(x_j,t_n)$, respectively. Furthermore, let u^n and v^n be the solution vector at time $t = t_n = n\tau$ with the components of $u(x_j,t_n)$ and $v(x_j,t_n)$, respectively.

In the proposed time-splitting technique, Eq. (8.3) is split into two equations. First the following equation

$$iu_t - \frac{\partial^\alpha u}{\partial |x|^\alpha} = 0, \tag{8.24}$$

is solved from time $t = t_n$ to time $t = t_{n+1}$, and then for the same time-step length τ, we solve

$$iu_t - uv = 0. \tag{8.25}$$

Using Fourier transform, Eq. (8.24) reduces to

$$i\hat{u}_t + |\mu_k|^\alpha \hat{u} = 0. \tag{8.26}$$

Now, Eq. (8.26) will be discretized in space by Fourier spectral method and integrated in time exactly. Next, integrating (8.25) from time $t = t_n$ to time $t = t_{n+1}$, and then approximating the integral on $[t_n, t_{n+1}]$ via the rectangular rule, we obtain

$$\begin{aligned} u(x, t_{n+1}) &= \exp\left[-i \int_{t_n}^{t_{n+1}} v(x, s)\mathrm{d}s\right] u(x, t_n) \\ &= \exp\left[-\frac{i\tau}{2}\left(v(x, t_{n+1} + v(x, t_n)\right)\right] u(x, t_n) \end{aligned} \tag{8.27}$$

Now, some of the mathematical definitions should be known regarding the discrete Fourier transform applied here.

For simplicity, let us introduce a generalized function $f(x, t)$ and assume that $f(x, t)$ satisfies the periodic boundary condition $f(a, t) = f(b, t)$ for $(x, t) \in \mathsf{R} \times [0, T]$. From t_n to t_{n+1}, the discrete Fourier transform of the sequence $\{f_j\}$ is defined as

$$\hat{f}_k(t) = F_k[f_j(t)] = \sum_{j=0}^{m-1} f_j(t) \exp(-i\mu_k(x_j - a)), k = -\frac{m}{2}, \ldots, \frac{m}{2} - 1 \tag{8.28}$$

and the formula for the inverse discrete Fourier transform is

$$f_j(t) = F_j^{-1}[\hat{f}_k(t)] = \frac{1}{m} \sum_{k=-\frac{m}{2}}^{\frac{m}{2}-1} \hat{f}_k(t) \exp(i\mu_k(x_j - a)), \quad j = 0, 1, 2, \ldots, m-1, \tag{8.29}$$

where μ_k is the transform parameter defined as $\mu_k = \frac{2\pi k}{b-a}$.

8.3.1 The Strang Splitting Spectral Method

From t_n to t_{n+1}, we split the Schrödinger-like Eq. (8.3) via Strang splitting. The technique of Strang splitting is presented by the following three equations

$$u_j^* = \exp\left[-i\frac{\tau}{4}(v^{n+1}+v^n)\right]_{x=x_j} u_j^n, \quad j=0,1,2,\ldots,m-1, \tag{8.30}$$

$$u_j^{**} = \frac{1}{m}\sum_{k=-\frac{m}{2}}^{\frac{m}{2}-1} \exp(i|\mu_k|^{\alpha}\tau)(\hat{u}^*)_k \exp(i\mu_k(x_j-a)), \quad j=0,1,2,\ldots,m-1, \tag{8.31}$$

$$u_j^{n+1} = \exp\left[-i\frac{\tau}{4}(v^{n+1}+v^n)\right]_{x=x_j} u_j^{**}, \quad j=0,1,2,\ldots,m-1, \tag{8.32}$$

where $(\hat{u}^*)_k$ is the discrete Fourier transform of u_j^*, defined as

$$(\hat{u}^*)_k = \frac{1}{m}\sum_{k=-\frac{m}{2}}^{\frac{m}{2}-1} (i\mu_k)u_j^* \exp(-i\mu_k(x_j-a)). \tag{8.33}$$

8.3.2 Crank–Nicolson Spectral Method for the KdV-like Equation

For the KdV-like Eq. (8.4), spatial derivatives are approximated using the pseudospectral method. Followed by application of the Crank–Nicolson spectral method (CNSP), we obtain

$$\begin{aligned}\frac{v_j^{n+1}-v_j^n}{\tau} = &-3(\theta v^{n+1}D_x v^{n+1}+(1-\theta)v^n D_x v^n)_{x=x_j} - \tfrac{1}{2}(\theta D_{xx}v^{n+1}+(1-\theta)D_{xx}v^n)_{x=x_j}\\ &+\tfrac{1}{2}(\theta D_x(u^{n+1}\bar{u}^{n+1})+(1-\theta)D_x(u^n\bar{u}^n))_{x=x_j}, \quad 0<\theta\le\tfrac{1}{2}\end{aligned} \tag{8.34}$$

where D_x and D_{xx} spectral differential operators approximating ∂_x and ∂_{xx} are defined as, respectively,

$$D_x v|_{x=x_j} = \frac{1}{m}\sum_{k=-\frac{m}{2}}^{\frac{m}{2}-1} (i\mu_k)(\hat{v})_k \exp(i\mu_k(x_j-a)), \tag{8.35}$$

$$D_{xx} v|_{x=x_j} = \frac{1}{m}\sum_{k=-\frac{m}{2}}^{\frac{m}{2}-1} (i\mu_k)^2(\hat{v})_k \exp(i\mu_k(x_j-a)). \tag{8.36}$$

The initial conditions (8.5) are discretized as

$$u_j^0 = u_0(x_j), \quad v_j^0 = v_0(x_j). \tag{8.37}$$

8.4 Properties of the Numerical Scheme and Stability Analysis for the Coupled Schrödinger–KdV Equations

Let $\mathbf{u} = (u_0, u_1, \ldots, u_{m-1})^T$. Let the discrete l_2-norm be defined on the interval (a, b) as

$$\|\mathbf{u}\|_{l_2} = \sqrt{\frac{b-a}{m}\sum_{j=0}^{m-1}|u_j|^2}. \tag{8.38}$$

For the stability of the Strang time-splitting spectral schemes (8.30), (8.31), and (8.32), the following theorem is proved, which shows that the total charge is conserved.

Theorem 8.1 *The time-splitting schemes* (8.30), (8.31), and (8.32) *for the coupled Schrödinger–KdV equations are unconditionally stable and possess the following conservative properties*:

$$\left\|\mathbf{u}^{n+1}\right\|_{l_2}^2 = \left\|u^0\right\|_{l_2}^2, \quad n = 0, 1, 2, \ldots \tag{8.39}$$

Proof For the schemes (8.30)–(8.32), using (8.28), (8.29), and (8.38), we have

$$\begin{aligned}
\frac{1}{b-a}\left\|\mathbf{u}^{n+1}\right\|_{l_2}^2 &= \frac{1}{m}\sum_{j=0}^{m-1}\left|u_j^{n+1}\right|^2 = \frac{1}{m}\sum_{j=0}^{m-1}\left|\exp\left(-\frac{i\tau}{4\varepsilon}(v_j^{n+1}+v_j^n)\right)u_j^{**}\right|^2 = \frac{1}{m}\sum_{j=0}^{m-1}\left|u_j^{**}\right|^2 \\
&= \frac{1}{m}\sum_{j=0}^{m-1}\left|\frac{1}{m}\sum_{k=-\frac{m}{2}}^{\frac{m}{2}-1}\exp(i|\mu_k|^\alpha\tau)(\hat{u}^*)_k\exp(i\mu_k(x_j-a))\right|^2 \\
&= \frac{1}{m^2}\sum_{k=-\frac{m}{2}}^{\frac{m}{2}-1}\left|\exp(i|\mu_k|^\alpha\tau)(\hat{u}^*)_k\right|^2 \\
&= \frac{1}{m^2}\sum_{k=-\frac{m}{2}}^{\frac{m}{2}-1}\left|(\hat{u}^*)_k\right|^2 = \frac{1}{m^2}\sum_{k=-\frac{m}{2}}^{\frac{m}{2}-1}\left|\sum_{j=0}^{m-1}\exp\left(-\frac{i\tau}{4}(v_j^{n+1}+v_j^n)\right)u_j^n\right|^2 \\
&\quad \exp(-i\mu_k(x_j-a)) \\
&= \frac{1}{m}\sum_{j=0}^{m-1}\left|u_j^n\right|^2 = \frac{1}{b-a}\|\mathbf{u}^n\|_{l_2}^2.
\end{aligned} \tag{8.40}$$

Here, the following identities have been used

$$\sum_{j=0}^{m-1} \mathrm{e}^{i2\pi(l-k)j/m} = \begin{cases} 0, & l-k \neq rm, \\ m, & l-k = rm, \end{cases} \quad r \text{ is an integer} \tag{8.41}$$

and

$$\sum_{k=-\frac{m}{2}}^{\frac{m}{2}-1} \mathrm{e}^{i2\pi(l-j)k/m} = \begin{cases} 0, & l-j \neq rm, \\ m, & l-j = rm, \end{cases} \quad r \text{ is an integer.} \tag{8.42}$$

The equality (8.39) can be obtained from Eq. (8.40) for the schemes (8.30)–(8.32), by induction. ■

The stability of the time-splitting spectral approximation for the Riesz fractional coupled Schrödinger–KdV equations manifests that the total density is conserved in the discretized level.

Now, the stability of the scheme (8.34) has been analyzed by using the von Neumann analysis for stability.

Theorem 8.2 *When* $\theta = \frac{1}{2}$, *the numerical scheme* (8.34) *is unconditionally stable. When* $0 < \theta < \frac{1}{2}$, *it is conditionally stable. The stability condition is*

$$\tau < \min_{-\frac{m}{2} \le k \le \frac{m}{2}-1, k \neq 0} \left[\frac{2}{(3A + \frac{1}{2}(i\mu_k)^2 - \frac{1}{2} i\mu_k B)(1-2\theta)} \right].$$

Proof Plugging

$$v_j^n = \frac{1}{m} \sum_{k=-\frac{m}{2}}^{\frac{m}{2}-1} (\hat{v})_k \exp(i\mu_k(x_j - a)), \quad j = 0, 1, 2 \ldots, m-1$$

into Eq. (8.34) and using the orthogonality of the Fourier function, we obtain

$$\begin{aligned} \frac{(\hat{v}^{n+1})_k - (\hat{v}^n)_k}{\tau} = & -3F_k \left[\theta v^{n+1} F_k^{-1} \left(i\mu_k (\hat{v}^{n+1})_k \right) + (1-\theta) v^n F_k^{-1} \left(i\mu_k (\hat{v}^n)_k \right) \right] \\ & - \frac{1}{2} \left[\theta (i\mu_k)^2 (\hat{v}^{n+1})_k + (1-\theta)(i\mu_k)^2 (\hat{v}^n)_k \right] \\ & + \frac{1}{2} (\theta i\mu_k F_k(u^{n+1}\bar{u}^{n+1}) + (1-\theta) i\mu_k F_k(u^n \bar{u}^n)). \end{aligned} \tag{8.43}$$

In the above discretization scheme (8.43), plugging $(\hat{v}^{n+1})_k = \xi (\hat{v}^n)_k$ with $\xi > 0$ being the amplification factor, we obtain the following equation

$$\xi = \frac{(1-\theta)(-3A\tau - \frac{1}{2}(i\mu_k)^2\tau + \frac{1}{2}i\mu_k B\tau) + 1}{1 + 3\theta A\tau + \frac{1}{2}\theta(i\mu_k)^2\tau - \frac{1}{2}i\theta\mu_k B\tau}. \tag{8.44}$$

Let us take $a = \tau z$,

where $z = 3A\tau + \frac{1}{2}(i\mu_k)^2\tau - \frac{1}{2}i\mu_k B\tau$. Without loss of generality, let us assume that $z > 0$.

Then from Eq. (8.44), we have

$$\xi = \frac{(1-\theta)(-z\tau) + 1}{1 + \theta z\tau} = \frac{(1-\theta)(-a) + 1}{1 + \theta a}. \tag{8.45}$$

From Eq. (8.45), we see that $|\xi| < 1$ if $\theta = \frac{1}{2}$. Therefore, in case of $\theta = \frac{1}{2}$, the numerical scheme is unconditionally stable.

When $0 < \theta < \frac{1}{2}$, we have

$$\left|1 - \frac{a}{1 + \theta a}\right| < 1. \tag{8.46}$$

This implies that

$$\frac{a}{1 + \theta a} < 2. \tag{8.47}$$

From the above Eq. (8.47), we get

$$\tau < \frac{2}{z(1 - 2\theta)}. \tag{8.48}$$

Hence, the stability condition for the case $0 < \theta < \frac{1}{2}$ is

$$\tau < \min_{-\frac{m}{2} \le k \le \frac{m}{2}-1, k \neq 0} \left[\frac{2}{(3A + \frac{1}{2}(i\mu_k)^2 - \frac{1}{2}i\mu_k B)(1 - 2\theta)}\right]. \tag{8.49}$$

■

8.5 Implicit Finite Difference Method for the Riesz Fractional Coupled Schrödinger–KdV Equations

The fractional centered difference has been used to discretize the Riesz fractional derivative. In this connection, the following property and lemma have been presented.

8.5.1 Approximation of Riesz Fractional Derivative by the Fractional Centered Difference

In [45], the fractional centered difference is defined by

$$\Delta_h^{\alpha}\phi(x) = \sum_{j=-\infty}^{\infty} \frac{(-1)^j \Gamma(\alpha+1)}{\Gamma\left(\frac{\alpha}{2}-j+1\right)\Gamma\left(\frac{\alpha}{2}+j+1\right)} \phi(x-jh), \quad \text{for } \alpha > -1$$

and it is shown that

$$\lim_{h\to 0} \frac{\Delta_h^{\alpha}\phi(x)}{h^{\alpha}} = \lim_{h\to 0} \frac{1}{h^{\alpha}} \sum_{j=-\infty}^{\infty} \frac{(-1)^j \Gamma(\alpha+1)}{\Gamma\left(\frac{\alpha}{2}-j+1\right)\Gamma\left(\frac{\alpha}{2}+j+1\right)} \phi(x-jh)$$

represents the Riesz fractional derivative (8.21) for $1 < \alpha \leq 2$.

Recently, Çelik and Duman [45] derived the interesting result that if $f^*(x)$ be defined as follows

$$f^*(x) = \begin{cases} f(x), & x \in [a,b] \\ 0, & x \notin [a,b] \end{cases}$$

such that $f^*(x) \in C^5(\mathsf{R})$ and all derivatives up to order five belong to $L_1(\mathsf{R})$, then for the Riesz fractional derivative of order $\alpha (1 < \alpha \leq 2)$

$$\frac{\partial^{\alpha} f(x)}{\partial |x|^{\alpha}} = -h^{-\alpha} \sum_{j=-\frac{b-x}{h}}^{\frac{x-a}{h}} g_j f(x-jh) + O(h^2), \tag{8.50}$$

where $h = \frac{b-a}{m}$, and m is the number of partitions of the interval $[a,b]$ and

$$g_j = \frac{(-1)^j \Gamma(\alpha+1)}{\Gamma(\alpha/2-j+1)\Gamma(\alpha/2+j+1)}. \tag{8.51}$$

Property 8.1 *The coefficients g_j of the fractional centered difference approximation have the following properties for $j = 0, \mp 1, \mp 2, \ldots$, and $\alpha > -1$:*

(i) $g_0 \geq 0$,
(ii) $g_{-j} = g_j \leq 0$ *for all* $|j| \geq 1$,
(iii) $g_{j+1} = \frac{j-\alpha/2}{\alpha/2+j+1} g_j$,
(iv) $g_j = O(j^{-\alpha-1})$.

Proof For the proof of the above properties, it may be referred to Ref. [45].

Lemma 8.1 *Let $f \in C^5(\mathsf{R})$ and all the derivatives up to order five belong to space $L_1(\mathsf{R})$ and the fractional centered difference be*

$$\Delta_h^{\alpha} f(x) = \sum_{j=-\infty}^{\infty} \frac{(-1)^j \Gamma(\alpha+1)}{\Gamma\left(\frac{\alpha}{2}-j+1\right)\Gamma\left(\frac{\alpha}{2}+j+1\right)} f(x-jh). \tag{8.52}$$

Then,

$$-h^{-\alpha}\Delta_h^{\alpha} f(x) = \frac{d^{\alpha} f(x)}{d|x|^{\alpha}} + O\left(h^2\right), \tag{8.53}$$

When $h \to 0, \frac{d^{\alpha} f(x)}{d|x|^{\alpha}}$ *represents the Riesz derivative of fractional order* α *for* $1 < \alpha \leq 2$.

Proof For proof of Lemma 8.1, it may be referred to Ref. [45]. ■

8.5.2 Numerical Scheme for Riesz Fractional Coupled Schrödinger–KdV Equations

The second-order implicit finite difference discretization for the coupled Schrödinger–KdV Eqs. (8.3) and (8.4) is given as

$$\begin{aligned}
&i\frac{u_j^{n+1}-u_j^n}{\tau} + \frac{h^{-\alpha}}{2}\left(\sum_{k=j-m}^{j} g_k\, u_{j-k}^{n+1} + \sum_{k=j-m}^{j} g_j\, u_{j-k}^{n}\right) - \frac{1}{2}\left(u_j^{n+1}v_j^{n+1} + u_j^n v_j^n\right) = 0,\\
&\frac{v_j^{n+1}-v_j^n}{\tau} + 3\left[v_j^{n+1}\left(\frac{v_{j+1}^{n+1}-v_{j-1}^{n+1}}{2h}\right) + v_j^n\left(\frac{v_{j+1}^n - v_{j-1}^n}{2h}\right)\right] + \frac{1}{2}\left(\frac{v_{j+2}^{n+1}-2v_{j+1}^{n+1}+2v_{j-1}^{n+1}-v_{j-2}^{n+1}}{2h^3}\right.\\
&\left. + \frac{v_{j+2}^{n}-2v_{j+1}^{n}+2v_{j-1}^{n}-v_{j-2}^{n}}{2h^3}\right) = \frac{1}{2}\left(\frac{u_{j+1}^{n+1}\bar{u}_{j+1}^{n+1}-u_{j-1}^{n+1}\bar{u}_{j-1}^{n+1}}{2h} + \frac{u_{j+1}^{n}\bar{u}_{j+1}^{n}-u_{j-1}^{n}\bar{u}_{j-1}^{n}}{2h}\right)
\end{aligned} \tag{8.54}$$

where the local truncation error $R_j^{n+\frac{1}{2}} = O(\tau^2 + h^2)$ and $i = \sqrt{-1}$.

8.5.3 Numerical Experiments and Discussion

In the present analysis, the following initial conditions [34, 35] have been taken into consideration for the fractional coupled S-K equations (8.3)–(8.4)

$$u(x,0) = 6\sqrt{2}e^{i\alpha x}k^2\mathrm{sech}^2(kx), v(x,0) = \frac{\alpha + 16k^2}{3} - 6k^2\tanh^2(kx). \quad (8.55)$$

In this case, the problem has been solved on the interval $[-40, 40]$ with vanishing boundary conditions. Moreover, this problem has been solved by both time-splitting spectral method (TSSM) and an implicit finite difference method, viz. Crank–Nicolson finite difference (CNFD) method in order to justify the efficiency and applicability of the proposed methods.

Figures 8.1, 8.2, and 8.3 show the comparison between the evolution of the TSSM solution and the CNFD solution at $t = 1$ for various fractional orders α. The results show that the curves of $|q(x,1)|$ and $r(x,1)$ obtained by TSSM coincide well with the CNFD solutions, respectively. Thus, there is a good agreement of results obtained by the proposed two methods.

Additionally, in Fig. 8.4, one-soliton 3-D solutions of $|q(x,t)|$ and the corresponding 2-D solution graph at $t = 1$ for fractional order $\alpha = 1.9$ have been presented. Also, one-soliton 3-D solutions of $r(x,t)$ and the corresponding 2-D solution graph at $t = 1$ for fractional order $\alpha = 1.9$ have been depicted in Fig. 8.5. The solution graphs in Figs. 8.4 and 8.5 have been drawn by the results obtained from TSSM.

In order to examine the accuracy of time-splitting method for the Riesz fractional coupled S-K equations (8.3)–(8.4), the L_2 and L_∞ error norms [46] have been calculated with regard to Crank–Nicolson finite difference method in Table 8.1. The obtained results quite establish the plausibility of the proposed methods for solving Riesz fractional coupled S-K equations (8.3)–(8.4).

8.6 New Proposed Technique for Riesz Fractional Chen–Lee–Liu Equation

In the present analysis, Riesz fractional CLL Eq. (8.14) has been solved by the following proposed numerical approach.

First, it has been chosen the spatial mesh size $h = \Delta x > 0$ with $h = (b-a)/m$ for m being an even positive integer and the time step $\tau = \Delta t > 0$. Then, the mesh points and time steps are taken as

$$x_j = a + jh, j = 0, 1, \ldots, m; t_n = n\tau, n = 0, 1, 2, \ldots.$$

Let q_j^n be the approximate value of $q(x_j, t_n)$. Furthermore, let $\mathbf{q}^n$ be the solution vector at time $t = t_n = n\tau$ with the components of $q(x_j, t_n)$.

In the new proposed approach, acquiring the concept of time-splitting technique Eq. (8.14) is split into two equations. First, the following equation

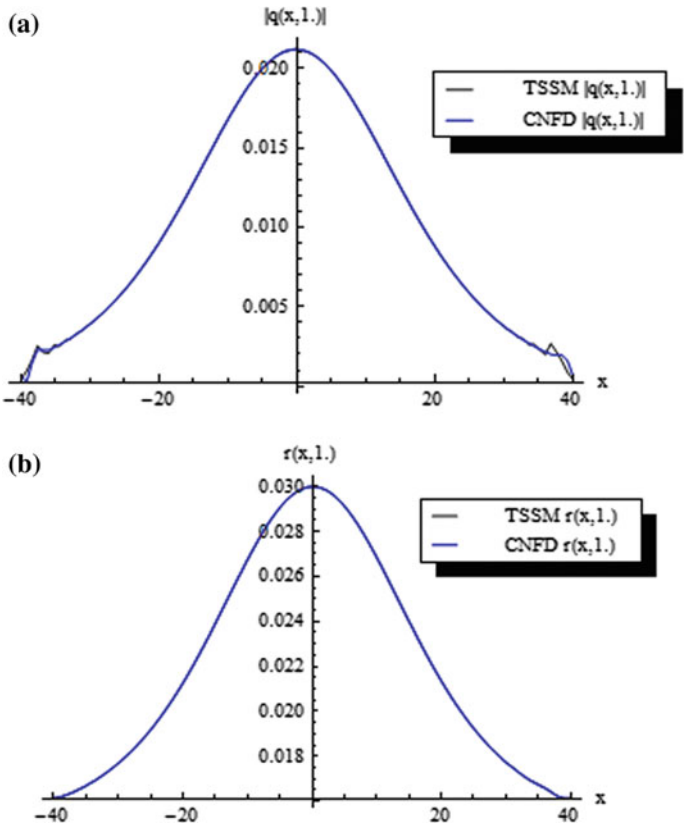

Fig. 8.1 Comparison of results obtained from TSSM and CNFD scheme for the Riesz fractional coupled S-K equations (8.3)–(8.4) with fractional order $\alpha = 1.75$ for **a** the solutions of $|q(x,1)|$ and **b** the solutions of $r(x,1)$, respectively

$$iq_t + \frac{\partial^\alpha q}{\partial |x|^\alpha} = 0, \tag{8.56}$$

is solved from time $t = t_n$ to $t = t_{n+1}$, and then for the same time-step length τ, it solves

$$iq_t + i|q|^2 q_x = 0. \tag{8.57}$$

With the help of Fourier transform, Eq. (8.56) reduces to

$$\hat{q}_t + i|\mu_k|^\alpha \hat{q} = 0. \tag{8.58}$$

Next, Eq. (8.58) will be discretized in space by Fourier spectral method and then integrated in time exactly. Now, from time $t = t_n$ to time $t = t_{n+1}$ Eq. (8.57) has

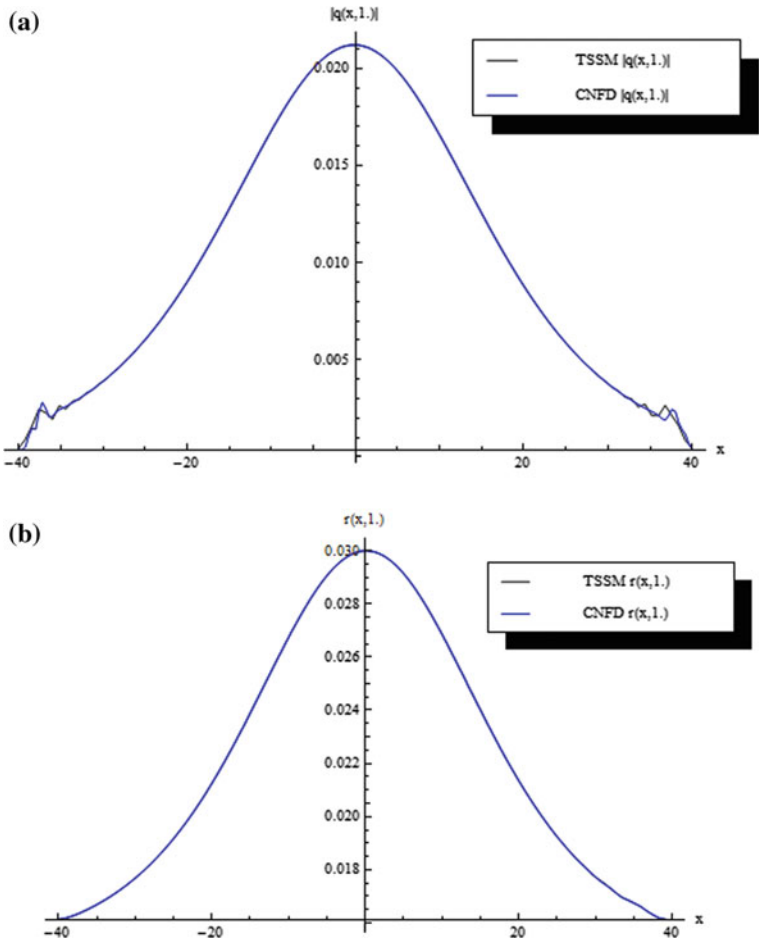

Fig. 8.2 Comparison of results obtained from TSSM and CNFD scheme for the Riesz fractional coupled S-K equations (8.3)–(8.4) with fractional order $\alpha = 1.8$ for **a** the solutions of $|q(x,1)|$ and **b** the solutions of $r(x,1)$, respectively

been integrated and has then approximated the integral on $[t_n, t_{n+1}]$ via the rectangular rule, yielding

$$\begin{aligned} q(x,t_{n+1}) &= \exp\left[-\int_{t_n}^{t_{n+1}} \bar{q}(x,s)q_x(x,s)\mathrm{d}s\right] q(x,t_n) \\ &= \exp\left[-\frac{\tau}{2}(\bar{q}(x,t_{n+1})q_x(x,t_{n+1}) + \bar{q}(x,t_n)q_x(x,t_n))\right] q(x,t_n) \end{aligned} \tag{8.59}$$

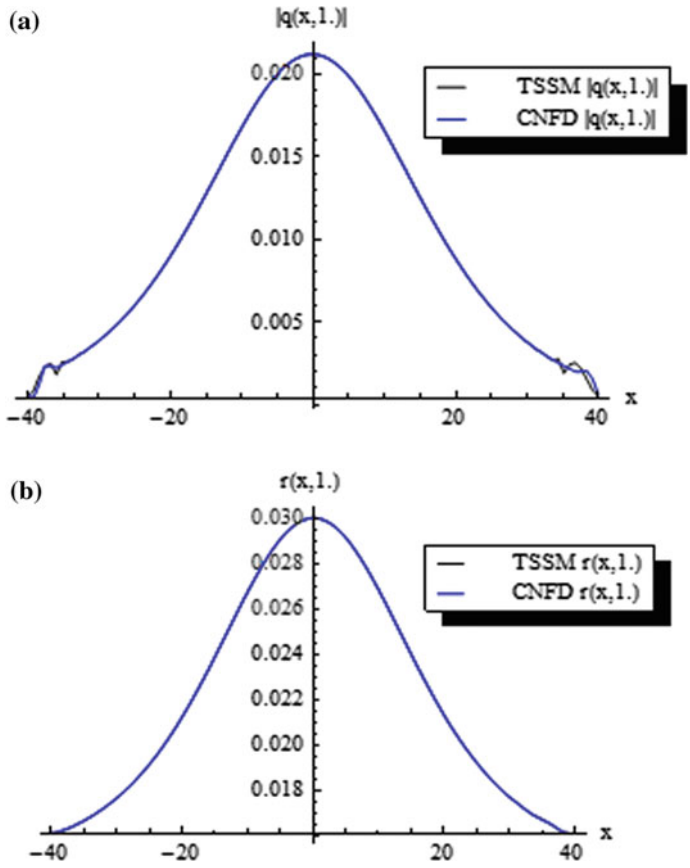

Fig. 8.3 Comparison of results obtained from TSSM and CNFD scheme for the Riesz fractional coupled S-K equations (8.3)–(8.4) with fractional order $\alpha = 1.9$ for **a** the solutions of $|q(x, 1)|$ and **b** the solutions of $r(x, 1)$, respectively

Now, regarding the implementation of a discrete Fourier transform, some mathematical definitions are essential for the subsequent study.

For the sake of convenience, let us consider a generalized function $\phi(x, t)$ and assume that $\phi(x, t)$ satisfies the periodic boundary condition $\phi(a, t) = \phi(b, t)$ for $(x, t) \in \mathsf{R} \times [0, T]$. From t_n to t_{n+1}, the discrete Fourier transform of the sequence $\{\phi_j\}$ is defined as

$$\hat{\phi}_k(t) = F_k[\phi_j(t)] = \sum_{j=0}^{m-1} \phi_j(t) \exp(-i\mu_k(x_j - a)), k = -\frac{m}{2}, \ldots, \frac{m}{2} - 1 \qquad (8.60)$$

and the corresponding inverse discrete Fourier transform is defined by

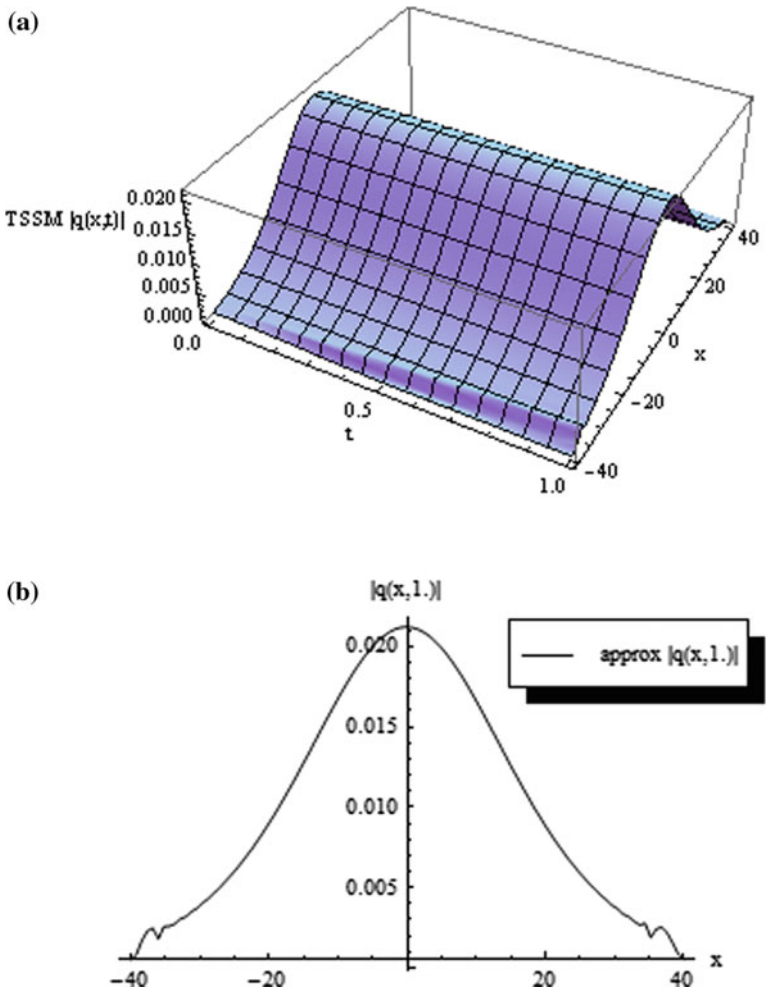

Fig. 8.4 **a** One-soliton wave 3-D solution of $|q(x,t)|$ and **b** the corresponding 2-D solution graph at $t = 1.0$ obtained by TSSM for the Riesz fractional coupled S-K equations (8.3)–(8.4) with fractional order $\alpha = 1.9$

$$\phi_j(t) = F_j^{-1}[\hat{\phi}_k(t)] = \frac{1}{m}\sum_{k=-\frac{m}{2}}^{\frac{m}{2}-1} \hat{\phi}_k(t)\exp(i\mu_k(x_j - a)), \quad j = 0, 1, 2, \ldots, m-1, \tag{8.61}$$

where μ_k is the transform parameter defined as $\mu_k = \frac{2\pi k}{b-a}$.

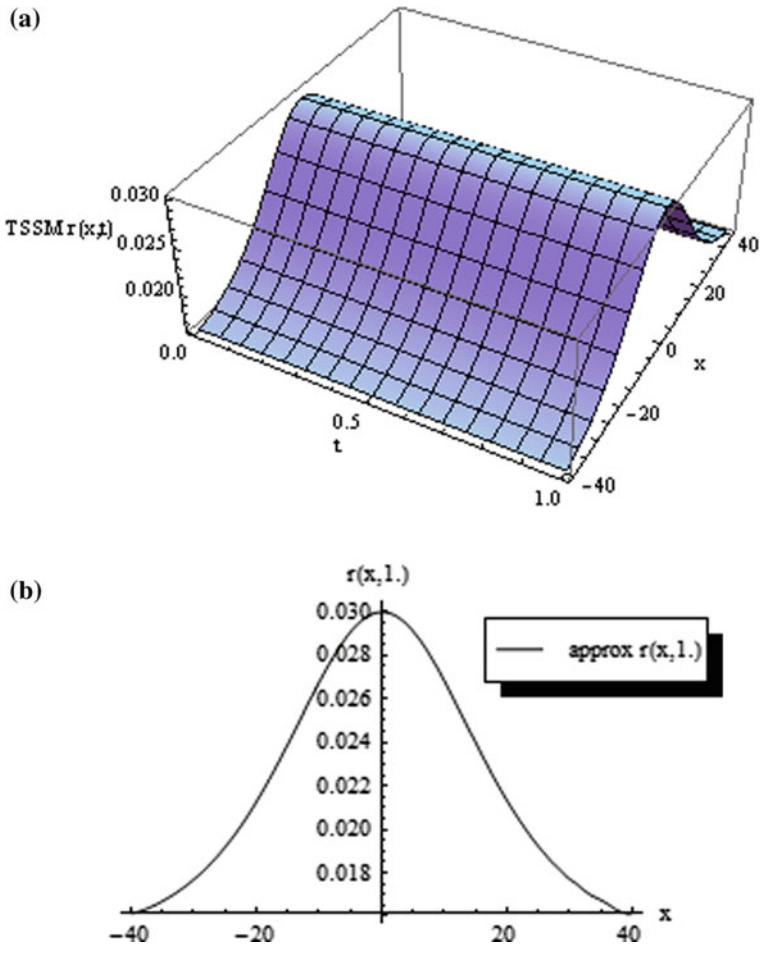

Fig. 8.5 **a** One-soliton wave 3-D solution of $r(x,t)$ and **b** the corresponding 2-D solution graph at $t = 1.0$ obtained by TSSM for the Riesz fractional coupled S-K equations (8.3)–(8.4) with fractional order $\alpha = 1.9$

Table 8.1 L_2 norm and L_∞ norm of errors between the solutions of TSSM and CNFD method at $t = 1$ for various values of fractional order α

t	$\alpha = 1.75$				$\alpha = 1.8$				$\alpha = 1.9$			
	L_2 error		L_∞ error		L_2 error		L_∞ error		L_2 error		L_∞ error	
	$\lvert q(x,t)\rvert$	$r(x,t)$	$\lvert q(x,t)\rvert$	$r(x,t)$	$\lvert q(x,t)\rvert$	$r(x,t)$	$\lvert q(x,t)\rvert$	$r(x,t)$	$\lvert q(x,t)\rvert$	$r(x,t)$	$\lvert q(x,t)\rvert$	$r(x,t)$
0.5	0.293308E−7	0.480306E−10	0.805285E−3	0.412279E−4	0.276652E−7	0.481225E−10	0.831127E−3	0.412538E−4	0.244033E−7	0.483519E−10	0.813834E−3	0.413466E−4
1.0	0.202791E−7	0.681797E−1	0.722753E−3	0.373995E−4	0.197543E−7	0.684439E−10	0.747454E−3	0.375156E−4	0.20052E−7	0.690599E−10	0.667E−3	0.376392E−4

8.7 The Strang Splitting Spectral Method

From time t_n to t_{n+1}, the Schrödinger-like Eq. (8.14) is split via Strang splitting. The proposed technique of Strang splitting is presented by the following three equations

$$q_j^* = \exp\left[-\frac{\tau}{4}\left[\bar{q}_j^{n+1} D_x\left(q^{n+1}\right)\big|_{x=x_j} + \bar{q}_j^n D_x(q^n)|_{x=x_j}\right]\right] q_j^n, \quad j = 0, 1, 2, \ldots, m-1, \tag{8.62}$$

$$q_j^{**} = \frac{1}{m}\sum_{k=-\frac{m}{2}}^{\frac{m}{2}-1} \exp(-i|\mu_k|^\alpha \tau)(\hat{q}^*)_k \exp(i\mu_k(x_j - a)), \quad j = 0, 1, 2, \ldots, m-1, \tag{8.63}$$

$$q_j^{n+1} = \exp\left[-\frac{\tau}{4}\left[\bar{q}_j^{n+1} D_x\left(q^{n+1}\right)\big|_{x=x_j} + \bar{q}_j^n D_x(q^n)|_{x=x_j}\right]\right] q_j^{**}, \quad j = 0, 1, 2, \ldots, m-1, \tag{8.64}$$

where $(\hat{q}^*)_k$ is the discrete Fourier transform of q_j^* as defined earlier and D_x, a spectral differential operator approximating ∂_x, is defined as

$$D_x q|_{x=x_j} = \frac{1}{m}\sum_{k=-\frac{m}{2}}^{\frac{m}{2}-1} (i\mu_k)(\hat{q})_k \exp(i\mu_k(x_j - a)). \tag{8.65}$$

8.8 Stability Analysis of Proposed Time-Splitting Spectral Scheme for Riesz Fractional Chen–Lee–Liu Equation

Let us define $\mathbf{q} = (q_0, q_1, \ldots, q_{m-1})^T$. Also, let the discrete L^2-norm be defined on the interval (a, b) as

$$\|\mathbf{q}\|_{l^2} = \sqrt{\frac{b-a}{m}\sum_{j=0}^{m-1} |q_j|^2}. \tag{8.66}$$

The following lemma is proved for the stability of the proposed Strang time-splitting spectral schemes (8.62), (8.63), and (8.64). This lemma also shows that the total charge is conserved.

Lemma 8.2 *The time-splitting schemes* (8.62), (8.63), *and* (8.64) *for the Riesz fractional CLL Eq.* (8.14) *are unconditionally stable and possess the following conservative properties:*

$$\left\|\mathbf{q}^{n+1}\right\|_{l^2}^2 = \left\|q^0\right\|_{l^2}^2, \quad n = 0, 1, 2, \ldots \tag{8.67}$$

Proof Using Eqs. (8.60), (8.61), and (8.66) for the schemes (8.62)–(8.64), yielding

$$\begin{aligned}
\frac{1}{b-a}\left\|\mathbf{q}^{n+1}\right\|_{l_2}^2 &= \frac{1}{m}\sum_{j=0}^{m-1}\left|q_j^{n+1}\right|^2 \\
&= \frac{1}{m}\sum_{j=0}^{m-1}\left|\exp\left[\frac{i\tau}{4}\left[iq_j^{n+1}\left(q_x^{n+1}\right)_j + iq_j^n\left(q_x^n\right)_j\right]\right]q_j^{**}\right|^2 \\
&= \frac{1}{m}\sum_{j=0}^{m-1}\left|q_j^{**}\right|^2 \\
&= \frac{1}{m}\sum_{j=0}^{m-1}\left|\frac{1}{m}\sum_{k=-\frac{m}{2}}^{\frac{m}{2}-1}\exp(-i|\mu_k|^\alpha\tau)(\hat{q}^*)_k\exp(i\mu_k(x_j-a))\right|^2 \\
&= \frac{1}{m^2}\sum_{k=-\frac{m}{2}}^{\frac{m}{2}-1}\left|\exp(-i|\mu_k|^\alpha\tau)(\hat{q}^*)_k\right|^2 \\
&= \frac{1}{m^2}\sum_{k=-\frac{m}{2}}^{\frac{m}{2}-1}\left|(\hat{q}^*)_k\right|^2 = \frac{1}{m^2}\sum_{k=-\frac{m}{2}}^{\frac{m}{2}-1}\left|\sum_{j=0}^{m-1}q_j^*\exp(-i\mu_k(x_j-a))\right|^2 \\
&= \frac{1}{m}\sum_{j=0}^{m-1}\left|q_j^*\right|^2 = \frac{1}{m}\sum_{j=0}^{m-1}\left|\exp\left[\frac{i\tau}{4}\left[iq_j^{n+1}\left(q_x^{n+1}\right)_j + iq_j^n\left(q_x^n\right)_j\right]\right]q_j^n\right|^2 \\
&= \frac{1}{m}\sum_{j=0}^{m-1}\left|q_j^n\right|^2 = \frac{1}{b-a}\|\mathbf{q}^n\|_{l^2}^2.
\end{aligned} \tag{8.68}$$

In the above analysis, the following identities have been used

$$\sum_{j=0}^{m-1}\mathrm{e}^{i2\pi(l-k)j/m} = \begin{cases} 0, & l-k \neq rm, \\ m, & l-k = rm, \end{cases} r \text{ is an integer} \tag{8.69}$$

and

$$\sum_{k=-\frac{m}{2}}^{\frac{m}{2}-1}\mathrm{e}^{i2\pi(l-j)k/m} = \begin{cases} 0, & l-j \neq rm, \\ m, & l-j = rm, \end{cases} r \text{ is an integer.} \tag{8.70}$$

The equality (8.67) can be obtained from Eq. (8.68) for the schemes (8.62)–(8.64), by the method of induction. ■

Lemma 8.2 for the stability of time-splitting spectral approximation for the Riesz fractional CLL equation establishes that the total density is conserved in the discretized level.

8.9 High-Order Approximations for Riemann–Liouville Fractional Derivatives

In this section, high-order approximations for Riemann–Liouville fractional derivatives have been presented. Let us first start with the introduction of the shifted Grünwald difference operator.

8.9.1 Shifted Grünwald–Letnikov Formula for Riesz Space Fractional Derivative

In [47], Meerschaert and Tadjeran reveal that standard Grünwald–Letnikov formula is often unstable for time-dependent problems. In this regard, they had first proposed the following shifted Grünwald–Letnikov formulae for the left and right Riemann–Liouville derivatives in order to overcome the stability.

The shifted Grünwald difference operators to approximate the left and right Riemann–Liouville fractional derivatives are given by

$$\mathcal{A}_{l_1}^{\alpha} u(x) = \frac{1}{h^{\alpha}} \sum_{k=0}^{\infty} \varpi_k^{(\alpha)} u(x - (k - l_1)h), \tag{8.71}$$

$$\mathcal{B}_{l_2}^{\alpha} u(x) = \frac{1}{h^{\alpha}} \sum_{k=0}^{\infty} \varpi_k^{(\alpha)} u(x - (k - l_2)h), \tag{8.72}$$

that have the first-order accuracy, i.e.,

$$\mathcal{A}_{l_1}^{\alpha} u(x) = {}_{-\infty}D_x^{\alpha} u(x) + O(h), \tag{8.73}$$

$$\mathcal{B}_{l_2}^{\alpha} u(x) = {}_{x}D_{+\infty}^{\alpha} u(x) + O(h), \tag{8.74}$$

where l_1 and l_2 are positive integers and

$$\varpi_k^{(\alpha)} = (-1)^k \binom{\alpha}{k}. \tag{8.75}$$

We know the binomial expansion of $(1-z)^{\alpha}$ as follows

$$(1-z)^{\alpha} = \sum_{k=0}^{\infty} (-1)^k \binom{\alpha}{k} z^k = \sum_{k=0}^{\infty} \varpi_k^{(\alpha)} z^k, \text{for all } |z| \le 1.$$

So, the coefficients $\varpi_k^{(\alpha)}$ are the binomial coefficients of $(1-z)^{\alpha}$ and they can be evaluated by the following recurrence relation

$$\varpi_0^{(\alpha)} = 1, \varpi_k^{(\alpha)} = \left(1 - \frac{\alpha+1}{k}\right) \varpi_{k-1}^{(\alpha)}, k = 1, 2, \ldots. \tag{8.76}$$

8.9.2 Weighted Shifted Grünwald–Letnikov Formula for Riesz Space Fractional Derivative

In view of the shifted Grünwald difference operators (8.71)–(8.72) and multistep method, the following second-order approximation for the Riemann–Liouville fractional derivatives has been derived by Tian et al. in [48].

$${}^{L}D_{l_1,l_2}^{\alpha} u(x) = \frac{\alpha - 2l_2}{2(l_1 - l_2)} \mathcal{A}_{l_1}^{\alpha} u(x) + \frac{2l_1 - \alpha}{2(l_1 - l_2)} \mathcal{A}_{l_2}^{\alpha} u(x), \tag{8.77}$$

$${}^{R}D_{l_1,l_2}^{\alpha} u(x) = \frac{\alpha - 2l_2}{2(l_1 - l_2)} \mathcal{B}_{l_1}^{\alpha} u(x) + \frac{2l_1 - \alpha}{2(l_1 - l_2)} \mathcal{B}_{l_2}^{\alpha} u(x). \tag{8.78}$$

Lemma 8.3 ([19]). *Suppose that* $1 < \alpha < 2$, *let* $u(x) \in L^1(\mathsf{R})$, ${}_{-\infty}D^{\alpha}u(x)$, $D^{\alpha}_{+\infty}u(x)$, *and their Fourier transforms belong to* $L^1(\boldsymbol{R})$, *then the weighted and shifted Grünwald difference operators satisfy*

$${}^{L}D_{l_1,l_2}^{\alpha} u(x) = {}_{-\infty}D_x^{\alpha} u(x) + O(h^2), \tag{8.79}$$

$${}^{R}D_{l_1,l_2}^{\alpha} u(x) = {}_xD^{\alpha}_{+\infty} u(x) + O(h^2), \tag{8.80}$$

uniformly for $x \in \boldsymbol{R}$, *where* l_1 and l_2 *are positive integers and* $l_1 \neq l_2$.

Let $u(x)$ be a function satisfying the assumptions in Lemma 8.3 on the bounded interval $[a, b]$. If $u(a) = 0$ or $u(b) = 0$, the function $u(x)$ can be zero extended for $x < a$ or $x > b$. Then, the α-order left and right Riemann–Liouville fractional

derivatives of $u(x)$ at each point x can be approximated with the second-order accuracy as follows

$$ {}_aD_x^{\alpha}u(x) = \frac{\mu_1}{h^{\alpha}}\sum_{k=0}^{\left[\frac{x-a}{h}\right]+l_1}\varpi_k^{(\alpha)}u(x-(k-l_1)h) + \frac{\mu_2}{h^{\alpha}}\sum_{k=0}^{\left[\frac{x-a}{h}\right]+l_2}\varpi_k^{(\alpha)}u(x-(k-l_2)h) + O(h^2), \tag{8.81} $$

$$ {}_xD_b^{\alpha}u(x) = \frac{\mu_1}{h^{\alpha}}\sum_{k=0}^{\left[\frac{b-x}{h}\right]+l_1}\varpi_k^{(\alpha)}u(x-(k-l_1)h) + \frac{\mu_2}{h^{\alpha}}\sum_{k=0}^{\left[\frac{b-x}{h}\right]+l_2}\varpi_k^{(\alpha)}u(x-(k-l_2)h) + O(h^2), \tag{8.82} $$

where

$$ \mu_1 = \frac{\alpha-2l_2}{2(l_1-l_2)} \text{ and } \mu_2 = \frac{2l_1-\alpha}{2(l_1-l_2)}. $$

Thus, weighted shifted Grünwald–Letnikov formula for Riesz space fractional derivative is given by

$$ \frac{d^{\alpha}u(x)}{d|x|^{\alpha}} = -\frac{1}{2\cos\left(\frac{\pi\alpha}{2}\right)}\left[\frac{\mu_1}{h^{\alpha}}\sum_{k=0}^{\left[\frac{x-a}{h}\right]+l_1}\varpi_k^{(\alpha)}u(x-(k-l_1)h) + \frac{\mu_2}{h^{\alpha}}\sum_{k=0}^{\left[\frac{x-a}{h}\right]+l_2}\varpi_k^{(\alpha)}u(x-(k-l_2)h) + \frac{\mu_1}{h^{\alpha}}\sum_{k=0}^{\left[\frac{b-x}{h}\right]+l_1}\varpi_k^{(\alpha)}u(x-(k-l_1)h) + \frac{\mu_2}{h^{\alpha}}\sum_{k=0}^{\left[\frac{b-x}{h}\right]+l_2}\varpi_k^{(\alpha)}u(x-(k-l_2)h)\right] + O(h^2), \tag{8.83} $$

where

$$ \mu_1 = \frac{\alpha-2l_2}{2(l_1-l_2)} \text{ and } \mu_2 = \frac{2l_1-\alpha}{2(l_1-l_2)}. $$

8.9.3 CN-WSGD Numerical Scheme

In this present analysis, consider the interval $[a,b]$ is partitioned into a uniform mesh with the space step $h=(b-a)/M$ and the time step $\tau = T/N$, where M,N are two positive integers. And the set of grid points are denoted by $x_j = jh$ and $t_n = n\tau$ for $j=1,\ldots,M$ and $n=0,\ldots,N$. Let $t_{n+1/2} = (t_n + t_{n+1})/2$ for $n=0,1,\ldots,N-1$, the following notations have been used

$$q_j^n = q(x_j, t_n), \text{ and } \delta_t q_j^n = (q_j^{n+1} - q_j^n)/\tau. \tag{8.84}$$

In space discretization, weighted shifted Grünwald–Letnikov formula (8.83) has been used to approximate Riesz fractional derivative and for the time discretization using the Crank–Nicolson technique in Eq. (8.14) leads to

$$\begin{aligned} i\delta_t q_j^n + \frac{1}{2}\Bigg[-\frac{1}{2\cos\left(\frac{\pi\alpha}{2}\right)h^\alpha}\Bigg[\sum_{k=0}^{j+1}\omega_k^{(\alpha)} q_{j-k+1}^{n+1} + \sum_{k=0}^{M-j+1}\omega_k^{(\alpha)} q_{j+k-1}^{n+1} \\ + \sum_{k=0}^{j+1}\omega_k^{(\alpha)} q_{j-k+1}^{n} + \sum_{k=0}^{M-j+1}\omega_k^{(\alpha)} q_{j+k-1}^{n}\Bigg]\Bigg] \\ + \frac{i}{2}\left[\left|q_j^{n+1}\right|^2\left(\frac{q_{j+1}^{n+1} - q_{j-1}^{n+1}}{2h}\right) + \left|q_j^n\right|^2\left(\frac{q_{j+1}^n - q_{j-1}^n}{2h}\right)\right] = \varepsilon_j^n, \end{aligned} \tag{8.85}$$

where

$$(l_1, l_2) = (1, 0), \omega_0^{(\alpha)} = \tfrac{\alpha}{2}\varpi_0^{(\alpha)}, \omega_k^{(\alpha)} = \tfrac{\alpha}{2}\varpi_k^{(\alpha)} + \tfrac{2-\alpha}{2}\varpi_{k-1}^{(\alpha)}, k \geq 1;$$

$$(l_1, l_2) = (1, -1), \omega_0^{(\alpha)} = \tfrac{2+\alpha}{4}\varpi_0^{(\alpha)}, \omega_1^{(\alpha)} = \tfrac{2+\alpha}{4}\varpi_1^{(\alpha)}, \omega_k^{(\alpha)} = \tfrac{2+\alpha}{4}\varpi_k^{(\alpha)} + \tfrac{2-\alpha}{4}\varpi_{k-2}^{(\alpha)}, k \geq 2;$$

$$\left|\varepsilon_j^n\right| \leq \tilde{c}(h^2 + \tau^2) \text{ and } i = \sqrt{-1}\,.$$

Multiplying Eq. (8.85) by τ and separating the time layers, we have

$$\begin{aligned} q_j^{n+1} - \frac{1}{2}\frac{v\tau}{h^\alpha}\sum_{k=0}^{j+1}\omega_k^{(\alpha)} q_{j-k+1}^{n+1} - \frac{1}{2}\frac{v\tau}{h^\alpha}\sum_{k=0}^{M-j+1}\omega_k^{(\alpha)} q_{j+k-1}^{n+1} + \frac{\tau}{2}\left|q_j^{n+1}\right|^2\left(\frac{q_{j+1}^{n+1} - q_{j-1}^{n+1}}{2h}\right) \\ = q_j^n + \frac{1}{2}\frac{v\tau}{h^\alpha}\sum_{k=0}^{j+1}\omega_k^{(\alpha)} q_{j-k+1}^{n} + \frac{1}{2}\frac{v\tau}{h^\alpha}\sum_{k=0}^{M-j+1}\omega_k^{(\alpha)} q_{j+k-1}^{n} - \frac{\tau}{2}\left|q_j^n\right|^2\left(\frac{q_{j+1}^n - q_{j-1}^n}{2h}\right) \\ + O(\tau h^2 + \tau^3), \end{aligned} \tag{8.86}$$

where $v = -\frac{i}{2\cos\left(\frac{\pi\alpha}{2}\right)}$.

Denoting $\tilde{q}_j^n$ as the numerical approximate value of q_j^n, the CN-WSGD scheme for Eq. (8.14) has been derived as

$$\tilde{q}_j^{n+1} - \frac{1}{2}\frac{v\tau}{h^\alpha}\sum_{k=0}^{j+1}\omega_k^{(\alpha)}\tilde{q}_{j-k+1}^{n+1} - \frac{1}{2}\frac{v\tau}{h^\alpha}\sum_{k=0}^{M-j+1}\omega_k^{(\alpha)}\tilde{q}_{j-k+1}^{n+1} + \frac{\tau}{2}\left|\tilde{q}_j^{n+1}\right|^2\left(\frac{\tilde{q}_{j+1}^{n+1} - \tilde{q}_{j-1}^{n+1}}{2h}\right)$$
$$= \tilde{q}_j^n + \frac{1}{2}\frac{v\tau}{h^\alpha}\sum_{k=0}^{j+1}\omega_k^{(\alpha)}\tilde{q}_{j-k+1}^n + \frac{1}{2}\frac{v\tau}{h^\alpha}\sum_{k=0}^{M-j+1}\omega_k^{(\alpha)}\tilde{q}_{j-k+1}^n - \frac{\tau}{2}\left|\tilde{q}_j^n\right|^2\left(\frac{\tilde{q}_{j+1}^n - \tilde{q}_{j-1}^n}{2h}\right), \tag{8.87}$$

$j = 1, 2, \ldots, M-1$ and $n = 1, 2, \ldots, N-1$,

$$\tilde{q}_j^0 = \gamma_0(x_j), j = 1, 2, \ldots, M-1, \tag{8.88}$$

$$\tilde{q}_0^n = \tilde{q}_M^n, \tilde{q}_{-1}^n = \tilde{q}_{M-1}^n, n = 1, 2, \ldots, N-1. \tag{8.89}$$

The system in Eq. (8.87) can be conveniently written into the following matrix form

$$\left(I - \frac{v\tau}{2h^\alpha}(A + A^T)\right)\tilde{\mathbf{q}}^{n+1} = \left(I + \frac{v\tau}{2h^\alpha}(A + A^T)\right)\tilde{\mathbf{q}}^n + \mathbf{G}^n - \tau\mathbf{F}^{n+1/2}. \tag{8.90}$$

where

I is an identity matrix, $\tilde{\mathbf{q}}^n = (\tilde{q}_1^n, \tilde{q}_2^n, \ldots, \tilde{q}_{M-1}^n)^T$,

$$A = \begin{pmatrix} \omega_1^{(\alpha)} & \omega_0^{(\alpha)} & & & \\ \omega_2^{(\alpha)} & \omega_1^{(\alpha)} & \omega_0^{(\alpha)} & & \\ \vdots & \omega_2^{(\alpha)} & \omega_1^{(\alpha)} & \ddots & \\ \omega_M^{(\alpha)} & \cdots & \ddots & \ddots & \omega_0^{(\alpha)} \\ \omega_{M-1}^{(\alpha)} & \omega_{M-2}^{(\alpha)} & \cdots & \omega_2^{(\alpha)} & \omega_1^{(\alpha)} \end{pmatrix} \text{ is a } (M-1)\times(M-1) \text{ matrix,}$$

$$\mathbf{G}^n = \frac{v\tau}{2h^\alpha}\begin{pmatrix} \omega_2^{(\alpha)} + \omega_0^{(\alpha)} \\ \omega_3^{(\alpha)} \\ \vdots \\ \omega_{M-1}^{(\alpha)} \\ \omega_M^{(\alpha)} \end{pmatrix}(\tilde{q}_0^n + \tilde{q}_0^{n+1}) + \frac{v\tau}{2h^\alpha}\begin{pmatrix} \omega_M^{(\alpha)} \\ \omega_{M-1}^{(\alpha)} \\ \vdots \\ \omega_3^{(\alpha)} \\ \omega_2^{(\alpha)} + \omega_0^{(\alpha)} \end{pmatrix}(\tilde{q}_M^n + \tilde{q}_M^{n+1}),$$

and

$$\mathbf{F}^{n+1/2}=\begin{pmatrix}\left|q_1^{n+1/2}\right|^2\left(\frac{\tilde{q}_2^{n+1/2}-\tilde{q}_0^{n+1/2}}{2h}\right)\\ \left|q_2^{n+1/2}\right|^2\left(\frac{\tilde{q}_3^{n+1/2}-\tilde{q}_1^{n+1/2}}{2h}\right)\\ \vdots\\ \left|q_{M-1}^{n+1/2}\right|^2\left(\frac{\tilde{q}_M^{n+1/2}-\tilde{q}_{M-2}^{n+1/2}}{2h}\right)\end{pmatrix}.$$

8.10 Stability and Convergence of CN-WSGD Scheme for Riesz Fractional Chen–Lee–Liu Equation

On the given domain $[a,b]\times[0,T]$, let us define $\Omega_h=\{x_j=jh: j=0,1,2,\ldots,M\}$, $\Omega_\tau=\{t_n=n\tau: n=0,1,2,\ldots,N\}$, $\Omega_{h\tau}=\Omega_h\times\Omega_\tau$. Suppose that, $V_{h,\tau}=\{v_j^n: j=0,1,2,\ldots,M; n=0,1,2,\ldots,N\}$ is a discrete function on $\Omega_{h\tau}$. Let us introduce the following notations:

$$<v^n,w^n>=h\sum_{j=1}^{M-1}v_j^n\overline{w_j^n},\quad \|v^n\|^2=<v^n,v^n>.$$

For any $v\in V_{h,\tau}$, we define the pointwise maximum norm

$$\|v^n\|_\infty=\max_{1\le j\le M-1}\left|v_j^n\right|, \tag{8.91}$$

and the following discrete l^2-norm

$$\|v^n\|_{l^2}=\sqrt{h\sum_{j=1}^{M-1}\left|v_j^n\right|^2}. \tag{8.92}$$

8.10.1 Stability Analysis

In Theorem 8.3, the stability of CN-WSGD scheme (8.87) has been analyzed in detail.

Theorem 8.3 *The CN-WSGD scheme* (8.87) *is unconditionally stable.*

Proof Let us denote $B=\frac{\nu\tau}{2h^2}(A+A^T)$. From Eq. (8.90), we have

$$\left(I-\frac{v\tau}{2h^{\alpha}}(A+A^{T})\right)\tilde{\mathbf{q}}^{n+1}=\left(I+\frac{v\tau}{2h^{\alpha}}(A+A^{T})\right)\tilde{\mathbf{q}}^{n}+\mathbf{G}^{n}-\tau\mathbf{F}^{n+1/2}. \tag{8.93}$$

If λ is a eigenvalue of matrix B, then $\left|\frac{1+\lambda}{1-\lambda}\right|$ is the eigenvalue of matrix $(I-B)^{-1}(I+B)$.

Now, when $1<\alpha\leq 2$, for $(l_1,l_2)=(1,-1)$, matrix A is negative definite, and the real parts of the eigenvalues λ of matrix $B=\frac{v\tau}{2h^{\alpha}}(A+A^{T})$ are less than 0. Thus, $\mathrm{Re}(\lambda)<0$, which implies that $\left|\frac{1+\lambda}{1-\lambda}\right|<1$. Therefore, the spectral radius of matrix $(I-B)^{-1}(I+B)$ is less than one.

Hence, the CN-WSGD scheme (8.87) is unconditionally stable. ■

8.10.2 Convergence Analysis

To prove the convergence, the following lemmas are needed.

Lemma 8.4 [49, 50] *The formula*

$$\mathrm{Im}\left(\sum_{l=1}^{M-1}\sum_{r=1}^{M-1}c_{l-r}\psi_r\overline{\psi_l}\right)=0,$$

holds, where "Im" *stands for the imaginary part.*

Lemma 8.5 (Grönwall's inequality) *Let* $\{G^n|n\geq 0\}$ *be a nonnegative sequence.*

If $G^{n+1}\leq(1+c\tau)G^n+\tau\sigma$, $n=0,1,2,\ldots$, where c and σ *are nonnegative constants. Then,* G^n *satisfies*

$$G^{n+1}\leq \mathrm{e}^{cn\tau}(G^0+\sigma/c).$$

Theorem 8.4 *The numerical solution* $\tilde{q}_j^n$ *of the finite difference scheme* (8.87) *is convergent to the true solution* q_j^n *with the error* $O(\tau^2+h^2)$ *in the discrete* L^2-norm.

Proof Let $q_j^n=q(x_j,t_n)$, $\tilde{q}_j^n=\tilde{q}(x_j,t_n)$, $e_j^n=q_j^n-\tilde{q}_j^n$,

$$\varepsilon_j^n=i\delta_t q_j^n+\frac{\gamma}{h^{\alpha}}\sum_{k=0}^{j+1}\omega_k^{(\alpha)}q_{j-k+1}^{n+1/2}+\frac{\gamma}{h^{\alpha}}\sum_{k=0}^{M-j+1}\omega_k^{(\alpha)}q_{j+k-1}^{n+1/2}+i\left|q_j^{n+1/2}\right|^2\left(\frac{q_{j+1}^{n+\frac{1}{2}}-q_{j-1}^{n+\frac{1}{2}}}{2h}\right), \tag{8.94}$$

$\gamma=-\frac{1}{2\cos\left(\frac{\pi\alpha}{2}\right)}$, $\mathbf{e}^n=(e_1^n,e_2^n,\ldots,e_{M-1}^n)^T$, and $\boldsymbol{\varepsilon}^{\boldsymbol{n}}=(\boldsymbol{\varepsilon}_{\boldsymbol{1}}^{\boldsymbol{n}},\boldsymbol{\varepsilon}_{\boldsymbol{1}}^{\boldsymbol{n}},\ldots,\boldsymbol{\varepsilon}_{\boldsymbol{M-1}}^{\boldsymbol{n}})^{\boldsymbol{T}}$.

From Eq. (8.94), we can write

$$\varepsilon_j^n = i\delta_t e_j^n + \frac{\gamma}{h^\alpha}\sum_{k=0}^{j+1}\omega_k^{(\alpha)} e_{j-k+1}^{n+1/2} + \frac{\gamma}{h^\alpha}\sum_{k=0}^{M-j+1}\omega_k^{(\alpha)} e_{j+k-1}^{n+1/2} + iH_j^{n+\frac{1}{2}}, \tag{8.95}$$

where

$$H_j^{n+\frac{1}{2}} = \left|q_j^{n+1/2}\right|^2\left(\frac{q_{j+1}^{n+\frac{1}{2}} - q_{j-1}^{n+\frac{1}{2}}}{2h}\right) - \left|\tilde{q}_j^{n+1/2}\right|^2\left(\frac{\tilde{q}_{j+1}^{n+\frac{1}{2}} - \tilde{q}_{j-1}^{n+\frac{1}{2}}}{2h}\right). \tag{8.96}$$

Now,

$$\left|H_j^{n+1/2}\right| \le (\max\{\left|q_j^{n+1/2}\right|, \left|\tilde{q}_j^{n+1/2}\right|\})^2\left|\frac{e_{j+1}^{n+1/2} - e_{j-1}^{n+1/2}}{2h}\right|. \tag{8.97}$$

It follows from Eq. (8.97) that there exists a constant $C_2 > 0$ such that

$$\left|H_j^{n+1/2}\right| \le C_2\left(\left|e_{j+1}^{n+1/2}\right| + \left|e_{j-1}^{n+1/2}\right|\right), \tag{8.98}$$

which implies that there exists a constant $C_3 > 0$ such that

$$\left\|\mathbf{H}^{n+1/2}\right\|^2 \le C_3\left(2\left\|\mathbf{e}^{n+1/2}\right\|^2 + h\left(\left|e_0^{n+1/2}\right|^2 - h\left|e_1^{n+1/2}\right|^2 + \left|e_M^{n+1/2}\right|^2 - \left|e_{M-1}^{n+1/2}\right|^2\right)\right). \tag{8.99}$$

From Eq. (8.99), it further follows that there exists a constant $\boldsymbol{M} > 0$ such that

$$\left\|\mathbf{H}^{n+1/2}\right\|^2 \le C_3\boldsymbol{M}\left\|\mathbf{e}^{n+1/2}\right\|^2 \tag{8.100}$$

Now, computing the inner product $<\boldsymbol{\varepsilon}^n, \overline{\mathbf{e}^{n+1}} + \overline{\mathbf{e}^n}>$, taking the imaginary part, and using Lemma 8.4, we have

$$\mathrm{Im}<\boldsymbol{\varepsilon}^n, 2\overline{\mathbf{e}^{n+1/2}}> \;= \frac{\left(\left\|\mathbf{e}^{n+1}\right\|^2 - \left\|\mathbf{e}^n\right\|^2\right)}{\tau} + \mathrm{Im}<i\mathbf{H}^{n+1/2}, 2\overline{\mathbf{e}^{n+1/2}}>. \tag{8.101}$$

Therefore,

$$\begin{aligned}\frac{\left(\left\|\mathbf{e}^{n+1}\right\|^2 - \left\|\mathbf{e}^n\right\|^2\right)}{\tau} &= \mathrm{Im}<\boldsymbol{\varepsilon}^n, 2\overline{\mathbf{e}^{n+1/2}}> + \mathrm{Im}< - i\mathbf{H}^{n+1/2}, 2\overline{\mathbf{e}^{n+1/2}}> \\ &\le \left(\left\|\boldsymbol{\varepsilon}^n\right\|^2 + 2\left\|\mathbf{e}^{n+1/2}\right\|^2\right) + \left(\left\|\mathbf{H}^{n+1/2}\right\|^2 + 2\left\|\mathbf{e}^{n+1/2}\right\|^2\right)\end{aligned} \tag{8.102}$$

Using Eqs. (8.100), (8.102) leads to

$$\begin{aligned}\left\|\mathbf{e}^{n+1}\right\|^2-\|\mathbf{e}^n\|^2 &\le \tau\left(\|\boldsymbol{\varepsilon}^n\|^2+2\left\|\mathbf{e}^{n+1/2}\right\|^2\right)+\tau\left(C_3\boldsymbol{M}\left\|\mathbf{e}^{n+1/2}\right\|^2+2\left\|\mathbf{e}^{n+1/2}\right\|^2\right)\\ &\le \tau\|\boldsymbol{\varepsilon}^n\|^2+2\tau\left(1+\frac{C_3\boldsymbol{M}}{4}\right)\left(\left\|\mathbf{e}^{n+1}\right\|^2+\|\mathbf{e}^n\|^2\right)\\ &\le \tau(b-a)\tilde{C}^2(h^2+\tau^2)^2+2\tau\left(1+\frac{C_3\boldsymbol{M}}{4}\right)\left(\left\|\mathbf{e}^{n+1}\right\|^2+\|\mathbf{e}^n\|^2\right).\end{aligned} \tag{8.103}$$

Therefore, there exists a constant τ_0: $0<\tau_0<1/\left(2+\frac{C_3\boldsymbol{M}}{2}\right)$ such that when $0<\tau\le\tau_0$, we have

$$\left\|\mathbf{e}^{n+1}\right\|^2 \le \left(1+\frac{\tau(4+C_3\boldsymbol{M})}{1-2\tau_0-\frac{C_3\boldsymbol{M}\tau_0}{2}}\right)\|\mathbf{e}^n\|^2+\frac{\tau(b-a)\tilde{C}^2(h^2+\tau^2)^2}{\left(1-2\tau_0-\frac{C_3\boldsymbol{M}\tau_0}{2}\right)}.$$

Let

$\sigma_1=\frac{(4+C_3\boldsymbol{M})}{1-2\tau_0-\frac{C_3\boldsymbol{M}\tau_0}{2}}$ and $\sigma_2=\frac{(b-a)\tilde{C}^2}{\left(1-2\tau_0-\frac{C_3\boldsymbol{M}\tau_0}{2}\right)}$, we then obtain

$$\left\|\mathbf{e}^{n+1}\right\|^2 \le (1+\sigma_1\tau)\|\mathbf{e}^n\|^2+\sigma_2\tau(h^2+\tau^2)^2. \tag{8.104}$$

Now, using Grönwall's inequality, we obtain

$$\left\|\mathbf{e}^{n+1}\right\|^2 \le \frac{\sigma_2}{\sigma_1}\mathrm{e}^{\sigma_1 T}(h^2+\tau^2)^2, n=0,1,2,\ldots \tag{8.105}$$

Hence, it is proved. ■

8.10.3 Numerical Experiments and Discussion

In this section, some numerical results concerning the solitary wave solutions for the Riesz fractional CLL Eq. (8.14) have been presented. The initial condition is chosen such that $q(x,0)=\gamma_0(x)$ decays to zero sufficiently fast as $|x|$ tending to the two boundary points. An appropriately long interval $[a,b]$ has been chosen for the computations such that the periodic boundary conditions do not introduce a significant error relative to the whole space problem.

In the present numerical experiment, the following initial condition [51] has been taken into consideration for the Riesz fractional CLL Eq. (8.14)

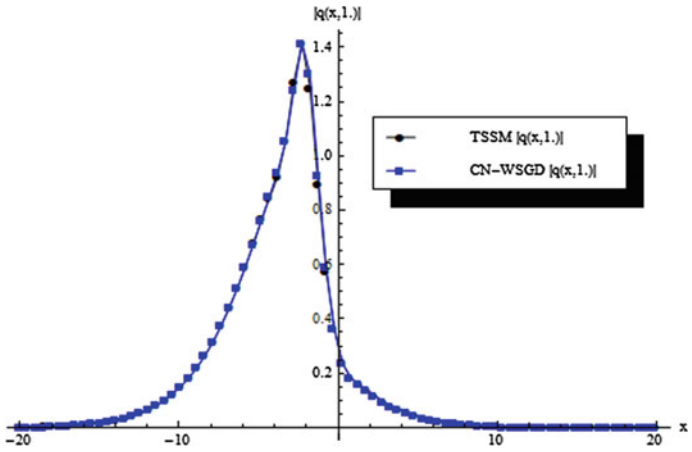

Fig. 8.6 Comparison of results for the solution of $|q(x,1)|$ obtained from TSSM and CN-WSGD scheme for the Riesz fractional CLL Eq. (8.14) with fractional order $\alpha = 1.75$

$$q(x,0) = \gamma_0(x) = 2i\Delta_1^2 B_0, \tag{8.106}$$

where

$$\begin{aligned}
\Delta_1 &= \exp\{2(2\beta-1)[if(x) + (\xi_1^2+\eta_1^2)(\xi_1^2-\eta_1^2)^{-1}g(x)]\}, \beta = 1/4\\
f(x) &= -g(x) + \frac{\xi_1\eta_1(\xi_1^2+\eta_1^2)\sinh(2X_1)}{(\xi_1^2-\eta_1^2)^2 + (\xi_1^4-\eta_1^4)\cosh(2X_1)}\\
g(x) &= \arctan[\xi_1^{-1}\eta_1\tanh(X_1)]\\
B_0 &= \frac{2i\xi_1\eta_1\exp(iY_1)}{\xi_1\cosh(X_1) + i\eta_1\sinh(X_1)}\\
X_1 &= 4\xi_1\eta_1 x + \delta_1\\
Y_1 &= -2(\xi_1^2-\eta_1^2)x + \mu_1
\end{aligned}$$

In this case, the problem has been solved on the interval $[-20, 20]$ with vanishing boundary conditions. The Riesz fractional CLL Eq. (8.14) along with the above initial condition (8.106) has been solved by both time-splitting spectral method (TSSM) and an implicit finite difference method, viz. CN-WSGD scheme, in order to justify the efficiency and applicability of the proposed methods.

Figures 8.6, 8.7, and 8.8 show the comparison between the evolutions of the TSSM solution and the CN-WSGD solution at $t = 1$ for various fractional orders α. The results show that the solution curves of $|q(x,1)|$ obtained by TSSM coincide well with the CN-WSGD solution curves, respectively. Thus, there is a good agreement of results obtained by the proposed two methods.

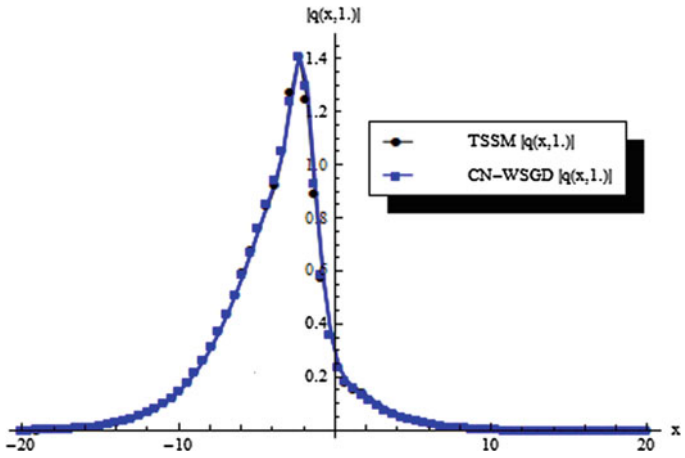

Fig. 8.7 Comparison of results for the solution of $|q(x, 1)|$ obtained from TSSM and CN-WSGD scheme for the Riesz fractional CLL Eq. (8.14) with fractional order $\alpha = 1.8$

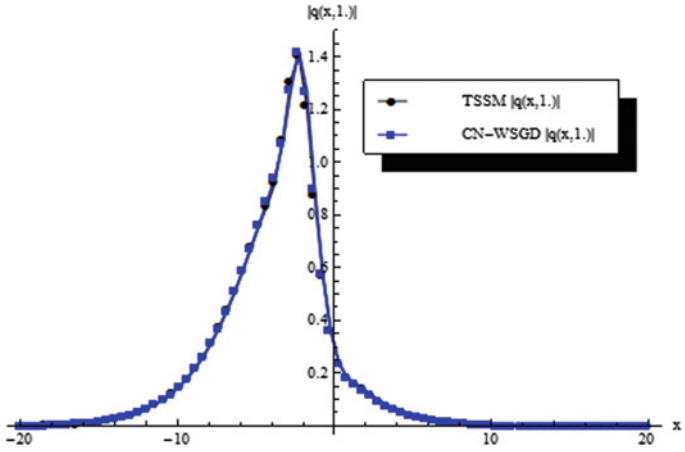

Fig. 8.8 Comparison of results for the solution of $|q(x, 1)|$ obtained from TSSM and CN-WSGD scheme for the Riesz fractional CLL Eq. (8.14) with fractional order $\alpha = 1.9$

In addition, in Fig. 8.9, the dynamic evolution of single-soliton 3-D solution of $|q(x, t)|$ and the corresponding 2-D solution graph at $t = 1$ for fractional order $\alpha = 1.9$ have been presented. Also, single-soliton 3-D surface solution of $|q(x, t)|$ and the corresponding 2-D solution graph at $t = 1$ for fractional order $\alpha = 1.75$ have been depicted in Fig. 8.10. The solution graphs in Figs. 8.9 and 8.10 have been drawn by the results obtained from TSSM.

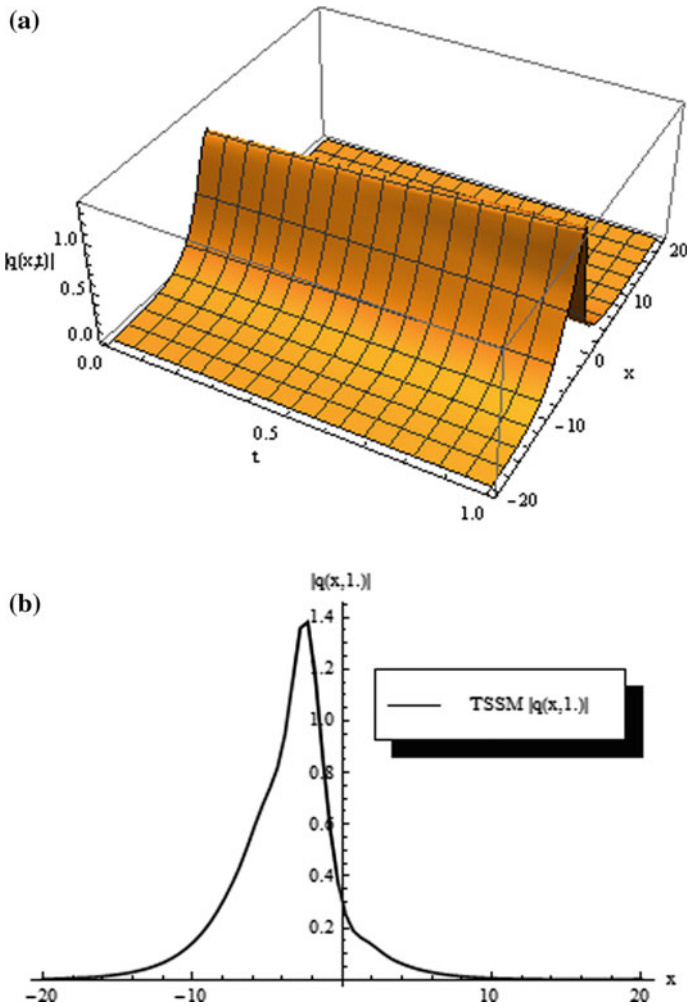

Fig. 8.9 **a** Dynamic evolution of single-soliton 3-D wave solution of $|q(x,t)|$ and **b** the corresponding 2-D solution graph at $t = 1.0$ obtained by TSSM for the Riesz fractional CLL Eq. (8.14) with fractional order $\alpha = 1.9$

To examine the accuracy of the time-splitting method for the Riesz fractional CLL Eq. (8.14), the L_2 and L_∞ error norms [46] for the results of TSSM have been calculated with regard to CN-WSGD results in Table 8.2. The comparison of results quite establishes the plausibility of the proposed methods for solving Riesz fractional CLL Eq. (8.14).

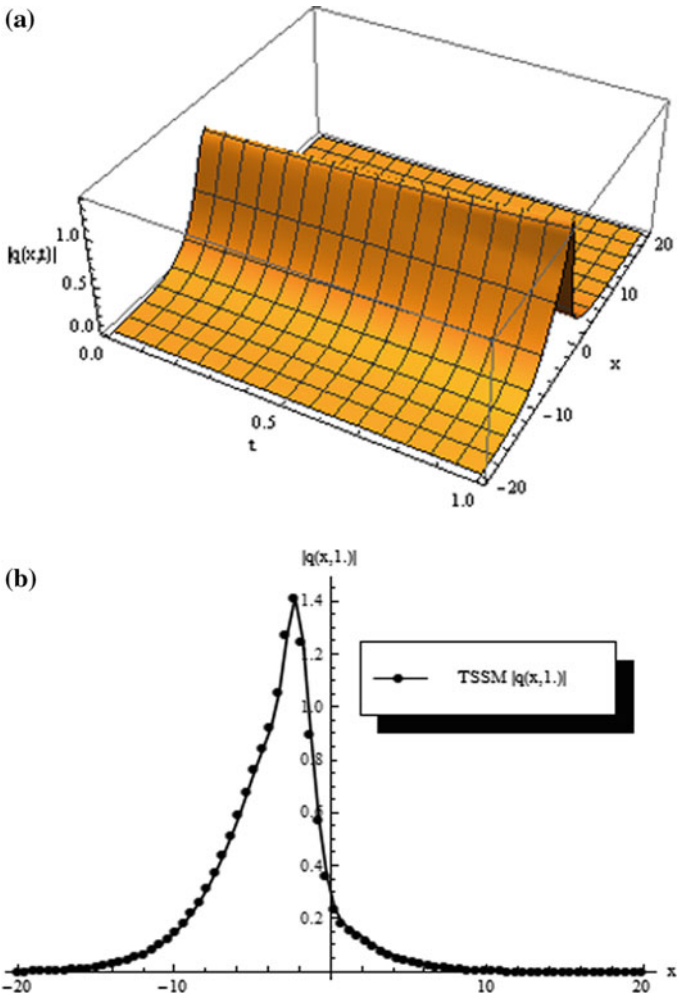

Fig. 8.10 **a** Dynamic evolution of single-soliton 3-D wave solution of $|q(x,t)|$ and **b** the corresponding 2-D solution graph at $t = 1.0$ obtained by TSSM for the Riesz fractional CLL Eq. (8.14) with fractional order $\alpha = 1.75$

Table 8.2 L_2 norm and L_∞ norm of errors between the solutions of TSSM and CNFD method for various values of fractional order α

t	$\alpha = 1.75$		$\alpha = 1.8$		$\alpha = 1.9$	
	L_2 error $\lvert q(x,t)\rvert$	L_∞ error $\lvert q(x,t)\rvert$	L_2 error $\lvert q(x,t)\rvert$	L_∞ error $\lvert q(x,t)\rvert$	L_2 error $\lvert q(x,t)\rvert$	L_∞ error $\lvert q(x,t)\rvert$
0.5	0.815537E−5	0.165953E−1	0.778329E−5	0.16581E−1	0.650155E−5	0.129859E−1
0.8	0.335717E−4	0.324358E−1	0.337131E−4	0.325136E−1	0.273365E−4	0.279851E−1
1.0	0.662656E−4	0.512437E−1	0.663821E−4	0.492266E−1	0.50869E−4	0.323696E−1

8.11 Conclusion

In this chapter, a new approach, viz. time-splitting spectral method, has been proposed for solving Riesz fractional coupled S-K equations. The proposed time-splitting spectral method is highly well suited for solving Riesz fractional coupled S-K equations. In addition, with the aid of fractional centered difference approximation for Riesz fractional derivative, an implicit finite difference technique, viz. Crank–Nicolson finite difference method, has been applied for Riesz fractional coupled S-K equations in order to assess the results of these proposed methods. It is found that there is a fine agreement between the results of both the techniques. In comparison with the implicit finite difference method, the proposed TSSM is also an efficient and simple tool to determine the approximate solution of Riesz fractional coupled S-K equations. The obtained results ascertain the reliability of the proposed methods and its applicability in solving Riesz fractional coupled S-K equations. The implementations of the proposed methods for the solutions of Riesz fractional coupled S-K equations quite well justify their applicability and efficiency.

A new approach, viz. time-splitting spectral method, has been proposed for solving Riesz fractional CLL equation. The TSSM is based on Strang splitting method in time coupled with trigonometric spectral approximation in space. In addition, with the aid of weighted shifted Grünwald–Letnikov formula for approximating Riesz fractional derivative, Crank–Nicolson implicit finite difference method has been applied for Riesz fractional CLL equation in order to examine the comparison results for these proposed methods. The numerical results obtained by the proposed TSSM highly agree with those obtained by CN-WSGD method. The obtained results ascertain the reliability of the proposed methods and its applicability in solving the Riesz fractional CLL equation. The successful implementations of the proposed methods for the solutions of Riesz fractional CLL equation quite well justify their applicability and efficiency. The numerical solutions obtained by TSSM for the Riesz fractional equations will be useful to analyze wave pattern in quantum mechanics, nonlinear optics, fluid mechanics, plasma physics, and magnetohydrodynamic wave equations [52, 53].

References

1. Leble, S., Reichel, B.: Coupled nonlinear Schrodinger equations in optic fibers theory: from general to solitonic aspects. Eur. Phys. J. Spec. Top. **173**, 5–55 (2009)
2. Kodama, Y.: Optical solitons in a monomode fiber. J. Stat. Phys. **39**, 597–614 (1985)
3. Bao, W., Jaksch, D.: An explicit unconditionally stable numerical method for solving damped nonlinear Schrodinger equations with a focusing nonlinearity. SIAM J. Numer. Anal. **41**, 1406–1426 (2003)
4. Fan, E.G.: A unified and explicit construction of *N*-soliton solutions for the nonlinear schrödinger equation. Commun. Theor. Phys. **36**(4), 401–404 (2001)

5. Bai, D., Zhang, L.: The finite element method for the coupled Schrödinger-KdV equations. Phys. Lett. A **373**, 2237–2244 (2009)
6. Yoshinaga, T., Wakamiya, M., Kakutani, T.: Recurrence and chaotic behavior resulting from nonlinear interaction between long and short waves. Phys. Fluids A **3**(1), 83–89 (1991)
7. Wazwaz, A.M.: Partial differential equations: methods and applications. Balkema, Lisse, The Netherlands (2002)
8. Debnath, L.: Nonlinear partial differential equations for scientists and engineers. Birkhäuser, Boston (2005)
9. Podlubny, I.: Fractional differential equations. Academic Press, New York (1999)
10. Oldham, K.B., Spainer, J.: The fractional calculus. Academic Press, New York (1974)
11. Saha Ray, S.: Fractional Calculus With Applications For Nuclear Reactor Dynamics. CRC Press, Taylor and Francis group, Boca Raton, New York, USA (2015)
12. Kilbas, A.A., Srivastava, H.M., Trujillo, J.J.: Theory and Applications of Fractional Differential Equations. Elsevier Science and Tech, Amsterdam, The Netherlands (2006)
13. Saha, Ray S., Gupta, A.K.: Wavelet Methods for Solving Partial Differential Equations and Fractional Differential Equations. Chapman and Hall/CRC, New York (2018)
14. Sabatier, J., Agrawal, O.P., Tenreiro Machado, J.A.: Advances in Fractional Calculus: Theoretical Developments and Applications in Physics and Engineering. Springer, Dordrecht, The Netherlands (2007)
15. Debnath, L., Bhatta, D.: Integral Transforms and Their Applications. CRC Press, Taylor and Francis Group, Boca Raton, New York, USA (2007)
16. Cui, M.: Compact finite difference method for the fractional diffusion equation. J. Comput. Phys. **228**, 7792–7804 (2009)
17. Saha Ray, S.: On Haar wavelet operational matrix of general order and its application for the numerical solution of fractional Bagley Torvik equation. Appl. Math. Comput. **218**, 5239–5248 (2012)
18. Aslan, İ.: Exact solutions for a local fractional DDE associated with a nonlinear transmission line. Commun. Theor. Phys. **66**(3), 315–320 (2016)
19. Aslan, İ.: Analytic investigation of a reaction–diffusion Brusselator model with the time-space fractional derivative. Int. J. Nonlinear Sci. Numer. Simul. **15**(2), 149–155 (2014)
20. Aslan, İ.: An analytic approach to a class of fractional differential-difference equations of rational type via symbolic computation. Math. Methods Appl. Sci. **38**, 27–36 (2015)
21. Aslan, İ.: Exact solutions for fractional DDEs via auxiliary equation method coupled with the fractional complex transform. Math. Methods Appl Sci. **39**(18), 5619–5625 (2016)
22. Saha Ray, S., Bera, R.K.: Analytical solution of a dynamic system containing fractional derivative of order one-half by Adomian decomposition method. Trans. ASME J. Appl. Mech. **72**(2), 290–295 (2005)
23. Saha Ray, S.: Exact solutions for time-fractional diffusion-wave equations by decomposition method. Phys. Scr., **75**(1), Article number 008, 53–61 (2007)
24. Saha Ray, S.: Numerical solutions and solitary wave solutions of fractional KdV equations using modified fractional reduced differential transform method. Comput. Math. Math. Phys. **53**(12), 1870–1881 (2013)
25. Saha Ray, S.: A novel method for travelling wave solutions of fractional whitham-broer-kaup, fractional modified boussinesq and fractional approximate long wave equations in shallow water. Math. Methods Appl. Sci. **38**(7), 1352–1368 (2015)
26. Lu, B.: The first integral method for some time fractional differential equations. J. Math. Anal. Appl. **395**, 684–693 (2012)
27. Saha Ray, S.: New exact solutions of nonlinear fractional acoustic wave equations in ultrasound. Comput. Math. Appl. **71**(2016) 859–868
28. Saha, Ray S., Sahoo, S.: Improved fractional sub-equation method for (3 + 1)-dimensional generalized fractional KdV-Zakharov-Kuznetsov equations. Comput. Math Appl. **70**(2), 158–166 (2015)
29. Zhang, S., Zhang, H.Q.: Fractional sub-equation method and its applications to nonlinear fractional PDEs. Phys. Lett. A **375**, 1069–1073 (2011)

30. Zhang, J., Liu, W., Qiu, D., Zhang, Y., Porsezian, K., He, J.: Rogue wave solutions of a higher-order Chen-Lee-Liu equation. Phys. Scr., **90**, Article ID 055207(18 Pages) (2015)
31. Triki, H., Babatin, M.M., Biswas, A.: Chirped bright solitons for Chen-Lee-Liu equation in optical fibers and PCF. Optics **149**, 300–303 (2017)
32. Kivshar, Y.S., Agrawal, G.P.: Optical Solitons: From Fibers to Photonic Crystals. Academic, New York
33. Agrawal, G.P.: Nonlinear Fiber Optics, 5th edn. Academic Press, San Diego, CA (2012)
34. Kaya, Dŏgan, El-Sayed, Salah M.: On the solution of the coupled Schrödinger–KdV equation by the decomposition method. Phys. Lett. A **313**(1–2), 82–88 (2003)
35. Fan, E., Hon, Y.C.: Applications of extended tanh method to 'special' types of nonlinear equations. Appl. Math. Comput. **141**, 351–358 (2003)
36. Fan, E.: Multiple travelling wave solutions of nonlinear evolution equations using a unified algebraic method. J. Phys. A: Math. Gen. **35**, 6853–6872 (2002)
37. Saha Ray, S.: On the soliton solution and Jacobi doubly periodic solution of the fractional coupled Schrödinger-KdV equation by a novel approach. Int. J. Nonlinear Sci. Numer. Simul. **16**, 79–95 (2015)
38. Küçükarslan, S.: Homotopy perturbation method for coupled Schrödinger–KdV equation. Nonlinear Analysis: Real World Applications **10**, 2264–2271 (2009)
39. Hirota, R.: The Direct Method in Soliton Theory. Cambridge University Press, Cambridge (2004)
40. Seadawy, A.R., El-Rashidy, K.: Classification of multiply travelling wave solutions for coupled burgers, Combined KdV-Modified KdV, and Schrödinger-KdV Equations, **2015**, Article ID 369294, 7 pages (2015)
41. Yang, Q., Liu, F., Turner, I.: Numerical methods for fractional partial differential equations with Riesz space fractional derivatives. Appl. Math. Model. **34**, 200–218 (2010)
42. Zhuang, P., Liu, F., Anh, V., Turner, I.: Numerical methods for the variable-order fractional advection–diffusion equation with a nonlinear source term. SIAM J. Numer. Anal. **47**, 1760–1781 (2009)
43. Chen, H.H., Lee, Y.C., Liu, C.S.: Integrability of nonlinear Hamiltonian system by inverse scattering method. Phys. Scr. **20**, 490–492 (1979)
44. Moses, J., Malomed, B.A., Wise, F.W.: Self-steepening of ultrashort optical pulses without self-phase-modulation. Phys. Rev. A, **76**, Article ID 021802 (2007)
45. Çelik, C., Duman, M.: Crank–Nicolson method for the fractional diffusion equation with the Riesz fractional derivative. J. Comput. Phys. **231**, 1743–1750 (2012)
46. Saha Ray, S.: A novel approach with time-splitting spectral technique for the coupled Schrödinger-Boussinesq equations involving Riesz fractional derivative. Commun. Theor. Phys. **68**(3), 301–308 (2017)
47. Meerschaert, M.M., Tadjeran, C.: Finite difference approximations for two-sided space-fractional partial differential equations. Appl. Numer. Math. **56**, 80–90 (2006)
48. Tian, W.Y., Zhou, H., Deng, W.H.: A class of second order difference approximation for solving space fractional diffusion equations. Math. Comput. **84**, 1703–1727 (2015)
49. Wang, D., Xiao, A., Yang, W.: Maximum-norm error analysis of a difference scheme for the space fractional CNLS. Appl. Math. Comput. **257**, 241–251 (2015)
50. Wang, D., Xiao, A., Yang, W.: Crank–Nicolson difference scheme for the coupled nonlinear Schrodinger equations with the Riesz space fractional derivative. J. Comput. Phys. **242**, 670–681 (2013)
51. Fan, E.: A family of completely integrable multi-Hamiltonian systems explicitly related to some celebrated equations. J. Math. Phys. **42**(9), 4327–4344 (2001)
52. Tarasov, V.E.: Fractional Dynamics: Applications of Fractional Calculus to Dynamics of Particles. Springer-Verlag, Berlin Heidelberg, New York, Fields and Media (2011)
53. Debnath, L.: Recent applications of fractional calculus to science and engineering. Int. J. Math. Math. Sci. **2003**, 3413–3442 (2003)

Chapter 9
Numerical Simulation of Stochastic Point Kinetics Equation in the Dynamical System of Nuclear Reactor

9.1 Introduction

In nuclear reactor dynamics, the point kinetics equations are the coupled differential equations for the neutron density and for the delayed neutron precursor concentrations. The point kinetics equations are the most vital model in nuclear engineering, and these equations model the time-dependent behavior of a nuclear reactor [1–4]. The time-dependent parameters in this system are the reactivity function and neutron source term. The dynamical process described by the point kinetics equations is stochastic in nature, and the neutron density and delayed neutron precursor concentrations vary randomly with time. At high power levels, random behavior is negligible. But at low power levels, such as at the beginning, random fluctuation in the neutron density and neutron precursor concentrations can be significant.

The point kinetics equations model a system of interacting populations, specifically the populations of neutrons and delayed neutron precursors. In this chapter, the physical dynamical system identified as a population process and the point kinetics equations have been analyzed to transform into a stochastic differential equation system that accurately models the random behavior of the process.

In the present chapter, the Euler–Maruyama method and Taylor 1.5 strong order approximation method have been applied efficiently and conveniently for the solution of stochastic point kinetics equation. The resulting systems of stochastic differential equations are solved over each time-step size in the partition. In the present investigation, the main attractive advantage, of these computational numerical methods, is their elegant applicability for solving stochastic point kinetics equations in a simple and efficient way.

S. Saha Ray, *Nonlinear Differential Equations in Physics*,
https://doi.org/10.1007/978-981-15-1656-6_9

9.2 Outline of the Present Study

In the present chapter, the numerical approximation methods, applied to efficiently calculate the solution for stochastic point kinetics equations [1, 3] in nuclear reactor dynamics, are investigated. A system of Itô stochastic differential equations has been analyzed to model the neutron density and the delayed neutron precursors in a point nuclear reactor. The resulting system of Itô stochastic differential equations is solved over each time-step size. The methods are verified by considering different initial conditions, experimental data, and over-constant reactivities. The computational results indicate that the methods are simple and worthy for solving stochastic point kinetics equations. In this work, a numerical investigation is made in order to observe the random oscillations in neutron and precursor population dynamics in subcritical and critical reactors.

9.3 Strong and Weak Convergence

In this section, a brief discussion on strong convergence and week convergence has been presented.

9.3.1 Strong Convergence

A discrete-time approximation method is said to converge strongly to the solution $X(t)$ at time t if

$$\lim_{\Delta t -> 0} E\left|X(t) - \widehat{X}(t)\right| = 0 \tag{9.1}$$

where $\widehat{X}(t)$ is the approximate solution computed with constant step size Δt and E denotes expected value.

A SDE method converges strongly with order α if the expected value of the error is of αth order in the step size, i.e., if for any time t

$$E\left|X(t) - \widehat{X}(t)\right| = \mathrm{O}((\Delta t)^{\alpha}) \tag{9.2}$$

for sufficiently small step size Δt [5].

9.3.2 Weak Convergence

A discrete-time approximation $\widehat{X}(t)$ with constant step size Δt is said to converge weakly to the solution *X(t)* at time t if

$$\lim_{\Delta t- > 0}\left|E(f(X(t))) - E\left(f(\widehat{X}(t))\right)\right| = 0 \tag{9.3}$$

for all smooth functions f in some class.

A SDE method converges weakly with order α if the error in the moments is of αth order in the step size

$$\left|E(f(X(t))) - E\left(f(\widehat{X}(t))\right)\right| = \mathrm{O}((\Delta t)^{\alpha}) \tag{9.4}$$

for sufficiently small step size Δt [5].

In other words, for a given time discretization $t_0 < t_1 < \ldots < t_n = T$,

- A method is said to have strong order of convergence α if there is a constant $K > 0$ such that

$$\sup_{t_k} E\left|X_{t_k} - \widehat{X}_{t_k}\right| < K(\Delta t_k)^{\alpha}$$

- A method is said to have weak order of convergence α if there is a constant $K > 0$ such that

$$\sup_{t_k}\left|E[X_{t_k}] - E[\widehat{X}_{t_k}]\right| < K(\Delta t_k)^{\alpha},$$

where $\Delta t_k = t_k - t_{k-1}$, X_{t_k} and $\widehat{X}_{t_k}$ represents the exact solution and approximate solution at time t_k.

The Euler–Maruyama method has strong convergence of order $\alpha = 1/2$, which is poorer of the convergence for the Euler method in the deterministic case, which is order $\alpha = 1$. However, the Euler–Maruyama method has week convergence of order $\alpha = 1$.

9.4 Evolution of Stochastic Neutron Point Kinetics Model

It is the most vital part of nuclear reactor dynamics, to derive the point kinetics equations in order to separate the birth and death process of neutron population. It will help us to form a stochastic model. The deterministic time-dependent equations satisfied by the neutron density and the delayed neutron precursors are as follows [1]

$$\frac{\partial N}{\partial t} = Dv\nabla^2 N - (\Sigma_a - \Sigma_f)vN + [(1-\beta)k_\infty \Sigma_a - \Sigma_f]vN + \sum_i \lambda_i C_i + S_0, \quad (9.5)$$

$$\frac{\partial C_i}{\partial t} = \beta_i k_\infty \Sigma_a vN - \lambda_i C_i, \quad i = 1, 2, \ldots, m, \quad (9.6)$$

where $N(r,t)$ is the neutron density at a point r at time t. The coefficients D, v, Σ_a *and* Σ_f are, respectively, diffusion constants, the neutron speed, the macroscopic neutron absorption, and fission cross sections. The capture cross section is $\Sigma_a - \Sigma_f$. If $\beta = \sum_{i=1}^{m} \beta_i$ is the delayed neutron fraction, the prompt neutron contribution to the source is $[(1-\beta)k_\infty \Sigma_a - \Sigma_f]vN$ and the prompt neutron fraction is $(1-\beta)$. The number of neutrons produced per neutrons absorbed is k_∞ (also called infinite-medium reproduction factor). The rate of transformations from neutron precursors to the neutron population is $\sum_{i=1}^{m} \lambda_i C_i$ where the delayed constant is λ_i and $C_i(r,t)$ is the density of the ith type of precursor for $i = 1, 2, \ldots, m$. Sources of neutrons extraneous to the fission process are represented by $S_0(r,t)$.

In the present analysis, captures (or leakages) of neutrons are considered as deaths. The fission process is considered a pure birth process where $v(1-\beta) - 1$ neutrons are born in each fission along with precursor fraction $v\beta$.

Let us assume that $N = f(r)n(t)$ and $C_i = g_i(r)c_i(t)$ are separable in time and space where $n(t)$ and $c_i(t)$ are the total number of neutrons and precursors of the ith type at time t, respectively.

Using these, Hetrick [1] and Hayes et al. [4] derived the deterministic point kinetics equation as

$$\frac{dn}{dt} = -\left[\frac{-\rho + 1 - \alpha}{l}\right] n + \left[\frac{1-\alpha-\beta}{l}\right] n + \sum_{i=1}^{m} \lambda_i c_i + q, \quad (9.7a)$$

$$\frac{dc_i}{dt} = \frac{\beta_i}{l} n - \lambda_i c_i, \quad i = 1, 2, \ldots, m, \quad (9.7b)$$

where $q(t) = \frac{S_0(r,t)}{f(r)}$, ρ is reactivity, neutron generation time $l = \frac{1}{k_\infty v \Sigma_a}$, α is defined as $\alpha = \frac{\Sigma_f}{\Sigma_a k_\infty} \approx \frac{1}{v}$, and v is the average number of neutrons per fission. Here, $n(t)$ is the population size of neutrons and $c_i(t)$ is the population size of the ith neutron precursor. The neutron reactions can be separated into three terms as follows:

$$\frac{dn}{dt} = \underbrace{-\left[\frac{-\rho + 1 - \alpha}{l}\right]}_{\text{deaths}} n + \underbrace{\left[\frac{1-\alpha-\beta}{l}\right]}_{\text{births}} n + \underbrace{\sum_{i=1}^{m} \lambda_i c_i}_{\text{transformations}} + q,$$

$$\frac{dc_i}{dt} = \frac{\beta_i}{l} n - \lambda_i c_i, \quad i = 1, 2, \ldots, m.$$

The neutron birth rate due to fission is $b = \frac{1-\alpha-\beta}{l(-1+(1-\beta)v)}$, where the denominator has the term $(-1+(1-\beta)v)$ which represents the number of neutrons (newborn) produced in each fission process. The neutron death rate due to captures or leakage is $d = \frac{-\rho+1-\alpha}{l}$. The transformation rate $\lambda_i c_i$ represents the rate that the ith precursor is transformed into neutrons and q represents the rate that source neutrons are produced.

To derive the stochastic dynamical system, we consider for simplicity only one precursor, i.e., $\beta = \beta_1$, where β is the total delayed neutron fraction for one precursor.

The point kinetics equations for one precursor are as follows

$$\frac{\mathrm{d}n}{\mathrm{d}t} = \left[\frac{-\rho+1-\alpha}{l}\right]n + \left[\frac{1-\alpha-\beta}{l}\right]n + \lambda_1 c_1 + q, \quad \frac{\mathrm{d}c_1}{\mathrm{d}t} = \frac{\beta_1}{l}n - \lambda_1 c_1.$$

Now, we consider in the small duration of time interval Δt where probability of more than one occurred event is small. There are four different possibilities for an event at this small time Δt. Let $[\Delta n, \Delta c_1]^{\mathrm{T}}$ be the change of n and c_1 in time Δt where the changes are assumed approximately normally distributed. The four possibilities for $[\Delta n, \Delta c_1]^{\mathrm{T}}$ are

$$E_1 = \begin{bmatrix} \Delta n \\ \Delta c_1 \end{bmatrix}_1 \equiv \begin{bmatrix} -1 \\ 0 \end{bmatrix},$$

$$E_2 = \begin{bmatrix} \Delta n \\ \Delta c_1 \end{bmatrix}_2 \equiv \begin{bmatrix} -1+(1-\beta)v \\ \beta_1 v \end{bmatrix},$$

$$E_3 = \begin{bmatrix} \Delta n \\ \Delta c_1 \end{bmatrix}_3 \equiv \begin{bmatrix} 1 \\ -1 \end{bmatrix},$$

$$E_4 = \begin{bmatrix} \Delta n \\ \Delta c_1 \end{bmatrix}_4 \equiv \begin{bmatrix} 1 \\ 0 \end{bmatrix},$$

where the first event E_1 denotes a death, the second event E_2 represents birth of $(-1+(1-\beta)v)$ neutrons and $\beta_1 v$ delayed neutron precursors produced in the fission process, the third event E_3 represents a transformation of a delayed neutron precursor to a neutron, and the last one E_4 event represents a neutron source. The respective probabilities of these events are

$$P(E_1) = n\Delta t d,$$

$$P(E_2) = n\Delta t b = \frac{1}{vl} n\Delta t\,, \quad \text{since } b = \frac{1-\alpha-\beta}{l(-1+(1-\beta)v)} \text{ and } \alpha = \frac{\Sigma_f}{\Sigma_a k_\infty} \approx \frac{1}{v}$$

$$P(E_3) = c_1 \Delta t \lambda_1,$$

$$P(E_4) = q\Delta t.$$

In this present analysis, it is assumed that the extraneous source randomly produces neutrons following Poisson process with intensity q.

According to our earlier assumption, the changes in neutron population and precursor concentration are approximately normally distributed with mean $E\left(\begin{bmatrix}\Delta n\\ \Delta c_1\end{bmatrix}\right)$ and variance $\mathrm{Var}\left(\begin{bmatrix}\Delta n\\ \Delta c_1\end{bmatrix}\right)$.

Here, the mean change in the small interval of time Δt

$$E\left(\begin{bmatrix}\Delta n\\ \Delta c_1\end{bmatrix}\right) = \sum_{k=1}^{4} P_k \begin{bmatrix}\Delta n\\ \Delta c_1\end{bmatrix}_k = \begin{bmatrix}\frac{\rho-\beta}{l} n + \lambda_1 c_1 + q\\ \frac{\beta_1}{l} n - \lambda_1 c_1\end{bmatrix} \Delta t,$$

and the variance of change in small time Δt

$$\mathrm{Var}\left(\begin{bmatrix}\Delta n\\ \Delta c_1\end{bmatrix}\right) = E\left(\begin{bmatrix}\Delta n\\ \Delta c_1\end{bmatrix}[\Delta n \quad \Delta c_1]\right) - \left(E\left(\begin{bmatrix}\Delta n\\ \Delta c_1\end{bmatrix}\right)\right)^2$$

$$= \sum_{k=1}^{4} P_k \begin{bmatrix}\Delta n\\ \Delta c_1\end{bmatrix}_k [\Delta n \quad \Delta c_1]_k = \widehat{B}\Delta t,$$

where

$$\widehat{B} = \begin{bmatrix} \gamma n + \lambda_1 c_1 + q & \frac{\beta_1}{l}(-1+(1-\beta)v)n - \lambda_1 c_1 \\ \frac{\beta_1}{l}(-1+(1-\beta)v)n - \lambda_1 c_1 & \frac{\beta_1^2 v}{l} n + \lambda_1 c_1 \end{bmatrix},$$

where

$$\gamma = \frac{-1-\rho+2\beta+(1-\beta)^2 v}{l}.$$

Now, by central limit theorem, the random variate

$$\frac{\begin{bmatrix}\Delta n\\ \Delta c_1\end{bmatrix} - E\left(\begin{bmatrix}\Delta n\\ \Delta c_1\end{bmatrix}\right)}{\sqrt{\mathrm{Var}\left(\begin{bmatrix}\Delta n\\ \Delta c_1\end{bmatrix}\right)}}$$

follows standard normal distribution. The above result implies

$$\begin{bmatrix}\Delta n\\ \Delta c_1\end{bmatrix} = E\left(\begin{bmatrix}\Delta n\\ \Delta c_1\end{bmatrix}\right) + \sqrt{\mathrm{Var}\left(\begin{bmatrix}\Delta n\\ \Delta c_1\end{bmatrix}\right)}\begin{bmatrix}\eta_1\\ \eta_2\end{bmatrix}, \quad \text{where } \eta_1, \eta_2 \sim N(0,1) \tag{9.8}$$

Thus, we have

$$\begin{bmatrix}n(t+\Delta t)\\ c_1(t+\Delta t)\end{bmatrix} = \begin{bmatrix}n(t)\\ c_1(t)\end{bmatrix} + \begin{bmatrix}\frac{\rho-\beta}{l}n + \lambda_1 c_1\\ \frac{\beta_1}{l}n + \lambda_1 c_1\end{bmatrix}\Delta t + \begin{bmatrix}q\\ 0\end{bmatrix}\Delta t + \widehat{B}^{1/2}\sqrt{\Delta t}\begin{bmatrix}\eta_1\\ \eta_2\end{bmatrix}, \tag{9.9}$$

where $\widehat{B}^{1/2}$ is the square root of the matrix $\widehat{B}$. Dividing both sides of Eq. (9.9) by Δt and then taking limit $\Delta t \to 0$, we achieve the following Itô stochastic differential equation system

$$\frac{d}{\mathrm{d}t}\begin{bmatrix}n\\ c_1\end{bmatrix} = \widehat{A}\begin{bmatrix}n\\ c_1\end{bmatrix} + \begin{bmatrix}q\\ 0\end{bmatrix} + \widehat{B}^{1/2}\frac{\mathrm{d}\overrightarrow{W}}{\mathrm{d}t}, \tag{9.10}$$

where

$$\widehat{A} = \begin{bmatrix}\frac{\rho-\beta}{l} & \lambda_1\\ \frac{\beta_1}{l} & -\lambda_1\end{bmatrix},$$

$$\widehat{B} = \begin{bmatrix}\gamma n + \lambda_1 c_1 + q & \frac{\beta_1}{l}(-1+(1-\beta)v)n - \lambda_1 c_1\\ \frac{\beta_1}{l}(-1+(1-\beta)v)n - \lambda_1 c_1 & \frac{\beta_1^2}{l}n + \lambda_1 c_1\end{bmatrix},$$

and

$$\overrightarrow{W}(t) = \begin{bmatrix}W_1(t)\\ W_2(t)\end{bmatrix},$$

where $W_1(t)$ and $W_2(t)$ are Wiener processes. Equation (9.10) represents the stochastic point kinetics equations for one precursor. Now generalizing the above argument to m precursors, we can obtain the following Itô stochastic differential equation system for m precursors

$$\frac{\mathrm{d}}{\mathrm{d}t}\begin{bmatrix} n \\ c_1 \\ c_2 \\ \vdots \\ c_m \end{bmatrix} = \widehat{A}\begin{bmatrix} n \\ c_1 \\ c_2 \\ \vdots \\ c_m \end{bmatrix} + \begin{bmatrix} q \\ 0 \\ 0 \\ \vdots \\ 0 \end{bmatrix} + \widehat{B}^{1/2}\frac{\mathrm{d}\overrightarrow{W}}{\mathrm{d}t}. \tag{9.11}$$

In Eq. (9.11), $\widehat{A}$ and $\widehat{B}$ are as follows

$$\widehat{A} = \begin{bmatrix} \frac{\rho-\beta}{l} & \lambda_1 & \lambda_2 & \cdots & \lambda_m \\ \frac{\beta_1}{l} & -\lambda_1 & 0 & \cdots & 0 \\ \frac{\beta_2}{l} & 0 & -\lambda_2 & \ddots & \vdots \\ \vdots & \vdots & \ddots & \ddots & 0 \\ \frac{\beta_m}{l} & 0 & \cdots & 0 & -\lambda_m \end{bmatrix}, \tag{9.12}$$

$$\widehat{B} = \begin{bmatrix} \zeta & a_1 & a_2 & \cdots & a_m \\ a_1 & r_1 & b_{2,3} & \cdots & b_{2,m+1} \\ a_2 & b_{3,2} & r_2 & \ddots & \vdots \\ \vdots & \vdots & \ddots & \ddots & b_{m,m+1} \\ a_m & b_{m+1,2} & \cdots & b_{m+1,m} & r_m \end{bmatrix}, \tag{9.13}$$

where

$$\zeta = \gamma n + \sum_{j=1}^{m} \lambda_j c_j + q,$$

$$\gamma = \frac{-1-\rho+2\beta+(1-\beta)^2 v}{l},$$

$$a_j = \frac{\beta_j}{l}(-1+(1-\beta)v)n - \lambda_j c_j,$$

$$b_{i,j} = \frac{\beta_{i-1}\beta_{j-1}v}{l}n,$$

and

$$r_i = \frac{\beta_i^2 v}{l} n + \lambda_i c_i.$$

Equation (9.11) represents the generalization of the standard point kinetics model since for $\widehat{B} = 0$, it reduces to the standard deterministic point kinetics model [3].

9.5 Application of Euler–Maruyama Method and Strong Order 1.5 Taylor Method for the Solution of Stochastic Point Kinetics Model

The stochastic point kinetics equations for m delayed groups are as follows

$$\frac{\mathrm{d}\overrightarrow{x}}{\mathrm{d}t} = A\overrightarrow{x} + B(t)\overrightarrow{x} + \overrightarrow{F}(t) + \widehat{B}^{1/2}\frac{\mathrm{d}\overrightarrow{W}}{\mathrm{d}t}, \tag{9.14}$$

where $\hat{B}$ is given in Eq. (9.13),

$$\overrightarrow{x} = \begin{bmatrix} n \\ c_1 \\ c_2 \\ \vdots \\ c_m \end{bmatrix}, \tag{9.15}$$

$$A = \begin{bmatrix} \frac{-\beta}{l} & \lambda_1 & \lambda_2 & \cdots & \lambda_m \\ \frac{\beta_1}{l} & -\lambda_1 & 0 & \cdots & 0 \\ \frac{\beta_2}{l} & 0 & -\lambda_2 & \ddots & \vdots \\ \vdots & \vdots & \ddots & \ddots & 0 \\ \frac{\beta_m}{l} & 0 & \cdots & 0 & -\lambda_m \end{bmatrix}, \tag{9.16}$$

$$B(t) = \begin{bmatrix} \frac{\rho(t)}{l} & 0 & 0 & \cdots & 0 \\ 0 & 0 & 0 & \cdots & 0 \\ 0 & 0 & 0 & \ddots & \vdots \\ \vdots & \vdots & \ddots & \ddots & 0 \\ 0 & 0 & \cdots & 0 & 0 \end{bmatrix}, \tag{9.17}$$

and

$$\overrightarrow{F}(t) = \begin{bmatrix} q(t) \\ 0 \\ 0 \\ \vdots \\ 0 \end{bmatrix}. \tag{9.18}$$

It can be noticed that $\widehat{A} = A + B(t)$.

9.5.1 Euler–Maruyama Method for the Solution of Stochastic Point Kinetics Model

This method is also known as order 0.5 strong Itô–Taylor approximation. By applying Euler–Maruyama method in Eq. (1.142) of Chap. 1 into Eq. (9.14), we obtain

$$\overrightarrow{x}_{i+1} = \overrightarrow{x}_i + (A + B_i)\overrightarrow{x}_i h + \overrightarrow{F}(t_i)h + B^{1/2}\sqrt{h}\,\overrightarrow{\eta}_i, \tag{9.19}$$

where $\mathrm{d}\overrightarrow{W}_i = \overrightarrow{W}_i - \overrightarrow{W}_{i-1} = \sqrt{h}\,\overrightarrow{\eta}_i$ and $h = t_{i+1} - t_i$. Here, $\overrightarrow{\eta}_i$ is a vector whose components are random numbers chosen from $N(0,1)$.

9.5.2 Strong Order 1.5 Taylor Method for the Solution of Stochastic Point Kinetics Model

We apply strong order 1.5 Taylor approximation method in Eq. (1.143) of Chap. 1 into Eq. (9.14) yielding

$$\overrightarrow{x}_{i+1} = \overrightarrow{x}_i + \left((A + B_i)\overrightarrow{x}_i + \overrightarrow{F}_i\right)h + \widehat{B}^{1/2}\sqrt{h}\,\overrightarrow{\eta}_i + (A + B_i)\widehat{B}^{1/2}\Delta Z_i + \frac{1}{2}\left((A + B_i)\overrightarrow{x}_i + \overrightarrow{F}_i\right)(A + B_i)h^2, \tag{9.20}$$

where $\Delta Z_i = \frac{1}{2}h(\Delta W_i + \Delta V_i/\sqrt{3})$ and $\Delta V_i = \sqrt{h}\,N(0,1)$.

9.5.3 Numerical Results and Discussion

In the present analysis, we consider the first example of nuclear reactor problem with the following parameters $\lambda_1 = 0.1, \quad \beta_1 = 0.05 = \beta, \quad v = 2.5, \quad v = 2.5,$ neutron source $q = 200, \quad l = 2/3$ and $\rho(t) = -1/3$ for $t \geq 0$. The initial condition is $\overrightarrow{x}(0) = [400 \quad 300]^{\mathrm{T}}$. We observe through 5000 trails, the good agreement between two methods with other available methods for 40 time intervals at time t = 2 s. The means and standard deviation of $n(2)$ and $c_1(2)$ are presented in Table 9.1.

In the second example, we assume the initial condition as

$$\overrightarrow{x}(0) = 100 \begin{bmatrix} 1 \\ \frac{\beta_1}{\lambda_1 l} \\ \frac{\beta_2}{\lambda_2 l} \\ \vdots \\ \frac{\beta_m}{\lambda_m l} \end{bmatrix}.$$

The following parameters are used in this example [1, 3] $\beta = 0.007$, $v = 2.5$, $l = 0.00002$, $q = 0$, $\lambda_i = [0.0127, 0.0317, 0.115, 0.311, 1.4, 3.87]$ and $\beta_i = [0.000266, 0.001491, 0.001316, 0.002849, 0.000896, 0.000182]$ with $m = 6$ delayed groups. The computational results at $t = 0.1$ and $t = 0.001$ are given in Tables 9.2 and 9.3, respectively, for Monte Carlo, stochastic PCA [4], Euler–Maruyama, and Taylor 1.5 strong order. It can be seen that there exist approximately close agreements between the three approaches in consideration of different step reactivities $\rho = 0.003$ and $\rho = 0.007$. The mean neutron density and two individual neutron samples are cited in Fig. 9.1. The mean precursor density and two precursor sample paths are cited in Fig. 9.2. For these calculations, we used 5000 trials in both Euler–Maruyama and Taylor 1.5 strong order method.

Table 9.1 Comparison of numerical computational methods for one precursor

	Monte Carlo	Stochastic PCA [4]	Euler–Maruyama approximation	Strong order 1.5 Taylor approximation
$E(n(2))$	400.03	395.32	412.23	412.10
$\sigma(n(2))$	27.311	29.411	34.391	34.519
$E(c_1(2))$	300.00	300.67	315.96	315.93
$\sigma(c_1(2))$	7.8073	8.3564	8.2656	8.3158

Table 9.2 Comparison for subcritical step reactivity $\rho = 0.003$

	Monte Carlo	Stochastic PCA [4]	Euler–Maruyama	Taylor 1.5 strong order
$E(n(0.1))$	183.04	186.31	208.599	199.408
$\sigma(n(0.1))$	168.79	164.16	255.954	168.547
$E(c_1(0.1))$	4.478×10^5	4.491×10^5	4.498×10^5	4.497×10^5
$\sigma(c_1(0.1))$	1495.7	1917.2	1233.38	1218.82

Table 9.3 Comparison for critical step reactivity $\rho = 0.007$

	Monte Carlo	Stochastic PCA [4]	Euler–Maruyama	Taylor 1.5 strong order
$E(n(0.001))$	135.67	134.55	139.568	139.569
$\sigma(n(0.001))$	93.376	91.242	92.042	92.047
$E(c_1(0.001))$	4.464×10^5	4.464×10^5	4.463×10^5	4.463×10^5
$\sigma(c_1(0.001))$	16.226	19.444	6.071	18.337

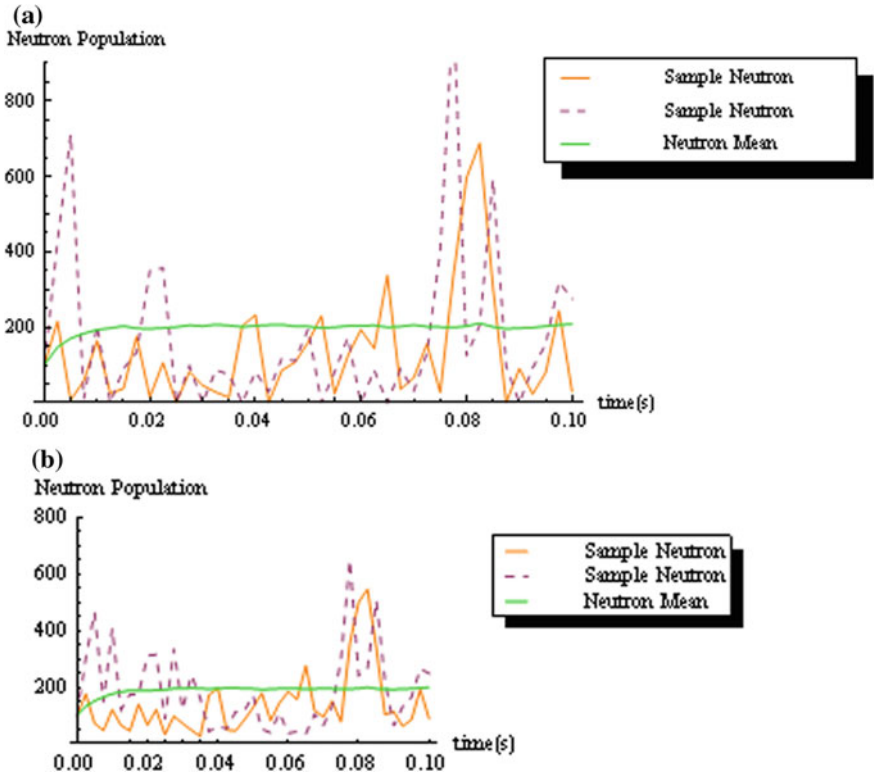

Fig. 9.1 **a** Neutron density obtained by Euler–Maruyama method using a subcritical step reactivity $\rho = 0.003$ and **b** neutron density obtained by strong 1.5 order Taylor method using a subcritical step reactivity $\rho = 0.003$

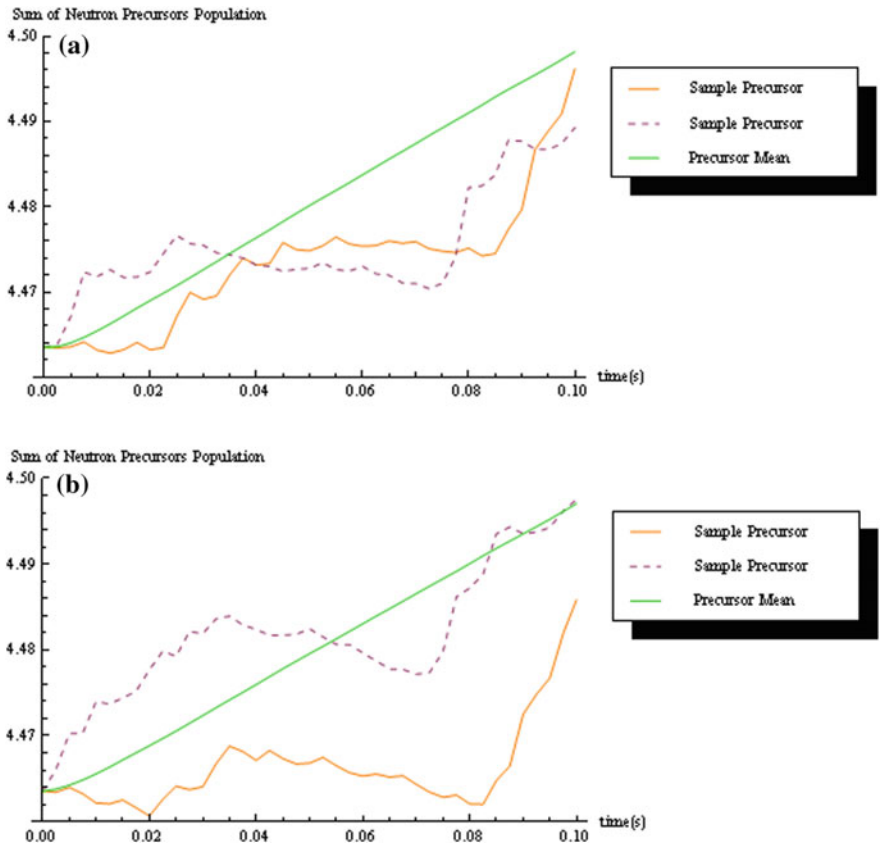

Fig. 9.2 **a** Precursor density obtained by Euler–Maruyama method using a subcritical step reactivity $\rho = 0.003$ and **b** precursor density obtained by strong 1.5 order Taylor method using a subcritical step reactivity $\rho = 0.003$

9.6 Conclusion

In this present research work, the stochastic point kinetics equations have been solved by using Euler–Maruyama and strong order 1.5 Taylor numerical methods having easier and efficient calculation in comparison with stochastic PCA method. The methods, in this investigation, are clearly effective numerical methods for solving the stochastic point kinetics equations. The methods are simple, efficient to calculate, and accurate with fewer round-off error. The derivation of stochastic point kinetics equations may be complicated but numerical solutions obtained more conveniently. The behavior of the stochastic neutron and precursor distributions within a reactor can be explicitly described by the stochastic point kinetics equations. The obvious reason seems to be that the intrinsic stochastic dynamic phenomena in the reactor system can be properly treated with the stochastic point

kinetics equations. In this chapter, a numerical investigation was performed in order to observe the random fluctuations in neutron and precursor population dynamics in subcritical and critical reactors.

References

1. Hetrick, D.L.: Dynamics of Nuclear Reactors. American Nuclear Society, Chicago, London (1993)
2. Duderstadt, J.J., Hamilton, L.J.: Nuclear Reactor Analysis. Wiley, Michigan, USA (1976)
3. Kinard, M., Allen, K.E.J.: Efficient numerical solution of the point kinetics equations in nuclear reactor dynamics. Ann. Nucl. Energy **31**, 1039–1051 (2004)
4. Hayes, J.G., Allen, E.J.: Stochastic point-kinetics equations in nuclear reactor dynamics. Ann. Nucl. Energy **32**, 572–587 (2005)
5. Sauer, T.: Numerical solution of stochastic differential equation in finance. Handbook of Computational Finance, pp. 529–550. Springer, NY (2012)